Extended computation of ultrasonic wavenumber in particulate dispersions

by

Terence James O'Neill

A thesis submitted to Keele University

for the Degree of Doctor of Philosophy

Ultrasonics and Digital Signal Processing Laboratory

Department of Physics

Keele University

Keele, Staffordshire ST5 5BG

United Kingdom

December 1998

Abstract

Methods to characterize dispersions in terms of concentration, sizes and size distribution of suspended particles promise significant commercial and industrial utility. Ultrasonic spectroscopy offers practical advantages over existing, mostly off-line, non-ultrasonic methods. A necessary function of a spectrometer would be the correlation of experimental with modelled ultrasonic spectra. These are derived from the complex ultrasonic wavenumber. There are a number of mathematical models to calculate the propagation wavenumber of ultrasound in a dispersion. Of these, that of Epstein & Carhart, extended by Allegra & Hawley and known as the ECAH model, offers the best compromise of inclusion of all significant loss mechanisms and ability to model a wide range of combinations of continuous and dispersed phase materials, frequencies, concentrations and particle sizes. Use of the ECAH model and some associated multiple scattering models in ultrasonic spectroscopy are evaluated and compared to experimental data. Although mathematically related, attenuation and phase velocity spectra are shown separately to contain information that might uniquely characterize a dispersion. Truncating the summation of the ultrasonic scattering wavenumber at low orders of its convergent infinite series solution is demonstrated to result sometimes in serious error. The orders required for limits of convergence for a variety of materials, frequencies and particle sizes are listed and analyzed. A relationship between the required order, frequency, particle size and compressive wave velocity in the continuous phase is established. Difficulties computing higher orders are examined and a solution, based on the work of Amos, developed. Also shown are modifications to the formulation of the ECAH model that substantially extend the limits of particle size and frequency that can be modelled without computational instability. Sensitivity of output to errors in temperature and values of physical properties of a modelled dispersion is examined and quantified. Spectral features that are indicators of concentration, size and size distribution of particles, that could be exploited in an on-line instrument to characterize dispersions, are identified and described.

Acknowledgements

I would like to thank my supervisor Professor Richard Challis: firstly, for giving me the opportunity of undertaking this research; secondly, for his trust, encouragement, guidance and advice throughout; and finally, for finding the necessary support funding when the task took longer than originally planned. I would also take the opportunity to thank Keele University, its Physics Department and former Electronics Department and my colleagues and friends in the UDSP Laboratory for contributing to such a helpful, enjoyable and stimulating environment in which to work and relax. In particular, I would like to thank Andrew Holmes, for the use of his experimental data, and John Tebbutt, for his early help when I was getting to grips with the theory of the project and, latterly, for his many hours of proof-reading and ensuing constructive criticisms, suggestions and comments.

Thank you also to Robert Jack of Malvern Instruments Ltd and Martin Garrood of the Institute of Food Research at Norwich for your contributions of advice and information.

I am grateful to the Engineering and Physical Sciences Research Council for funding most of this research project under Grant Number 94701560.

Lastly, but most importantly, none of this would have been possible without my greatest supporters - my wife Susan, daughter Josephine and son, Timothy. There is no doubt that they have had to put up with a lot, and missed out on a lot, while I have been totally immersed in this research. I consider myself fortunate to have such family and friends.

Table of contents

List of figures

List of tables

1. Propagation of sound through a medium - a brief overview

1.1 Introduction

This thesis investigates the interaction of sound with dispersions. Dispersions comprise particles of suspended material, be they gaseous, liquid or solid, in a continuous medium, which can be gaseous, liquid or solid. A subset of this definition encompasses colloids, conventionally described as particles of solid in a liquid or an emulsion of a liquid in a liquid. The usual size criterion ascribed to colloids is that the particles are of a diameter small enough to be subject to Brownian motion (<1μm) but large enough not to be subject to quantum effects (>50nm). The techniques described in this thesis seek to model the acoustic behaviour of particles in the extended range of 10nm to 1mm in diameter and that the model not be limited by the physical phase of the suspended or continuous media. Many of the underlying mathematical principles used to model and predict the interaction of sound with materials are based on the assumption that the scale of wavelength of the sound in relation to particle size is large. Therefore, in view of the particle sizes of interest, the term *sound* implies acoustic frequencies of hundreds of kilohertz up to hundreds of megahertz – and is usually called ultrasound. Dispersions containing particles in the size range under consideration are of considerable academic and commercial interest and include:

a. Foodstuffs such as mayonnaise, sauces etc

b. Paints, inks and coatings

c. Fogs and mists

d. Polymer latices

e. Constituents of ceramics

f. Controlled-release or topically applied drugs

g. Cosmetics

h. Lubricants

i. Abrasive materials and polishes

These examples are by no means exhaustive but do have something in common other than being dispersions. Critically, not only do they depend upon the type of suspended material but also upon its shape, size, size-distribution and % v/v concentration (a measure of volume of suspended phase as a proportion of total volume of both suspended and continuous phases –sometimes referred to as volume fraction) for the properties or quality of the end-product. Monitoring and/or controlling these parameters are of vital importance both in the laboratory and in commercial-scale operations. The object of this thesis is to demonstrate the feasibility of modelling the behaviour of sound propagation through the described media accurately enough to enable the correlation of modelled and experimentally measured acoustic propagation. By the back-fitting of modelled to experimentally measured results it should then be possible to ascertain the size and % v/v concentration of a dispersion from its measured acoustic characteristics.

There are a number of other ways of deriving the size and % v/v concentration properties of a dispersion. Some of them are well established and others are under development. Many are invasive and require the removal and/or dilution of test samples that might be destroyed in the process while others enable on-line measurements to be made. They include microscopy, optical light measurements, sedimentation rate measurement, analysis of various electrical properties, magnetic resonance, sub-atomic particle or X-ray scattering and electro-acoustic methods. As yet, none offers the ultimate goal of in-line, real-time

measurement over a full range of materials, particle sizes and % v/v concentrations. It is unlikely that acoustic methods alone will achieve that goal either, but probably will help complement other methods to achieve better solutions to the problems of science and industry.

As far as the author is aware, no current models incorporate all the loss mechanisms described, but concentrate upon a few of the more important ones. Therefore, this chapter gives a brief overview of some of the more significant physical mechanisms that influence the acoustic behaviour of a dispersion and it goes on to describe some of those mechanisms that must be borne in mind when selecting or formulating a model for a particular application. By judicious choice of model, there can be excellent agreement between even the most limited model and experimentally measured data if the overall contribution of loss mechanisms not catered for by the chosen model is insignificant for the dispersion materials, sizes, % v/v concentrations and frequency ranges of interest.

1.2 Energy content of a dispersion

Sound takes a finite time to pass from a source, through a medium, to a receiver and, in all practical circumstances, some energy is lost in transit. These two properties of sound transmission, couched in terms of sound velocity and attenuation, are functions of the physical media and the frequency of the sound. In media that consist of inhomogeneous mixtures of particles within a suspending continuous phase, sound attenuation and phase velocity dispersion (the variation of phase velocity with frequency) depend upon the physical nature of each of the continuous and dispersed phases, the shape, size and size distribution of the particles, the temperature and pressure. A useful analogy used by

Litovitz (Litovitz, 1959) is that the energy contained within a dispersion is contained within a great number of boxes, each containing a different type of energy. Some of the more obvious boxes might be:

a. Molecular vibrational energy
b. Translational energy
c. Lattice vibrational energy
d. Molecular structural states (rotational isomers)
e. Lattice structural energy (degree of order in the liquid)

These boxes are all coupled to each other by physical mechanisms and are in equilibrium. If the energy of one box is raised it is possible for energy to be redistributed to other boxes to re-establish equilibrium. The time taken to reach equilibrium is dependent upon the nature of the coupling process. Two important classes of coupling process are:

a. *Oscillatory*, where the energy is exchanged and overshoots back and forth at a certain frequency
b. *Relaxational*, where the energy in a higher energy box will decrease exponentially, as it flows into a lower energy box, with its own characteristic time constant dependent upon the nature of the energy translation

1.2.1 Relaxational coupling of energy

A sound wave passing through a given point in a medium raises the energy in one or more boxes as the compression takes place but that energy can be returned to the ordered elastic energy of the wave as decompression takes place. However, because of relaxational coupling, some of the translational energy of the wave is coupled to other energy boxes by relaxational processes that are sensitive to the time available to reach equilibrium. This time is a function of frequency. At certain frequencies the compression-decompression cycle and exchange of energy between boxes can become significant but out of phase with each other; consequently, the energy is irretrievably lost to the elastic wave and the effective attenuation per wavelength spectrum of the medium passes through a characteristically broad maximum. As the frequency increases there is less time for the energy to transfer between boxes. Inevitably, a smaller fraction of the energy gets shared and this tends to decrease the loss from the acoustic wave. At very high frequencies almost no energy is shared and the effective attenuation per wavelength due to relaxational processes drops towards zero. A schematic representation of a typical relaxation effect on attenuation per wavelength and phase velocity appears in Figure 1.1.

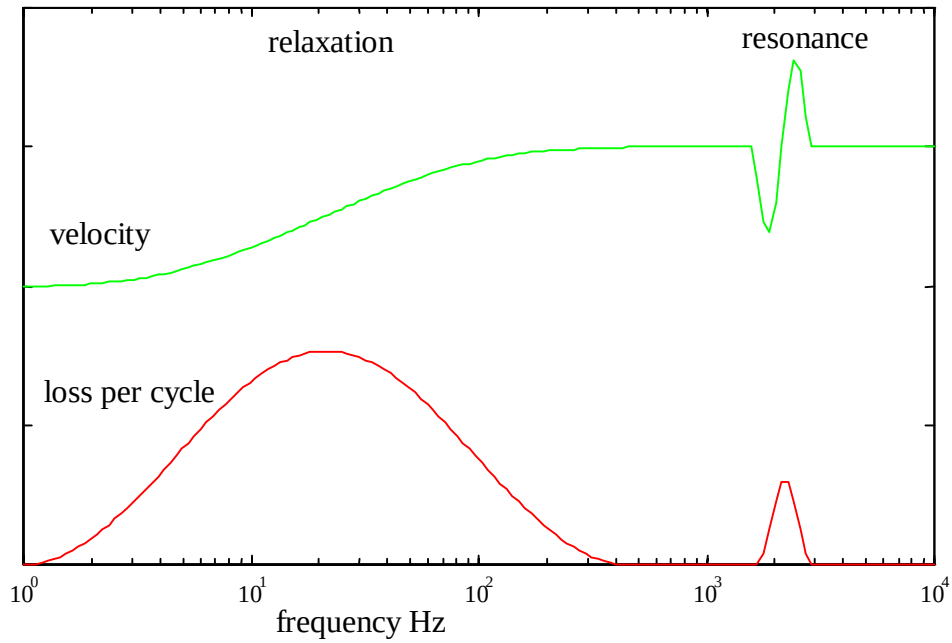

Figure 1.1 Schematic diagram in arbitrary units versus frequency of relaxation and resonance effects on attenuation and phase velocity (based on Litovitz, 1959)

1.2.2 Resonant coupling of energy

Resonant coupling occurs when a feature of the medium such as suspended particles of similar dimensions to the wavelength of the exciting sound resonate together over a relatively narrow frequency band. Such resonances produce characteristically sharp maxima in the attenuation spectrum and closely associated minima and maxima in the phase velocity spectrum. A schematic representation of a typical resonance effect on attenuation and velocity also appears in Figure 1.1.

1.3 Acoustic loss mechanisms

The physical mechanisms by which sound energy is redirected or lost within a dispersion are many and include the following:

a. Viscous losses

b. Thermal losses

c. Scattering losses.

d. Intrinsic losses

e. Electrokinetic effects.

f. Structural losses

g. Chemical relaxation

h. Melting, crystallization or other phase transition relaxation

Each of these loss mechanisms is explained briefly in the following paragraphs.

1.3.1 Viscous losses

When considering the propagation of a plane compression wave through a fluid single-phase system the attenuation coefficient can be derived from first principles using linear terms representing viscosity and thermal conductivity (Temkin, 1981). For a viscous, non-heat conducting (ideal) fluid, the coefficient of attenuation, α, the low-frequency sound speed, c, angular frequency in radians, ω and the viscous relaxation time, $\tau_{v,}$ are related by the expression

$$\left(\frac{\alpha c}{\omega}\right)^2 = \frac{1}{2}\left(\frac{1}{\sqrt{1+\omega^2\tau_v^2}} - \frac{1}{1+\omega^2\tau_v^2}\right) \quad \textbf{(1.1)}$$

Where

$$\omega\tau_v = \frac{4}{3}\frac{\omega\,\nu'}{c^2} \quad \textbf{(1.2)}$$

$$\nu' = \frac{\eta}{\rho}\left(1+\frac{3}{4}\frac{K}{\eta}\right) \quad \textbf{(1.3)}$$

and K represents the bulk or expansion viscosity, η the shear or dynamic viscosity and ρ the mass density of the fluid. Consequently, the term $\omega\tau_v$ represents the speed of viscous momentum transfer relative to the speed c, with which momentum is transmitted by wave motion in an ideal fluid (Temkin, 1981). Attenuation α increases with increasing $\omega\tau_v$.

When the transmitting medium consists of continuous and dispersed phases another viscous loss mechanism comes into play. If a particle and its suspending continuous phase possess different mass densities they will not move in phase when subjected to an oscillating acoustic pressure field, because of the inertia of the particle. This gives rise to oscillating shear waves propagating from the surface of the particle both inwards into the particle and outwards into the suspending medium. Most of the energy contained in these waves will be lost to the propagating elastic compression wave. The amplitude of the shear wave decays exponentially with the distance from the particle surface (Stokes, 1845). A useful metric of this effect is the distance over which the shear wave decays by a factor of $1/e$. This distance is usually termed *oscillatory boundary layer thickness* or *viscous skin depth*, δ_v, and expressed as

$$\delta_v = \sqrt{\frac{2\eta}{\rho\omega}} \qquad \textbf{(1.4)}$$

1.3.2 Thermal losses

In any practical sound-conducting medium thermal conduction will be possible. Therefore, heat will tend to flow from adiabatically heated zones of compression into adjacent adiabatically cooled zones of rarefaction. This is a relaxational process, dependent upon

the thermophysical properties of the medium, and will take place within the continuous medium and also within the suspended particles. In the presence of suspended particles, oscillating temperature gradients inside and outside the particle will be generated adjacent to its surface and a useful metric of this effect is termed *thermal skin depth*, denoted by δ_T, and expressed as

$$\delta_T = \sqrt{\frac{2\kappa}{\omega \rho C_p}} \qquad \textbf{(1.5)}$$

Where κ is thermal conductivity and C_p is specific heat capacity at constant pressure. Thermal skin depth into the particle or outwards into the surrounding medium is found by substituting either the dispersed or continuous phase's thermal conductivity, specific heat and mass density figures into Equation 1.5.

1.3.3 Scattering losses

Acoustic scattering is analogous to light scattering. The first in-depth treatment of the phenomena appeared in 1877 in Lord Rayleigh's *Theory of Sound* (Rayleigh, 1877) and the scattering of sound waves, the wavelength of which is much larger than the diameter of the scatterer, is known as long-wavelength regime or *Rayleigh Scattering*. Most of the mathematical treatments of acoustic scattering in the literature assume particles to have clearly defined geometries such as spheres, cylinders or plates and reflection to be non-specular and in the long wavelength regime. Such scattering does not, in principle, cause attenuation but diverts energy away from the transmitter to receiver path and therefore appears at the receiver as a loss of sound energy. In reality there will be some losses due to mode conversion and scattering at the particle surface and at the boundary of real-life

systems such as test cell walls. The methods of calculating scattering losses are complicated and are examined in some detail in Chapter 4.

1.3.4 Intrinsic losses

The term *intrinsic losses* is used by many workers to denote losses due to each individual phase. Below 200MHz, the frequency range of interest of this thesis, the viscous and thermal effects already described are the primary causes of intrinsic losses. Molecular resonance losses can be significant, but at much higher frequencies.

1.3.5 Electrokinetic effects

All practical dispersions of particles possess electrical properties. A particle with an electrical charge potential will attract and keep an adjacent layer of oppositely charged ions from the suspending fluid if these ions are available. This combination of an electrically charged particle with an oppositely charged, spherically symmetrical 'cloud' of ions around it is known as an electrical double layer. It is in electrical equilibrium if undisturbed and the centres of electrical charge for each of the components will be co-located. However, motion of the particle relative to the surrounding fluid will lead to asymmetry of the double layer and the centres of charge will no longer coincide. A steady relative motion, such as that caused by gravity, leads to a constant *sedimentation potential* (Booth, 1954).

Through a similar mechanism to that of the sedimentation potential, the oscillating disturbance caused by the passage of an elastic compressive wave will set up an *acoustophoretic* oscillating electric dipole (Enderby, 1951) at each particle. The acoustophoretic effect over a system of suspended particles is macroscopically additive and

results in an induced electric field that opposes the motion of the charged particles relative to the fluid. This phenomenon, termed colloid vibration potential, tends to *counteract* the viscous attenuation of sound although a relatively small amount of acoustic energy will be irretrievably converted to electromagnetic energy, resulting in acoustic attenuation.

1.3.6 Structural losses

Liquids such as water and ethyl alcohol exhibit structural or volume relaxational losses. For example, water is assumed to exist in two energy states (Hall, 1948). In the higher energy state the water molecules are more closely packed than in the lower energy state. Water normally exists in the lower energy state. The passage of a compressional wave is assumed to promote the transfer of molecules from one state to the other and the two-way process, being relaxational in nature, can cause frequency dependent losses. The effects of this phenomenon can be significant but are usually taken into account indirectly by incorporating them into a hypothetical bulk viscosity when predicting absorption.

1.3.7 Chemical relaxation

Many liquids, particularly aqueous electrolytes, exhibit absorption caused by ionic energy exchange. In the case of seawater, the relatively low concentration of magnesium sulphate is responsible for significant absorption of sound, increasing $\alpha\lambda$ by an order of magnitude between 10kHz and 100kHz, but the effect becomes negligible by 1MHz. The phenomenon is believed to be associated with the dissociation of $MgSO_4$ to give a complex with one water molecule inserted between the Mg^{2+} and the SO_4^{2-} ions (Stephens, 1970). At higher frequencies a second absorption peak is found due to the insertion of a second water molecule. There are many other phenomena of a similar nature: ionic atmospheric

relaxation, hydrolysis, formation of complexes, hydration of solute molecules (eg sugars), changes in the co-ordination number, formation and disintegration of clathrate structures, monomer-micelle exchange in surfactants, and the equilibrium between monomer and dimer as in acetic acid. An excellent review of these phenomena can be found in Batia (1967).

1.3.8 Melting, crystallization or other phase-transition relaxation phenomena

A number of physical effects can be caused by the passage of a compressional elastic wave, usually triggered by the change in pressure leading to a localized change in mass density and temperature. If the variation in pressure, mass density and temperature spans the range in which suspended particles of solid, liquid or gas change phase then that change will usually be relaxational in nature and lead to attenuation. For example, a mixture of soluble particles in a saturated solution will vary in its % v/v concentration of suspended particles if the solubility and degree of saturation are functions of temperature that can be varied by the passage of a sound wave. This effect, as well as causing relaxational absorption of sound energy, will complicate the scattering mechanisms as the sizes of the scattering particles oscillate. A related phenomenon is isomeric relaxation. When a molecule possesses a number of isomeric forms each is usually associated with a different energy level or energy is temporarily required to convert from one isomeric form to another. This has been shown to result in relaxational isomeric absorption (Karpovich, 1954).

1.4 Acoustic phase propagation velocity

Although velocity has been mentioned as a measurable property of sound passing through a dispersion, discussion has so far dwelled upon acoustic attenuation. However, when a medium exhibits properties of attenuating acoustic propagation in a frequency dependent way which is invariably the case, the *Kramers-Kronig* relationship implies that the wave propagation will exhibit velocity variation in a frequency dependent way (Kronig & Kramers, 1928). This is known as phase velocity dispersion. In mathematical terms the Kramers-Kronig relationship enables the localized frequency attenuation to be calculated given the phase velocity dispersion *for all frequencies.* Conversely, the frequency localized velocity dispersion (rate of change of phase velocity) can be calculated given the attenuation values *for all frequencies.* In practical terms, it is impossible to know the values of attenuation or velocity dispersion for all frequencies. However, providing the attenuation or phase velocity dispersion varies smoothly within a certain frequency band of interest (no sharp resonance effects) it is possible to use the Kramers-Kronig relationship over such a bounded frequency range to illustrate the relationship. Although what is usually regarded as a simple model is used as a basis for the illustration, the Kramers-Kronig relationship is true for all attenuated acoustic waves *irrespective of the loss mechanisms involved* (O'Donnell *et al*, 1978). The following example is a brief overview of work carried out by O'Donnell and co-workers at Washington University (O'Donnell *et al*, 1978 & 1981) and the interested reader is referred to the latter reference for a more rigorous mathematical treatment of the Kramers-Kronig relationship, as applicable to acoustic waves. In a perfect (lossless) sound-transmitting fluid the velocity of sound in the medium can be calculated from its physical properties. Wood's equation (Wood, 1941) states that the velocity can be expressed as

$$c = \sqrt{\frac{1}{\beta\rho}} \tag{1.6}$$

where β represents the bulk compressibility of the medium. From this velocity, *c*, the wavenumber *k* of the medium can be calculated for any frequency

$$k = \frac{\omega}{c} \tag{1.7}$$

Nevertheless, there are no known perfect media, all practical materials exhibit some acoustic losses to a greater or lesser extent. To incorporate attenuation the wavenumber must be complex and includes α as an imaginary term that represents the loss in energy *E* over a distance *x* in the following way

$$\frac{E_{out}}{E_{in}} = e^{-2\alpha x} \tag{1.8}$$

The wavenumber for a practical medium can now be expressed as

$$k = \frac{\omega}{c} + i\alpha \tag{1.9}$$

Where $i = \sqrt{-1}$. In this case, Wood's equation, Equation (1.6) still holds true, but the compressibility term β is now deemed to be complex. Also, if we restrict our attention to media in which both the attenuation and velocity of propagating sound exhibit frequency dependence (real media of practical interest) β and *c* are also dependent upon frequency and can be denoted as frequency domain functions β(ω) and *c*(ω). Recasting Wood's equation, Equation (1.6), in terms of complex wavenumber instead of phase velocity leads to

$$k^2 = \omega^2\rho\beta(\omega) \tag{1.10}$$

Where the frequency domain compressibility $\beta(\omega)$ can be split into its real and imaginary parts

$$\beta(\omega) = \beta_1(\omega) + i\beta_2(\omega) \tag{1.11}$$

Equation (1.10) can now be re-expressed by expanding the left-hand side using the identity given in Equation (1.9) and expanding the right-hand side using the identity given in Equation (1.11) to give

$$\frac{\omega^2}{c^2(\omega)} - \alpha^2(\omega) + \frac{i2\omega\alpha(\omega)}{c(\omega)} = \omega^2\rho\left[\beta_1(\omega) + i\beta_2(\omega)\right] \tag{1.12}$$

The real and imaginary parts of each side of Equation (1.12) can now be equated to give

$$\frac{\omega^2}{c^2(\omega)} - \alpha^2(\omega) = \omega^2\rho\beta_1(\omega) \tag{1.13}$$

$$\frac{2\omega\alpha(\omega)}{c(\omega)} = \omega^2\rho\beta_2(\omega) \tag{1.14}$$

In the usual case in which the magnitude of the real part of the complex wavenumber is much greater than the magnitude of the imaginary part

$$\alpha(\omega)\frac{c(\omega)}{\omega} << 1 \tag{1.15}$$

for all frequencies, rearrangement of Equations (1.13) and (1.14) gives explicit approximations for attenuation and phase velocity

$$c(\omega) \cong \frac{1}{\sqrt{\rho\beta_1}(\omega)} \tag{1.16}$$

$$\alpha(\omega) \cong \frac{\rho c(\omega)}{2}\omega\beta_2(\omega) \tag{1.17}$$

It can be shown (op cit) that for slowly varying attenuation and phase velocity dispersion (no sharp resonance effects) that the following, based on exact non-local relationships, is a useful local approximation of the complex compressibility

$$\frac{d\beta_1(\omega)}{d\omega} \cong -\frac{2}{\rho c^3(\omega)}\frac{dc(\omega)}{d\omega} \tag{1.18}$$

$$\beta_2(\omega) \cong -\frac{\pi}{2}\frac{d\beta_1(\omega)}{d\omega} \tag{1.19}$$

The explicit attenuation and phase velocity dispersion relationships in Equations (1.16) and (1.17) can now be re-expressed, using the approximations of Equations (1.18) and (1.19) as

$$\frac{dc(\omega)}{d\omega} \cong \frac{2c^2(\omega)\alpha(\omega)}{\pi\omega^2} \tag{1.20}$$

$$\alpha(\omega) \cong \frac{\pi\omega^2}{2c^2(\omega)}\frac{dc(\omega)}{d\omega} \tag{1.21}$$

If Equation (1.20) is transposed to give

$$\frac{dc(\omega)}{c^2(\omega)} \cong \frac{2\alpha(\omega)}{\omega^2}d\omega \tag{1.22}$$

and each side is integrated over some range ω_0 to ω, then the relationship of phase velocity to the attenuation coefficient is given by

$$\frac{1}{c_0} - \frac{1}{c(\omega)} \cong \frac{2}{\pi}\int_{\omega_0}^{\omega}\frac{\alpha(\omega)}{\omega^2}d\omega \tag{1.23}$$

where c_0 denotes the sound velocity at ω_0. Based on the assumption that the value of phase velocity dispersion is usually small (in relation to the value of the attenuation coefficient) Equations (1.20) and (1.21) can now be simplified to give

$$\Delta c = c(\omega) - c_0 = \frac{2c_0^2}{\pi}\int_{\omega_0}^{\omega}\frac{\alpha(\omega)}{\omega^2}d\omega \tag{1.24}$$

$$\alpha(\omega) = \frac{\pi\omega^2}{2c_0^2}\frac{dc(\omega)}{d\omega} \qquad \textbf{(1.25)}$$

Where

$$c(\omega) \cong c_0 + \Delta c(\omega), \quad \Delta c(\omega) << c_0 \qquad \textbf{(1.26)}$$

and higher than first order frequency derivatives of $c(\omega)$ are ignored.

As an illustration of their applicability, Equations (1.24) and (1.25) were used to predict both phase velocity dispersion and attenuation from data generated by a relatively well-proven mathematical model based on Allegra and Hawley single scattering (Allegra & Hawley, 1972). Figure 1.2 shows modelled velocity against frequency for 1μm radius silica particles, 10% by volume in a water dispersion, at 25°C. The model was run to within 0.01% convergence of both phase velocity and attenuation at all frequency points. It can be seen that the phase velocity exhibits a peak at about 30MHz such that its frequency derivative passes through zero. Therefore, Equation (1.25), which is linearly dependent upon the frequency derivative of velocity, indicates that the attenuation would be zero, an impossible situation in practice. Even more revealing is that after the phase velocity in Figure 1.2 passes through the peak at about 30MHz its slope is negative which, from Equation (1.24), would indicate that the attenuation would be negative - again, an impossible situation in practice. Nevertheless, the Kramers-Kronig predictions show good agreement with the model within certain limits. Figure 1.3 shows modelled and predicted α/f^2 against frequency of 1μm radius silica. The predictions use Equation (1.25) and modelled phase velocity data. It can be seen that agreement is reasonable throughout the range 100kHz to 100MHz and is very good in the centre range of 2MHz to 30MHz.

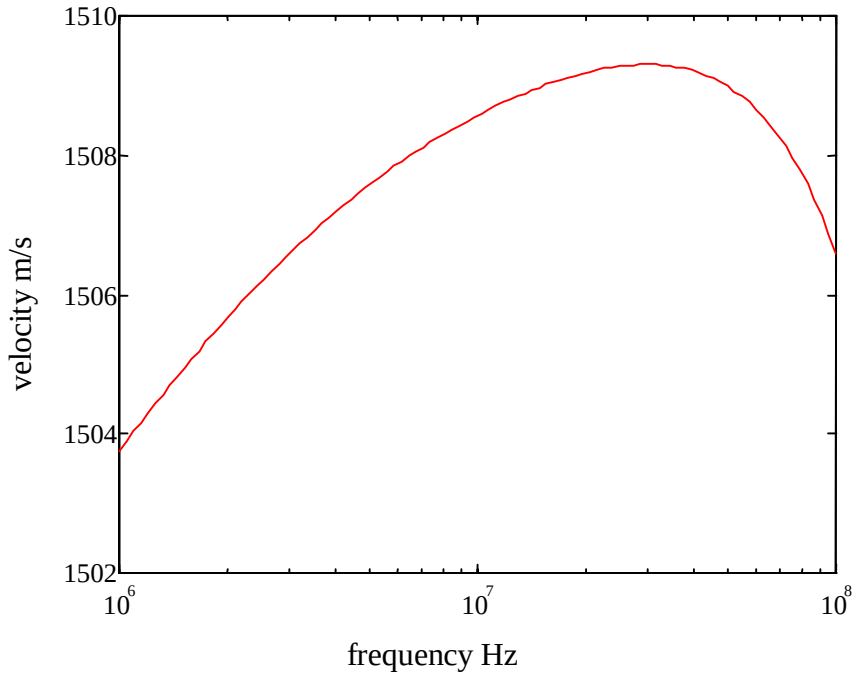

Figure 1.2 Modelled phase velocity versus frequency of 10% v/v 1μm radius aqueous silica dispersion

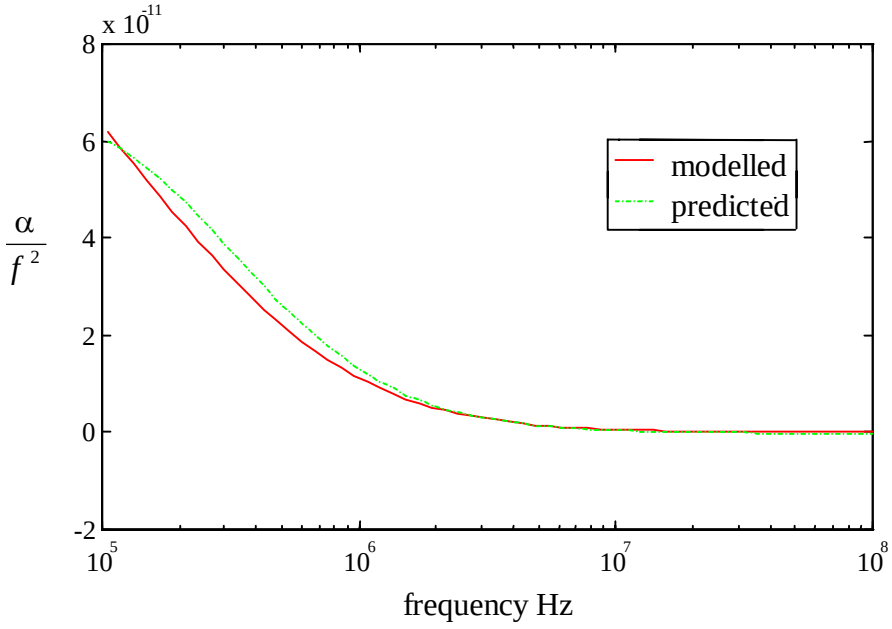

Figure 1.3 Modelled and predicted attenuation versus frequency of 10% v/v 1μm radius aqueous silica dispersion

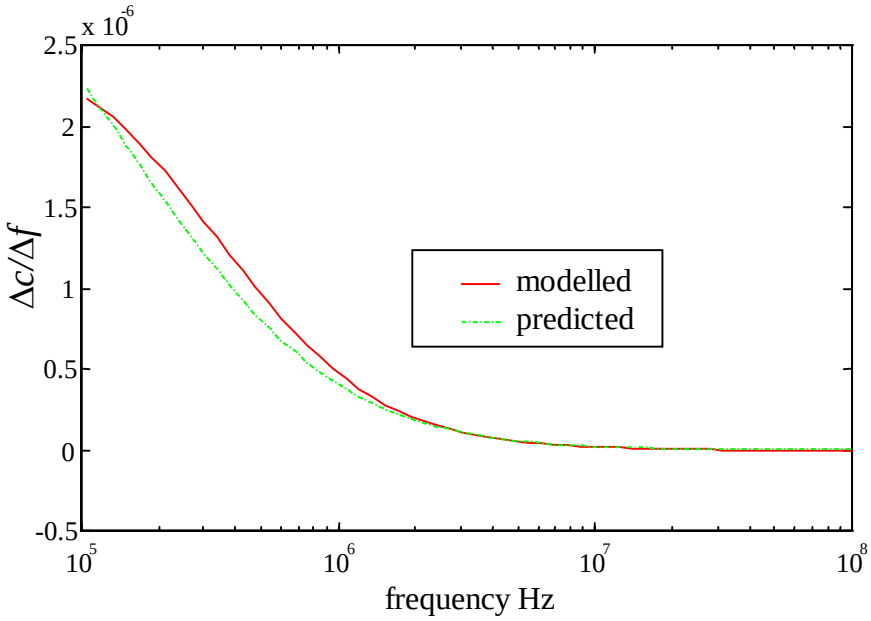

Figure 1.4 Modelled and predicted phase velocity gradient versus frequency of 10% v/v 1μm radius aqueous silica dispersion

Figure 1.4 shows modelled and predicted $\Delta c/\Delta f$ against frequency of 1μm radius silica. The predictions use Equation (1.24) and modelled attenuation data. Again, it can be seen that agreement is reasonable throughout the range 100kHz to 100MHz and is very good in the centre range of 2MHz to 30MHz.

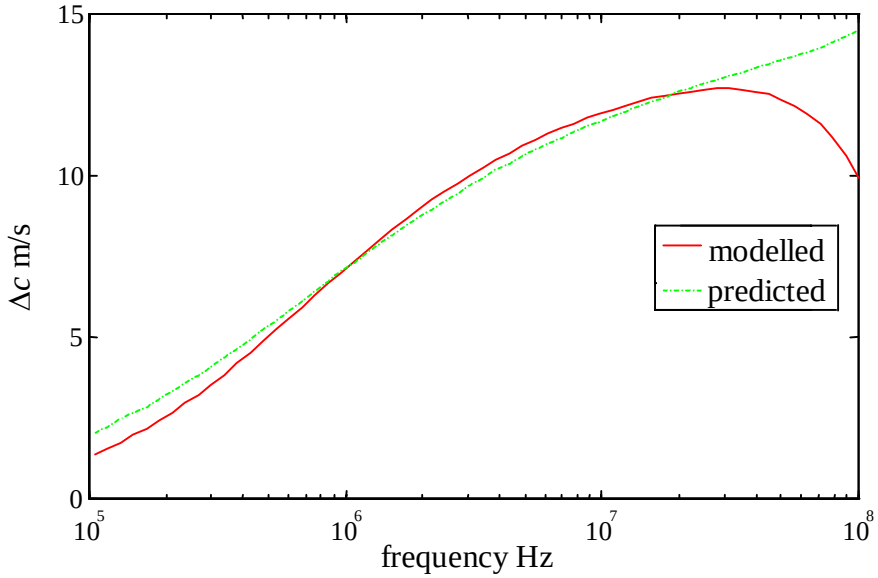

Figure 1.5 Modelled and predicted normalized velocity dispersion versus frequency of 1μm radius 10% v/v aqueous silica dispersion

Figure 1.5 shows the modelled and predicted change in phase velocity with respect to the modelled velocity at 10kHz, for a 1μm radius 10% v/v aqueous silica dispersion. The predictions use Equation (1.24) and modelled attenuation data to calculate Δc that is then integrated over the frequency interval $\Delta\omega$. It can be seen that agreement is reasonable over the range 100kHz to 30MHz but the employment of such a localized integral is wholly inappropriate when the slope of the modelled phase velocity passes through zero and goes negative.

1.5 Summary

When sound propagates through a dispersion of particles it is subjected to attenuating losses, and phase velocity dispersion by association. Each is a characteristic of the physical properties of the dispersion and sound frequency. Both dispersed and continuous phases can be gaseous, liquid or solid. For the particle size range of interest, 10nm to 1mm in diameter which subsumes the size range of colloids and colloidal emulsions, the constraints of available mathematical models make them applicable usually only to ultrasound of frequencies between a few hundreds of kilohertz and a few hundreds of megahertz. There are numerous different loss mechanisms affecting the propagation of ultrasound in dispersions and it is important to understand which ones make the most significant contributions to overall losses for the media and frequency range of interest. Only then can the most suitable simulation model be chosen because no one model takes into account all loss processes. Often, by judicious choice of even a very simple model, good agreement between experimental and modelled attenuation and phase velocity spectra can be obtained. However, for more general applicability, more complicated models usually are needed. The ability to accurately model and predict experimental spectra could enable deduction of unknown parameters, such as particle sizes and % v/v concentration, when other parameters are known or can be measured. Such ability would be useful over a wide range of academic and industrial applications.

1.6 Outline of the thesis

This thesis builds upon earlier work on the computational modelling of ultrasonic attenuation and phase velocity dispersion caused by the scattering of sound waves by suspended particles. Chapter 2 offers a review of the Allegra & Hawley model of scattering by a single, spherical particle and goes on to examine the widely held assumption that only the first three orders of the partial wave expansions are required for adequate modelling of ultrasonic attenuation and phase velocity dispersion. The relationship between particle radius-frequency product and required order, *n*, of the partial wave expansion that needs to be computed for acceptable levels of convergence is described and tabulated. A heuristic relationship between particle radius-frequency product and required order *n* is presented as a useful rule of thumb for incorporation into algorithms used to compute ultrasonic attenuation and phase velocity dispersion. Chapter 3 examines one of the main difficulties in reliably computing higher orders of the partial wave expansions, which is the stable computation of spherical Bessel and Hankel functions. The other major source of instability and limit to the range of particle size and frequency that could be successfully modelled, the solution of the 6×6 matrix in six unknowns, is examined in Chapter 5. This chapter describes a number of theoretical and practical measures to extend the range of particle size and frequency that can be successfully modelled. The problem of incorporating the calculated scattering wavenumber of a single particle into an expression that adequately describes the complex wavenumber due to multiple scattering by a dispersion of many particles is investigated in Chapter 4. Four multiple scattering models of differing levels of complication are compared and the ability of each adequately to model ultrasonic attenuation and phase velocity dispersion is assessed. Chapter 6 identifies some of the distinctive features and morphology of ultrasonic attenuation and phase

velocity dispersion spectra. The intention of this is to enable comparison of modelled and experimentally derived spectra over an *optimally minimum* range of defined frequencies, when it is undertaken for the purpose of predicting unknown particle sizes and/or concentration of a dispersion. Thereby, obviating the time and cost involved in the collection of unnecessary data. Therefore, if designing an instrument to classify unknown characteristics of dispersions over a predetermined range of materials, particle sizes and concentrations, the optimal band of operating frequencies could be incorporated into a cost-effective design. Chapter 7 summarizes, reviews and discusses the results and findings in detail and draws conclusions.

2. Mathematical model of acoustic scattering

2.1 Introduction

In Chapter 1 it was explained that there is a great number of different physical mechanisms which cause energy to be lost from a wave propagating through a dispersion of particles. Some of the more important of those mechanisms were discussed. Mathematical models have been proposed to simulate acoustic losses in dispersions of:

a. Liquids in fluids (Sewell, 1910), (Epstein, 1941), (Epstein & Carhart, 1953), (Lamb, 1945), (Urick, 1947), (Allegra & Hawley, 1972), (Evans & Attenborough, 1997).

b. Solids in fluids (Sewell, 1910), (Lamb, 1945), (Knudsen, 1946), (Urick, 1947), (Urick & Ament, 1949), (Allegra & Hawley, 1972), (Harker & Temple, 1988), (Strout, 1991).

c. Fluids in solids (Biot, 1956a, 1956b, 1962a, 1962b).

d. Solids in solids (Ying & Truell, 1956), (Flax, Gaunaurd & Ueberall, 1981), (Challis *et al*, 1999).

Although none of the models incorporate the physics of more than a few of the acoustic loss mechanisms, if used within appropriate constraints, the models agree well with experimental evidence and most have been reviewed elsewhere (Anson & Chivers, 1993), (Tebbutt, 1996). If the purpose of modelling is to compare the predicted attenuation and phase velocity spectra with those of an unknown dispersion in order to deduce particle sizes and their distribution and/or % v/v concentration, the choice of model is governed by a number of factors that might include:

a. The dominant loss mechanisms in the combination of media and acoustic frequency range of interest

b. The availability of the physical parameters of the media which are needed by the model

c. The computational time and effort needed to accurately model the losses

d. Whether some information, such as % v/v concentration or particle size, is known *a priori*

2.2 Early models

The investigation of acoustic losses in fluids has a long history. Of the intrinsic losses associated with non-ideal fluids discussed in Chapter 1, viscous losses owing to shear viscosity were quantified by Stokes (Stokes, 1845) and those losses owing to heat conduction by Kirchoff (Kirchoff, 1868). Rayleigh (1871, 1894) further developed the work of Stokes and Kirchoff and also investigated the physics of attenuation caused by suspended particles scattering light or sound of a wavelength longer (by a factor of approximately ten or greater) than the diameter of the particles. This is the so-called fourth power law in which the amplitude A_s of a wave of wavelength λ scattered in any direction making an angle θ with the incident wave, A_i, is inversely proportional to the fourth power of the wavelength

$$A_s \propto A_i \frac{1+\cos\theta}{\lambda^4} \qquad \textbf{(2.1)}$$

He mathematically represented the disturbance of a plane wave by a small particle by using a partial wave expansion. Rayleigh concluded that the magnitude of the expansion's zero-order term is a function of the compressibility difference between the particle and suspending fluid and acts in the manner of a pulsating sphere; and the first-order term is a function of the density difference and acts as a dipole radiator. The characteristics of the

first-order term point to its being caused by viscous drag opposing the relative motion of the particle and its surrounding medium. On this basis Sewell (1910) derived an expression for the attenuation of sound caused by inelastic, immovable particles suspended in a gas. Lamb refined Sewell's expression to remove the restriction that the particles be immovable. Up until the 1940s a great deal of research was undertaken to investigate and quantify the intrinsic acoustic losses in fluids and solids but it was not until 1949 that the first practically useful model for calculating acoustic attenuation and phase velocity in a dispersion of particles was published. Urick (1947, 1948) derived equations for the attenuation and velocity of sound propagating through a dispersion by using the effective medium approach. This treats a dispersion as an equivalent homogeneous medium in order to calculate the velocity using Wood's Equation (see Equation (1.6)) and a development of the work of Lamb (1945) to calculate attenuation. This model is limited in that it is wholly independent of frequency and velocity is independent of the size of the particles. Soon afterwards Urick & Ament (1949) developed a model which used a single equation to express the complex wavenumber (see Equation (1.9)) of an effective medium from which both attenuation and phase velocity could be derived. It offers a useful method of calculating frequency and particle-size dependent attenuation and phase velocity as long as the following assumptions are true:

a. The particles are spherical, compressible and mobile.

b. Absorption by the continuous phase is negligible.

c. Multiple scattering of energy is negligible.

d. The particles occupy negligible volume.

e. Thermal losses are negligible.

However, the subject of the last assumption, thermal losses, was shown by Isakovich (1948) to be a significant source of attenuation under certain conditions, owing to thermal diffusion from regions of adiabatic compression and rarefaction. A significant proportion of current research into the modelling of acoustic loss mechanisms can be categorized into two distinct approaches: scattering theory models and coupled phase models. Only the former will be examined in this thesis.

2.3 The Epstein & Carhart and Allegra & Hawley scattering model

The work of Epstein & Carhart (1953) differed from the effective medium approach already described in that it first modelled the scattering from the surface of an individual particle as a plane compression wave impinged upon it. This formed the basis for calculating the bulk effect of a dispersion of such particles on acoustic propagation. Their work was aimed at modelling fogs, that is to say, dispersions of water particles in air. Epstein (1941) had already refined the Sewell-Lamb scattering equation to remove the restriction that the particle be incompressible. They also took account of thermal loss mechanisms. Allegra & Hawley (1972) refined the Epstein & Carhart model (which will be collectively referred to as the ECAH model) and widened its applicability to dispersions of liquid or solid particles in a liquid continuous phase. Challis and his co-workers (1999) further extended the ECAH model and applied it to solid in solid composites with and without thermal terms. They showed that the ECAH model without its thermal terms is analytically equivalent to the mathematical model of Ying and Truell (1956). Their results demonstrated that the inclusion of thermal terms gave better agreement when compared with experimental acoustic phase velocity and attenuation results than models which did not consider thermal processes (Challis *et al*, 1999).

2.3.1 The ECAH field equations

The derivation by Epstein & Carhart dealt only with fluids and so restricted itself to equating velocity potentials. Allegra & Hawley allowed for the inclusion of a solid dispersed phase by equating velocity and displacement potentials and eliminating time dependency by the relationships

$$\mu = -i\omega\eta\,,\ \frac{\partial}{\partial t} = -i\omega \tag{2.2}$$

Where ω denotes angular frequency and μ and η denote shear modulus and viscosity respectively. By employing these relationships within Euler's (1755) linearized conservation of mass and momentum equations for a solid element, combining the Navier-Stokes additional term which incorporates viscosity made applicable to a solid by using Equation (2.2), and incorporating an additional thermodynamic relationship leads to the following field equations

$$\frac{\partial \rho}{\partial t} + \rho\nabla.\dot{\mathbf{u}} = 0 \tag{2.3}$$

$$\rho\ddot{\mathbf{u}}_j + \rho\left(\dot{\mathbf{u}}.\nabla\right)\dot{\mathbf{u}} = -\frac{\partial P_{ij}}{\partial x_i} \tag{2.4}$$

$$\rho\left(\frac{\partial U}{\partial t}\right) + P\nabla.\dot{\mathbf{u}} = \nabla.\left(\kappa\nabla T\right) \tag{2.5}$$

Where ρ denotes mass density, U specific internal energy, P pressure, P_{ij} the viscous stress tensor, $\mathbf{u}$ the displacement vector of a volume element, x_i the Cartesian coordinate, κ the thermal conductivity, T the temperature. The Einstein summation convention is employed. For an elastic isotropic solid, the stress tensor can be expressed as

$$P_{ij} = \beta S\delta_{ij} - 2\mu S_{ij} \tag{2.6}$$

Where S is the trace and S_{ij} (the trace of which is empty) denote the fractional change in volume, δ_{ij} the Kronecker delta function and β the bulk modulus, the reciprocal of compressibility. Therefore, the hydrostatic pressure can be expressed as

$$P = -\beta S, \quad P_{ij} = \delta_{ij}\left(P - 2\mu\right) \tag{2.6a}$$

Two variables, pressure $P(\rho,T)$ and specific internal energy $U(\rho,T)$, incorporate pressure-temperature relationships into the system of equations. Because $\mathbf{u}$ is a vector in three dimensional space, Equations (2.3), (2.4) and (2.5) can be separated into seven equations in seven unknowns, $\mathbf{u}$, ρ, μ, P, and T, and rearranged to give

$$\frac{\partial^3 \mathbf{u}}{\partial t^3} = \frac{-c_1^2\beta}{\gamma}\nabla\dot{T} + \frac{\mu}{\rho_0}\nabla^2\dot{\mathbf{u}} + \nabla\left(\nabla.\dot{\mathbf{u}}\right)\left[\frac{c_1^2}{\gamma} + \frac{\mu}{3\rho_0}\right] \tag{2.7}$$

$$\frac{\left(\gamma-1\right)}{\beta}\nabla.\dot{\mathbf{u}} + \dot{T} = \gamma\sigma\nabla^2 T \tag{2.8}$$

Where γ is the ratio of specific heats C_p/C_v and c_1 is spherical wave speed given by

$$c_1^2 = c^2 - \frac{4\mu}{3\rho} \tag{2.9}$$

2.3.2 The ECAH wave equations

By separating the displacement vector of an elastic isotropic solid into its longitudinal and transverse components, the field equations can be de-coupled into three ordinary differential equations which can be solved separately. This can be accomplished by using the Helmholtz vector relationship given by

$$\mathbf{u} = -\nabla\bar{\phi} + \nabla\times\mathbf{A}, \quad \nabla.\mathbf{A} = \mathbf{0} \tag{2.10}$$

$$\mathbf{v} = -\nabla\bar{\phi}' + \nabla\times\mathbf{A}', \quad \nabla.\mathbf{A}' = \mathbf{0} \tag{2.11}$$

Where $\overline{\phi} = \phi_c + \phi_T$ and denotes the wave potential scalar, **v** the velocity vector and **A** the shear wave potential vector. A prime indicates a variable associated with the dispersed phase. Wave equations for the three potentials, compressional ϕ_c, thermal ϕ_T and viscous (or shear) **A,** can now be derived from the field equations to give

$$\phi_c \left(\nabla^2 + k_c^2\right) = 0 \qquad \textbf{(2.12)}$$

$$\phi_T \left(\nabla^2 + k_T^2\right) = 0 \qquad \textbf{(2.13)}$$

$$\mathbf{A}\left(\nabla^2 + k_s^2\right) = 0 \qquad \textbf{(2.14)}$$

Where

$$k_c = \frac{\omega}{c} + i\alpha \qquad \textbf{(2.15)}$$

$$k_T = (1+i)\left(\frac{1}{\delta_T}\right) \qquad \textbf{(2.16)}$$

$$k_s = (1+i)\left(\frac{1}{\delta_v}\right) \qquad \textbf{(2.17)}$$

Equation (1.4) gives the definition of viscous skin depth δ_v and Equation (1.5) the definition of thermal skin depth δ_T . The wave equation in Equation (2.15) is equally applicable to a viscous fluid or a solid and so are Equations (2.16) and (2.17) by employing the conventions in Equation (2.2).

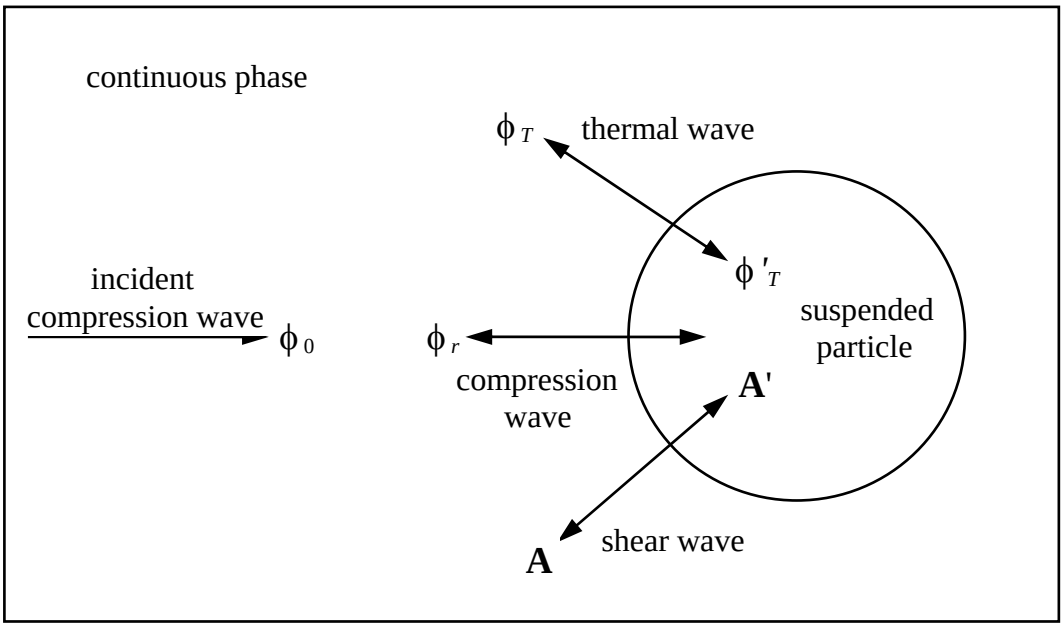

Figure 2.1 Schematic illustration of the translation of an incoming compressional wave into scattered and transmitted compressional, viscous and thermal waves (based on Tebbutt (1996))

When a plane compressional wave impinges upon a sphere of radius *R* in a continuous suspending medium the sphere translates some of the compressional energy into thermal and viscous waves. This gives rise to compressional, shear and thermal waves travelling from the surface of the sphere both outwards into the suspending medium and inwards into the sphere. The concept is represented diagrammatically in Figure 2.1. At the surface of the sphere, there is continuity of radial and angular velocities, temperature, heat flux, and compressive and shear stresses. These conditions are expressed in Equations (2.27) to (2.30). The solutions to the wave equations in Equations (2.12), (2.13) and (2.14) are solved in terms of spherical Bessel functions and Legendre polynomials. Spherical Bessel functions of the first kind, denoted $j_n(z)$, are defined at the origin and therefore are used to

represent inwards travelling transmitted waves which pass through zero radius. Spherical Bessel functions of the first type and third kind, usually called spherical Hankel functions and denoted $h_n^{(1)}(z)$, are defined at infinity and therefore are used to represent reflected waves travelling outwards towards infinity. For clarity the superscript denoting first type will be omitted.

2.3.3 Simplifications due to axial symmetry

The spherical polar coordinate system, with its origin at the centre of the particle, describes any point within or outside the particle in terms of distance from the origin, *r*, and azimuth angle, ψ, and elevation angle, θ, from the direction of acoustic propagation. Assuming axial symmetry, the angular dependence of scattered or transmitted waves can be expressed in the form of Legendre polynomials or associated Legendre polynomials of the first kind, denoted by P_n and P_n^1 respectively. The simplification afforded by assuming axial symmetry also causes the potentials $\overline{\phi}$ and **A** in spherical co-ordinates to assume simpler vector identities given by

$$\overline{\phi}(r,\theta,\psi) = \overline{\phi}(r,\theta,0) \qquad \textbf{(2.18)}$$

$$\mathbf{A} = \mathbf{A}(0,0,r\sin\theta A_\psi) \qquad \textbf{(2.19)}$$

Allegra & Hawley (1972) showed that only the A_ψ component of **A** is non-zero; therefore, the vector $\mathbf{A} = A_\psi$ can be adequately represented by the scalar A. Using these conventions, the series solutions to the wave equations in terms of spherical polar coordinates are given by:

The incident compressional wave

$$\phi_0 = \sum_{n=0}^{\infty} i^n (2n+1) j_n(k_c r) P_n(\cos\theta) \qquad \textbf{(2.20)}$$

The scattered compressional wave

$$\phi_r = \sum_{n=0}^{\infty} i^n (2n+1) A_n h_n(k_c r) P_n(\cos\theta) \qquad \textbf{(2.21)}$$

The scattered thermal wave

$$\phi_T = \sum_{n=0}^{\infty} i^n (2n+1) B_n h_n(k_T r) P_n(\cos\theta) \qquad \textbf{(2.22)}$$

The scattered shear wave

$$\mathrm{A} = \sum_{n=0}^{\infty} i^n (2n+1) C_n h_n(k_s r) P_n^1(\cos\theta) \qquad \textbf{(2.23)}$$

The transmitted compressional wave

$$\phi_c' = \sum_{n=0}^{\infty} i^n (2n+1) A_n' j_n(k_c' r) P_n(\cos\theta) \qquad \textbf{(2.24)}$$

The transmitted thermal wave

$$\phi_T' = \sum_{n=0}^{\infty} i^n (2n+1) B_n' j_n(k_T' r) P_n(\cos\theta) \qquad \textbf{(2.25)}$$

The transmitted shear wave

$$\mathrm{A}' = \sum_{n=0}^{\infty} i^n (2n+1) C_n' j_n(k_s' r) P_n^1(\cos\theta) \qquad \textbf{(2.26)}$$

Variables associated with the dispersed phase are denoted by a prime and P_n and P_n^1 are Legendre polynomials and associated Legendre polynomials of the first kind, both of order *n*, respectively. All the variables and coefficients in Equations (2.20) to (2.26), except the complex scattering coefficients A_n, B_n, C_n, A_n', B_n', *and* C_n', are known or can be determined explicitly. In order to determine the scattering coefficients it is necessary to apply the

relationships of Equations (2.20) to (2.26) to known boundary conditions at the surface of a single particle at each value of *n* using the *comparing coefficients* technique.

2.3.4 Continuity at the boundary between the particle and continuous phase

At $r = R$ the following six boundary conditions must be satisfied:

Continuity of radial and angular velocities

$$v_r = v_r', \quad v_\theta = v_\theta' \tag{2.27}$$

Continuity of temperature

$$T = T' \tag{2.28}$$

Continuity of heat flux

$$\kappa \frac{\partial T}{\partial r} = \kappa' \frac{\partial T'}{\partial r'} \tag{2.29}$$

Continuity of compressive and shear stresses

$$P_{rr} = P_{rr}', \quad P_{r\theta} = P_{r\theta}' \tag{2.30}$$

Epstein and Carhart (1953) gave detailed derivations of v_r and v_θ that were modified by Allegra and Hawley (1972) to give

$$v_r' = -i\omega\left(-\frac{\partial \bar{\phi}'}{\partial r} + \frac{1}{r \sin\theta} \frac{\partial}{\partial \theta} A' \sin\theta \right) \tag{2.31}$$

$$v_\theta' = -i\omega\left(-\frac{1}{r} \frac{\partial \bar{\phi}'}{\partial r} + \frac{1}{r} \frac{\partial}{\partial r} A' r \right) \tag{2.32}$$

The temperature-related boundary conditions of Equations (2.28) and (2.29) were derived by Allegra and Hawley (op cit), expressing them in terms of acoustic potentials given by

$$T' = b_c'\phi_c' + b_T'\phi_T' \tag{2.33}$$

Where the thermal boundary condition coefficients are given by

$$b_c' = \frac{-\gamma'}{\beta_T' c_1'^2}\left[\omega^2 - \left(\frac{c_1'^2}{\gamma'} + \frac{4\mu'}{3\rho'}\right)k_c'^2\right] \tag{2.34}$$

$$b_T' = \frac{-\gamma'}{\beta_T' c_1'^2}\left[\omega^2 - \left(\frac{c_1'^2}{\gamma'} + \frac{4\mu'}{3\rho'}\right)k_T'^2\right] \tag{2.35}$$

Where β_T denotes thermal dilatability (coefficient of expansion). The right hand side of the boundary condition equations for compressive and shear stresses given by Equations (2.30) were derived by Epstein and Carhart (1953) and modified by Allegra and Hawley (1972) to give

$$P_{rr}' = \left(-\omega^2\rho' + 2\mu' k_c'^2\right)\phi_c' + \left(-\omega^2\rho' + 2\mu' k_T'^2\right)\phi_T' + 2\mu'\left\{\frac{\partial^2\bar{\phi}'}{\partial r^2} + \frac{1}{\sin\theta}\frac{\partial}{\partial\theta}\left[\sin\theta\left(\frac{A'}{r^2} - \frac{1}{r}\frac{\partial A}{\partial r}\right)\right]\right\}$$

(2.36)

$$P_{r\theta}' = -\mu'\left\{-2\frac{\partial}{\partial\theta}\left(\frac{1}{r}\frac{\partial\bar{\phi}'}{\partial r} - \frac{\bar{\phi}'}{r^2}\right) - \left(\frac{\partial^2 A'}{\partial r^2} - \frac{2A'}{r^2}\right) + \frac{1}{r^2}\frac{\partial}{\partial\theta}\left(\frac{1}{\sin\theta}\frac{\partial}{\partial\theta}A'\sin\theta\right)\right\} \tag{2.37}$$

The arguments of the Bessel functions are complex compressive, shear or thermal wavenumber-radius products and are abbreviated as follows: $a_c \equiv k_c R$, $a_s \equiv k_s R$, $a_T \equiv k_T R$. The use of primed variables denotes properties of the dispersed phase but the use of single and double primed Bessel functions denotes first and second derivatives respectively. They are differentiated with respect to their arguments.

2.3.5 Unified series of equations for solid or fluid phases by use of effective μ

By exploiting the relationships given by Equation (2.2) all occurrences of η or η′ can be replaced by a notional *effective* μ which is complex and frequency dependent. This effective μ may also be used in Equations (2.34) to (2.37) in the case of a fluid dispersed phase. By this device, using values of actual or effective μ for both phases, the same set of six equations in six unknowns can be used for numerical calculation of the scattering coefficients for any permutation of solid or liquid continuous and dispersed phases. By employing this convention and applying the boundary equation coefficients the six equations in six unknowns, which are the complex scattering coefficients A_n, B_n, C_n, A_n', B_n', and C_n', are given by

$$b_c\left[j_n(a_c)+A_n h_n(a_c)\right]+b_T B_n h_n(a_T)=-i\omega\left[b_c' A_n' j_n(a_c')+b_T' B_n' j_n(a_T')\right] \quad \textbf{(2.38)}$$

$$\kappa\left\{a_c b_c\left[j_n'(a_c)+A_n h_n'(a_c)\right]+B_n b_T a_T h_n'(a_T)\right\}=-i\omega\kappa'\left[A_n' b_c' a_c' j_n'(a_c')+B_n' b_T' a_T' j_n'(a_T')\right] \quad \textbf{(2.39)}$$

$$a_c j_n'(a_c)+A_n a_c h_n'(a_c)+B_n a_T h_n'(a_T)-C_n n(n+1)h_n(a_s)=$$

$$-i\omega\left[A_n' a_c' j_n'(a_c')+B_n' a_T' j_n'(a_T')-C_n' n(n+1) j_n(a_s')\right] \quad \textbf{(2.40)}$$

$$j_n(a_c)+A_n h_n(a_c)+B_n h_n(a_T)-C_n\left[h_n(a_s)+a_s h_n'(a_s)\right]=$$

$$-i\omega\left\{A_n' j_n(a_c')+B_n' j_n(a_T')-C_n'\left[j_n(a_s')+a_s' j_n'(a_s')\right]\right\} \quad \textbf{(2.41)}$$

$$\frac{\mu}{-i\omega}\left\{\left[\left(a_s^2-2a_c^2\right)j_n(a_c)-2a_c^2 j_n''(a_c)\right]+A_n\left[\left(a_s^2-2a_c^2\right)h_n(a_c)-2a_c^2 h_n''(a_c)\right]+\right.$$

$$\left.B_n\left[\left(a_s^2-2a_T^2\right)h_n(a_T)-2a_T^2 h_n''(a_T)\right]+C_n 2n(n+1)\left[a_s h_n'(a_s)-h_n(a_s)\right]\right\}=$$

$$A_n'\left[\left(\omega^2\rho' R^2-2\mu' a_c'^2\right)j_n(a_c')-2\mu' a_c'^2 j_n''(a_c')\right]+$$

$$B_n'\left[\left(\omega^2\rho' R^2-2\mu' a_T'^2\right)j_n(a_T')-2\mu' a_T'^2 j_n''(a_T')\right]+C_n' 2\mu' n(n+1)\left[a_s' j_n'(a_s')-j_n(a_s')\right] \quad \textbf{(2.42)}$$

$$\frac{\mu}{-i\omega}\left\{a_c j_n'(a_c) - j_n(a_c) + A_n\left[a_c h_n'(a_c) - h_n(a_c)\right] + B_n\left[a_T h_n'(a_T) - h_n(a_T)\right]\right.$$
$$\left. - \frac{C_n}{2}\left[a_s^2 h_n''(a_s) + \left(n^2 + n - 2\right) h_n(a_s)\right]\right\} =$$

$$\mu'\left\{A_n'\left[a_c' j_n'(a_c') - j_n(a_c')\right] + B_n'\left[a_T' j_n'(a_T') - j_n(a_T')\right] - \frac{C_n'}{2}\left[a_s'^2 j_n''(a_s') + \left(n^2 + n - 2\right) j_n(a_s')\right]\right\}$$

(2.43)

2.3.6 Expressing the system of six equations as an augmented matrix

Equations (2.38) to (2.43) can be transposed into matrix format such that they take the form **Mx** = **C**. Because the 6×6 matrix **M** and 6×1 column vector **C** are explicitly known, the system can be solved for **x**, the column vector of the complex scattering coefficients A_n, B_n, C_n, A_n', B_n', and C_n'. As the matrix must be solved for each order of n the subscript on the scattering coefficients will be omitted for clarity. Acoustic attenuation and velocity dispersion are usually measured experimentally only in terms of the relationship between the longitudinal compression waves transmitted by a transmitter transducer, along a path of known length through the dispersion, and those received by the receiver transducer. For this reason only the compressive complex scattering wavenumber of the continuous phase, A_n , is of interest and needs to be evaluated. Therefore, in **Mx** = **C** format, the cells of the matrix, using the convention M_{column}^{row} are given by

$$\begin{bmatrix} M_1^1 & M_2^1 & M_3^1 & M_4^1 & M_5^1 & M_6^1 \\ M_1^2 & M_2^2 & M_3^2 & M_4^2 & M_5^2 & M_6^2 \\ M_1^3 & M_2^3 & M_3^3 & M_4^3 & M_5^3 & M_6^3 \\ M_1^4 & M_2^4 & M_3^4 & M_4^4 & M_5^4 & M_6^4 \\ M_1^5 & M_2^5 & M_3^5 & M_4^5 & M_5^5 & M_6^5 \\ M_1^6 & M_2^6 & M_3^6 & M_4^6 & M_5^6 & M_6^6 \end{bmatrix} \begin{bmatrix} A \\ B \\ C \\ A' \\ B' \\ C' \end{bmatrix} = \begin{bmatrix} C_1 \\ C_2 \\ C_3 \\ C_4 \\ C_5 \\ C_6 \end{bmatrix} \qquad \textbf{(2.44)}$$

Where

$$M_1^1 = a_c\, h_n'(a_c) \tag{2.45}$$

$$M_1^2 = h_n(a_c) \tag{2.46}$$

$$M_1^3 = b_c\, h_n(a_c) \tag{2.47}$$

$$M_1^4 = \kappa\, a_c b_c\, h_n'(a_c) \tag{2.48}$$

$$M_1^5 = \frac{\mu}{-i\omega}\left[\left[h_n(a_c)\left(a_s^2 - 2a_c^2\right)\right] - 2a_c^2\, h_n''(a_c)\right] \tag{2.49}$$

$$M_1^6 = \frac{\mu}{-i\omega}\left[a_c\, h_n'(a_c) - h_n(a_c)\right] \tag{2.50}$$

$$M_2^1 = a_T\, h_n'(a_T) \tag{2.51}$$

$$M_2^2 = h_n(a_T) \tag{2.52}$$

$$M_2^3 = b_T\, h_n(a_T) \tag{2.53}$$

$$M_2^4 = \kappa\, a_T b_T\, h_n'(a_T) \tag{2.54}$$

$$M_2^5 = \frac{\mu}{-i\omega}\left[\left[h_n(a_T)\left(a_s^2 - 2a_T^2\right)\right] - 2a_T^2\, h_n''(a_T)\right] \tag{2.55}$$

$$M_2^6 = \frac{\mu}{-i\omega}\left[a_T\, h_n'(a_T) - h_n(a_T)\right] \tag{2.56}$$

$$M_3^1 = -n(n+1)\, h_n(a_s) \tag{2.57}$$

$$M_3^2 = -\left[h_n(a_s) + a_s\, h_n'(a_s)\right] \tag{2.58}$$

$$M_3^3 = 0 \tag{2.59}$$

$$M_3^4 = 0 \tag{2.60}$$

$$M_3^5 = 2n(n+1)\frac{\mu}{-i\omega}\left[a_s\, h_n'(a_s) - h_n(a_s)\right] \tag{2.61}$$

$$M_3^6 = \frac{\mu}{i2\omega}\left[a_s^2\, h_n''(a_s) + (n-1)(n+2)\, h_n(a_s)\right] \quad \textbf{(2.62)}$$

$$M_4^1 = i\omega\, a_c'\, j_n'(a_c') \quad \textbf{(2.63)}$$

$$M_4^2 = i\omega\, j_n(a_c') \quad \textbf{(2.64)}$$

$$M_4^3 = i\omega\, b_c'\, j_n(a_c') \quad \textbf{(2.65)}$$

$$M_4^4 = i\omega\, \kappa' a_c' b_c'\, j_n'(a_c') \quad \textbf{(2.66)}$$

$$M_4^5 = -j_n(a_c')\left(\omega^2 R^2 \rho' - 2\mu' a_c'^2\right) + 2\mu' a_c'^2\, j_n''(a_c') \quad \textbf{(2.67)}$$

$$M_4^6 = -\mu'\left[a_c'\, j_n'(a_c') - j_n(a_c')\right] \quad \textbf{(2.68)}$$

$$M_5^1 = i\omega\, a_T'\, j_n'(a_T') \quad \textbf{(2.69)}$$

$$M_5^2 = i\omega\, j_n(a_T') \quad \textbf{(2.70)}$$

$$M_5^3 = i\omega\, b_T'\, j_n(a_T') \quad \textbf{(2.71)}$$

$$M_5^4 = i\omega\, \kappa' a_T' b_T'\, j_n'(a_T') \quad \textbf{(2.72)}$$

$$M_5^5 = -j_n(a_T')\left(\omega^2 R^2 \rho' - 2\mu' a_T'^2\right) + 2\mu' a_T'^2\, j_n''(a_T') \quad \textbf{(2.73)}$$

$$M_5^6 = -\mu'\left[a_T'\, j_n'(a_T') - j_n(a_T')\right] \quad \textbf{(2.74)}$$

$$M_6^1 = -i\omega n(n+1) j_n'(a_s') \quad \textbf{(2.75)}$$

$$M_6^2 = -i\omega\left[j_n(a_s') + a_s'\, j_n'(a_s')\right] \quad \textbf{(2.76)}$$

$$M_6^3 = 0 \quad \textbf{(2.77)}$$

$$M_6^4 = 0 \quad \textbf{(2.78)}$$

$$M_6^5 = -2n(n+1)\mu'\left[a_s'\, j_n'(a_s') - j_n(a_s')\right] \quad \textbf{(2.79)}$$

$$M_6^6 = \frac{\mu'}{2}\left[a_s'^2\, j_n''(a_s') + (n-1)(n+2) j_n(a_s')\right] \quad \textbf{(2.80)}$$

$$C_1 = -a_c\, j_n'(a_c) \tag{2.81}$$

$$C_2 = -j_n(a_c) \tag{2.82}$$

$$C_3 = -b_c\, j_n(a_c) \tag{2.83}$$

$$C_4 = -\kappa\, a_c b_c\, j_n'(a_c) \tag{2.84}$$

$$C_5 = \frac{\mu}{i\omega}\left[\left[j_n(a_c)\left(a_s^2 - 2a_c^2\right)\right] - 2a_c^2\, j_n''(a_c)\right] \tag{2.85}$$

$$C_6 = \frac{\mu}{i\omega}\left[a_c\, j_n'(a_c) - j_n(a_c)\right] \tag{2.86}$$

2.3.7 Solving the matrix

There are numerous methods that can be used to find the solutions of a system of equations of this kind. They differ markedly in their degree of sophistication and, as a corollary to that, their mathematical complexity and computational cost. The matrix in Equation (2.44) is intrinsically poorly conditioned because on the same row of the matrix some elements become exponentially larger simultaneously with some elements becoming exponentially smaller when input arguments, for example frequency or particle radius, are varied. The causes and effects of instabilities when solving the matrix, and techniques to minimize them, are examined in Chapter 5. Inspection of the matrix Equations (2.45) to (2.86) reveals that a number of them possess n as a multiplicand. Therefore, when $n = 0$ these equations also are identical to zero and the matrix reduces to a 4×4 series of equations. For the sake of computational simplicity, this case is treated as a sparse 6×6 matrix and the same methods are used for the solution of both 4×4 and 6×6 matrices.

2.4 A simple single-scattering model

It is possible to model the phase velocity and attenuation of sound propagation through a dispersion by a number of methods. Of the methods that model acoustic scattering all but the most unsophisticated require the computation and use of scattering coefficients, A_n , of order *n*. The attenuation of a plane compressive wave by a single suspended sphere was calculated by Allegra and Hawley (1972) as the energy absorbed in the vicinity of the particle as well as that scattered to infinity in directions other than the direction of propagation. They derived an expression for the total energy absorbed by a dispersion of spheres by representing the total velocity potential at infinity in terms of incoming and outgoing waves on a single sphere summed over the number of particles per unit volume. The difference in the energy carried by these waves is the energy absorbed by the dispersion. The compressional wavenumber β was found to be determined by an infinite series containing coefficients of the reflected compression wave, A_n, and if the ratio of wavenumbers β/k_c is close to unity an approximation of the attenuation α is given by

$$\alpha = \frac{-3\phi}{2k_c^2 R^3}\sum_{n=0}^{\infty}(2n+1)\ \mathrm{Re}(A_n) \qquad \textbf{(2.87)}$$

This is the imaginary part of the complex scattering wavenumber in the direction of propagation, $f(0)$, derived by Foldy (1945) which uses both parts of the complex scattering compressive wavenumber of a single particle, A_n, permitting total attenuation and phase velocity to be derived explicitly

$$\beta^2 = k_c^2 + \frac{3\phi}{i\,k_c R^3}\sum_{n=0}^{\infty}(2n+1)\ A_n \qquad \textbf{(2.88)}$$

Where β is the complex wavenumber of the dispersion defined as

$$\beta = \frac{\omega}{c(\omega)} + i\alpha(\omega) \qquad \textbf{(2.89)}$$

The calculation of β is then straightforward using De Moivre's formula. These derivations assume that the net effect of a number of scatterers is simply additive. This assumption is valid only for those dilute dispersions where multiple scattering and inter-particle interactions are insignificant. More complicated models which take multiple scattering into consideration are examined in Chapter 4.

2.5 Convergence of phase velocity and attenuation with increasing order *n* of A_n

Much of the published literature that requires the incorporation of the A_n values in the numerical calculation of attenuation and phase velocity is restricted to orders $n = 0$, $n = 1$ and at the most $n = 2$ because low orders lend themselves to simplified analytical solutions and physical interpretation. This was due to the difficulty in solving the matrix numerically before the widespread availability of digital computers and also because of the added complexity of computing higher orders of spherical functions. The need to compute higher orders of A_n was investigated and the inaccuracy resulting from truncating the A_n series at $n = 2$ was examined by establishing the order n required, for various limits of convergence to a final value, for a range of materials and frequencies. A brief examination of the tables in Appendix C will show that limiting the computation of scattering coefficients to order $n = 0$ to $n = 2$ is generally unsatisfactory. For some materials, especially those with high mass density or acoustic contrasts between the two phases, the effect of truncation at low orders of n was found to lead to significant errors in modelled attenuation and phase velocity. It followed that for any dispersions with large compressive wavenumber-particle radius products it was essential to compute higher orders n of A_n for accurate results.

Throughout this thesis, in order to investigate the behaviour of the models, numerical experiments were undertaken that incorporated the physical properties of practical materials. These included

a. 1-bromo-hexadecane (abbreviated to 1-b-hex)
b. Dow Corning 200 fluid: 350cSt silicone oil (abbreviated to silicone)
c. Hexadecane (abbreviated to hex)
d. Metallic iron (abbreviated to iron)
e. Polystyrene (abbreviated to poly)
f. Silica (abbreviated to silica)
g. Soya oil (abbreviated to soya)
h. Titanium dioxide AHR pigment (abbreviated to tiox)
i. Water (parameterized at 25°C)

The physical constants for each of these materials are listed in Appendix E.

As an illustration of the need to compute higher orders n of A_n for accurate results, a theoretical 10% v/v concentration dispersion of 1mm diameter titanium dioxide AHR pigment spheres in water was modelled. Because the order of n required for convergence increases with frequency and particle size, the choice of such a large diameter demonstrates the phenomenon more clearly. The dependence of calculated attenuation and phase velocity values on the choice of order n at which the single scattering computation was truncated is illustrated in Figures 2.2 to 2.7 inclusive.

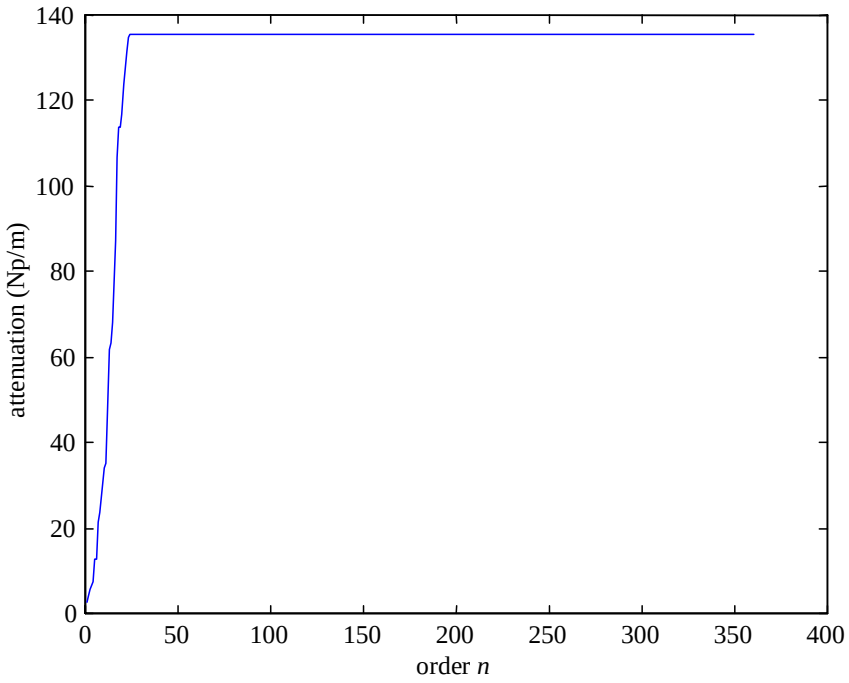

Figure 2.2 Attenuation versus order *n* of a dispersion of 1mm diameter titanium dioxide AHR pigment spheres in water at 25ºC and 10MHz

Figure 2.2 shows the effect of premature truncation of the series in Equation (2.88) on the value of modelled attenuation at 10MHz. It is obvious that premature truncation at $n < 25$ could introduce a significant error when compared to the fully converged value of attenuation.

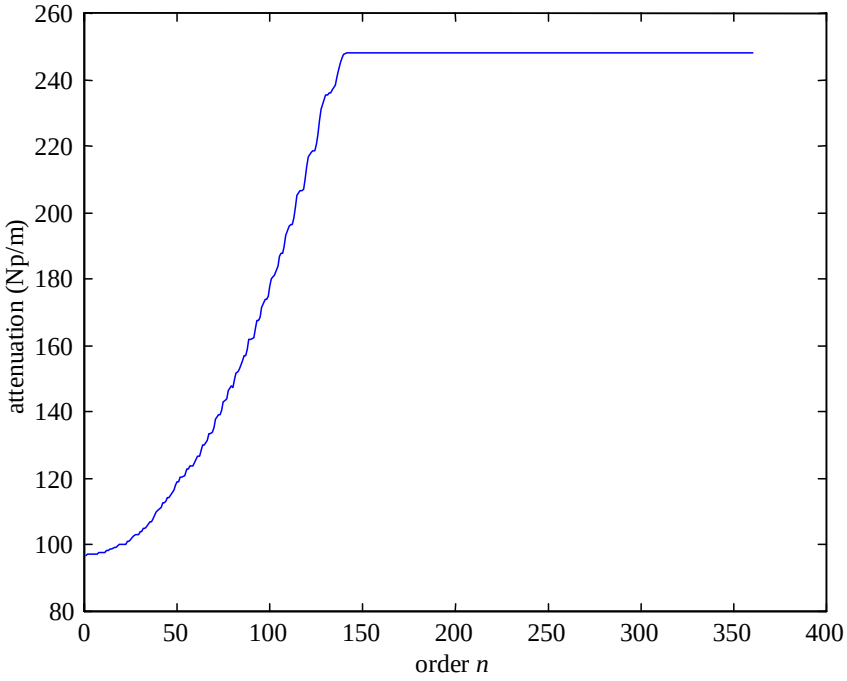

Figure 2.3 Attenuation versus order *n* of a dispersion of 1mm diameter titanium dioxide AHR pigment spheres in water at 25ºC and 65MHz

Comparison of Figures 2.2 and 2.3 shows that as frequency is increased from 10MHz to 65MHz there is a need to calculate the series from $n = 25$ to an increased value of $n = 145$ for adequate convergence.

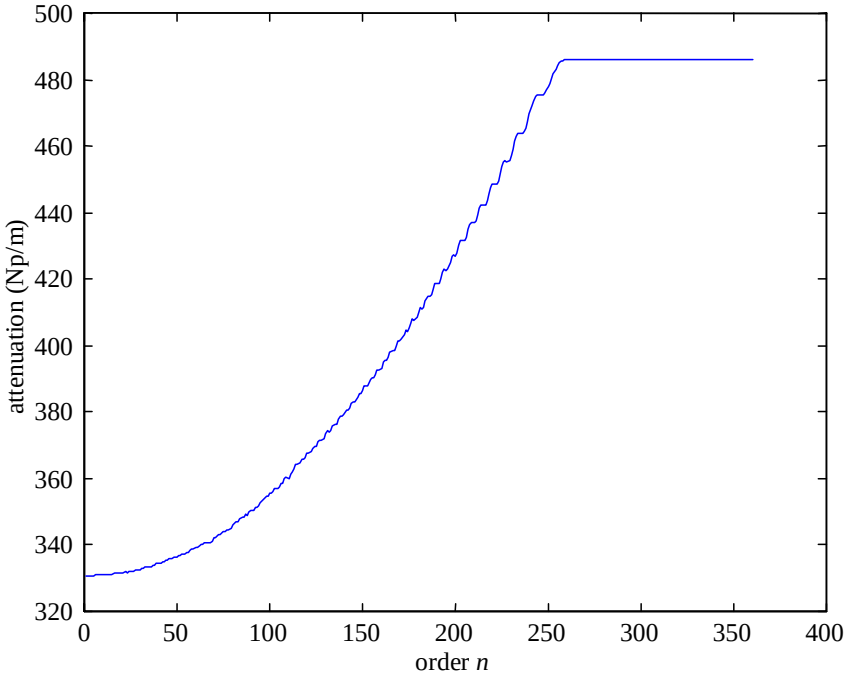

Figure 2.4 Attenuation versus order *n* of a dispersion of 1mm diameter titanium dioxide AHR pigment spheres in water at 25°C and 120MHz

The information shown in Figure 2.4 reinforces the need to compute the series to higher orders of n for increased frequency. In this case the series must be computed to $n = 261$ to ensure adequate convergence when the frequency is 120MHz. However, it is notable that the percentage error resulting from premature truncation of the series gets *less* as frequency is increased.

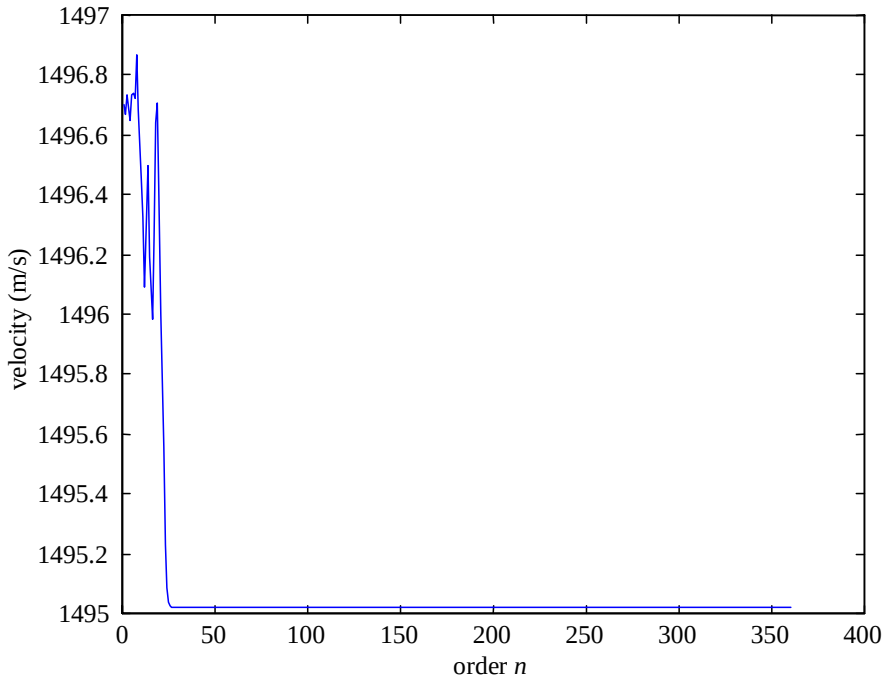

Figure 2.5 Phase velocity versus order *n* through a dispersion of 1mm diameter titanium dioxide AHR pigment spheres in water at 25ºC and 10MHz

Figure 2.5 shows that premature truncation of the series when calculating the phase velocity at a frequency of 10MHz can lead to an error of over 1.8 m/s when compared to the fully converged final value. Interestingly, as the frequency is increased the phenomenon of premature truncation of the series resulting in a correspondingly reduced relative error in the values of modelled attenuation is paralleled in the case of phase velocity, but is even more marked. Although full convergence to the final phase velocity value is only achieved by including higher orders of *n* when there is an increase in frequency, the relative error caused by truncating the computation at low values of *n* decreases significantly as frequency increases.

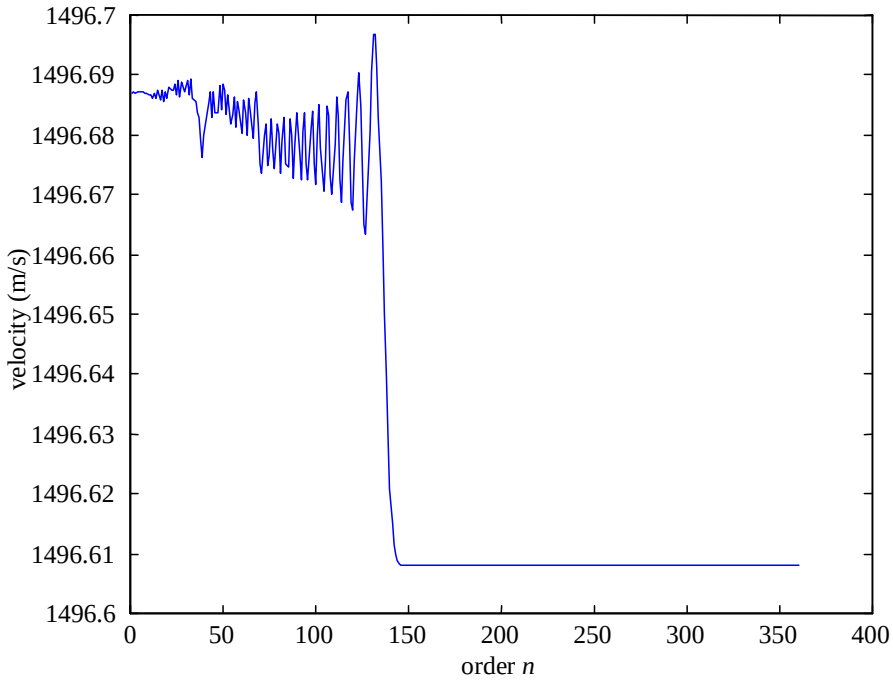

Figure 2.6 Phase velocity versus order *n* through a dispersion of 1mm diameter titanium dioxide AHR pigment spheres in water at 25ºC and 65MHz

Figures 2.6 and 2.7 illustrate that the possible error caused by premature truncation reduces to approximately 0.09 m/s at 65MHz and approximately 0.035 m/s at 120MHz. Nevertheless, the latter case requires computation to an order $n \cong 260$ for full and stable convergence to within machine epsilon of a final value. Machine epsilon is the smallest possible relative difference between a computer's representation of two floating-point numbers. It is a function of machine architecture and type of floating-point representation used and will be dealt with in more detail in Chapter 3. However, throughout this chapter the definition of fully converged to within machine epsilon is to within 19 decimal places using 80-bit arithmetic.

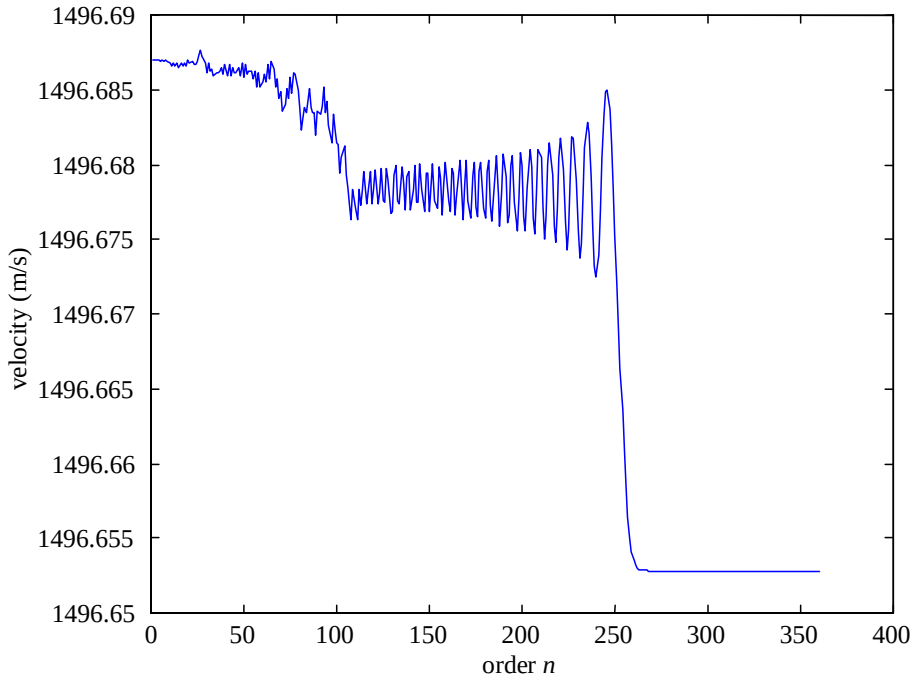

Figure 2.7 Phase velocity versus order *n* through a dispersion of 1mm diameter titanium dioxide AHR pigment spheres in water at 25ºC and 120MHz

2.5.1 Relationship between order *n* needed for series convergence and particle size-wavenumber product

The orders of *n* to which the infinite series must be calculated to achieve convergence to within a predetermined threshold percentage of fully converged attenuation or phase velocity values are listed in Appendix C. It includes values of *n* associated with a range of material combinations, particle sizes and frequencies. The values of *n* required for convergence to within 0.01% of final value for 1mm diameter particles of a range of materials over the range 0.1MHz to 150MHz are shown in Figure 2.8.

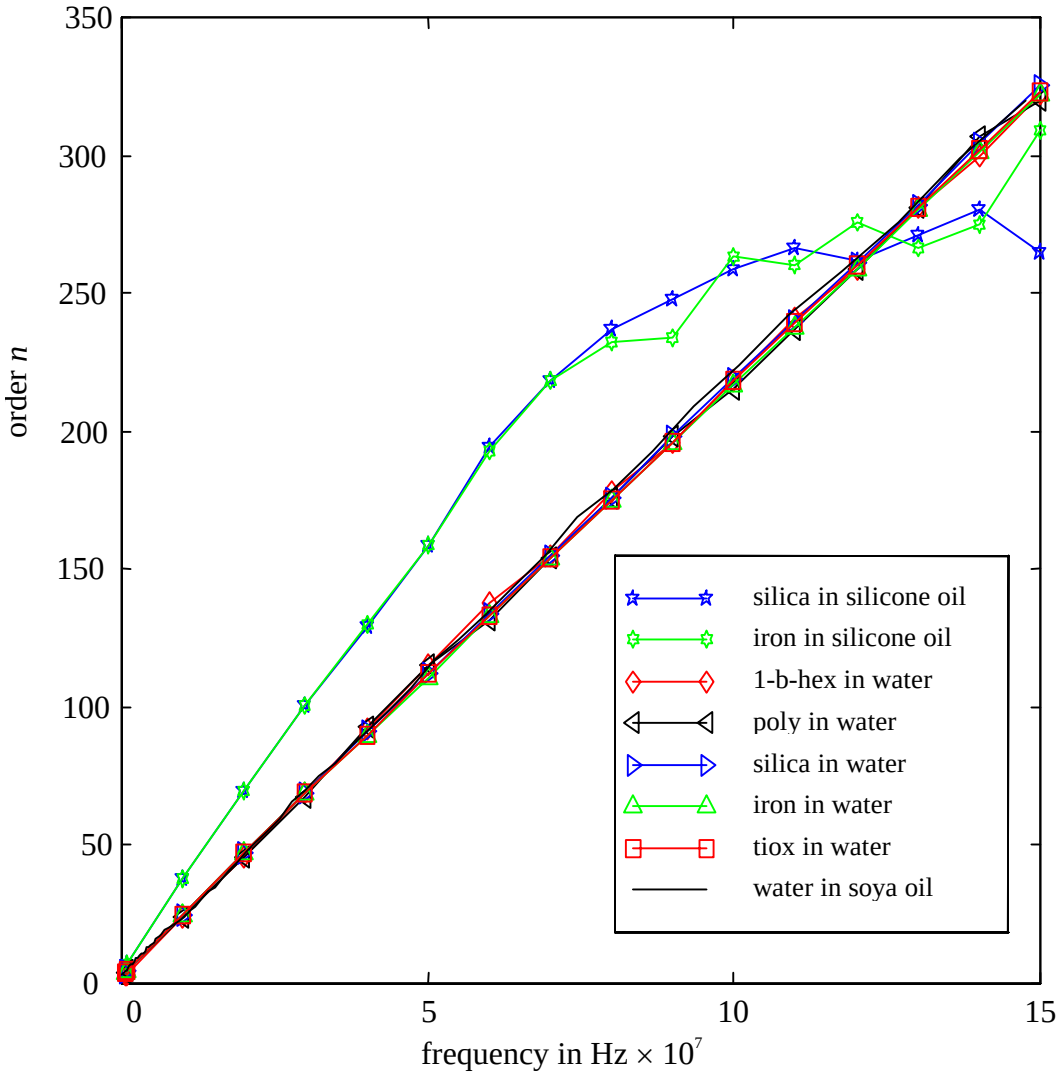

Figure 2.8 Order *n* needed for convergence to within 0.01% of final value of attenuation versus frequency in dispersions of 1mm diameter particles (see Appendix E for a key to the abbreviations and for a listing of each material's physical properties)

Over the whole frequency range of all the modelled dispersions in which the continuous phase was water or soya oil, and for silicone oil continuous phase dispersions up to about 70MHz, it was found that:

a. n is proportional to particle diameter and acoustic frequency

b. n is inversely proportional to compressive wave velocity in the continuous phase

The linear relationship is evident for all particle sizes above 1μm diameter, and the relationship between order n and particle diameter-frequency product over wave velocity is roughly a constant for each of the three categories of dispersion. This relationship was tested using a range of notional values for compressive wave velocity between 500 and 4000 m/s and found to hold true. Therefore, as a rough working guide: the order n needed for convergence of the series to within 0.01% of final value of attenuation or phase velocity is 3 for particle diameters up to 1μm for all the material combinations and frequencies modelled. For particle diameters above 1μm in dispersions: the order n needed for convergence of the series to within 0.01% of final value of attenuation or phase velocity is given by

$$n \cong 3.3\frac{Df}{c} + 4\,, \qquad \frac{Df}{c} < 70 \tag{2.90}$$

rounded up to the nearest integer, where D is the diameter of the particle in metres, f is the frequency in Hz and c is the compressive wave velocity in the continuous phase. Equation (2.90) was found to give reasonably accurate results up to $\frac{Df}{c} < 70$ for all the modelled dispersions, and it remained equally valid up to a modelled limit of $\frac{Df}{c} \le 100$ for water or soya oil continuous phase dispersions.

2.6 Application of the simple scattering model to polydispersity

Discussion of the mechanisms that give rise to attenuation and phase velocity dispersion so far has considered only dispersions of identically sized spheres, known as *monodisperse* dispersions. Although almost monodisperse systems do exist in practice, they are usually found only in the laboratory. The particulate dispersions encountered in industry and commerce, some of which are listed in Chapter 1, most frequently span a range of particle sizes within the same dispersion and are known as *polydisperse*. By assuming the same conditions of superposition as those for monodisperse single scattering, viz the net effect of a number of scatterers is simply additive, polydisperse systems can be modelled. Again, this assumption is valid only for those dilute dispersions where multiple scattering and particle-particle interactions are insignificant. It is possible to compute a polydisperse single-scattering model using a function to represent particle size distribution, for example the lognormal distribution. However, it is computationally simpler to divide the distribution into a number, *B,* of particle size-% v/v concentration bins. Each bin *b* is associated with a particle radius R_b and a % v/v concentration ϕ_b . One advantage that this method offers is that attenuation and phase velocity can be modelled using sizing information in a form frequently encountered as the output of commercial sizing instruments. This facilitates the more accurate modelling of real dispersions for comparison with experimental results. This method can be computationally expensive when there is a large number of bins because each R_b value necessitates the calculation of its associated compressive scattering wavenumber series $A_{b,n}$ to convergence. The polydispersity-modified form of Equation (2.88) is given by

$$\beta^2 = k_c^2 + \frac{3}{ik_c}\sum_{b=1}^{B}\frac{\phi_b}{R_b^3}\sum_{n=0}^{\infty}(2n+1)\ A_{b,n} \qquad \textbf{(2.91)}$$

2.7 Summary

A brief outline is given of the development of the mathematical scattering theory that is used to model acoustic attenuation and phase velocity dispersion in particulate dispersions, culminating in the ECAH model. A modification to the original ECAH equations is described which incorporates effective μ for liquids and so uses the same set of equations for any permutation of solid and liquid dispersed and continuous phases. The Foldy simple scattering model is used to incorporate series values of A_n into an expression from which acoustic attenuation and phase velocity can be derived. Using this model it is demonstrated that truncation of the series at low orders of n can lead to significant errors in the calculation of acoustic attenuation and phase velocity. The orders of n that need to be computed for predetermined thresholds of convergence are tabulated for a range of different materials, acoustic frequencies and particle sizes. A relationship between compressive wavenumber-particle size product and order n required for convergence is demonstrated. This requirement to compute the partial wave expansion to orders beyond $n = 2$ for larger particles and/or higher frequencies leads to a complementary requirement to compute higher orders of spherical Bessel and Hankel functions. Before the recent advances and wider availability of affordable computing power, this was a major obstacle. However, work was undertaken in the 1970s and early 1980s at Sandia Laboratories as part of the United States Atomic Weapons Program to calculate complicated high-order, three-dimensional wave functions of extremely large and extremely small complex arguments. The routines were intended to run on what were then state-of-the-art supercomputers but they are now capable of being run at an acceptable speed on any reasonably modern desktop PC. The mathematical development and numerical techniques used to maximize the accuracy and stability of the functions, and the modifications to the mathematics,

numerical techniques and translation to a different programming language required to adapt the routines for use in modelling acoustic scattering are described in Chapter 3.

3. Numerical computation of Bessel functions

3.1 Introduction

Chapter 2 described how the equations of Allegra & Hawley (1972) model the propagation of compressive, shear and thermal waves through a continuous medium, in the presence of particles of a dispersed medium, by the numerical computation of a number of mathematical functions each taking a complex argument. These are spherical Bessel functions of the first kind and their first and second derivatives expressed as $j_n(z)$, $j_n'(z)$ and $j_n''(z)$ respectively and spherical Bessel functions of the third kind, usually called spherical Hankel functions, of the first type expressed as $h_n^1(z)$, $h_n'^1(z)$ and $h_n''^1(z)$. For each function *n* denotes the real, non-negative integer order of the function, and *z* denotes the complex argument of the function. The phase velocity and attenuation of ultrasound propagation through a dispersion is modelled by using the solution of Allegra and Hawley's equations. Out of the selection of ways of numerically computing the values of Bessel functions the choice for a particular combination of order, argument modulus and argument phase is critical to the stability, accuracy and computational efficiency of calculation. The criteria and algorithms employed in choosing a method of computing values of a Bessel function, and details of the various methods, are described in this chapter.

The numerical computation of the required Bessel functions needed for the ECAH model has resulted in the production of a package of software. It includes a C++ translation of part of the original Amos (March 1986) library of subroutines, originally written in Fortran 66 and Fortran 77 primarily for the CDC6600 mainframe computer. The package also incorporates a number of modifications enabling compatibility with C++ code for the

solution of Allegra and Hawley's equations and the 32-bit Intel based computer environment. This chapter describes in detail the algorithmic development of the software.

3.2 Calculation of cylindrical modified Bessel functions $I_\nu(z)$ and $K_\nu(z)$

The kernel of the Amos routines computes cylindrical modified Bessel functions of the first kind $I_\nu(z)$, and second kind $K_\nu(z)$, in the right half z plane, $\mathrm{Re}(z) \geq 0$, where ν denotes the real, non-negative fractional order of the function. The relationship of the required Bessel functions to the kernel functions is detailed in Equations (3.1) and (3.2). They use the usual Watson (1922) convention, in which functions expressed in upper-case *J, Y, I, K* and *H* denote specific kinds of cylindrical functions and the same letters in lower-case denote corresponding functions taking spherical arguments

$$H_\nu^{(1)}(z) = \frac{2}{i\pi} e^{\frac{-i\pi\nu}{2}} K_\nu\left(ze^{\frac{-i\pi}{2}}\right), \quad \mathrm{Re}(z) \geq 0 \qquad \textbf{(3.1)}$$

$$J_\nu(z) = e^{\frac{\mp i\pi\nu}{2}} I_\nu\left(ze^{\frac{\pm i\pi}{2}}\right), \quad \mathrm{Re}(z) \geq 0 \qquad \textbf{(3.2)}$$

These functions are made analytically continuous over the whole of the branch cut complex plane $-\pi < \arg z < \pi$ through the formulae

$$K_\nu\left(ze^{\pm i\pi}\right) = e^{\mp i\pi\nu} K_\nu(z) \mp i\pi\, I_\nu(z), \quad \mathrm{Re}(z) \geq 0 \qquad \textbf{(3.3)}$$

$$I_\nu\left(ze^{\pm i\pi}\right) = e^{\pm i\pi\nu} I_\nu(z), \quad \mathrm{Re}(z) \geq 0 \qquad \textbf{(3.4)}$$

$$J_\nu\left(ze^{\pm i\pi}\right) = e^{\pm i\pi\nu} J_\nu(z), \quad \mathrm{Re}(z) > 0 \qquad \textbf{(3.5)}$$

Positive rotation of *z* from the third into the fourth quadrant and negative rotation of *z* from the second into the first quadrant satisfies $-\pi < \arg\left(ze^{\pm i\pi}\right) \leq \pi$ in Equations (3.1) and (3.2) and $-\pi/2 \leq \arg z \leq \pi/2$ in Equations (3.3), (3.4) and (3.5).

3.3 Numerical considerations

The power series for small $|z|$ and asymptotic series for large $|z|$ have proven to be satisfactory methods for numerically computing *I* and *K* functions (Abramowitz & Stegun, 1972) and are used in the software that has been developed; however, values of $|z|$ between these extremes are more problematic and the software draws on the work of Temme (1975a) on the computation of $K_\nu(z)$ and on the work of Olver & Sookne (1972) and Sookne (1973) on the ratios of $\dfrac{I_{\nu+1}(z)}{I_\nu(z)}$. These references gave detailed analyses of truncation errors enabling the selection and optimization by Amos (March 1983) of algorithms to compute $I_\nu(z)$ and $K_\nu(z)$ efficiently and to a predetermined level of precision. The software is also configured to offer the option of returning the results of computation with exponential scaling $e^{iz} H_\nu^1(z)$ and $e^{-|y|} J_\nu(z)$ where $z = x + iy$, to remove the dominant growth for $z \to \infty$. The algorithms detect underflow and overflow by estimating function magnitudes and testing them in logarithmic form against the largest machine number and smallest positive machine number. Unit round-off, or machine epsilon ε, representing the lower bound of truncation errors, is used to terminate infinite processes after the highest possible precision has been computed. This varies by machine

architecture but, for 32-bit Intel architecture (which includes for this purpose Intel 486 and Pentium machines) using 64-bit arithmetic, $\varepsilon = 2^{-52}$ or approximately 2.22×10^{-16}. The 32-bit Intel co-processor internal floating-point-unit uses 80-bit arithmetic as its native mode. If software code is written to exploit this, machine epsilon reduces to $\varepsilon = 2^{-64}$ or approximately 5.42×10^{-20}. Unfortunately, 80-bit arithmetic is supported by only a limited number of compilers and translation software packages. Therefore, for the sake of future portability, 80-bit arithmetic is restricted to parts of the software where its use is considered essential.

3.4 Choice of kernel Bessel functions

In view of the kinds of Bessel function specified in §3.1 that are required to be computed, it might appear evident that the well known relationship

$$H_\nu^1(z) = J_\nu(z) + iY_\nu(z) \qquad \textbf{(3.6)}$$

can form the primary, and relatively straightforward, starting point for computing the desired functions. Hence, computation would be restricted to determining $J_\nu(z)$ and $Y_\nu(z)$ as kernel functions. However, there are practical disadvantages. As $|z|$ grows larger, heavy loss of significance occurs when z moves away from the real axis. As an example, Table 3.1 shows the effect of moving a vector $|z| = 500$ off the real axis.

Function	Value of Real Part	Value of Imaginary Part
z_1	+500	0
z_2	+300	+400
$J_0(z_1)$	$-3.410055688073200\times10^{-2}$	0
$J_0(z_2)$	$-3.142409030809552\times10^{+171}$	$+8.771727070688033\times10^{+171}$
$iY_0(z_1)$	0	$+1.050670873983137\times10^{-2}$
$iY_0(z_2)$	$+3.142409030809552\times10^{+171}$	$-8.771727070688033\times10^{+171}$
$J_0(z_1) + iY_0(z_1)$	$-3.410055688073200\times10^{-2}$	$+1.050670873983137\times10^{-2}$
$J_0(z_2) + iY_0(z_2)$	0	0
$H_0^1(z_1)$	$-3.410055688073200\times10^{-2}$	$+1.050670873983137\times10^{-2}$
$H_0^1(z_2)$	$-6.528277832091689\times10^{-176}$	$-2.015874043748228\times10^{-176}$

Table 3.1 Numerical values of $J_0(z) + iY_0(z)$ and directly computed $H_0^1(z)$

The displayed precision of 16 digits is representative of 64-bit arithmetic. In this extreme case, loss of significance is total as $J_0(z_2) + iY_0(z_2)$ is less than machine epsilon although the true value of $H_0^1(z_2)$, computed by using Equation (3.1), is over 135 orders of magnitude larger than even the smallest machine number using only 64-bit arithmetic. Moreover, another inherent disadvantage of computer floating-point complex arithmetic is that if the real and imaginary part of a number differ by more than a few orders of magnitude the smaller component does not contain full significance, although the larger part and the complex modulus do retain full significance. This is permissible in some applications where only the complex modulus and phase angle are of interest but, in the computation of attenuation and phase velocity, the separation of real and imaginary components at the highest possible precision of each is highly desirable as it helps to extend the limits of particle size and frequency that can be successfully modelled.

3.5 Transformation of cylindrical to spherical Bessel functions and their derivatives

Spherical Bessel functions can be expressed in terms of higher orders of cylindrical Bessel functions of the same kinds and types. In the following expression *j* and *J* are interchangeable with *h* and *H* respectively; also, because Hankel functions exclusively of the first type are used in the equations derived by Allegra and Hawley, the superscript (1) is considered implicit and subsequently omitted for clarity

$$h_n(z) = \sqrt{\frac{\pi}{2z}}\, H_{(n+1/2)}(z) \tag{3.7}$$

$$h_n'(z) = \frac{n}{z} h_n(z) - h_{(n+1)}(z) = \sqrt{\frac{\pi}{2z}} \left[\frac{n}{z} H_{(n+1/2)}(z) - H_{(n+3/2)}(z) \right] \tag{3.8}$$

$$h_n''(z) = \frac{n^2 - n}{z^2} h_n(z) - h_{(n+2)}(z) = \sqrt{\frac{\pi}{2z}} \left[\frac{n^2 - n}{z^2} H_{(n+1/2)}(z) - \frac{n-1}{z} H_{(n+3/2)}(z) + H_{(n+5/2)}(z) \right] \tag{3.9}$$

3.6 Choice of computational method

There are a number of methods for deriving numerical values of the *I* and *K* functions. Figure 3.1 and Figure 3.2 show, in schematic form that is not to scale, the optimal selection arrived at by Amos (May 1983) of computational method over the $(|z|, \nu)$ plane. The optimal selection of computational method used in each particular case is a trade-off between accuracy, numerical stability and, all other factors being equal, speed of execution.

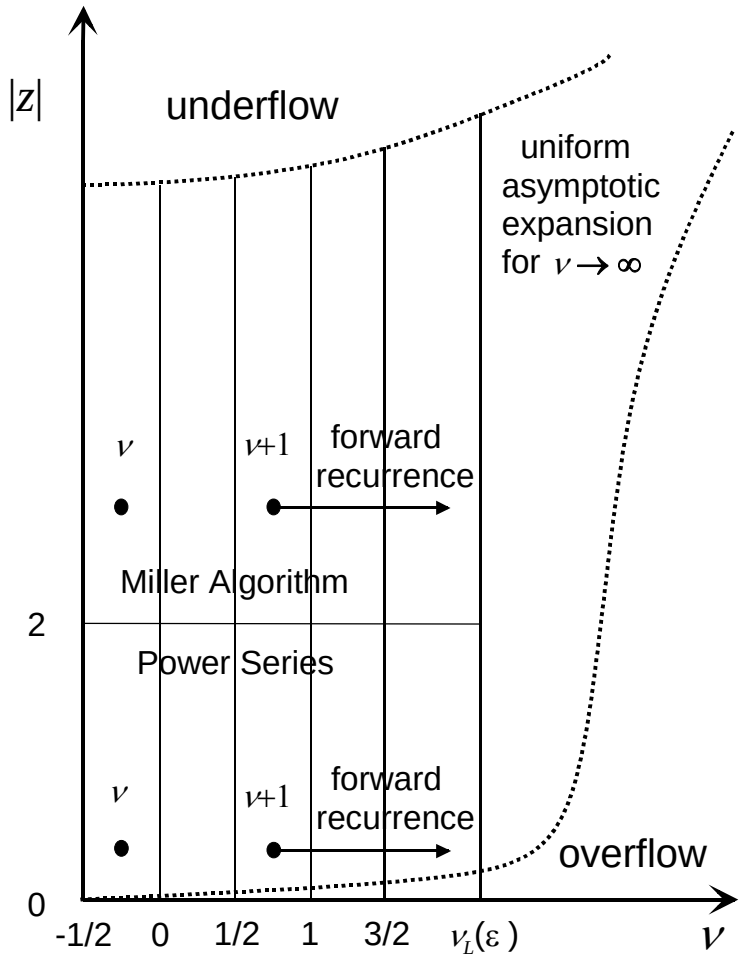

Figure 3.1 Computation Diagram for $K_\nu(z)$ after Amos (May 1983)

The computationally valid region of Figure 3.1, for orders up to $\nu_L(\varepsilon)$, is horizontally separated into two areas representing the optimum applicability of the power series and Miller algorithm (Miller, 1952) to compute $K_\nu(z)$ and $K_{\nu+1}(z)$ for $-\frac{1}{2} \le \nu < \frac{1}{2}$. The computation of $\nu_L(\varepsilon)$ is detailed in Appendix A. Higher order function values for the same value of z can then be found by forward recurrence into ν values not covered by the fundamental formula by employing the relationship

$$K_{\nu+1}(z) = \frac{2\nu}{z} K_{\nu}(z) + K_{\nu-1}(z) \qquad \textbf{(3.10)}$$

up to an arbitrary limit of $\nu = \nu_L(\varepsilon)$ after which uniform asymptotic expansions for $\nu \to \infty$ are used to compute both *I* and *K* numerical values and, under certain circumstances, explicit numerical values of *J* and *H*. The $\nu = \nu_L(\varepsilon)$ threshold is a function of machine epsilon. It is the point beyond which uniform asymptotic expansions for $\nu \to \infty$ are computationally more efficient and more accurate than recurrence methods, as there is a loss of accuracy owing to round-off error resulting from the high number of iterations necessary to compute K_ν by recurrence or I_ν by Wronskian. Uniform asymptotic expansions for $\nu \to \infty$ are described in detail in §3.15. The area above the Wronskian in Figure 3.2 is computed efficiently by backward recurrence from the asymptotic expansion since that entails fewer iterations than the Wronskian method because the degree of recurrence implicit in the latter method increases proportionally with increase in $|z|$.

3.7 Computation of $K_\nu(z)$ for $|z| \le 2$ and $\mathrm{Re}(z) \ge 0$, $-\frac{1}{2} < \nu < \frac{1}{2}$

The case of computing $K_\nu(z)$ when $\nu = \pm \frac{1}{2}$ is a special one and can be expressed explicitly as

$$K_{-1/2}(z) = K_{1/2}(z) = e^{-z}\sqrt{\frac{\pi}{2z}} \qquad \textbf{(3.11)}$$

However, when $|z| \le 2$, $\mathrm{Re}(z) \ge 0$ and $-\frac{1}{2} < \nu < \frac{1}{2}$, $K_\nu(z)$ is computed by expanding the power series. Expressions for $K_\nu(z)$ and $K_{\nu+1}(z)$ were given by Temme (1975a) as

$$K_v(z) = \sum_{k=0}^{\infty} C_k f_k \tag{3.12}$$

$$K_{v+1}(z) = \frac{2}{z}\sum_{k=0}^{\infty} C_k\left(p_k - kf_k\right) \tag{3.13}$$

Where

$$f_0 = \frac{\pi v}{\sin \pi v}\left[\Gamma_1(v)\cosh \mu + \Gamma_2(v)\ln\left(\frac{2}{z}\right)\frac{\sinh \mu}{\mu}\right] \tag{3.14}$$

$$p_0 = \frac{1}{2}\left(\frac{z}{2}\right)^{-v}\Gamma(1+v) \tag{3.15}$$

$$q_0 = \frac{1}{2}\left(\frac{z}{2}\right)^{v}\Gamma(1-v) \tag{3.16}$$

$$C_0 = 1 \tag{3.17}$$

$$f_k = \frac{\left(kf_{k-1} + p_{k-1} + q_{k-1}\right)}{\left(k^2 - v^2\right)} \tag{3.18}$$

$$p_k = \frac{p_{k-1}}{(k-v)} \quad , \quad k \geq 1 \tag{3.19}$$

$$q_k = \frac{q_{k-1}}{(k+v)}, \quad k \geq 1 \tag{3.20}$$

$$C_k = \frac{\left(\frac{z^2}{2}\right)^k}{k!} \tag{3.21}$$

$$\mu = v\ln\left(\frac{2}{z}\right) \tag{3.22}$$

$$\Gamma_1(v) = \frac{1}{2v}\left[\frac{1}{\Gamma(1-v)} - \frac{1}{\Gamma(1+v)}\right] \tag{3.23}$$

$$\Gamma_2(v) = \frac{1}{2}\left[\frac{1}{\Gamma(1-v)} + \frac{1}{\Gamma(1+v)}\right] \tag{3.24}$$

In his algorithm, Amos (March 1983) computed the gamma function by evaluating the asymptotic expansion

$$\ln\Gamma(z) \sim (z - \tfrac{1}{2})\ln z - z + \tfrac{1}{2}\ln(2\pi) + \sum_{m=1}^{M} \frac{B_{2m}}{2m(2m-1)z^{2m-1}} + R_M \qquad \textbf{(3.25)}$$

for $z \geq X$, where X is an integer, and B_{2m}, $m = 1,2,\ldots$ are Bernoulli numbers (Abramowitz & Stegun, 1972, p810) and the notation of $f(x) \sim g(x)$ denotes $f(x)$ is asymptotic to $g(x)$ following the convention due to Bachmann and Landau (Landau, 1927). The Gamma function is then computed by backward recurrence using the equality

$$\Gamma(x) = \frac{\Gamma(x+1)}{x} \qquad \textbf{(3.26)}$$

But computed in the logarithmic domain for computational efficiency

$$\ln\Gamma(x) = \ln\Gamma(z) - \ln\left[x(x+1)\ldots(x+k-1)\right] \qquad \textbf{(3.27)}$$

Where

$$0 < x < X, \quad z = x + k, \quad k = (x - X) + 1 \qquad \textbf{(3.28)}$$

Amos' numerical experiments showed that accuracy is guaranteed to at least 18 decimal digits with recursion of 22 terms or less (Amos, March 1983). Duplication of calculation is reduced by using the relationship

$$\Gamma(1-\nu) = \frac{\pi\,\nu}{\sin\pi\,\nu}\frac{1}{\Gamma(1+\nu)} \qquad \textbf{(3.29)}$$

and taking into account that it is already necessary to compute $\sin(\pi\nu)/\pi\nu$ to evaluate f_0 in Equation (3.14) as a seed of Equations (3.12) and (3.13).

Although the problem does not arise in the calculation of A_n , Allegra and Hawley's scattering coefficients, there is an instability in the computation of gamma functions when $v \to 0$ for the equation

$$\Gamma_1(v) = \frac{1}{2v}\left[\frac{1}{\Gamma(1-v)} - \frac{1}{\Gamma(1+v)}\right] \qquad \textbf{(3.30)}$$

Therefore, for the sake of ensuring robust design of the software, the Taylor expansion about $v = 0$ is incorporated into the algorithm which provides a stable method of computing the Gamma function by employing Psi and Riemann Zeta functions when $v \to 0$. Amos (op. cit) deals with the method of implementation in detail.

Equation (3.12) is a rearrangement of the standard definition

$$K_v(z) = \frac{\pi}{2}\frac{I_{-v}(z) - I_v(z)}{\sin \pi v} \qquad \textbf{(3.31)}$$

It employs the power series for $I_{-v}(z)$ and $I_v(z)$. Therefore, it is reasonable to assume that Equation (3.12) and, by implication, Equation (3.13) will not converge any faster than either of their constituents, $I_{-v}(z)$ or $I_v(z)$. Since the former constituent dominates the latter, convergence is based on the error test for $I_{-v}(z)$

$$I_{-v}(z) = \left(\frac{z}{2}\right)^{-v} \sum_{k=0}^{\infty}\left[\frac{\left(\frac{z^2}{4}\right)^k}{k!\Gamma(k+1-v)}\right], \quad -½ < v < ½, \quad |z| \le 2 \qquad \textbf{(3.32)}$$

Which can be expressed as

$$I_{-\nu}(z) = \frac{\left(\frac{z}{2}\right)^{-\nu}}{\Gamma(1-\nu)}\left[\sum_{k=0}^{M} A_k + R_M\right] \tag{3.33}$$

where $A_0 = 1$ and

$$A_{k+1} = \frac{A_k\left(\frac{z^2}{4}\right)}{(k+1)(k-\nu+1)}, \quad k \geq 0 \tag{3.34}$$

It is then possible to make the remainder term R_M explicit as

$$R_M = \sum_{M+1}^{\infty} A_k \tag{3.35}$$

Which, by inserting the limits $|z^2/4| \leq 1$, $-½ < \nu < ½$ and Equation (3.34) can be bounded as follows

$$\begin{aligned} |R_M| \leq \sum_{M+1}^{\infty} |A_k| &\leq \frac{|A_m|}{(M+1)(M-\nu+1)} + \frac{|A_M|}{(M+1)(M-\nu+1)(M+2)(M-\nu+2)} + \quad \cdots \\ &\leq \frac{|A_M|}{(M+1)(M-\nu+1)}\left[1 + \frac{1}{\left(M+\frac{3}{2}\right)^2} + \frac{1}{\left(M+\frac{3}{2}\right)^4} + \quad \cdots\right] \\ &\leq \frac{|A_m|}{(M+1)(M-\nu+1)} \frac{\left(M+\frac{3}{2}\right)^2}{M^2+3M+\frac{5}{4}} = \frac{|A_m|}{(M+1)(M-\nu)}\left[1 + \frac{1}{M^2+3M+\frac{5}{4}}\right] \\ &< \frac{1.2|A_M|}{(M+1)(M+1-\nu)}, \quad M \geq 1 \end{aligned} \tag{3.36}$$

Consequently, the computation of $K_\nu(z)$ for $|z| \leq 2$, $\mathrm{Re}(z) \geq 0$ and $-½ < \nu < ½$ is terminated, summed and an accurate result returned when the following numerical comparison test is true

$$\frac{1.2\left|A_M\right|}{\left(M+1\right)\left(M+\frac{1}{2}\right)} \le 0.5\left|A_M\right| < \varepsilon \qquad \textbf{(3.37)}$$

3.8 Computation of $K_\nu(z)$ for $|z| > 2$, $\mathrm{Re}(z) \ge 0$ and $-½ < \nu < ½$

In Figure 3.1 the computation of $K_\nu(z)$ and $K_{\nu+1}(z)$ in the section of the diagram bounded by $|z| > 2$, $\mathrm{Re}(z) \ge 0$, $-½ < \nu < ½$ and $\nu_L(\varepsilon)$ is accomplished using the Miller algorithm that exploits the relationship of $K_\nu(z)$ and $K_{\nu+1}(z)$ to confluent hypergeometric functions, sometimes called Kummer functions, of the second kind and denoted by $U(x, y, z)$. Temme (1975a) analyzed the Miller algorithm for the computation of $K_\nu(z)$ and $K_{\nu+1}(z)$ and derived a numerical approximation of its associated explicit error term E_M for real values of z. However, numerical experiments by Amos (September 1975) showed that Temme's E_M in Equation (3.47) is valid for complex z in the right-half z plane. Therefore, it is used to terminate the algorithm after satisfactory convergence is achieved. The Miller algorithm is based upon the association given by

$$K_\nu(z) = \sqrt{\pi}(2z)^\nu e^{-z}\, U\left(\nu + ½, 2\nu + 1, 2z\right) \qquad \textbf{(3.38)}$$

It employs the recurrence relationship

$$K_{\nu+1}(z) = K_\nu(z)\frac{\left[\nu + ½ + z - \dfrac{k_1(z)}{k_0(z)}\right]}{z} \qquad \textbf{(3.39)}$$

In order to compute the confluent hypergeometric function the algorithm first uses the backward recurrence relationship

$$k_{n+1}(z) - b_n(z)k_n(z) + a_n(z)k_{n-1}(z) = 0\,, \quad n \ge 1 \qquad \textbf{(3.40)}$$

Where the a_n and b_n components can be expressed explicitly as

$$a_n = \frac{\left(n - \tfrac{1}{2}\right)^2 - v^2}{n(n+1)} \tag{3.41}$$

and

$$b_n = \frac{2(n+z)}{n+1} \tag{3.42}$$

Also, the k_n coefficient of Equation (3.40) can be expressed as

$$k_n(z) = (-1)^n (v, n)\, U\left(v + \tfrac{1}{2} + n,\, 2v+1,\, 2z\right), \quad -\tfrac{1}{2} \le v < \tfrac{1}{2} \tag{3.43}$$

Where

$$(v, n) = \frac{\Gamma\left(v + \tfrac{1}{2} + n\right)}{n!\,\Gamma\left(v + \tfrac{1}{2} - n\right)} = \frac{(-1)^n \cos(\pi v)}{n!\, v}\,\Gamma\left(v + \tfrac{1}{2} + n\right)\Gamma\left(\tfrac{1}{2} - v + n\right) \tag{3.44}$$

The reason for using backward recurrence is detailed in §3.9. Ultimately, the sparse system of equations can be normalized by using the equality

$$\sum_{n=0}^{\infty} k_n(z) = (2z)^{-v-\frac{1}{2}} \tag{3.45}$$

Equations (3.40) and (3.45) are treated as a tridiagonal matrix of equations and solved as a truncated $M \times M$ system. Coefficients $k_n^M(z)$, n = 0,…, M denote the approximate, pre-normalized values and are derived as follows: p_n of Equation (3.46) is generated by a forward recurrence relationship, taking as its seeds $p_0 = 0$ and $p_1 = 1$, given by

$$p_{n+1} = b_n p_n - a_n p_{n-1}, \quad n \ge 1 \tag{3.46}$$

Iterations continue for increasing integer n until the explicit error term E_M is less than machine epsilon such that

$$E_M = \frac{\cos \pi \nu}{-M|z|\left|p_M\right|} < \varepsilon \qquad \textbf{(3.47)}$$

At this point the index M is used to insert values for the bottom-right elements of the truncated tridiagonal matrix where

$$k_{M+1}^{M} = 0 \text{ and } k_M^M = \varepsilon \qquad \textbf{(3.48)}$$

These values provided the seeds for the backward recurrence in Equation (3.40) generating approximate values of $k_n^M(z)$ scaled by $k_n(z)$. Evaluation of the normalizing Equation (3.45) truncated at $n = M$ gives the scaling factor

$$S_M = \sum_{n=0}^{M} k_n^M(z) \qquad \textbf{(3.49)}$$

that is needed for complete solution of the matrix by substitution into Equation (3.43). Finally, the computed k_0 , k_1 , and S_M numerical coefficients can be inserted into Equations (3.38) and (3.39) to give

$$K_\nu(z) \sim e^{-z}\sqrt{\frac{\pi}{2z}}\frac{k_0^M}{S_M}, \quad -\tfrac{1}{2} \le \nu < \tfrac{1}{2} \qquad \textbf{(3.50)}$$

$$K_{\nu+1}(z) \sim \frac{K_\nu(z)}{z}\left[z + \nu + \tfrac{1}{2} - \frac{k_1^M(z)}{k_0^M(z)}\right], -\tfrac{1}{2} \le \nu < \tfrac{1}{2} \qquad \textbf{(3.51)}$$

By setting $k_M^M = \varepsilon$ it follows that as n decreases k_n^M increases, thereby ensuring that the matrix remains well scaled and, therefore, numerically stable.

3. 9 Derivation of an explicit expression for the terminating coefficient *M*

In the vicinity of $|z| = 2$ in Figure 3.1, the value of M, derived from Equation (3.46), can be in excess of 130 on a 32-bit Intel platform using only 64-bit arithmetic. M forward

recurrences on Equation (3.46) and M backward recurrences of Equation (3.42) generate K_ν and $K_{\nu+1}$. Hence, computation of K_ν and $K_{\nu+1}$ can require over 260 recurrence calculations and the allocation of over 130 double (complex) 2×64-bit storage locations, with their associated computational overhead, for each of the coefficients a_n and b_n. Derivation of an explicit value for M obviates the forward recurrence computation of p_m in Equation (3.46) and thereby halves the computation and storage burden. Equation (3.46), together with its seeds $p_0 = 0$ and $p_1 = 1$, form a homogeneous three term recurrence relationship with a solution p_n which in turn can be expressed as a linear combination of the two independent solutions of Equation (3.40). Putting those solutions in place of k_n in Equation (3.40) gives a second independent solution y_n in Equation (3.52) dependent upon Φ which is the confluent hypergeometric function of the first kind

$$y_n = \frac{\Gamma\left(\tfrac{1}{2} + v + n\right)}{\Gamma(n+1)} \Phi\left(v + \tfrac{1}{2} + n, 2v+1, 2z\right) \qquad \textbf{(3.52)}$$

The solution p_n, expressed as a linear combination of the independent solutions of Equations (3.40) and (3.52), is given by

$$p_n = C_1 k_n + C_2 y_n \qquad \textbf{(3.53)}$$

It has been shown that the y_n solution is dominant while the k_n solution is recessive (Temme, 1975a & 1975b) such that

$$\lim_{n\to\infty} \frac{k_n}{y_n} = 0 \qquad \textbf{(3.54)}$$

and that only backward recurrence ensures arrival at the minimal solution k_n. Because minimal solutions are unique up to a multiplicative constant (that is to say, identical, relative to a multiplicative constant), p_n is a dominant solution for large n shown by

$$\lim_{n\to\infty}\frac{k_n}{p_n}=\lim_{n\to 0}\frac{k_n}{C_1k_n+C_2y_n}=0,\quad C_2\neq 0 \tag{3.55}$$

It follows that

$$p_n\sim C_2y_n,\quad n\to\infty \tag{3.56}$$

and C_1 and C_2 can readily be determined from the initial conditions $p_0 = 0$ and $p_1 = 1$

$$C_1k_0+C_2y_0=0 \tag{3.57}$$

$$C_1k_1+C_2y_1=1 \tag{3.58}$$

Which can be substituted and transposed to give

$$C_1=\frac{-y_0}{\left(k_0y_1-k_1y_0\right)}=\frac{-1}{k_0\left(\frac{y_1}{y_0}-\frac{k_1}{k_0}\right)} \tag{3.59}$$

$$C_2=\frac{-k_0}{\left(k_0y_1-k_1y_0\right)}=\frac{1}{y_0\left(\frac{y_1}{y_0}-\frac{k_1}{k_0}\right)} \tag{3.60}$$

To numerically solve Equation (3.56), values of y_0, y_1/y_0 and k_1/k_0 are needed. As a first step Equation (3.39) is rearranged to give

$$\frac{k_1}{k_0}=\nu+\tfrac{1}{2}+z-z\left(\frac{K_{\nu+1}(z)}{K_\nu(z)}\right) \tag{3.61}$$

Equation (3.52), the confluent form, is combined with an elementary relation of Kummer's confluent hypergeometric function (Erdelyi, 1953, p254) given by

$$\tfrac{1}{2}\frac{d}{dz}\left[(2z)^{\nu+1}\Phi\left(\nu+\tfrac{1}{2},2\nu+1,2z\right)\right]=\left(\nu+\tfrac{1}{2}\right)(2z)^{\nu-\frac{1}{2}}\Phi\left(\nu+\tfrac{3}{2},2\nu+1,2z\right) \tag{3.62}$$

and a relationship between confluent hypergeometric functions and Bessel functions (Erdelyi, 1953, p265) given by

$$\frac{y_0}{\Gamma\left(v+\tfrac{1}{2}\right)} = \Phi\left(v+\tfrac{1}{2}, 2v+1, 2z\right) = \Gamma(v+1)\left(\frac{z}{2}\right)^{-v} e^z I_v(z) \qquad \textbf{(3.63)}$$

Altogether, these combinations give

$$2^v \Gamma(v+1)\frac{d}{dz}\left[z^{\frac{1}{2}} e^z I_\upsilon(z)\right] = \frac{v+\tfrac{1}{2}}{\Gamma\left(v+\tfrac{3}{2}\right)} z^{v-\frac{1}{2}} y_1 \qquad \textbf{(3.64)}$$

This, in turn, evaluates to

$$2^v \Gamma(v+1)\,\Gamma\left(v+\tfrac{1}{2}\right)\left[e^z\left(v+\tfrac{1}{2}+z\right) I_v(z) + z e^z I_{v+1}(z)\right] = z^v y_1 \qquad \textbf{(3.65)}$$

Equations (3.63) and (3.65) are rearranged and combined to give

$$\frac{y_0}{y_1} = \left(v+\tfrac{1}{2}+z+z\frac{I_{v+1}(z)}{I_v(z)}\right) \qquad \textbf{(3.66)}$$

Which, in conjunction with the Wronskian

$$I_v(z)K_{v+1}(z) + I_{v+1}(z)K_v(z) = \frac{1}{z} \qquad \textbf{(3.67)}$$

and Equation (3.61), all join to give

$$\frac{y_1}{y_0} - \frac{k_1}{k_0} = \frac{1}{I_v(z)K_v(z)} \qquad \textbf{(3.68)}$$

Therefore, Equation (3.56) becomes

$$p_n \sim \frac{y_n\left(\frac{z}{2}\right)^v e^{-z} K_v(z)}{\Gamma\left(v+\tfrac{1}{2}\right)\Gamma(v+1)}, \qquad |z| > 2 \qquad \textbf{(3.69)}$$

From Slater (1960, p88) the first term of the asymptotic expansion of the confluent hypergeometric function of the first kind $\Phi(a, b, 2z)$ when $a \to \infty$ is

$$\Phi\left(a, b, 2z\right) \sim \frac{\Gamma(b)\left(\frac{2}{u}\right)^{b-1}}{\left(\sqrt{2z}\right)^{b-1}} e^{z} I_{b-1}\left(u\sqrt{2z}\right) \tag{3.70}$$

Where

$$u = 2\sqrt{a - \frac{b}{2}} \tag{3.71}$$

$$a = \nu + \tfrac{1}{2} + n \tag{3.72}$$

$$b = 2\nu + 1 \tag{3.73}$$

The numerical value of Equation (3.70), the leading term expression, reliably indicates the order of magnitude of the summation of the convergent series and from that it is possible to ascertain order of magnitude estimates for a number of related functions as given by

$$I_{\nu}(z) \sim \frac{e^{z}}{\sqrt{2\pi z}} \tag{3.74}$$

$$K_{\nu}(z) \sim e^{-z}\sqrt{\frac{\pi}{2z}} \tag{3.75}$$

$$\frac{\Gamma\left(\nu + \tfrac{1}{2} + n\right)}{\Gamma(n+1)} \sim n^{\nu - \tfrac{1}{2}} \tag{3.76}$$

and for $|z| > 2$, $|\nu|$ small and n large, Equation (3.52) becomes

$$y_{n} \sim \frac{\Gamma(2\nu+1)}{2\sqrt{\pi}\, n^{\frac{3}{4}}} \frac{e^{z+2\sqrt{2nz}}}{(2z)^{\nu+\frac{1}{4}}} \tag{3.77}$$

Substituting the Gamma function duplication formula (Abramowitz & Stegun, 1972, p256) given by

$$\Gamma(2\nu+1) = \frac{2^{2\nu}\Gamma\left(\nu + \tfrac{1}{2}\right)\Gamma(\nu+1)}{\sqrt{\pi}} \tag{3.78}$$

into Equation (3.77), p_n in Equation (3.69) becomes

$$p_n \sim \frac{e^{-z+2\sqrt{nz}}}{2\sqrt{\pi}\,(2nz)^{3/4}} \tag{3.79}$$

By converting to polar co-ordinates, $z \equiv |z|e^{i\theta}$, the modulus of Equation (3.79) is

$$|p_n| \sim \frac{e^{|z|\cos\theta+2\sqrt{2n|z|}\frac{\cos\theta}{2}}}{2\sqrt{\pi}\,(2n|z|)^{3/4}} \tag{3.80}$$

and the error estimate in Equation (3.47) transposes to give

$$2M|z|\,|p_M| > \frac{2\cos(v\pi)}{\pi\,\varepsilon} \tag{3.81}$$

Combining Equations (3.80) and (3.81) gives

$$e^{2\sqrt{2M|z|}\frac{\cos\theta}{2}} > \frac{4\cos(v\pi)\,e^{|z|\cos\theta}}{\varepsilon\,\sqrt{\pi}\,(2M|z|)^{1/4}} \tag{3.82}$$

Which is recast as an approximate numerical equality (treating all floating point numerical values as approximations) with M on the left hand side and a right hand side, very weakly varying with M, together given by

$$M = \frac{1}{2|z|}\left(\frac{\ln C - \tfrac{1}{4}\ln M + |z|\cos\theta}{2\cos\frac{\theta}{2}}\right)^2, \quad |z| > 2, \quad -\pi \le \theta \le \pi \tag{3.83}$$

By neglecting the $(-\tfrac{1}{4}\ln M)$ term the equality is made explicit and any consequential error is safely in the direction of making M (conservatively) bigger. This is expressed as

$$M = \frac{1}{2|z|}\left(\frac{\ln C + |z|\cos\theta}{2\cos\frac{\theta}{2}}\right)^2 \tag{3.84}$$

Where

$$C = \frac{4\cos\nu\,\pi}{\varepsilon\sqrt{\pi}\left(2|z|\right)^{1/4}} \tag{3.85}$$

This value of *M* has been found to be valid when |*z*| is not large. If |*z*| is large, it leads to an excessively small value of *M* which causes premature termination of the expansion and truncation of its return value at less than optimum accuracy. However, these conclusions led to extensive numerical studies by Amos (1983, March 1986, May 1986) that resulted in his modified value of *M*, which proved to be quite accurate even when *M* was small, given by

$$M = \frac{0.97}{2|z|}\frac{\left(\ln C + \dfrac{|z|\cos A\theta}{1+0.008|z|}\right)^2}{\left(2\cos B\theta\right)^2} + 1.5, \quad |z| > 2, \quad -\pi \le \theta \le \pi \tag{3.86}$$

Where

$$A = \frac{3}{1+|z|} \tag{3.87}$$

$$B = \frac{14.7}{28+|z|} \tag{3.88}$$

$$C = \frac{4\cos\nu\,\pi}{\varepsilon\sqrt{\pi}\,\left(2|z|\right)^{1/4}} \tag{3.89}$$

With *M* derived explicitly, the need for forward recurrence in the Miller algorithm is eliminated with the savings in computation, memory and associated overhead already described.

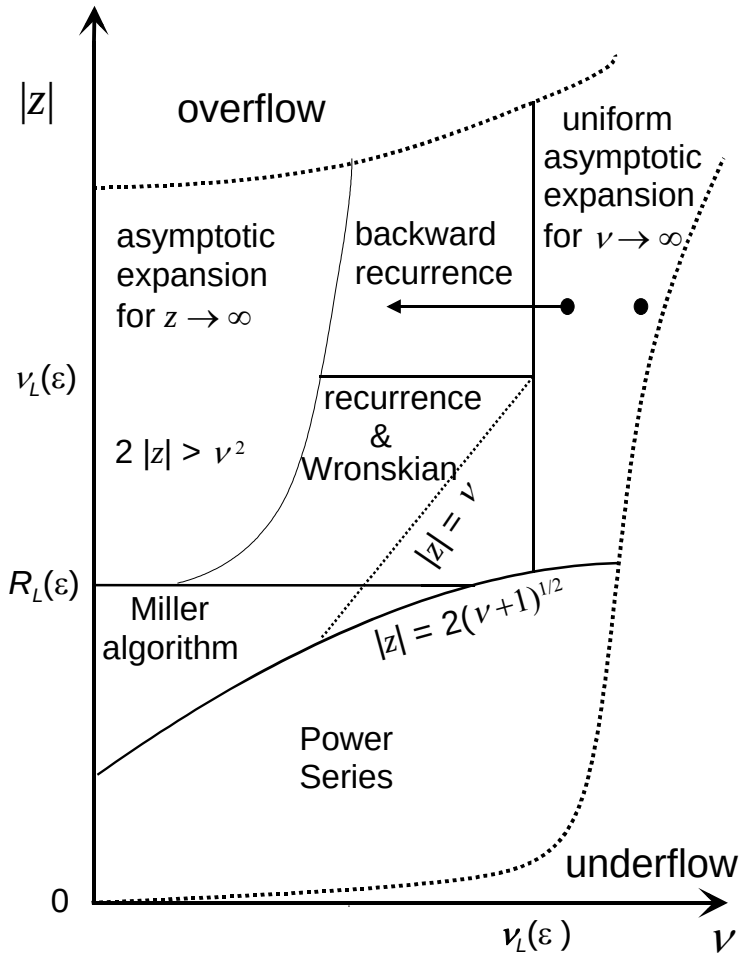

Figure 3.2 Computation Diagram for $I_\nu(z)$ after Amos (May 1983)

(See Table 3.2 for values of $R_L(\varepsilon)$ and Appendix A for corresponding values of $\nu_L(\varepsilon)$ and ε)

3.10 Computation of $I_\nu(z)$ for $|z| \le 2\,(\nu + 1)^{1/2}$

The computationally valid area in Figure 3.2 bounded by the line $|z| \le 2\,(\nu + 1)^{1/2}$ is computed in the right half of the z plane using the power series (cf. Equations (3.32), (3.33) and (3.34)) given by

$$I_\nu(z) = \left(\frac{z}{2}\right)^\nu \sum_{k=0}^{\infty} \frac{\left(\frac{z^2}{4}\right)^k}{k!\Gamma(k+1+\nu)} = \frac{\left(\frac{z}{2}\right)^\nu}{\Gamma(1+\nu)}\left[\sum_{k=0}^{M} A_k + R_M\right] \quad \textbf{(3.90)}$$

Where

$$A_0 = 1 \quad \textbf{(3.91)}$$

$$A_{k+1} = \frac{A_k\left(\frac{z^2}{4}\right)}{(k+1)(k+\nu+1)}, \quad k = 0, 1, \ldots \quad \textbf{(3.92)}$$

and it has been shown (Amos & Daniel, 1975) that R_M is bounded, as expressed by

$$|R_M| \le \frac{2|A_M|}{M}, \quad M \ge 1 \quad \textbf{(3.93)}$$

In a slightly modified form of Equation (3.37) the recurrence is terminated and the numerical value of $I_\nu(z)$ returned when the following inequality is true

$$|R_M| \le \frac{2|A_M|}{M} < \varepsilon, \quad M \ge 1 \quad \textbf{(3.94)}$$

3.11 Computation of $I_\nu(z)$ for $|z| \to \infty$

There is a value of $|z|$, the $R_L(\varepsilon)$ boundary shown in Figure 3.2, above which the asymptotic expansion for $|z| \to \infty$ reliably converges in fewer terms than is the case if the Miller algorithm is used. Derivation of a numerical value of $|z|$ corresponding to $R_L(\varepsilon)$ is shown in this section. The boundaries that delimit the use of asymptotic expansions for $|z| \to \infty$ with forward or backward recurrence or Wronskian methods, as shown in Figure 3.2, are detailed in §3.10. The expansions for complex z in the first and fourth quadrants given by

$$I_v(z) \sim \frac{e^z}{\sqrt{2\pi\ z}}\left[1+\sum_{k=1}^{\infty}(-1)^{\ k}\ A_k(z)\right]+\frac{e^{f-z}}{\sqrt{2\pi z}}\left[1+\sum_{k=1}^{\infty}A_k(z)\right] \quad \textbf{(3.95)}$$

Where

$$A_k(z)=\frac{\left(4v^{\,2}-1^2\right)....\left(4v^{\,2}-(2k-1)^2\right)}{k!(8z)^k} \quad \textbf{(3.96)}$$

$$f\ =i\pi\left(v+\tfrac{1}{2}\right),\quad 0<\arg z<\frac{\pi}{2} \quad \textbf{(3.97)}$$

$$f\ =-i\pi\left(v+\tfrac{1}{2}\right),\quad \frac{3\pi}{2}<\arg z<0 \quad \textbf{(3.98)}$$

These equations clearly indicate that the factorial term dominates when k is small and $|8z|>4v^2$, which simplifies to $|2z|>v^2$. In the worst case, when $v = 0$, it has been shown (Gatto & Seery, 1981) that effective convergence occurs before

$$k=2\left(R_L\left(\varepsilon\ \right)\right)+2 \quad \textbf{(3.99)}$$

Where $R_L(\varepsilon)$ is the smallest value of $|z|$ needed to terminate the Equation (3.95) by rendering the modulus of the term less than machine epsilon. Conservative values for E, D and $R_L(\varepsilon)$ were derived empirically by Amos (March 1983) to be

$$R_L(\varepsilon) = 1.2D + 2.4 \quad \textbf{(3.100)}$$

$$D = E\ \log_{10}(2) \quad \textbf{(3.101)}$$

$$2^{-E+1} = \varepsilon \quad \textbf{(3.102)}$$

For the purposes of software implementation using 64-bit or 80-bit arithmetic on a 32-bit Intel architecture machine Table 3.2 gives the numerical values of E, D and $R_L(\varepsilon)$.

	64-bit arithmetic	80-bit arithmetic
E	53	65
D	15.95	19.57
$R_L(\varepsilon)$	21.54	25.88

Table 3.2 Values of E, D and $R_L(\varepsilon)$ for 64-bit and 80-bit Intel arithmetic

$R_L(\varepsilon)$ equates to the modulus of z, below which asymptotic expansion of $|z|$ within the region $|z| > \frac{\nu^2}{2}$ is truncated because $|z|$ becomes too small to make e^{f-z} small in comparison with e^z when z is real. In the latter case the second term of the expansion of Equation (3.95), which is imaginary on the real axis and asymptotic only to zero, would become dominant. Therefore, it is essential for reliable numerical results that

$$e^{-2|z|} < \varepsilon \tag{3.103}$$

Or, expressed logarithmically

$$|z| > -\tfrac{1}{2}\ln\varepsilon \sim \frac{D\ln 10}{2} \sim 1.15D \tag{3.104}$$

Comparison of Equation (3.100) with Equation (3.104) shows that the former, implemented in software, is the more conservative and the essential condition of Equation (3.104) is comfortably satisfied. Also, the expansion converges relative to the k=1 term because when z is wholly imaginary, $z = iy$, then

$$I_\nu(iy) = e^{\frac{i\nu\pi}{2}} J_\nu(y) \tag{3.105}$$

$$J_\nu(y) \sim \sqrt{\frac{2}{\pi y}}\left\{\cos\chi_\nu\left[1+\sum_{k=1}^{\infty}(-1)^k A_{2k}(z)\right] - \sin\chi_\nu\left[\sum_{k=1}^{\infty}(-1)^k A_{2k-1}(z)\right]\right\} \tag{3.106}$$

$$\chi_\nu = y - \frac{\pi}{4} - \frac{\nu\pi}{2} \tag{3.107}$$

Hence, when $\cos \chi_\nu$ is small $A_1(z)$ is dominant. Usefully, the dominant term

$$\left| \frac{e^x}{\sqrt{2\pi\, z}} \right| = \frac{e^x}{\sqrt{2\,\pi\,|z|}} \tag{3.108}$$

when expressed in logarithmic form given by

$$x - \frac{\ln\left(2 - |z|\right)}{2} \tag{3.109}$$

can be, and is, used as a safe and convenient overflow test when compared against the logarithm of the maximum machine number.

In summary, the range of applicability of Equation (3.95) that is the asymptotic expansion of $\mathrm{I}_\nu(z)$ for $z \to \infty$, as shown in Figure 3.2 is given by

$$|z| > \max\{R_L(\varepsilon),\ \nu^2/2\} \tag{3.110}$$

3.12 Computation of $I_\nu(z)$ for medium values of $|z|$ and ν

The methods employed for the efficient calculation of $I_\nu(z)$ within the computationally valid regions of $|z| < 2\sqrt{\nu+1}$ and $R_L(\varepsilon) < \nu^2/2 < |z|$ are described in §3.10 and §3.11. As well as describing the computational method there is a justification of the choice of boundary lines delineating those regions on the $(|z|,\ \nu)$ plane shown in Figure 3.2. In the region of the $(|z|,\ \nu)$ plane bounded by $|z| > 2\sqrt{\nu+1}$, $2|z| < \nu^2$ and $\nu_L(\varepsilon)$ there is a choice of viable options available to compute $I_\nu(z)$. These comprise the Miller algorithm, Wronskian, and recurrence from an adjacent ν region. Conclusions drawn from the computation of $K_\nu(z)$, described in §3.7 and §3.8, are equally applicable to the computation of $I_\nu(z)$ in that the Wronskian algorithm converges slowly near $|z| = 2$, but converges rapidly when $|z|$ is

large (Amos, March 1983, Table 1). Conversely, the Miller algorithm $I_\nu(z)$ is shown to converge quickly for small to medium values of $|z|$. These results give a choice of computational methods which are complementary over the intermediate area of the ($|z|$, ν) plane and enable selection of the most efficient method for particular subsets of intermediate value ($|z|$, ν) combinations.

3.13 Computation of $I_\nu(z)$ for $2(\nu + 1)^{1/2} < |z| < R_L(\varepsilon)$ using the Miller algorithm

In the region $2(\nu + 1)^{1/2} < |z| < R_L(\varepsilon)$ the Miller algorithm has been shown to be computationally efficient (Olver & Sookne, 1972). A three term recurrence relation

$$I_{\nu-1}(z) = \frac{2\nu}{z} I_\nu(z) + I_{\nu+1}(z) \tag{3.111}$$

is used to generate ratios, $r_\nu(z)$, given by

$$r_\nu(z) = \frac{I_{\nu+1}(z)}{I_\nu(z)} \tag{3.112}$$

Which are subsequently normalized using the relationship

$$\sum_{k=0}^{\infty} \lambda_k I_{\nu+k}(z) = \frac{\left(\frac{z}{2}\right)^\nu e^z}{\Gamma(1+\nu)}, \quad 0 \le \nu < 1 \tag{3.113}$$

$$\lambda_k = 1, \quad k = 0 \tag{3.114}$$

$$\lambda_k = \frac{2(\nu + k)\Gamma(2\nu + k)}{k!\,\Gamma(2\nu + 1)}, \quad k \ge 1 \tag{3.115}$$

Thereby enabling derivation of values for $I_\nu(z)$ to be made directly.

The advantages and method of computing an explicit value of M with which to terminate an infinite series on its Mth term, within the confines of good computational efficiency and

without introducing truncation errors, are described in §3.9 as applicable to the computation of $K_\nu(z)$. An analogous scheme applicable to the computation of $I_\nu(z)$, although not identical to that of §3.9, was devised by Olver & Sookne (1972). This allows the explicit derivation of the truncation index M for use in the computation of numerically accurate ratios of the type given by Equation (3.112).

The scheme expanded Equation (3.111) into a tridiagonal system of equations that are solved by simple Gaussian elimination. The elimination operation and eventual error testing require a solution, denoted by the term p_m, of Equation (3.111) which is generated by forward recurrence on the three term relationship $p_{\bar{\nu}} = 0, \quad p_{\bar{\nu}+1} = 1$ and

$$p_{m+1} = p_{m-1} - \frac{2m}{z} p_m , \qquad m = \bar{\nu} + 1, \quad \bar{\nu} + 2, \ldots, \tag{3.116}$$

Where

$$\bar{\nu} \geq \left[|z| \right] \tag{3.117}$$

The convention $[x]$ refers to the integer part of a real number x such that $[x] < x$. Recurrence continues until

$$|p_m| > T_1 = \sqrt{\frac{|p_L|\,|p_{L+1}|}{\varepsilon}} \tag{3.118}$$

Where

$$L = \max\left\{ \left[|z| \right] + 1, \quad \left[\nu \right] + 1 \right\} \tag{3.119}$$

is satisfied at index $m = N_1$ where ν is the required order. Using the N_1 and T_1 coefficients, recurrence resumes until the comparison test

$$\left|p_m\right| \geq T_1 \sqrt{\frac{\rho_{N_1}}{\rho_{N_1}^2 - 1}} \tag{3.120}$$

is satisfied at index $m = M$ where

$$\rho_m = \min\left(\beta_m, \left|k_m\right|\right) \tag{3.121}$$

$$\beta_m = \frac{m+1}{|z|} + \sqrt{\left(\frac{m+1}{|z|}\right)^2 - 1} \tag{3.122}$$

$$k_m = \frac{p_{m+1}}{p_m} = \frac{2m}{z} - \frac{p_{m-1}}{p_m} \tag{3.123}$$

Backward recurrence of Equation (3.111) from $m = M$ using the three term recurrence relationship $y_{M+1}^M = 0$, $y_M^M = \varepsilon$ and

$$y_{m-1}^M = y_m^M \left(\frac{2\left(v_f + \bar{v} + m\right)}{z}\right) + y_{m+1}^M, \quad m = M, M-1, \ldots, 1 \tag{3.124}$$

ensures that the *I* function ratios, beginning at $\bar{v} + v_f$ where $v_f = v - [v]$, given by

$$r_{\bar{v}+v_f+m}^M = \frac{y_{m+1}^M}{y_m^M}, \quad m = L, L-1, \ldots, 0 \tag{3.125}$$

are accurate to maximum machine precision, that is to say, have relative errors no greater than machine epsilon.

The largest possible value of $\bar{v} = \max\left\{[|z|], [v]\right\}$ is used as the starting point. Then Equation (3.118) can be expressed as

$$\left|p_m\right| > T_1 = \sqrt{\frac{\left|p_{\bar{v}+2}\right|}{\varepsilon}} \tag{3.126}$$

However, if the required order is less than the modulus of the argument, $\nu < |z|$, further backward recurrence from $\bar{\nu} + \nu_f$ to ν using Equation (3.124) and its seeds is used.

The scaling factor for the normalizing relation is given by

$$S_M = y_0^M + \sum_{k=1}^{M} \lambda_k y_k^M + R_M \qquad \textbf{(3.127)}$$

Where an approximation of the relative truncation error R_M is derived by Sookne (1973) and used in its modulus form in the equality test given by

$$\left|R_M\right| = \frac{2\rho_{\bar{\nu}+2}^{2}\left(M+1\right)^2}{\left(\rho_{\bar{\nu}+2}^{2}-1\right)\left(\rho_{\bar{\nu}+2}-1\right)\left|p_M\right|} < \varepsilon \qquad \textbf{(3.128)}$$

$$\rho_{\bar{\nu}+2} = \beta_{\bar{\nu}+2} \qquad \textbf{(3.129)}$$

for the index M if $\nu < |z|$. However, if $\nu \geq |z|$ then the maximum of $[\nu]+M$ in Equation (3.125) and $[|z|]+M$ in Equation (3.128), $\max\{[\nu]+M, [|z|]+M\}$, is used to start backward recurrence. If ν is much larger than $|z|$, some re-scaling is necessary during backward recurrence as a precaution against values of y_m^M increasing too much in magnitude and eventually leading to machine overflow. Seeding Equation (3.124) with $y_m^M = \varepsilon$ extends the computable range of parameters. Term $(M+1)^2$ of Equation (3.128) which does not appear in the formulae of Sookne's (1973) derivation is an approximation to

$$\frac{\lambda_k}{2} = \frac{(k+\nu)\Gamma(k+2\nu)}{k!\,\Gamma(1+2\nu)} \sim k^{2\nu-1}(k+\nu) \leq (k+1)^2 \qquad \textbf{(3.130)}$$

in the region $0 \leq \nu < 1$ to cater for the necessity of a different normalizing relation.

The method described by Sookne (1973) for *I* functions of integer order follows a slightly different algorithm, taking the minimal value of $\bar{\nu}$, but is not described here because it is not used in the computation of integer order spherical Bessel functions.

3.14 Computation of $I_\nu(z)$ for $2(\nu+1)^{1/2} < |z| < R_L(\varepsilon)$ using the Wronskian

Computation of $I_\nu(z)$ from the Wronskian in the form

$$I_\nu(z) = \frac{1}{z\left[K_{\nu+1}(z) + r_\nu(z)K_\nu(z)\right]} \qquad \textbf{(3.131)}$$

is most efficient when $|z|$ and ν are relatively large but less than $\nu_L(\varepsilon)$. The computation of $\nu_L(\varepsilon)$ is detailed in Appendix A. The computation of $r_\nu(z)$ is described in §3.13. The computation of $K_\nu(z)$ and $K_{\nu+1}(z)$ is described in §3.7, §3.8 and §3.9. If either $K_\nu(z)$ or $K_{\nu+1}(z)$ underflow or overflow during computation, Equation (3.131) is predetermined to respectively overflow or underflow. In either case, the invalid and therefore nugatory computation is not carried out; although the software, as with all the described methods of computing *I* and *K* functions, returns a 'soft' error. That is to say: overflow returns a value corresponding to maximum machine number, underflow returns a value corresponding to minimum machine number or zero, and an appropriate error flag is signalled to the calling software routine.

3.15 Uniform asymptotic expansion for $\nu \to \infty$

Computation of Bessel functions using uniform asymptotic expansions for $\nu \to \infty$ involves the use of one of a choice of two elaborate and complicated algorithms. However, they are

computationally more efficient than power series or recurrence methods for values of ν greater than $\nu_L(\varepsilon)$; moreover, their computational efficiency increases with increasing ν.

Both algorithms are based on well-established relationships (Abramowitz & Stegun, 1972) and are due to the work of Olver (1974). They were implemented practically and numerically tested by Amos (May 1983). In common with algorithms already described, they are valid only for non-negative orders in the right half of the complex z plane. They are rendered analytically continuous throughout the whole of the branch-cut z plane, $-\pi \leq \arg z \leq \pi$, using transformations given by Equations (3.3), (3.4) and (3.5) and vector rotation conventions detailed in §3.2. The first method adheres to the convention of computing kernel functions, $K_\nu(z)$ and $I_\nu(z)$, for reasons explained in §3.4, before using those kernel functions to compute $J_\nu(z)$ and $H_\nu(z)$. The expansions are given by

$$I_\nu(z) \sim \sqrt{\frac{t}{2\pi\nu}} e^{\nu\xi} \left[1 + \sum_{k=1}^{\infty} \frac{U_k(t)}{\nu^k} \right] \qquad \textbf{(3.132)}$$

$$K_\nu(z) \sim \sqrt{\frac{\pi t}{2\nu}} e^{-\nu\xi} \left[1 + \sum_{k=1}^{\infty} \frac{(-1)^k U_k(t)}{\nu^k} \right] \qquad \textbf{(3.133)}$$

Where t and ξ are mappings from the z plane and $U_k(t)$ is a complicated polynomial containing both integrals and derivatives. These are defined, for the purposes of Equations (3.132) and (3.133) as

$$t = \frac{1}{\sqrt{1 + \left(\frac{z}{\nu}\right)^2}} \qquad \textbf{(3.134)}$$

$$\xi = -\left\{ \ln\left[\frac{1+\sqrt{1+\left(\frac{z}{\nu}\right)^2}}{\left(\frac{z}{\nu}\right)} \right] - \sqrt{1+\left(\frac{z}{\nu}\right)^2} \right\} \qquad \textbf{(3.135)}$$

$$U_0(t) = 1 \qquad \textbf{(3.136)}$$

$$U_{k+1}(t) = \tfrac{1}{2} t^2\left(1-t^2\right)U_k'(t) + \tfrac{1}{8}\int_0^t \left(1-5y^2\right)U_k(y)\,dy, \quad k>1 \qquad \textbf{(3.137)}$$

Where

$$-\frac{\pi}{2} < \arg z < \frac{\pi}{2} \qquad \textbf{(3.138)}$$

Although the literature ascribes the applicability of Equations (3.132) and (3.133) to the whole of the region $-\frac{\pi}{2} < \arg z < \frac{\pi}{2}$ of the complex plane (Abramowitz & Stegun, 1972) (Olver, 1974), numerical experiments by Amos (May 1983) showed that as arg z approaches $\pm\,\pi$ accuracy deteriorates unless order ν grows dramatically. This is inappropriate for the intended purpose of the software described in this chapter. In practice, the useful region for the applicability of Equations (3.132) and (3.133) is cited by Amos to be subject to the condition $|\arg z| < \frac{\pi}{3}$ and their use is restricted to that region. For conditions where $\left|\arg z\right| > \frac{\pi}{3}$ Olver's (1974) explicit expansions for $J_\nu(z)$ and $H_\nu(z)$ (see also Abramowitz & Stegun, 1972) are employed. They are given by the asymptotes

$$J_\nu(z) \sim \phi(z)\left\{ \mathrm{Ai}(\alpha)\,S_1(z,\nu) + \frac{\mathrm{Ai}'(\alpha)}{\nu^{4/3}}\,S_2(z,\nu) \right\}, \qquad \pi < \arg z < \pi \qquad \textbf{(3.139)}$$

$$H_v(z) \sim 2e^{-i\frac{\pi}{3}}\phi(z)\left\{\mathrm{Ai}(\beta)S_1(z,v)+\frac{e^{i\frac{2\pi}{3}}\mathrm{Ai}'(\beta)}{v^{4/3}}S_2(z,v)\right\}, \quad \pi < \arg z < \pi \quad \textbf{(3.140)}$$

Where Ai(z) and Ai′(z) denote Airy functions and derivatives of Airy functions with respect to z. The complex plane mappings α, β, and ζ are defined as

$$\alpha = v^{2/3}\zeta \quad \textbf{(3.141)}$$

$$\beta = e^{i\frac{2\pi}{3}}\alpha \quad \textbf{(3.142)}$$

$$\frac{2}{3}\zeta^{3/2} = \left[\ln\frac{1+\sqrt{1+\left(\frac{z}{v}\right)^2}}{\left(\frac{z}{v}\right)} - \sqrt{1-\left(\frac{z}{v}\right)^2}\right] \quad \textbf{(3.143)}$$

The infinite series complex polynomials S_1, S_2, A_k and B_k are defined as

$$S_1(z,v) = \sum_{k=0}^{\infty}\frac{A_k(\xi)}{v^{2k}} \quad \textbf{(3.144)}$$

$$S_2(z,v) = \sum_{k=0}^{\infty}\frac{B_k(\xi)}{v^{2k}} \quad \textbf{(3.145)}$$

$$A_k(\zeta) = \sum_{s=0}^{2k}\frac{\mu_s U_{2k-s}(t)}{\zeta^{\frac{3s}{2}}} \quad \textbf{(3.146)}$$

$$B_k(\zeta) = \sum_{s=0}^{2k+1}\frac{\lambda_s U_{2k-s+1}(t)}{\zeta^{\frac{(3s+1)}{2}}} \quad \textbf{(3.147)}$$

The coefficients λ_0, λ_s and μ_s are defined as

$$\lambda_0 = 1 \quad \textbf{(3.148)}$$

$$\lambda_s = \frac{(2s+1)(2s+3)\ldots(6s-1)}{s!(144)^s}, \qquad s = 0, 1, 2,\ldots \quad \textbf{(3.149)}$$

$$\mu_s = -\frac{6s+1}{6s-1}\lambda_s, \qquad s = 0, 1, 2,\ldots \tag{3.150}$$

The complex plane mapping $\phi(z)$ is defined as

$$\phi(z) = \frac{1}{\nu^{1/3}}\left[\frac{4\zeta}{1-\left(\frac{z}{\nu}\right)^2}\right]^{1/4} \tag{3.151}$$

and the definitions of the t function and the $U(t)$ polynomials are the same as those defined in Equations (3.134), (3.136) and (3.137) but valid over an extended range bounded by

$$\pi < \arg z < \pi \tag{3.152}$$

The latter of the two algorithms appears the more versatile and usable over the whole of the complex plane, through use of complex rotation transformations given by Equations (3.3), (3.4) and (3.5) and vector rotation conventions detailed in §3.2. Nevertheless, it carries considerable penalties in the form of additional computational complexity and storage requirements. Therefore, the algorithm defined by Equations (3.132) and (3.133) is used when $|\arg z| < \frac{\pi}{3}$ and the algorithm defined by Equations (3.139) and (3.140) is used when $|\arg z| > \frac{\pi}{3}$.

3.16 Uniform asymptotic expansion for $\nu \to \infty$ and $|\mathbf{arg}z| < \frac{\pi}{3}$

The recurrence relationship between orders of $U_k(t)$ given by Equations (3.136) and (3.137) contain continuous integrals and consequently cannot be numerically evaluated directly. However, the $U_k(t)$ polynomials have the canonical form

$$U_k(t) = t^k \sum_{j=0}^{k} C_j(k) t^{2j} \tag{3.153}$$

and the unknown $C_j(k)$ coefficients can be generated in a straightforward way by substituting Equation (3.153) into Equations (3.136) and (3.137) and equating like powers of t. This gives the seed terms of a k+1 square recurrence matrix

$$C_0(0) = 1 \tag{3.154}$$

$$C_0(k+1) = C_0(k)\left[\frac{k}{2} + \frac{1}{8(k+1)}\right], \qquad k > 0 \tag{3.155}$$

$$\begin{aligned} C_j(k+1) = {} & C_j(k)\left[\frac{2j+k}{2} + \frac{1}{8(2j+k+1)}\right] \\ & - C_{j-1}(k)\left[\frac{2j+k-2}{2} + \frac{5}{8(2j+k+1)}\right] \end{aligned}, \qquad 1 < j < k \tag{3.156}$$

$$C_{k+1}(k+1) = -C_k(k)\left[\frac{3k}{2} + \frac{5}{8(3k+3)}\right], \qquad k > 0 \tag{3.157}$$

Which can be evaluated analytically for Equation (3.153). As an example, the first three $U(t)$ polynomials generated are

$$U_0(t) = 1 \tag{3.158}$$

$$U_1(t) = \frac{\left(3t - 5t^3\right)}{24} \tag{3.159}$$

$$U_2(t) = \frac{\left(81t^2 - 462t^4 + 385t^6\right)}{1152} \tag{3.160}$$

The number of summations required for convergence of dependent equations governs the choice of a value of k, which dictates the matrix size. The sums S_1 and S_2 in Equations (3.144) and (3.145) terminate on reciprocal powers as small as ν^{-10} and the sum $U_{k+1}(t)$ in Equation (3.137) terminates on even smaller reciprocal powers of ν^{-11} when $k = 11$ is

chosen. This enables the $C_j(k)$ coefficients, being arithmetically related to their matrix position and independent of z or ν to be pre-calculated to 18 digits, and stored in an 11×11 look-up table. The hard coding of the coefficients to 18 digits offers compatibility with the precision needed if the option of 80-bit arithmetic is used.

3.17 Uniform asymptotic expansion for $\nu \to \infty$ and $|\mathbf{arg}z| > \frac{\pi}{3}$

If the complex z vector argument of $J_\nu(z)$ and $H_\nu(z)$ lies outside of the region bounded by $\pm\frac{\pi}{3}$, the uniform asymptotic expansions given by Equations (3.139) and (3.140), although computationally more expensive, must be used. From inspection of Equations (3.139) and (3.140) it can be seen that they are dependent upon numerical values of Airy functions. From standard definitions (Abramowitz & Stegun, 1972, p447) Airy functions of the first kind and their derivatives with respect to z can be expressed as

$$\mathrm{Ai}(z) = \frac{1}{\pi}\sqrt{\frac{z}{3}}\,K_{1/3}(\zeta) \qquad \textbf{(3.161)}$$

$$\mathrm{Ai}'(z) = \frac{-z}{\pi\sqrt{3}}\,K_{2/3}(\zeta) \qquad \textbf{(3.162)}$$

Where

$$\zeta = \frac{2}{3}z^{3/2} \qquad \textbf{(3.163)}$$

When $|z| > 1$ these relationships are computed directly using the algorithms described in §3.7 and §3.8 to obtain values for $K_{1/3}(\zeta)$ and the same algorithms with forward recurrence to compute $K_{2/3}(\zeta)$. However, there is a danger of numerical instability as $z \to 0$.

Therefore, substituting the Bessel function power series definition for $K_\nu(z)$ when $|z|<1$ resolves the indeterminacy about $z = 0$ and the Airy functions of the first kind and their derivatives can be re-expressed as

$$\mathrm{Ai}(z) = C_1\, f(z) - C_2\, g(z) \tag{3.164}$$

$$\mathrm{Ai}'(z) = C_1\, f'(z) - C_2\, g'(z) \tag{3.165}$$

Where

$$f(z) = \sum_{k=0}^{\infty} 3^k \left(\frac{1}{3}\right)_k \frac{z^{3k}}{(3k)!} \tag{3.166}$$

$$g(z) = z\sum_{k=0}^{\infty} 3^k \left(\frac{2}{3}\right)_k \frac{z^{3k}}{(3k+1)!} \tag{3.167}$$

$$f'(z) = \frac{z^2}{2}\left[2\sum_{k=0}^{\infty} 3^{k+1} \left(\frac{1}{3}\right)_{k+1} \frac{z^{3k}}{(3k+2)!}\right] \tag{3.168}$$

$$g'(z) = \sum_{k=0}^{\infty} 3^k \left(\frac{2}{3}\right)_k \frac{z^{3k}}{(3k)!} \tag{3.169}$$

$$C_1 = \frac{3^{-2/3}}{\Gamma\left(\frac{2}{3}\right)} \tag{3.170}$$

$$C_2 = \frac{3^{1/3}}{\Gamma\left(\frac{1}{3}\right)} \tag{3.171}$$

The notation $(X)_N$ denotes Pochhammer's symbol, sometimes called the rising factorial, where $(X)_N = X(X+1)\ldots(X+N-1) = \dfrac{\Gamma(X+N)}{\Gamma(X)}$. Fortunately, when $|z|<1$ the constituent series in Equations (3.164) and (3.165) converge rapidly. The numerical lower bound of

the truncation error for the series $f(z)$ in Equation (3.166) is computed from the recurrence relations $A_0 = 1$ and

$$A_{k+1} = \frac{A_k z^3}{(3k+2)(3k+3)} \tag{3.172}$$

Which give, when $|z| < 1$ and $|A_0| = 1$,

$$|A_{k+1}| = \frac{|A_k||z^3|}{(3k+2)(3k+3)} < \frac{|A_k|}{(3k+2)^2} \tag{3.173}$$

Similarly, the numerical lower bound of the truncation error for the series $g(z)$ in Equation (3.167) is computed from the recurrence relations $A_0 = 1$ and

$$A_{k+1} = \frac{A_k z^3}{(3k+3)(3k+4)} \tag{3.174}$$

Which give, when $|z| < 1$ and $|A_0| = 1$,

$$|A_{k+1}| = \frac{|A_k||z^3|}{(3k+3)(3k+4)} < \frac{|A_k|}{(3k+2)^2} \tag{3.175}$$

Therefore, the remainder for both series is given by the same expression

$$R_M = \sum_{k=M+1}^{\infty} A_k \tag{3.176}$$

The upper bound of which is given by

$$|R_M| < C_M \left[1 + \frac{1}{(3M+2)^2} + \frac{1}{(3M+2)^4} + \ldots\right] < C_M \left[1 + \frac{1}{9M^2 + 12M + 3}\right] < 1.05\, C_M \tag{3.177}$$

Where $M > 1$ and

$$C_M^f = \frac{|A_M|}{(3M+2)(3M+3)} \tag{3.178}$$

and

$$C_M^g = \frac{|A_M|}{(3M+3)(3M+4)} \tag{3.179}$$

The process is repeated in an identical fashion for the series $f'(z)$ and $g'(z)$. Therefore, the numerical lower bound of the truncation error for the series $f'(z)$ of Equation (3.168) is computed from the recurrence relations $A_0 = 1$ and

$$A_{k+1} = \frac{A_k z^3}{(3k+3)(3k+5)} \tag{3.180}$$

Similarly, the numerical lower bound of the truncation error for the series $g'(z)$ in Equation (3.169) is computed from the recurrence relations $A_0 = 1$ and

$$A_{k+1} = \frac{A_k z^3}{(3k+1)(3k+3)} \tag{3.181}$$

Which, following the steps detailed in Equations (3.173) and (3.175), give a remainder term common to both series $f'(z)$ and $g'(z)$

$$|R_M| < C_M\left[1 + \frac{1}{9M^2 + 6M}\right] < 1.07\, C_M \tag{3.182}$$

Where

$$C_M^{f'} = \frac{|A_M|}{(3M+3)(3M+5)} \tag{3.183}$$

and

$$C_M^{g'} = \frac{|A_M|}{(3M+1)(3M+3)} \tag{3.184}$$

The remainder terms described by Equations (3.177) and (3.182) are used in the usual way in the equality test

$$|R_M| < \varepsilon \tag{3.185}$$

and if true the relevant series is terminated and values returned to the calling functions described by equations (3.139) and (3.140).

3.18 Summary

In this chapter there was a brief explanation of the use of Bessel functions of complex argument in the context of calculating the phase velocity and attenuation of acoustic propagation in particulate dispersions. The software that is used for the Bessel function computation was modified and translated from obsolescent Fortran 66 and 77 to C++. It calculated *I* and *K* cylindrical Bessel functions. The reasons for initially computing *I* and *K* cylindrical functions directly and the transformations used to obtain the required *j* and *h* spherical Bessel functions indirectly, which are used in the derivation of scattering coefficients, were expounded in detail.

A variety of methods available for the computation of each of the *I* and *K* cylindrical functions was described. Each method was best suited for use over specific regions of the $(|z|, \nu)$ plane, shown graphically by Figures 3.1 for the *K* functions and 3.2 for the *I* functions. Every method chosen was justified in terms of numerical accuracy, stability and computational efficiency and the implementation of its algorithm described in detail. An item of practical importance for the implementation in software was the precise delineation of the different regions that employed different methods of computation. These boundaries were investigated and their properties derived in explicit terms for use in method selection algorithms.

Examples of the degree of recurrence needed for convergence and the final accuracy attainable using different methods of computation were given both in general terms and specifically for the Intel 32-bit computer architecture using either 64-bit or 80-bit internal arithmetic.

All the software routines were designed to return ‘soft’ errors which means that machine arithmetic overflows during computation were detected and made to return maximum machine number. Conversely, machine arithmetic underflows during computation were detected and made to return zero or minimum positive machine number. In each case an error flag was set to warn the calling software routine of the error condition. This procedure could permit computation to continue, frequently with minimal effect on accuracy.

The algorithms described enable accurate and reliable computation of high orders of Bessel and Hankel functions with large complex arguments. The importance of such algorithms in the calculation of attenuation and phase velocity in particulate dispersions was outlined in Chapter 2 and will be discussed more extensively in Chapter 4.

4. Multiple scattering models

4.1 Introduction

The development of the single scattering model that incorporates scattering, thermal and hydrodynamic (frequently referred to as visco-inertial) loss mechanisms was examined in Chapter 2. The mathematical treatment was presented in a form such that dispersions of solid particles in a liquid, emulsions or fogs of fluid particles in a fluid and matrices of solid particles in a solid could be modelled. From this model the complex wavenumbers of compressive, shear and thermal waves propagating into and scattered away from a single suspended particle, at any single frequency, can be derived. However, this procedure deals with the hypothetical case of the effect of a sound wave when it impinges upon a single particle, the so-called diffraction problem. In practical applications, dispersions comprising a great number of scatterers are of interest. This chapter examines and compares some of the theoretical schemes that are used to model the behaviour of an array of scatterers in a dispersion. Comparison between modelled and experimental results will be presented in Chapter 6.

4.2 The Foldy model

Chapter 2 briefly mentioned the work of Foldy (1945) who derived Equation (2.88), an expression for the cumulative effect of a number of scatterers randomly dispersed in a volume. The equation expresses the averaged complex compressive wavenumber of a dispersion in terms of % v/v concentration and radius of the suspended particles and the complex compressive wavenumbers of both suspended particles and the continuous phase. He introduced the concept of *configurational* averaging which used the joint probability

distribution for the occurrence of a given configuration of isotropic point scatterers to average the resulting wave over all configurations.

In experimental and practical applications of ultrasonic spectroscopy it is usual that the transducer used to detect the sound waves after they have passed through a dispersion is sensitive only to coherent compressive waves integrated over the whole face of the transducer. Therefore, only the compressive single-scattering coefficient, A_n, and the overall compressive wavenumber, β, of the dispersion (referred to sometimes as the compressive refractive index) is of interest. Equation (2.89) shows how the attenuation and velocity of coherent compressive sound waves at a single frequency can, in turn, be derived from β. In formulating his model, Foldy made a number of assumptions, explicitly or implicitly, including:

a. When the incident wave is scattered away from its forward path by a particle its energy is lost and none of it resumes its original path, coherent with the original incident wave, after re-scattering by any other particle or particles.
b. Following on from (a), no particle is disturbed by the behaviour of an adjacent particle, that is to say, there are no inter-particle interactions.
c. Scattering is isotropic, that is to say, the particles are effectively spherical and their scattering is monopolar.
d. The particles are randomly distributed with a normal distribution of inter-particle distances, and do not conform to any long-range order or lattice structure.

e. There is no movement of particles, they are immobile scatterers; therefore, there is no translation of energy between frequencies due to the Doppler effect and, together with the assumptions in (c), scattering amplitude is independent of direction.

f. The exciting scalar field that would exist at a point in the dispersion is the same whether a scattering particle is located there or not.

With an axis of symmetry about the direction of propagation of an incident plane sound wave of wavenumber k and amplitude ϕ_i, the far-field amplitude of the scattered wave at a distance r from the scatterer and at an angle θ to the axis can be expressed as

$$\phi(\theta, r) = \phi_i f(\theta) \frac{e^{ikr}}{r} \qquad \textbf{(4.1)}$$

Where $f(\theta)$ represents the far field scattering amplitude, derived from the plane wave expansion of the Green function for unbounded space (for a detailed derivation see p1483 of Morse & Feshbach, 1953) given by

$$f(\theta) = -\sum_{n=0}^{\infty} (2n+1) \mathbf{T}_n P_n(\cos\theta) \qquad \textbf{(4.2)}$$

The scattering matrix $\mathbf{T}_n$ represents compressive $\left(T_n^{cc}\right)$, thermal $\left(T_n^{TT}\right)$ and two orthogonal shear $\left(T_n^{ss} \text{and} T_n^{tt}\right)$ partial waves of order n perpendicular to the axis. It also represents mode conversions between different types of wave and can be expressed as

$$\mathbf{T}_n = \begin{bmatrix} T_n^{cc} & T_n^{cs} & T_n^{ct} & T_n^{cT} \\ T_n^{sc} & T_n^{ss} & T_n^{st} & T_n^{sT} \\ T_n^{tc} & T_n^{ts} & T_n^{tt} & T_n^{tT} \\ T_n^{Tc} & T_n^{Ts} & T_n^{Tt} & T_n^{TT} \end{bmatrix} \qquad \textbf{(4.3)}$$

Because only the compressive wave is of interest and mode conversions are assumed to be negligible, the variable $\mathbf{T}_n$ in Equation (4.2) can be replaced by the complex variable $\frac{A_n}{ik_c}$ derived by the procedure described in Chapter 2. Therefore, the general case can now be expressed as

$$f(\theta) = \frac{1}{ik_c} \sum_{n=0}^{\infty} (2n+1)\, A_n\, P_n(\cos\theta) \qquad \textbf{(4.4)}$$

It follows that the particular cases, when $\theta = 0$ and $\theta = \pi$, give

$$f(0) = \frac{1}{ik_c} \sum_{n=0}^{\infty} (2n+1) A_n \qquad \textbf{(4.5)}$$

$$f(\pi) = \frac{1}{ik_c} \sum_{n=0}^{\infty} (-1)^n (2n+1) A_n \qquad \textbf{(4.6)}$$

Foldy (1945) considered only forward scattering in a dilute dispersion of point scatterers (where $\theta = 0$ and coherent re-scattering is negligible) to give the expression

$$\beta^2 = k_c{}^2 + \frac{3\phi}{R^3} f(0) \qquad \textbf{(4.7)}$$

Where β is the complex compressive wavenumber averaged for the whole dispersion.

4.3 Incorporation of re-directed back scattering into the model

Waterman and Truell (1961) extended Foldy's model, incorporating the work of Urick and Ament (1949). They considered the effect of back scattering (where $\theta = \pi$ and up to second order coherent re-scattering is significant) in a thin slab of the dispersion. By treating the

dispersion as a concatenation of a number of such slabs they derived an expression for the square of the complex compressive wavenumber averaged for the whole dispersion as

$$\beta^2 = k_c^2 + \frac{3\phi\ f(0)}{R^3} + \frac{9\phi^2}{4k_c^2 R^6}\left[f^2(0) - f^2(\pi)\right] \qquad \textbf{(4.8)}$$

4.4 Incorporation of re-directed back scattering and radial scattering into the model

Lloyd and Berry (1967) also considered second-order coherent re-scattering as significant and re-derived the term for back scattering in the general case. This assumed spherically propagating back scattering without the simplification of a slab approximation. In their derivation they introduced an additional term for radial scattering in all directions. Assuming axial symmetry about the direction of propagation, Lloyd and Berry's expression for the square of the complex compressive wavenumber averaged for the whole dispersion is given by

$$\beta^2 = k_c^2 + \frac{3\phi f(0)}{R^3} + \frac{9\phi^2}{4k_c^2 R^6}\left[f^2(\pi) - f^2(0) - \int_{\theta=0}^{\pi} \frac{\frac{d}{d\theta} f^2(\theta)}{\sin\left(\frac{\theta}{2}\right)} d\theta \right] \qquad \textbf{(4.9)}$$

When numerical values for A_n to the required order of n have been computed it is a relatively trivial task to complete the summations that comprise $f(0)$ and $f(\pi)$, defined in Equations (4.5) and (4.6). However, to the authors knowledge there is no closed form solution in terms of A_n to the third component of Lloyd and Berry's expression for second-order scattering given by

$$\int_{\theta=0}^{\pi} \frac{\frac{d}{d\theta} f^2(\theta)}{\sin\left(\frac{\theta}{2}\right)} d\theta \qquad \textbf{(4.10)}$$

Explicit solutions of Equation (4.10) in terms of A_n have, to the author's knowledge, appeared in the literature (Anson & Chivers, 1993) only up to order n = 2. An explicit solution of Equation (4.10) in terms of A_n up to order n = 18 was derived by the current author and is listed in Appendix B2. This order is high enough to enable the computation of the series summation constituents of Equation (4.6) to within 0.01% of absolute convergence, for particle diameters of up to 100μm at an ultrasonic frequency of 70MHz.

4.5 Revision of the Waterman & Truell model

It should be noted that the derivation of back scattering in the general case by Lloyd and Berry, dispensing with the slab approximation, results in reversed polarity of the second order $f(0)$ and $f(\pi)$ terms in the model of Waterman and Truell. If the term for second-order radial scattering of Lloyd and Berry is neglected, a revised expression can be devised analogous to the model of Waterman and Truell without the incorrect slab approximation. This is given by

$$\beta^2 = k_c^2 + \frac{3\phi f(0)}{R^3} + \frac{9\phi^2}{4k_c^2 R^6}\left[f^2(\pi) - f^2(0)\right] \qquad \textbf{(4.11)}$$

4.6 The Javanaud and Thomas model

Another model, which incorporates the work of Foldy (1945) and incorporates second-order effects, is that of Javanaud and Thomas (1988). Their model is represented by the equation

$$\beta^2 = k_c^2\left(1 + \frac{3}{2}\frac{\phi f(0)}{k_c^2 R^3}\right)^2 - \frac{9}{4}\frac{\phi^2 f(0) f(\pi)}{k_c^2 R^6} \qquad \textbf{(4.12)}$$

Which can be transposed, into a form that eases comparison with the foregoing models, to give

$$\beta^2 = k_c^2 + \frac{3\phi f(0)}{R^3} + \frac{9\phi^2}{4k_c^2 R^6}\left[f^2(0) - f(0)f(\pi)\right] \qquad \textbf{(4.13)}$$

This second-order part of Equation (4.13) does not agree with those of the other models represented by Equations (4.9) or (4.11). Also, their derivation assumed a % v/v concentration of no more than 1% and that the particle size-wavenumber product ($k_c r$) must be greater than approximately unity. These assumptions limit its applicability. For these reasons this model will not be considered further in this thesis.

4.7 Comparison of the models

In Figure 4.1 to Figure 4.6 the key to the legend annotations is as follows:

a. *Foldy* – the Foldy model of superposition of a number of single scatterers, described in §4.2 and expressed by Equation (4.7)

b. *W&T* – the original model of Waterman and Truell incorporating second-order scattering resulting from back-scattering, based on the concatenation of slabs approximation, described in §4.3 and expressed by Equation (4.8)

c. *W&T(2)* – the model of Waterman and Truell revised by Lloyd and Berry, dispensing with the concatenation of slabs approximation, described in §4.5 and expressed by Equation (4.11)

d. L&B – the Lloyd and Berry model incorporating second-order scattering resulting from first-order scattering in all directions, described in §4.4 and expressed by Equation (4.9)

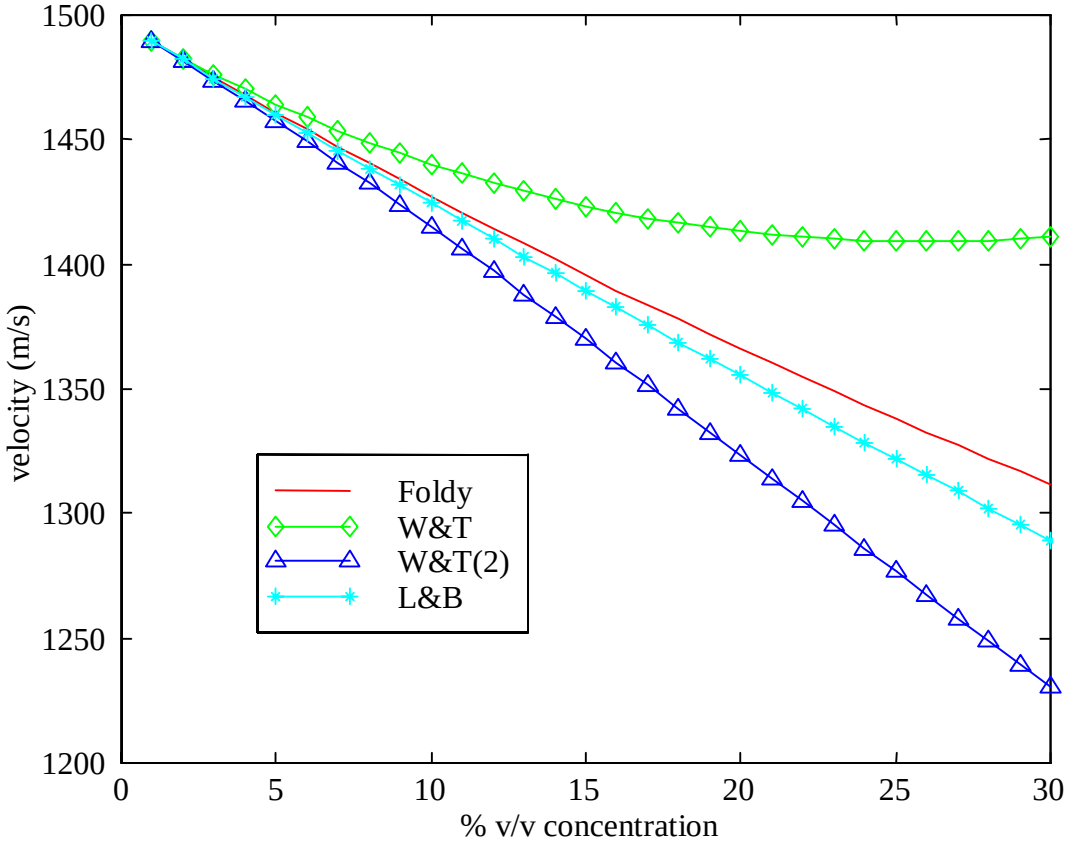

Figure 4.1 Modelled phase velocity versus % v/v concentration through a hypothetical dispersion of 500nm diameter titanium dioxide AHR pigment spheres in water at 25ºC and 5MHz

Inspection of Figures 4.1 to 4.6 reveals that the different models can produce significantly different results in terms of modelled attenuation and phase velocity spectra.

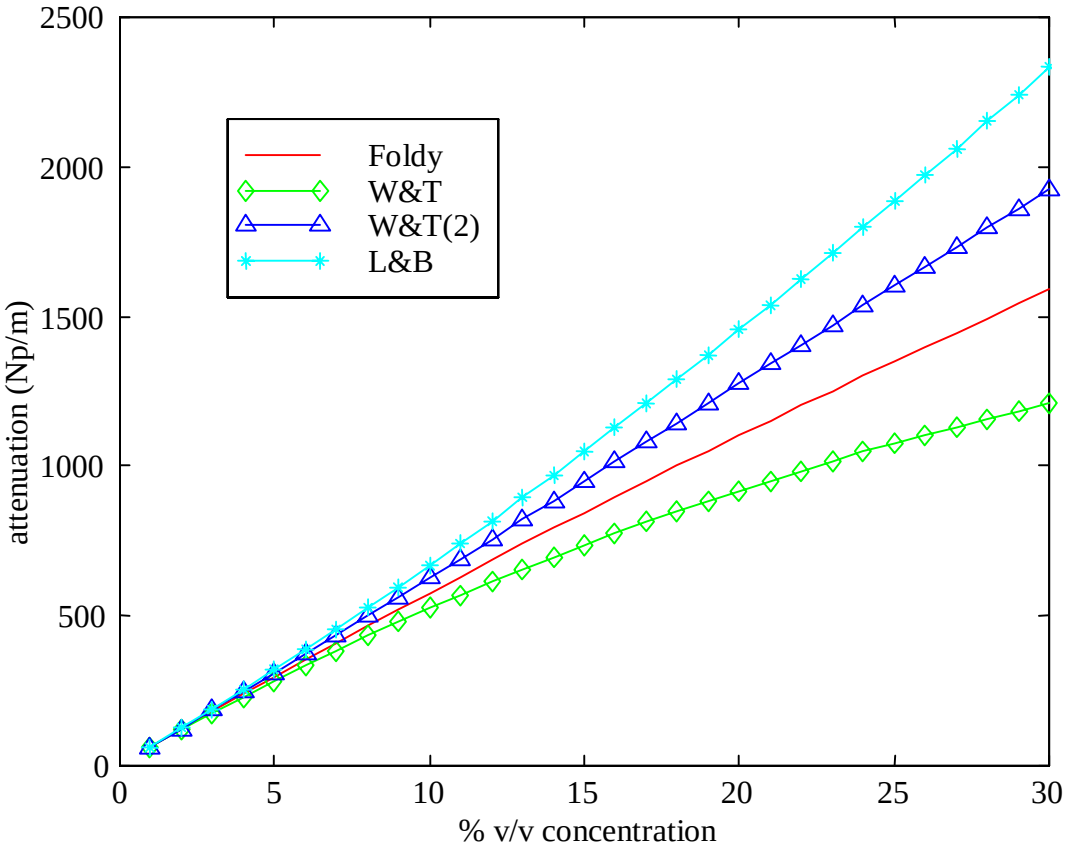

Figure 4.2 Modelled attenuation versus % v/v concentration through a hypothetical dispersion of 500nm diameter titanium dioxide AHR pigment spheres in water at 25ºC and 5MHz

The spectra depicted in Figures 4.1 to 4.4 clearly highlight a number of features. It is obvious that the effect on both phase velocity and attenuation of including only forward and backward second-order scattering terms, as is the case in the Waterman & Truell models, is particularly significant as the % v/v concentration is increased, for both the 5MHz and 50MHz frequencies. The only difference between the models that produced the

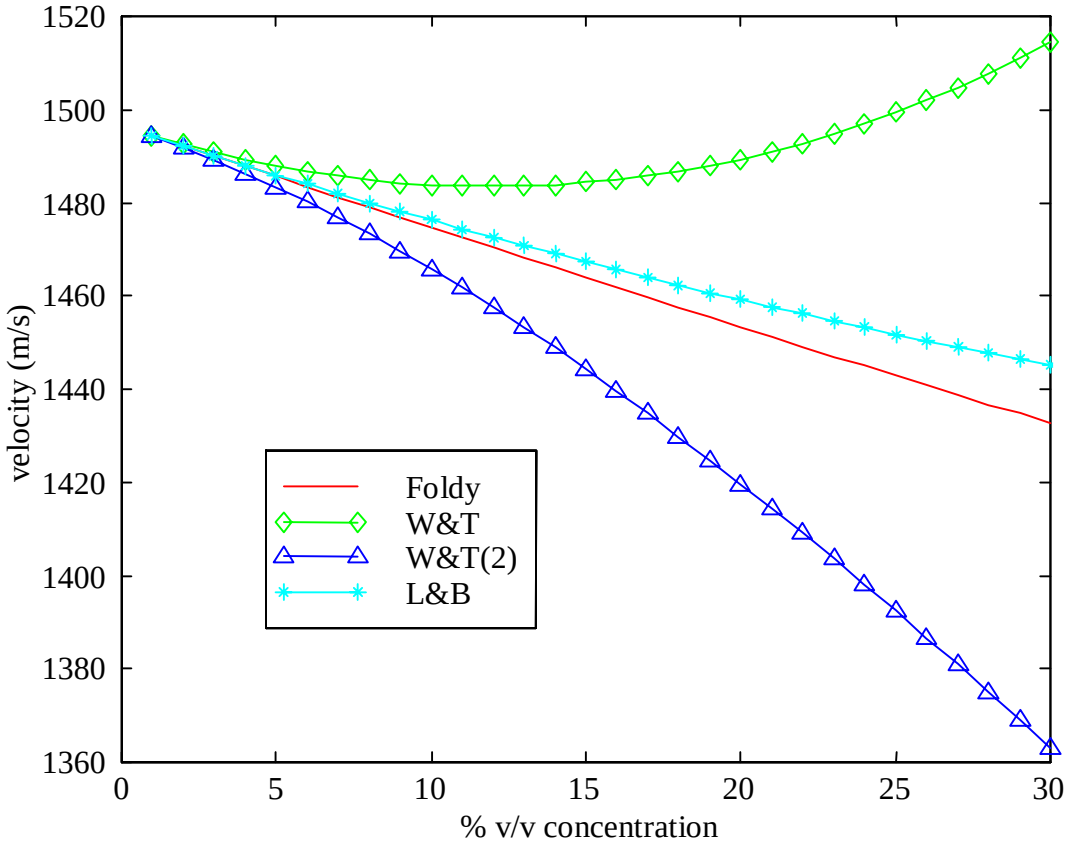

Figure 4.3 Modelled phase velocity versus % v/v concentration through a hypothetical dispersion of 500nm diameter titanium dioxide AHR pigment spheres in water at 25ºC and 50MHz

Waterman & Truell and revised Waterman & Truell plots is the polarity of the second-order terms. It can also be seen that as % v/v concentration increases, the third term, incorporating $f(\theta)$, in the Lloyd & Berry model makes an increasingly important contribution to the modelled phase velocity at low and high frequencies. Similarly, it also makes an increasingly important contribution to modelled attenuation at the lower frequency.

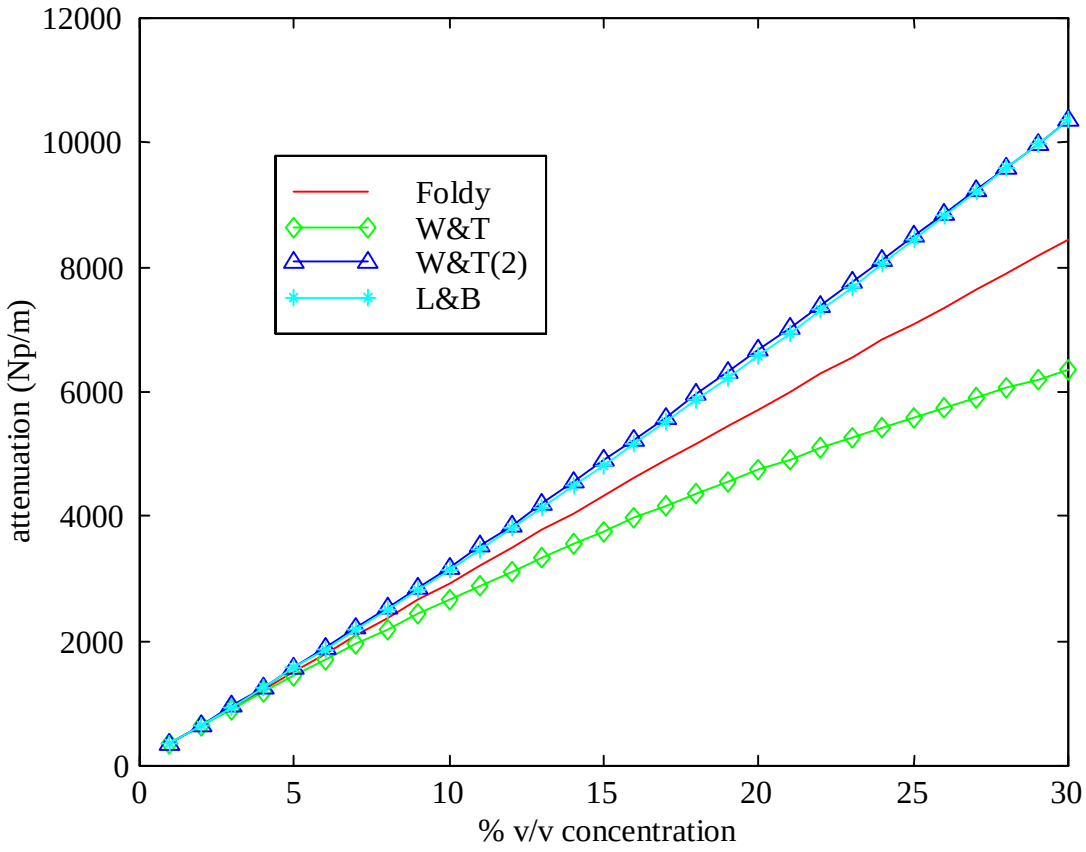

Figure 4.4 Modelled attenuation versus % v/v concentration through a hypothetical dispersion of 500nm diameter titanium dioxide AHR pigment spheres in water at 25ºC and 50MHz

It is worth noting that the incorrect polarity of the second-order terms that resulted from Waterman & Truell's concatenation of slabs approximation produces a very significant error in phase velocity and attenuation at higher % v/v concentrations and at higher frequencies.

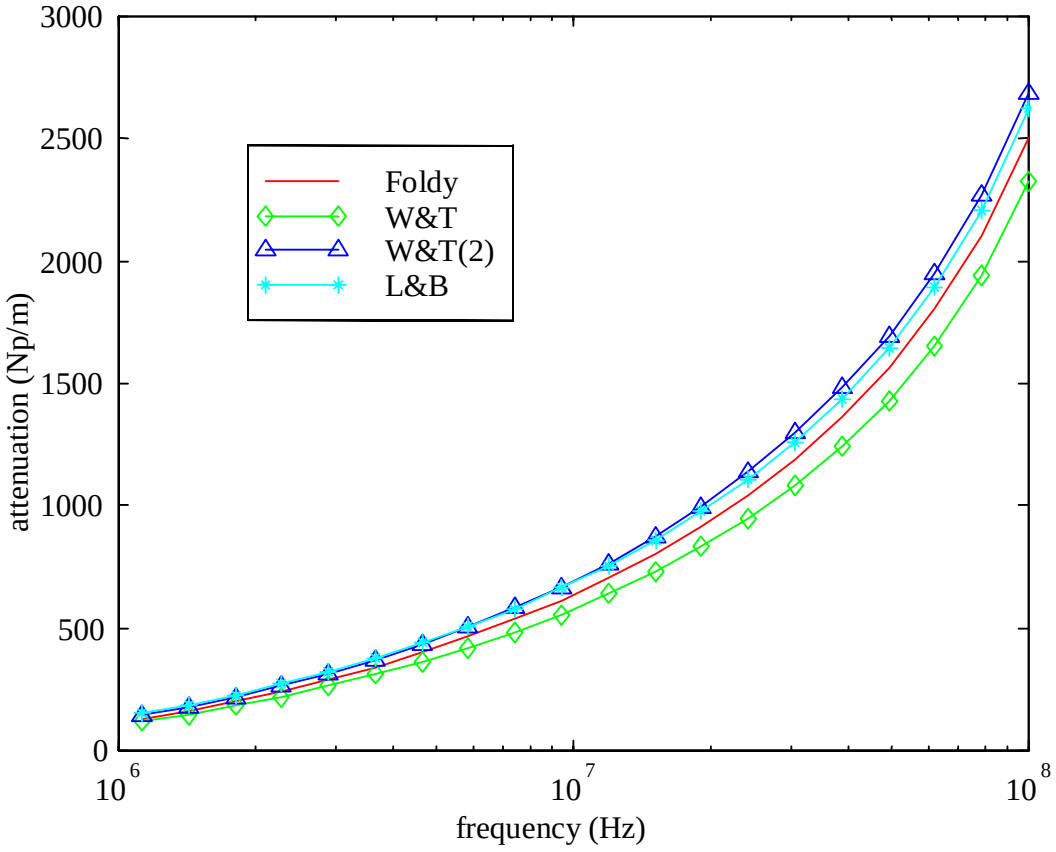

Figure 4.5 Modelled attenuation versus frequency through a hypothetical 10% v/v dispersion of 1μm diameter titanium dioxide AHR pigment spheres in water at 25ºC

Figures 4.5 and 4.6 show that for a particle diameter of 1μm and 10% v/v concentration, the contribution of the third term, incorporating $f(\theta)$, in the Lloyd & Berry model makes an insignificant contribution to attenuation. However, it makes a significant contribution to modelled phase velocity over the whole of the modelled frequency range. Consequently, the revised Waterman & Truell model and the Lloyd & Berry model exhibit very similar results for attenuation over the whole range between 1MHz and 100MHz.

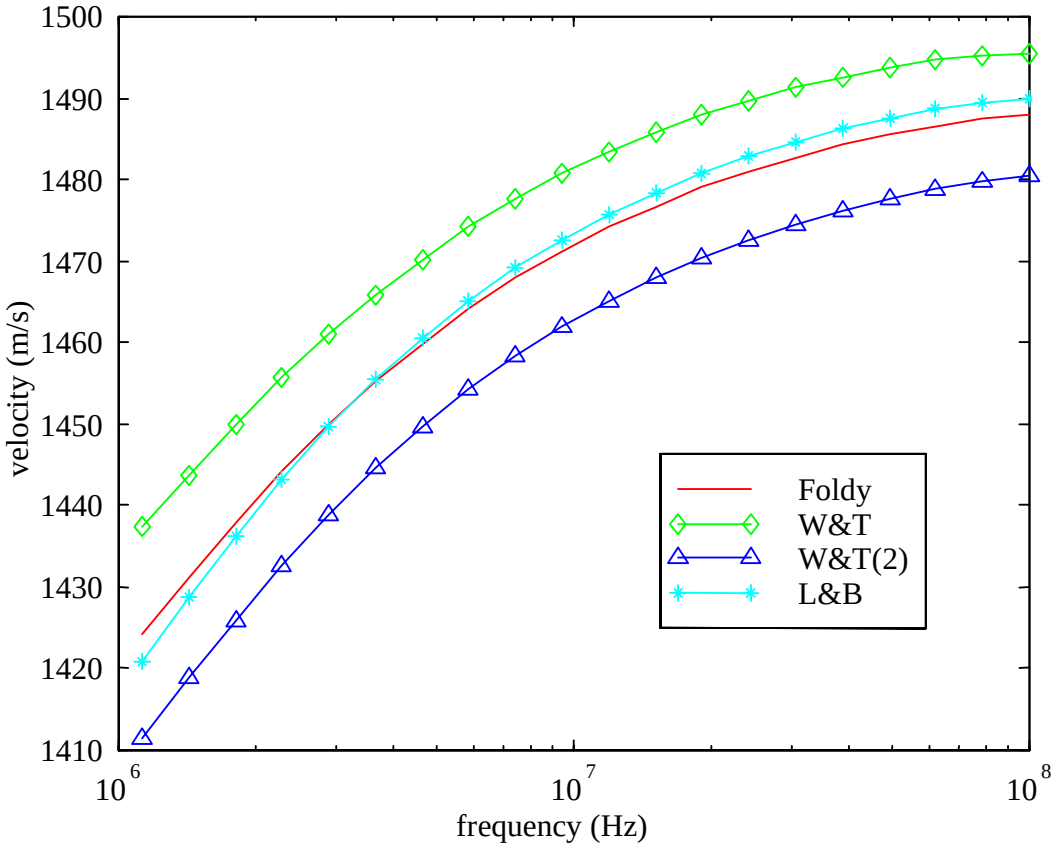

Figure 4.6 Modelled phase velocity versus frequency through a hypothetical 10% v/v dispersion of 1μm diameter titanium dioxide AHR pigment spheres in water at 25ºC

The plots depicted in Figure 4.6 show that the Lloyd & Berry model yields a phase velocity spectrum that is very similar to that produced by the Foldy model. The contribution of the second-order term incorporating $f(\theta)$ cancels out the contribution of the other second-order terms. In contrast, the Waterman & Truell models give a very similar phase velocity dispersion curve to that of the Foldy model but each with a relatively constant velocity displacement, which clearly shows their opposing polarities, over the whole of the modelled frequency range.

4.8 Modelling the effects of polydispersity

The Foldy model described by Equation (4.7) represents only first-order scattering by superposition of a number of monodisperse particles; however, it lends itself to the simple modification described in Chapter 2 and depicted in Equation (2.91) to accommodate polydispersity. The models of Waterman & Truell and Lloyd & Berry represented by Equations (4.8), (4.9) and, the revised model of Waterman & Truell, (4.10) are all based on the assumption that the dispersions are monodisperse. The underlying mathematics assume, in the case of second-order scattering, that any secondary-scattered wave has been scattered twice by the same size of scatterer. In polydisperse systems this cannot be taken for granted, indeed, it is most unlikely. Extending the principle of superposition used in Equation (2.91) to accommodate polydispersity in the models of Waterman & Truell and Lloyd & Berry provides an expression to include the effects of second-order scattering in polydisperse systems. The Waterman & Truell model, modified to include polydispersity is given by

$$\beta^2 = k_c^2 + \sum_{b=1}^{B}\left\{\frac{3\phi_b f_b(0)}{R_b^3} + \frac{9\phi_b^2}{4k_c^2 R_b^6}\left[f_b^2(0) - f_b^2(\pi)\right]\right\} \qquad \textbf{(4.14)}$$

The Lloyd & Berry model, modified to include polydispersity is given by

$$\beta^2 = k_c^2 + \sum_{b=1}^{B}\left\{\frac{3\phi_b f_b(0)}{R_b^3} + \frac{9\phi_b^2}{4k_c^2 R_b^6}\left[f_b^2(\pi) - f_b^2(0) - \int_{\theta=0}^{\pi}\frac{\frac{d}{d\theta} f_b^2(\theta)}{\sin\left(\frac{\theta}{2}\right)}d\theta\right]\right\} \qquad \textbf{(4.15)}$$

The revised Waterman & Truell model, modified to include polydispersity is given by

$$\beta^2 = k_c^2 + \sum_{b=1}^{B}\left\{\frac{3\phi_b f_b(0)}{R_b^3} + \frac{9\phi_b^2}{4k_c^2 R_b^6}\left[f_b^2(\pi) - f_b^2(0)\right]\right\} \qquad \textbf{(4.16)}$$

The notation used in Equations (4.14), (4.15) and (4.16) to accommodate polydispersity is the same as that used in Equation (2.91). Apart from the assumption in Equations (4.14) to (4.16) that second-order re-scattering is caused by a particle of the same size species as the primary scatterer there is a more significantly erroneous assumption. That is, after a wave has been re-radiated by a primary scatterer of a particular size species it will not 'see' scatterers of any other species and will only impinge upon secondary scatterers of the same species as the primary. If any of Equations (4.14) to (4.16) were used to represent a system with a large number, *B*, of size bins then the implied degree of secondary scattering is much less than really would be the case. As an illustration and a test of self-consistency of Equations (4.14) to (4.16), two dispersions of identical particle size distribution and % v/v concentration were compared, using the Foldy, revised Waterman & Truell and Lloyd & Berry models. The first dispersion modelled was a 30% v/v concentration, 1μm particle diameter monodisperse aqueous dispersion of titanium dioxide AHR pigment spheres at 25°C. The second dispersion modelled was an identical system but considered to be composed of 30 identical particle size bins of 1% each. Therefore, the first, monodisperse dispersion, was modelled using Equations (4.4), (4.6) and (4.11). The second, polydisperse dispersion, was modelled using Equations (2.91), (4.15) and (4.16). The results of the modelling appear as Figures 4.7 and 4.8.

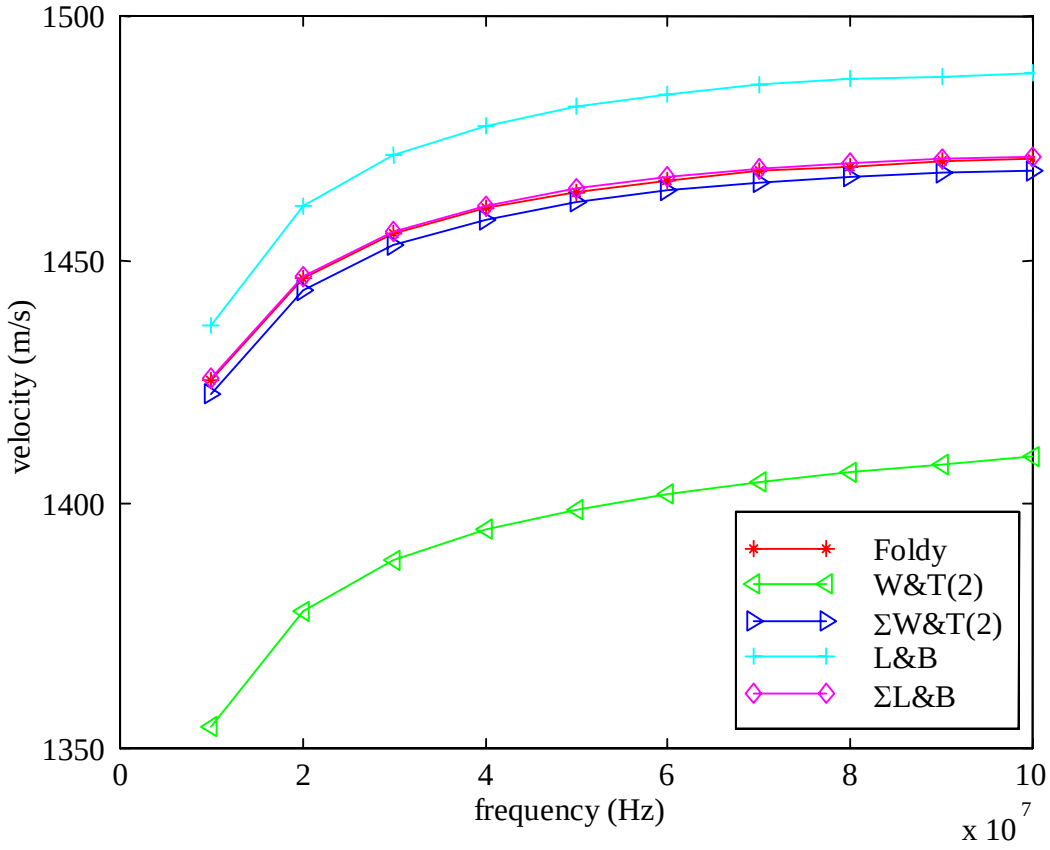

Figure 4.7 Modelled phase velocity versus frequency through a hypothetical 30% v/v dispersion of 1μm diameter titanium dioxide AHR pigment spheres in water at 25ºC

The key to the legends of Figures 4.7 and 4.8 are the same as those of Figures 4.1 to 4.6 with the addition of the summation sign to denote the result of a polydispersity summation over 30 size bins. The phase velocity and attenuation results from modelling the monodisperse and polydisperse versions of the Foldy equation, Equations (4.7) and (2.91), agreed to within 14 significant figures. Therefore, only the results from the monodisperse version of the Foldy equation are plotted in Figures 4.7 and 4.8. It can be seen that the second-order scattering terms, contained in the revised Waterman & Truell and Lloyd &

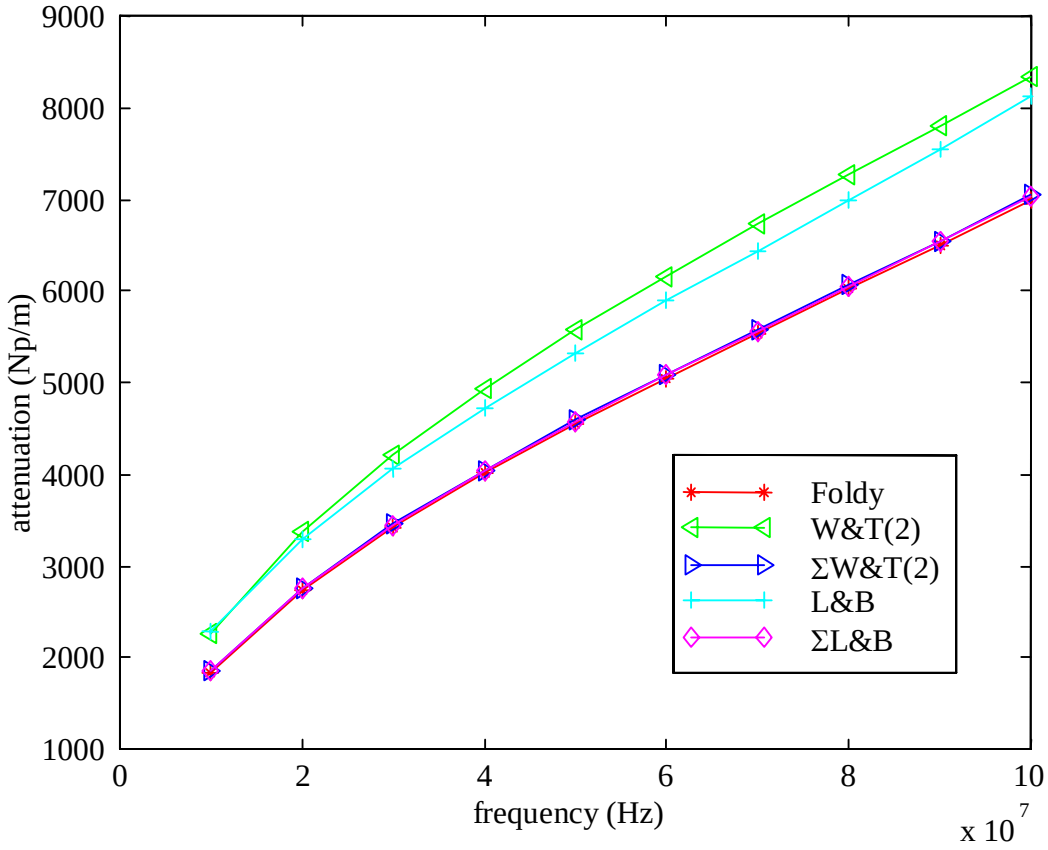

Figure 4.8 Modelled attenuation versus frequency through a hypothetical 30% v/v dispersion of 1μm diameter titanium dioxide AHR pigment spheres in water at 25ºC

Berry models of a 30% v/v concentration monodisperse dispersion, cause significant differences in their attenuation and phase velocity spectra when compared to that of the first-order-only Foldy models. This is in general agreement with findings already covered in this chapter. However, it is clear that the 30-bin summation of secondary-scattering terms in the revised Waterman & Truell and Lloyd & Berry polydisperse models does not cause a significant change to their respective attenuation and phase velocity spectra when compared to that of the first-order-only Foldy models.

4.9 Summary

There are three principal models that incorporate the scattering due to a single particle into an expression to represent multiple scattering. They range from the simplest, the Foldy model, that assumes that the scattering due to a dispersion can be represented by the superposition of the total number of individual scatterers. It assumes that the scatterers are far enough apart to ensure that any scattering not in the forward direction will not be reflected upon any other scatterer and its energy will be irretrievably lost. However, the attenuation and phase velocity spectra produced from the Foldy model differ little from those produced from more complicated models when restricted to modelling dilute dispersions. Moreover, it is mathematically straightforward and valid to incorporate polydispersity into the Foldy model for dilute dispersions.

The revised Waterman & Truell model includes the contribution of second-order scattering that has been shown to be significant for more concentrated dispersions of particles. Nevertheless, this model has been shown sometimes to exaggerate the secondary scattering contribution when compared to the more comprehensive Lloyd & Berry model. It is relatively straightforward to use the model up to high orders of n when this is necessitated by the requirement to compute values of β which correspond to high frequency-particle radius products. The original Waterman & Truell model has been shown to be incorrect but has been included in the analysis to better highlight the contribution of second-order scattering.

The Lloyd & Berry model is the most complicated. However, its use is justified at higher concentrations of particles in dispersion because the inclusion of the third secondary-

scattering term, a function of $f(\theta)$, results in significantly different attenuation and phase velocity spectra than those produced by the revised Waterman & Truell and Foldy models. An explicit solution for the third secondary-scattering term has been evaluated to order $n = 20$ and is tabulated in Appendix B2 up to order $n = 18$. This limits the application of this model to particles of approximately 100μm in diameter and up to a frequency of 80MHz, although higher orders of n could be calculated by using computationally expensive numerical methods.

Simple summation of the revised Waterman & Truell and Lloyd & Berry models over a range of size bins does not successfully incorporate second-order scattering into the modelling of a polydisperse dispersion. The resulting attenuation and phase velocity spectra are little different to those produced by the Foldy model despite their being far more computationally expensive.

This chapter has gone some way to highlighting the applicability of the different models for adequately representing the behaviour of dispersions. In Chapter 5 the numerical methods employed to implement the models will be presented. A comparison between modelled spectra, using the Lloyd & Berry model to represent monodisperse systems and the Foldy model to represent polydisperse systems, and experimental spectra will be presented in Chapter 6.

5. Modelling software

5.1 Introduction

The computation of attenuation and phase velocity in a dispersion can be regarded as comprising two main parts: the computation of the complex scattering coefficient, A_n, for a single particle, and the incorporation of that scattering coefficient into an expression taking account of the volume concentration of the dispersed phase. Paradoxically, the first part of the problem, computation of the complex scattering coefficient A_n for a single particle, is clearly defined mathematically but presents difficulties when a numerical implementation is attempted. The second part of the problem, the incorporation of that scattering coefficient into an expression taking account of the volume concentration of dispersed phase and the interaction and multiple scattering between particles, is the subject of ongoing research. Although the underlying mathematics of the limited models that do exist is complicated, they are relatively straightforward to implement numerically. The mathematics of the single and multiple scattering models and the translation of analytical results to a numerical implementation are dealt with in Chapter 4. The more intractable problem of computing functions which can result in extremely large floating-point complex numbers and the solution of a very poorly conditioned 6×6 matrix, both situations encountered together when dealing with realistic sizes of particle and frequencies, is the topic examined in this chapter.

5.2 Bessel and Hankel function arguments

The computation of the scattering coefficients from the 6×6 matrix in Equation (2.44) relies on accurate and stable numerical computation of spherical Bessel and Hankel functions. The actual methods employed to derive numerical values for spherical Bessel and Hankel

functions, and their first and second derivatives, are explained in some depth in Chapter 3. However, a brief look at the problems inherent in their use gives a valuable insight into the design and limitations of ECAH modelling software. Although the ECAH model uses spherical functions, Equations (3.7) to (3.9) show they are closely related to cylindrical Bessel and Hankel functions and, for the purposes of assessing their stability, an investigation into the stability of cylindrical functions will serve the same purpose. The arguments passed to the computer code for the calculation of spherical functions are the compressive, shear and thermal wavenumber-particle radius products for both phases. The arguments are usually complex.

Numerical experiments were undertaken over the frequency range of 100kHz to 200MHz, and over the particle diameter range of 10nm to 1mm, for some of the range of materials listed in Chapter 2. The key to the abbreviation and physical constants for each of these materials are listed in Appendix E. When using this range of sizes and frequencies it was found that the real parts of the wavenumber-radius products lie within the range 10^{-7} to 10^{5} and the imaginary parts of the wavenumber-radius products lie within the range 10^{-20} to 10^{5}

$$10^{-7} > \mathrm{Re}(kR) > 10^{5},\ \ 10^{-20} > \mathrm{Im}(kR) > 10^{5} \qquad \textbf{(5.1)}$$

Where k denotes either compressive, shear or thermal wavenumber in either the continuous or the dispersed phase and R denotes particle radius.

5.3 Numerical stability in the computation of Bessel and Hankel functions

Numerical experiments to establish the stability map of Bessel and Hankel functions on the complex plane encompassed by Equation (5.1) showed that when the imaginary part of the argument was larger than a certain threshold then overflow occurred in the computation of Bessel functions. It followed that underflow occurred in the computation of Hankel functions. The computation was not sensitive to the size of the real part of the argument or the order of the function, within the limits of those sizes and orders of practical interest ($n < 1000$). The overflow-underflow threshold of the imaginary part of the argument is a function of machine arithmetic, specifically on an Intel PC machine using 64-bit arithmetic. If the imaginary part of the argument exceeds a threshold value of approximately 692 for Hankel functions or 700 for Bessel functions the return value of the resulting computation is outside the possible range of 64-bit machine numbers

$$\mathrm{Im}(kR) > 692 \rightarrow H_n(kR) < 1.7 \times 10^{-308}, \text{ 64-bit arithmetic} \quad \textbf{(5.2)}$$

$$\mathrm{Im}(kR) > 700 \rightarrow J_n(kR) > 1.7 \times 10^{308}, \text{ 64-bit arithmetic} \quad \textbf{(5.3)}$$

Similarly, on Intel PC machines using 80-bit arithmetic the corresponding threshold values are approximately 1135 for Hankel functions and 1136 for Bessel functions

$$\mathrm{Im}(kR) > 1136 \rightarrow H_n(kR) < 3.4 \times 10^{-4932}, \text{ 80-bit arithmetic} \quad \textbf{(5.4)}$$

$$\mathrm{Im}(kR) > 1135 \rightarrow J_n(kR) > 1.1 \times 10^{4932}, \text{ 80-bit arithmetic} \quad \textbf{(5.5)}$$

Within the frequency and particle size ranges of interest it follows that the stability of the computation of Bessel and Hankel functions depends completely upon the imaginary part of the wavenumber-particle radius product argument. This dependency upon the radius of the particle and also upon the imaginary part of the wavenumber can be seen from Equation

(1.9) to represent compressive, shear or thermal attenuation. Table 5.1 lists attenuation coefficients and their relationship to frequency, for a range of materials. The coefficients are *invariant to whether the materials constitute the continuous or dispersed phase*.

	α_c $\left(\mathrm{Im}(k_c) = \frac{\alpha_c}{f^2}\right)$	α_s $\left(\mathrm{Im}(k_s) = \frac{\alpha_s}{\sqrt{f}}\right)$	α_T $\left(\mathrm{Im}(k_T) = \frac{\alpha_T}{\sqrt{f}}\right)$
iron	5.7×10^{-14}	0	3.53×10^{2}
silica	2.6×10^{-22}	0	1.75×10^{3}
tiox	1.3×10^{-16}	0	1.58×10^{3}
poly	1.00×10^{-13}	0	5.86×10^{3}
1-b-hex	1.45×10^{-13}	6.88×10^{2}	6.84×10^{3}
soya	2.19×10^{-13}	7.55×10	5.00×10^{3}
silicone	2.5×10^{-12}	9.47×10	5.37×10^{3}
water	2.2×10^{-14}	1.88×10^{3}	4.69×10^{3}

Table 5.1 Attenuation coefficients and their relationships to frequency

Inspection of Table 5.1 shows clearly that as the frequency-particle radius product is increased the thermal wavenumber will be by far the largest of all the wavenumbers and, therefore, the first one to cause computational overflow or underflow. By using the attenuation coefficient, the lower of the two threshold wavenumbers for overflow/underflow and the relationship to frequency given in Table 5.1, it is easy to model the particle-radius and frequency combinations, above which the computation would become unstable. Figure 5.1 shows the stability thresholds for a continuous range of particle-radius and frequency combinations, for a number of materials, for a machine using 64-bit arithmetic.

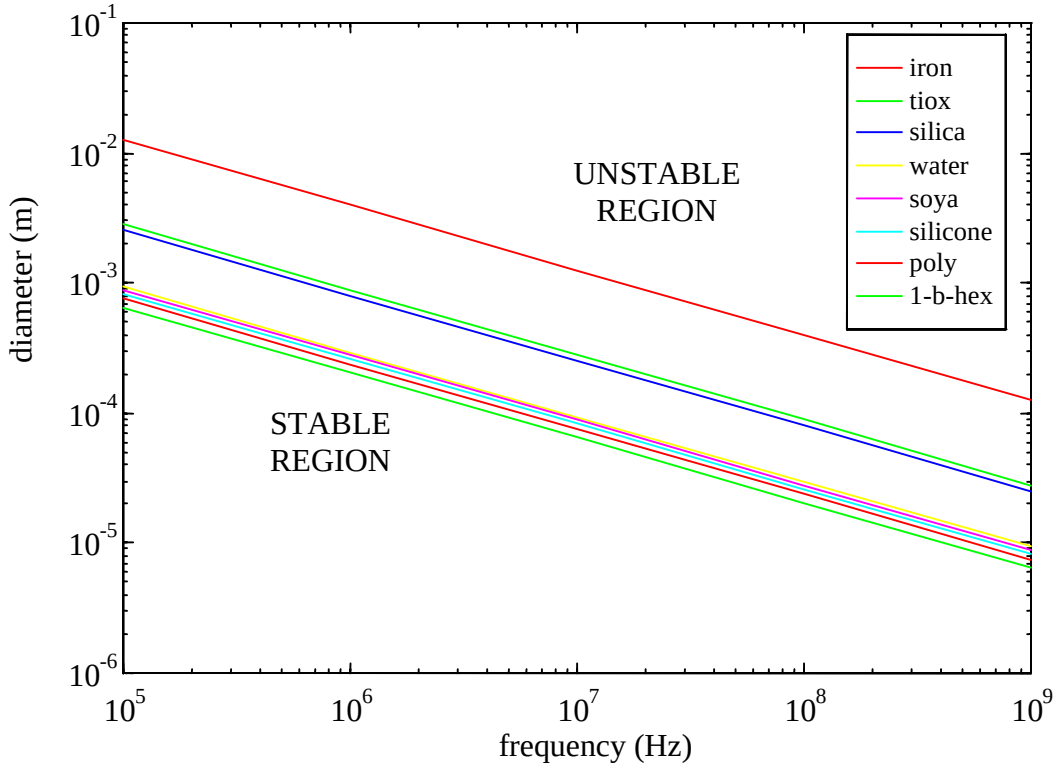

Figure 5.1 64-bit arithmetic diameter-frequency stability thresholds for a number of different materials

Figure 5.2 shows the stability thresholds for a continuous range of particle-radius and frequency combinations, for a number of materials, for a machine using 80-bit arithmetic. For the sake of clarity, the legends in Figures 5.1 and 5.2 denote the materials in the same order that they appear in the plots. It can be seen that because the Bessel and Hankel functions grow exponentially with the growth of the imaginary part of the argument, the additional numerical range afforded by 80-bit arithmetic is not as dramatic as might be expected. The increased stability threshold translates to the ability to compute the thermal wavenumber of larger particles by a factor of approximately (1135-692)/692 = 0.64 or to higher frequencies by a factor of approximately $(1135/692)^2 \cong 2.69$.

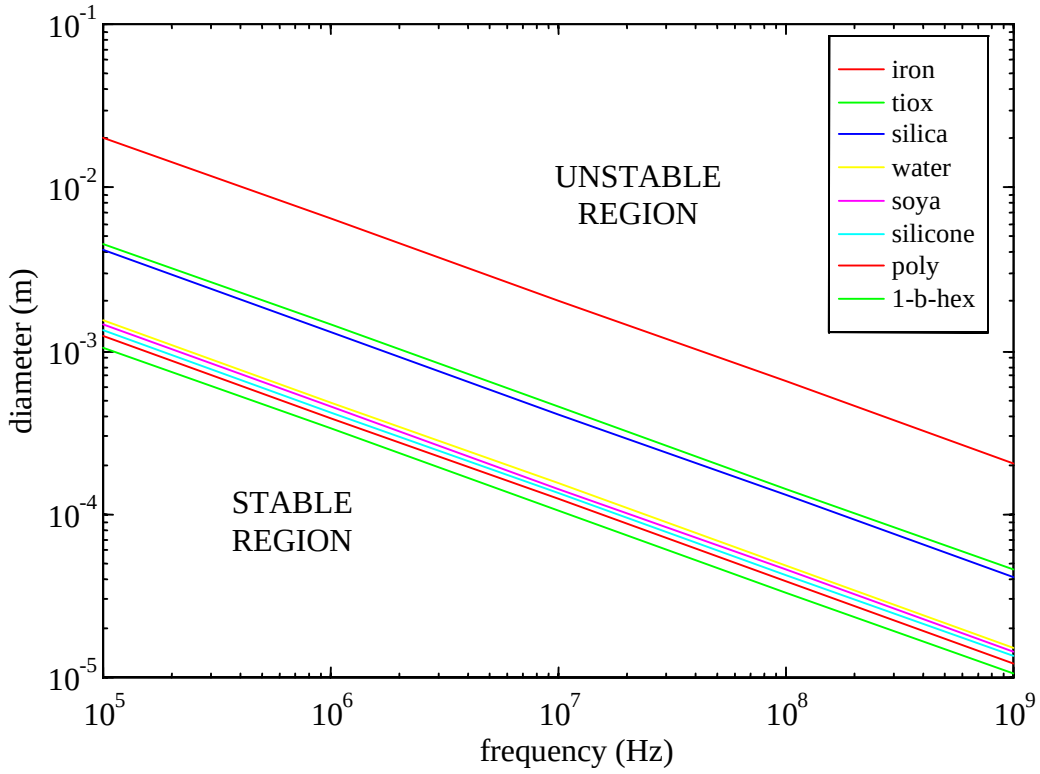

Figure 5.2 80-bit arithmetic diameter-frequency stability thresholds for a number of different materials

5.4 Solution of the series of six equations in six unknowns

Once the complex compressive, shear and thermal wavenumbers in spherical coordinates have been computed from the Bessel and Hankel functions of their respective linear wavenumber-radius products they are related to known physical parameters and calculated boundary conditions in a series of six equations in six unknowns. These equations appear as Equations (2.38) to (2.43) and are expressed in augmented matrix form in Equation (2.44).

5.4.1 Stability of solutions to the matrix

There is a great number of methods that can be used to find the solutions to a system of equations of this kind. They differ markedly in their degree of sophistication and as a corollary to that, their mathematical complexity and computational cost. The simplest method is Gaussian elimination, which works satisfactorily only on well-conditioned matrices and can be used to invert the matrix. Matrix inversion is computationally efficient such that the solution to equation $\mathbf{Mx} = \mathbf{D}$, where $\mathbf{x}$ is the unknown vector, is given by

$$\mathbf{x} = \mathbf{M}^{-1}\mathbf{D} \qquad (5.6)$$

Where $\mathbf{M}^{-1}$ is the matrix inverse of $\mathbf{M}$. The ratio of the largest singular value of a matrix to the smallest singular value is known as the 2-norm condition number. A value close to unity indicates that the matrix is well conditioned and small errors due to computational rounding or noise in input data do not have a significant effect on the solutions. However, as an example, during the relatively modestly demanding computation of A_2, using the physical parameters of an aqueous dispersion of polystyrene particles 200nm in diameter, at a frequency of 60MHz, the condition number of the matrix in Equation (2.44) is in excess of 10^{29}. This indicates that the matrix is very badly conditioned and highly singular. Small perturbations of the matrix can produce large swings in the output. The condition number of the matrix during the computation of A_n for higher values of n, and/or larger diameter particles and/or higher frequencies is even higher. Nevertheless, stable solutions for significantly larger particles than 200nm in diameter and higher frequencies than 60MHz have been achieved using Cramer's rule by Tebbutt (1996). This method was found by the author to be more robust than matrix inversion, Gaussian elimination, LU decomposition and even the computationally expensive Singular Value Decomposition method, although the use of Cramer's rule is computationally relatively expensive. The greatest drawback

with the Cramer's rule method is, however, the inevitable overflow or underflow that can occur during the intermediate multiplication essential for the calculation of the determinants if the product of two multiplicand elements of the matrix falls outside the range of possible machine numbers. Careful redesign of the ECAH matrix layout (op cit) can result in a stable computation of the determinant despite some of its elements, for example Equation (2.71), containing floating point numbers of up to 6×10^{296} which is close to the maximum machine number of 1.1×10^{308}. In practical terms this limit equates to the successful modelling of ultrasonic propagation in an aqueous polystyrene dispersion of 16μm diameter particles at more than 150MHz. Another common source of floating point overflow and underflow, worth mentioning at this point in the discussion of computing with large numbers, is the use of complex arithmetic subroutines. For example, some complex division routines widely used in numerical modelling use the square of each component of the complex divisor as an intermediate result. The practical effect of using such a routine is to limit the components of a complex divisor to the square root of maximum or minimum machine number if overflow or underflow is to be avoided - a serious limitation.

5.4.2 Analytical optimization of the six equations in six unknowns

Inspection of Figures 5.1 and 5.2 reveals that there are finite limits on the diameter of a particle and upper frequency that can be computed using the methods discussed so far. For example, using 80-bit arithmetic, at 100MHz the maximum sized 1-bromo-hexadecane particles that can be modelled are less than 30μm in diameter. Using 64-bit arithmetic the diameter is less than 20μm in diameter. Particles of these orders of diameter are common at the upper end of the particle size distribution range of polydisperse emulsions encountered in commercial processes; therefore, the ability to model them is of more than

academic interest. The alternatives available to enable modelling above these computational ceilings are:

a. To resort to greater than 80-bit arithmetic, available in native mode only on expensive workstation, mini or mainframe computers

b. To employ variable machine precision in software, resulting in drastically more complicated software and computational overhead (execution times several orders of magnitude longer than when using native mode arithmetic)

c. To modify the method of computing and using Bessel and Hankel functions, and adapt the matrix accordingly

In view of the desirability of keeping the software and the necessary platform upon which to execute it as simple and inexpensive as possible, the last alternative was the one implemented. It exploits the fact that the algorithms described in Chapter 3 to compute Bessel and Hankel functions calculate values using recurrence relationships and convergent series that are subsequently normalized. Normalization typically requires multiplication in the logarithmic domain by factors dominated by z^{v} and e^{z} where complex z is the argument of a function and real, positive v its order (see, for example, normalizing Equation (3.113) used by the Miller algorithm). By returning un-normalized values it is possible to scale Bessel and Hankel functions in a systematic way before exponentiating them out of the logarithmic domain. It is important to bear in mind that Bessel and Hankel functions are oscillatory and as a consequence their values pass through zero. This can cause problems when exponentiating out of the logarithmic domain, causing 'log of zero' run-time errors. Although it is a relatively trivial measure to trap such errors it is essential that they are trapped for the stable execution of the computation. In the process of transforming some of the computation into the logarithmic domain it is possible to reduce the complexity of the

matrix, building upon the simplifications already incorporated, and explained in Chapter 2, by the use of effective $\frac{\mu}{-i\omega}$ in place of η. The first step is to divide both sides of Equations (2.42) and (2.43) by $\frac{\mu}{-i\omega}$, divide both sides of Equation (2.39) by κ and then substitute into the system of 6 Equations (2.38) to (2.43) in 6 unknowns the following identities

$$a_s'^2 = \omega^2 \frac{\rho'}{\mu'} R^2 \quad \textbf{(5.7)}$$

$$\tilde{r}_n(z) \equiv \frac{r(z)}{r(z)} = 1 \quad \textbf{(5.8)}$$

$$\tilde{r}_n'(z) \equiv \frac{z r_n'(z)}{r_n(z)} \quad \textbf{(5.9)}$$

$$\tilde{r}_n''(z) \equiv \frac{z^2 r_n''(z)}{r_n(z)} \quad \textbf{(5.10)}$$

Where $r(z)$ represents either a spherical Bessel or a spherical Hankel function, $\tilde{r}(z)$ is defined as a scaled version of the corresponding function and all the variables and the primes have the same meaning as in Chapter 2. The effect of substituting Equations (5.8) to (5.10) in a systematic way into the system of 6×6 equations is to inversely scale the corresponding parts of the **x** vector when expressed in the form **Mx** = **C**. The redefined identities of those parts of the **x** vector thus scaled are

$$\tilde{\tilde{B}}_n = B_n h_n\left(a_T\right) \tag{5.11}$$

$$\tilde{\tilde{C}}_n = C_n h_n\left(a_s\right) \tag{5.12}$$

$$\tilde{\tilde{A}}'_n = \frac{A'_n j_n\left(a_c\right)}{-i\omega} \tag{5.13}$$

$$\tilde{\tilde{B}}'_n = \frac{B'_n j_n\left(a_T\right)}{-i\omega} \tag{5.14}$$

$$\tilde{\tilde{C}}'_n = \frac{C'_n j_n\left(a_s\right)}{-i\omega} \tag{5.15}$$

This results in a revised system of 6×6 equations in 6 unknowns in which the A_n and **C** vector coefficients expressed in the form of Equation (2.44) remain intact, leading to direct derivation of the required A_n coefficient without the need for subsequent re-scaling. For reasons already described in Chapter 2, only the A_n coefficient is of interest. Therefore, the re-scaling factors inherent in Equations (5.11) to (5.15) are detailed for the sake of completeness and clarity of analysis and, in practice, do not need to be implemented numerically. Also, Equations (5.8) to (5.10) not only simplify the expression for the revised system of 6×6 equations in 6 unknowns but also numerically scale the expression returned by the function used to evaluate the Bessel and Hankel functions. The numerical values of a Bessel function and its first and second derivatives, irrespective of the size of function argument, are within an order of magnitude of each other. Hankel functions and their first and second derivatives behave in a similar way. Therefore, even when large imaginary components of their arguments would otherwise cause the return value of functions to numerically overflow or underflow, the values are scaled by a factor of numerically similar size to themselves. This is done logarithmically to safeguard against the occurrence of overflow or underflow while computing intermediate results. The Bessel

and Hankel function software calculates spherical functions from cylindrical functions, denoted by $R(z)$ and $r(z)$ respectively, using the following relationships

$$r_n(z) = \sqrt{\frac{\pi}{2z}}\, R_{(n+1/2)}(z) \tag{5.16}$$

$$r_n'(z) = \frac{n}{z} r_n(z) - r_{(n+1)}(z) = \sqrt{\frac{\pi}{2z}} \left[\frac{n}{z} R_{(n+1/2)}(z) - R_{(n+3/2)}(z) \right] \tag{5.17}$$

$$r_n''(z) = \frac{n^2 - n}{z^2} r_n(z) - r_{(n+2)}(z) =$$

$$\sqrt{\frac{\pi}{2z}} \left[\frac{n^2 - n}{z^2} R_{(n+1/2)}(z) - \frac{2n+1}{z} R_{(n+3/2)}(z) + R_{(n+5/2)}(z) \right] \tag{5.18}$$

Equations (5.16) to (5.18) are combined with Equations (5.9) and (5.10) and, after some transposition and cancellation lead to the much simplified expressions given by

$$\tilde{r}_n'(z) = n - z \left(\frac{R_{(n+3/2)}(z)}{R_{(n+1/2)}(z)} \right) \tag{5.19}$$

$$\tilde{r}_n''(z) = n^2 - n - z\tilde{r}_n'(z) + z^2 \left(\frac{R_{(n+5/2)}(z)}{R_{(n+1/2)}(z)} \right) \tag{5.20}$$

Using the modified definitions, the matrix cells containing scaled Bessel and Hankel functions would all be within a few orders of magnitude of each other were it not for the multiplicative effect of the boundary equation coefficients, defined in Equations (2.34) and (2.35). They possess complex values and are functions of fixed physical parameters and frequency squared. An approximate guide to the magnitudes of the boundary coefficients in an aqueous polystyrene dispersion appears in Table 5.2.

frequency (Hz)	b_c	b_c'	b_T	b_T'
10^5	10^7	10^8	10^{17}	10^{17}
10^6	10^8	10^{10}	10^{18}	10^{18}
10^7	10^{11}	10^{12}	10^{19}	10^{19}
10^8	10^{13}	10^{14}	10^{20}	10^{20}
10^9	10^{15}	10^{16}	10^{21}	10^{21}

Table 5.2 Approximate magnitude values of the boundary coefficients of an aqueous polystyrene dispersion

After scaling of the spherical Bessel and Hankel functions and their first and second derivatives the boundary coefficients detract from the condition of an otherwise well-conditioned series of equations. Therefore, by dividing each one by b_c, all boundary coefficients can be normalized. By this means the numerical value of each of the relevant matrix cells is reduced towards the ideal of close to unity by between 7 and 15 orders of magnitude. By these means, the matrix is rendered much better conditioned and analytically and numerically optimized. Numerical experiments to test stability using only 64-bit arithmetic were undertaken. They showed that by using scaled Bessel and Hankel functions and the scaled and optimized matrix it was possible to compute a smoothly varying series of values of the complex scattering coefficient A_n. The range of values computed corresponded to values of frequency of up to 200MHz, particle diameter greater than 80cm to an order n greater than 10,000 without numerical over or underflow. This particle size and frequency corresponds to $k_c R \cong 3.35\times10^5$ in water.

5.4.3 The optimized and scaled matrix

Equations (2.38) to (2.43) can now be re-expressed as

$$a_c j_n'(a_c) + A_n a_c h_n'(a_c) + \tilde{B}_n \tilde{h}_n'(a_T) - \tilde{C}_n n(n+1) = \tilde{A}_n' \tilde{j}_n'(a_c') + \tilde{B}_n' \tilde{j}_n'(a_T') - \tilde{C}_n' n(n+1) \quad \textbf{(5.21)}$$

$$j_n(a_c) + A_n h_n(a_c) + \tilde{B}_n - \tilde{C}_n\left[\tilde{h}_n'(a_s) + 1\right] = \tilde{A}_n' + \tilde{B}_n' - \tilde{C}_n'\left[\tilde{j}_n'(a_s') + 1\right] \quad \textbf{(5.22)}$$

$$j_n(a_c) + A_n h_n(a_c) + \frac{b_T}{b_c}\tilde{B}_n = \frac{b_c'}{b_c}\tilde{A}_n' + \frac{b_T'}{b_c}\tilde{B}_n' \quad \textbf{(5.23)}$$

$$a_c\left[j_n'(a_c) + A_n h_n'(a_c)\right] + \tilde{B}_n \frac{b_T}{b_c}\tilde{h}_n'(a_T) = K\left[\tilde{A}_n' \frac{b_c'}{b_c}\tilde{j}_n'(a_c') + \tilde{B}_n' \frac{b_T'}{b_c}\tilde{j}_n'(a_T')\right] \quad \textbf{(5.24)}$$

$$\left(\frac{a_s^2}{2} - a_c^2\right) j_n(a_c) - a_c^2 j_n''(a_c) + A_n\left[\left(\frac{a_s^2}{2} - a_c^2\right) h_n(a_c) - a_c^2 h_n''(a_c)\right] +$$

$$\tilde{B}_n\left[\frac{a_s^2}{2} - a_T^2 - \tilde{h}_n''(a_T)\right] + \tilde{C}_n n(n+1)\left[\tilde{h}_n'(a_s) - 1\right] =$$

$$-U\left\{\tilde{A}_n'\left[a_c'^2 - \frac{a_s'^2}{2} + \tilde{j}_n''(a_c')\right] + \tilde{B}_n'\left[a_T'^2 - \frac{a_s'^2}{2} + \tilde{j}_n''(a_T')\right] - \tilde{C}_n' n(n+1)\left[\tilde{j}_n'(a_s') - 1\right]\right\} \quad \textbf{(5.25)}$$

$$a_c j_n'(a_c) - j_n(a_c) + A_n\left[a_c h_n'(a_c) - h_n(a_c)\right] + \tilde{B}_n\left[\tilde{h}_n'(a_T) - 1\right] - \frac{\tilde{C}_n}{2}\left[\tilde{h}_n''(a_s) + (n+2)(n-1)\right] =$$

$$U\left\{\tilde{A}_n'\left[\tilde{j}_n'(a_c') - 1\right] + \tilde{B}_n'\left[\tilde{j}_n'(a_T') - 1\right] - \frac{\tilde{C}_n'}{2}\left[\tilde{j}_n''(a_s') + (n+2)(n-1)\right]\right\} \quad \textbf{(5.26)}$$

The augmented matrix of Equation (2.44) and its associated components, Equations (2.45) to (2.86) can now be expressed as

$$M_1^1 = a_c\, h_n'(a_c) \quad \textbf{(5.27)}$$

$$M_1^2 = h_n(a_c) \quad \textbf{(5.28)}$$

$$M_1^3 = h_n(a_c) \quad \textbf{(5.29)}$$

$$M_1^4 = a_c\, h_n'(a_c) \tag{5.30}$$

$$M_1^5 = \left(\frac{a_s^2}{2} - a_c^2\right) h_n(a_c) - a_c^2\, h_n''(a_c) \tag{5.31}$$

$$M_1^6 = a_c\, h_n'(a_c) - h_n(a_c) \tag{5.32}$$

$$M_2^1 = \tilde{h}_n'(a_T) \qquad \text{`} \tag{5.33}$$

$$M_2^2 = 1 \tag{5.34}$$

$$M_2^3 = \frac{b_T}{b_c} \tag{5.35}$$

$$M_2^4 = \frac{b_T}{b_c}\tilde{h}_n'(a_T) \tag{5.36}$$

$$M_2^5 = \frac{a_s^2}{2} - a_T^2 - \tilde{h}_n''(a_T) \tag{5.37}$$

$$M_2^6 = \tilde{h}_n'(a_T) - 1 \tag{5.38}$$

$$M_3^1 = -n(n+1) \tag{5.39}$$

$$M_3^2 = -\left(\tilde{h}_n'(a_s) + 1\right) \tag{5.40}$$

$$M_3^3 = 0 \tag{5.41}$$

$$M_3^4 = 0 \tag{5.42}$$

$$M_3^5 = n(n+1)\left(\tilde{h}_n'(a_s) - 1\right) \tag{5.43}$$

$$M_3^6 = -\frac{1}{2}\left(\tilde{h}_n''(a_s) + (n-1)(n+2)\right) \tag{5.44}$$

$$M_4^1 = \tilde{j}_n'(a_c') \tag{5.45}$$

$$M_4^2 = 1 \tag{5.46}$$

$$M_4^3 = \frac{b_c'}{b_c} \tag{5.47}$$

$$M_4^4 = K\frac{b_c'}{b_c}\tilde{j}_n'(a_c') \tag{5.48}$$

$$M_4^5 = -U\left(a_c'^2 - \frac{a_s'^2}{2} + \tilde{j}_n''(a_c')\right) \tag{5.49}$$

$$M_4^6 = U\left(\tilde{j}_n'(a_c') - 1\right) \tag{5.50}$$

$$M_5^1 = \tilde{j}_n'(a_T') \tag{5.51}$$

$$M_5^2 = 1 \tag{5.52}$$

$$M_5^3 = \frac{b_T'}{b_c} \tag{5.53}$$

$$M_5^4 = K\frac{b_T'}{b_c}\tilde{j}_n'(a_T') \tag{5.54}$$

$$M_5^5 = -U\left(a_T'^2 - \frac{a_s'^2}{2} + \tilde{j}_n''(a_T')\right) \tag{5.55}$$

$$M_5^6 = U\left(\tilde{j}_n'(a_T') - 1\right) \tag{5.56}$$

$$M_6^1 = -n(n+1) \tag{5.57}$$

$$M_6^2 = -\left(\tilde{j}_n'(a_s') + 1\right) \tag{5.58}$$

$$M_6^3 = 0 \tag{5.59}$$

$$M_6^4 = 0 \tag{5.60}$$

$$M_6^5 = U\,n(n+1)\left(\tilde{j}_n'(a_s') - 1\right) \tag{5.61}$$

$$M_6^6 = \frac{-U}{2}\left[\tilde{j}_n''(a_s') + (n-1)(n+2)\right] \tag{5.62}$$

$$C_1 = -a_c\, j_n'(a_c) \tag{5.63}$$

$$C_2 = -j_n(a_c) \tag{5.64}$$

$$C_3 = -j_n(a_c) \tag{5.65}$$

$$C_4 = -a_c\, j_n'(a_c) \tag{5.66}$$

$$C_5 = a_c^2\, j_n''(a_c) - j_n(a_c)\left(\frac{a_s^2}{2} - a_c^2\right) \tag{5.67}$$

$$C_6 = j_n(a_c) - a_c\, j_n'(a_c) \tag{5.68}$$

Where

$$K = \frac{\kappa'}{\kappa} \text{ and } U = \frac{\mu'}{\mu} \tag{5.69}$$

The use of the ratios in Equation (5.69) instead of absolute values improves the condition of the matrix and reduces the number of computations required. Moreover, in the case of emulsions, the U of a particular dispersed-continuous phase combination is a fixed parameter that does not vary with frequency, as each *effective* μ would if used alone. This feature offers significant savings in computational effort.

5.5 Summary

A straightforward translation of the mathematics of the ECAH model is feasible but is limited in the ranges of frequency and particle size it can successfully model before floating-point overflow and underflow occur. This happens when an increase in the imaginary part of the input argument causes the numerical return value of Bessel or Hankel functions to grow or shrink exponentially to beyond the finite limits of machine arithmetic. Extending the precision of machine arithmetic either by hardware or software means is

usually prohibitively expensive either in hardware cost or computational overhead. Moreover, it is shown that extending machine precision is of limited effectiveness in extending the range of frequency or particle sizes that can be modelled. Scaling of the pre-normalized Bessel and Hankel functions in the logarithmic domain is shown to be equally effective whether the numerical value of the function is very large or very small. Scaling, when used in conjunction with other measures to optimize the ECAH matrix, results in significantly fewer computations than a literal translation of the ECAH equations. Also, the frequency-particle size combination capable of being modelled increases from 14μm to 80cm in diameter for an aqueous dispersion of polystyrene at 200MHz. Of equal value is that the condition of the matrix is significantly improved, thereby increasing confidence in the accuracy of the matrix solution at extreme values of particle size and frequency.

The ability to model the attenuation and phase velocity spectra of dispersions over an extended range enables scrutiny and comparison of the spectra to identify spectral features which might be characteristic of certain particle sizes and concentration. This could help in the design process of an instrument by specifying the optimum frequency band over which it should operate for reliable but cost-effective categorization of a known range of dispersions. Chapter 6 seeks to identify some of those spectral features.

6. Characteristics of modelled spectra

6.1 Introduction

Two of the main reasons for seeking to model the propagation of a sound wave through a dispersion of particles are to gain an understanding of the physical processes which take place and, therefore, to be able to predict the complex ultrasonic wavenumber of a real dispersion. Comparing modelled ultrasonic refractive indices with experimentally derived data from practical dispersions could enable the determination of unknown particle sizes and/or unknown concentrations of dispersed particles in continuous phases. Successful and efficient inversion of experimental data would depend upon a number of factors, which include:

a. The model used caters for all the significant physical loss mechanisms
b. The model used is numerically accurate
c. The frequency range over which model and experimental data are compared provides a unique ‘signature’ of the particle sizes and phase concentration to enable unambiguous matching, with an acceptable level of confidence
d. Availability of sufficiently accurate values of physical properties for each of the phases
e. The ability of an inversion algorithm to generate and compare the minimum amount of modelled data with experimentally derived data to achieve a match
f. Availability of sufficiently accurate and reliable experimental data

This thesis is concerned primarily with the first four factors. Chapter 2 described the ECAH model that is complicated but includes a range of the most common loss mechanisms encountered in practical dispersions. Chapters 3, 4 and 5 examined issues that

affect numerical accuracy, and offered some solutions. This chapter seeks to examine the problem described in (c) above, and to identify and recommend the optimum frequency range over which to extract experimental data and compare it with modelled. It also examines the sources of error when evaluating the differences between experimental and modelled data, which include the issue mentioned above in (d).

6.2 The limits of experimental and modelled data

As a rule, it is easier, cheaper and faster to model data than to obtain it experimentally. Also, as a general rule in dispersions with a fluid continuous phase, the limitations on experimentally derived data are frequency dependent. That is to say, it is difficult to obtain good quality ultrasonic propagation data at very high or very low frequencies. Particle size or concentration *per se* does not usually limit experimental data (unless the dispersion becomes so attenuative that the signal to noise ratio causes the data to be unreliable). However, the computational stability of numerical models, being sensitive to the magnitude of the frequency-particle radius product, means that modelling has a finite range in both particle size and frequency.

6.3 Experimental data

Wide bandwidth attenuation and phase velocity spectra of sound propagation through silica in water dispersions were obtained from the fast Fourier transform (FFT) of short acoustic pulses. The spectral data is that described by Holmes, Challis & Wedlock (1994). The experimental method and signal processing techniques employed are detailed by Challis *et al* (1991). The three dispersions were all of a mass fraction of 7.8% w/w (mass fraction will be referred to in terms of % w/w concentration) and comprised narrow size distribution

(commercially available model particles sold as near-monodisperse) aqueous dispersions of silica with mean diameters of 125nm, 320nm and 520nm. Other statistical moments of the size distribution are not known. The multiple scattering models described in Chapter 4 all require the inclusion of the number of particles per unit volume, expressed as a function of % v/v concentration and particle size. For the purposes of modelling, the experimental dispersions were regarded as monodisperse and the % v/v concentration related to the % w/w concentration by the equation given by

$$\phi_v = \frac{\phi_m}{\left(\frac{\rho'}{\rho}\right)(1-\phi_m)+\phi_m} \qquad \textbf{(6.1)}$$

Where ϕ_v denotes % v/v concentration, ϕ_m % w/w concentration, ρ mass density of the continuous phase and ρ' mass density of the dispersed phase. It can be seen from Equation (6.1) and Equations (4.7), (4.8) and (4.9) that the % v/v concentration ϕ_v and, therefore, the accuracy of the modelled data are heavily dependent upon $\left(\frac{\rho'}{\rho}\right)$, the relative values of the mass density of the continuous and dispersed phases. The mass density of pure water at the temperature of the experiment (30 ± 0.1ºC) is known to a high degree of precision (Kell, 1975). However, ascertaining the precise physical properties of other materials to an adequate level of accuracy can be a problem and this topic will be examined further in §6.10. The mass density of silica is given by a great number of sources in the literature and there is considerable disagreement between them. This is to be expected, as it is highly likely that the techniques used in the manufacture of small silica particles could result in real differences in mass density, possibly due to differences in porosity or crystal structure. Some suppliers of model particles undertake some analysis to ascertain physical properties

of their products but many appear to use established values from the literature. For example, a major supplier of high purity silica (Goodfellow, 1998) quotes a mass density of 2180 kg/m^3 for SiO_2 silica. The CRC Handbook (Weast, 1988) Table F1 quotes a mass density of 2210 kg/m^3 for fused transparent silica and 2070 kg/m^3 for translucent. Kaye & Laby (1995) give the mass density of silica to be 1970 kg/m^3. This selection of values is by no means exhaustive or even representative of extremes but, nevertheless, spans the range 1970 to 2210 kg/m^3. The given dispersed phase mass concentration of the experimental dispersions is 7.8% w/w. These values substituted into Equation (6.1) give a range of % v/v concentrations in water at 30ºC from 4.1%, corresponding to mass density of 1970 kg/m^3, to 3.67%, corresponding to a mass density of 2210 kg/m^3. This discrepancy in the % v/v concentration figures, if used for multiple scattering calculations, can lead to significant errors. Different mass density values can also lead to significant variations in the calculated scattering wavenumber using the ECAH model. These factors will be quantified in §6.9. In addition, the stated limits of experimental error in temperature, while having little effect on attenuation, are of critical importance when modelling and making comparisons of experimental phase velocities.

6.4 Modelled data

Aqueous dispersions of silica were modelled, using the physical properties for water and silica tabulated in Appendix E. The Lloyd & Berry model was run to within 0.01% of convergence to produce results of attenuation and phase velocity. These corresponded to the 90 experimentally obtained frequency points between 1.95 and 19.33 MHz of the 125nm and 320nm dispersions and the 80 experimentally obtained frequency points between 1.95 and 17.38 MHz of the 520nm dispersion. A value of attenuation and phase

velocity was generated for each frequency point over a linear range of 40 particle sizes between 10nm and 1000nm and a linear range of 40 % v/v concentration values between 0.01% and 8.00%. This was used to construct a size-% v/v concentration 40×40 matrix with 80 or 90 frequency points in each matrix element for attenuation and an analogous matrix for phase velocity. Three pairs of these matrices were produced, corresponding to modelled dispersions at 29.5ºC, 30.0ºC and 30.5ºC to investigate the effect of experimental temperature tolerances. In each model, the silica physical properties remained constant and only the water physical properties were varied in accordance with a fifth-order polynomial fit to the tabulated values given by the sources of physical properties listed in Appendix E.

6.5 Comparison between experimental and modelled data

The 80 or 90 points of experimental data corresponding to 125nm, 320nm and 520nm diameter particulate dispersions were compared to each element of the appropriate modelled attenuation or modelled phase velocity matrices. At each frequency point the difference between the experimental and modelled value was squared, the square root of the sum of the squared differences for all 80 or 90 frequency points gave the RMS difference for a single size-% v/v concentration point on the appropriate 40×40 matrix. Therefore, if a modelled attenuation or phase velocity spectrum formed a perfect match with an experimentally obtained spectrum the RMS difference would be zero. Such a fit was considered highly unlikely and to accentuate goodness of fit a contour plot was constructed showing the reciprocal of RMS difference. Peaks of reciprocal RMS difference appear as points on the plot surrounded sometimes by contours of equal value. Comparison of experimental and modelled spectra using the RMS technique does not apply weighting to any part of the spectrum *per se*. However, the choice of how attenuation is represented

before comparisons are undertaken can make a significant difference to the apparent RMS difference. If values of alpha (defined in Equation (1.7)) are compared, any difference between experimental and modelled spectra is accentuated at high frequencies but low frequency differences are much less obvious. Whereas, the exact reverse is usually the case if values of alpha over frequency squared are compared. A good compromise that shows differences over the whole frequency range is comparison of values of alpha over frequency. The other two representations were found virtually to ignore quite significant differences at either one of the extreme ends of the frequency range. However, for the sake of comparison and to illustrate the effect of choice of the attenuation representation, all three schemes are depicted in Figures 6.1, 6.2 and 6.3 and observable differences between them are subsequently discussed.

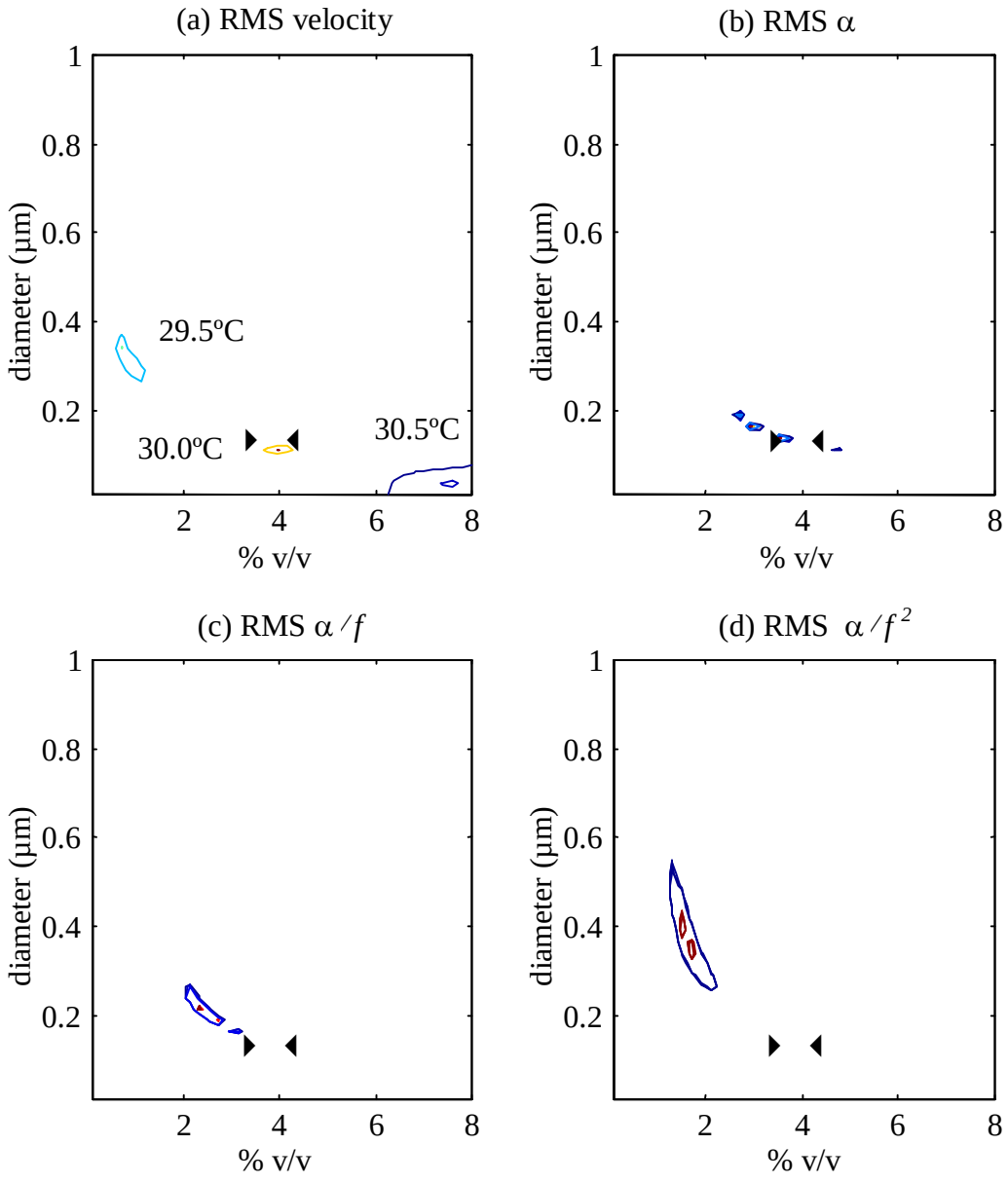

Figure 6.1 Contour plots showing reciprocal of RMS difference between experimental data from a nominally 125nm diameter and between 3.67 and 4.1% v/v concentration (range denoted by ▸ ◂) aqueous silica dispersion and modelled data over the 10nm to 1000nm and 0.01% to 8.00% size-% v/v concentration space, at modelled temperatures of 29.5ºC, 30.0ºC and 30.5ºC (the contours corresponding to each of the three temperatures effectively overlay each other on the attenuation plots)

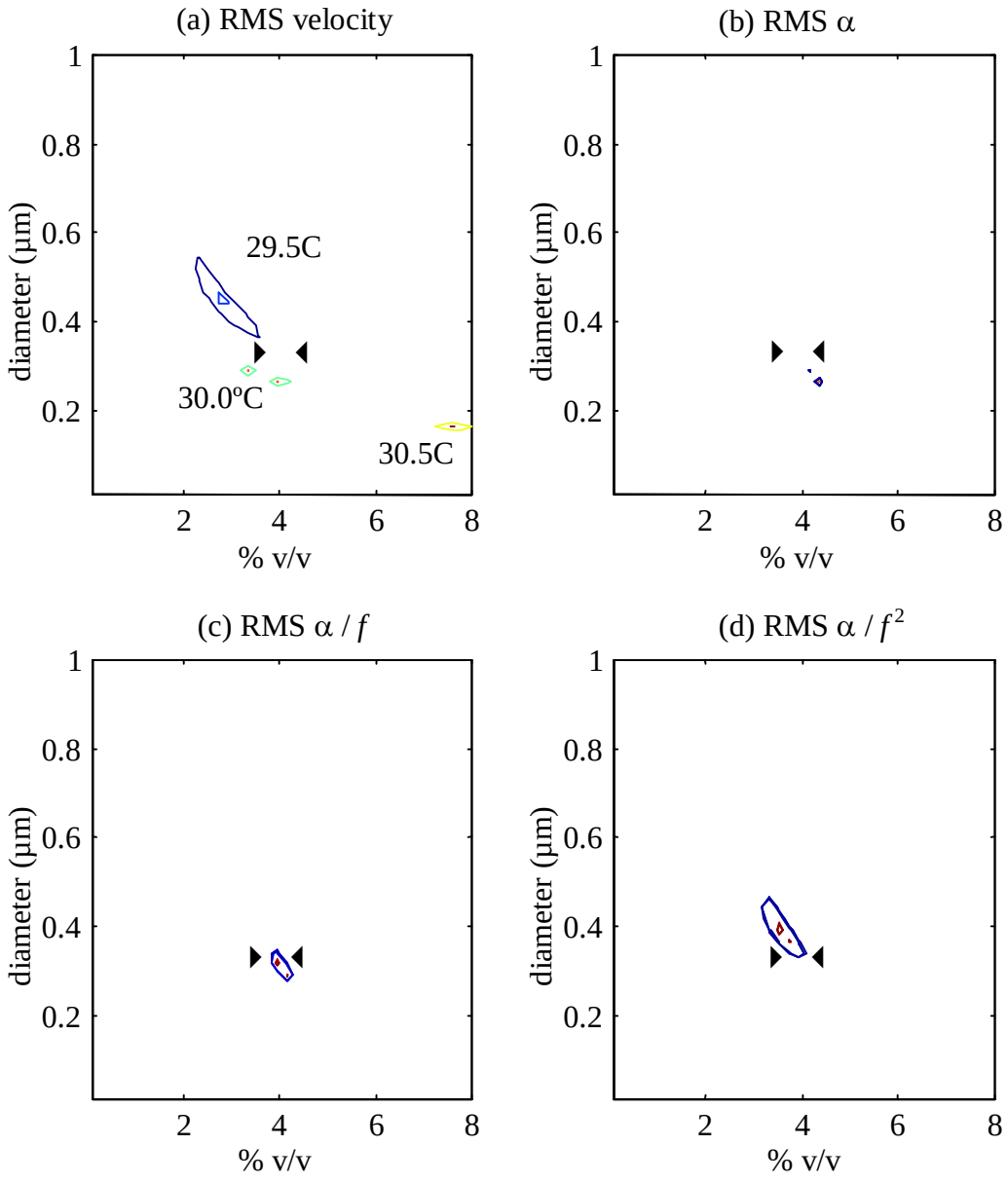

Figure 6.2 Contour plots showing reciprocal of RMS difference between experimental data from a nominally 320nm diameter and between 3.67 and 4.1% v/v concentration (range denoted by ▸ ◂) aqueous silica dispersion and modelled data over the 10nm to 1000nm and 0.01% to 8.00% size-% v/v concentration space, at modelled temperatures of 29.5ºC, 30.0ºC and 30.5ºC (the contours corresponding to each of the three temperatures effectively overlay each other on the attenuation plots)

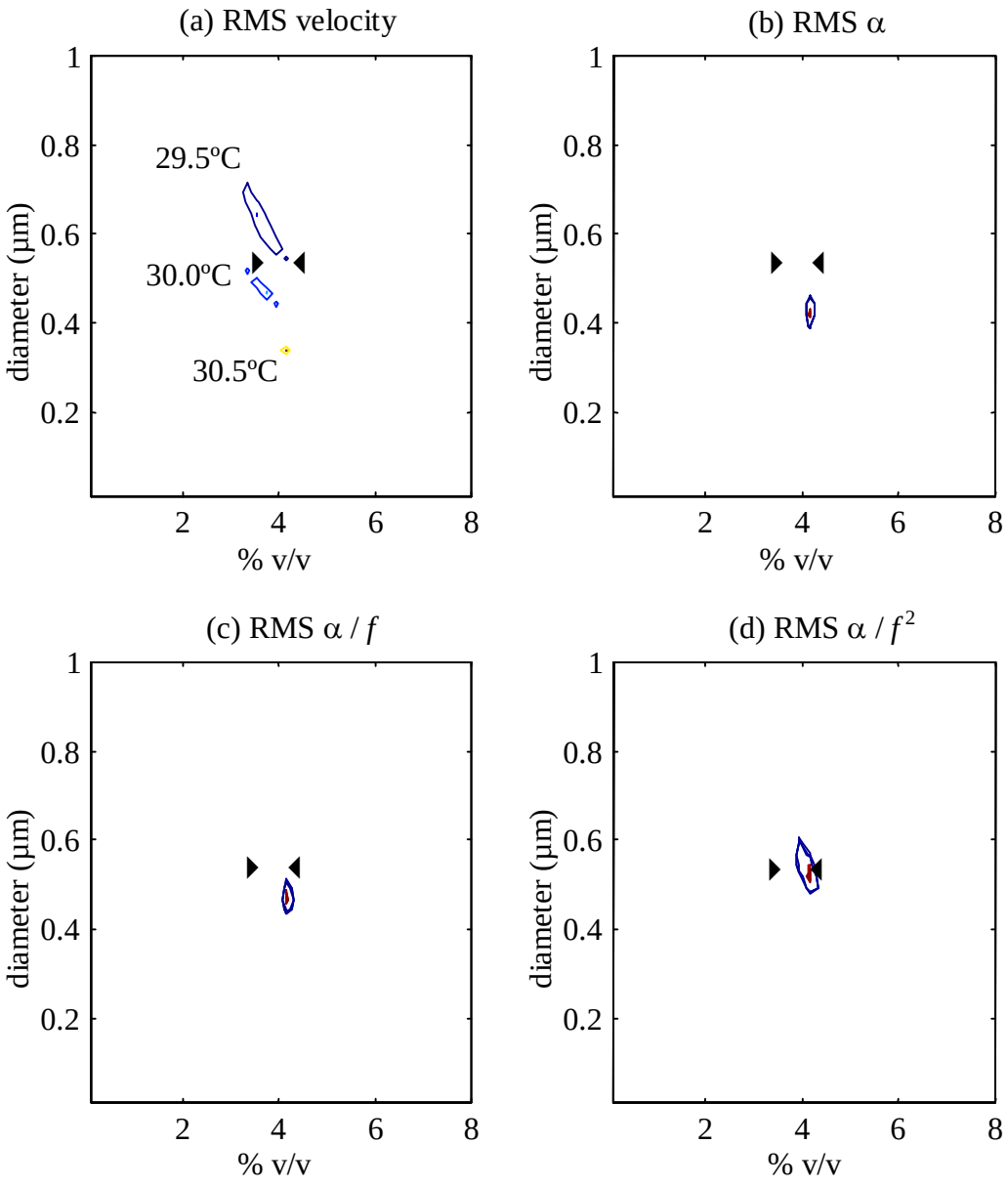

Figure 6.3 Contour plots showing reciprocal of RMS difference between experimental data from a nominally 520nm diameter and between 3.67 and 4.1% v/v concentration (range denoted by ▸ ◂) aqueous silica dispersion and modelled data over the 10nm to 1000nm and 0.01% to 8.00% size-% v/v concentration space, at modelled temperatures of 29.5ºC, 30.0ºC and 30.5ºC (the contours corresponding to each of the three temperatures effectively overlay each other on the attenuation plots)

6.6 Observations and discussion on the comparison between experimental and modelled data

It can be seen from Figures 6.1, 6.2 and 6.3 that the reciprocal RMS matrix is reasonably effective at highlighting the best agreement between experimental and modelled data. The comparison of RMS phase velocity in Figures 6.1(a), 6.2(a) and 6.3(a) show quite clearly the importance of accurate temperature control if phase velocity is to be used in a particle-size or % v/v concentration discriminator. As a very crude rule of thumb, both variations of temperature and variations in % v/v concentration result in vertical translation of the velocity spectrum. It is obvious, therefore, that temperature error would very likely result in an analogous error in the interpretation of % v/v concentration of a dispersion from its velocity spectrum. For each particle size and attenuation representation, all the attenuation plots that correspond to different temperatures effectively overlay each other; but, when comparing phase velocities, variations of only one half of a degree either side of a central value can introduce apparently large variations. In the case of the 125nm dispersion, the indicated particle size and % v/v concentrations range from approximately 20nm at 7.4%, through 115nm at 4%, to approximately 340nm at 0.6%. Less marked but nevertheless significant variations apply in the cases of 320nm and 520nm. It is interesting to note that as the particle size increases the difference in temperature versus % v/v concentration rule of thumb becomes more applicable. In the case of the 520nm particle diameter plots, variations in temperature result in the movement of the reciprocal RMS centroid almost vertically along the % v/v concentration axis.

6.6.1 Choice of attenuation representation

The attenuation plots also clearly illustrate the difference in apparent size-% v/v concentration matches, depending upon which of the alpha, alpha over frequency or alpha over frequency squared metrics was used for comparison. The reason for the latter discrepancies has already been alluded to by reference to the fact that some choices of attenuation representation are tantamount to applying bias to the RMS algorithm, in favour of high or low frequencies. This becomes clearer if the individual attenuation over frequency and phase velocity spectra in Figures 6.4, 6.5 and 6.6 are examined. All the spectra in Figures 6.4, 6.5 and 6.6 represent aqueous silica dispersions at a temperature of 30.0ºC modelled using the Lloyd & Berry model run to within 0.01% of convergence. The phase velocity plot in Figure 6.4 shows how the temperature induced errors apparent in Figure 6.1 are caused if the experimental phase velocity spectra of the 125nm dispersion is imagined to simply translate vertically, as is usually the case for small variations in temperature. The significant differences between Figures 6.1(b), 6.1(c) and 6.1(d) can be understood by reference to the attenuation spectra in Figure 6.4. The experimental spectrum agrees well with the modelled 125nm 4% v/v spectrum only at higher frequencies. Agreement is poor at lower frequencies. Therefore, if alpha is used to calculate RMS difference the lack of agreement at lower frequencies is ignored and Figure 6.1(b) shows good agreement with the true size and % v/v concentration values.

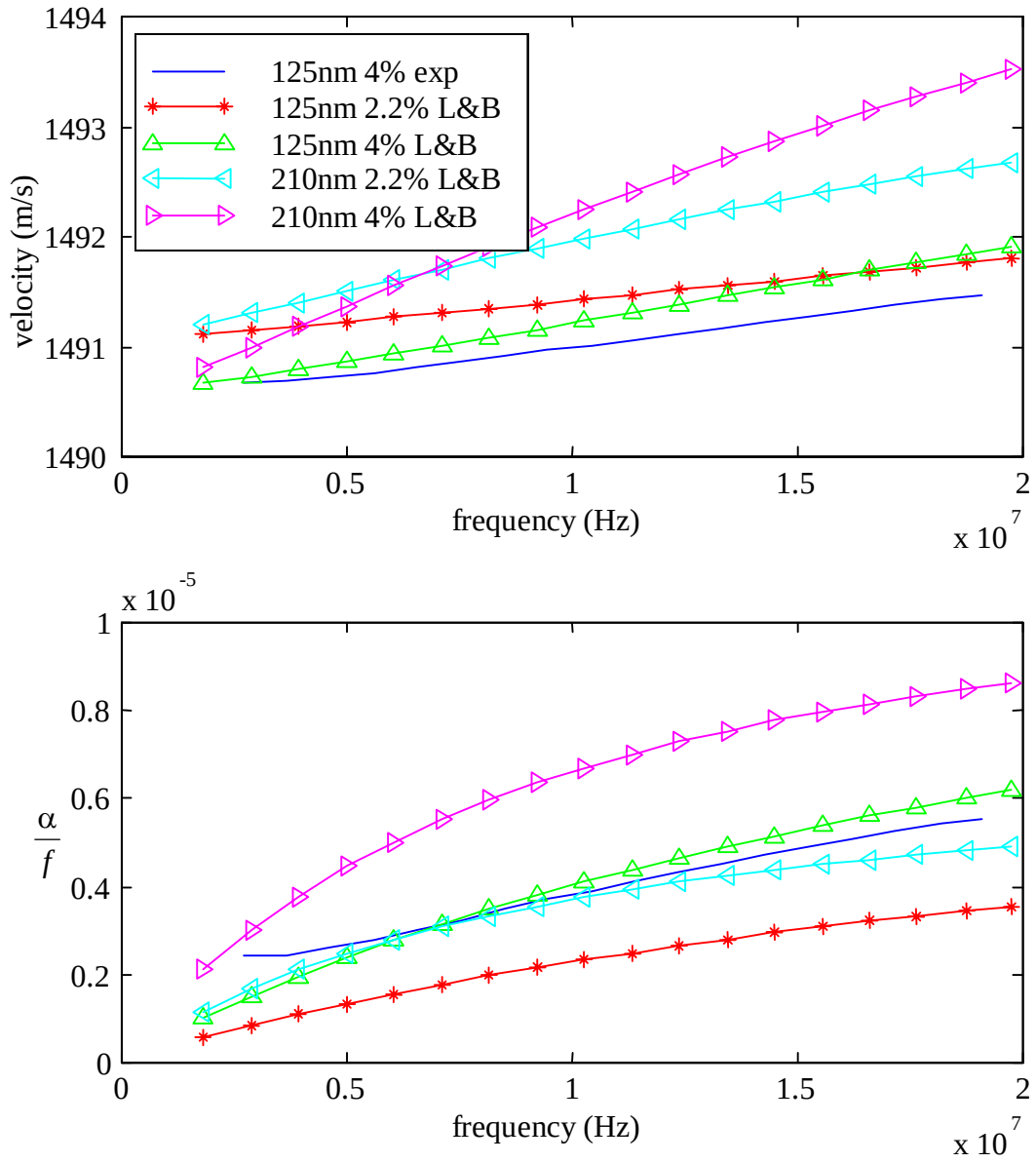

Figure 6.4 Comparison of experimental phase velocity and attenuation spectra from a nominally 125nm diameter, approximately 4% v/v concentration, aqueous silica dispersion and modelled spectra of similar shape at 30°C

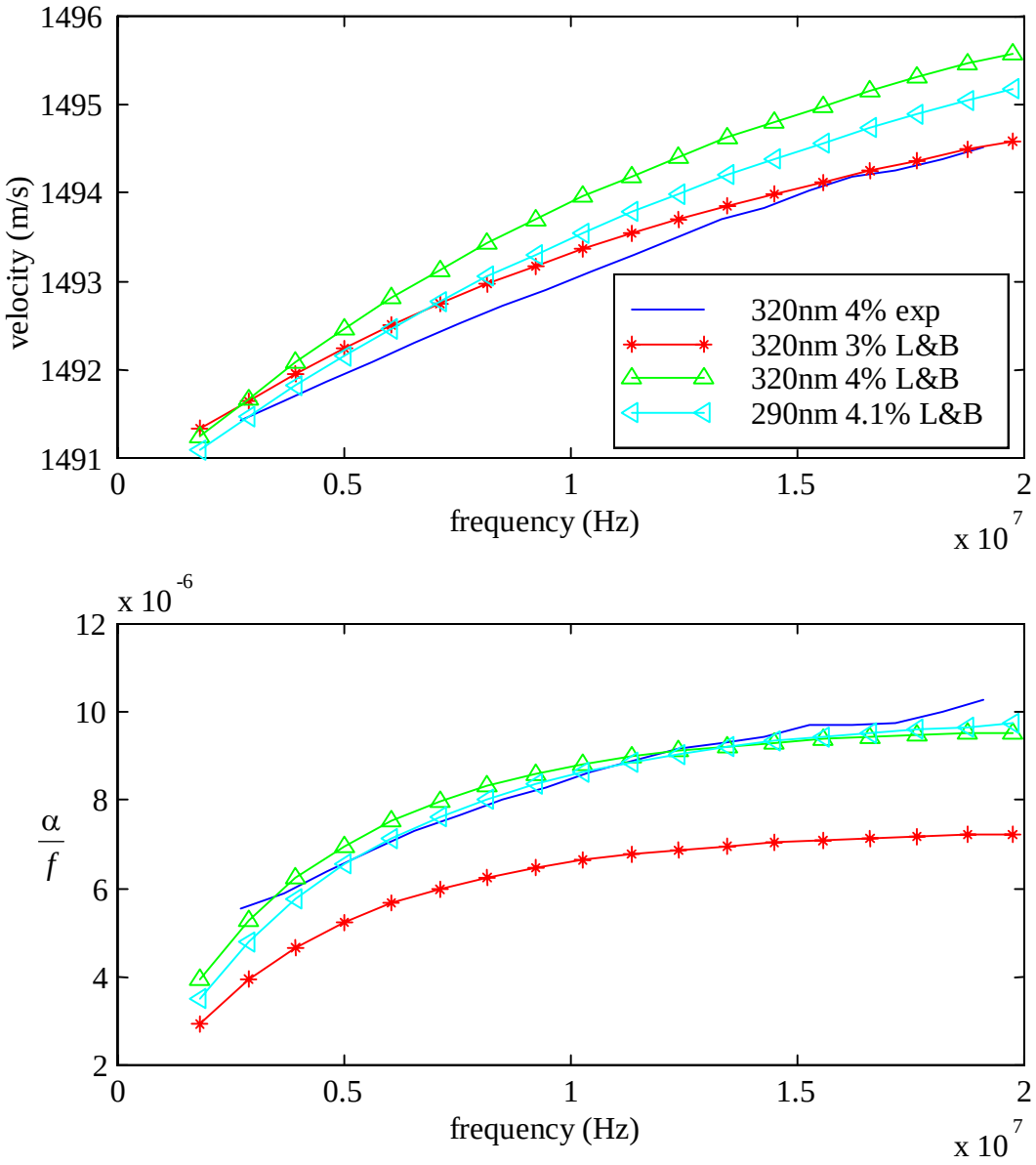

Figure 6.5 Comparison of experimental phase velocity and attenuation spectra from a nominally 320nm diameter, approximately 4% v/v concentration, aqueous silica dispersion and modelled spectra of similar shape at 30°C

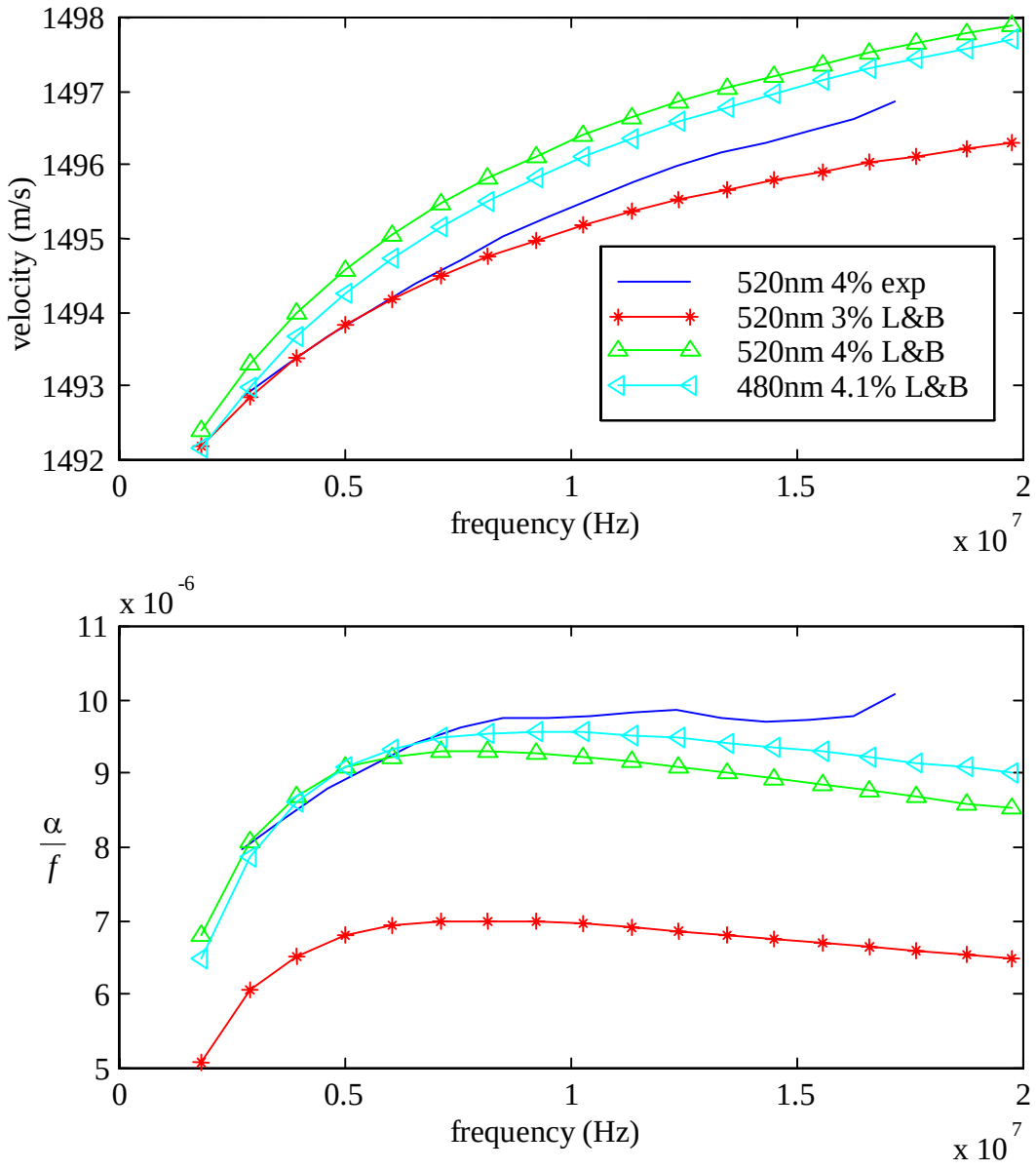

Figure 6.6 Comparison of experimental phase velocity and attenuation spectra from a nominally 520nm diameter, approximately 4% v/v concentration, aqueous silica dispersion and modelled spectra of similar shape at 30ºC

However, a comparison using alpha over frequency, depicted in Figure 6.1(c), agrees less well. Not surprisingly, alpha over frequency squared largely ignores the good agreement at higher frequencies shown in Figure 6.4 and instead bases its fit on the lower frequencies, and Figure 6.1(d) indicates a best fit with a much higher particle size and a much lower % v/v concentration. The spectra of such small particles as 125nm diameter are plotted as relatively straight lines, lacking any characteristic curvature, and this can make them ambiguous and difficult to classify. If they are distorted by problems with noise, lack of bandwidth at extremes of spectrum frequency or systematic errors such as whole spectrum scaling of attenuation they easily assume the characteristics of quite different dispersions.

6.6.2 Spectral shape

As particle size increases the degree of curvature apparent in both the phase velocity and attenuation spectra increases. This is illustrated by inspection of the spectra depicted in Figures 6.5 and 6.6. The curvature depicted in the attenuation plot in Figure 6.6 is notable in that it forms a distinct peak where the gradient of the modelled alpha over frequency passes through zero. This occurs at approximately 7 MHz and it can also be seen that the peak turning point frequency is the same for 520nm particles at a number of different % v/v concentrations. The experimental data appears to peak at 10 MHz. The possible reasons for this discrepancy will be examined in §6.10. Figures 6.7 and 6.8 depict the modelled phase velocity and attenuation spectra of 600nm diameter monodisperse, 1-10% v/v concentration incremented in 1% steps, aqueous silica dispersions at 30ºC.

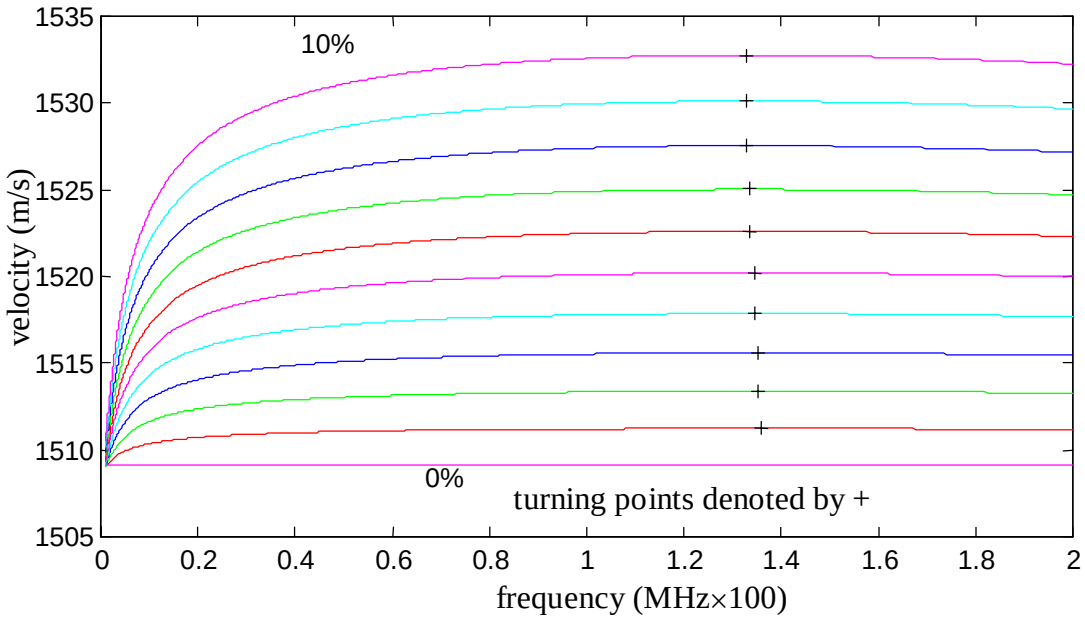

Figure 6.7 Modelled phase velocity spectra of 600nm diameter monodisperse, 0-10% v/v concentration incremented in 1% steps, aqueous silica dispersions at 30ºC

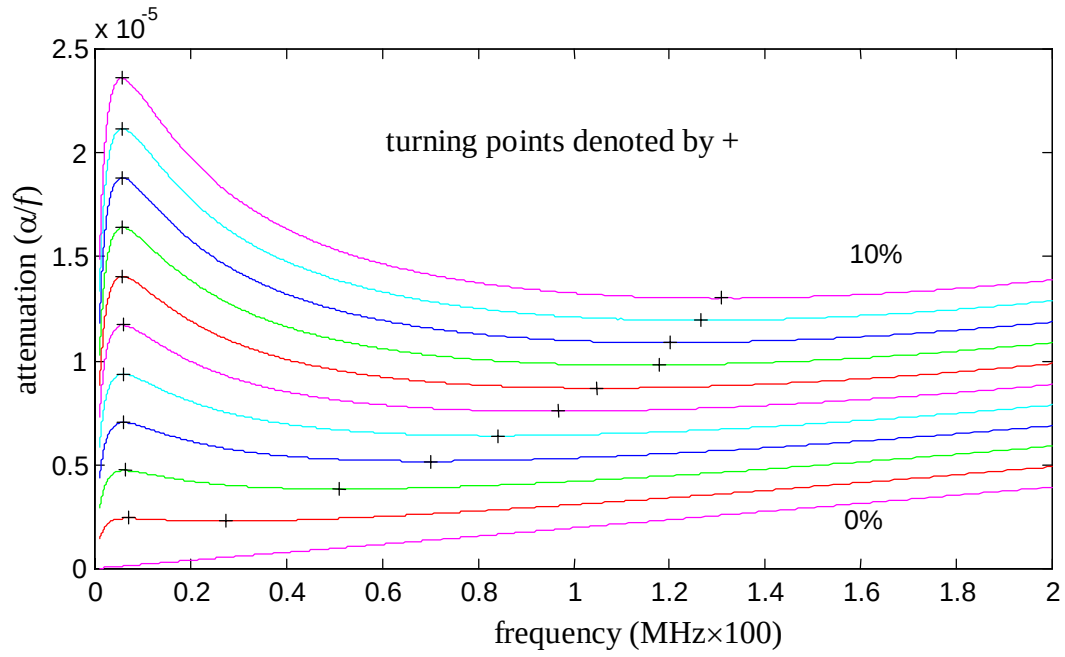

Figure 6.8 Modelled attenuation spectra of 600nm diameter monodisperse, 0-10% v/v concentration incremented in 1% steps, aqueous silica dispersions at 30ºC

From Figures 6.7 and 6.8 it can be seen that the frequency value of the peaks, referred to as maximum turning points, do not vary with % v/v concentration, within the range 1% to 10% v/v (alignment is almost vertical when considering round-off error and the discrete nature of the data). Equally interesting are the troughs, referred to as minimum turning points, in the attenuation spectra where the spectral gradient passes through zero (it is worth noting that phase velocity also exhibits such troughs but at much higher particle diameter-wavenumber products than those depicted). The attenuation and phase velocity spectra of a number of aqueous dispersions with differing dispersed phase materials and diameters, all at 10% v/v concentration, were modelled and plotted to compare the natural log of the particle diameter versus the natural log of the frequency at which the turning points occurred. Such plots for silica, titanium dioxide, hexadecane and polystyrene appear as Figure 6.9.

6.7 Relationships between spectral shape, particle size and concentration

It can be seen from Figure 6.9 that there appears to be a power-law relationship between particle size and the characteristic frequencies at which maximum and minimum turning points occur. Additional modelling, not detailed here, reinforced the conclusions that can be drawn from Figure 6.8, that is, the frequency at which maximum turning points occur for a particular combination of continuous and dispersed phases is solely a function of particle size, and is independent of % v/v concentration.

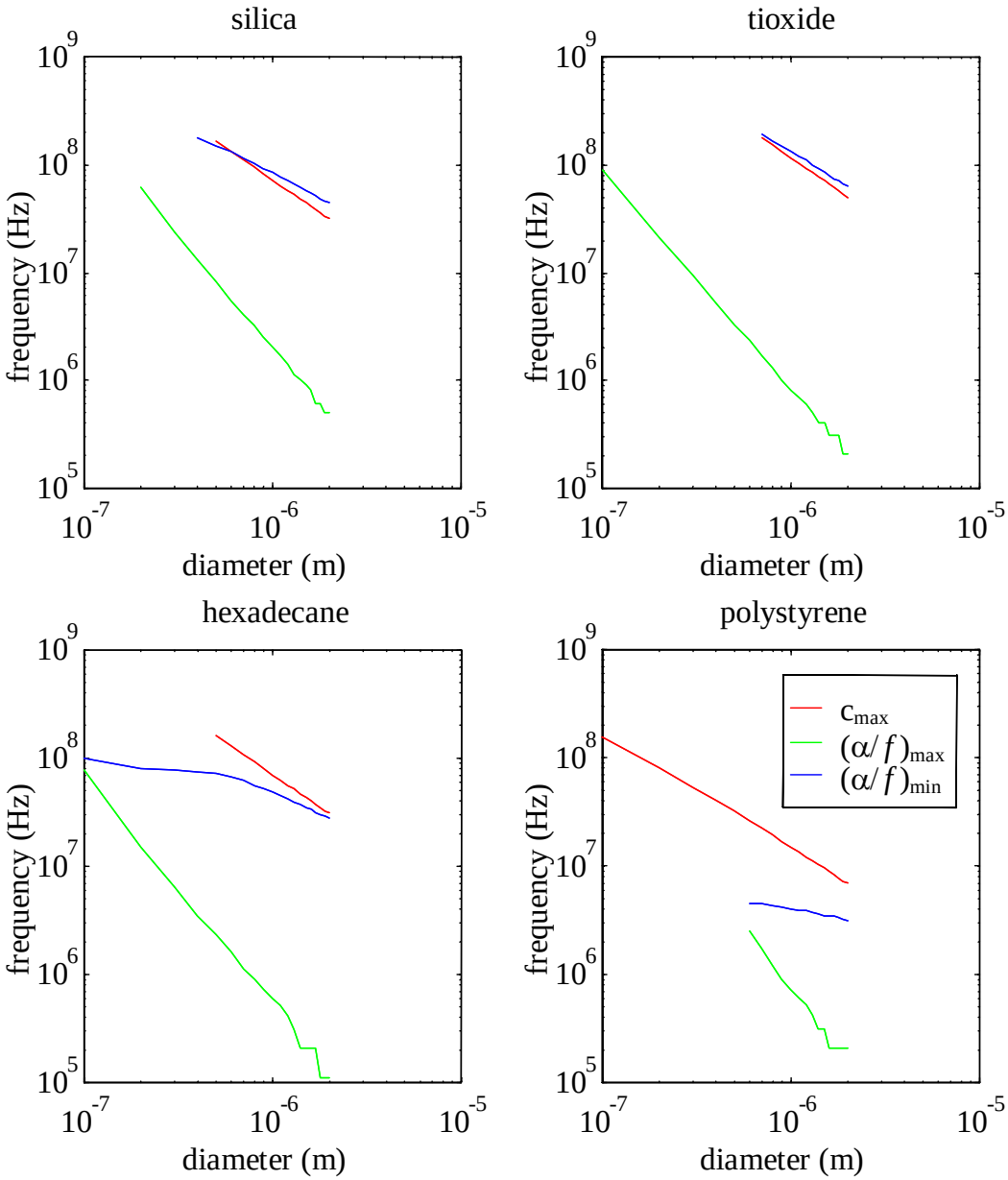

Figure 6.9 Logarithmic axes plots of maximum and minimum turning points for a range of aqueous dispersions of materials and particle diameters versus frequency, all at 10% v/v concentration and 30ºC

From the logarithmic relationships evident in Figure 6.9 it was found that the maximum turning point frequency, *f*, and particle diameter, *d*, were linked by the relationship

$$d = xf^{y} \qquad \textbf{(6.2)}$$

Where *x* and *y* are coefficients. In addition, it was found that for *any particular % v/v concentration* the minimum turning point also obeyed the relationship in Equation (6.2). Therefore, for a particular combination of continuous and dispersed phases, the *x* and *y* coefficients associated with maximum turning points are a function of particle size, but the *x* and *y* coefficients associated with the minimum turning points are a function of particle size and % v/v concentration. In practical terms this means that, for a particular combination of continuous and dispersed phases, if the maximum and minimum turning points are known: *the unique particle size and % v/v concentration combination can be determined*. As an example, the *x* and *y* coefficients applicable to aqueous dispersions of silica, titanium dioxide AHR pigment, hexadecane emulsion and polystyrene are listed in Table 6.1. Although the *x* and *y* coefficients for the maximum turning points are independent of % v/v concentration it must be stressed that those listed for the minimum turning points apply only to a 10% v/v concentration dispersion. Although an expression to relate the *x* and *y* coefficients of minimum turning points to % v/v concentration, ϕ, was derived it was found to be ill-conditioned (accurate results were obtained only by using coefficients calculated to 10 decimal places). This problem would merit further research. Nevertheless, if the coefficients were needed to form part of an algorithm to determine particle size and % v/v concentration from experimentally obtained maximum and minimum turning point frequencies, it would be straightforward to derive a range of modelled values to construct a look-up table from which values could be interpolated.

material	turning point	$d = xf^{y}$		$f = xd^{y}$	
		x	*y*	*x*	*y*
silica	c_{max}	3.9189	-0.83903	5.0932	-1.1918
	$(\alpha/f)_{max}$	1.0832×10^{-3}	-0.48137	7.1499×10^{-7}	-2.0750
	$(\alpha/f)_{min}$	872.79	-1.1293	414.93	-0.88319
tioxide	c_{max}	4.1908	-0.82107	5.7270	-1.2179
	$(\alpha/f)_{max}$	9.2613×10^{-4}	-0.50044	9.0078×10^{-7}	-1.9956
	$(\alpha/f)_{min}$	45.214	-0.94291	57.026	-1.0604
hexadecane	c_{max}	3.5687	-0.83499	4.5915	-1.1976
	$(\alpha/f)_{max}$	4.4081×10^{-4}	-0.46242	6.6106×10^{-8}	-2.1499
	$(\alpha/f)_{min}$	1.3018×10^{9}	-1.9777	8.0499×10^{4}	-0.45679
polystyrene	c_{max}	5.8644	-0.94398	6.6492	-1.0579
	$(\alpha/f)_{max}$	4.2842×10^{-4}	-0.44789	5.4232×10^{-8}	-2.1897
	$(\alpha/f)_{min}$	8.5063×10^{14}	-3.1715	5.4776×10^{4}	-0.31008

Table 6.1 Relationship between particle diameter and the frequency of turning points

(Diameter is in metres and frequency in Hz)

6.8 The effect on spectral shape of particle polydispersity

Monodisperse dispersions of particles are difficult and expensive to prepare synthetically and are rarely found outside the laboratory or special industrial or pharmaceutical processes where the property of monodispersity is important enough to justify the extra cost of production and quality testing. Virtually all practical dispersions are found to be polydisperse. In nature, the sizes of particles in dispersion and their relative proportions of the whole of the dispersed phase are rarely random or discontinuous, but more often together make a continuous distribution between the largest and smallest particle size. Although there are exceptions, the most common way of representing continuous particle size distributions is by the lognormal distribution. The familiar normal distribution, $g(x)$, is given by

$$g(x) = \frac{\exp\left[\frac{(x-\mu)^2}{2\sigma^2}\right]}{\sigma\sqrt{2\pi}} \qquad \textbf{(6.3)}$$

Where x is the continuous function, in this case particle size, μ is the mean particle diameter and σ is the standard deviation. The lognormal distribution has the shape of the normal distribution when plotted on a logarithmic horizontal axis. The lognormal distribution, $g(w)$, can be expressed as

$$g(w) = \frac{\exp\left[\frac{\left(\log_e(w)-\mu_{\log}\right)^2}{2\sigma_{\log}^2}\right]}{\sigma_{\log} w\sqrt{2\pi}} \qquad \textbf{(6.4)}$$

Where w is the logarithmic continuous function and the logarithmic mean, $\mu_{\log}$, is not the same as the normal mean but is related by the expression

$$\mu_{\log} = \exp\left(\log_e \mu + \sigma_{\log}^2\right), \qquad \sigma_{\log}^2 = \exp\left(2\mu + \sigma^2\right)\left(\exp\sigma^2 - 1\right) \qquad \textbf{(6.5)}$$

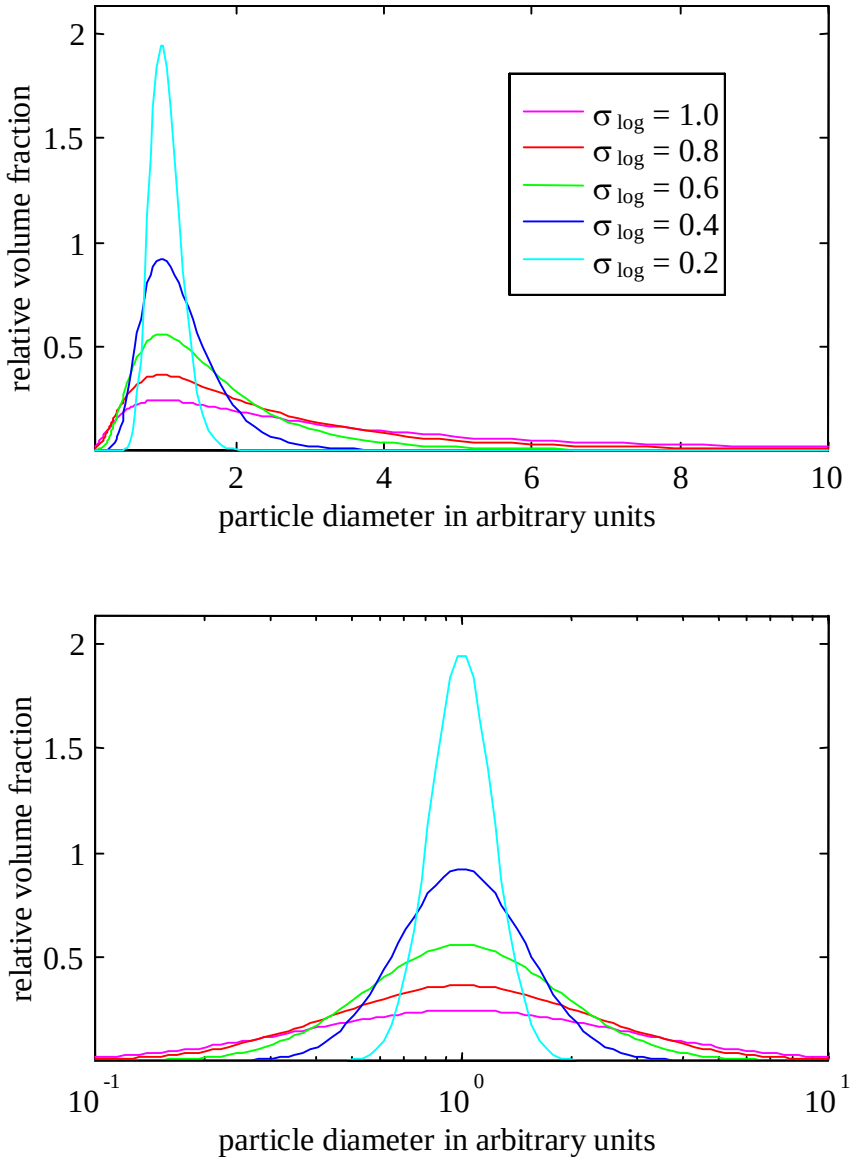

Figure 6.10 An illustration of the relationship between normal and lognormal distributions, for different values of σ_{log}. The distributions are all centred on unity and relative % v/v concentrations are given such that the area under the curve of each distribution is unity

Also, the logarithmic standard deviation σ_{log} is not the same as normal standard deviation, although it is a measure of the width of the distribution in an analogous way. Figure 6.10 illustrates the relationships between the normal and lognormal distributions.

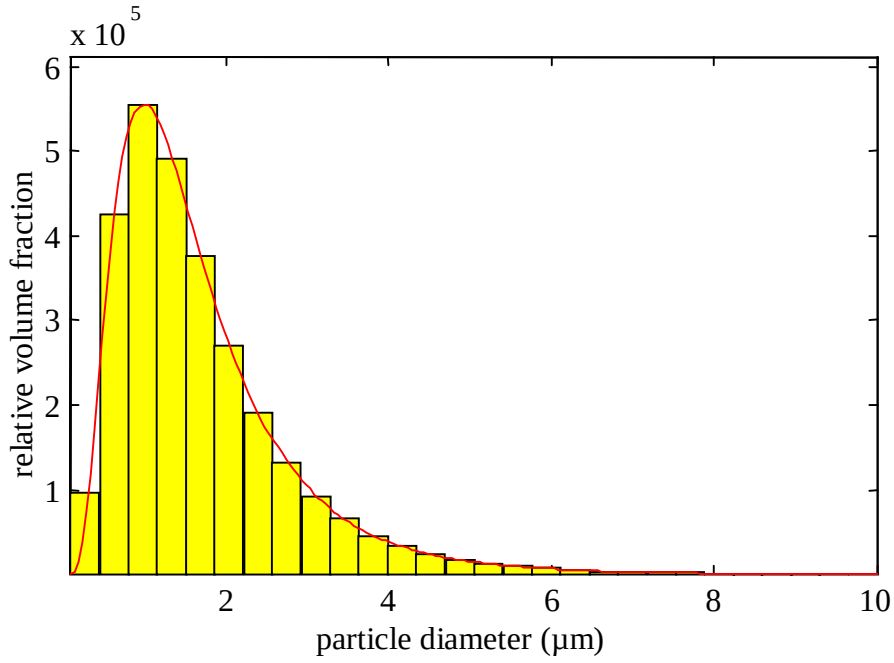

Figure 6.11 Lognormal distribution centred on 1μm diameter and logarithmic standard deviation, $\sigma_{log,}$ of 0.6 overlaid with its discrete evenly-spaced size bin representation (the area under the curve is unity)

Multi-modal distributions with more than one distinct peak value of particle size are often represented as superpositioned lognormal distributions. Distributions that have a distinct peak at a certain particle size but in which the distribution tails off towards the smaller end of the particle size spectrum, for example as the result of a sieving process, are common but are difficult to represent analytically. When modelling a dispersion with a particle size distribution using the procedure described in §2.6 it is relatively straightforward to generate the necessary size-bin versus % v/v concentration pairs from any distribution. For example, Figure 6.11 shows a continuous lognormal distribution overlaid with its discrete analogue. It is worthy of note that the lognormal distribution depicted in Figure 6.11 is centred on a modal value of 1μm but that is *not* the logarithmic mean value, which, from

Equation (6.5) can be derived to be 1.43μm. A range of lognormal distributions, all centred on modal values of 1μm diameter, with corresponding logarithmic means appear in Table 6.2. The difficulty in analytically representing distributions with long tails towards the smaller size end of the distribution can present problems when model inversion is the aim, that is to say, the fitting of experimental data onto closely matched modelled data. This is because the most efficient algorithms that fit experimental data would fit it to an analytic function of the variables of interest. Fitting experimental data iteratively to a number of sets of modelled data until a good fit is found is computationally wasteful and prone to errors. However, such fitting would be required in particle sizing system based on ultrasound. Thus it is instructive to investigate the effects of a small particle-size tail as a determinant of ultrasonic wavenumber. A simple investigation to reveal any differences between the effect on attenuation spectra of polydispersity versus monodispersity was undertaken. A plot of the resulting spectra appears as Figure 6.12. In this figure all the plots represent relatively narrow particle size distributions or monodisperse dispersions. It can be seen that there is a similarity between the shapes of the spectra when plotted on a logarithmic frequency axis. Indeed, in the region around their maximum turning points, the spectra of monodisperse dispersions apparently are identical but translated in absolute values of frequency and attenuation. It is interesting to note that even when modelling such narrow particle size distributions, modelled monodisperse dispersions clearly exhibit higher attenuation values at their maximum turning points than polydisperse dispersions of similar concentration.

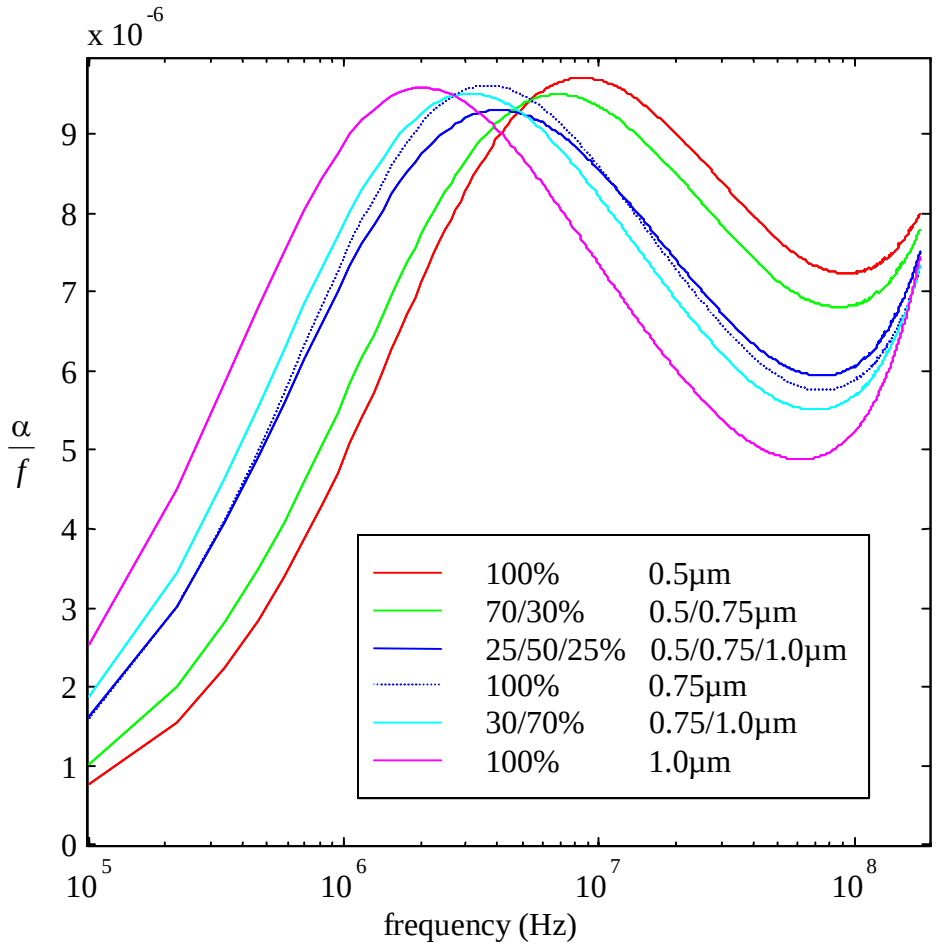

Figure 6.12 Modelled attenuation versus frequency spectra of 4% v/v aqueous silica dispersions at 30°C showing the relationship of spectral shape to particle diameter and polydispersity

Figure 6.12 illustrates the changes to the spectra of dispersions that go in stages through:

a. 0.5µm monodisperse

b. 70% 0.5µm and 30% 0.75µm

c. 25% 0.5µm, 50% 0.75µm and 25% 1µm

d. 0.75µm monodisperse

e. 30% 0.75μm and 70% 1μm

f. 1μm monodisperse

Inspection of Figure 6.12 shows the general rule how, as the mean diameter of a dispersion's particle size distribution increases, the frequency of the maximum turning point decreases. Conversely, as the width of a dispersion's particle size distribution increases the value of attenuation at the maximum turning point decreases. Another point worthy of note is that the frequency of the maximum turning point for a symmetrical particle size distribution centred on 750nm, described in (c) above, has a higher value than that for a 750nm monodisperse modelled dispersion. Other numerical experiments showed the same effect, that in the case of a symmetrically distributed particle size distribution the smaller particles dominate the scattering effects. This could be visualized as the 'centre of effect' or *effective mean* of a distribution is to the left (smaller in diameter) of the statistical mean, although it is not simply related to the number of scatterers.

Figure 6.13 illustrates the effects on phase velocity and attenuation spectra of greater degrees of polydispersity than those depicted in Figure 6.12. Some of the statistics of the plots in Figure 6.13 are listed in Table 6.2. It is clear from Figure 6.13 that the degree of polydispersity in a size distribution is reflected in the kurtosis of the modelled attenuation spectrum. As the standard deviation, σ_{log}, of a lognormal particle size distribution is increased, then the modelled attenuation spectrum becomes flatter, and both the frequency and attenuation values at the maximum turning point decrease.

If this modelled phenomenon accurately reflects the behaviour of practical dispersions, the polydispersity of the particle size distribution of particles in a dispersion could be ascertained from the shape of the attenuation spectra around the maximum turning point.

Close inspection and comparison of the plots for monodisperse and symmetrical distributions in Figure 6.12 reveal a degree of similarity or proportionality in the gradient of the relatively-straight line portion on the left and right flank of each curve before and after the maximum turning point.

The assymetrical distributions appear to have assymetrical left and right flanks. When an assymetrical distribution is dominated by smaller particles, as in distribution (b), it appears to exhibit greater similarity to the right flank of the monodisperse spectrum, and when an assymetrical distribution is dominated by larger particles, as in distribution (e), it appears to exhibit greater similarity to the left flank of the monodisperse spectrum. This topic would merit further research.

modal particle diameter (μm)	σ_{log}	μ_{log} (μm)	f_{max} (MHz) predicted by μ	modelled f_{max} (MHz)	diameter (μm) predicted by modelled f_{max}
1.0	0.1	1.0100	1.9739	2.008	1.0017
1.0	0.2	1.0408	1.8547	1.948	1.0165
1.0	0.3	1.0942	1.6718	1.839	1.0450
1.0	0.4	1.1735	1.4458	1.680	1.0915
1.0	0.5	1.2840	1.1996	1.511	1.1487
1.0	0.6	1.4333	0.9548	1.342	1.2162
1.0	0.7	1.6323	0.7290	1.014	1.3918
1.0	0.8	1.8965	0.5340	0.8057	1.5547
1.0	0.9	2.2479	0.3753	0.6069	1.7819
1.0	1.0	2.7183	0.2530	0.5945	1.7997

Table 6.2 Comparison of modelled and predicted particle diameter versus frequency of maximum turning point, f_{max}, for 1μm modal particle size distributions with varying standard deviations, σ_{log}.

An investigation was undertaken to see if the maximum turning point frequency of a polydisperse particulate dispersion and the statistical moments of the particle size distribution were related. Table 6.2 lists the numerical values of the modelled frequency of the maximum turning points of the plots depicted in Figure 6.13, which correspond to

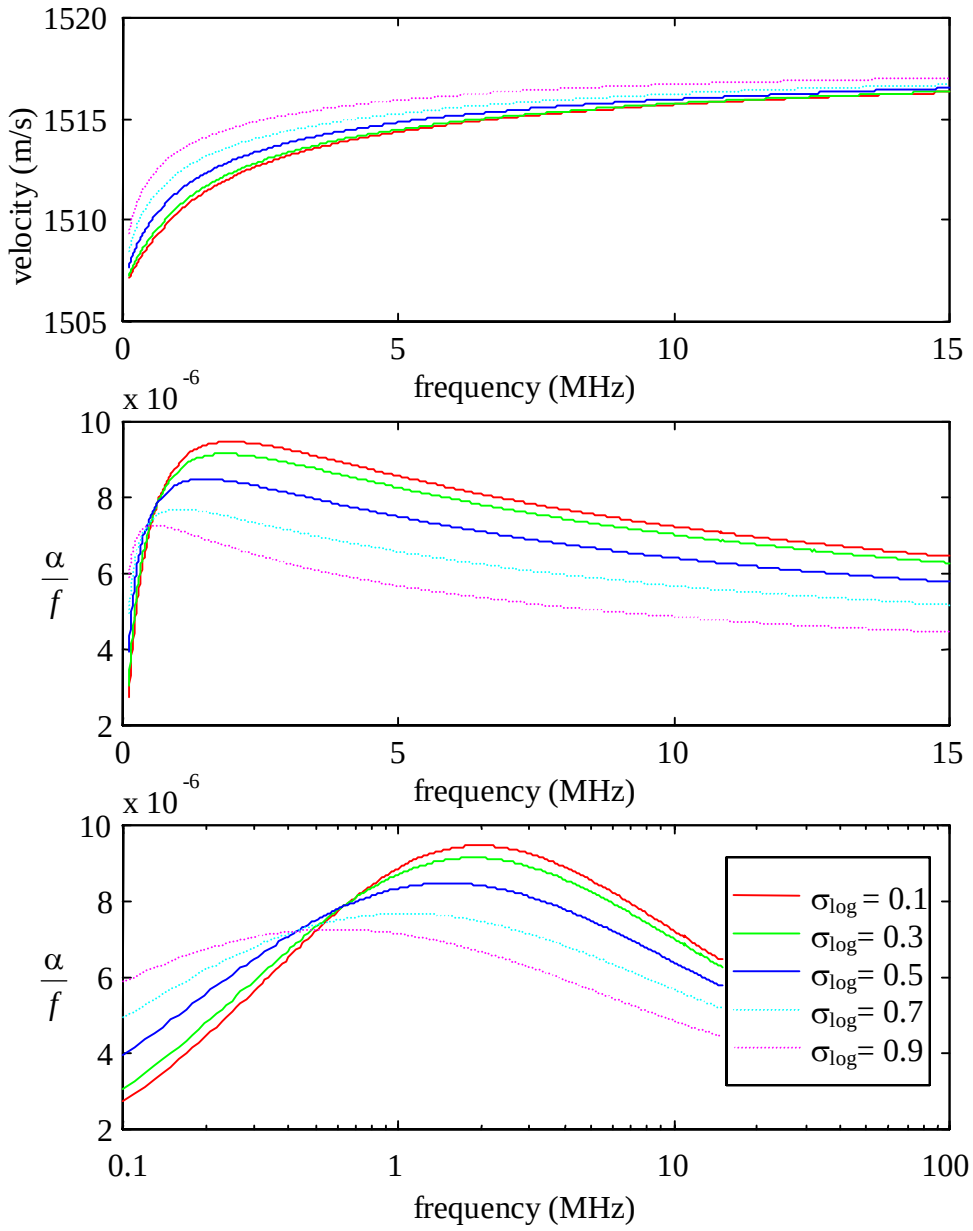

Figure 6.13 Phase velocity and attenuation versus frequency spectra of 4% v/v modal value of 1μm aqueous silica dispersions at 30°C, showing the relationship of spectral maximum turning point frequency location and kurtosis to particle diameter and degree of polydispersity. All the particle size distributions are lognormal. The attenuation plots are of the same data on different frequency axes

different particle size distributions, all centred on a modal diameter of 1μm. A predicted frequency value of the maximum turning point, based on the logarithmic mean and using the relationship given by Equation (6.2) and Table 6.1, was calculated and is shown. The predicted frequencies of maximum turning points and those modelled do not match, although there appears to be a straight line correlation between them. Conversely, the relationship given by Equation (6.2) and Table 6.1 was used to predict the effective mean particle diameter of each particle size distribution, based on the modelled maximum turning points. Again, it was found that the *effective mean* particle diameter is always to the left (smaller) than the statistical mean particle diameter of a given distribution. The relationship between statistical mean, standard deviation and effective mean is not a simple one and would merit further research.

6.9 Sensitivity of modelled attenuation and phase velocity spectra to variations of input values of physical properties

The problems associated with ascertaining sufficiently accurate physical properties of the constituent materials of a modelled dispersion were mentioned briefly in §6.3. The problem is complicated by the need not only to know the value of a physical property but also the sensitivity of the model to variations or errors in that property. The latter point is of crucial importance if it is accepted that practical dispersions will consist of materials that are themselves of variable quality, origin or structure. It then follows that there is no 'correct and accurate' value for a particular physical property – it is a variable that occupies a probability distribution in its parameter space. Hence, the use of the word 'physical constant' can be misleading. The only exceptions might be where properties of the material in question can be tightly controlled, for example, the case of extremely pure water as the

continuous phase. Even this would be difficult or impractical outside a laboratory or pharmaceutical setting.

6.9.1 Sensitivity of modelled attenuation and phase velocity spectra to particle coatings and addition of particle dispersing agents

Another complicating factor is the effect of chemical and electrical phenomena at the particle-continuous phase interface. These phenomena can give rise to what is effectively a 'third phase', an interfacial boundary layer with physical properties not shared with either of the dispersed or continuous phases. The thickness and nature of this third phase could vary with such factors as the presence of surfactants, presence and ionic strength of electrolytes, and electrical activity (which can be affected by such things as gravity, agitation, changes of speed or direction of flow). The contribution of third phase effects would almost certainly grow as particle size decreases because the thickness and volume of the third phase would become progressively greater, relative to the radius and volume of the particle. The addition of dispersing agents could also have significant effects on the physical properties of the continuous phase.

6.9.2 General investigation of the sensitivity of modelled attenuation and phase velocity spectra to variations in the physical properties of the continuous and dispersed phases

The ECAH model requires seven physical properties of each of the two phases as inputs to the calculations. Varying the value of any one property up or down can affect the

attenuation and phase velocity output of the model at a particular frequency point. The size and direction of the variation in output will be a function of:

a. The nature of the dispersed phase
b. The nature of the continuous phase
c. The output being considered
d. The property being varied
e. The frequency value
f. The particle size
g. The % v/v concentration of the dispersion
h. The temperature of the dispersion

All of these factors might act alone or in combination. To reduce the scale of an investigation into the problem of sensitivity of the model to variations in input properties, the number of variables was reduced. A sensitivity analysis was undertaken using the following assumptions:

a. Only five dispersed phase materials would be examined, these were chosen to represent a contrasting range of categories of materials with diverse physical properties
b. Only aqueous dispersions would be examined
c. The effect on total velocity and total attenuation would be examined
d. Each of the possible 14 input physical properties would be varied individually and in isolation using an increment of 1% to +20% and –20% of a central value

e. The effects would be examined at fixed frequency points of 100kHz, 1MHz, 10MHz, 100MHz and 200MHz
f. The effects would be examined at fixed dispersed phase particle sizes of 10nm, 100nm, 1μm, 10μm, 100μm and 1mm diameter.
g. The dispersed phase concentration was fixed at 10% v/v, which was considered a concentration encountered in practical applications but high enough to ensure that subtle effects were not lost due to computer floating point arithmetic rounding
h. The temperature was fixed at 25ºC

The full results of the above investigation amount to (working through the foregoing Subparagraphs a to h) 5×2×14×41×5×6 = 172,000 individual results, each of which consisted of a floating point number to 19 decimal places. Therefore, only a synopsis of the results and a generalized analysis of them appear as Appendix D.

6.10 Effect of variations in the physical properties of the continuous and dispersed phases on the comparison between experimental and modelled attenuation and phase velocity spectra

Appendix D examines the effects on modelled attenuation and phase velocity spectra of variations in the values of physical properties used in the calculation of the ECAH model. As a corollary to that, it is highly likely that such variations would cause a change in predicted particle size and/or % v/v concentration by a system of spectral matching such as the inverse RMS difference algorithm described in §6.5. Variations in predicted particle size and/or % v/v concentration caused by the use of values for physical properties that

differ from the actual values pertaining to the materials of interest, which might be the subject of ultrasonic spectroscopy in the laboratory or as part of an industrial process, are of great practical interest. For this reason a more specialized investigation than that detailed in Appendix D was undertaken, specifically looking at the differences between the experimental and modelled 125nm, 320nm and 520nm 4% v/v concentration aqueous silica dispersions described in §6.3 and §6.4. Figures 6.2, 6.3 and, to a lesser extent, Figure 6.1 show reasonably good agreement with expectations. Nevertheless, there was some deviation from expectations, particularly with respect to particle size. This was highlighted in Figures 6.4, 6.5 and 6.6 which show that the experimental and appropriate modelled spectra are generally similar in the level of attenuation or phase velocity but show some marked differences in slope or degree of curvature. The latter is particularly noticeable in Figure 6.6 where the maximum turning point of the modelled 520nm aqueous silica (which is independent of concentration) is about 7.8MHz but that of the experimental data, although apparently distorted by noise, is clearly higher at above 10MHz. This difference is significant and, using the heuristics detailed in §6.5 the experimental maximum turning point indicates the predominance of about 460nm diameter silica particles, using the physical properties listed in Appendix E. Consequently, the frequency and attenuation value of the maximum turning point of the alpha over frequency spectrum was made the focus of attention in the subsequent investigation.

The investigation of the effects of polydispersity on modelled spectra detailed in §6.8 indicated that if the particles used in the experiments possessed a narrow polydisperse size distribution as opposed to being truly monodisperse, that would account for the effective mean particle diameter being less than the statistical mean. However, for the purposes of

the following analysis, the 125nm, 320nm and 520nm particles are assumed to be monodisperse.

Each of the 7 physical properties were varied by up to ±50% and the effect on the maximum turning point was noted. The effect of varying the thermo-physical properties of either phase was of limited significance, which is not surprising in a density-contrast dominated combination such as aqueous silica. Moreover, with the exception of temperature, μ' and η, variation of the other parameters tended to change the absolute values of attenuation and phase velocity without causing any significant change in spectral gradient or degree of curvature. Variations in μ' did, however, cause some movement in frequency of the maximum turning point and from this investigation it was found that, in the case of aqueous silica dispersions, there was a straight-line relationship between the x of Equation (6.2) and μ'. Although the frequency of the maximum turning point moved in response to μ', the spectrum maintained roughly the same shape. The greatest variation in modelled attenuation spectra was caused by variations in the values of η and temperature. The latter acted almost solely through its indirect effect of modifying the value of η for water. Even slight variations in the viscosity value for the water continuous phase caused significant changes in the modelled attenuation spectra, both in the frequencies of the maximum turning points and in the general slope and degree of curvature of spectra. If all other properties were as detailed in Appendix E except the viscosity of the aqueous continuous phase, η, which was increased in value from 8×10^{-4} Pascal seconds to 10×10^{-4} Pascal seconds, then the maximum turning points of the modelled and experimental attenuation spectra of the 520nm diameter particle dispersion coincided.

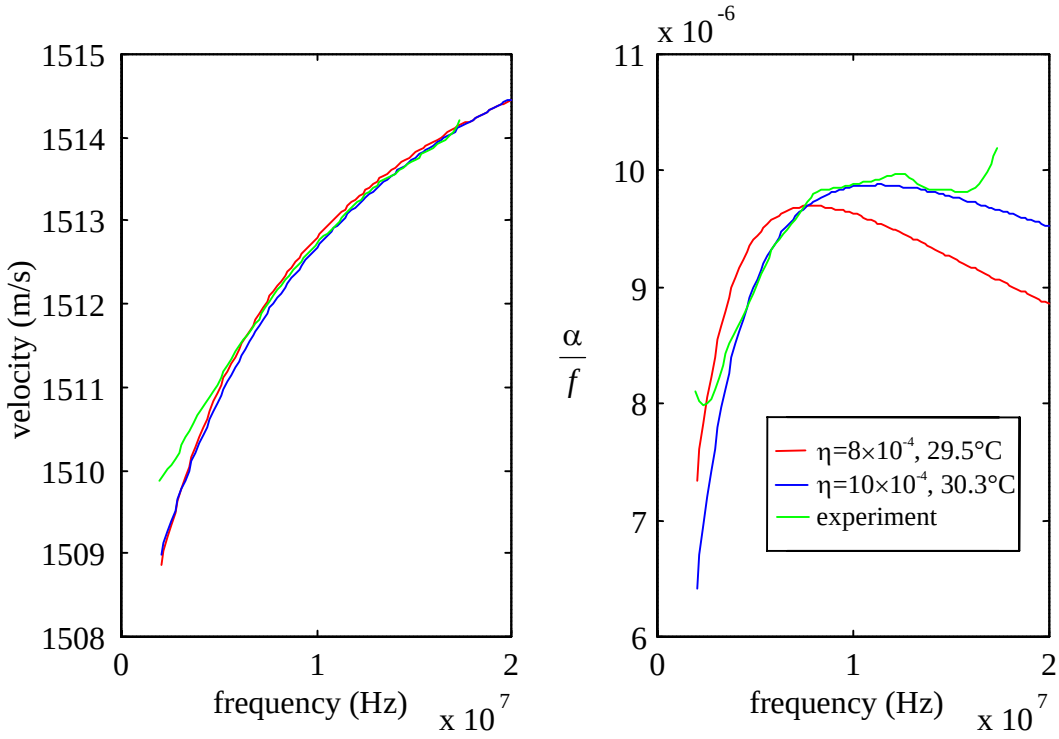

Figure 6.14 Comparison of experimental and modelled phase velocity and attenuation versus frequency of an aqueous silica dispersion of 520nm particles at 4.05% v/v using two alternative values of continuous phase viscosity

This is shown in Figure 6.14. The values of modelled % v/v concentration and temperature were chosen to provide visually good agreement between plotted experimental and modelled 520nm phase velocity. Inspection of Figure 6.14 reveals much better agreement, over most of the frequency range of interest, between experimental and modelled attenuation when a viscosity value of $\eta=10\times10^{-4}$ was used instead of $\eta=8\times10^{-4}$ to model the data. To ascertain whether the revised viscosity value merely fitted the modelled data onto the experimental data in a concidental manner, the revised viscosity value was also used to model aqueous silica dispersions of 125nm and 320nm diameter particles.

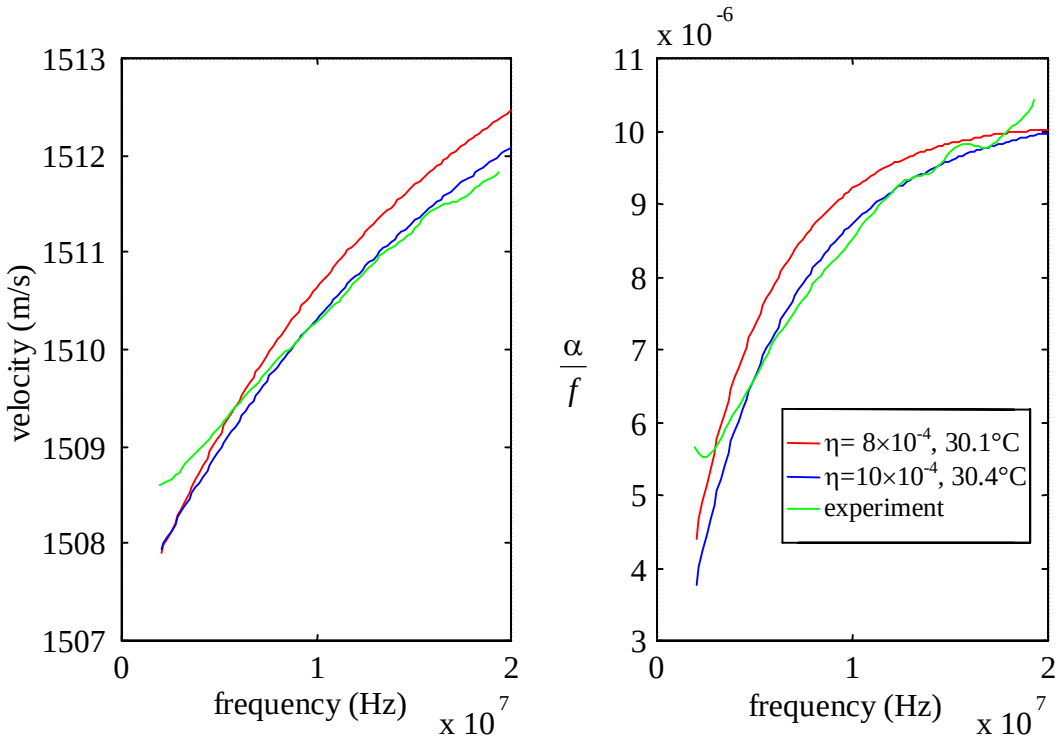

Figure 6.15 Comparison of experimental and modelled phase velocity and attenuation versus frequency of an aqueous silica dispersion of 320nm particles at 4% v/v using two alternative values of continuous phase viscosity

Comparisons of the revised modelled data with experimental data for the 320nm dispersions appears as Figure 6.15 and the same comparisons for the 125nm dispersions appears as Figure 6.16. The values of modelled % v/v concentration and temperature were chosen to provide visually good agreement between plotted experimental and modelled phase velocity of 320nm and 125nm dispersions respectively.

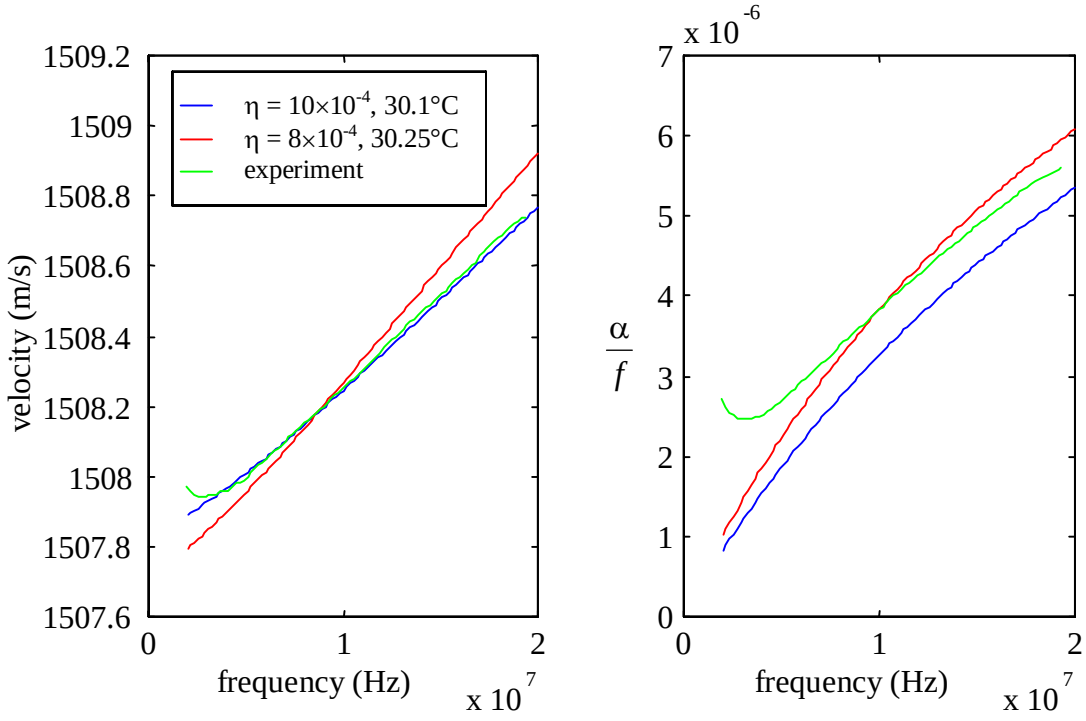

Figure 6.16 Comparison of experimental and modelled phase velocity and attenuation versus frequency of an aqueous silica dispersion of 125nm particles at 4% and using two alternative values of continuous phase viscosity

Inspection of Figure 6.15 reveals good agreement, over most of the frequency range of interest, between experimental and modelled phase velocity and attenuation when a viscosity value of $\eta=10\times10^{-4}$ was used instead of $\eta=8\times10^{-4}$ to model the data. In Figure 6.16, although the absolute values of experimental and modelled attenuation do not agree closely, the spectrum modelled using the revised viscosity value shows greater similarities in gradient and degree of curvature than that modelled using the original value of viscosity. From the evidence in Figures 6.14, 6.15 and 6.16, which represent three separate experiments using different sized particles (but provided from the same source, so in all probability sharing the same physical properties of continuous and dispersed phases), it

appears that the viscosity (or *effective viscosity*) was higher than that assumed for pure water. The viscosity could be modified by:

a. The presence of dispersing agents or dissolved contaminants
b. An effect of particle concentration leading to un-modelled phenomena such as inter-particle interactions or particle surface effects
c. An artifact of the model

The fact that the revised viscosity gave best results for the larger particles, but still gave better results for all three sizes would tend to discount the latter two hypotheses and strongly suggests that the effective viscosity of the continuous phase was greater than the measured viscosity of pure water at the experimental temperature (water possesses a viscosity of approximately 8×10^{-4} at a temperature of 30°C and 10×10^{-4} at 20°C).

Based on an assumption that the revised viscosity value was correct, the inverse RMS comparison procedure described in §6.5 was repeated using modelled spectra incorporating the revised viscosity value. The comparison plots, analogous to those of Figures 6.1, 6.2 and 6.3, appear as Figures 6.17, 6.18 and 6.19. The comparisons of the 125nm spectra in Figure 6.17 are, like their counterparts in Figure 6.1, inconclusive. However, the 320nm and 520nm comparisons depicted in Figures 6.18 and 6.19 do show even better agreement between experiment and model than the corresponding Figures 6.2 and 6.3.

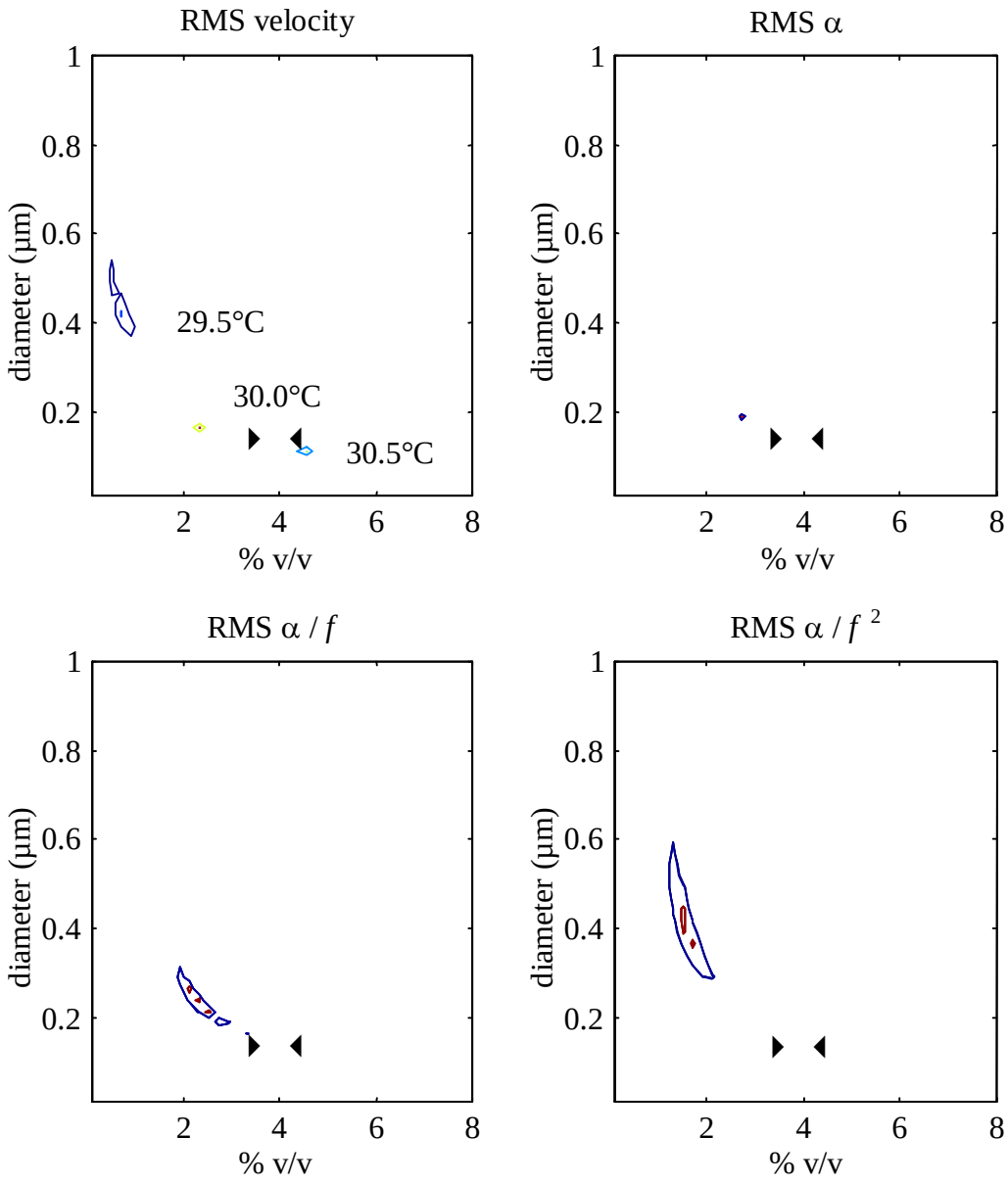

Figure 6.17 Contour plots showing reciprocal of RMS difference between experimental data from a nominally 125nm diameter and between 3.67 and 4.1% v/v concentration (range denoted by ▸ ◂) aqueous silica dispersion and modelled data over the 10nm to 1000nm and 0.01% to 8.00% size-% v/v concentration space, at modelled temperatures of 29.5ºC, 30.0ºC and 30.5ºC, and using a revised value for viscosity of the continuous phase (the contours corresponding to each of the three temperatures effectively overlay each other on the attenuation plots)

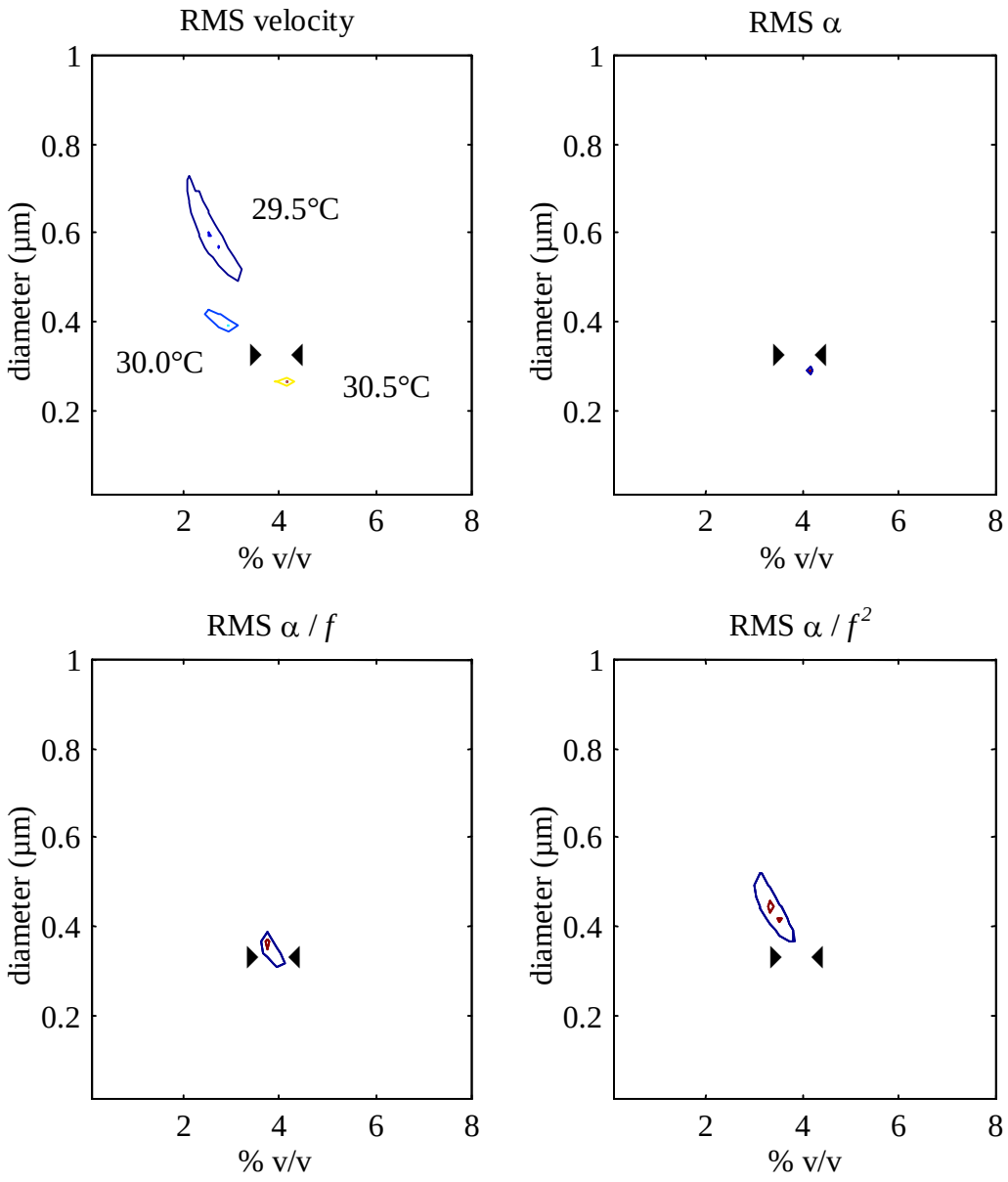

Figure 6.18 Contour plots showing reciprocal of RMS difference between experimental data from a nominally 320nm diameter and between 3.67 and 4.1% v/v concentration (range denoted by ▶ ◀) aqueous silica dispersion and modelled data over the 10nm to 1000nm and 0.01% to 8.00% size-% v/v concentration space, at modelled temperatures of 29.5ºC, 30.0ºC and 30.5ºC, and using a revised value for viscosity of the continuous phase (the contours corresponding to each of the three temperatures effectively overlay each other on the attenuation plots)

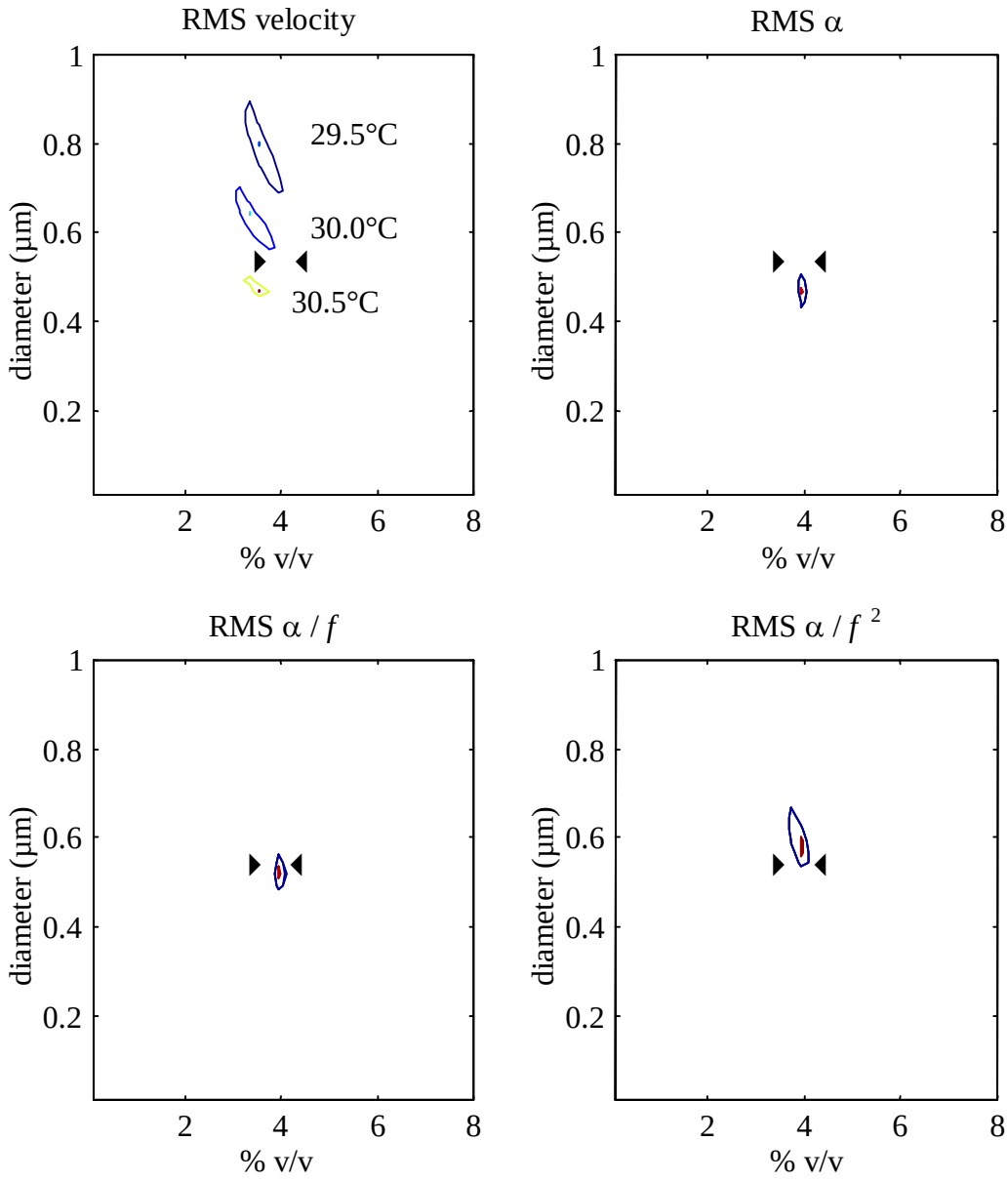

Figure 6.19 Contour plots showing reciprocal of RMS difference between experimental data from a nominally 520nm diameter and between 3.67 and 4.1% v/v concentration (range denoted by ▸ ◂) aqueous silica dispersion and modelled data over the 10nm to 1000nm and 0.01% to 8.00% size-% v/v concentration space, at modelled temperatures of 29.5ºC, 30.0ºC and 30.5ºC, and using a revised value for viscosity of the continuous phase (the contours corresponding to each of the three temperatures effectively overlay each other on the attenuation plots)

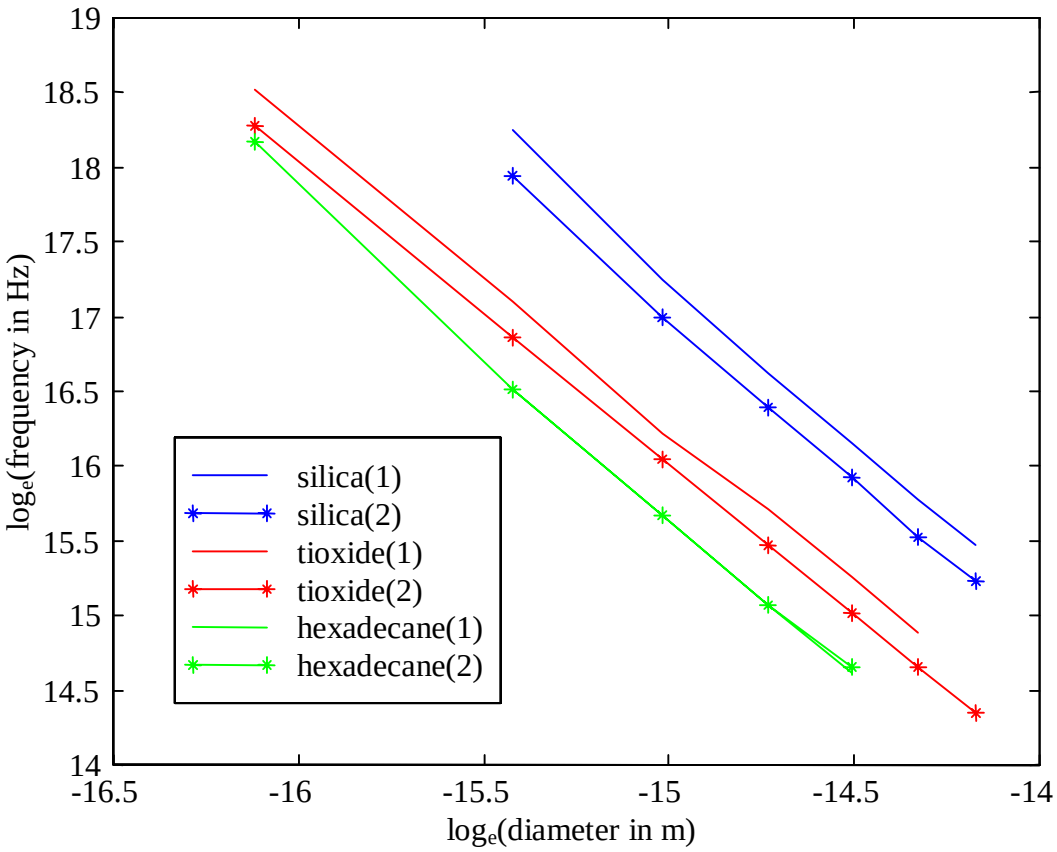

Figure 6.20 Modelled log$_e$ of frequency of maximum turning point versus log$_e$ of particle diameter for aqueous suspensions of silica, titanium dioxide AHR pigment and hexadecane using two alternative values for viscosity of the continuous phase: 8×10^{-4} denoted by (1) and 10×10^{-4} denoted by (2)

The strong linkage observed between continuous phase viscosity and the frequency of maximum turning point, described at the beginning of this section, was investigated for materials other than silica. The straight line relationship in the logarithmic domain between particle diameter versus frequency of maximum turning point, described in §6.6, was plotted for silica, titanium dioxide AHR pigment and hexadecane using the both values of continuous phase viscosity. The plots appear as Figure 6.20.

From Figure 6.20 it can be seen that, for silica and titanium dioxide, a change in continuous phase viscosity results in a similar, but shifted in the logarithmic domain, relationship between particle size and the spectral shape of attenuation. However, the continuous phase change in viscosity appears to have little or no effect on the attenuation spectral shape of an aqueous hexadecane dispersion. The most likely explanation for this is that, within the frequency range of interest, the dominant loss mechanism for aqueous silica and titanium dioxide dispersions is hydrodynamic whereas the dominant loss mechanisms in aqueous hexadecane dispersions are compressive and thermal. Continuous phase viscosity is a major factor in hydrodynamic loss mechanisms but does not contribute significantly to compressive or thermal losses. A topic for further research would be the contribution of continuous phase viscosity in high density contrast dispersions, and compressibility and thermal properties in low density contrast dispersions, to the *y* coefficient of Equation (6.2).

6.11 Summary

This chapter examined those properties of phase velocity and attenuation spectra that might collectively form the unique signature of a dispersion. Because a single value of attenuation or phase velocity at a single frequency value might form part of the spectra of an infinite number of different dispersions, it follows that a sequence of such values is required for a unique signature. The properties of a sequence of phase velocity or attenuation values could be summarized as an absolute value and gradient at a given value of frequency. Together, these have been referred to as spectral shape. A highly distinctive combination of absolute values and gradient occurs over the maximum turning point in phase velocity and the alpha over frequency representation of attenuation. A similarly distinctive combination of absolute values and gradient occurs over the minimum turning

point in phase velocity and the alpha over frequency representation of attenuation. It was found that the maximum turning point obeyed a predictable relationship with particle diameter while the minimum turning point obeyed a predictable relationship with particle diameter and concentration. If all physical properties were known accurately, it would be possible to uniquely identify a monodisperse particulate dispersion in terms of particle diameter and concentration from a knowledge of only two frequencies – the maximum and minimum turning points.

For a polydisperse system the situation is more complicated. However, there is a relationship between degree of polydispersity and the kurtosis of the spectrum around the maximum turning point. There also appears to be a relationship between the gradient of the left and right spectral flanks before and after the maximum turning point and whether the mode of the particle size distribution is skewed left (smaller diameter) or right (larger diameter). These features could be exploited as the basis of an algorithmic inversion of experimental data to derive particle size, particle size distribution and concentration of a dispersion.

The success of such an algorithmic inversion of experimental data would depend upon the accuracy of the model and the number of physical processes it describes that, in turn, depend upon an accurate knowledge of a number of physical properties of the continuous and dispersed phases and experimental temperature. The relative importance of each of the physical properties was examined. The numerical modelling was cross-referenced to experimental results to corroborate some of the points raised above. A crude algorithm to determine particle size and concentration of a dispersion using experimental results was

demonstrated. It gave reasonable agreement with *a priori* knowledge of the dispersions and served to highlight the problems inherent with numerical models that seek to reproduce a comprehensive range of acoustic loss mechanisms.

7. Summary, conclusions and recommendations for further research

7.1 Summary and general conclusions

Many commercially important products consist of or include particulate dispersions. Frequently, the particle size, particle size distribution and concentration of the dispersed phase are of crucial importance to the nature or quality of the finished product. Therefore, a reliable method of ascertaining these properties of the dispersed phase would be of significant commercial and industrial utility. Some methods are already available but often they suffer from significant disadvantages, such as their being restricted to optically transparent dispersions, narrow ranges of particle sizes, or dispersions that possess particular electrical properties. An instrument using ultrasonic spectroscopy would be able to categorize optically transparent or opaque dispersions of almost any combination of materials over a wide range of particle sizes and concentrations, without the need for any off-line preparation such as dilution. An instrument to achieve these goals ideally would consist of two parts. The first would measure the ultrasonic attenuation and phase velocity spectra through a dispersion. The second would model an appropriate number of similar dispersions for comparison against the practical measurements to find a close match that would indicate dispersed phase particle size, size distribution and concentration. Of the second part, accurate modelling of particulate dispersions and the optimum method of comparing modelled and experimentally measured data present a number of difficulties. These are the topics of this thesis.

The ultrasonic attenuation and phase velocity spectra characteristic of a particulate dispersion are linked by the Kramers-Kronig relationship although, over the restricted

frequencies obtainable in practice, both contain independent information. The spectra of some dispersions, over certain frequency intervals, are primarily the result of only one or two simply modelled loss mechanisms. In these instances some of the simple models reviewed in Chapter 1 are entirely adequate for comparison with practical measurements. However, their applicability has strict limits. If it is desired to employ a single, comprehensive model over a wide range of frequencies and with particulate dispersions possessing material properties lying anywhere within the range encountered in practice, then a more complicated model incorporating all the most significant loss mechanisms is essential. Such a comprehensive model is that of Epstein & Carhart, which was extended by Allegra and Hawley, and collectively known as the ECAH model.

The most significant loss mechanisms include intrinsic losses, compressive scattering away from the direction of propagation, and irretrievable conversion of compressive energy into shear and thermal waves. As a corollary to incorporating these loss mechanisms, the physical properties, which are necessary to calculate the losses in both phases of the dispersion, must be incorporated into the model. In the case of the ECAH model, as well as the temperature of the dispersion and the frequency value of interest, seven physical properties of each phase are required. Chapter 2 detailed the nature of these properties and their place in the calculations. For some materials, for example pure water, all of the properties pertaining to a wide range of temperatures are well known and documented. However, for many materials this is not the case and it is a major difficulty when intending to use the model. Particularly, thermal and acoustic properties for solids can be difficult or impossible to find in the literature. Even the commonest continuous phase encountered in industrial dispersions – impure water containing dissolved contaminants, surfactants or

ionic dispersing agents – presents a problem. In addition, common sense reveals that the variability of industrial grade materials that might make up a dispersed phase are unlikely to possess a single, accurate set of values of physical properties that could be universally applied in all modelling. The effect on the output phase velocity and attenuation values of variations in each of the seven physical properties was calculated, tabulated and analyzed in Appendix D. Chapter 6 includes a more specific examination of this problem and its potential effect on the process of predicting particle size and concentration of a dispersion from experimental results. It is in the form of a case study, the results from three dispersions containing different diameters of particle almost certainly composed of the same variety of silica.

Mathematically, the ECAH model enables the calculation of the amplitude of compressive, shear and thermal waves reflected, refracted and diffracted by a single particle in any given direction. To model the effect of a number of scattering particles, which together comprise a particulate dispersion, requires the incorporation of the numerical results of ECAH single scattering into a multiple scattering model. Multiple scattering models were reviewed and compared in Chapter 4. The simplest of these, and mathematically the most versatile, is the Foldy model. It is easily adapted to incorporate polydispersity but, because it does not include second order terms that represent re-scattering of already scattered waves, it is limited to situations where second order scattering is insignificant, that is to say, dilute dispersions. The most comprehensive and complicated of the multiple scattering models is that of Lloyd & Berry. It incorporates second order scattering in the purely forward, purely backward and all radial directions. However, it incorporates neither higher than second

order scattering nor, in common with all the other multiple scattering models, does it model particle to particle interactions. The significance of one or both of these mechanisms would increase with concentration, especially at higher levels - above about 8% v/v for some dispersions. The usefulness of the Lloyd & Berry model is limited by its being mathematically restricted to monodisperse dispersions but, when modelling such systems, it is shown to offer worthwhile advantages of improved accuracy over the simpler models.

The ECAH model is mathematically complicated and poses some difficulties when incorporating it into computer software. It requires the computation of an infinite series of terms, each containing: a complex scattering coefficient, A_n; spherical Bessel and Hankel functions of compressive, shear and thermal complex wavenumber argument; and ordinary and associated Legendre polynomials that are functions of scattering direction. The first order multiple scattering model of Foldy and the relatively simple second order multiple scattering models, for example that of Waterman & Truell, consider only forward and backward scattering. For this reason the computation of Legendre polynomials is trivial as they assume one of only two values of ± 1 associated with scattering angles of 0 or π. The Lloyd & Berry model requires the computation of a complicated term that integrates an infinite series containing Legendre polynomials over a continuum between 0 and π. This can be accomplished using either numerical quadrature techniques that are computationally very expensive or evaluated directly, but only if the closed form solution to the integral is known. Closed form solutions of the Lloyd & Berry integral terms for the infinite series truncated at orders of up to 20 were calculated and those up to 18 are listed in Appendix B2. However, irrespective of which of the multiple scattering models is used, they all

require the computation of the scattering coefficient A_n, and Bessel and Hankel functions as part of the constituent ECAH model. Although explicit formulae for low orders of Bessel and Hankel functions exist, for higher orders they must be calculated recursively. When attempting to calculate Bessel or Hankel functions with very small or very large arguments, intermediate values in the calculation can cause arithmetic overflow or underflow in a conventional computer program. Also, high orders of n necessitate a similarly high number of recursive calculations that can result in significant rounding errors and loss of accuracy. As the imaginary part of the complex argument passed to Hankel and Bessel functions increases linearly, the value of the function returned respectively decreases and increases exponentially. Both the thermal and shear wavenumbers are obtained by multiplying real coefficients by $(1 + i)$ before being multiplied by the particle radius and passed as arguments to the Hankel and Bessel function calculating software. Therefore, extreme care is needed in the computation of Hankel and Bessel functions if the boundaries of computational stability, which directly translates to the boundaries of particle diameter-wavenumber product, are to be extended upwards and downwards as far as possible. Chapter 3 explains how the many years of specialized research in the field of cylindrical functions, much of it undertaken as part of the US Atomic Weapons Program at Sandia Laboratories, was adapted for use in the calculation of spherical functions for use in the ECAH model. The calculation of the compressive scattering coefficient, A_n, included the results from the calculation of the spherical functions into a series of six equations in six unknowns. This problem, expressed in the form of a 6×6 and single column augmented matrix, contained instances of the returned results from the computation of Bessel and Hankel functions on each of the lines of the matrix. Consequently, as the frequency or particle size varies linearly, different matrix components on the same line are increasing

and decreasing exponentially. Therefore each line contains six numerical values, some of which are approaching the limits of the largest floating point number simultaneously as some others are approaching the limits of the smallest floating point number. Pre-scaling or conditioning of the matrix in this form is impossible. In this situation, the matrix is ill conditioned and its solution becomes unreliable as the particle size-wavenumber product becomes very large or very small. Complicated techniques to calculate spherical functions in the logarithmic domain and to incorporate them into the matrix as pre-scaled functions without affecting the solution to the matrix are explained in Chapter 5.

The infinite series that comprises the solution of the ECAH model does not have a closed form solution so, when it is computed numerically, it is truncated. The choice of the order at which the series is truncated will affect the accuracy of the final numerical result. The polar diagrams in Appendix B3 that correspond to different orders of scattering show that scattering of order zero is monopolar. This corresponds to the scattering intuitively associated with the thermal properties and compressibility of the scattering particle. Similarly, the first order scattering polar diagram is dipolar and is intuitively associated with the backwards and forwards oscillation of the particle causing shear in the continuous phase around the particle. Intuitive physical explanations for higher orders of scattering are difficult to visualize but are probably due to distortion of the particle and interaction or superposition of waves within and outside the particle. For these reasons it has been usual for workers in this field to consider the main loss mechanisms included in the ECAH model to be adequately covered by the zero and first order terms of the infinite series. As a consequence, most of the literature is limited to considering only the zero, first and

sometimes second order terms. It was shown in Chapter 2 that such an assumption can lead to errors much greater than those associated with reasonable experimental accuracy. An investigation was undertaken over a range of material combinations, frequencies and particle sizes, which computed the series up to a point where it converged beyond oscillation to a single complex value, within the confines of 80-bit Intel arithmetic – 19 decimal places. This point was called the fully converged final value. For each combination of continuous and dispersed phase materials, particle size and frequency, the order of n required for convergence to within 10%, 1%, 0.1%, and 0.01% of final value was calculated and is tabulated in Appendix C. Some of the results appear as plots in Chapter 2 and reveal a straight line relationship over a practically useful range, which links particle diameter, frequency and compressive wave velocity in the continuous phase to the order of n required for convergence to within 0.01% of final value.

Inspection of the tables in Appendix C shows that at high frequencies and large particle sizes, the order of n required for convergence to within 0.01% of final value is very much higher than the order 2 mentioned earlier. For particles 1mm in diameter and at frequencies around 200MHz, order of $n \cong 450$ is required for convergence to within 0.01% of final value in attenuation. Calculation using the Lloyd & Berry model, which incorporates the most sophisticated representation of second order terms, is not a practical proposition beyond order $n = 20$. This implies an upper limit to its use of the real part of the compressive wavenumber-particle radius product, $k_c r$, of approximately 17 which roughly equates to a frequency of 80MHz and a particle diameter of 100μm in an aqueous continuous phase. For dispersions with the real part of their compressive wavenumber-particle radius products above 17 the Waterman & Truell or Foldy models are the

alternatives. The concentration of the dispersion being modelled, which governs the significance of second order scattering, might influence the choice of model although second order scattering in polydisperse systems is not modelled adequately by any of the models reviewed. For this reason, if the dispersion being modelled is polydisperse, Chapter 4 showed that the Foldy model gives almost equally as good results as any other reviewed model at considerably lower computational cost.

Chapter 6 illustrated the phenomena of maximum and minimum turning points and outlined the development of a relationship between the particle size and concentration of a dispersion and the frequencies at which they occurred. It showed that the coefficients used to construct an equation for that relationship were related to physical property values. The spectrum around such turning points also provided a predictable, distinctive and characteristic feature, which was useful for comparison between experimental and modelled data. There was some evidence that the kurtosis and gradient of the flanks of a spectrum around the maximum turning point bore a relationship to the moments of the associated particle size distribution. The characteristic turning points for the 320nm and 520nm diameter particulate dispersions were within or near to the range of experimental data, and reasonably good matches using the inverse RMS matrix were obtained. However, the characteristic turning points for the 125nm diameter particulate dispersion was much higher than the range of experimental data and matching was less conclusive. One surprising result was the robustness of the relatively unsophisticated inverse RMS matrix, which produced reasonably good agreement with *a priori* knowledge of particle size and concentration even when using apparently suspect physical property values. The value of phase velocity data, either stand-alone or as an *a priori* adjunct to the attenuation data, was

demonstrated. This was particularly true in the case of the smallest particle diameter where the velocity correlation was of better quality than the attenuation correlation.

In Chapter 1 the stated object of this thesis was to demonstrate the feasibility of modelling the behaviour of sound propagation through a combination of media accurately enough to enable the correlation of modelled and experimentally measured acoustic attenuation and phase velocity. The feasibility of this proposition has been demonstrated, although more work needs to be done on the back fitting of experimental to modelled data. As an integral part of the back-fitting process it is highly desirable that algorithms exploit the characteristic features of ultrasonic spectra described in Chapter 6 to achieve a best fit over a carefully selected frequency range in preference to an indiscriminate minimum distance correlation over an arbitrary frequency range. Algorithms that exploit those characteristic features are likely to be more robust than minimum distance correlation methods and, most importantly, much faster. It should be possible to dispense with comprehensive sets of look-up tables for point by point comparisons and replace them with a rule-based discriminator. This would enable real-time characterization of particulate dispersions using relatively modest monitoring equipment and computing capacity – making it a viable method of on-line monitoring in industrial applications.

7.2 Principal conclusions of this thesis

The principal conclusions of this thesis are (an asterisk * following a conclusion denotes work that is presented as original in this thesis):

a. A way of characterizing particle concentration, size and size distribution, on-line and applicable to a wide range of dispersed materials and concentrations, would be of considerable commercial and industrial utility

b. A method of particle sizing using ultrasonic spectroscopy offers significant advantages over alternative methods, including the ability to work on-line and over a wide range of concentrations and particle sizes.

c. An essential function of an ultrasonic spectrometer is the ability to model accurate ultrasonic spectra for correlation with experimental data

d. Although mathematically related, there is complementary useful information suitable for correlation purposes contained in both phase velocity and attenuation spectra

e. Of the models available the most versatile is the ECAH model that can be used to calculate each order of an infinite series representation of the ultrasonic wavenumber

f. A drawback of such a comprehensive model as the ECAH that incorporates all of the significant acoustic loss mechanisms is that it requires values for a wide range of physical properties

g. The values of physical properties are sometimes difficult or impossible to find in the literature and, if they are available, sources often disagree. Variations in the composition and manufacture of materials make it likely that there is no absolutely accurate value for a given physical property

h. Another drawback of the ECAH model is that its use requires the solution of a 6×6 matrix that becomes increasingly ill-conditioned and computationally unstable as

modelled particle diameter or frequency approach upper or lower limits. Modifications to the formulation of the ECAH model that significantly extend both the upper and lower limits were developed by the author *

i. The ECAH model is used in conjunction with a multiple scattering model in order to represent practical systems of scatterers and calculate phase velocity and attenuation

j. Sensitivity of modelled phase velocity and attenuation to variations of an input value of a physical property might or might not be significant, depending upon the property being varied and the nature of the continuous and dispersed phases. The sensitivity to variations of each of the input properties for a range of materials in aqueous dispersion was quantified and analyzed *

k. Knowledge of the nature of the sensitivity of modelled phase velocity and attenuation to variations of an input value can enable the identification and revision of critical input properties to better fit experimental data from dispersions of known characteristics. This procedure could be automated to derive unknown or effective values of physical properties *

l. Truncation of summation of the infinite series representation of the ultrasonic wavenumber at order $n = 2$ can lead to serious errors in the calculation of phase velocity and attenuation. This was demonstrated *

m. The order n at which the infinite series representation of the ultrasonic wavenumber can be safely truncated at a satisfactorily converged summation is an explicit function of compressive wavenumber and particle diameter, and can be determined *a priori* *

n. Summation of the infinite series representation of the ultrasonic wavenumber to higher orders requires the calculation of correspondingly higher orders of spherical Bessel and Hankel functions that are prone to either inaccuracies, errors or excessive computational overhead unless complicated optimizing algorithms, which are described, are employed

o. There can be significant discrepancies in modelled phase velocity and attenuation values between the most comprehensive multiple scattering model of Lloyd & Berry and simpler models

p. The Lloyd & Berry model is the best choice when modelling less-dilute monodisperse systems where second-order scattering is significant but, in common with the Waterman & Truell model, when modelling polydisperse systems it offers no significant advantages over the mathematically and computationally much simpler Foldy model *

q. The Foldy model does not incorporate higher than first order scattering or, like all the models reviewed, particle to particle interactions. Therefore its use is limited to dilute dispersions

r. Use of the Lloyd & Berry model requires the analytical or numerical solution of a complicated integral term. The numerical solution of the integral term is computationally very expensive and an analytical solution only up to order $n = 2$ is available in the literature; an analytical solution up to order $n = 18$ was derived and is presented by the author *

s. A crude scheme that calculates point by point RMS difference between modelled and experimental phase velocity and attenuation spectra can form a reasonably accurate discriminator to determine particle size and concentration of practical dispersions; it

appears to be remarkably robust to significant errors in the modelled spectra apparently caused by incorrect critical input physical properties *

t. Both phase velocity and α/f representations of attenuation exhibit characteristic maximum and minimum turning points where the gradient of the spectrum passes through zero

u. The maximum turning point is an explicit function of effective particle diameter and is independent of concentration *

v. The minimum turning point is an explicit function of effective particle diameter and concentration *

w. The kurtosis of the maximum turning point is a function of the degree of polydispersity of a particulate dispersion *

x. The skew of the maximum turning point is a function of the shape of the particle size distribution of a polydisperse particulate dispersion *

y. The statistical moments of maximum and minimum turning points could form the basis of a robust and computationally efficient particle sizing system capable of operating in real time *

7.3 Recommendations for further research

Although of limited value, the translation of the software used to evaluate Bessel and Hankel functions from using 64-bit to 80-bit arithmetic would extend the effective range of particle size-wavenumber products that the software package could successfully model. This could be of use, particularly if the intention is to model dispersions of very small particles.

There is a pressing need for multiple scattering models to include in their formulation the following features: particle to particle interactions; higher than second order re-scattering; and, most importantly, at least second order and preferably higher re-scattering in polydisperse particulate dispersions. The last of these modifications would enable more accurate modelling of less dilute polydisperse particulate dispersions and could prove crucial in significantly moving the ultrasonic technology out of the laboratory and into industrial applications.

Also of importance if the technology is to be commercially exploited is a way of overcoming the strong dependence of the modelling aspect of acoustic spectroscopy on the availability of values of material properties. The use of alternative models that use a smaller set of physical properties is limited to a more narrow range of applicability than the more comprehensive ECAH model. In Appendix D some of the results are listed and a limited analysis undertaken of the effects of errors in values of material properties. Only variations of a single physical property at one time were investigated. The effects of a combination of errors involving changes to more than one physical property would merit further study. Moreover, a great deal more work remains to be done on the effects of such errors on a system designed to interpret attenuation and phase velocity spectra and render particle size information and concentration.

More sophisticated algorithms to match experimental and modelled data than the inverse RMS matrix would be most useful. It was shown in Chapter 6 that variations in most of the values of physical properties resulted in no effect or simple vertical translation of absolute values of whole spectra. If a matching-algorithm based on shape and value and not simply

on absolute values could be devised it might prove to be relatively immune to errors in many of the physical property values. In the dispersion under scrutiny, only variations in one physical property, viscosity of the dispersed phase, resulted in significant changes to the maximum turning points and general shape of the modelled spectra. It would be useful to extend the scope of the investigation to find the critical physical properties for a range of types of dispersion. It could be possible to automate the back fitting that was done by eye in Chapter 6 to arrive at a value of the critical physical property that provided a better fit of the modelled to experimental data.

If work is to be undertaken to model less dilute and polydisperse particulate dispersions, a suitable range of corresponding, reliable experimental data would be essential for benchmarking the models. Also, if reliable experimental data corresponding to dispersions of different materials and particle size distributions covering a range of modes and standard deviations were available, the relationships between the shape of ultrasonic spectra and the moments of particle size distributions could be corroborated, refined and established quantitatively. Such data, as far as the author is aware, is not available at the moment.

Although largely of academic interest, the list of Lloyd & Berry coefficients in Appendix B2 are all integers or rational numbers. Together they form a complicated but clearly discernable pattern that appears to be a geometric progression. If the analytical form of the progression could be derived it would enable the efficient calculation of Lloyd & Berry coefficients beyond the present upper limit. This would enable the use of the Lloyd & Berry model above a compressive wavenumber-particle radius product, $k_c r$, of

approximately 17 which roughly equates to a frequency of 80MHz and a particle diameter of 100μm in a water continuous phase.

References

Abramowitz M, Stegun IA. *Handbook of Mathematical Functions.* National Bureau of Standards, reprinted with corrections to 10th ed. Dover Publications Inc, New York (1972)

Allegra JR, Hawley *SA. Attenuation of Sound in Suspensions and Emulsions: Theory and Experiments.* J. Acoust. Soc. Am., **51**(5) Part2 1545-1564 (1972)

Amos DE. *Computation of Bessel Functions of a Complex Argument.* Sandia Laboratories Report, **SAND83-0086** (March 1983)

Amos DE. *Computation of Bessel Functions of a Complex Argument and Large Order.* Sandia Laboratories Report, **SAND83-0643** (May 1983)

Amos DE. *Algorithm 644 - A Portable Package for Bessel Functions of a Complex Argument and Non-negative Order.* ACM Transactions on Mathematical Software, **12**(3), (September 1986)

Amos DE & Daniel SL. *A CDC 6600 Subroutine for Bessel Functions* $I_v(x), v \geq 0, x \geq 0$. Sandia Laboratories Report, **SAND75-0152** (September 1975)

Anson LW & Chivers RC *Ultrasonic Velocity in Suspensions of Solids in Solids - a Comparison of Theory and Experiment.* J. Phys. D: Appl. Phys. **26** 1566-1575 (1993)

Batia AB. *Ultrasonic Absorption*: *An Introduction to the Theory of Sound Absorption and Dispersion in Gases, Liquids and Solids*. Clarendon Press. Oxford (1967)

Biot MA. *Theory of Propagation of Elastic Waves in a Fluid-saturated Porous Solid. I. Low Frequency Range.* J. Acoust. Soc. Am. **28(2)** 168-178 (1956)

Biot MA. *Theory of Propagation of Elastic Waves in a Fluid-saturated Porous Solid. II. Higher Frequency Range.* J. Acoust. Soc. Am. **28(2)** 179-191 (1956)

Biot MA *Mechanics of Deformation and Acoustic Propagation in Porous Media.*
J. Appl. Phys. **33(4)** 1482-1498 (1962)

Biot MA *Generalized Theory of Acoustic Propagation in Porous Dissipative Media.*
J. Appl. Phys. **34(9)** 1254-1264 (1962)

Booth F. *Sedimentation Potential and Velocity of Solid Spherical Particles.*
J. Chem. Phys. **22** 1956-1968 (1954)

Challis RE, Holmes AK, Tebbutt JS, Cocker RP *Scattering of Ultrasonic Compressional Waves by Particulate Filler in a Cured Epoxy Continuum.*
J. Acoust. Soc. Am. **103(3)** 1413-1420 (1998)

Challis RE, Harrison JA, Holmes AK, Cocker RP. *A Wide Bandwidth Spectrometer for Rapid Ultrasonic Absorption Measurements in Liquids.*
J. Acoust. Soc. Am. **90** 730-740 (1991)

Challis RE, Tebbutt JS, Holmes AK. *Equivalence between Three Scattering Formulations for Ultrasonic Wave Propagation in Particulate Mixtures.* J. Phys. D. **31** 3481-3497 (1999)

Enderby JA. *On Electrical Effects Due to Sound Waves in Colloidal Suspensions.*
Proc. R. Soc. (London) **A207** 329-342 (1951)

Ensminger D *Ultrasonics; fundamentals, technology, applications.* 2nd edn. Marcel Dekker Inc, New York (1988)

Erdelyi A, Magnus M, Oberhettinger F, Tricomi FG. *Higher Transcendental Functions*. **1**. McGraw Hill, New York (1953)

Epstein PS. *On the Absorption of Sound by Suspensions and Emulsions.* Contributions to Applied Mechanics, Theodore von Karman Anniversary Volume. California Institute of Technology, Pasadena (1941)

Epstein PS & Carhart RR. *The Absorption of Sound in Suspensions and Emulsions: I. Water Fog in Air*. J. Acoust. Soc. Am. **25** 553 (1953)

Euler L, *Principes Généraux du Mouvement des Fluides* Hist. de l'Acad. de Berlin (1755)

Evans JM & Attenborough K. *Coupled Phase Theory for Sound Propagation in Emulsions.* J. Acoust. Soc. Am. **102(1)** 278-282 (1997)

Flax L, Gaunaurd GC & Ueberall H. *The Theory of Resonance Scattering.* Physical Acoustics **15** Eds. Mason PW & Thurston RN. Academic Press New York (1981)

Foldy LL. *The Multiple Scattering of Waves.* Phys Rev. **67** 107-119 (1945)

Gatto MA & Seery JB. *Numerical Evaluation of the Modified Bessel Functions I and K.* Comp. & Maths. with Applications, **7**, 203-209, (1981)

Gladwell N, Javanaud C, Anson LW & Chivers RC. *Measurement and Interpretation of Ultrasonic Velocity and Attenuation in Low Concentration Polystyrene Dispersions*. Proc. Ultrasonics International '87, 555-560, Butterworth, Guildford UK (1987)

Gray DE (ed). *American Institute of Physics Handbook*. 2nd edn. McGraw Hill, New York (1963)

Del Grosso VA & Mader CW. *Speed of Sound in Pure Water*. J. Acoust. Soc. Am. **52** 1442 (1972)

Hall L. *The Origin of Ultrasonic Absorption in Water.* Phys. Rev. **73** No7 775-781 (1948)

Harker AH & Temple JAG. *Velocity and Attenuation of Ultrasound in Suspensions of Particles in Fluids.* J. Phys. D: Applied Phys **21** 1576-1588 (1988)

Holmes AK, Challis RE, Wedlock DJ. *A Wide-bandwidth Study of Suspensions: The Variation of Velocity and Attenuation with Particle Size.* J. Colloid & Interface Science **168** 339-348 (1994)

Isakovich MA. Zh. Eksperim. i Teor. Fiz. **18** 907 (1948)

Javanaud C, Thomas A. *Multiple Scattering Using The Foldy-Twersky Integral Equation.* Ultrasonics **26** 341-3 (1988)

Karpovich J. J. Chem. Phys. **22(10)** 1767-1773 (1954)

Kaye GWC & Laby TH. *Tables of Physical and Chemical Constants,* 16th edn. Longman, Harlow UK (1995)

Kell GS. J. Chem. Eng. Data. **20(1)** 97 (1975)

Kirchoff G. Annln. Phys. 134, 177. (1868)

Knudsen VO. *The Propagation of Sound in the atmosphere - Attenuation and Fluctuations.* J. Acoust. Soc. Am. **18(1)** 90-96 (1946)

Kronig R & Kramers HA. *Absorption and Dispersion in X-ray Spectra.* Zeits. f. Phys. **48** 174 (1928)

Lamb H. *Hydrodynamics.* 6th Edition, Dover Publications, New York (1945)

Landau E. *Vorlesungen über Zahlentheorie.* **Sec.1** Hirzel Stuttgart (1927). Reprinted by Chelsea, Bronx New York (1947)

Litovitz TA. *Ultrasonic Spectroscopy in Liquids.* J. Acoust. Soc. Am. **31(6)** 681-691 (1959)

Lloyd P, Berry MV. *Wave Propagation Through an Assembly of Spheres. IV. Relations Between Different Multiple Scattering Theories.* Proc. Phys. Soc., **91** (1967)

Marczak W. *Water As a Standard in the Measurement of the Speed Of Sound In Liquids.* J. Acoust. Soc. Am. **102(5)** Pt1 2776 (1997)

Miller JCP. *A Method for the Determination of Converging Factors, Applied to the Asymptotic Expansions for the Parabolic Cylinder Functions.* Proc. Cambridge Philos. Soc. **48**, 243-254 (1952)

Morse PM, Feshbach H. *Methods of Theoretical Physics.* Vol 2**.** McGraw-Hill. New York (1953)

O'Donnell M, Jaynes ET, Miller JG. *General Relationships between ultrasonic Attenuation and Dispersion.* J.Acoust.Soc.Amer. **63(6)** 1935-1937 (1978)

O'Donnell M, Jaynes ET, Miller JG. *Kramers-Kronig Relationship Between Ultrasonic Attenuation and Phase Velocity.* J.Acoust.Soc.Amer. **69(3)** 696-701 (1981)

Olver FWJ. *Numerical Solution of Second-order Linear Difference Equations.* J. Res. NBS-B **71b** Nos 2&3 (1967)

Olver FWJ. *Asymptotics and Special Functions*. Academic Press. New York (1974)

Olver FJW, Sookne DJ. *Note on Backward Recurrence Algorithms.* Math. Comp **26**, 941-947 (1972)

Rayleigh, Lord. Phil. Mag. **41** 107, 274 (1871)

Rayleigh, Lord. Phil. Mag. **47** 308 (1877)

Rayleigh, Lord. *Theory of Sound.* 2nd edn. Macmillan, London (1894) (first published 1877)

Reynolds O. *An Experimental Investigation of The Circumstances Which Determine Whether The Motion of Water Shall Be Direct or Sinuous, and The Law Of Resistance in Parallel Channels*. Phil. Trans. R. Soc. **174** 935-82 (1883)

Sewell CJT. *On the Extinction of Sound in a Viscous Atmosphere by Small Obstacles of Cylindrical and Spherical Form* Phil. Trans. R. Soc. (London) **A210** 239 (1910)

Slater LJ. *Confluent Hypergeometric Functions*. Cambridge University Press. Cambridge (1960)

Smith MC & Beyer RT. *Ultrasonic Absorption in Water in The Temperature Range O°C – 80°C.* J.Acoust.Soc.Amer. **20(5)** 608-610 (Sept 1948)

Sookne DJ. *Bessel Functions I and J of Complex Argument and Integer Order.* J. Res. NBS-B, Math Sciences. **77B**, Nos 3 & 4, 125-132 (July-December 1973)

Stephens RWB (ed). *The Sea as an Acoustic Medium*. Wiley (1970)

Stokes GG. *Trans. Camb. Phil. Soc.* **8**, 287 (1845)

Strout T. *Attenuation of Sound in High-concentration Suspensions: Development and Application of an Oscillatory Cell Model.* PhD Thesis, University of Maine (1991)

Temme NM. *On the Numerical Evaluation of the Modified Bessel Functions of the Third Kind.* J. Comp. Physics. **19**, 324-337 (1975)

Tebbut JS. *Ultrasonic Absorption and Phase Velocity Spectra in Colloids: Theory, Simulation and Experiment*. PhD Thesis. University of Keele (1996)

Temkin S. *Elements of Acoustics.* John Wiley & Sons, New York (1981)

Temme NM. *On the Numerical Evaluation of the Modified Bessel Functions of the Third Kind.* J. Comp. Physics. **19**, 324-337 (1975a)

Temme NM. *Numerical Evaluations of Functions Arising from Transformations of Formal Series.* J. Mathematical Analysis and Applications. **51**, 678-694 (1975b)

Urick RJ *A Sound Velocity Method for Determining the Compressibility of Finely Divided Substances.* J. Appl. Phys. **18** 983-987 (1947)

Urick RJ J. Acoust. Soc. Am. **20** 283 (1948)

Urick RJ & Ament WS *The Propagation of Sound in Composite Media*
J. Acoust. Soc. Am. **21** 115-119 (1949)

Waterman PC & Truell R. *Multiple Scattering of Waves.*
J. Math. Phys. **2(4)** 512-537 (1961)

Watson GN. *A Treatise on the Theory of Bessel Functions.* MacMillan, London (1922)

Weast RC (ed). *Handbook of Chemistry and Physics.*
CRC Press, New York, 68th edn. (1988)

Wood AB. *A Textbook of Sound.* 2nd edn. Bell, London (1941)

Ying CF & Truell R. *Scattering of a Plane Longitudinal Wave by a Spherical Obstacle in an Isotropically Elastic Solid.* J. Appl. Phys. **27(9)** 1086-1097 (1956)

Appendix A: Bessel function conformal mapping

A1.1 Algorithmic coding of uniform asymptotic expansion for $\nu \to \infty$

This description of the Algorithmic coding of uniform asymptotic expansion for $\nu \to \infty$ closely follows the description given by Amos (Amos, May 1983) and is given here for the sake of completeness and to clarify some of the nomenclature used in Chapter 3.

The coding of uniform asymptotic expansions employs several stages of transformation represented by intricate mappings between conformal complex planes. If the *w* plane mapping given by

$$w = \left\{ \ln\left[\frac{1+\sqrt{1+z^2}}{z} \right] - \sqrt{1+z^2} \right\}^{2/3} = \left[\tfrac{1}{2} \ln \frac{1+\sqrt{1-z^2}}{1-\sqrt{1-z^2}} - \sqrt{1-z^2} \right]^{2/3} \qquad \textbf{(A1.1)}$$

is compared to Equation (3.143) it can be seen that the *z* of Equation (3.183) simply replaces the $\frac{z}{\nu}$ of Equation (3.143) and by a slightly less straightforward transposition $\left(\frac{3}{2}\right)^{2/3} w$ replaces ζ. The ξ mapping of Equations (3.132) and (3.133) is undertaken in a similar fashion. The *z* to *w* transform expressed by Equation (3.183) is shown graphically as a conformal mapping with exemplar points by Figures A1.1 and A1.2.

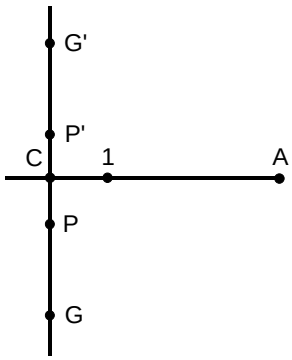

Figure A1.1 *z* plane

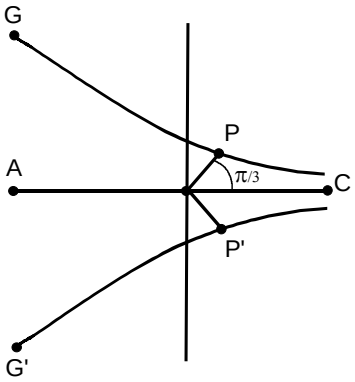

Figure A1.2 *w* plane

For clarity and as an aid to understanding the algorithm, Figures A1.3 to A1.8 outline the individual steps involved in mapping the *z* plane, including exemplar points, to the conformal *w* plane.

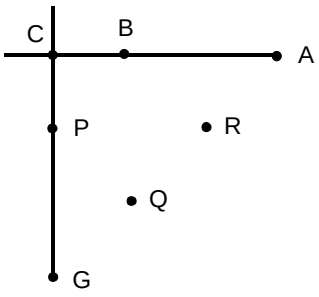

Figure A1.3 *z* plane

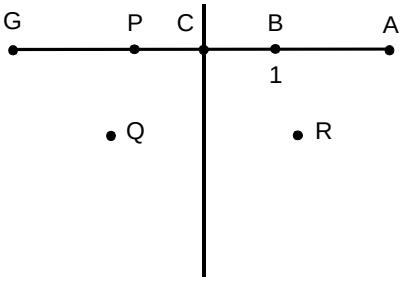

Figure A1.4 $w_1 = z^2$ plane

The principal square root $w_3 = \sqrt{w_2}$ maps the upper half plane of Figure A1.5 into the first quadrant of Figure A1.6 while the negative axis maps to the positive imaginary axis, as it should. However, if the first quadrant of Figure A1.3 is mapped Figure A1.5 would be the lower half plane. For continuity, the negative axis under the mapping $w_3 = \sqrt{w_2}$ would

map into the negative imaginary axis, a mapping not achieved by the principal square root. Therefore, the fourth quadrant is treated as a canonical region and conjugated to achieve first quadrant results.

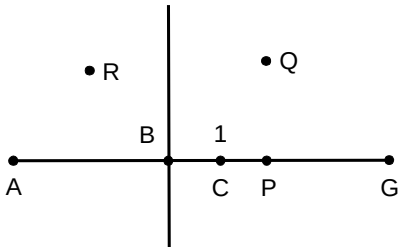

Figure A1.5 $w_2 = 1 - \left(w_1\right)^2$ **plane**

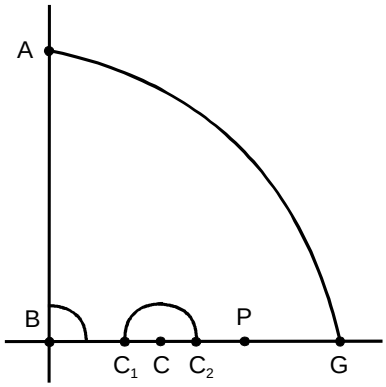

Figure A1.6 $w_3 = \sqrt{w_2}$ **plane**

The mapping

$$w_4 = \tfrac{1}{2}\ln\frac{1+w_3}{1-w_3} - w_3 \text{ ,} \qquad w_3 = a + ib \tag{A1.2}$$

maps Figure A1.6 to Figure A1.7. The positive imaginary axis $w_3 = ib$ maps over to the negative imaginary axis

$$w_4 = \tfrac{1}{2}\ln\frac{1+ib}{1-ib} - ib \;=\; i\left(\left(\arctan b\right) - b\right) \;=\; -i\left(b - \left(\arctan b\right)b\right) \tag{A1.3}$$

The direction of the negative imaginary axis of Figure A1.7 is not the conventional $\frac{\pi}{2}$ but $\frac{3\pi}{2}$ because the power series for Equation (A1.2) when $w_3 = be^{i\pi/2}$, and for small v, becomes

$$w_4 = \frac{(w_3)^3}{3} + \ldots = \frac{b^3 e^{\frac{i\,3\pi}{2}}}{3} + \ldots \qquad \textbf{(A1.4)}$$

Therefore, if an argument $\theta = \arg w_4$ is to be computed for Figure A1.7, θ has to be within the bounds $0 < \theta < \frac{3\pi}{2}$. The segment C_2PG in Figure A1.6 maps directly to the straight line C_2PG in Figure A1.7 since

$$w_4 = \tfrac{1}{2}\ln\frac{1+a}{1-a} - a\,,\ w_3 = a + ib\,,\ b = 0 \qquad \textbf{(A1.5)}$$

$$= \tfrac{1}{2}\ln\frac{1+a}{a-1} - a + \frac{i\pi}{2}\,,\ a > 1 \qquad \textbf{(A1.6)}$$

and the imaginary part is constant.

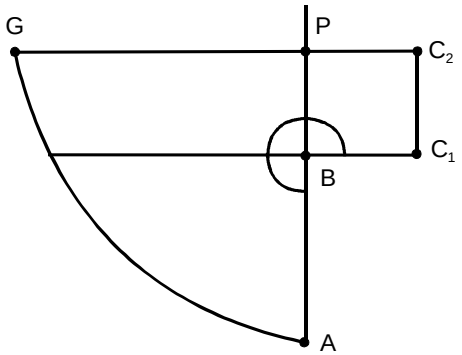

Figure A1.7 $w_4 = \tfrac{1}{2}\ln\frac{1+w_3}{1-w_3} - w_3$ **plane**

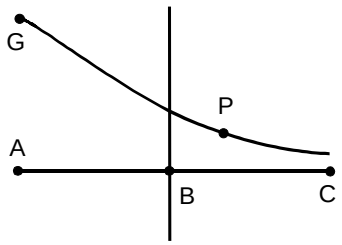

Figure A1.8 $w_5 = (w_4)^{\frac{2}{3}}$ **plane**

By tracing the mappings through the Figures: the point P in Figure A1.6 comes from the point $z = -0.6628i$, and the point P in Figure A1.8 has the coordinates

$$w_5 = 0.67559 + 1.1703i\ ,\quad \arg w_5 \sim \frac{\pi}{3}$$

The mapping for Equation (3.143) with all modifying coefficients moved to the right is given by

$$\zeta = \left\{ \frac{3}{2} \left[\ln \frac{1+\sqrt{1+\left(\frac{z}{\nu}\right)^2}}{\left(\frac{z}{\nu}\right)} - \sqrt{1-\left(\frac{z}{\nu}\right)^2} \right] \right\}^{2/3} \qquad \textbf{(A1.7)}$$

which has the properties obtained for Equation (A1.1) with the *z* plane scaled by $\frac{1}{\nu}$ and the *w* plane scaled by $\left(\frac{3}{2}\right)^{2/3}$. The ξ mapping for Equations (3.132) and (3.133) can be traced from Figure A1.3 through Figure A1.5 with the modification $w_2 = 1+\left(w_1\right)^2$. In this case, the first quadrant is the canonical region because the relation $w_3 = \sqrt{w_2}$ must map the negative real axis properly using the principal square root, where the first quadrant under the mapping $w_2 = 1+z^2$ goes into the upper half w_2 plane, which includes the negative real axis.

A1.2 Derivation of $\nu_L(\varepsilon)$

For the sake of computational efficiency each series has to terminate within a reasonable number of terms. The reasonable number was taken by Amos (Amos, May 1983) to be 30. To achieve this a compromise between minimum order ν_L and the magnitude of w^2 had to be made. Again, to preserve the option of using high-precision (in the current application, 80-bit) arithmetic it was necessary to aim for at least 18 digit accuracy. The upper bound of $|w^2| < 0.25$ was chosen such that $\left(0.25\right)^{30} = 2^{-60} \cong 10^{-18}$ and took a value of ν_L such that any losses of significance for $|w^2|$ slightly larger than 0.25 in Equations (3.139) and (3.140)

were compensated for by a lower magnitude term. Amos found that the choice of 30 terms was consistent with the apparent convergence properties of each series and the choice of value of $\nu_L(\varepsilon)$ was applicable to both Figures 3.1 and 3.2 and to Equations (3.139) and (3.140). Therefore, $\nu_L(\varepsilon)$ was found to be a machine dependent parameter and numerical experiments (op. cit) indicated that a linear relation with $\nu_L = 10$ for 3 digit accuracy and $\nu_L = 100$ for 18 digit accuracy was conservative. The value of $\nu_L(\varepsilon)$ was given by

$$\nu_L(\varepsilon) = 10 + 6(D-3) \qquad \textbf{(A1.8)}$$

Where

$$10^{-D} = 2^{-E+1} = \varepsilon \quad \text{or} \quad D = (E-1)\log_{10}2 \qquad \textbf{(A1.9)}$$

This value of $\nu_L(\varepsilon)$ was derived to be approximately 104 for 64-bit arithmetic and 125 for 80-bit arithmetic on an Intel 32-bit architecture platform and the $\nu_L(\varepsilon)$ boundary on the $\left(|z|,\nu\right)$ plane was set automatically by the software by an in-built function to detect machine epsilon.

Appendix B: The Lloyd & Berry integral term

B1 Lloyd and Berry scattering model

Lloyd and Berry's expression for the square of the complex propagation quantity β, from which the components of phase velocity and attenuation are obtained, is given by

$$\beta^2 = k_c^2 + \frac{3\phi\ f(0)}{R^3} + \frac{9\phi^2}{4k_c^2 R^6}\left[f^2(\pi) - f^2(0) - \int_{\theta=0}^{\pi} \frac{\frac{d}{d\theta} f^2(\theta)}{\sin\left(\frac{\theta}{2}\right)} \quad d\theta \right] \tag{B1.1}$$

Where the $f(\theta)$ term given by

$$f(\theta) = -\sum_{n=0}^{\infty} (2n+1)\ A_n\ P_n(\cos\theta) \tag{B1.2}$$

represents the radially scattered components and the expression $P_n(\cos\theta)$ in Equation (B1.2) denotes a Legendre polynomial or zonal harmonic of order n and argument $\cos\theta$ expressed by the expansion of the closed form

$$P_n(\cos\theta) = \sum_{k=0}^{N} (-1)^k \frac{(2n-2k)!}{2^n k!(n-k)(n-2k)} (\cos\theta)^{n-2k}, \quad \begin{cases} N = \frac{n}{2}, & n \text{ even} \\ N = \frac{n-1}{2}, & n \text{ odd} \end{cases} \tag{B1.3}$$

Where

$$P_0(\cos\theta) = 1 \tag{B1.4}$$

$f(\pi)$ and $f(0)$ are merely special cases of $f(\theta)$, respectively representing the forward scattered component

$$f(0) = \frac{-i}{k_c} \sum_{n=0}^{\infty} (2n+1)\ A_n \tag{B1.5}$$

and the backwards scattered component

$$f(\pi) = \frac{-i}{k_c} \sum_{n=0}^{\infty} (-1)^n (2n+1)\, A_n \qquad \text{(B1.6)}$$

A representation of the different orders of radial scattering, denoted by polar diagrams of the magnitude of each of the Legendre polynomial orders from zero to 18, give an insight into the physical processes involved and are reproduced in Appendix B3. The net contribution of the complicated radial scattering patterns to the overall scattering in the forward direction, detected by an integrating transducer target, is the integral term of Equation (B1.1). That integral is expressed as an infinite series denoted by

$$\left[\int_{\theta=0}^{\pi} \frac{\frac{d}{d\theta} f^2(\theta)}{\sin\left(\frac{\theta}{2}\right)} \, d\theta \right] = \sum_{m=0}^{\infty} \sum_{n=0}^{\infty} C_n^m A_m A_n \qquad \text{(B1.7)}$$

and evaluated analytically for the orders from zero to 18. The resulting coefficients are commutative in that the coefficients $C(A_j A_k)$ and $C(A_k A_j)$ are equivalent and identical and, therefore, combine to form a diagonal permutation matrix of rank 19. The coefficients, expressed in the form $C_n^m = C(A_m A_n)$, are reproduced in Appendix B2. With the exception of the $C(A_0 A_0) = 0$ coefficient, all the elements of the permutation matrix are non-zero, real and negative integers or rational numbers.

B2 Lloyd and Berry integral term coefficients

$C(A_0 A_0)$ = 0

$C(A_0 A_1)$ = -24

$C(A_0 A_2)$ = -40

$C(A_0 A_3)$ = -112

$C(A_0 A_4)$ = -144

$C(A_0 A_5)$ = -264

$C(A_0 A_6)$ = -312

$C(A_0 A_7)$ = -480

$C(A_0 A_8)$ = -544

$C(A_0 A_9)$ = -760

$C(A_0 A_{10})$ = -840

$C(A_0 A_{11})$ = -1104

$C(A_0 A_{12})$ = -1200

$C(A_0 A_{13})$ = -1512

$C(A_0 A_{14})$ = -1624

$C(A_0 A_{15})$ = -1984

$C(A_0 A_{16})$ = -2112

$C(A_0 A_{17})$ = -2520

$C(A_0 A_{18})$ = -2664

$C(A_1 A_1)$ = -24

$C(A_1 A_2)$ = -192

$C(A_1 A_3)$ = -264

$C(A_1 A_4)$ = -552

$C(A_1 A_5)$ = -672

$C(A_1 A_6)$ = -1104

$C(A_1 A_7)$ = -1272

$C(A_1 A_8)$ = -1848

$C(A_1 A_9)$ = -2064

$C(A_1 A_{10})$ = -2784

$C(A_1 A_{11})$ = -3048

$C(A_1 A_{12})$ = -3912

$C(A_1 A_{13})$ = -4224

$C(A_1 A_{14})$ = -5232

$C(A_1 A_{15})$ = -5592

$C(A_1 A_{16})$ = -6744

$C(A_1 A_{17})$ = -7152

$C(A_1 A_{18})$ = -8448

$C(A_2 A_2)$ = -920/7

$C(A_2 A_3)$ = -1864/3

$C(A_2 A_4)$ = -60120/77

$C(A_2 A_5)$ = -538/39

$C(A_2 A_6)$ = -17824/11

$C(A_2 A_7)$ = -543720/221

$C(A_2 A_8)$ = -52824/19

$C(A_2 A_9)$ = -4593/119

$C(A_2 A_{10})$ = -18616/437

$C(A_2 A_{11})$ = -195304/35

$C(A_2 A_{12})$ = -12544/207

$C(A_2 A_{13})$ = -1104912/145

$C(A_2 A_{14})$ = -22822/279

$C(A_2 A_{15})$ = -3183640/319

$C(A_2 A_{16})$ = -2304552/217

$C(A_2 A_{17})$ = -51526/407

$C(A_2 A_{18})$ = -12175/91

$C(A_3 A_3)$ = -12656/33

$C(A_3 A_4)$ = -2050/143

$C(A_3 A_5)$ = -66760/39

$C(A_3 A_6)$ = -15251/561

$C(A_3 A_7)$ = -143645712/46189

$C(A_3 A_8)$ = -1100016/247

$C(A_3 A_9)$ = -1938264/391

$C(A_3 A_{10})$ = -246530424/37145

$C(A_3 A_{11})$ = -6201152/855

$C(A_3 A_{12})$ = -556399/6003

$C(A_3 A_{13})$ = -10334968/103385

$C(A_3 A_{14})$ = -1894878/15345

$C(A_3 A_{15})$ = -37864016/2871

$C(A_3 A_{16})$ = -5280963/3326

$C(A_3 A_{17})$ = -27602020/164021

$C(A_3 A_{18})$ = -116394088/5863

$C(A_4 A_4)$ = -842256/1001

$C(A_4 A_5)$ = -608184/221

$C(A_4 A_6)$ = -11294280/3553

$C(A_4 A_7)$ = -216527280/46189

$C(A_4 A_8)$ = -328827024/62491

$C(A_4 A_9)$ = -256351464/35581

$C(A_4 A_{10})$ = -2943307/37145

$C(A_4 A_{11})$ = -3376532064/327845

$C(A_4 A_{12})$ = -43854000/392863

$C(A_4 A_{13})$ = -15887490408/1137235

$C(A_4 A_{14})$ = -5873610/39215

$C(A_4 A_{15})$ = -2150237/11803

$C(A_4 A_{16})$ = -58630217488/3026933

$C(A_4 A_{17})$ = -1214471595/5270837

$C(A_4 A_{18})$ = -13314310493/54707653

$C(A_5 A_5)$ = -19730216/12597

$C(A_5 A_6)$ = -45518/969

$C(A_5 A_7)$ = -512216040/96577

$C(A_5 A_8)$ = -210475592/28405

$C(A_5 A_9)$ = -6250507/76245

$C(A_5 A_{10})$ = -151732688976/14003665

$C(A_5 A_{11})$ = -1542063400/13066965

$C(A_5 A_{12})$ = -899681937800/60108039

$C(A_5 A_{13})$ = -31646285136/1964315

$C(A_5 A_{14})$ = -23512221152/1187145

$C(A_5 A_{15})$ = -3049855027/14437215

$C(A_5 A_{16})$ = -22470276953/88645895

$C(A_5 A_{17})$ = -61393629877280/2287064091

$C(A_5 A_{18})$ = -6509982868/20604181

$C(A_6 A_6)$ = -214037512/81719

$C(A_6 A_7)$ = -30206289/408595

$C(A_6 A_8)$ = -197291528/24035

$C(A_6 A_9)$ = -18720089/170085

$C(A_6 A_{10})$ = -4020353057/33393355

$C(A_6 A_{11})$ = -22455451752/1451885

$C(A_6 A_{12})$ = -346361453/2072691

$C(A_6 A_{13})$ = -2822038415426/13591095485

$C(A_6 A_{14})$ = -55124948085/248113305

$C(A_6 A_{15})$ = -14967858761/55651145

$C(A_6 A_{16})$ = -66412176664/232548515

$C(A_6 A_{17})$ = -3276425389250/9676040385

$C(A_6 A_{18})$ = -29279425673888/819412429

$C(A_7 A_7)$ = -227080416/55913

$C(A_7 A_8)$ = -90281072/823745

$C(A_7 A_9)$ = -54905169240/4569617

$C(A_7 A_{10})$ = -1354371335800/86822723

$C(A_7 A_{11})$ = -1292032464/76415

$C(A_7 A_{12})$ = -5243671859760/247110827

$C(A_7 A_{13})$ = -281381632977/1235554135

$C(A_7 A_{14})$ = -1068695596566/3842999413

$C(A_7 A_{15})$ = -34997366587099/118214162209

$C(A_7 A_{16})$ = -31002097054267/87670790155

$C(A_7 A_{17})$ = -3390314466944578/9065159702027

$C(A_7 A_{18})$ = -16358876417208984/372832655195

$C(A_8 A_8)$ = -152036005344/25536095

$C(A_8 A_9)$ = -625810123/4032015

$C(A_8 A_{10})$ = -33090995448/1964315

$C(A_8 A_{11})$ = -202023998032/9479955

$C(A_8 A_{12})$ = -999748487632/43607793

$C(A_8 A_{13})$ = -84084162465528/2979865855

$C(A_8 A_{14})$ = -399140240085544/13255265355

$C(A_8 A_{15})$ = -49410221440452/13640095639

$C(A_8 A_{16})$ = -30058787956865048/78290015608415

$C(A_8 A_{17})$ = -43142386965144772328/951841768712835

$C(A_8 A_{18})$ = -372387880527267/779559188135

$C(A_9 A_9)$ = -44066916904/5272635

$C(A_9 A_{10})$ = -13785213429/65029165

$C(A_9 A_{11})$ = -1935866038/8482065

$C(A_9 A_{12})$ = -452119482734/1599717459

$C(A_9 A_{13})$ = -3464009152196256/114646417895

$C(A_9 A_{14})$ = -433846502642128/11859974265

$C(A_9 A_{15})$ = -11915796561467/30673899285

$C(A_9 A_{16})$ = -71647836582831794 4/15531217671305

$C(A_9 A_{17})$ = -19602869596751920/402470092479

$C(A_9 A_{18})$ = -493752299297289884/867649376394255

$C(A_{10} A_{10})$ = -14003924991224/1235554135

$C(A_{10} A_{11})$ = -61922432944344/2202509545

$C(A_{10} A_{12})$ = -13099464853351800/435656388001

$C(A_{10} A_{13})$ = -796744743218790/2178281940005

$C(A_{10} A_{14})$ = -2605634101842/6698897545

$C(A_{10}\,A_{15})$ = -631413003776225/1359876201635

$C(A_{10}\,A_{16})$ = -667700189127735/1359876201635

$C(A_{10}\,A_{17})$ = -1937009843673384/3359814435017

$C(A_{10}\,A_{18})$ = -2506405314487448592/41316636971155

$C(A_{11}\,A_{11})$ = -74491597101648/4984626865

$C(A_{11}\,A_{12})$ = -6203759411362048/170474238783

$C(A_{11}\,A_{13})$ = -101342628015323/261839517085

$C(A_{11}\,A_{14})$ = -26379545668002776/568823778495

$C(A_{11}\,A_{15})$ = -78449570669328/1597974385

$C(A_{11}\,A_{16})$ = -2071919381852206128/35789327677355

$C(A_{11}\,A_{17})$ = -9355394539613028/15338283290295

$C(A_{11}\,A_{18})$ = -205764405702972376/2901837379245

$C(A_{12}\,A_{12})$ = -20866444545462587600/10840156007319

$C(A_{12}\,A_{13})$ = -55586884035337704/1204461778591

$C(A_{12}\,A_{14})$ = -127826920804047400/2616589381077

$C(A_{12}\,A_{15})$ = -394530043605628400/6828009980841

$C(A_{12}\,A_{16})$ = -143291819146523 72/23518701045119

$C(A_{12}\,A_{17})$ = -501541078506423 5240/70556103135357

$C(A_{12}\,A_{18})$ = -8398704631306 1431/112508380675299

$C(A_{13}\,A_{13})$ = -5048371121540184/207665823895

$C(A_{13}\,A_{14})$ = -2332227130964472/4054948456055

$C(A_{13}\,A_{15})$ = -87245846425505016/1438852677955

$C(A_{13}\,A_{16})$ = -83391916884853727/117593505225595

$C(A_{13}\,A_{17})$ = -8124548288974239911/10902597841630165

$C(A_{13}\,A_{18})$ = -9851778764252044872/11438352035322065

$C(A_{14}\,A_{14})$ = -1211865518608183032 8/401439897149445

$C(A_{14}\,A_{15})$ = -91434698925062669 6/12949674101595

$C(A_{14}\,A_{16})$ = -17745990608554711224/239241958907245

$C(A_{14}\,A_{17})$ = -11819778979416555140 00/13759830379436691

$C(A_{14}\,A_{18})$ = -11713548369738810865 28/13016055764332005

$C(A_{15}\,A_{15})$ = -3136263033454492608/84892307999345

$C(A_{15}\,A_{16})$ = -31565960858522554 3/368979097913615

$C(A_{15}\,A_{17})$ = -80729579808801262243 60/90104695710504783

$C(A_{15}\,A_{18})$ = -707901764853057741 1/6882262304562645

$C(A_{16}\,A_{16})$ = -30754772417880016359 04/68896120398800345

$C(A_{16}\,A_{17})$ = -24510252219610464417576/239210753434344055

$C(A_{16}\,A_{18})$ = -32448967641202117460 39/3032157928667766535

$C(A_{17}\,A_{17})$ = -80596106047392542554 0456/15111285024095277303

$C(A_{17}\,A_{18})$ = -17363563447749337089077/1429445880657661366533

$C(A_{18}\,A_{18})$ = -29881946787956601621524760/473623068457905132767

B3 Legendre polynomials of orders zero to 18

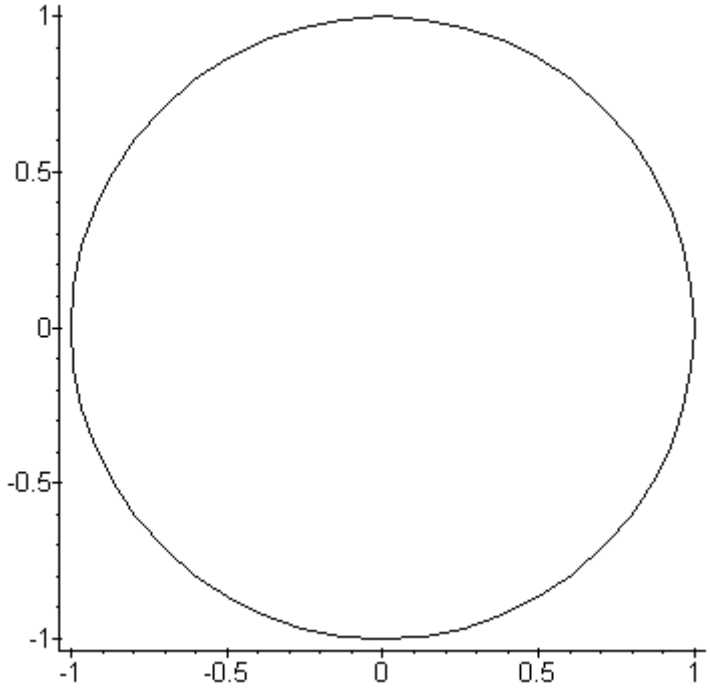

Figure B3.1 Polar diagram of the magnitude of $P_0(\cos\theta)$

$$P_0(\cos\theta) = 1 \tag{B3.1}$$

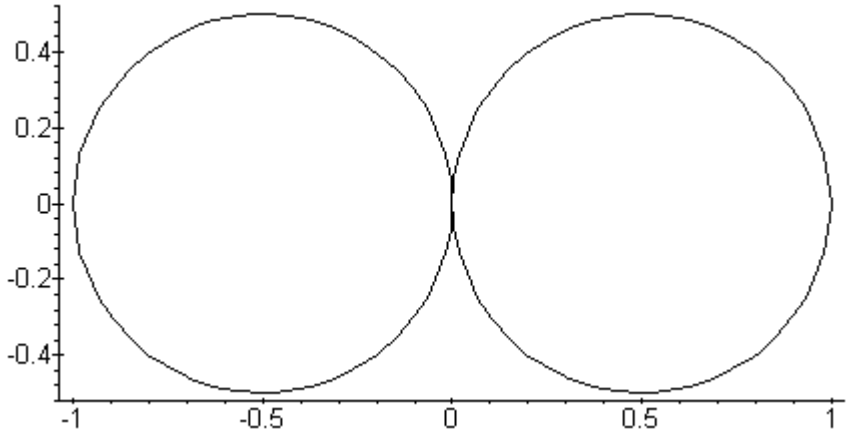

Figure B3.2 Polar diagram of the magnitude of $P_1(\cos\theta)$

$$P_1(\cos\theta) = \cos\theta \tag{B3.2}$$

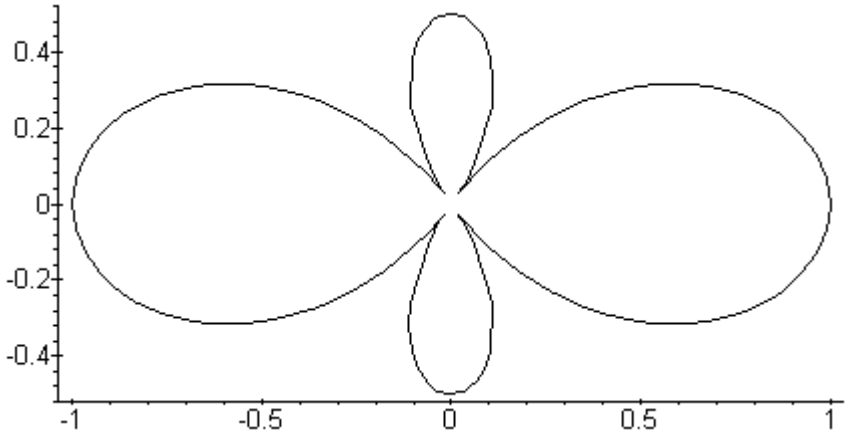

Figure B3.3 Polar diagram of the magnitude of $P_2(\cos\theta)$

$P_2(\cos\theta)$ =

$$\frac{3}{2}\cos(\theta)^2 - \frac{1}{2} \tag{B3.3}$$

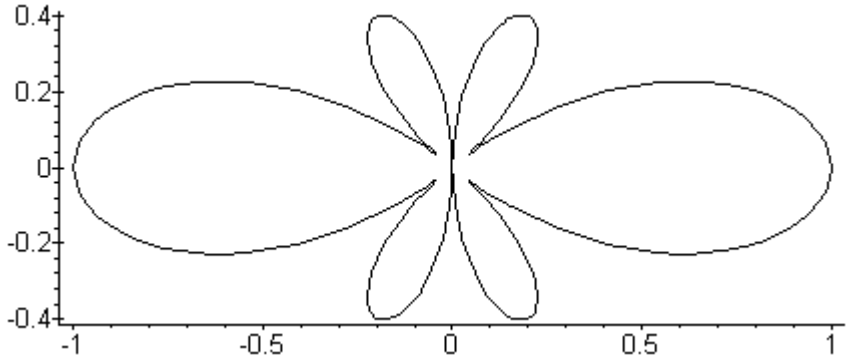

Figure B3.4 Polar diagram of the magnitude of $P_3(\cos\theta)$

$P_3(\cos\theta)$ =

$$\frac{5}{2}\cos(\theta)^3 - \frac{3}{2}\cos(\theta) \tag{B3.4}$$

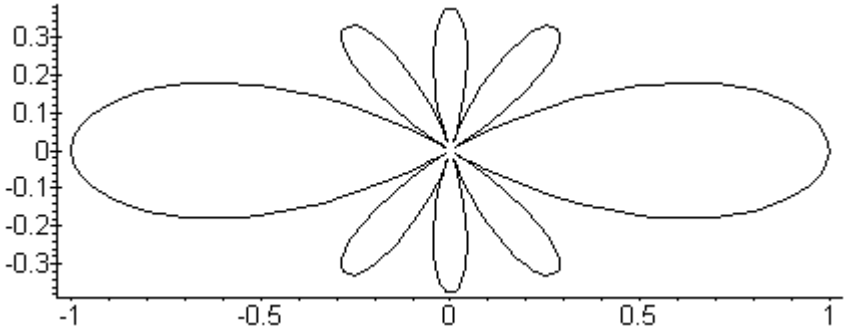

Figure B3.5 Polar diagram of the magnitude of $P_4(\cos\theta)$

$P_4(\cos\theta)$ =

$$\frac{35}{8}\cos(\theta)^4 - \frac{15}{4}\cos(\theta)^2 + \frac{3}{8} \tag{B3.5}$$

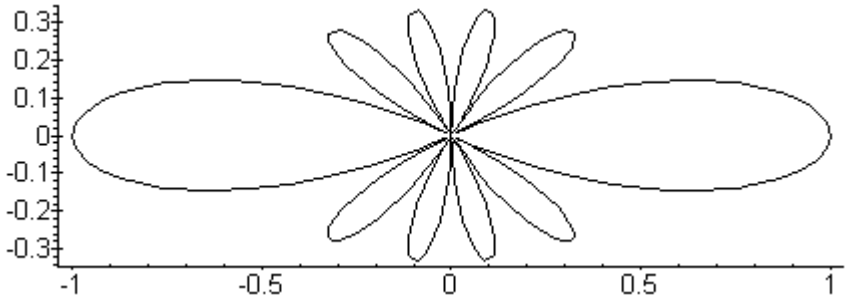

Figure B3.6 Polar diagram of the magnitude of $P_5(\cos\theta)$

$P_5(\cos\theta)$ =

$$\frac{63}{8}\cos(\theta)^5 - \frac{35}{4}\cos(\theta)^3 + \frac{15}{8}\cos(\theta) \tag{B3.6}$$

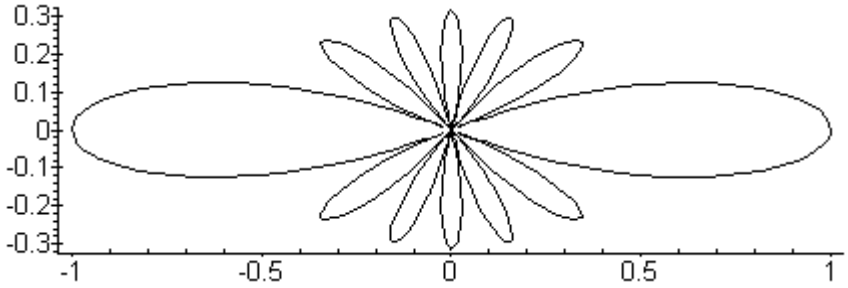

Figure B3.7 Polar diagram of the magnitude of $P_6(\cos\theta)$

$P_6(\cos\theta)$ =

$$\frac{231}{16}\cos(\theta)^6 - \frac{315}{16}\cos(\theta)^4 + \frac{105}{16}\cos(\theta)^2 - \frac{5}{16} \tag{B3.7}$$

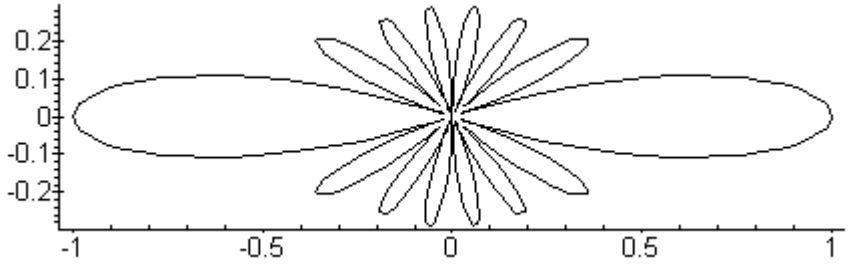

Figure B3.8 Polar diagram of the magnitude of $P_7(\cos\theta)$

$P_7(\cos\theta)$ =

$$\frac{429}{16}\cos(\theta)^7 - \frac{693}{16}\cos(\theta)^5 + \frac{315}{16}\cos(\theta)^3 - \frac{35}{16}\cos(\theta) \tag{B3.8}$$

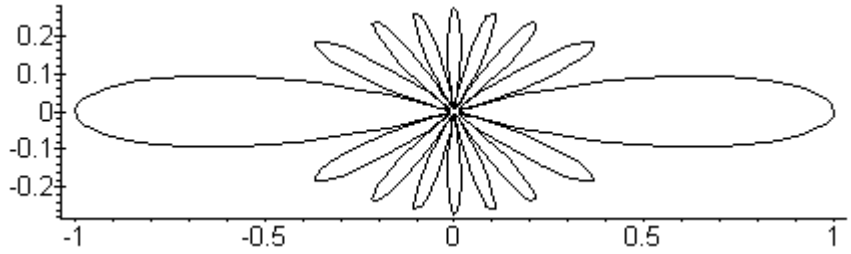

Figure B3.9 Polar diagram of the magnitude of $P_8(\cos\theta)$

$P_8(\cos\theta)$ =

$$\frac{6435}{128}\cos(\theta)^8 - \frac{3003}{32}\cos(\theta)^6 + \frac{3465}{64}\cos(\theta)^4 - \frac{315}{32}\cos(\theta)^2 + \frac{35}{128} \qquad \text{(B3.9)}$$

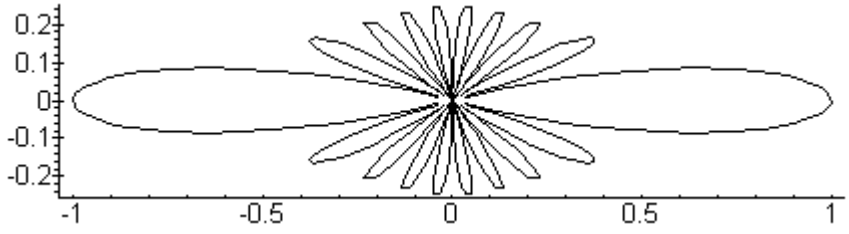

Figure B3.10 Polar diagram of the magnitude of $P_9(\cos\theta)$

$P_9(\cos\theta)$ =

$$\frac{12155}{128}\cos(\theta)^9 - \frac{6435}{32}\cos(\theta)^7 + \frac{9009}{64}\cos(\theta)^5 - \frac{1155}{32}\cos(\theta)^3 + \frac{315}{128}\cos(\theta) \qquad \text{(B3.10)}$$

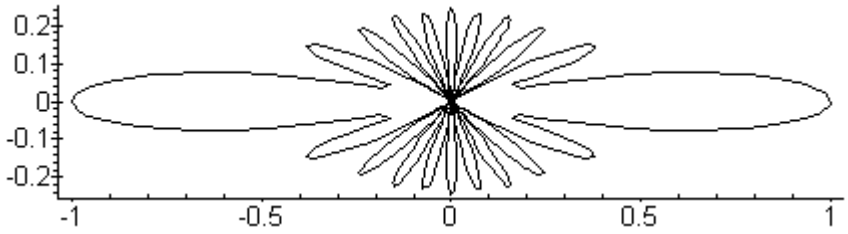

Figure B3.11 Polar diagram of the magnitude of $P_{10}(\cos\theta)$

$P_{10}(\cos\theta)$ =

$$\frac{46189}{256}\cos(\theta)^{10} - \frac{109395}{256}\cos(\theta)^{8} + \frac{45045}{128}\cos(\theta)^{6} - \frac{15015}{128}\cos(\theta)^{4} + \frac{3465}{256}\cos(\theta)^{2} - \frac{63}{256} \tag{B3.11}$$

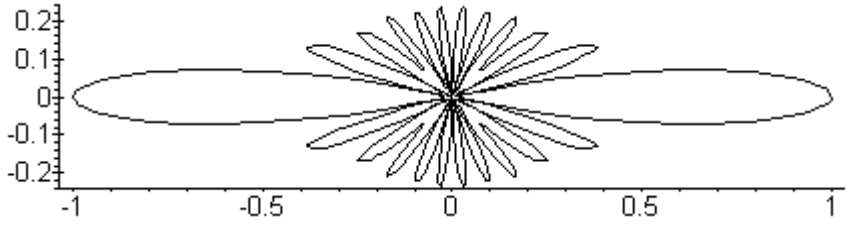

Figure B3.12 Polar diagram of the magnitude of $P_{11}(\cos\theta)$

$P_{11}(\cos\theta)$ =

$$\frac{88179}{256}\cos(\theta)^{11} - \frac{230945}{256}\cos(\theta)^{9} + \frac{109395}{128}\cos(\theta)^{7} - \frac{45045}{128}\cos(\theta)^{5} + \frac{15015}{256}\cos(\theta)^{3} - \frac{693}{256}\cos(\theta) \tag{B3.12}$$

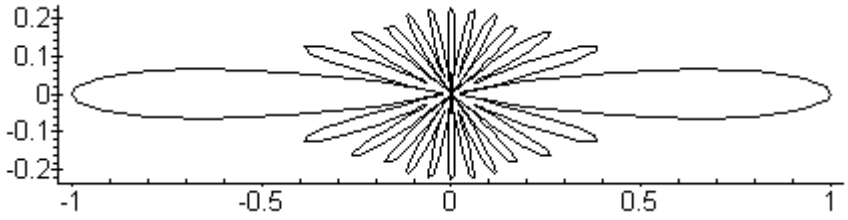

Figure B3.13 Polar diagram of the magnitude of $P_{12}(\cos\theta)$

$$P_{12}(\cos\theta) = \frac{676039}{1024}\cos(\theta)^{12} - \frac{969969}{512}\cos(\theta)^{10} + \frac{2078505}{1024}\cos(\theta)^{8} - \frac{255255}{256}\cos(\theta)^{6} + \frac{225225}{1024}\cos(\theta)^{4} - \frac{9009}{512}\cos(\theta)^{2} + \frac{231}{1024} \quad \text{(B3.13)}$$

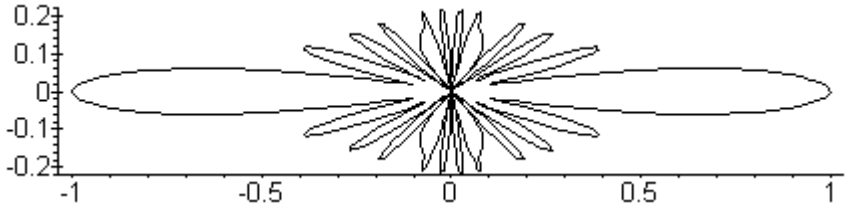

Figure B3.14 Polar diagram of the magnitude of $P_{13}(\cos\theta)$

$$P_{13}(\cos\theta) = \frac{1300075}{1024}\cos(\theta)^{13} - \frac{2028117}{512}\cos(\theta)^{11} + \frac{4849845}{1024}\cos(\theta)^{9} - \frac{692835}{256}\cos(\theta)^{7} + \frac{765765}{1024}\cos(\theta)^{5} - \frac{45045}{512}\cos(\theta)^{3} + \frac{3003}{1024}\cos(\theta) \quad \text{(B3.14)}$$

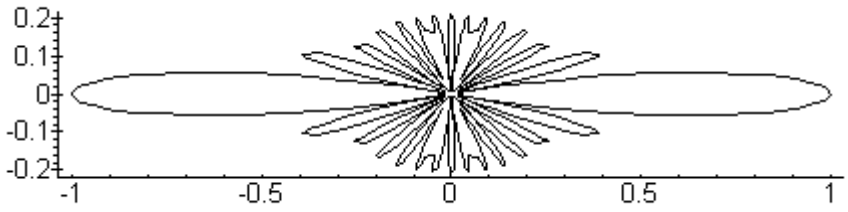

Figure B3.15 Polar diagram of the magnitude of $P_{14}(\cos\theta)$

$P_{14}(\cos\theta) =$

$$\frac{5014575}{2048}\cos(\theta)^{14} - \frac{16900975}{2048}\cos(\theta)^{12} + \frac{22309287}{2048}\cos(\theta)^{10} - \frac{14549535}{2048}\cos(\theta)^{8} + \frac{4849845}{2048}\cos(\theta)^{6} - \frac{765765}{2048}\cos(\theta)^{4} + \frac{45045}{2048}\cos(\theta)^{2} - \frac{429}{2048} \tag{B3.15}$$

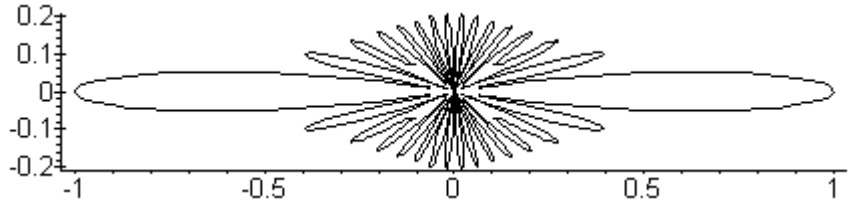

Figure B3.16 Polar diagram of the magnitude of $P_{15}(\cos\theta)$

$P_{15}(\cos\theta) =$

$$\frac{9694845}{2048}\cos(\theta)^{15} - \frac{35102025}{2048}\cos(\theta)^{13} + \frac{50702925}{2048}\cos(\theta)^{11} - \frac{37182145}{2048}\cos(\theta)^{9} + \frac{14549535}{2048}\cos(\theta)^{7} - \frac{2909907}{2048}\cos(\theta)^{5} + \frac{255255}{2048}\cos(\theta)^{3} - \frac{6435}{2048}\cos(\theta) \tag{B3.16}$$

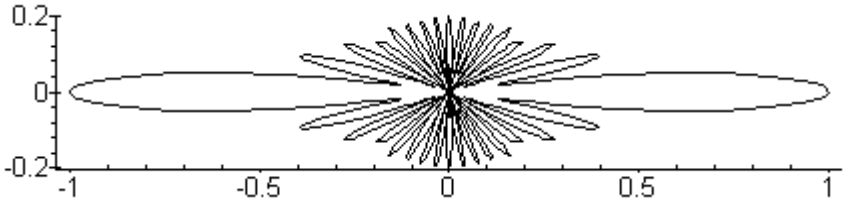

Figure B3.17 Polar diagram of the magnitude of $P_{16}(\cos\theta)$

$P_{16}(\cos\theta)$ =

$$\frac{300540195}{32768}\cos(\theta)^{16} - \frac{145422675}{4096}\cos(\theta)^{14} + \frac{456326325}{8192}\cos(\theta)^{12} - \frac{185910725}{4096}\cos(\theta)^{10} + \frac{334639305}{16384}\cos(\theta)^{8} - \frac{20369349}{4096}\cos(\theta)^{6} + \frac{4849845}{8192}\cos(\theta)^{4} - \frac{109395}{4096}\cos(\theta)^{2} + \frac{6435}{32768} \quad \text{(B3.17)}$$

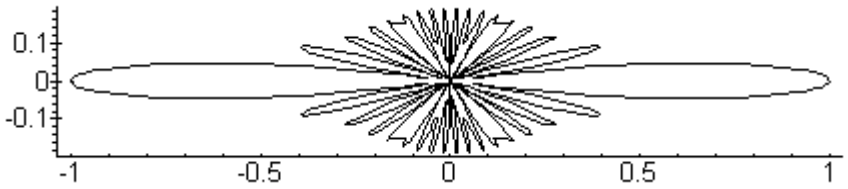

Figure B3.18 Polar diagram of the magnitude of $P_{17}(\cos\theta)$

$P_{17}(\cos\theta)$ =

$$\frac{583401555}{32768}\cos(\theta)^{17} - \frac{300540195}{4096}\cos(\theta)^{15} + \frac{1017958725}{8192}\cos(\theta)^{13} - \frac{456326325}{4096}\cos(\theta)^{11} + \frac{929553625}{16384}\cos(\theta)^{9} - \frac{66927861}{4096}\cos(\theta)^{7} + \frac{20369349}{8192}\cos(\theta)^{5} - \frac{692835}{4096}\cos(\theta)^{3} + \frac{109395}{32768}\cos(\theta) \quad \text{(B3.18)}$$

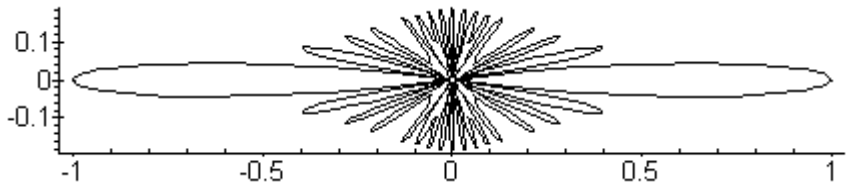

Figure B3.19 Polar diagram of the magnitude of $P_{18}(\cos\theta)$

$$P_{18}(\cos\theta) = \frac{2268783825}{65536}\cos(\theta)^{18} - \frac{9917826435}{65536}\cos(\theta)^{16} + \frac{4508102925}{16384}\cos(\theta)^{14} - \frac{4411154475}{16384}\cos(\theta)^{12} + \frac{5019589575}{32768}\cos(\theta)^{10} - \frac{1673196525}{32768}\cos(\theta)^{8} + \frac{156165009}{16384}\cos(\theta)^{6} - \frac{14549535}{16384}\cos(\theta)^{4} + \frac{2078505}{65536}\cos(\theta)^{2} - \frac{12155}{65536} \quad \text{(B3.19)}$$

Appendix C: Tables of order of *n* required for convergence of phase velocity and attenuation

Tables were compiled to indicate the orders n of A_n it is necessary to compute for satisfactory convergence, to a final value of phase velocity and attenuation, for a particular dispersed/continuous phase and radius/frequency combination. The convergence criteria were to within 0.01%, 0.1%, 1%, and 10% of fully converged total attenuation in Nepers per metre and total velocity in metres per second. In this context fully converged means numerically converged to within machine epsilon of a final value which is stable for the next 10 values of n. The materials were chosen to encompass a range of mass density, acoustic and thermal contrasts. They are: aqueous suspensions of polystyrene, silica, iron and titanium dioxide; an aqueous emulsion of hexadecane; and suspensions of iron and silica in Dow Corning 350 centistokes silicone oil. The physical parameters of each material are shown in Appendix E. At each of the frequencies 0.5MHz, 1MHz, 10MHz and at 10MHz steps up to and including 150MHz, the phase velocity and attenuation were computed from the single scattering model using orders n of the A_n scattering coefficient up to and including 400. The convergence was plotted to ensure by visual inspection that convergence had been achieved in all cases. The phase velocity and attenuation value at each frequency point was subsequently regressed backwards for reducing order n to derive the value of n at which the phase velocity and attenuation values had converged to within 0.01%, 0.1%, 1% and 10% of the fully converged values. Those converged values are also incorporated into the tables. Some of the predicted values for phase velocity at high frequencies in the silicone oil suspensions were surprising but experimental corroboration

is impractical using currently available equipment owing to the extremely high attenuation associated with these materials at these frequencies.

Table C1 10% v/v monodisperse 10nm diameter model X in water at 25ºC

freq (MHz)	0.01%/0.1%/1%/10% alpha convergence	0.01%/0.1%/1%/10% velocity convergence	alpha in Nepers/m	velocity in m/s
0.5	3/3/3/1	2/2/1/1	5.9893666439e-03	1517.20174
1.0	3/3/3/1	2/2/0/0	2.3957035130e-02	1517.20174
10.0	3/3/3/0	2/2/0/0	2.3953855000e+00	1517.20175
20.0	3/3/3/0	2/2/0/0	9.5807737926e+00	1517.20178
30.0	3/3/3/0	2/2/0/0	2.1555419812e+01	1517.20181
40.0	3/3/3/0	2/2/0/0	3.8318774622e+01	1517.20185
50.0	3/3/3/0	2/2/0/0	5.9870383669e+01	1517.20190
60.0	3/3/3/0	2/2/0/0	8.6209852620e+01	1517.20194
70.0	3/3/3/0	2/2/0/0	1.1733683038e+02	1517.20200
80.0	3/3/3/0	2/2/0/0	1.5325099910e+02	1517.20205
90.0	3/3/3/0	2/2/0/0	1.9395206770e+02	1517.20210
100.0	3/3/3/0	2/2/0/0	2.3943976737e+02	1517.20216
110.0	3/3/3/0	2/2/0/0	2.8971384827e+02	1517.20222
120.0	3/3/3/0	2/2/0/0	3.4477407704e+02	1517.20228
130.0	3/3/3/0	2/2/0/0	4.0462023488e+02	1517.20234
140.0	3/3/3/0	2/2/0/0	4.6925211598e+02	1517.20240
150.0	3/3/3/0	2/2/0/0	5.3866952623e+02	1517.20247

Table C2 10% v/v monodisperse 100nm diameter model X in water at 25ºC

freq (MHz)	0.01%/0.1%/1%/10% alpha convergence	0.01%/0.1%/1%/10% velocity convergence	alpha in Nepers/m	velocity in m/s
0.5	3/3/3/1	2/2/1/1	7.8783432992e-03	1517.20189
1.0	3/3/3/1	2/2/0/0	3.1107897382e-02	1517.20215
10.0	3/3/3/0	2/2/0/0	2.8645030114e+00	1517.20910
20.0	3/3/3/0	2/2/0/0	1.1032464495e+01	1517.21679
30.0	3/3/3/0	2/2/0/0	2.4244497021e+01	1517.22334
40.0	3/3/3/0	2/2/0/0	4.2389040862e+01	1517.22868
50.0	3/3/3/0	2/2/0/0	6.5409155334e+01	1517.23289
60.0	3/3/3/0	2/2/0/0	9.3275507409e+01	1517.23607
70.0	3/3/3/0	2/2/0/0	1.2597436247e+02	1517.23831
80.0	3/3/3/0	2/2/0/0	1.6350127220e+02	1517.23970
90.0	3/3/3/0	2/2/0/0	2.0585745236e+02	1517.24031
100.0	3/3/3/1	2/2/0/0	2.5304759703e+02	1517.24021
110.0	3/3/3/1	2/2/0/0	3.0507852024e+02	1517.23945
120.0	3/3/3/1	2/2/0/0	3.6195829786e+02	1517.23809
130.0	3/3/3/1	2/2/0/0	4.2369572173e+02	1517.23616
140.0	3/3/3/1	2/2/0/0	4.9029995274e+02	1517.23370
150.0	3/3/3/1	2/2/0/0	5.6178030253e+02	1517.23074

Table C3 10% v/v monodisperse 1μm diameter model X in water at 25ºC

freq (MHz)	0.01%/0.1%/1%/10% alpha convergence	0.01%/0.1%/1%/10% velocity convergence	alpha in Nepers/m	velocity in m/s
0.5	3/3/2/2	2/2/1/1	6.2615235639e-02	1517.23854
1.0	3/3/3/2	2/2/0/0	1.5824663962e-01	1517.26160
10.0	3/3/3/2	2/2/0/0	3.6837860627e+00	1517.32807
20.0	3/3/3/3	2/2/0/0	1.2250682207e+01	1517.30906
30.0	3/3/3/3	2/2/0/0	2.6233360394e+01	1517.25952
40.0	3/3/3/3	3/2/0/0	4.5967853679e+01	1517.18620
50.0	4/3/3/3	3/2/0/0	7.1742215630e+01	1517.09110
60.0	4/3/3/3	3/2/0/0	1.0383513509e+02	1516.97500
70.0	4/3/3/3	3/2/0/0	1.4253028952e+02	1516.83825
80.0	4/3/3/3	3/2/0/0	1.8812347605e+02	1516.68093
90.0	4/3/3/3	3/2/0/0	2.4092687070e+02	1516.50300
100.0	4/3/3/3	3/2/0/0	3.0127196057e+02	1516.30431
110.0	4/3/3/3	3/2/0/0	3.6951183613e+02	1516.08461
120.0	4/4/3/3	3/2/0/0	4.4602321134e+02	1515.84357
130.0	4/4/3/3	3/3/0/0	5.3120840483e+02	1515.58080
140.0	4/4/3/3	3/3/0/0	6.2549745593e+02	1515.29582
150.0	4/4/3/3	3/3/0/0	7.2935052468e+02	1514.98806

Table C4 10% v/v monodisperse 10μm diameter model X in water at 25ºC

freq (MHz)	0.01%/0.1%/1%/10% alpha convergence	0.01%/0.1%/1%/10% velocity convergence	alpha in Nepers/m	velocity in m/s
0.5	3/3/3/2	2/2/1/1	4.3510945640e-02	1517.37659
1.0	3/3/3/2	2/2/0/0	8.4773557607e-02	1517.37850
10.0	4/4/3/3	3/2/0/0	4.9722624256e+00	1516.45952
20.0	4/4/3/3	3/3/0/0	3.0760497559e+01	1513.52485
30.0	4/4/3/3	3/3/0/0	1.0486529270e+02	1507.85060
40.0	5/4/4/3	4/3/3/0	2.9329458217e+02	1496.78102
50.0	5/4/3/3	4/3/3/0	1.1100645465e+03	1467.92361
60.0	4/4/3/3	4/4/3/1	5.4174700163e+04	1386.53712
70.0	5/4/4/3	5/4/3/0	4.2048825709e+03	1582.72086
80.0	5/5/4/4	5/4/4/0	3.1003834980e+03	1532.00733
90.0	5/4/4/4	5/4/4/0	3.7848426824e+04	1579.61508
100.0	6/5/5/4	5/5/4/0	4.3961180541e+03	1555.62378
110.0	6/5/5/2	6/5/4/0	1.1900329120e+04	1514.58394
120.0	6/6/5/5	6/5/5/0	1.0180222280e+04	1577.46473
130.0	7/6/6/4	6/6/1/0	6.6941419869e+03	1550.85945
140.0	7/6/6/6	6/6/1/0	1.0052428893e+04	1530.63756
150.0	7/7/6/4	7/6/1/0	7.5211149747e+03	1544.51475

Table C5 10% v/v monodisperse 100μm diameter model X in water at 25ºC

freq (MHz)	0.01%/0.1%/1%/10% alpha convergence	0.01%/0.1%/1%/10% velocity convergence	alpha in Nepers/m	velocity in m/s
0.5	4/3/3/3	3/2/1/1	2.4409733185e-02	1517.18471
1.0	4/4/3/3	3/2/0/0	1.5292853853e-01	1516.50933
10.0	5/5/4/4	5/5/4/0	3.8790530398e+02	1557.31934
20.0	8/8/6/3	8/6/1/0	8.5743564343e+02	1522.75740
30.0	10/8/6/6	10/6/0/0	2.2695013635e+03	1507.56863
40.0	12/10/9/9	11/9/0/0	2.6638064282e+03	1497.55311
50.0	14/13/12/11	12/11/0/0	1.8227127863e+03	1498.24163
60.0	16/15/15/11	15/0/0/0	1.7066709069e+03	1496.66058
70.0	19/18/17/13	17/1/0/0	1.7374110311e+03	1499.04689
80.0	21/20/20/16	20/1/0/0	1.9615517354e+03	1498.52908
90.0	24/23/23/19	23/0/0/0	1.9386425487e+03	1497.72032
100.0	26/26/26/1	22/0/0/0	1.9944654601e+03	1497.16916
110.0	29/29/29/21	25/0/0/0	1.7828586652e+03	1497.30156
120.0	32/32/28/24	27/0/0/0	1.9869583101e+03	1497.58719
130.0	35/35/31/1	26/0/0/0	2.0513691385e+03	1497.62099
140.0	38/34/30/1	29/0/0/0	2.2571440261e+03	1497.49301
150.0	41/33/33/1	32/0/0/0	2.2809720307e+03	1496.67495

Table C6 10% v/v monodisperse 200μm diameter model X in water at 25ºC

freq (MHz)	0.01%/0.1%/1%/10% alpha convergence	0.01%/0.1%/1%/10% velocity convergence	alpha in Nepers/m	velocity in m/s
0.5	4/3/3/3	3/2/1/1	6.1458317639e-02	1516.51609
1.0	4/4/3/3	3/3/0/0	6.4260488601e-01	1513.68698
10.0	8/8/6/3	8/6/1/0	4.2148598000e+02	1522.98464
20.0	12/10/9/9	11/9/0/0	1.3189634161e+03	1497.29947
30.0	16/15/15/11	15/0/0/0	8.2892384430e+02	1496.62007
40.0	21/20/20/16	20/0/0/0	9.4243548609e+02	1498.54848
50.0	26/26/26/22	26/0/0/0	9.4794282380e+02	1497.22851
60.0	32/32/28/24	28/0/0/0	9.1608362454e+02	1497.51022
70.0	38/34/30/1	29/0/0/0	1.0253872521e+03	1497.48378
80.0	40/36/35/1	35/0/0/0	9.3241511329e+02	1496.83716
90.0	45/41/38/1	1/0/0/0	9.4551870190e+02	1497.19970
100.0	47/47/47/1	1/0/0/0	1.0439443008e+03	1496.96353
110.0	53/49/49/1	1/0/0/0	1.0484997284e+03	1496.99440
120.0	55/55/51/1	1/0/0/0	1.1612856975e+03	1496.99702
130.0	61/57/56/1	0/0/0/0	1.1654693348e+03	1496.65690
140.0	66/62/59/1	1/0/0/0	1.2032324785e+03	1496.87507
150.0	72/68/64/1	1/0/0/0	1.3136485319e+03	1496.82901

Table C7 10% v/v monodisperse 400μm diameter model X in water at 25ºC

freq (MHz)	0.01%/0.1%/1%/10% alpha convergence	0.01%/0.1%/1%/10% velocity convergence	alpha in Nepers/m	velocity in m/s
0.5	4/4/3/3	3/3/1/1	2.9659238794e-01	1513.70068
1.0	4/4/3/3	4/3/3/0	3.7866737712e+00	1497.62059
10.0	11/9/9/9	11/9/0/0	6.5555033292e+02	1497.11638
20.0	21/20/20/16	20/1/0/0	4.6135059216e+02	1498.56648
30.0	32/32/28/24	28/0/0/0	4.3707911102e+02	1497.45598
40.0	39/36/35/1	35/0/0/0	4.3229575469e+02	1496.83010
50.0	47/47/47/1	0/0/0/0	4.6872605151e+02	1496.98339
60.0	55/55/51/1	1/0/0/0	5.0262698092e+02	1496.99349
70.0	66/62/59/1	1/0/0/0	4.9288756239e+02	1496.87046
80.0	74/74/70/1	0/0/0/0	5.3612486982e+02	1496.79608
90.0	82/78/78/1	0/0/0/0	5.7990636813e+02	1496.74818
100.0	93/93/85/1	0/0/0/0	6.1711498241e+02	1496.80876
110.0	97/97/93/1	0/0/0/0	6.5181685905e+02	1496.77985
120.0	108/104/101/1	0/0/0/0	6.9988904589e+02	1496.74408
130.0	116/116/108/1	0/0/0/0	7.6924869423e+02	1496.70480
140.0	124/120/116/1	0/0/0/0	8.3157087808e+02	1496.75918
150.0	135/128/124/1	0/0/0/0	8.8676235852e+02	1496.77439

Table C8 10% v/v monodisperse 600μm diameter model X in water at 25ºC

freq (MHz)	0.01%/0.1%/1%/10% alpha convergence	0.01%/0.1%/1%/10% velocity convergence	alpha in Nepers/m	velocity in m/s
0.5	4/4/3/3	3/3/1/1	8.2560910140e-01	1508.24958
1.0	4/4/3/3	4/4/3/3	7.5257657503e+02	1284.17275
10.0	16/15/14/11	15/0/0/0	2.7027834998e+02	1496.57549
20.0	32/32/28/24	28/0/0/0	2.8634127602e+02	1497.43476
30.0	45/41/41/1	1/0/0/0	2.7355079790e+02	1497.21409
40.0	55/55/51/1	1/0/0/0	3.1793426824e+02	1496.99151
50.0	72/72/64/1	1/0/0/0	3.2639275956e+02	1496.84047
60.0	82/78/78/1	0/0/0/0	3.4651946851e+02	1496.74703
70.0	95/95/91/1	0/0/0/0	3.6356329709e+02	1496.74101
80.0	108/104/101/1	0/0/0/0	3.9616904272e+02	1496.74369
90.0	118/118/114/1	0/0/0/0	4.3606216955e+02	1496.74995
100.0	135/128/124/1	0/0/0/0	4.8136990244e+02	1496.77476
110.0	145/141/137/1	0/0/0/0	5.2592596643e+02	1496.73080
120.0	158/158/146/1	0/0/0/0	5.7979269785e+02	1496.71207
130.0	168/168/1/1	0/0/0/0	6.3044645349e+02	1496.71570
140.0	185/181/1/1	0/0/0/0	6.8762337798e+02	1496.71276
150.0	194/191/1/1	0/0/0/0	7.4684554281e+02	1496.71064

Table C9 10% v/v monodisperse 800μm diameter model X in water at 25ºC

freq (MHz)	0.01%/0.1%/1%/10% alpha convergence	0.01%/0.1%/1%/10% velocity convergence	alpha in Nepers/m	velocity in m/s
0.5	4/4/3/3	4/3/3/1	1.8188832455e+00	1497.66708
1.0	4/4/4/3	5/4/4/0	3.0901869484e+01	1533.80538
10.0	21/20/20/16	20/1/0/0	2.2810856705e+02	1498.58140
20.0	39/36/35/1	35/0/0/0	2.0773459209e+02	1496.81634
30.0	55/55/51/1	1/0/0/0	2.3207422023e+02	1496.99017
40.0	74/70/70/1	0/0/0/0	2.3276057330e+02	1496.80118
50.0	93/93/85/1	0/0/0/0	2.5308470444e+02	1496.80821
60.0	108/104/101/1	0/0/0/0	2.7069514505e+02	1496.74345
70.0	124/120/120/1	0/0/0/0	3.0828711687e+02	1496.75812
80.0	143/139/131/1	0/0/0/0	3.2936670227e+02	1496.74486
90.0	158/158/146/1	0/0/0/0	3.7538049176e+02	1496.71249
100.0	181/170/155/1	0/0/0/0	4.1021462534e+02	1496.72895
110.0	189/189/1/1	0/0/0/0	4.6184933380e+02	1496.69757
120.0	208/208/1/1	0/0/0/0	5.0854502935e+02	1496.71277
130.0	227/219/1/1	0/0/0/0	5.6393595157e+02	1496.70837
140.0	246/235/1/1	0/0/0/0	6.2744072421e+02	1496.70412
150.0	258/254/1/1	0/0/0/0	6.8624237975e+02	1496.70608

Table C10 10% v/v monodisperse 1mm diameter model X in water at 25ºC

freq (MHz)	0.01%/0.1%/1%/10% alpha convergence	0.01%/0.1%/1%/10% velocity convergence	alpha in Nepers/m	velocity in m/s
0.5	4/4/3/3	4/3/3/1	5.5294201311e+00	1470.40823
1.0	5/5/4/4	5/5/4/0	3.7640026256e+01	1557.87660
10.0	26/26/26/22	26/0/0/0	1.8526871753e+02	1497.36653
20.0	47/47/47/1	1/0/0/0	1.7569581801e+02	1497.00408
30.0	72/72/64/1	1/0/0/0	1.8233969283e+02	1496.84473
40.0	93/93/85/1	1/0/0/0	1.9354240200e+02	1496.80800
50.0	114/114/103/1	0/0/0/0	2.1560244035e+02	1496.76845
60.0	135/131/124/1	0/0/0/0	2.3617640235e+02	1496.77556
70.0	156/149/145/1	0/0/0/0	2.6376529796e+02	1496.72749
80.0	181/170/166/1	0/0/0/0	2.9301520987e+02	1496.72873
90.0	202/191/1/1	0/0/0/0	3.2936611781e+02	1496.71057
100.0	216/212/1/1	0/0/0/0	3.7101978192e+02	1496.72032
110.0	237/233/1/1	0/0/0/0	4.1814781618e+02	1496.70148
120.0	258/254/1/1	0/0/0/0	4.6992029868e+02	1496.70616
130.0	279/275/1/1	0/0/0/0	5.2525221163e+02	1496.69539
140.0	300/296/1/1	0/0/0/0	5.8591118844e+02	1496.70222
150.0	321/317/1/1	0/0/0/0	6.5086212447e+02	1496.69250

Table C11 10% v/v monodisperse 10nm diameter silica in water at 25ºC

freq (MHz)	0.01%/0.1%/1%/10% alpha convergence	0.01%/0.1%/1%/10% velocity convergence	alpha in Nepers/m	velocity in m/s
0.5	3/3/3/2	2/2/2/1	7.0155088932e-03	1496.61112
1.0	3/3/3/2	2/2/2/0	2.8051034579e-02	1496.61114
10.0	3/3/3/2	2/2/2/0	2.7967791689e+00	1496.61154
20.0	3/3/3/2	2/2/2/0	1.1167013461e+01	1496.61228
30.0	3/3/3/2	2/2/2/0	2.5091181749e+01	1496.61321
40.0	3/3/3/2	2/2/2/0	4.4554844577e+01	1496.61429
50.0	3/3/3/2	2/2/2/0	6.9545974486e+01	1496.61551
60.0	3/3/3/2	2/2/2/0	1.0005406031e+02	1496.61683
70.0	3/3/3/2	2/2/2/0	1.3606966227e+02	1496.61825
80.0	3/3/3/2	2/2/2/0	1.7758415113e+02	1496.61975
90.0	3/3/3/2	2/2/2/0	2.2458953925e+02	1496.62134
100.0	3/3/3/2	2/2/2/0	2.7707836352e+02	1496.62300
110.0	3/3/3/2	2/2/2/0	3.3504360039e+02	1496.62473
120.0	3/3/3/2	2/2/2/0	3.9847860170e+02	1496.62652
130.0	3/3/3/2	2/2/2/0	4.6737704481e+02	1496.62837
140.0	3/3/3/2	2/2/2/0	5.4173289305e+02	1496.63028
150.0	3/3/3/2	2/2/2/0	6.2154036348e+02	1496.63225

Table C12 10% v/v monodisperse 100nm diameter silica in water at 25ºC

freq (MHz)	0.01%/0.1%/1%/10% alpha convergence	0.01%/0.1%/1%/10% velocity convergence	alpha in Nepers/m	velocity in m/s
0.5	3/3/2/2	2/2/2/1	8.7475413088e-02	1496.61543
1.0	3/3/2/2	2/2/2/0	3.3896666496e-01	1496.62272
10.0	3/3/2/2	2/2/2/0	2.6539278443e+01	1496.87393
20.0	3/3/2/2	2/2/2/0	9.0937980581e+01	1497.22414
30.0	3/3/2/2	2/2/2/0	1.8139825785e+02	1497.58321
40.0	3/3/3/2	2/2/2/0	2.9132924694e+02	1497.93341
50.0	3/3/3/2	2/2/2/0	4.1647139469e+02	1498.26854
60.0	3/3/3/2	2/2/2/0	5.5389900777e+02	1498.58654
70.0	3/3/3/2	2/2/2/0	7.0152651311e+02	1498.88712
80.0	3/3/3/2	2/2/2/0	8.5782810783e+02	1499.17079
90.0	3/3/3/2	2/2/2/0	1.0216656432e+03	1499.43840
100.0	3/3/3/2	2/2/2/0	1.1921773137e+03	1499.69094
110.0	3/3/3/2	2/2/2/0	1.3687028765e+03	1499.92945
120.0	3/3/3/2	2/2/2/0	1.5507319032e+03	1500.15491
130.0	3/3/3/2	2/2/2/0	1.7378670977e+03	1500.36826
140.0	3/3/3/2	2/2/2/0	1.9297977657e+03	1500.57038
150.0	3/3/3/2	2/2/2/0	2.1262802916e+03	1500.76206

Table C13 10% v/v monodisperse 1μm diameter silica in water at 25ºC

freq (MHz)	0.01%/0.1%/1%/10% alpha convergence	0.01%/0.1%/1%/10% velocity convergence	alpha in Nepers/m	velocity in m/s
0.5	3/2/2/2	2/2/2/1	3.5594178221e+00	1498.26989
1.0	3/2/2/2	2/2/2/0	9.5067881828e+00	1499.69964
10.0	3/3/2/2	2/2/2/0	9.5965899310e+01	1506.18513
20.0	3/3/2/2	2/2/2/0	1.6130499281e+02	1507.53959
30.0	3/3/3/2	2/2/2/0	2.1921890793e+02	1508.12208
40.0	3/3/3/2	3/2/2/0	2.7605175163e+02	1508.42965
50.0	3/3/3/2	3/2/2/0	3.3463728439e+02	1508.59506
60.0	3/3/3/2	3/2/2/0	3.9669099652e+02	1508.67114
70.0	3/3/3/2	3/2/2/0	4.6346730123e+02	1508.68375
80.0	4/3/3/2	3/2/2/0	5.3600510442e+02	1508.64739
90.0	4/3/3/2	3/2/2/0	6.1523625161e+02	1508.57101
100.0	4/3/3/2	3/2/2/0	7.0203839606e+02	1508.46057
110.0	4/3/3/3	3/2/2/0	7.9726191892e+02	1508.32033
120.0	4/3/3/3	3/2/2/0	9.0174343175e+02	1508.15344
130.0	4/3/3/3	3/3/2/0	1.0163118061e+03	1507.96241
140.0	4/3/3/3	3/3/2/0	1.1417898172e+03	1507.74926
150.0	4/3/3/3	3/3/2/0	1.2789931315e+03	1507.51571

Table C14 10% v/v monodisperse 10μm diameter silica in water at 25ºC

freq (MHz)	0.01%/0.1%/1%/10% alpha convergence	0.01%/0.1%/1%/10% velocity convergence	alpha in Nepers/m	velocity in m/s
0.5	3/2/2/2	2/2/2/1	2.6827844321e+00	1508.88603
1.0	3/3/2/2	2/2/2/0	4.0216727233e+00	1509.54685
10.0	4/3/3/2	3/2/2/0	2.0322050855e+01	1509.68360
20.0	4/4/3/3	3/3/2/0	7.7434488876e+01	1507.18375
30.0	4/4/3/3	3/3/2/0	2.3783502711e+02	1503.51531
40.0	4/4/3/3	4/3/2/0	5.3994109718e+02	1499.21546
50.0	5/4/3/3	4/3/3/0	9.8695007115e+02	1494.48632
60.0	5/4/3/3	4/4/3/0	1.5837996140e+03	1489.32198
70.0	5/4/4/3	4/4/3/0	2.3869903809e+03	1483.80539
80.0	5/4/4/3	5/4/3/0	3.5037172785e+03	1478.39995
90.0	5/5/4/3	5/4/3/0	4.9885927862e+03	1473.94725
100.0	6/5/4/3	5/4/3/0	6.6962970141e+03	1471.14319
110.0	6/5/4/3	5/5/3/0	8.3113490759e+03	1469.88050
120.0	6/5/4/3	6/5/3/0	9.6135737794e+03	1469.40440
130.0	6/5/4/4	6/5/4/0	1.0621976185e+04	1469.17252
140.0	6/6/5/4	6/5/4/0	1.1428774216e+04	1469.21159
150.0	7/6/5/4	6/5/4/0	1.2020407915e+04	1469.68826

Table C15 10% v/v monodisperse 100μm diameter silica in water at 25ºC

freq (MHz)	0.01%/0.1%/1%/10% alpha convergence	0.01%/0.1%/1%/10% velocity convergence	alpha in Nepers/m	velocity in m/s
0.5	3/3/3/2	3/2/2/1	3.4595320494e-01	1510.71542
1.0	4/3/3/2	3/2/2/0	7.9898529911e-01	1510.07349
10.0	5/4/4/3	5/4/3/0	6.0878176287e+02	1471.57521
20.0	7/7/6/5	7/6/1/0	1.0622746107e+03	1475.79210
30.0	10/9/8/7	9/8/0/0	1.1152514049e+03	1488.85036
40.0	12/11/10/9	12/10/0/0	1.6823213680e+03	1489.79405
50.0	15/13/13/11	14/12/0/0	1.5133014437e+03	1490.06898
60.0	17/16/15/14	16/1/0/0	1.4510916310e+03	1492.62408
70.0	19/18/17/15	18/1/0/0	1.6637945285e+03	1494.00644
80.0	21/20/19/17	20/1/0/0	1.7942317120e+03	1493.79785
90.0	24/22/21/15	22/1/0/0	1.6838076959e+03	1494.31046
100.0	26/25/23/16	24/1/0/0	1.8097701406e+03	1494.93873
110.0	28/27/26/18	26/1/0/0	1.8806923925e+03	1495.10011
120.0	30/29/28/1	28/0/0/0	1.9905545397e+03	1495.22200
130.0	33/31/30/1	30/0/0/0	1.9839705687e+03	1495.34298
140.0	35/33/32/1	32/0/0/0	2.0811563300e+03	1495.74570
150.0	37/35/34/1	34/0/0/0	2.1785693697e+03	1495.70863

Table C16 10% v/v monodisperse 200μm diameter silica in water at 25ºC

freq (MHz)	0.01%/0.1%/1%/10% alpha convergence	0.01%/0.1%/1%/10% velocity convergence	alpha in Nepers/m	velocity in m/s
0.5	4/3/3/2	3/2/2/1	3.2224722737e-01	1510.12635
1.0	4/3/3/2	3/3/2/0	2.3561258510e+00	1507.58151
10.0	7/7/6/5	7/6/1/0	5.2501246688e+02	1475.81020
20.0	12/11/10/9	12/10/0/0	8.2702990304e+02	1489.78503
30.0	17/16/15/14	16/1/0/0	7.0039482838e+02	1492.61239
40.0	21/20/19/17	20/1/0/0	8.5573880790e+02	1493.78098
50.0	26/25/23/16	24/1/0/0	8.4406366985e+02	1494.92182
60.0	30/29/28/20	28/0/0/0	9.0944391425e+02	1495.20406
70.0	35/33/32/1	32/0/0/0	9.2792516132e+02	1495.72073
80.0	39/38/36/1	36/0/0/0	9.5191478763e+02	1495.76823
90.0	43/42/41/1	1/0/0/0	1.0140250397e+03	1495.95073
100.0	48/46/45/1	1/0/0/0	1.0517097131e+03	1496.09456
110.0	52/51/49/1	1/0/0/0	1.0999028644e+03	1496.18471
120.0	57/55/53/1	1/0/0/0	1.1400277952e+03	1496.23998
130.0	61/59/58/1	1/0/0/0	1.2082989292e+03	1496.30174
140.0	65/63/62/1	1/0/0/0	1.2651711995e+03	1496.35118
150.0	70/68/66/1	1/0/0/0	1.3277414967e+03	1496.39861

Table C17 10% v/v monodisperse 400μm diameter silica in water at 25ºC

freq (MHz)	0.01%/0.1%/1%/10% alpha convergence	0.01%/0.1%/1%/10% velocity convergence	alpha in Nepers/m	velocity in m/s
0.5	4/3/3/2	3/3/2/1	1.1259913403e+00	1507.61512
1.0	4/3/3/1	4/3/2/0	1.0996407803e+01	1499.77335
10.0	12/11/10/9	12/10/0/0	4.0944271631e+02	1489.77925
20.0	21/20/19/17	20/1/0/0	4.1688438575e+02	1493.76914
30.0	30/29/28/20	28/0/0/0	4.3256452406e+02	1495.19158
40.0	39/38/36/1	36/0/0/0	4.3858864780e+02	1495.75653
50.0	48/46/45/1	1/0/0/0	4.6864791875e+02	1496.08256
60.0	56/55/53/1	1/0/0/0	4.8891429475e+02	1496.22877
70.0	65/63/62/1	1/0/0/0	5.2286797250e+02	1496.34048
80.0	74/72/70/1	1/0/0/0	5.5547515251e+02	1496.41328
90.0	82/81/79/1	1/0/0/0	5.9563877233e+02	1496.47852
100.0	91/89/87/1	1/0/0/0	6.4255874186e+02	1496.50578
110.0	100/98/96/1	1/0/0/0	6.8261991528e+02	1496.54775
120.0	108/106/104/1	0/0/0/0	7.4049024944e+02	1496.56472
130.0	117/115/112/1	0/0/0/0	7.8637261144e+02	1496.56932
140.0	125/123/121/1	0/0/0/0	8.4957365069e+02	1496.60942
150.0	134/132/129/1	0/0/0/0	9.1429662184e+02	1496.59847

Table C18 10% v/v monodisperse 600μm diameter silica in water at 25ºC

freq (MHz)	0.01%/0.1%/1%/10% alpha convergence	0.01%/0.1%/1%/10% velocity convergence	alpha in Nepers/m	velocity in m/s
0.5	4/3/3/2	3/3/2/1	2.9398190497e+00	1504.00675
1.0	4/3/3/3	4/4/3/0	2.2417290791e+01	1490.11502
10.0	17/16/15/14	16/1/0/0	2.2719778640e+02	1492.60135
20.0	30/29/28/20	28/0/0/0	2.8327774707e+02	1495.18611
30.0	43/42/41/1	40/0/0/0	2.9626704334e+02	1495.93383
40.0	56/55/53/1	1/0/0/0	3.0774776907e+02	1496.22384
50.0	69/68/66/1	1/0/0/0	3.3081377234e+02	1496.38266
60.0	82/80/79/1	1/0/0/0	3.5695341056e+02	1496.47391
70.0	95/93/92/1	1/0/0/0	3.8627192979e+02	1496.51670
80.0	108/106/104/1	0/0/0/0	4.2268323819e+02	1496.56066
90.0	121/119/117/1	0/0/0/0	4.6060370787e+02	1496.57478
100.0	134/132/129/1	0/0/0/0	4.9912839621e+02	1496.59568
110.0	146/144/142/1	0/0/0/0	5.4219272800e+02	1496.61226
120.0	159/157/153/1	0/0/0/0	5.9165184135e+02	1496.63389
130.0	172/170/1/1	0/0/0/0	6.4614031443e+02	1496.63812
140.0	185/183/1/1	0/0/0/0	7.0538575842e+02	1496.64967
150.0	198/195/1/1	0/0/0/0	7.6924444139e+02	1496.66150

Table C19 10% v/v monodisperse 800μm diameter silica in water at 25ºC

freq (MHz)	0.01%/0.1%/1%/10% alpha convergence	0.01%/0.1%/1%/10% velocity convergence	alpha in Nepers/m	velocity in m/s
0.5	4/3/3/1	4/3/2/1	5.4482406708e+00	1499.80424
1.0	4/4/3/3	5/4/3/0	3.7788390638e+01	1479.27391
10.0	21/20/19/17	20/1/0/0	2.0546935370e+02	1493.76081
20.0	39/37/36/1	36/0/0/0	2.0970205568e+02	1495.74834
30.0	56/55/53/1	1/0/0/0	2.2393740601e+02	1496.22092
40.0	74/72/70/1	1/0/0/0	2.4199949390e+02	1496.40593
50.0	91/89/87/1	1/0/0/0	2.6563005781e+02	1496.49906
60.0	108/106/104/1	0/0/0/0	2.9035668309e+02	1496.55825
70.0	125/123/121/1	0/0/0/0	3.1651545145e+02	1496.60274
80.0	142/140/138/1	0/0/0/0	3.4774656858e+02	1496.62803
90.0	159/157/154/1	0/0/0/0	3.8431787134e+02	1496.63200
100.0	176/174/1/1	0/0/0/0	4.2790767508e+02	1496.63719
110.0	193/191/1/1	0/0/0/0	4.7642800423e+02	1496.65380
120.0	210/208/1/1	0/0/0/0	5.2472155461e+02	1496.66635
130.0	227/225/1/1	0/0/0/0	5.7600596223e+02	1496.67465
140.0	244/242/1/1	0/0/0/0	6.3540250140e+02	1496.67061
150.0	261/259/1/1	0/0/0/0	6.9969027969e+02	1496.67466

Table C20 10% v/v monodisperse 1mm diameter silica in water at 25ºC

freq (MHz)	0.01%/0.1%/1%/10% alpha convergence	0.01%/0.1%/1%/10% velocity convergence	alpha in Nepers/m	velocity in m/s
0.5	4/3/3/1	4/3/3/1	8.2302384382e+00	1495.19422
1.0	5/4/4/3	5/4/3/0	5.9405100732e+01	1471.72599
10.0	25/24/23/16	24/1/0/0	1.5841735101e+02	1494.90081
20.0	47/46/45/1	1/0/0/0	1.7345273861e+02	1496.07219
30.0	69/68/66/1	1/0/0/0	1.8493296120e+02	1496.37785
40.0	91/89/87/1	1/0/0/0	2.0356985390e+02	1496.49734
50.0	112/110/109/1	0/0/0/0	2.2075937254e+02	1496.57469
60.0	134/132/130/1	0/0/0/0	2.4642741243e+02	1496.59270
70.0	155/153/151/1	0/0/0/0	2.7396916299e+02	1496.62945
80.0	176/174/171/1	0/0/0/0	3.0707088736e+02	1496.63622
90.0	198/195/1/1	0/0/0/0	3.4273859006e+02	1496.65841
100.0	219/217/1/1	0/0/0/0	3.8446404388e+02	1496.65346
110.0	240/238/1/1	0/0/0/0	4.3087376207e+02	1496.66922
120.0	261/259/1/1	0/0/0/0	4.8060724561e+02	1496.67372
130.0	282/280/1/1	0/0/0/0	5.3664534335e+02	1496.67579
140.0	304/301/1/1	0/0/0/0	5.9271303789e+02	1496.67761
150.0	325/322/1/1	0/0/0/0	6.5877325206e+02	1496.67730

Table C21 10% v/v monodisperse 10nm diameter polystyrene in water at 25ºC

freq (MHz)	0.01%/0.1%/1%/10% alpha convergence	0.01%/0.1%/1%/10% velocity convergence	alpha in Nepers/m	velocity in m/s
0.5	3/3/3/1	2/2/1/1	7.1613489261e-03	1525.20437
1.0	3/3/3/1	2/2/0/0	2.8642311032e-02	1525.20437
10.0	3/3/3/0	2/2/0/0	2.8620170763e+00	1525.20443
20.0	3/3/3/0	2/2/0/0	1.1443062441e+01	1525.20446
30.0	3/3/3/0	2/2/0/0	2.5738836118e+01	1525.20442
40.0	3/3/3/0	2/2/0/0	4.5746696303e+01	1525.20432
50.0	3/3/3/0	2/2/0/0	7.1464857121e+01	1525.20415
60.0	3/3/3/0	2/2/0/0	1.0289210649e+02	1525.20391
70.0	3/3/3/0	2/2/0/0	1.4002766102e+02	1525.20358
80.0	3/3/3/0	2/2/0/0	1.8287107826e+02	1525.20318
90.0	3/3/3/0	2/2/0/0	2.3142219851e+02	1525.20270
100.0	3/3/3/0	2/2/0/0	2.8568110339e+02	1525.20214
110.0	3/3/3/0	2/2/0/0	3.4564808525e+02	1525.20150
120.0	3/3/3/0	2/2/0/0	4.1132362349e+02	1525.20079
130.0	3/3/3/0	2/2/0/0	4.8270836595e+02	1525.19999
140.0	3/3/3/0	2/2/0/0	5.5980311374e+02	1525.19912
150.0	3/3/3/0	2/2/0/0	6.4260880887e+02	1525.19817

Table C22 10% v/v monodisperse 100nm diameter polystyrene in water at 25ºC

freq (MHz)	0.01%/0.1%/1%/10% alpha convergence	0.01%/0.1%/1%/10% velocity convergence	alpha in Nepers/m	velocity in m/s
0.5	3/3/3/1	2/2/1/1	2.8189081222e-02	1525.20554
1.0	3/3/3/1	2/2/0/0	1.0990851657e-01	1525.20750
10.0	3/3/3/0	2/2/0/0	9.1496461223e+00	1525.28033
20.0	3/3/3/0	2/2/0/0	3.2184373081e+01	1525.39484
30.0	3/3/3/0	2/2/0/0	6.4583885769e+01	1525.51374
40.0	3/3/3/0	2/2/0/0	1.0365292610e+02	1525.62114
50.0	3/3/3/0	2/2/0/0	1.4820134985e+02	1525.71148
60.0	3/3/3/0	2/2/0/0	1.9794751615e+02	1525.78485
70.0	3/3/3/0	2/2/0/0	2.5302291916e+02	1525.84352
80.0	3/3/3/0	2/2/0/0	3.1369155632e+02	1525.89025
90.0	3/3/3/0	2/2/0/0	3.8022392908e+02	1525.92752
100.0	3/3/3/0	2/2/0/0	4.5285253865e+02	1525.95735
110.0	3/3/3/0	2/2/0/0	5.3176330007e+02	1525.98132
120.0	3/3/3/0	2/2/0/0	6.1710027859e+02	1526.00063
130.0	3/3/3/0	2/2/0/0	7.0897394155e+02	1526.01619
140.0	3/3/3/0	2/2/0/0	8.0746917458e+02	1526.02868
150.0	3/3/3/0	2/2/0/0	9.1265191087e+02	1526.03864

Table C23 10% v/v monodisperse 1μm diameter polystyrene in water at 25ºC

freq (MHz)	0.01%/0.1%/1%/10% alpha convergence	0.01%/0.1%/1%/10% velocity convergence	alpha in Nepers/m	velocity in m/s
0.5	3/2/2/1	2/2/1/1	7.2513452114e-01	1525.76475
1.0	3/3/2/1	2/2/0/0	1.3499569497e+00	1526.06408
10.0	3/3/3/2	2/2/0/0	9.3013618767e+00	1526.53973
20.0	3/3/3/1	2/2/0/0	2.3136805685e+01	1526.56941
30.0	3/3/3/1	2/2/0/0	4.4123245929e+01	1526.53578
40.0	3/3/3/3	3/2/0/0	7.2861884687e+01	1526.46610
50.0	3/3/3/3	3/2/0/0	1.0976836200e+02	1526.36753
60.0	4/3/3/3	3/2/0/0	1.5521093880e+02	1526.24295
70.0	4/3/3/3	3/2/0/0	2.0954981945e+02	1526.09374
80.0	4/3/3/3	3/2/0/0	2.7315282151e+02	1525.92065
90.0	4/3/3/3	3/2/0/0	3.4640278676e+02	1525.72410
100.0	4/3/3/3	3/2/0/0	4.2970142563e+02	1525.50431
110.0	4/3/3/3	3/2/0/0	5.2347140964e+02	1525.26137
120.0	4/3/3/3	3/2/0/0	6.2815754726e+02	1524.99528
130.0	4/3/3/3	3/3/0/0	7.4422748946e+02	1524.70595
140.0	4/4/3/3	3/3/0/0	8.7217223835e+02	1524.39324
150.0	4/4/3/3	3/3/0/0	1.0125066506e+03	1524.05694

Table C24 10% v/v monodisperse 10μm diameter polystyrene in water at 25ºC

freq (MHz)	0.01%/0.1%/1%/10% alpha convergence	0.01%/0.1%/1%/10% velocity convergence	alpha in Nepers/m	velocity in m/s
0.5	3/3/2/2	2/2/1/1	1.5380830666e-01	1526.69534
1.0	3/3/3/2	2/2/0/0	2.4962051014e-01	1526.72052
10.0	4/3/3/3	3/2/0/0	7.1546876788e+00	1525.71047
20.0	4/4/3/3	3/3/0/0	4.3914936760e+01	1522.49521
30.0	4/4/3/3	3/3/0/0	1.4796215903e+02	1516.77127
40.0	5/4/3/3	4/3/3/0	3.7526753381e+02	1507.11284
50.0	5/4/3/3	4/3/3/0	9.4029685921e+02	1488.36095
60.0	5/4/3/3	4/4/3/0	4.7912893662e+03	1433.51825
70.0	4/4/3/3	5/4/3/0	3.3826586954e+04	1678.62027
80.0	5/4/4/3	5/4/3/0	6.6027820701e+03	1576.68033
90.0	5/5/4/4	5/4/4/0	6.5124503348e+03	1526.05427
100.0	5/4/4/4	5/5/4/0	3.8227127180e+04	1584.31038
110.0	6/5/5/4	6/5/4/0	9.0755118751e+03	1570.44495
120.0	6/6/5/5	6/5/5/0	8.8798696614e+03	1530.34530
130.0	6/5/5/5	6/5/5/0	2.9913780942e+04	1586.06415
140.0	7/6/5/5	6/6/5/0	1.2651350337e+04	1561.11113
150.0	7/6/6/4	7/6/1/0	1.2688745844e+04	1541.83691

Table C25 10% v/v monodisperse 100μm diameter polystyrene in water at 25ºC

freq (MHz)	0.01%/0.1%/1%/10% alpha convergence	0.01%/0.1%/1%/10% velocity convergence	alpha in Nepers/m	velocity in m/s
0.5	4/3/3/3	3/2/1/1	4.2207889449e-02	1526.54413
1.0	4/3/3/3	3/2/0/0	2.3954565963e-01	1525.77388
10.0	5/5/4/4	5/5/4/0	4.7250451339e+03	1574.87784
20.0	8/8/7/4	8/7/1/0	1.3970625432e+03	1532.11493
30.0	11/11/8/5	11/8/0/0	1.8533046580e+03	1508.12446
40.0	12/11/9/7	12/1/0/0	1.6320948613e+03	1494.01425
50.0	14/13/10/10	13/0/0/0	1.7192532407e+03	1494.86177
60.0	16/15/13/12	13/0/0/0	1.8838616785e+03	1497.57028
70.0	18/17/16/15	16/1/0/0	2.0167092773e+03	1498.44219
80.0	20/19/18/18	18/0/0/0	1.8228902149e+03	1497.01524
90.0	23/21/21/20	21/0/0/0	1.6148839336e+03	1497.51435
100.0	25/24/23/23	22/0/0/0	1.9739008412e+03	1497.50771
110.0	27/26/26/1	26/0/0/0	1.9989518128e+03	1497.30061
120.0	30/29/28/23	28/0/0/0	2.0928595530e+03	1497.06900
130.0	32/31/31/26	27/0/0/0	1.9626045294e+03	1496.73828
140.0	35/34/29/1	26/0/0/0	1.9975511010e+03	1497.31294
150.0	37/36/32/1	31/0/0/0	2.1571469780e+03	1497.21595

Table C26 10% v/v monodisperse 200μm diameter polystyrene in water at 25ºC

freq (MHz)	0.01%/0.1%/1%/10% alpha convergence	0.01%/0.1%/1%/10% velocity convergence	alpha in Nepers/m	velocity in m/s
0.5	4/3/3/3	3/2/1/1	9.9745771067e-02	1525.78243
1.0	4/4/3/3	3/3/0/0	1.0872803119e+00	1522.66713
10.0	8/7/7/4	8/7/1/0	6.9589224470e+02	1532.17645
20.0	12/11/9/7	12/1/0/0	7.9907462195e+02	1494.00887
30.0	16/14/13/12	13/1/0/0	9.1363638755e+02	1497.55868
40.0	20/19/18/18	18/0/0/0	8.7198512075e+02	1496.98764
50.0	25/24/23/23	22/0/0/0	9.2904910162e+02	1497.44530
60.0	30/29/28/23	28/0/0/0	9.6968292789e+02	1497.04720
70.0	34/34/29/29	26/0/0/0	8.8875547210e+02	1497.33671
80.0	39/39/34/1	34/0/0/0	9.8520013084e+02	1497.03907
90.0	44/40/40/1	39/0/0/0	9.4089308369e+02	1496.99074
100.0	46/45/45/1	1/0/0/0	1.0444344521e+03	1496.82990
110.0	55/50/50/1	0/0/0/0	1.0628546842e+03	1496.92432
120.0	56/55/51/1	1/0/0/0	1.1355435719e+03	1496.88572
130.0	61/57/56/1	0/0/0/0	1.1598243683e+03	1496.81093
140.0	66/66/57/1	1/0/0/0	1.2509276682e+03	1496.88591
150.0	68/67/62/1	0/0/0/0	1.2835010596e+03	1496.78309

Table C27 10% v/v monodisperse 400μm diameter polystyrene in water at 25ºC

freq (MHz)	0.01%/0.1%/1%/10% alpha convergence	0.01%/0.1%/1%/10% velocity convergence	alpha in Nepers/m	velocity in m/s
0.5	4/3/3/1	3/3/1/1	5.1567327892e-01	1522.68154
1.0	4/4/3/3	4/3/3/0	5.9546048998e+00	1507.83819
10.0	12/11/9/7	12/1/0/0	3.9444191097e+02	1494.00302
20.0	20/19/18/18	18/0/0/0	4.2531921101e+02	1496.97338
30.0	29/29/28/23	28/0/0/0	4.6573984347e+02	1497.03564
40.0	39/39/34/1	34/0/0/0	4.5854858889e+02	1497.05362
50.0	46/45/45/1	1/0/0/0	4.6657361696e+02	1496.81503
60.0	56/55/51/1	1/0/0/0	4.8874550729e+02	1496.88487
70.0	66/66/61/1	1/0/0/0	5.2036922046e+02	1496.88584
80.0	73/72/72/1	0/0/0/0	5.5365929553e+02	1496.83808
90.0	83/78/78/1	0/0/0/0	5.8264017303e+02	1496.80953
100.0	93/89/84/1	0/0/0/0	6.1039502164e+02	1496.79248
110.0	99/99/90/1	0/0/0/0	6.5970582553e+02	1496.75363
120.0	106/105/101/1	0/0/0/0	7.1306799746e+02	1496.78209
130.0	116/111/107/1	0/0/0/0	7.5991516080e+02	1496.76783
140.0	126/122/117/1	0/0/0/0	8.1953301523e+02	1496.73946
150.0	132/128/123/1	0/0/0/0	8.8357031594e+02	1496.72523

Table C28 10% v/v monodisperse 600μm diameter polystyrene in water at 25ºC

freq (MHz)	0.01%/0.1%/1%/10% alpha convergence	0.01%/0.1%/1%/10% velocity convergence	alpha in Nepers/m	velocity in m/s
0.5	4/4/3/1	3/3/1/1	1.4333394707e+00	1517.16049
1.0	4/3/3/3	4/4/3/0	5.0497235691e+01	1437.05845
10.0	16/14/13/12	13/0/0/0	2.9736752847e+02	1497.54823
20.0	29/28/28/23	28/0/0/0	3.0627212634e+02	1497.03160
30.0	44/40/40/1	39/0/0/0	2.7104382404e+02	1497.01219
40.0	56/55/51/1	1/0/0/0	3.0822797915e+02	1496.88438
50.0	67/67/62/1	0/0/0/0	3.1595273843e+02	1496.77630
60.0	83/78/78/1	1/0/0/0	3.4935937872e+02	1496.80851
70.0	94/94/89/1	0/0/0/0	3.6552978902e+02	1496.73713
80.0	106/105/101/1	0/0/0/0	4.0496191891e+02	1496.78392
90.0	121/121/112/1	0/0/0/0	4.3684105579e+02	1496.72683
100.0	132/128/128/1	0/0/0/0	4.7869255018e+02	1496.72433
110.0	148/139/135/1	0/0/0/0	5.2914487236e+02	1496.72489
120.0	155/155/138/1	0/0/0/0	5.7464163655e+02	1496.73145
130.0	171/166/1/1	0/0/0/0	6.2702842899e+02	1496.71361
140.0	182/182/1/1	0/0/0/0	6.9068695738e+02	1496.70570
150.0	198/189/1/1	0/0/0/0	7.5309359166e+02	1496.71672

Table C29 10% v/v monodisperse 800μm diameter polystyrene in water at 25ºC

freq (MHz)	0.01%/0.1%/1%/10% alpha convergence	0.01%/0.1%/1%/10% velocity convergence	alpha in Nepers/m	velocity in m/s
0.5	4/4/3/1	4/3/3/1	2.9126090954e+00	1507.87763
1.0	5/4/3/3	5/4/3/0	7.6808565981e+01	1579.90896
10.0	20/18/18/18	18/0/0/0	2.0970159825e+02	1496.96648
20.0	39/39/34/1	34/0/0/0	2.2098491136e+02	1497.06634
30.0	56/55/51/1	1/0/0/0	2.2455791352e+02	1496.88406
40.0	72/72/72/1	0/0/0/0	2.4271557281e+02	1496.83212
50.0	93/89/84/1	0/0/0/0	2.5028862038e+02	1496.79809
60.0	106/105/101/1	0/0/0/0	2.7731627719e+02	1496.78478
70.0	126/122/117/1	0/0/0/0	3.0158925067e+02	1496.74184
80.0	143/138/134/1	0/0/0/0	3.3445054187e+02	1496.72561
90.0	159/155/145/1	0/0/0/0	3.7160755645e+02	1496.73238
100.0	176/176/154/1	0/0/0/0	4.1379710295e+02	1496.70522
110.0	197/188/1/1	0/0/0/0	4.5942963879e+02	1496.71095
120.0	209/205/1/1	0/0/0/0	5.0955680187e+02	1496.70793
130.0	226/221/1/1	0/0/0/0	5.6637399098e+02	1496.70562
140.0	242/238/1/1	0/0/0/0	6.2240583801e+02	1496.70307
150.0	259/259/1/1	0/0/0/0	6.8896218924e+02	1496.70314

Table C30 10% v/v monodisperse 1mm diameter polystyrene in water at 25ºC

freq (MHz)	0.01%/0.1%/1%/10% alpha convergence	0.01%/0.1%/1%/10% velocity convergence	alpha in Nepers/m	velocity in m/s
0.5	4/3/3/3	4/3/3/1	5.7911100907e+00	1489.96950
1.0	5/5/4/4	5/5/4/0	5.0772642484e+02	1568.23398
10.0	24/23/23/23	22/0/0/0	1.7386149703e+02	1497.36487
20.0	46/45/45/1	1/0/0/0	1.7280406488e+02	1496.80182
30.0	67/67/62/1	0/0/0/0	1.7608003906e+02	1496.77461
40.0	93/88/84/1	0/0/0/0	1.9144239538e+02	1496.79945
50.0	115/110/106/1	0/0/0/0	2.1472260222e+02	1496.73588
60.0	132/128/128/1	0/0/0/0	2.3424439592e+02	1496.72325
70.0	154/154/145/1	0/0/0/0	2.6617175338e+02	1496.71602
80.0	176/176/160/1	0/0/0/0	2.9571327665e+02	1496.70419
90.0	198/189/1/1	0/0/0/0	3.3334746225e+02	1496.71724
100.0	215/211/1/1	0/0/0/0	3.7531395633e+02	1496.70672
110.0	237/233/1/1	0/0/0/0	4.1951507500e+02	1496.70659
120.0	259/259/1/1	0/0/0/0	4.7207324210e+02	1496.70335
130.0	281/272/1/1	0/0/0/0	5.2427764798e+02	1496.70092
140.0	307/294/1/1	0/0/0/0	5.8504887731e+02	1496.70204
150.0	320/316/1/1	0/0/0/0	6.4697852237e+02	1496.69753

Table C31 10% v/v monodisperse 10nm diameter iron in water at 25ºC

freq (MHz)	0.01%/0.1%/1%/10% alpha convergence	0.01%/0.1%/1%/10% velocity convergence	alpha in Nepers/m	velocity in m/s
0.5	3/3/2/2	2/2/2/2	7.1513281753e-02	1212.26529
1.0	3/3/2/2	2/2/2/2	2.8534395802e-01	1212.26566
10.0	3/3/2/2	2/2/2/2	2.8008587455e+01	1212.28354
20.0	3/3/2/2	2/2/2/2	1.1074674005e+02	1212.31785
30.0	3/3/2/2	2/2/2/2	2.4693438897e+02	1212.36272
40.0	3/3/2/2	2/2/2/2	4.3559585463e+02	1212.41622
50.0	3/3/2/2	2/2/2/2	6.7589623881e+02	1212.47721
60.0	3/3/2/2	2/2/2/2	9.6708736373e+02	1212.54493
70.0	3/3/2/2	2/2/2/2	1.3084812822e+03	1212.61877
80.0	3/3/2/2	2/2/2/2	1.6994349457e+03	1212.69829
90.0	3/3/2/2	2/2/2/2	2.1393404051e+03	1212.78311
100.0	3/3/2/2	2/2/2/2	2.6276181125e+03	1212.87290
110.0	3/3/2/2	2/2/2/2	3.1637121180e+03	1212.96740
120.0	3/3/2/2	2/2/2/2	3.7470864921e+03	1213.06637
130.0	3/3/2/2	2/2/2/2	4.3772225851e+03	1213.16960
140.0	3/3/2/2	2/2/2/2	5.0536168763e+03	1213.27690
150.0	3/3/2/2	2/2/2/2	5.7757792531e+03	1213.38810

Table C32 10% v/v monodisperse 100nm diameter iron in water at 25ºC

freq (MHz)	0.01%/0.1%/1%/10% alpha convergence	0.01%/0.1%/1%/10% velocity convergence	alpha in Nepers/m	velocity in m/s
0.5	2/2/2/2	2/2/2/2	6.0108968467e+00	1212.47647
1.0	2/2/2/2	2/2/2/2	2.3284866719e+01	1212.87003
10.0	2/2/2/2	2/2/2/2	1.6633598543e+03	1229.68735
20.0	3/2/2/2	2/2/2/2	4.9467419456e+03	1253.11944
30.0	3/2/2/2	2/2/2/2	8.5895195742e+03	1274.45787
40.0	3/2/2/2	2/2/2/2	1.2150932411e+04	1292.56191
50.0	3/2/2/2	2/2/2/2	1.5496890853e+04	1307.69263
60.0	3/2/2/2	2/2/2/2	1.8603292176e+04	1320.36639
70.0	3/2/2/2	2/2/2/2	2.1483527536e+04	1331.06851
80.0	3/2/2/2	2/2/2/2	2.4161816464e+04	1340.19542
90.0	3/2/2/2	2/2/2/2	2.6663509817e+04	1348.05745
100.0	3/2/2/2	2/2/2/2	2.9011795954e+04	1354.89488
110.0	3/2/2/2	2/2/2/2	3.1226840032e+04	1360.89400
120.0	3/2/2/2	2/2/2/2	3.3325822541e+04	1366.20021
130.0	3/2/2/2	2/2/2/2	3.5323275030e+04	1370.92803
140.0	3/2/2/2	2/2/2/2	3.7231478461e+04	1375.16856
150.0	3/3/2/2	2/2/2/2	3.9060837649e+04	1378.99497

Table C33 10% v/v monodisperse 1μm diameter iron in water at 25ºC

freq (MHz)	0.01%/0.1%/1%/10% alpha convergence	0.01%/0.1%/1%/10% velocity convergence	alpha in Nepers/m	velocity in m/s
0.5	2/2/2/2	2/2/2/2	1.5425981460e+02	1307.67725
1.0	2/2/2/2	2/2/2/2	2.8735487932e+02	1354.86858
10.0	3/2/2/2	2/2/2/0	1.0946490620e+03	1443.81673
20.0	3/2/2/2	2/2/2/0	1.5428401126e+03	1454.70745
30.0	3/3/2/2	2/2/2/0	1.8898631279e+03	1459.37650
40.0	3/3/2/2	3/2/2/0	2.1899157604e+03	1462.08366
50.0	3/3/2/2	3/2/2/0	2.4638419708e+03	1463.87024
60.0	3/3/2/2	3/2/2/0	2.7227876122e+03	1465.13325
70.0	3/3/2/2	3/2/2/0	2.9739400532e+03	1466.06176
80.0	3/3/3/2	3/2/2/0	3.2225677200e+03	1466.75920
90.0	3/3/3/2	3/2/2/0	3.4729058044e+03	1467.28790
100.0	3/3/3/2	3/2/2/0	3.7285907052e+03	1467.68824
110.0	3/3/3/2	3/2/2/0	3.9928897008e+03	1467.98801
120.0	4/3/3/2	3/2/2/0	4.2688272877e+03	1468.20721
130.0	4/3/3/2	3/2/2/0	4.5592550682e+03	1468.36087
140.0	4/3/3/2	3/3/2/0	4.8668888911e+03	1468.46071
150.0	4/3/3/2	3/3/2/0	5.1943261372e+03	1468.51612

Table C34 10% v/v monodisperse 10μm diameter iron in water at 25ºC

freq (MHz)	0.01%/0.1%/1%/10% alpha convergence	0.01%/0.1%/1%/10% velocity convergence	alpha in Nepers/m	velocity in m/s
0.5	2/2/2/2	2/2/2/1	2.3885676728e+01	1464.18983
1.0	3/2/2/2	2/2/2/0	3.3471475836e+01	1468.86997
10.0	3/3/3/2	3/2/2/0	1.1650537481e+02	1475.44311
20.0	4/3/3/2	3/3/2/0	2.8968714706e+02	1473.89661
30.0	4/3/3/2	3/3/2/0	7.3793532311e+02	1472.00366
40.0	4/4/3/2	4/3/2/0	1.5197457609e+03	1471.45697
50.0	4/4/3/2	4/3/3/0	2.5007135169e+03	1472.48489
60.0	5/4/3/2	4/4/3/0	3.4718084752e+03	1474.18050
70.0	5/4/3/3	4/4/3/0	4.3452252061e+03	1475.50132
80.0	5/4/3/3	5/4/3/0	5.1911451080e+03	1476.17358
90.0	5/4/4/3	5/4/3/0	6.0849626799e+03	1476.62767
100.0	6/5/4/3	5/4/3/0	6.9810337311e+03	1477.28693
110.0	6/5/4/3	5/4/3/0	7.7677499601e+03	1478.13076
120.0	6/5/4/3	6/5/3/0	8.4007053267e+03	1478.91344
130.0	6/5/4/4	6/5/1/0	8.9214885154e+03	1479.55161
140.0	7/6/5/4	6/5/1/0	9.3695945439e+03	1480.16044
150.0	7/6/5/4	6/5/0/0	9.7344723091e+03	1480.83896

Table C35 10% v/v monodisperse 100μm diameter iron in water at 25ºC

freq (MHz)	0.01%/0.1%/1%/10% alpha convergence	0.01%/0.1%/1%/10% velocity convergence	alpha in Nepers/m	velocity in m/s
0.5	3/3/2/2	3/2/2/1	2.3754034983e+00	1478.26070
1.0	3/3/3/2	3/2/2/0	4.2150762691e+00	1477.90165
10.0	5/4/4/3	5/4/3/0	6.3992328106e+02	1478.00246
20.0	7/7/6/5	7/6/0/0	9.2227706228e+02	1485.07737
30.0	10/9/8/7	9/8/0/0	9.2192884388e+02	1490.93629
40.0	12/11/10/6	11/10/0/0	1.2961408985e+03	1491.80248
50.0	15/13/12/8	13/11/0/0	1.2425796443e+03	1493.23125
60.0	17/16/15/10	15/1/0/0	1.2964104118e+03	1494.52546
70.0	19/18/17/11	17/1/0/0	1.4635078811e+03	1495.15028
80.0	21/20/19/13	19/1/0/0	1.5406218080e+03	1494.94937
90.0	24/22/21/15	21/1/0/0	1.4765023623e+03	1495.20615
100.0	26/24/23/17	23/0/0/0	1.5238207319e+03	1495.72172
110.0	28/27/25/19	25/0/0/0	1.6944397358e+03	1495.94193
120.0	30/29/27/1	27/0/0/0	1.7792941656e+03	1495.70254
130.0	33/31/29/1	29/0/0/0	1.7219431052e+03	1495.76408
140.0	35/33/31/1	31/0/0/0	1.7742319565e+03	1496.13802
150.0	37/35/33/1	33/0/0/0	1.9745450946e+03	1496.20999

Table C36 10% v/v monodisperse 200μm diameter iron in water at 25ºC

freq (MHz)	0.01%/0.1%/1%/10% alpha convergence	0.01%/0.1%/1%/10% velocity convergence	alpha in Nepers/m	velocity in m/s
0.5	3/3/3/2	3/2/2/1	1.6167880691e+00	1478.23518
1.0	4/3/3/2	3/3/2/0	7.9870182001e+00	1475.89912
10.0	7/7/6/5	7/6/0/0	4.5531524645e+02	1485.13489
20.0	12/11/10/6	11/10/0/0	6.3464570695e+02	1491.82673
30.0	17/16/15/10	15/1/0/0	6.2343220220e+02	1494.54102
40.0	21/20/19/13	19/1/0/0	7.2955541574e+02	1494.96002
50.0	26/24/23/17	23/0/0/0	7.0112692866e+02	1495.72736
60.0	30/29/27/21	27/0/0/0	8.0324288352e+02	1495.70102
70.0	35/33/31/24	31/0/0/0	7.7237290764e+02	1496.14171
80.0	39/37/36/1	35/0/0/0	8.7730590566e+02	1496.01508
90.0	43/42/40/1	1/0/0/0	8.8688340446e+02	1496.31779
100.0	48/46/44/1	1/0/0/0	9.6362487065e+02	1496.21167
110.0	52/50/48/1	1/0/0/0	9.6791400797e+02	1496.38144
120.0	56/54/52/1	1/0/0/0	1.0727925466e+03	1496.35396
130.0	61/59/56/1	1/0/0/0	1.0748400820e+03	1496.48350
140.0	65/63/60/1	1/0/0/0	1.1770220534e+03	1496.39734
150.0	69/67/64/1	1/0/0/0	1.2178249123e+03	1496.52558

Table C37 10% v/v monodisperse 400μm diameter iron in water at 25ºC

freq (MHz)	0.01%/0.1%/1%/10% alpha convergence	0.01%/0.1%/1%/10% velocity convergence	alpha in Nepers/m	velocity in m/s
0.5	3/3/2/2	3/3/2/1	3.7345788640e+00	1476.06842
1.0	3/3/2/2	4/3/2/0	3.1791733194e+01	1472.97176
10.0	12/11/10/6	11/10/0/0	3.1350565441e+02	1491.84461
20.0	21/20/19/13	19/1/0/0	3.5403457755e+02	1494.96805
30.0	30/29/27/21	27/0/0/0	3.7936012096e+02	1495.69947
40.0	39/37/36/1	35/0/0/0	4.0128055945e+02	1496.01766
50.0	47/46/44/1	1/0/0/0	4.2453984033e+02	1496.20954
60.0	56/54/52/1	1/0/0/0	4.5464660468e+02	1496.35884
70.0	65/63/61/1	1/0/0/0	4.7808465909e+02	1496.39793
80.0	73/71/69/1	1/0/0/0	5.1524797914e+02	1496.46886
90.0	82/80/77/1	1/0/0/0	5.5516459074e+02	1496.51865
100.0	90/88/85/1	0/0/0/0	5.8939412226e+02	1496.57850
110.0	99/97/86/1	0/0/0/0	6.4523538435e+02	1496.56735
120.0	107/105/94/1	0/0/0/0	6.9441273165e+02	1496.56678
130.0	116/113/102/1	0/0/0/0	7.4750965285e+02	1496.59343
140.0	124/122/110/1	0/0/0/0	8.0887057158e+02	1496.60955
150.0	133/130/118/1	0/0/0/0	8.7102621651e+02	1496.61712

Table C38 10% v/v monodisperse 600μm diameter iron in water at 25ºC

freq (MHz)	0.01%/0.1%/1%/10% alpha convergence	0.01%/0.1%/1%/10% velocity convergence	alpha in Nepers/m	velocity in m/s
0.5	3/3/2/2	3/3/2/1	8.9948585454e+00	1473.84219
1.0	4/3/3/2	4/3/3/0	5.1614933496e+01	1475.44231
10.0	16/15/14/10	15/1/0/0	2.0171302267e+02	1494.55812
20.0	30/29/27/21	27/0/0/0	2.4780536249e+02	1495.69904
30.0	43/41/40/1	1/0/0/0	2.5400615590e+02	1496.31931
40.0	56/54/52/1	1/0/0/0	2.8470343842e+02	1496.36090
50.0	69/67/65/1	1/0/0/0	2.9399363617e+02	1496.52429
60.0	82/80/77/1	1/0/0/0	3.2973994072e+02	1496.51936
70.0	95/92/89/1	0/0/0/0	3.4788539611e+02	1496.57095
80.0	107/105/94/1	0/0/0/0	3.9176435062e+02	1496.56733
90.0	120/118/106/1	0/0/0/0	4.2114337962e+02	1496.61375
100.0	133/130/118/1	0/0/0/0	4.6988791004e+02	1496.61637
110.0	145/143/130/1	0/0/0/0	5.1078341375e+02	1496.62482
120.0	158/155/142/1	0/0/0/0	5.6913893701e+02	1496.63536
130.0	171/168/1/1	0/0/0/0	6.1764042867e+02	1496.64209
140.0	183/180/1/1	0/0/0/0	6.8113653918e+02	1496.65624
150.0	196/193/1/1	0/0/0/0	7.4422319291e+02	1496.64297

Table C39 10% v/v monodisperse 800μm diameter iron in water at 25ºC

freq (MHz)	0.01%/0.1%/1%/10% alpha convergence	0.01%/0.1%/1%/10% velocity convergence	alpha in Nepers/m	velocity in m/s
0.5	3/3/2/2	4/3/2/1	1.5745844881e+01	1473.05565
1.0	4/3/3/3	5/4/3/0	5.8185412725e+01	1477.32679
10.0	21/20/19/13	19/1/0/0	1.7413581234e+02	1494.97397
20.0	38/37/36/1	35/0/0/0	1.9106424751e+02	1496.01975
30.0	56/54/52/1	1/0/0/0	2.0656846622e+02	1496.36205
40.0	73/71/69/1	1/0/0/0	2.2149515268e+02	1496.46935
50.0	90/88/85/1	0/0/0/0	2.3856545955e+02	1496.58064
60.0	107/105/101/1	0/0/0/0	2.6707176739e+02	1496.56769
70.0	124/122/111/1	0/0/0/0	2.9547243299e+02	1496.60923
80.0	141/139/127/1	0/0/0/0	3.2953069274e+02	1496.63869
90.0	158/155/143/1	0/0/0/0	3.6702962261e+02	1496.63544
100.0	175/172/158/1	0/0/0/0	4.0582824953e+02	1496.63724
110.0	192/189/1/1	0/0/0/0	4.5302413654e+02	1496.65743
120.0	209/206/1/1	0/0/0/0	5.0567678264e+02	1496.66232
130.0	226/222/1/1	0/0/0/0	5.5909517439e+02	1496.66081
140.0	242/239/1/1	0/0/0/0	6.1769184891e+02	1496.66502
150.0	259/255/1/1	0/0/0/0	6.8440742341e+02	1496.66475

Table C40 10% v/v monodisperse 1mm diameter iron in water at 25ºC

freq (MHz)	0.01%/0.1%/1%/10% alpha convergence	0.01%/0.1%/1%/10% velocity convergence	alpha in Nepers/m	velocity in m/s
0.5	4/3/2/2	4/3/2/1	2.1776888328e+01	1473.90788
1.0	5/4/4/3	5/4/3/0	6.2611277893e+01	1478.23740
10.0	25/24/23/17	23/0/0/0	1.2987978147e+02	1495.73769
20.0	47/46/44/1	1/0/0/0	1.5575784284e+02	1496.20861
30.0	69/67/65/1	1/0/0/0	1.6286277230e+02	1496.52367
40.0	90/88/85/1	0/0/0/0	1.8181722144e+02	1496.58143
50.0	111/109/106/1	0/0/0/0	1.9983118913e+02	1496.59709
60.0	133/130/119/1	0/0/0/0	2.2862533896e+02	1496.61546
70.0	154/151/139/1	0/0/0/0	2.5372224084e+02	1496.63401
80.0	175/172/159/1	0/0/0/0	2.8928761612e+02	1496.63760
90.0	196/193/1/1	0/0/0/0	3.2724440508e+02	1496.64326
100.0	217/214/1/1	0/0/0/0	3.6986334815e+02	1496.65566
110.0	238/235/1/1	0/0/0/0	4.1760548418e+02	1496.66196
120.0	259/256/1/1	0/0/0/0	4.6801661021e+02	1496.66459
130.0	280/276/1/1	0/0/0/0	5.2371677810e+02	1496.66909
140.0	301/297/1/1	0/0/0/0	5.8245471443e+02	1496.67168
150.0	322/318/1/1	0/0/0/0	6.4737555016e+02	1496.67250

Table C41 10% v/v monodisperse 10nm diameter titanium dioxide in water at 25ºC

freq (MHz)	0.01%/0.1%/1%/10% alpha convergence	0.01%/0.1%/1%/10% velocity convergence	alpha in Nepers/m	velocity in m/s
0.5	3/3/3/2	2/2/2/2	2.5879729127e-02	1349.94589
1.0	3/3/3/2	2/2/2/2	1.0329681584e-01	1349.94603
10.0	3/3/3/2	2/2/2/2	1.0165453380e+01	1349.95273
20.0	3/3/3/2	2/2/2/2	4.0262226152e+01	1349.96534
30.0	3/3/3/2	2/2/2/2	8.9897403481e+01	1349.98160
40.0	3/3/3/2	2/2/2/2	1.5877568891e+02	1350.00079
50.0	3/3/3/2	2/2/2/2	2.4664758048e+02	1350.02247
60.0	3/3/3/2	2/2/2/2	3.5329211519e+02	1350.04637
70.0	3/3/3/2	2/2/2/2	4.7850835377e+02	1350.07227
80.0	3/3/3/2	2/2/2/2	6.2211041688e+02	1350.10000
90.0	3/3/3/2	2/2/2/2	7.8392428887e+02	1350.12942
100.0	3/3/3/2	2/2/2/2	9.6378561684e+02	1350.16043
110.0	3/3/3/2	2/2/2/2	1.1615381194e+03	1350.19292
120.0	3/3/3/2	2/2/2/2	1.3770323925e+03	1350.22682
130.0	3/3/3/2	2/2/2/2	1.6101249864e+03	1350.26206
140.0	3/3/3/2	2/2/2/2	1.8606776758e+03	1350.29855
150.0	3/3/3/2	2/2/2/2	2.1285568701e+03	1350.33626

Table C42 10% v/v monodisperse 100nm diameter titanium dioxide in water at 25ºC

freq (MHz)	0.01%/0.1%/1%/10% alpha convergence	0.01%/0.1%/1%/10% velocity convergence	alpha in Nepers/m	velocity in m/s
0.5	3/2/2/2	2/2/2/2	1.8686964672e+00	1350.02267
1.0	3/2/2/2	2/2/2/2	7.2462883933e+00	1350.16112
10.0	3/2/2/2	2/2/2/2	5.4425342259e+02	1355.74092
20.0	3/2/2/2	2/2/2/2	1.7375667753e+03	1363.80220
30.0	3/2/2/2	2/2/2/2	3.2214133587e+03	1371.72989
40.0	3/2/2/2	2/2/2/2	4.8217348795e+03	1378.99259
50.0	3/2/2/2	2/2/2/2	6.4510814478e+03	1385.49119
60.0	3/2/2/2	2/2/2/2	8.0655524824e+03	1391.26402
70.0	3/2/2/2	2/2/2/2	9.6437589717e+03	1396.38987
80.0	3/3/2/2	2/2/2/2	1.1176166756e+04	1400.95318
90.0	3/3/2/2	2/2/2/2	1.2659541057e+04	1405.03195
100.0	3/3/2/2	2/2/2/2	1.4093979323e+04	1408.69421
110.0	3/3/2/2	2/2/2/2	1.5481296106e+04	1411.99791
120.0	3/3/2/2	2/2/2/2	1.6824132808e+04	1414.99187
130.0	3/3/2/2	2/2/2/2	1.8125464806e+04	1417.71712
140.0	3/3/2/2	2/2/2/2	1.9388330442e+04	1420.20814
150.0	3/3/2/2	2/2/2/2	2.0615685533e+04	1422.49402

Table C43 10% v/v monodisperse 1μm diameter titanium dioxide in water at 25ºC

freq (MHz)	0.01%/0.1%/1%/10% alpha convergence	0.01%/0.1%/1%/10% velocity convergence	alpha in Nepers/m	velocity in m/s
0.5	2/2/2/2	2/2/2/2	6.3909572300e+01	1385.49549
1.0	2/2/2/2	2/2/2/2	1.3853342524e+02	1408.71137
10.0	3/2/2/2	2/2/2/0	7.1206623744e+02	1466.62292
20.0	3/3/2/2	2/2/2/0	1.0426322052e+03	1474.72652
30.0	3/3/2/2	2/2/2/0	1.3001905171e+03	1478.20172
40.0	3/3/2/2	3/2/2/0	1.5246973563e+03	1480.20043
50.0	3/3/2/2	3/2/2/0	1.7316624944e+03	1481.50094
60.0	3/3/2/2	3/2/2/0	1.9294921441e+03	1482.40092
70.0	3/3/3/2	3/2/2/0	2.1237089133e+03	1483.04243
80.0	3/3/3/2	3/2/2/0	2.3184504741e+03	1483.50331
90.0	3/3/3/2	3/2/2/0	2.5171182645e+03	1483.83062
100.0	3/3/3/2	3/2/2/0	2.7226933202e+03	1484.05497
110.0	4/3/3/2	3/2/2/0	2.9379009397e+03	1484.19751
120.0	4/3/3/2	3/2/2/0	3.1652990604e+03	1484.27358
130.0	4/3/3/2	3/2/2/0	3.4073250074e+03	1484.29478
140.0	4/3/3/2	3/3/2/0	3.6663181871e+03	1484.27026
150.0	4/3/3/2	3/3/2/0	3.9445283168e+03	1484.20738

Table C44 10% v/v monodisperse 10μm diameter titanium dioxide in water at 25ºC

freq (MHz)	0.01%/0.1%/1%/10% alpha convergence	0.01%/0.1%/1%/10% velocity convergence	alpha in Nepers/m	velocity in m/s
0.5	2/2/2/2	2/2/2/1	1.6605405406e+01	1481.85400
1.0	3/2/2/2	2/2/2/0	2.3632434711e+01	1485.35775
10.0	3/3/3/2	3/2/2/0	8.6969915690e+01	1489.88807
20.0	4/3/3/2	3/3/2/0	2.3796888556e+02	1487.73621
30.0	4/4/3/2	3/3/2/0	6.3924647386e+02	1485.02611
40.0	4/4/3/2	4/3/2/0	1.3426263714e+03	1483.19804
50.0	4/4/3/2	4/3/3/0	2.2437713258e+03	1482.43048
60.0	5/4/3/2	4/4/3/0	3.1883540219e+03	1482.02404
70.0	5/4/3/3	4/4/3/0	4.1224149881e+03	1481.25371
80.0	5/4/3/3	5/4/3/0	5.1104370272e+03	1480.05627
90.0	5/4/4/3	5/4/3/0	6.2013046701e+03	1478.93512
100.0	6/5/4/3	5/4/3/0	7.3151140756e+03	1478.31818
110.0	6/5/4/3	5/4/3/0	8.3016438297e+03	1478.14307
120.0	6/5/4/3	6/5/3/0	9.0865424109e+03	1478.09059
130.0	6/5/4/4	6/5/3/0	9.6999185496e+03	1478.02006
140.0	7/6/5/4	6/5/1/0	1.0179677236e+04	1478.03057
150.0	7/6/5/4	6/5/1/0	1.0511072061e+04	1478.22362

Table C45 10% v/v monodisperse 100μm diameter titanium dioxide in water at 25ºC

freq (MHz)	0.01%/0.1%/1%/10% alpha convergence	0.01%/0.1%/1%/10% velocity convergence	alpha in Nepers/m	velocity in m/s
0.5	3/3/2/2	3/2/2/1	1.7443972514e+00	1492.28288
1.0	3/3/3/2	3/2/2/0	3.2609536909e+00	1491.73172
10.0	5/4/4/3	5/4/3/0	6.7217219990e+02	1479.00646
20.0	7/7/6/5	7/6/0/0	8.6627365173e+02	1481.52463
30.0	10/9/8/7	9/8/0/0	9.6099583383e+02	1489.86650
40.0	12/11/10/9	11/10/0/0	1.2525927236e+03	1493.49444
50.0	15/13/12/8	13/11/0/0	1.4945249268e+03	1493.08665
60.0	17/16/15/10	15/1/0/0	1.3740532939e+03	1493.00644
70.0	19/18/17/11	18/1/0/0	1.2868940274e+03	1494.48206
80.0	21/20/19/13	20/0/0/0	1.4862867714e+03	1495.61716
90.0	24/22/21/15	22/0/0/0	1.6601919377e+03	1495.39456
100.0	26/24/23/17	23/1/0/0	1.6992797698e+03	1495.07502
110.0	28/27/25/19	25/0/0/0	1.6016029332e+03	1495.19363
120.0	30/29/27/20	27/0/0/0	1.6188810093e+03	1495.74866
130.0	33/31/29/1	29/0/0/0	1.7523851054e+03	1496.36427
140.0	35/33/31/1	31/0/0/0	2.0245629204e+03	1496.04320
150.0	37/35/34/1	33/0/0/0	2.0137866827e+03	1495.72927

Table C46 10% v/v monodisperse 200μm diameter titanium dioxide in water at 25ºC

freq (MHz)	0.01%/0.1%/1%/10% alpha convergence	0.01%/0.1%/1%/10% velocity convergence	alpha in Nepers/m	velocity in m/s
0.5	3/3/3/2	3/2/2/1	1.2705574695e+00	1491.98167
1.0	4/3/3/2	3/3/2/0	7.0106449690e+00	1489.26142
10.0	7/7/6/5	7/6/1/0	4.2690836386e+02	1481.58441
20.0	12/11/10/9	11/10/0/0	6.1273549806e+02	1493.51537
30.0	17/16/15/10	15/1/0/0	6.6179868966e+02	1493.02049
40.0	21/20/19/13	19/0/0/0	7.0213692761e+02	1495.62038
50.0	26/24/23/17	23/1/0/0	7.8824026389e+02	1495.08089
60.0	30/29/27/21	27/0/0/0	7.2457100925e+02	1495.75022
70.0	34/33/31/1	31/0/0/0	8.9658453639e+02	1496.04079
80.0	39/37/36/1	35/0/0/0	8.2387192882e+02	1495.87385
90.0	43/42/40/1	1/0/0/0	9.2139879744e+02	1496.32233
100.0	48/46/44/1	1/0/0/0	9.6481686327e+02	1496.13323
110.0	52/50/48/1	1/0/0/0	9.8053723139e+02	1496.28930
120.0	56/54/52/1	1/0/0/0	1.0894845297e+03	1496.39128
130.0	61/59/57/1	1/0/0/0	1.0895196508e+03	1496.33092
140.0	65/63/61/1	1/0/0/0	1.1701856095e+03	1496.48604
150.0	69/67/65/1	1/0/0/0	1.2706546242e+03	1496.42311

Table C47 10% v/v monodisperse 400μm diameter titanium dioxide in water at 25ºC

freq (MHz)	0.01%/0.1%/1%/10% alpha convergence	0.01%/0.1%/1%/10% velocity convergence	alpha in Nepers/m	velocity in m/s
0.5	4/3/2/2	3/3/2/1	3.3121358067e+00	1489.39027
1.0	4/3/2/2	4/3/2/0	2.8594702075e+01	1484.44219
10.0	12/11/10/9	11/10/0/0	3.0248993594e+02	1493.53131
20.0	21/20/19/13	19/0/0/0	3.4020940079e+02	1495.62425
30.0	30/29/27/21	27/0/0/0	3.4037685096e+02	1495.75210
40.0	39/37/36/1	35/0/0/0	3.7452692152e+02	1495.87611
50.0	47/46/44/1	1/0/0/0	4.2478136342e+02	1496.13426
60.0	56/54/52/1	1/0/0/0	4.6251208940e+02	1496.38876
70.0	65/63/61/1	1/0/0/0	4.7476124983e+02	1496.48227
80.0	73/71/69/1	1/0/0/0	5.0348705527e+02	1496.44084
90.0	82/80/77/1	1/0/0/0	5.4526162888e+02	1496.45073
100.0	90/88/86/1	1/0/0/0	5.9958189042e+02	1496.49900
110.0	99/97/94/1	0/0/0/0	6.4831424250e+02	1496.56248
120.0	108/105/102/1	0/0/0/0	6.9328290004e+02	1496.57732
130.0	116/114/102/1	0/0/0/0	7.5131105687e+02	1496.57135
140.0	125/122/110/1	0/0/0/0	8.1282143222e+02	1496.57243
150.0	133/130/118/1	0/0/0/0	8.8543173908e+02	1496.59309

Table C48 10% v/v monodisperse 600μm diameter titanium dioxide in water at 25ºC

freq (MHz)	0.01%/0.1%/1%/10% alpha convergence	0.01%/0.1%/1%/10% velocity convergence	alpha in Nepers/m	velocity in m/s
0.5	3/3/2/2	3/3/2/1	8.0964456097e+00	1486.46829
1.0	4/3/3/2	4/4/3/0	4.7643777887e+01	1483.18450
10.0	16/16/15/10	15/1/0/0	2.1434402368e+02	1493.03476
20.0	30/29/27/21	27/0/0/0	2.2187723299e+02	1495.75315
30.0	43/41/40/1	1/0/0/0	2.6502871451e+02	1496.31920
40.0	56/54/53/1	1/0/0/0	2.8986963993e+02	1496.38793
50.0	69/67/65/1	1/0/0/0	3.1044158230e+02	1496.42176
60.0	82/80/78/1	1/0/0/0	3.2316365041e+02	1496.45119
70.0	95/93/90/1	0/0/0/0	3.5581128744e+02	1496.56139
80.0	107/105/102/1	0/0/0/0	3.9095034463e+02	1496.57635
90.0	120/118/114/1	0/0/0/0	4.3195776247e+02	1496.62356
100.0	133/130/118/1	0/0/0/0	4.7901190715e+02	1496.59292
110.0	146/143/130/1	0/0/0/0	5.1463337306e+02	1496.60635
120.0	158/156/142/1	0/0/0/0	5.7255729055e+02	1496.63772
130.0	171/168/1/1	0/0/0/0	6.2318991708e+02	1496.62376
140.0	184/181/1/1	0/0/0/0	6.7872062118e+02	1496.65137
150.0	196/193/1/1	0/0/0/0	7.5463671461e+02	1496.64818

Table C49 10% v/v monodisperse 800μm diameter titanium dioxide in water at 25ºC

freq (MHz)	0.01%/0.1%/1%/10% alpha convergence	0.01%/0.1%/1%/10% velocity convergence	alpha in Nepers/m	velocity in m/s
0.5	3/3/2/2	4/3/2/1	1.4180084506e+01	1484.51104
1.0	4/3/3/3	5/4/3/0	5.7396787121e+01	1481.17736
10.0	21/20/19/13	19/0/0/0	1.6717534491e+02	1495.62778
20.0	39/37/36/28	35/0/0/0	1.7764838633e+02	1495.87758
30.0	56/54/53/1	1/0/0/0	2.1041740354e+02	1496.38752
40.0	73/71/69/1	1/0/0/0	2.1567047007e+02	1496.44068
50.0	90/88/86/1	1/0/0/0	2.4369332363e+02	1496.49901
60.0	107/105/102/1	0/0/0/0	2.6642937734e+02	1496.57582
70.0	124/122/118/1	0/0/0/0	2.9746609750e+02	1496.57289
80.0	141/139/126/1	0/0/0/0	3.3507981526e+02	1496.63005
90.0	158/156/142/1	0/0/0/0	3.6953683414e+02	1496.63676
100.0	175/173/158/1	0/0/0/0	4.1193684258e+02	1496.65006
110.0	192/189/1/1	0/0/0/0	4.5217672412e+02	1496.64241
120.0	209/206/1/1	0/0/0/0	5.0581135406e+02	1496.64195
130.0	226/223/1/1	0/0/0/0	5.6204191834e+02	1496.64980
140.0	243/240/1/1	0/0/0/0	6.2521839973e+02	1496.65761
150.0	260/256/1/1	0/0/0/0	6.8949299723e+02	1496.66461

Table C50 10% v/v monodisperse 1mm diameter titanium dioxide in water at 25ºC

freq (MHz)	0.01%/0.1%/1%/10% alpha convergence	0.01%/0.1%/1%/10% velocity convergence	alpha in Nepers/m	velocity in m/s
0.5	4/3/3/2	4/3/3/1	1.9739573919e+01	1483.66915
1.0	5/4/4/3	5/4/3/0	6.5794686538e+01	1479.23438
10.0	25/24/23/17	23/0/0/0	1.4716623595e+02	1495.08861
20.0	47/46/44/1	1/0/0/0	1.5577849628e+02	1496.13503
30.0	69/67/65/1	1/0/0/0	1.7251301403e+02	1496.42140
40.0	90/88/86/1	1/0/0/0	1.8593062866e+02	1496.49898
50.0	112/109/107/1	0/0/0/0	2.0717112569e+02	1496.58897
60.0	133/131/127/1	0/0/0/0	2.3388155408e+02	1496.59263
70.0	154/152/139/1	0/0/0/0	2.5877367465e+02	1496.61639
80.0	175/173/158/1	0/0/0/0	2.9407867271e+02	1496.64929
90.0	196/194/1/1	0/0/0/0	3.3311651811e+02	1496.64712
100.0	218/215/1/1	0/0/0/0	3.7274267842e+02	1496.64066
110.0	239/236/1/1	0/0/0/0	4.1838280110e+02	1496.66374
120.0	260/256/1/1	0/0/0/0	4.7199128988e+02	1496.66403
130.0	281/277/1/1	0/0/0/0	5.2524167414e+02	1496.65510
140.0	302/298/1/1	0/0/0/0	5.8419896043e+02	1496.66862
150.0	323/319/1/1	0/0/0/0	6.4886379095e+02	1496.66724

Table C51 10% v/v monodisperse 10nm diameter iron in silicone oil at 25°C

freq (MHz)	0.01%/0.1%/1%/10% alpha convergence	0.01%/0.1%/1%/10% velocity convergence	alpha in Nepers/m	velocity in m/s
0.5	3/3/3/3	2/2/2/2	1.2748341346e+00	796.22311
1.0	3/3/3/3	2/2/2/2	5.2012930333e+00	796.20752
10.0	3/3/3/3	2/2/2/2	5.1936308853e+02	796.27764
20.0	3/3/3/3	3/2/2/2	2.0741217601e+03	796.49049
30.0	3/3/3/3	3/2/2/2	4.6574511949e+03	796.83684
40.0	3/3/3/3	3/3/2/2	8.2595562788e+03	797.31362
50.0	3/3/3/3	3/3/2/2	1.2867707729e+04	797.91733
60.0	3/3/3/3	3/3/2/2	1.8466517023e+04	798.64386
70.0	3/3/3/3	3/3/2/2	2.5038215032e+04	799.48871
80.0	3/3/3/3	3/3/2/2	3.2563008418e+04	800.44691
90.0	3/3/3/3	3/3/2/2	4.1019452161e+04	801.51321
100.0	3/3/3/3	3/3/2/2	5.0384868891e+04	802.68208
110.0	3/3/3/3	3/3/2/2	6.0635677719e+04	803.94785
120.0	3/3/3/3	3/3/2/2	7.1747779096e+04	805.30476
130.0	3/3/3/3	3/3/3/2	8.3696894347e+04	806.74707
140.0	3/3/3/3	3/3/3/2	9.6458837597e+04	808.26914
150.0	3/3/3/3	3/3/3/2	1.1000978282e+05	809.86544

Table C52 10% v/v monodisperse 100nm diameter iron in silicone oil at 25°C

freq (MHz)	0.01%/0.1%/1%/10% alpha convergence	0.01%/0.1%/1%/10% velocity convergence	alpha in Nepers/m	velocity in m/s
0.5	3/3/3/3	2/2/2/2	3.3742733671e+00	796.28924
1.0	3/3/3/3	2/2/2/2	1.2656285660e+01	796.42698
10.0	3/3/3/3	2/2/2/2	7.8581141540e+02	799.11956
20.0	3/3/3/3	3/2/2/2	2.6235636677e+03	800.90074
30.0	3/3/3/3	3/2/2/2	5.4210431053e+03	802.11818
40.0	3/3/3/3	3/2/2/2	9.1796028302e+03	803.12380
50.0	3/3/3/3	3/3/2/2	1.3897888194e+04	804.05604
60.0	3/3/3/3	3/3/2/2	1.9569720473e+04	804.97827
70.0	3/3/3/3	3/3/2/2	2.6185350322e+04	805.92263
80.0	3/3/3/3	3/3/2/2	3.3732417402e+04	806.90639
90.0	3/3/3/3	3/3/2/2	4.2196589844e+04	807.93896
100.0	3/3/3/3	3/3/2/2	5.1562014486e+04	809.02527
110.0	3/3/3/3	3/3/2/2	6.1811657900e+04	810.16750
120.0	3/3/3/3	3/3/2/2	7.2927580469e+04	811.36612
130.0	3/3/3/3	3/3/2/2	8.4891165673e+04	812.62044
140.0	3/3/3/3	3/3/3/2	9.7683316589e+04	813.92903
150.0	3/3/3/3	3/3/3/2	1.1128462638e+05	815.28993

Table C53 10% v/v monodisperse 1um diameter iron in silicone oil at 25°C

freq (MHz)	0.01%/0.1%/1%/10% alpha convergence	0.01%/0.1%/1%/10% velocity convergence	alpha in Nepers/m	velocity in m/s
0.5	3/3/3/1	2/2/2/2	1.6230299722e+01	802.49306
1.0	3/3/3/2	2/2/2/2	3.4991774947e+01	803.60782
10.0	3/3/3/3	2/2/2/2	1.4429846315e+03	807.06875
20.0	3/3/3/3	2/2/2/2	5.2651078693e+03	810.30321
30.0	4/3/3/3	2/2/2/2	1.1173838899e+04	814.03567
40.0	4/3/3/3	3/2/2/2	1.8941123321e+04	818.10193
50.0	4/3/3/3	3/2/2/2	2.8398541768e+04	822.39409
60.0	4/3/3/3	3/2/2/2	3.9420678198e+04	826.85513
70.0	4/3/3/3	3/2/2/2	5.1911610537e+04	831.46159
80.0	4/4/3/3	3/3/2/2	6.5793925195e+04	836.21136
90.0	4/4/3/3	3/3/2/2	8.0999844212e+04	841.11528
100.0	4/4/3/3	3/3/2/2	9.7464144011e+04	846.19133
110.0	4/4/3/3	3/3/2/2	1.1511863403e+05	851.46031
120.0	4/4/3/3	4/3/2/2	1.3388805184e+05	856.94257
130.0	4/4/3/3	4/3/2/2	1.5368730204e+05	862.65546
140.0	4/4/3/3	4/3/2/2	1.7442000721e+05	868.61131
150.0	4/4/3/3	4/3/2/2	1.9597834536e+05	874.81583

Table C54 10% v/v monodisperse 10μm diameter iron in silicone oil at 25°C

freq (MHz)	0.01%/0.1%/1%/10% alpha convergence	0.01%/0.1%/1%/10% velocity convergence	alpha in Nepers/m	velocity in m/s
0.5	3/3/2/2	2/2/2/2	1.5587580865e+02	822.59838
1.0	3/3/2/2	2/2/2/2	4.3273284709e+02	843.08751
10.0	4/3/3/2	3/3/2/2	3.8568907622e+03	937.58704
20.0	4/4/3/3	4/3/2/0	7.6688235899e+03	953.08359
30.0	5/4/4/3	4/3/3/0	1.2717742462e+04	962.91991
40.0	5/5/4/3	4/4/3/0	1.8366176738e+04	971.59630
50.0	6/5/4/3	5/4/3/0	2.4220185559e+04	978.89301
60.0	6/5/5/4	5/4/3/0	2.9922138564e+04	984.91851
70.0	7/6/5/4	5/4/3/0	3.5345468373e+04	989.30722
80.0	7/6/5/4	5/4/3/0	4.0623118292e+04	992.39108
90.0	7/7/6/4	5/4/0/0	4.5818152480e+04	994.59238
100.0	8/7/6/5	5/4/0/0	5.1029979693e+04	996.20854
110.0	8/7/6/5	6/4/0/0	5.6357741009e+04	997.49029
120.0	8/8/6/5	7/4/0/0	6.1904684870e+04	998.58403
130.0	9/8/7/5	7/6/0/0	6.7782876140e+04	999.57480
140.0	9/8/7/5	8/6/0/0	7.4096052090e+04	1000.49382
150.0	9/8/7/1	8/7/0/0	8.0934512512e+04	1001.33325

Table C55 10% v/v monodisperse 100μm diameter iron in silicone oil at 25°C

freq (MHz)	0.01%/0.1%/1%/10% alpha convergence	0.01%/0.1%/1%/10% velocity convergence	alpha in Nepers/m	velocity in m/s
0.5	3/3/3/2	3/2/2/1	7.5402536662e+01	968.21916
1.0	4/3/3/2	3/3/2/0	1.1487772715e+02	973.48942
10.0	8/7/6/4	6/5/1/0	1.6540679742e+03	989.65053
20.0	11/10/9/7	10/8/0/0	2.7425237656e+03	997.35329
30.0	15/14/12/1	12/7/0/0	4.0382538987e+03	999.47182
40.0	18/17/15/1	13/0/0/0	5.8626055461e+03	1000.49306
50.0	22/20/18/1	16/0/0/0	8.1699465127e+03	1001.12157
60.0	25/23/20/1	18/0/0/0	1.0828684623e+04	1001.29223
70.0	28/26/23/1	24/0/0/0	1.4158574903e+04	1001.40552
80.0	31/29/25/0	27/0/0/0	1.7748352963e+04	1001.59278
90.0	33/31/23/0	30/0/0/0	2.2089056754e+04	1001.39725
100.0	35/34/22/0	33/0/0/0	2.6702306190e+04	1001.84956
110.0	38/36/24/0	36/0/0/0	3.1989741033e+04	1001.02872
120.0	43/39/27/0	40/14/0/0	3.7960859257e+04	1002.51567
130.0	46/42/34/0	43/27/0/0	4.3153899423e+04	1000.66212
140.0	49/44/37/0	46/30/0/0	5.3109243008e+04	1002.42414
150.0	53/47/40/0	49/34/0/0	5.4571749765e+04	1002.11505

Table C56 10% v/v monodisperse 200μm diameter iron in silicone oil at 25°C

freq (MHz)	0.01%/0.1%/1%/10% alpha convergence	0.01%/0.1%/1%/10% velocity convergence	alpha in Nepers/m	velocity in m/s
0.5	4/3/3/2	3/3/2/1	4.0313304983e+01	978.01584
1.0	4/4/3/2	3/3/2/0	8.6854007792e+01	978.69225
10.0	11/10/9/7	10/8/0/0	1.0244064631e+03	997.04567
20.0	18/17/15/1	15/1/0/0	1.8650773972e+03	1000.05735
30.0	25/23/21/1	19/0/0/0	3.1355353991e+03	1000.96100
40.0	31/30/27/1	24/0/0/0	4.8781320606e+03	1001.31623
50.0	38/35/26/1	27/0/0/0	7.1209607798e+03	1001.49139
60.0	44/41/1/0	33/0/0/0	9.8908706249e+03	1001.62522
70.0	49/46/1/0	39/0/0/0	1.3229924447e+04	1001.58286
80.0	54/52/31/0	44/0/0/0	1.7036004960e+04	1001.32896
90.0	59/57/40/0	53/0/0/0	2.1561494139e+04	1001.43747
100.0	68/63/50/0	59/36/0/0	2.5766954279e+04	1000.04188
110.0	75/69/56/0	66/48/0/0	2.8921094042e+04	995.57131
120.0	81/75/67/44	72/60/0/0	2.7954644617e+04	1004.33252
130.0	87/81/75/57	82/68/47/0	2.9743321783e+04	1022.72446
140.0	96/94/92/86	88/77/63/0	1.6676217297e+03	1054.80507
150.0	99/93/87/74	96/90/78/61	1.2852397328e+05	1658.66353

Table C57 10% v/v monodisperse 400μm diameter iron in silicone oil at 25°C

freq (MHz)	0.01%/0.1%/1%/10% alpha convergence	0.01%/0.1%/1%/10% velocity convergence	alpha in Nepers/m	velocity in m/s
0.5	4/4/3/2	3/3/2/1	3.3854636145e+01	980.91533
1.0	5/4/4/3	4/4/3/0	1.1300582722e+02	983.82746
10.0	18/17/15/9	16/1/0/0	6.4976507377e+02	999.83543
20.0	31/30/27/1	25/0/0/0	1.4248549808e+03	1001.11075
30.0	44/42/32/1	26/0/0/0	2.6844980579e+03	1001.40795
40.0	57/54/1/0	32/0/0/0	4.4479920852e+03	1001.37825
50.0	68/65/1/0	47/0/0/0	6.6682305848e+03	1001.27535
60.0	79/76/38/0	58/0/0/0	9.2439460158e+03	1001.49699
70.0	90/88/60/0	75/0/0/0	1.2424215225e+04	1002.10352
80.0	105/100/80/0	89/60/0/0	1.7489876698e+04	1002.71725
90.0	118/111/94/60	105/86/0/0	2.5754579594e+04	998.03034
100.0	130/123/108/86	120/102/73/0	3.7467428944e+04	911.78148
110.0	140/130/115/90	133/121/102/68	1.7279064032e+05	920.25918
120.0	141/128/106/77	148/139/124/103	1.9395652115e+06	2636.69261
130.0	148/136/116/90	150/138/119/94	3.8651717100e+06	279.77813
140.0	153/138/118/88	149/131/110/76	1.2874476715e+07	38.60231
150.0	161/149/130/104	160/145/125/97	3.0660790756e+07	18.56124

Table C58 10% v/v monodisperse 600μm diameter iron in silicone oil at 25°C

freq (MHz)	0.01%/0.1%/1%/10% alpha convergence	0.01%/0.1%/1%/10% velocity convergence	alpha in Nepers/m	velocity in m/s
0.5	5/4/3/2	4/3/2/1	4.3516008982e+01	982.44271
1.0	6/5/4/3	5/4/3/0	1.1847261272e+02	986.89326
10.0	25/23/22/1	21/0/0/0	5.1964368430e+02	1000.65010
20.0	44/42/39/1	0/0/0/0	1.2845585138e+03	1001.32830
30.0	63/60/1/0	0/0/0/0	2.5448397073e+03	1001.37450
40.0	81/77/1/0	0/0/0/0	4.2371923509e+03	1001.43185
50.0	98/94/1/0	71/0/0/0	6.5399588987e+03	1001.77301
60.0	115/112/81/0	93/0/0/0	9.5532111775e+03	1001.08953
70.0	137/130/109/51	116/87/0/0	1.0983254292e+04	1000.23994
80.0	157/149/136/111	141/121/80/0	1.0902921098e+04	1043.78360
90.0	168/154/137/107	164/149/127/82	1.8373162996e+05	1172.03307
100.0	183/171/152/125	177/161/137/107	3.8386811199e+05	493.81003
110.0	185/168/146/115	202/190/174/151	4.9210667161e+06	2721.53852
120.0	183/165/134/92	192/177/149/119	4.4070309339e+07	57.70274
130.0	201/183/158/128	202/186/164/135	1.1148678656e+08	9.98772
140.0	209/192/169/141	208/189/168/137	4.7461621899e+08	1.34097
150.0	198/176/147/102	209/186/162/130	1.4783725014e+10	0.22823

Table C59 10% v/v monodisperse 800μm diameter iron in silicone oil at 25°C

freq (MHz)	0.01%/0.1%/1%/10% alpha convergence	0.01%/0.1%/1%/10% velocity convergence	alpha in Nepers/m	velocity in m/s
0.5	5/4/3/3	4/4/3/1	5.0695310765e+01	984.87172
1.0	6/6/5/4	6/5/3/0	1.1454841939e+02	989.27349
10.0	31/30/28/1	26/0/0/0	4.5257248717e+02	1000.98302
20.0	57/55/44/1	0/0/0/0	1.2151539578e+03	1001.32510
30.0	82/78/1/0	0/0/0/0	2.4395731092e+03	1001.40931
40.0	106/101/1/0	55/0/0/0	4.2330064111e+03	1001.49132
50.0	128/124/81/0	100/0/0/0	6.1763126996e+03	1000.54191
60.0	152/148/122/0	131/88/0/0	8.7728834251e+03	1005.57249
70.0	175/164/143/102	162/137/83/0	2.6875689426e+04	979.39558
80.0	199/192/174/148	190/170/143/86	4.2563873466e+04	850.55707
90.0	202/183/150/102	208/192/166/130	2.4179838425e+06	707.32338
100.0	216/195/169/126	217/194/168/128	8.5396279789e+06	66.89806
110.0	240/224/200/170	233/211/189/154	1.4089238651e+07	15.42576
120.0	229/207/175/133	237/214/186/151	7.1571546101e+08	2.28743
130.0	247/223/198/163	222/197/159/106	1.2516503309e+09	0.05538
140.0	245/223/195/156	241/219/191/151	5.9614710671e+10	0.01118
150.0	252/229/200/162	237/207/174/128	4.9478240240e+11	0.00036

Table C60 10% v/v monodisperse 1mm diameter iron in silicone oil at 25°C

freq (MHz)	0.01%/0.1%/1%/10% alpha convergence	0.01%/0.1%/1%/10% velocity convergence	alpha in Nepers/m	velocity in m/s
0.5	5/5/4/3	5/4/3/1	5.3065187888e+01	986.58102
1.0	7/6/5/4	6/5/1/0	1.0268325623e+02	991.03524
10.0	38/36/34/1	27/0/0/0	4.1276352255e+02	1001.14818
20.0	70/67/1/1	0/0/0/0	1.1659313590e+03	1001.32461
30.0	101/96/1/0	0/0/0/0	2.4164967777e+03	1001.49777
40.0	130/125/1/0	80/0/0/0	4.0768915228e+03	1001.07193
50.0	159/146/109/0	129/0/0/0	6.4263404666e+03	1002.00901
60.0	193/185/160/118	167/134/1/0	7.6012935020e+03	995.13870
70.0	218/207/184/153	209/188/158/90	5.1211771184e+04	1154.09862
80.0	232/213/185/143	230/209/178/131	9.2116642462e+05	410.80495
90.0	234/209/178/118	246/225/197/157	1.3852692647e+07	169.84708
100.0	263/241/211/173	273/254/229/199	5.1390350559e+07	57.63607
110.0	260/238/204/161	255/226/192/142	6.5650083892e+08	0.52790
120.0	276/249/219/179	257/225/187/133	4.6009613833e+09	0.02747
130.0	266/237/201/148	284/258/228/190	4.5546573023e+11	0.00969
140.0	275/245/210/163	269/238/202/152	7.5874298086e+12	0.00007
150.0	309/283/257/222	289/261/229/188	3.0011773216e+13	0.00000

Table C61 10% v/v monodisperse 10nm diameter silica in silicone oil at 25°C

freq (MHz)	0.01%/0.1%/1%/10% alpha convergence	0.01%/0.1%/1%/10% velocity convergence	alpha in Nepers/m	velocity in m/s
0.5	3/3/3/1	2/2/2/1	6.4795146372e-01	1005.90941
1.0	3/3/3/3	2/2/2/0	4.8341477378e+00	1005.96857
10.0	3/3/3/3	3/2/2/0	4.8335914854e+02	1006.06328
20.0	3/3/3/3	3/2/2/0	1.9312179946e+03	1006.40724
30.0	3/3/3/3	3/2/2/0	4.3369714343e+03	1006.98399
40.0	3/3/3/3	3/3/2/0	7.6901271961e+03	1007.78501
50.0	3/3/3/3	3/3/2/0	1.1976504917e+04	1008.80459
60.0	3/3/3/3	3/3/2/0	1.7178509094e+04	1010.03647
70.0	3/3/3/3	3/3/2/0	2.3275723911e+04	1011.47284
80.0	3/3/3/3	3/3/2/0	3.0245150258e+04	1013.10534
90.0	3/3/3/3	3/3/2/0	3.8061876531e+04	1014.92491
100.0	3/3/3/3	3/3/3/0	4.6699585227e+04	1016.92184
110.0	3/3/3/3	3/3/3/0	5.6130940651e+04	1019.08620
120.0	3/3/3/3	3/3/3/0	6.6328091185e+04	1021.40802
130.0	3/3/3/3	3/3/3/0	7.7263151703e+04	1023.87726
140.0	3/3/3/3	3/3/3/0	8.8908449585e+04	1026.48416
150.0	3/3/3/3	3/3/3/0	1.0123701135e+05	1029.21924

Table C62 10% v/v monodisperse 100nm diameter silica in silicone oil at 25°C

freq (MHz)	0.01%/0.1%/1%/10% alpha convergence	0.01%/0.1%/1%/10% velocity convergence	alpha in Nepers/m	velocity in m/s
0.5	3/3/3/3	2/2/2/1	1.4975896850e+00	1005.95899
1.0	3/3/3/3	2/2/2/0	5.8901056455e+00	1005.98525
10.0	3/3/3/3	3/2/2/0	5.3385264389e+02	1006.65987
20.0	3/3/3/3	3/2/2/0	2.0581396818e+03	1007.48159
30.0	3/3/3/3	3/2/2/0	4.5365524499e+03	1008.39150
40.0	3/3/3/3	3/3/2/0	7.9519118973e+03	1009.42426
50.0	3/3/3/3	3/3/2/0	1.2289100264e+04	1010.59819
60.0	3/3/3/3	3/3/2/0	1.7532204981e+04	1011.92219
70.0	3/3/3/3	3/3/2/0	2.3663834318e+04	1013.39987
80.0	3/3/3/3	3/3/2/0	3.0665003403e+04	1015.03163
90.0	3/3/3/3	3/3/2/0	3.8515210120e+04	1016.81584
100.0	3/3/3/3	3/3/2/0	4.7192582867e+04	1018.74956
110.0	3/3/3/3	3/3/3/0	5.6674056195e+04	1020.82888
120.0	3/3/3/3	3/3/3/0	6.6935555651e+04	1023.04924
130.0	3/3/3/3	3/3/3/0	7.7952182809e+04	1025.40558
140.0	3/3/3/3	3/3/3/0	8.9698395720e+04	1027.89248
150.0	3/3/3/3	3/3/3/0	1.0214818207e+05	1030.50427

Table C63 10% v/v monodisperse 1μm diameter silica in silicone oil at 25°C

freq (MHz)	0.01%/0.1%/1%/10% alpha convergence	0.01%/0.1%/1%/10% velocity convergence	alpha in Nepers/m	velocity in m/s
0.5	3/3/3/3	2/2/2/1	5.2771592465e+00	1007.84172
1.0	3/3/3/3	2/2/2/0	1.2853725163e+01	1008.52316
10.0	3/3/3/3	2/2/2/0	5.2646776587e+02	1010.09576
20.0	4/3/3/3	3/2/2/0	2.0098957977e+03	1010.45561
30.0	4/3/3/3	3/2/2/0	4.4689120553e+03	1010.82006
40.0	4/3/3/3	3/2/2/0	7.9070630826e+03	1011.27139
50.0	4/4/3/3	3/3/2/0	1.2326346013e+04	1011.83713
60.0	4/4/3/3	3/3/2/0	1.7727008287e+04	1012.53413
70.0	4/4/3/3	3/3/2/0	2.4106968055e+04	1013.37550
80.0	4/4/3/3	3/3/2/0	3.1461160561e+04	1014.37241
90.0	4/4/3/3	3/3/2/0	3.9780888827e+04	1015.53449
100.0	4/4/3/3	4/3/2/0	4.9053225345e+04	1016.86970
110.0	4/4/3/3	4/3/2/0	5.9260507786e+04	1018.38415
120.0	4/4/3/3	4/3/2/0	7.0379972816e+04	1020.08172
130.0	4/4/3/3	4/3/3/0	8.2383571374e+04	1021.96368
140.0	4/4/3/3	4/3/3/0	9.5238004054e+04	1024.02845
150.0	4/4/3/3	4/3/3/0	1.0890500573e+05	1026.27122

Table C64 10% v/v monodisperse 10μm diameter silica in silicone oil at 25°C

freq (MHz)	0.01%/0.1%/1%/10% alpha convergence	0.01%/0.1%/1%/10% velocity convergence	alpha in Nepers/m	velocity in m/s
0.5	3/3/3/3	2/2/2/1	4.3080028335e+00	1010.59554
1.0	3/3/3/3	2/2/2/0	1.3550256038e+01	1010.96421
10.0	4/4/3/3	3/3/2/0	7.4003454984e+02	1011.54956
20.0	5/4/4/3	4/3/2/0	2.9727370084e+03	1006.68530
30.0	5/4/4/3	4/3/3/0	7.1358631136e+03	1000.95769
40.0	5/5/4/3	4/4/3/0	1.3299599826e+04	996.80813
50.0	6/5/4/3	5/4/3/0	2.0862367855e+04	995.58052
60.0	6/6/5/4	5/4/3/0	2.8581554564e+04	996.29430
70.0	7/6/5/4	5/4/3/0	3.5727864759e+04	996.94470
80.0	7/6/5/4	5/4/3/0	4.2221348690e+04	997.07968
90.0	7/7/6/4	5/4/0/0	4.8082335044e+04	996.91052
100.0	8/7/6/5	5/4/0/0	5.3451284567e+04	996.71526
110.0	8/7/6/5	6/4/0/0	5.8518788794e+04	996.75982
120.0	8/8/6/5	7/4/0/0	6.3515642306e+04	997.17267
130.0	9/8/7/5	7/6/0/0	6.8703723499e+04	997.97554
140.0	9/8/7/5	8/6/0/0	7.4339601859e+04	999.09381
150.0	9/8/7/1	8/7/0/0	8.0648532115e+04	1000.38334

Table C65 10% v/v monodisperse 100μm diameter silica in silicone oil at 25°C

freq (MHz)	0.01%/0.1%/1%/10% alpha convergence	0.01%/0.1%/1%/10% velocity convergence	alpha in Nepers/m	velocity in m/s
0.5	4/3/3/3	3/2/2/1	8.6763557324e+00	1017.13371
1.0	4/4/3/3	3/3/2/0	2.0709481873e+01	1016.34547
10.0	8/7/6/4	6/5/1/0	1.8464907116e+03	987.79283
20.0	11/10/9/7	10/8/0/0	2.7988912483e+03	996.74779
30.0	15/14/12/1	12/7/0/0	4.0492685074e+03	1000.14722
40.0	18/17/15/1	13/1/0/0	5.9517467719e+03	999.95896
50.0	22/20/18/1	16/0/0/0	8.2395357732e+03	1001.40938
60.0	25/23/21/1	21/0/0/0	1.0806610456e+04	1001.10224
70.0	28/26/23/1	24/0/0/0	1.4259081358e+04	1001.55780
80.0	31/29/25/0	27/0/0/0	1.7702330943e+04	1001.65464
90.0	33/31/23/0	30/0/0/0	2.2059749622e+04	1001.30773
100.0	35/34/21/0	34/0/0/0	2.6700397969e+04	1001.63631
110.0	37/36/24/0	37/0/0/0	3.2352849365e+04	1001.22426
120.0	43/39/31/0	40/18/0/0	3.7943180289e+04	1002.07688
130.0	46/42/34/0	43/27/0/0	4.3043275038e+04	1000.92446
140.0	50/44/37/0	46/30/0/0	5.1113228816e+04	1001.61416
150.0	53/47/40/0	49/36/0/0	5.8103130207e+04	1002.32750

Table C66 10% v/v monodisperse 200μm diameter silica in silicone oil at 25°C

freq (MHz)	0.01%/0.1%/1%/10% alpha convergence	0.01%/0.1%/1%/10% velocity convergence	alpha in Nepers/m	velocity in m/s
0.5	4/4/3/3	3/3/2/1	7.5310428000e+00	1017.15356
1.0	4/4/3/3	4/3/2/0	3.0659819533e+01	1012.67608
10.0	11/10/9/7	10/8/0/0	1.0497258900e+03	996.24505
20.0	18/17/15/1	15/1/0/0	1.9136590388e+03	999.50167
30.0	25/23/21/1	19/0/0/0	3.1371634931e+03	1000.80418
40.0	31/30/27/1	24/0/0/0	4.8760550224e+03	1001.36072
50.0	38/35/31/1	30/0/0/0	7.1297899000e+03	1001.46932
60.0	44/41/27/0	33/0/0/0	9.9100462211e+03	1001.59011
70.0	49/46/29/0	39/0/0/0	1.3157677403e+04	1001.47343
80.0	54/52/31/0	47/0/0/0	1.6897403523e+04	1001.57272
90.0	59/57/40/0	53/0/0/0	2.1423129185e+04	1001.50629
100.0	68/63/50/0	60/36/0/0	2.5440439216e+04	1000.51998
110.0	75/69/56/0	66/50/0/0	3.1347245701e+04	1001.57633
120.0	81/75/64/41	72/60/0/0	3.5597560254e+04	995.08211
130.0	87/81/73/55	82/68/47/0	3.7768890107e+04	997.40397
140.0	93/87/78/64	88/77/63/0	7.0932005950e+04	1029.37272
150.0	99/97/91/79	94/85/71/45	3.3368070629e+04	868.61605

Table C67 10% v/v monodisperse 400μm diameter silica in silicone oil at 25°C

freq (MHz)	0.01%/0.1%/1%/10% alpha convergence	0.01%/0.1%/1%/10% velocity convergence	alpha in Nepers/m	velocity in m/s
0.5	4/4/3/3	3/3/2/1	1.2481375049e+01	1013.30047
1.0	5/4/4/3	4/4/3/0	6.9833251331e+01	1002.25999
10.0	18/17/15/9	16/1/0/0	6.7477036290e+02	999.22066
20.0	32/30/28/1	25/0/0/0	1.4301843086e+03	1001.12796
30.0	44/42/38/1	28/0/0/0	2.6978954627e+03	1001.40420
40.0	57/54/1/0	32/0/0/0	4.4359607065e+03	1001.42136
50.0	68/65/1/0	49/0/0/0	6.6514278954e+03	1001.34050
60.0	79/76/35/0	63/0/0/0	9.3981665108e+03	1001.26738
70.0	90/88/64/0	77/0/0/0	1.2747591944e+04	1001.70266
80.0	105/100/80/0	92/65/0/0	1.6658252016e+04	1001.21621
90.0	119/112/97/70	105/86/0/0	1.5343359196e+04	992.15385
100.0	130/123/109/88	121/107/80/0	3.6708879953e+04	1015.80747
110.0	137/127/108/83	134/125/107/79	3.9131739970e+05	1255.89528
120.0	146/138/121/97	144/136/120/94	7.0526880902e+05	746.51263
130.0	155/144/129/110	146/132/113/81	8.4204833509e+05	133.78634
140.0	157/146/130/106	166/155/140/121	9.9797496738e+06	372.61448
150.0	156/140/119/89	152/137/113/81	6.1067622980e+07	10.75027

Table C68 10% v/v monodisperse 600μm diameter silica in silicone oil at 25°C

freq (MHz)	0.01%/0.1%/1%/10% alpha convergence	0.01%/0.1%/1%/10% velocity convergence	alpha in Nepers/m	velocity in m/s
0.5	5/4/4/3	4/3/2/1	2.1687692019e+01	1008.25785
1.0	6/5/4/3	5/4/3/0	1.1185448505e+02	992.81794
10.0	25/23/22/1	21/1/0/0	5.2384302739e+02	1000.44766
20.0	44/42/39/1	0/0/0/0	1.2949336541e+03	1001.32201
30.0	63/61/1/0	0/0/0/0	2.5404201410e+03	1001.38478
40.0	81/77/1/0	0/0/0/0	4.2745036085e+03	1001.37230
50.0	98/95/46/0	71/0/0/0	6.5089947408e+03	1001.29651
60.0	115/112/83/0	96/0/0/0	9.0205492644e+03	1000.76218
70.0	136/130/107/0	119/89/0/0	1.2686091793e+04	1003.12331
80.0	157/149/136/113	141/118/80/0	9.8451420987e+03	1000.83942
90.0	167/160/142/114	163/149/124/82	1.0760170007e+05	1097.46930
100.0	175/162/140/104	173/158/135/91	9.8004665296e+05	387.88981
110.0	179/159/132/87	183/165/142/105	8.3562648914e+06	155.81623
120.0	191/172/148/111	193/175/153/119	2.7678639417e+07	39.28020
130.0	184/163/134/61	202/183/162/133	3.5007185662e+08	21.98101
140.0	199/181/156/118	209/194/171/144	1.2371279141e+09	3.06831
150.0	210/189/166/135	213/195/172/143	6.7692193646e+09	0.25174

Table C69 10% v/v monodisperse 800μm diameter silica in silicone oil at 25°C

freq (MHz)	0.01%/0.1%/1%/10% alpha convergence	0.01%/0.1%/1%/10% velocity convergence	alpha in Nepers/m	velocity in m/s
0.5	5/4/4/3	4/4/3/1	3.1361421425e+01	1002.92945
1.0	6/6/5/4	6/5/3/0	1.2994630487e+02	989.31597
10.0	31/30/28/1	25/0/0/0	4.5707324651e+02	1000.96584
20.0	57/55/43/1	0/0/0/0	1.2151623955e+03	1001.33977
30.0	82/78/1/0	0/0/0/0	2.4573961472e+03	1001.38151
40.0	105/101/1/0	55/0/0/0	4.2097255716e+03	1001.40556
50.0	128/124/79/0	100/0/0/0	6.4984416738e+03	1001.56241
60.0	152/149/122/0	131/88/0/0	8.7128394594e+03	1001.30637
70.0	180/173/151/116	162/139/90/0	1.3593849817e+04	1010.31954
80.0	205/197/181/159	186/170/139/75	1.5270493280e+04	731.69406
90.0	207/192/168/128	209/193/171/132	1.3892114475e+06	535.00150
100.0	219/201/177/137	215/195/165/124	5.5316162998e+06	55.14698
110.0	249/234/214/188	215/189/162/110	1.5166042977e+06	5.68227
120.0	237/214/188/151	229/207/175/137	3.2518233829e+08	1.05572
130.0	245/223/198/160	242/220/192/155	3.5395463760e+09	0.15714
140.0	227/197/162/93	239/214/182/139	2.0973137860e+11	0.01304
150.0	238/211/176/127	225/198/160/90	1.6152164164e+12	0.00025

Table C70 10% v/v monodisperse 1mm diameter silica in silicone oil at 25°C

freq (MHz)	0.01%/0.1%/1%/10% alpha convergence	0.01%/0.1%/1%/10% velocity convergence	alpha in Nepers/m	velocity in m/s
0.5	5/5/4/3	5/4/3/1	4.1271413944e+01	997.59633
1.0	7/6/5/4	6/5/4/0	1.1897937663e+02	988.43780
10.0	38/36/34/1	27/0/0/0	4.1867849402e+02	1001.12477
20.0	70/67/1/1	0/0/0/0	1.1662980916e+03	1001.34841
30.0	101/96/1/0	0/0/0/0	2.4130565291e+03	1001.37796
40.0	129/125/1/0	80/0/0/0	4.1761420477e+03	1001.47446
50.0	159/154/114/0	129/0/0/0	6.3162128614e+03	1002.24679
60.0	194/187/169/131	170/134/1/0	4.6152328771e+03	996.54350
70.0	218/211/190/163	204/183/146/0	2.3176993167e+04	839.03344
80.0	237/217/192/155	231/210/180/133	5.9440557650e+05	376.91018
90.0	248/224/195/158	250/230/200/167	6.7513201111e+06	127.27721
100.0	259/238/210/169	235/207/164/69	1.6965606347e+07	3.01412
110.0	266/245/214/172	259/231/198/154	4.4382108909e+08	0.60932
120.0	262/233/197/147	250/220/180/101	1.4132020449e+10	0.02170
130.0	271/243/208/161	259/229/188/111	2.1897464301e+11	0.00130
140.0	280/253/223/180	265/233/196/122	3.6142292461e+12	0.00005
150.0	265/237/197/124	253/216/176/100	3.2117150543e+14	0.00000

Table C71 10% v/v monodisperse 10nm diameter hexadecane in water at 25ºC

freq (MHz)	0.01%/0.1%/1%/10% alpha convergence	0.01%/0.1%/1%/10% velocity convergence	alpha in Nepers/m	velocity in m/s
0.5	3/3/3/1	2/1/1/1	7.6183658297e-03	1463.49655
1.0	3/3/3/1	2/0/0/0	3.0439047883e-02	1463.49657
10.0	3/3/3/0	2/0/0/0	3.0186877026e+00	1463.49765
20.0	3/3/3/0	2/0/0/0	1.2014687885e+01	1463.49952
30.0	3/3/3/0	2/0/0/0	2.6930970032e+01	1463.50179
40.0	3/3/3/0	2/0/0/0	4.7726501514e+01	1463.50435
50.0	3/3/3/0	2/0/0/0	7.4367918325e+01	1463.50713
60.0	3/3/3/0	2/0/0/0	1.0682669832e+02	1463.51008
70.0	3/3/3/0	2/0/0/0	1.4507774573e+02	1463.51317
80.0	3/3/3/0	2/0/0/0	1.8909855555e+02	1463.51637
90.0	3/3/3/0	2/0/0/0	2.3886866943e+02	1463.51967
100.0	3/3/3/0	2/0/0/0	2.9436929727e+02	1463.52306
110.0	3/3/3/0	2/0/0/0	3.5558304116e+02	1463.52652
120.0	3/3/3/0	2/0/0/0	4.2249368655e+02	1463.53004
130.0	3/3/3/0	2/0/0/0	4.9508603967e+02	1463.53361
140.0	3/3/3/0	2/0/0/0	5.7334579810e+02	1463.53723
150.0	3/3/3/0	2/0/0/0	6.5725944566e+02	1463.54088

Table C72 10% v/v monodisperse 100nm diameter hexadecane in water at 25ºC

freq (MHz)	0.01%/0.1%/1%/10% alpha convergence	0.01%/0.1%/1%/10% velocity convergence	alpha in Nepers/m	velocity in m/s
0.5	3/3/1/1	2/1/1/1	2.1655243121e-01	1463.50919
1.0	3/3/1/1	2/0/0/0	8.3341324665e-01	1463.53099
10.0	3/3/1/0	2/0/0/0	5.9734156646e+01	1464.37524
20.0	3/3/1/0	2/0/0/0	1.7881258187e+02	1465.57717
30.0	3/3/1/0	2/0/0/0	3.0618159589e+02	1466.64100
40.0	3/3/0/0	2/0/0/0	4.2448308911e+02	1467.46910
50.0	3/3/0/0	2/0/0/0	5.3240349290e+02	1468.08918
60.0	3/3/0/0	2/0/0/0	6.3325590289e+02	1468.55390
70.0	3/3/0/0	2/0/0/0	7.3059781099e+02	1468.90856
80.0	3/3/3/0	2/0/0/0	8.2714850850e+02	1469.18593
90.0	3/3/3/0	2/0/0/0	9.2477301333e+02	1469.40844
100.0	3/3/3/0	2/0/0/0	1.0246999904e+03	1469.59121
110.0	3/3/3/0	2/0/0/0	1.1277316661e+03	1469.74450
120.0	3/3/3/0	2/0/0/0	1.2343975551e+03	1469.87535
130.0	3/3/3/0	2/0/0/0	1.3450566284e+03	1469.98870
140.0	3/3/3/0	2/0/0/0	1.4599621728e+03	1470.08809
150.0	3/3/3/0	2/0/0/0	1.5793019131e+03	1470.17612

Table C73 10% v/v monodisperse 1μm diameter hexadecane in water at 25ºC

freq (MHz)	0.01%/0.1%/1%/10% alpha convergence	0.01%/0.1%/1%/10% velocity convergence	alpha in Nepers/m	velocity in m/s
0.5	2/1/1/1	2/1/1/1	4.6961123743e+00	1468.13972
1.0	3/1/1/1	2/1/0/0	7.5985612231e+00	1469.67959
10.0	3/3/1/0	2/0/0/0	3.0195341113e+01	1471.89907
20.0	3/3/3/0	2/0/0/0	5.1227006546e+01	1472.17939
30.0	3/3/3/0	2/0/0/0	7.5947400303e+01	1472.29674
40.0	3/3/3/0	2/0/0/0	1.0574904213e+02	1472.36053
50.0	3/3/3/0	2/0/0/0	1.4121428669e+02	1472.39793
60.0	4/3/3/0	2/0/0/0	1.8269660398e+02	1472.41939
70.0	4/3/3/0	2/0/0/0	2.3046215565e+02	1472.42991
80.0	4/3/3/0	2/0/0/0	2.8473972905e+02	1472.43226
90.0	4/3/3/0	2/0/0/0	3.4574270995e+02	1472.42815
100.0	4/3/3/0	2/0/0/0	4.1368027979e+02	1472.41869
110.0	4/3/3/0	2/0/0/0	4.8876369831e+02	1472.40464
120.0	4/3/3/0	2/0/0/0	5.7121003051e+02	1472.38660
130.0	4/3/3/0	2/0/0/0	6.6124439699e+02	1472.36499
140.0	4/3/3/3	2/0/0/0	7.5910129588e+02	1472.34017
150.0	4/4/3/3	2/0/0/0	8.6502529911e+02	1472.31246

Table C74 10% v/v monodisperse 10μm diameter hexadecane in water at 25ºC

freq (MHz)	0.01%/0.1%/1%/10% alpha convergence	0.01%/0.1%/1%/10% velocity convergence	alpha in Nepers/m	velocity in m/s
0.5	3/3/1/1	2/1/1/1	6.3152967610e-01	1472.45102
1.0	3/3/1/1	2/0/0/0	9.1839378118e-01	1472.57840
10.0	4/3/3/0	2/0/0/0	6.7536132368e+00	1472.66102
20.0	4/4/3/0	2/0/0/0	2.7593834566e+01	1472.33250
30.0	4/4/3/0	2/2/0/0	8.5356699514e+01	1471.85763
40.0	4/4/3/0	2/2/0/0	2.0775368882e+02	1471.40292
50.0	5/4/3/0	3/2/0/0	4.1321274280e+02	1471.15059
60.0	5/4/3/0	3/2/0/0	6.9245958798e+02	1471.21609
70.0	5/4/3/0	3/2/0/0	1.0069432012e+03	1471.54915
80.0	5/4/3/2	3/2/0/0	1.3204687080e+03	1471.94808
90.0	5/4/3/2	4/3/0/0	1.6373611627e+03	1472.22830
100.0	6/5/3/2	4/3/1/0	1.9983868639e+03	1472.37863
110.0	6/5/3/2	4/3/1/0	2.4337510228e+03	1472.53687
120.0	6/5/3/2	4/3/1/0	2.9266831603e+03	1472.82210
130.0	6/5/4/3	4/3/1/0	3.4338895566e+03	1473.21136
140.0	6/5/4/3	5/4/1/0	3.9392501410e+03	1473.59502
150.0	7/5/4/3	5/4/1/0	4.4691229308e+03	1473.92169

Table C75 10% v/v monodisperse 100μm diameter hexadecane in water at 25ºC

freq (MHz)	0.01%/0.1%/1%/10% alpha convergence	0.01%/0.1%/1%/10% velocity convergence	alpha in Nepers/m	velocity in m/s
0.5	3/3/ 3/1	2/1/1/1	7.5738173832e-02	1472.81310
1.0	4/3/3/1	2/0/0/0	1.8905523972e-01	1472.72931
10.0	5/3/3/2	4/3/1/0	1.6835376827e+02	1472.27490
20.0	6/5/5/4	6/5/1/0	6.5055389819e+02	1475.28823
30.0	8/7/7/6	8/7/1/0	1.3009177083e+03	1479.63646
40.0	10/10/9/8	10/8/0/0	1.9611148361e+03	1484.68445
50.0	13/12/11/10	12/10/0/0	2.4720639608e+03	1489.64046
60.0	15/14/13/12	14/1/0/0	2.7309174180e+03	1493.83075
70.0	17/16/15/14	16/0/0/0	2.7243368133e+03	1496.83295
80.0	20/19/18/17	18/1/0/0	2.5040727984e+03	1498.53476
90.0	22/21/20/19	20/1/0/0	2.1699541571e+03	1499.03771
100.0	25/23/22/21	23/1/0/0	1.8599525189e+03	1498.64488
110.0	27/26/25/24	25/0/0/0	1.6810693566e+03	1497.85073
120.0	29/28/27/26	27/0/0/0	1.6549694102e+03	1497.05630
130.0	31/30/29/28	29/0/0/0	1.7705875933e+03	1496.44369
140.0	34/32/31/1	31/0/0/0	1.9975513746e+03	1496.16392
150.0	36/34/33/1	32/0/0/0	2.2388647877e+03	1496.25605

Table C76 10% v/v monodisperse 200μm diameter hexadecane in water at 25ºC

freq (MHz)	0.01%/0.1%/1%/10% alpha convergence	0.01%/0.1%/1%/10% velocity convergence	alpha in Nepers/m	velocity in m/s
0.5	3/3/3/1	2/1/1/1	7.3142967813e-02	1472.73846
1.0	4/3/1/1	2/0/0/0	5.9632999025e-01	1472.38788
10.0	6/5/5/4	6/5/1/0	3.2212328246e+02	1475.25407
20.0	10/9/9/8	10/8/0/0	9.7307646404e+02	1484.60098
30.0	15/14/13/12	14/1/0/0	1.3545483151e+03	1493.80068
40.0	19/19/18/17	18/1/0/0	1.2264105027e+03	1498.61762
50.0	24/23/22/21	23/1/0/0	8.6898244494e+02	1498.74905
60.0	29/28/27/26	27/0/0/0	7.3166352697e+02	1497.06077
70.0	33/32/31/1	31/0/0/0	8.8507170356e+02	1496.06206
80.0	38/37/36/1	34/0/0/0	1.0803860836e+03	1496.47499
90.0	42/41/40/1	1/0/0/0	1.1181620952e+03	1497.10409
100.0	47/46/45/1	1/0/0/0	1.0075778357e+03	1497.18902
110.0	51/50/49/1	1/0/0/0	9.9171521745e+02	1496.86346
120.0	56/55/54/1	0/0/0/0	1.1025266329e+03	1496.56684
130.0	60/59/58/1	0/0/0/0	1.2274210823e+03	1496.68367
140.0	65/64/63/1	1/0/0/0	1.2883951521e+03	1496.88030
150.0	69/68/62/1	1/0/0/0	1.2801832128e+03	1496.88769

Table C77 10% v/v monodisperse 400μm diameter hexadecane in water at 25ºC

freq (MHz)	0.01%/0.1%/1%/10% alpha convergence	0.01%/0.1%/1%/10% velocity convergence	alpha in Nepers/m	velocity in m/s
0.5	3/3/1/1	2/1/1/1	2.8308588870e-01	1472.39249
1.0	3/3/1/1	2/2/0/0	3.7506427910e+00	1471.43543
10.0	10/9/9/8	10/8/0/0	4.8466261599e+02	1484.55883
20.0	19/18/18/17	18/1/0/0	6.0685613503e+02	1498.66022
30.0	29/28/27/26	27/0/0/0	3.4162889617e+02	1497.06293
40.0	37/36/36/1	36/0/0/0	5.0943304871e+02	1496.45147
50.0	47/46/45/1	1/0/0/0	4.4515139520e+02	1497.23283
60.0	56/55/54/1	0/0/0/0	4.7060417824e+02	1496.50756
70.0	65/64/63/1	1/0/0/0	5.4504868558e+02	1496.91644
80.0	74/73/67/1	0/0/0/0	5.0712057233e+02	1496.77724
90.0	83/82/76/1	0/0/0/0	5.9556416371e+02	1496.69737
100.0	92/91/85/1	0/0/0/0	6.0916594240e+02	1496.81802
110.0	101/95/94/1	0/0/0/0	6.5696799709e+02	1496.69022
120.0	110/104/103/1	0/0/0/0	7.1964015412e+02	1496.76481
130.0	119/113/106/1	0/0/0/0	7.5253410955e+02	1496.72522
140.0	124/122/115/1	0/0/0/0	8.3089276881e+02	1496.71630
150.0	133/131/124/1	0/0/0/0	8.8167781083e+02	1496.73816

Table C78 10% v/v monodisperse 600μm diameter hexadecane in water at 25ºC

freq (MHz)	0.01%/0.1%/1%/10% alpha convergence	0.01%/0.1%/1%/10% velocity convergence	alpha in Nepers/m	velocity in m/s
0.5	3/3/1/1	2/2/1/1	8.5639588352e-01	1471.90592
1.0	3/2/2/1	3/2/0/0	9.4244257890e+00	1471.20917
10.0	15/14/13/12	14/1/0/0	4.4911896776e+02	1493.78025
20.0	29/28/27/26	27/0/0/0	2.2234892134e+02	1497.06365
30.0	42/41/40/1	39/0/0/0	3.3918581190e+02	1497.14081
40.0	55/54/54/1	0/0/0/0	2.9576101529e+02	1496.48330
50.0	69/68/68/1	1/0/0/0	3.1317495728e+02	1496.92400
60.0	83/82/76/1	0/0/0/0	3.5909962211e+02	1496.68728
70.0	96/96/89/1	0/0/0/0	3.5549465605e+02	1496.73599
80.0	110/104/103/1	0/0/0/0	4.1088361993e+02	1496.77318
90.0	124/118/111/1	0/0/0/0	4.3823263629e+02	1496.69430
100.0	133/131/125/1	0/0/0/0	4.7677165681e+02	1496.74535
110.0	146/145/126/1	0/0/0/0	5.3126585754e+02	1496.71230
120.0	160/154/1/1	0/0/0/0	5.7184407592e+02	1496.71016
130.0	173/167/1/1	0/0/0/0	6.3208843488e+02	1496.71922
140.0	187/181/1/1	0/0/0/0	6.8962965601e+02	1496.70266
150.0	196/194/1/1	0/0/0/0	7.5134505911e+02	1496.71007

Table C79 10% v/v monodisperse 800μm diameter hexadecane in water at 25ºC

freq (MHz)	0.01%/0.1%/1%/10% alpha convergence	0.01%/0.1%/1%/10% velocity convergence	alpha in Nepers/m	velocity in m/s
0.5	3/2/1/1	2/2/1/1	1.8630547186e+00	1471.43753
1.0	3/3/2/2	3/2/0/0	1.3730354500e+01	1471.89826
10.0	19/18/18/17	18/0/0/0	3.0184854845e+02	1498.68177
20.0	37/36/36/1	36/0/0/0	2.4708863213e+02	1496.43952
30.0	55/54/54/1	1/0/0/0	2.1506502374e+02	1496.47011
40.0	73/73/67/1	0/0/0/0	2.1511447374e+02	1496.77889
50.0	92/91/85/1	1/0/0/0	2.4933491891e+02	1496.83829
60.0	110/104/103/1	0/0/0/0	2.8238784394e+02	1496.77834
70.0	124/122/116/1	0/0/0/0	3.1053106997e+02	1496.70876
80.0	142/140/134/1	0/0/0/0	3.3525538181e+02	1496.69564
90.0	160/159/1/1	0/0/0/0	3.6863504841e+02	1496.70856
100.0	178/172/1/1	0/0/0/0	4.1166683352e+02	1496.71924
110.0	192/190/1/1	0/0/0/0	4.6064365989e+02	1496.71427
120.0	209/203/1/1	0/0/0/0	5.1154751874e+02	1496.70478
130.0	227/221/1/1	0/0/0/0	5.6492841254e+02	1496.69986
140.0	245/239/1/1	0/0/0/0	6.2301677090e+02	1496.69999
150.0	259/252/1/1	0/0/0/0	6.8671797356e+02	1496.70068

Table C80 10% v/v monodisperse 1mm diameter hexadecane in water at 25ºC

freq (MHz)	0.01%/0.1%/1%/10% alpha convergence	0.01%/0.1%/1%/10% velocity convergence	alpha in Nepers/m	velocity in m/s
0.5	3/2/2/1	3/2/1/1	3.2287351244e+00	1471.16675
1.0	3/3/3/2	4/3/1/0	1.6502217974e+01	1472.26733
10.0	24/23/22/21	23/1/0/0	1.6395036119e+02	1498.83665
20.0	46/45/45/1	1/0/0/0	1.6380744591e+02	1497.26177
30.0	69/68/68/1	1/0/0/0	1.7401536439e+02	1496.93196
40.0	92/91/91/1	1/0/0/0	1.9071864871e+02	1496.84372
50.0	115/109/108/1	0/0/0/0	2.0898338177e+02	1496.78349
60.0	138/131/125/1	0/0/0/0	2.3269965429e+02	1496.75414
70.0	155/154/148/1	0/0/0/0	2.6077440501e+02	1496.73408
80.0	178/172/164/1	0/0/0/0	2.9373464232e+02	1496.72120
90.0	196/194/1/1	0/0/0/0	3.3118722945e+02	1496.71302
100.0	218/212/1/1	0/0/0/0	3.7305707634e+02	1496.70750
110.0	241/235/1/1	0/0/0/0	4.1931195953e+02	1496.70374
120.0	259/253/1/1	0/0/0/0	4.6993346826e+02	1496.70105
130.0	281/275/1/1	0/0/0/0	5.2492741135e+02	1496.69907
140.0	300/293/1/1	0/0/0/0	5.8429726485e+02	1496.69757
150.0	322/315/1/1	0/0/0/0	6.4804761590e+02	1496.69639

Appendix D: Modelled attenuation and phase velocity sensitivity to variation of physical properties

D1.1 Introduction

The Allegra and Hawley equations require the provision of a number of specific physical properties applicable to both the dispersed and continuous phases to model the behaviour of sound waves propagating through a dispersion. Those properties for a range of selected media are listed in Appendix E. The choice of media was determined by availability of data, particularly thermal properties, and the coverage of an exemplar range media in terms of mass density, thermal and acoustic properties. Water was chosen as the continuous phase for all of the dispersions, despite its unusual thermal properties, because its properties are well characterized and documented and the regularity with which it occurs in dispersions of practical interest.

The properties listed in Table D1.1 illustrate the range of material property contrasts available using the selected media.

Medium in Water	Mass Density Contrast	Acoustic Contrast	Thermal Contrast
polystyrene	low	low	medium
1-bromo - hexadecane	low	medium	medium
silica	medium	high	low
titanium dioxide	high	high	medium
iron	high	medium	high

Table D1.1 Physical property contrasts of continuous and dispersed media

It is assumed, using the effective media concept, that a comparison of dispersions which consist of materials identical in all but one property would owe any difference in attenuation or phase velocity dispersion to the effects of that one property. Therefore, it follows that by carefully selecting combinations of continuous and dispersed phases, it is possible to model the effects of errors in physical property values in dispersions where viscous, thermal or acoustic mismatch effects dominate. The dispersions were all modelled at a temperature of 25ºC and 10% v/v concentration. The dispersed phase physical properties listed in Appendix E were individually varied from a central value, in 1% increments, between ±20%. The sensitivity of alpha and phase velocity to each variation, for each dispersion, was noted. Initially, the measurements were made over a range of frequency and particle size combinations which equated to dispersed phase compressive wavenumber-radius products ($k_c r$) of 10^{-4}, 10^{-3}, 10^{-2}, 10^{-1}, 1, 10 and 100. However, often it was found that the effect of varying a property was *different at two radius-frequency combinations*, although they shared the same $k_c r$ value. Therefore it was necessary to repeat the experiment over a range of explicit frequencies and particle sizes. The frequencies chosen were 100kHz, 1MHz, 10MHz, 100MHz and 200MHz and the particle sizes were 10nm, 100nm, 1μm, 10μm, 100μm and 1mm diameter. All 14 properties were individually varied for each of the frequency-radius combinations. The model computed attenuation and phase velocity values, for each dispersion, in excess of those of the pure continuous water medium

$$\alpha_{excess} = \alpha_{suspension} - \alpha_{water} \qquad \textbf{(D1.1)}$$

$$c_{excess} = c_{suspension} - c_{water} \qquad \textbf{(D1.2)}$$

All the excess attenuation and phase velocity values resulting from n% variation of input properties were normalized as a proportional increase or decrease over the output attenuation and phase velocity values corresponding to zero input perturbation

$$\alpha_n = \frac{\alpha_{excess(n\%)} - \alpha_{excess(0\%)}}{\alpha_{excess(0\%)}} \qquad \textbf{(D1.3)}$$

$$c_n = \frac{c_{excess(n\%)} - c_{excess(0\%)}}{c_{excess(0\%)}} \qquad \textbf{(D1.4)}$$

This resulted in tables that gave the proportional error of modelled attenuation and phase velocity for a given error of a single input property. An abbreviated form of those tables, showing the results after ± 5%, ±10% and ±20% variation of each physical property for each of the five material combinations appears as Appendix D3. These tables were subjected to further analysis to ascertain the ±% variation of input property permissible before a certain threshold of output attenuation and phase velocity variation resulted. Two threshold output variations were chosen: 0.01% and 0.1%. Either of these thresholds might be considered reasonable experimental margins of error for measured phase velocity and attenuation, depending upon the available equipment and the intended use of the measurements. Those tables appear as Appendix D2. As an example, Table D2.20, aqueous metallic iron dispersion - continuous phase alpha, κ, 1MHz, 10μm shows *9/8/20/20*. The first pair of numbers, *9/8*, indicates that at a frequency of 1MHz the κ property of a 10% v/v concentration monodisperse dispersion of 10μm diameter metallic iron particles in water can be varied by $+9\%$ and -8% before the modelled attenuation varies by more than 0.01% from the value modelled using completely accurate input properties. The second pair of numbers, *20/20*, indicates that the κ property of this

dispersion can be varied by *at least* the +20% and *at least* -20% before the modelled attenuation varies by more than 0.1% from the value modelled using completely accurate input properties. The use of unprimed variables indicates properties of the continuous phase and the use of primed variables indicates properties of the dispersed phase.

D1.2 Analysis of Results

	poly		**1-b- hex**		**silica**		**tiox**		**iron**	
	$c(\omega)$	$\alpha(\omega)$	$c(\omega)$	$\alpha(\omega)$	$c(\omega)$	$\alpha(\omega)$	$c(\omega)$	$\alpha(\omega)$	$c(\omega)$	$\alpha(\omega)$
c '	LMH	LMH	LMH	LMH	LMH	LMH	MH	H	MH	H
c	LMH	LMH	LMH	LMH	LMH	LMH	LMH	LMH	LMH	LMH
ρ'	LMH	LMH	LMH	LMH	LMH	LMH	LMH	LMH	LMH	LMH
ρ	LMH	LMH	LMH	LMH	LMH	LMH	LMH	LMH	LMH	LMH
μ'/η'	LMH	LMH		LM	LMH	LMH	H	H	MH	L H
μ/η	MH	LM	M	LM	MH	LM	MH	LM	MH	LM
κ'	M	LM	M	LM	M	M				
κ		LM	M	LM	M	LM				
C_p'	LM	LM	LM	LM	LM	LM		M		L
C_p	LM	LM	LM	LM	LM	LM		L		
α'/f^2	H	LM	H	LM		L				L
α/f^2	H	LM	H	LM	H	LM	H	L	H	L
β'	LM	LM	LM	LM	LM	LM				L
β	LM	LM	LM	LM	LM	LM	LM	LM	M	LM

Table D1.2 Sensitivity of modelled attenuation and phase velocity to variations in input physical properties

D1.3 Key to interpreting Table D1.2

Table D1.2 represents an attempt to summarize all of the information contained in Tables D2.1 to D2.20. The most obvious relationships linking sensitivity of modelled output to variations in physical property input appear to be gradations in frequency and particle size, although inspection of Appendix D2 reveals numerous exceptions. In order to render the large amount of data down to a more manageable level, values spanning the range from 10nm-0.1MHz through to 1mm-200MHz are divided into three bands. The bands represent low, medium and high $k_c r$ and are denoted L, M and H. Table D1.2 denotes the sensitivity of modelled attenuation, α, and phase velocity, c, in both continuous and dispersed phases to variations of each input physical property. Therefore, if a modelled output is sensitive to a particular input over the whole range of $k_c r$ that is denoted by LMH in the relevant box. An underlined number indicates that an output is weakly sensitive over that range. It follows that ranges where modelled outputs are relatively insensitive to variations of a certain input property are immediately obvious by the absence of numbers in the corresponding box.

D1.4 Assumptions and generalizations made in Table D1.2

Inspection of Appendix D2 shows that a variation in modelled output in response to a variation in input property sometimes differs for the same percentage variation, depending whether the input property is varied positively or negatively. Although this asymmetry is occasionally quite marked, as a general rule the variation is symmetrical. For this reason no indication of asymmetry appears in Table D1.2. Also worthy of note is that for certain particle sizes the sensitivity of output attenuation and phase velocity to input variations of

α/f^2, and to a less marked extent β, is frequently a stronger function of frequency, therefore exhibiting some independence of particle size.

D1.5 Synopsis of results analysis

D1.5.1 Sensitivity of modelled attenuation and phase velocity in aqueous polystyrene dispersions to variations in input physical properties

Modelled attenuation and phase velocity output are strongly sensitive at all values of $k_c r$ to variations in the input properties of 'static' sound velocity and mass density for both continuous and dispersed phases. Output is strongly sensitive to variation in input shear modulus for all values of $k_c r$. Phase velocity output at low values of $k_c r$ and attenuation output at high values of $k_c r$ are sensitive to variations in continuous phase η. Output attenuation is sensitive to variations in continuous or dispersed phase properties of thermal conductivity at low and medium values of $k_c r$. Output phase velocity is sensitive to variations in properties of thermal conductivity at medium values of $k_c r$ in the dispersed phase but insensitive to variations in those of the continuous phase. Both modelled attenuation and phase velocity are sensitive to variations in the specific heat property of the continuous and dispersed phases at low and medium values of $k_c r$. Similarly, both modelled attenuation and phase velocity are sensitive to variations in the thermal dilatability (coefficient of expansion) property of the continuous and dispersed phases at low and medium values of $k_c r$. The effect of varying the α'/f^2 and α/f^2 properties is a good deal more complicated than it appears even in Table D1.2. Very roughly, output phase velocity is insensitive to variation of either property at all but high values of $k_c r$ and,

conversely, output attenuation is sensitive to variation of either property at all but high values of $k_c r$.

D1.5.2 Sensitivity of modelled attenuation and phase velocity in aqueous 1-bromo-hexadecane dispersions to variations in input physical properties

Modelled attenuation and phase velocity output are strongly sensitive at all values of $k_c r$ to variations in the input properties of 'static' sound velocity and mass density for both continuous and dispersed phases. Phase velocity output is insensitive at all values of $k_c r$ and attenuation output is insensitive at high values of $k_c r$ to variations in η'. Phase velocity output at nearly all values of $k_c r$ and attenuation output at high values of $k_c r$ are insensitive to variations in continuous phase η. Output attenuation is sensitive to variations in continuous or dispersed phase properties of thermal conductivity at low and medium values of $k_c r$. Output phase velocity is sensitive to variations in continuous or dispersed phase properties of thermal conductivity at medium values of $k_c r$. Both modelled attenuation and phase velocity are sensitive to variations in the specific heat property of the continuous and dispersed phases at low and medium values of $k_c r$. Similarly, both modelled attenuation and phase velocity are sensitive to variations in the thermal dilatability (coefficient of expansion) property of the continuous and dispersed phases at low and medium values of $k_c r$. The effect of varying the α'/f^2 and α/f^2 properties is a good deal more complicated than it appears even in Table D1.2. Very roughly, output phase velocity is insensitive to variation of either property at all but high values of $k_c r$ and, conversely, output attenuation is sensitive to variation of either property at all but high values of $k_c r$.

D1.5.3 Sensitivity of modelled attenuation and phase velocity in aqueous silica dispersions to variations in input physical properties

Modelled attenuation and phase velocity output is strongly sensitive at all values of $k_c r$ to variations in the input properties of 'static' sound velocity and mass density for both continuous and dispersed phases. Output is strongly sensitive to variation in input shear modulus for all values of $k_c r$. Phase velocity output at low values of $k_c r$ and attenuation output at high values of $k_c r$ are sensitive to variations in continuous phase η. Output attenuation is sensitive to variations in continuous-phase properties of thermal conductivity at low and medium values of $k_c r$, and to variations of dispersed-phase properties at low and high values of $k_c r$. Both modelled attenuation and phase velocity are sensitive to variations in the specific heat property of the continuous and dispersed phases at low and medium values of $k_c r$. Similarly, both modelled attenuation and phase velocity are sensitive to variations in the thermal dilatability (coefficient of expansion) property of the continuous and dispersed phases at low and medium values of $k_c r$. The effect of varying the α'/f^2 and α/f^2 properties is a good deal more complicated than it appears even in Table D1.2. Very roughly, output phase velocity is only sensitive to variation in the property for the continuous phase at high values of $k_c r$ and, conversely, output attenuation is sensitive to variation of either property at all but medium or high values of $k_c r$.

D1.5.4 Sensitivity of modelled attenuation and phase velocity in aqueous titanium dioxide dispersions to variations in input physical properties

Modelled attenuation and phase velocity output is strongly sensitive at most values of $k_c r$ to variations in the input properties of 'static' sound velocity and mass density for both continuous and dispersed phases. The exceptions are some insensitivity of phase velocity at low $k_c r$ and alpha at low to medium $k_c r$ to variations in *c*'. Both phase velocity and attenuation output is strongly sensitive to variation in input shear modulus for low and medium values of $k_c r$. Phase velocity output at low values of $k_c r$ and attenuation output at high values of $k_c r$ are sensitive to variations in continuous phase η. All outputs are insensitive to variations in continuous or dispersed phase properties of thermal conductivity. Modelled phase velocity is insensitive to variations in the specific heat property of the continuous and dispersed phases and the attenuation is only weakly sensitive at low or medium values of $k_c r$. Similarly, both modelled attenuation and phase velocity are sensitive to variations in the thermal dilatability (coefficient of expansion) property of the dispersed phase at low or medium values of $k_c r$ but insensitive to variations in β'. The effect of varying the α'/f^2 and α/f^2 properties is a good deal more complicated than it appears even in Table D1.2. Very roughly, output phase velocity and attenuation are insensitive to variation of α'/f^2; however, varying α/f^2 of the continuous phase effects the output phase velocity at high values of $k_c r$ and the output attenuation, albeit weakly, at low values of $k_c r$.

D1.5.5 Sensitivity of modelled attenuation and phase velocity in aqueous metallic iron dispersions to variations in input physical properties

Modelled attenuation and phase velocity output is strongly sensitive at most values of $k_c r$ to variations in the input properties of 'static' sound velocity and mass density for both continuous and dispersed phases. The exceptions are some insensitivity of phase velocity at low $k_c r$ and alpha at low to medium $k_c r$ to variations in *c*'. Phase velocity output is sensitive to variation in input shear modulus for low values of $k_c r$ and attenuation at medium values of $k_c r$. Phase velocity output at low values of $k_c r$ and attenuation output at high values of $k_c r$ are sensitive to variations in continuous phase η. All outputs are insensitive to variations in continuous or dispersed phase properties of thermal conductivity. Modelled phase velocity is insensitive to variations in the specific heat property of the continuous and dispersed phases and the attenuation is only weakly sensitive to variations in C_p' at low values of $k_c r$. Similarly, both modelled attenuation and phase velocity are sensitive to variations in the thermal dilatability (coefficient of expansion) property of the dispersed phase at low or medium values of $k_c r$ but insensitive or only weakly sensitive to variations in β'. The effect of varying the α'/f^2 and α/f^2 properties is a good deal more complicated than it appears even in Table D1.2. Very roughly, output phase velocity and attenuation are insensitive or only weakly sensitive to variation of α'/f^2; however, varying α/f^2 of the continuous phase effects the output phase velocity at high values of $k_c r$ and the output attenuation, albeit weakly, at low values of $k_c r$.

D2 Tables of permissible percentage variations in input property that result in defined limits of variation in modelled phase velocity and attenuation

Table D2.1 10% v/v aqueous polystyrene - dispersed phase at 25ºC (permissible + & - % variation in input property for 0.01% and 0.1% variation in output phase velocity)

property	frequency	10nm	100nm	1μm	10μm	100μm	1mm
c'	0.1MHz	0/0/0/0	0/0/0/0	0/0/0/0	0/0/0/0	0/0/0/0	0/0/0/0
c'	1MHz	0/0/0/0	0/0/0/0	0/0/0/0	0/0/0/0	0/0/0/0	0/0/0/0
c'	10MHz	0/0/0/0	0/0/0/0	0/0/0/0	0/0/0/0	0/0/0/0	0/0/0/0
c'	100MHz	0/0/0/0	0/0/0/0	0/0/0/0	0/0/0/0	0/0/0/0	0/0/0/0
c'	200MHz	0/0/0/0	0/0/0/0	0/0/0/0	1/1/17/20	0/0/0/0	1/0/1/0
ρ'	0.1MHz	0/0/0/0	0/0/0/0	0/0/0/0	0/0/0/0	0/0/0/0	0/0/0/0
ρ'	1MHz	0/0/0/0	0/0/0/0	0/0/0/0	0/0/0/0	0/0/0/0	0/0/0/0
ρ'	10MHz	0/0/0/0	0/0/0/0	0/0/0/0	0/0/0/0	0/0/0/0	0/0/0/0
ρ'	100MHz	0/0/0/0	0/0/0/0	0/0/0/0	0/0/0/0	0/0/0/0	0/0/0/0
ρ'	200MHz	0/0/0/0	0/0/0/0	0/0/0/0	0/0/0/0	0/0/0/0	0/0/0/0
μ'	0.1MHz	0/0/0/0	0/0/0/0	0/0/0/0	0/0/0/0	0/0/0/0	0/0/0/0
μ'	1MHz	0/0/0/0	0/0/0/0	0/0/0/0	0/0/0/0	0/0/0/0	0/0/0/0
μ'	10MHz	0/0/0/0	0/0/0/0	0/0/0/0	0/0/0/0	0/0/0/0	0/0/0/0
μ'	100MHz	0/0/0/0	0/0/0/0	0/0/0/0	0/0/2/0	0/0/0/0	0/0/0/0
μ'	200MHz	0/0/0/0	0/0/0/0	0/0/0/0	0/0/0/0	0/0/0/0	0/0/0/0
κ'	0.1MHz	20/20/20/20	20/20/20/20	4/4/20/20	3/3/20/20	20/20/20/20	20/20/20/20
κ'	1MHz	20/20/20/20	20/20/20/20	0/0/9/9	12/11/20/20	20/20/20/20	20/20/20/20
κ'	10MHz	20/20/20/20	9/7/20/20	3/3/20/20	20/20/20/20	20/20/20/20	20/20/20/20
κ'	100MHz	20/20/20/20	0/0/9/8	9/8/20/20	20/20/20/20	20/20/20/20	20/20/20/20
κ'	200MHz	20/20/20/20	1/1/10/9	9/9/20/20	20/20/20/20	20/20/20/20	20/20/20/20
C_p'	0.1MHz	0/0/1/1	0/0/1/1	0/0/1/1	0/0/7/6	7/6/20/20	20/20/20/20
C_p'	1MHz	0/0/1/1	0/0/1/1	0/0/2/2	3/2/20/20	20/20/20/20	20/20/20/20
C_p'	10MHz	0/0/1/1	0/0/1/1	1/1/18/11	17/11/20/20	20/20/20/20	20/20/20/20
C_p'	100MHz	0/0/2/2	0/0/6/5	6/5/20/20	20/20/20/20	20/20/20/20	20/20/20/20
C_p'	200MHz	0/0/3/3	1/0/11/8	9/7/20/20	20/20/20/20	20/20/20/20	20/20/20/20
α'/f^2	0.1MHz	20/20/20/20	20/20/20/20	20/20/20/20	20/20/20/20	20/20/20/20	20/20/20/20
α'/f^2	1MHz	20/20/20/20	20/20/20/20	20/20/20/20	20/20/20/20	20/20/20/20	20/20/20/20
α'/f^2	10MHz	20/20/20/20	20/20/20/20	20/20/20/20	20/20/20/20	4/4/20/20	5/5/20/20
α'/f^2	100MHz	20/20/20/20	1/1/17/17	20/20/20/20	0/0/4/4	0/0/3/2	4/18/15/20
α'/f^2	200MHz	6/6/20/20	1/1/10/10	20/20/20/20	0/0/6/5	0/0/1/1	7/4/7/4
β'	0.1MHz	0/0/0/0	0/0/0/0	0/0/0/0	0/0/5/5	5/6/20/20	20/20/20/20
β'	1MHz	0/0/0/0	0/0/0/0	0/0/1/1	1/1/11/13	11/12/20/20	17/20/20/20
β'	10MHz	0/0/0/0	0/0/0/0	0/0/2/2	2/2/20/20	6/6/20/20	12/16/20/20
β'	100MHz	0/0/0/0	0/0/0/0	0/0/5/5	6/6/20/20	7/7/20/20	20/20/20/20
β'	200MHz	0/0/0/0	0/0/0/0	0/0/4/5	10/10/20/20	5/8/20/20	20/20/20/20

Table D2.2 10% v/v aqueous polystyrene - continuous phase at 25ºC (permissible + & - % variation in input property for 0.01% and 0.1% variation in output phase velocity)

property	frequency	10nm	100nm	1μm	10μm	100μm	1mm
c	0.1MHz	0/0/0/0	0/0/0/0	0/0/0/0	0/0/0/0	0/0/0/0	0/0/0/0
c	1MHz	0/0/0/0	0/0/0/0	0/0/0/0	0/0/0/0	0/0/0/0	0/0/0/0
c	10MHz	0/0/0/0	0/0/0/0	0/0/0/0	0/0/0/0	0/0/0/0	0/0/0/0
c	100MHz	0/0/0/0	0/0/0/0	0/0/0/0	0/0/0/0	0/0/0/0	0/0/0/0
c	200MHz	0/0/0/0	0/0/0/0	0/0/0/0	0/0/0/0	0/0/0/0	0/0/0/0
ρ	0.1MHz	0/0/0/0	0/0/0/0	0/0/0/0	0/0/0/0	0/0/0/0	0/0/0/0
ρ	1MHz	0/0/0/0	0/0/0/0	0/0/0/0	0/0/0/0	0/0/0/0	0/0/0/0
ρ	10MHz	0/0/0/0	0/0/0/0	0/0/0/0	0/0/0/0	0/0/0/0	0/0/0/0
ρ	100MHz	0/0/0/0	0/0/0/0	0/0/0/0	0/0/0/0	0/0/8/2	0/0/1/1
ρ	200MHz	0/0/0/0	0/0/0/0	0/0/0/0	0/0/2/1	0/0/2/8	0/0/0/0
η	0.1MHz	20/20/20/20	20/20/20/20	20/20/20/20	10/10/20/20	20/20/20/20	20/20/20/20
η	1MHz	20/20/20/20	20/20/20/20	17/13/20/20	20/20/20/20	20/20/20/20	0/0/3/3
η	10MHz	20/20/20/20	20/20/20/20	9/8/20/20	6/6/20/20	0/0/1/1	0/0/2/2
η	100MHz	20/20/20/20	17/13/20/20	1/1/20/18	0/0/3/3	0/0/0/0	1/0/4/2
η	200MHz	20/20/20/20	8/7/20/20	0/0/5/5	0/0/8/8	0/0/0/0	7/3/7/3
κ	0.1MHz	20/20/20/20	20/20/20/20	6/5/20/20	18/14/20/20	20/20/20/20	20/20/20/20
κ	1MHz	20/20/20/20	20/20/20/20	5/4/20/20	20/20/20/20	20/20/20/20	20/20/20/20
κ	10MHz	20/20/20/20	9/7/20/20	20/16/20/20	20/20/20/20	20/20/20/20	20/20/20/20
κ	100MHz	20/20/20/20	5/5/20/20	20/20/20/20	20/20/20/20	20/20/20/20	20/20/20/20
κ	200MHz	20/20/20/20	7/6/20/20	20/20/20/20	20/20/20/20	20/20/20/20	20/20/20/20
C_p	0.1MHz	0/0/2/2	0/0/2/2	0/0/2/2	1/1/19/15	19/15/20/20	20/20/20/20
C_p	1MHz	0/0/2/2	0/0/2/2	0/0/5/5	6/5/20/20	20/20/20/20	20/20/20/20
C_p	10MHz	0/0/3/2	0/0/3/2	2/1/20/17	20/17/20/20	20/20/20/20	20/20/20/20
C_p	100MHz	0/0/3/3	0/0/6/6	6/6/20/20	20/20/20/20	20/20/20/20	20/20/20/20
C_p	200MHz	0/0/4/3	0/0/10/9	9/7/20/20	20/20/20/20	20/20/20/20	20/20/20/20
α/f^2	0.1MHz	20/20/20/20	20/20/20/20	20/20/20/20	20/20/20/20	20/20/20/20	20/20/20/20
α/f^2	1MHz	20/20/20/20	20/20/20/20	20/20/20/20	20/20/20/20	20/20/20/20	20/20/20/20
α/f^2	10MHz	20/20/20/20	20/20/20/20	20/20/20/20	20/20/20/20	20/20/20/20	20/20/20/20
α/f^2	100MHz	20/20/20/20	15/15/20/20	20/20/20/20	5/5/20/20	3/3/20/20	1/1/3/4
α/f^2	200MHz	20/20/20/20	10/10/20/20	20/20/20/20	3/3/20/20	1/1/15/16	1/0/1/0
β	0.1MHz	0/0/2/2	0/0/2/2	0/0/2/2	1/1/19/18	20/18/20/20	20/20/20/20
β	1MHz	0/0/2/2	0/0/2/2	0/0/5/5	5/5/20/20	20/20/20/20	20/20/20/20
β	10MHz	0/0/2/2	0/0/2/2	1/1/17/15	16/14/20/20	20/20/20/20	20/20/20/20
β	100MHz	0/0/2/1	0/0/4/4	4/4/20/20	20/20/20/20	20/20/20/20	20/20/20/20
β	200MHz	0/0/2/2	0/0/5/5	5/4/20/20	20/20/20/20	8/12/20/20	20/20/20/20

Table D2.3 10% v/v aqueous 1-bromo-hexadecane - dispersed phase at 25ºC (permissible + & - % variation in input property for 0.01% and 0.1% variation in output phase velocity)

property	frequency	10nm	100nm	1μm	10μm	100μm	1mm
c'	0.1MHz	0/0/0/0	0/0/0/0	0/0/0/0	0/0/0/0	0/0/0/0	0/0/0/0
c'	1MHz	0/0/0/0	0/0/0/0	0/0/0/0	0/0/0/0	0/0/0/0	0/0/0/0
c'	10MHz	0/0/0/0	0/0/0/0	0/0/0/0	0/0/0/0	0/0/0/0	0/0/0/0
c'	100MHz	0/0/0/0	0/0/0/0	0/0/0/0	0/0/0/0	0/0/0/0	0/0/0/0
c'	200MHz	0/0/0/0	0/0/0/0	0/0/0/0	0/0/0/0	0/0/0/0	0/0/0/0
ρ'	0.1MHz	0/0/0/0	0/0/0/0	0/0/0/0	0/0/0/0	0/0/0/0	0/0/0/0
ρ'	1MHz	0/0/0/0	0/0/0/0	0/0/0/0	0/0/0/0	0/0/0/0	0/0/0/0
ρ'	10MHz	0/0/0/0	0/0/0/0	0/0/0/0	0/0/0/0	0/0/0/0	0/0/0/0
ρ'	100MHz	0/0/0/0	0/0/0/0	0/0/5/1	0/0/0/0	0/0/0/0	0/0/0/0
ρ'	200MHz	0/0/0/0	0/0/0/0	0/0/0/0	0/0/0/0	0/0/0/0	0/0/0/0
η'	0.1MHz	20/20/20/20	20/20/20/20	20/20/20/20	1/1/14/12	14/12/20/20	20/20/20/20
η'	1MHz	20/20/20/20	20/20/20/20	13/10/20/20	5/5/20/20	20/20/20/20	20/20/20/20
η'	10MHz	20/20/20/20	20/20/20/20	1/1/17/13	14/12/20/20	16/16/20/20	20/20/20/20
η'	100MHz	20/20/20/20	14/11/20/20	2/2/20/20	1/1/14/14	20/20/20/20	20/20/20/20
η'	200MHz	20/20/20/20	5/4/20/20	1/1/18/18	0/0/8/8	1/1/11/11	20/20/20/20
κ'	0.1MHz	20/20/20/20	20/20/20/20	0/0/8/7	0/0/5/5	5/5/20/20	20/20/20/20
κ'	1MHz	20/20/20/20	20/20/20/20	0/0/1/1	1/1/17/15	17/15/20/20	20/20/20/20
κ'	10MHz	20/20/20/20	1/1/16/11	0/0/5/5	4/4/20/20	20/20/20/20	20/20/20/20
κ'	100MHz	20/20/20/20	0/0/1/1	1/1/15/14	18/16/20/20	20/20/20/20	20/20/20/20
κ'	200MHz	20/20/20/20	0/0/2/2	2/1/20/18	20/20/20/20	6/4/20/20	20/20/20/20
C_p'	0.1MHz	0/0/0/0	0/0/0/0	0/0/0/0	0/0/1/1	1/1/12/9	12/9/20/20
C_p'	1MHz	0/0/0/0	0/0/0/0	0/0/0/0	0/0/4/4	4/4/20/20	20/20/20/20
C_p'	10MHz	0/0/0/0	0/0/0/0	0/0/2/2	2/1/20/15	20/18/20/20	20/20/20/20
C_p'	100MHz	0/0/0/0	0/0/0/0	0/0/10/7	12/9/20/20	20/13/20/20	20/20/20/20
C_p'	200MHz	0/0/0/0	0/0/1/1	1/1/20/14	20/20/20/20	5/4/20/20	20/20/20/20
α'/f^2	0.1MHz	20/20/20/20	20/20/20/20	20/20/20/20	20/20/20/20	20/20/20/20	20/20/20/20
α'/f^2	1MHz	20/20/20/20	20/20/20/20	20/20/20/20	20/20/20/20	20/20/20/20	20/20/20/20
α'/f^2	10MHz	20/20/20/20	20/20/20/20	20/20/20/20	20/20/20/20	7/7/20/20	0/0/7/7
α'/f^2	100MHz	20/20/20/20	1/1/16/16	12/11/20/20	0/0/6/6	0/0/0/0	0/0/0/0
α'/f^2	200MHz	5/5/20/20	0/0/8/8	15/18/20/20	0/0/1/1	0/0/0/0	17/6/17/6
β'	0.1MHz	0/0/0/0	0/0/0/0	0/0/0/0	0/0/0/0	0/0/8/9	8/9/20/20
β'	1MHz	0/0/0/0	0/0/0/0	0/0/0/0	0/0/1/1	1/1/17/20	20/20/20/20
β'	10MHz	0/0/0/0	0/0/0/0	0/0/0/0	0/0/3/4	4/5/20/20	8/8/20/20
β'	100MHz	0/0/0/0	0/0/0/0	0/0/0/0	1/1/10/11	1/1/15/19	20/16/20/20
β'	200MHz	0/0/0/0	0/0/0/0	0/0/0/0	2/2/20/20	0/0/2/2	3/20/3/20

Table D2.4 10% v/v aqueous 1-bromo-hexadecane - continuous phase at 25ºC (permissible + & - % variation in input property for 0.01% and 0.1% variation in output phase velocity)

property	frequency	10nm	100nm	1μm	10μm	100μm	1mm
c	0.1MHz	0/0/0/0	0/0/0/0	0/0/0/0	0/0/0/0	0/0/0/0	0/0/0/0
c	1MHz	0/0/0/0	0/0/0/0	0/0/0/0	0/0/0/0	0/0/0/0	0/0/0/0
c	10MHz	0/0/0/0	0/0/0/0	0/0/0/0	0/0/0/0	0/0/0/0	0/0/0/0
c	100MHz	0/0/0/0	0/0/0/0	0/0/0/0	0/0/0/0	0/0/0/0	0/0/0/0
c	200MHz	0/0/0/0	0/0/0/0	0/0/0/0	0/0/0/0	0/0/0/0	0/0/0/0
ρ	0.1MHz	0/0/0/0	0/0/0/0	0/0/0/0	0/0/0/0	0/0/0/0	0/0/0/0
ρ	1MHz	0/0/0/0	0/0/0/0	0/0/0/0	0/0/0/0	0/0/0/0	0/0/0/0
ρ	10MHz	0/0/0/0	0/0/0/0	0/0/0/0	0/0/0/0	0/0/0/0	0/0/0/0
ρ	100MHz	0/0/0/0	0/0/0/0	0/0/0/0	0/0/0/0	0/0/1/1	0/0/5/3
ρ	200MHz	0/0/0/0	0/0/0/0	0/0/0/0	0/0/0/0	0/0/0/0	0/1/0/1
η	0.1MHz	20/20/20/20	20/20/20/20	12/9/20/20	0/0/7/6	8/7/20/20	20/20/20/20
η	1MHz	20/20/20/20	20/20/20/20	1/1/12/10	2/2/20/20	20/20/20/20	20/20/20/20
η	10MHz	20/20/20/20	20/14/20/20	0/0/6/6	7/7/20/20	20/20/20/20	20/20/20/20
η	100MHz	20/20/20/20	1/1/17/13	2/2/20/20	8/9/20/20	19/16/20/20	1/20/20/20
η	200MHz	20/20/20/20	1/1/11/9	4/4/20/20	4/4/20/20	3/2/20/20	20/20/20/20
κ	0.1MHz	20/20/20/20	20/20/20/20	0/0/10/8	1/1/20/16	19/15/20/20	20/20/20/20
κ	1MHz	20/20/20/20	18/13/20/20	0/0/7/6	6/5/20/20	20/20/20/20	20/20/20/20
κ	10MHz	20/20/20/20	1/1/14/11	2/2/20/18	20/17/20/20	20/20/20/20	20/20/20/20
κ	100MHz	20/19/20/20	0/0/8/7	6/6/20/20	20/20/20/20	20/20/20/20	20/20/20/20
κ	200MHz	15/11/20/20	1/1/11/10	10/9/20/20	20/20/20/20	20/20/20/20	20/20/20/20
C_p	0.1MHz	0/0/1/1	0/0/1/1	0/0/1/1	0/0/5/4	4/4/20/20	20/20/20/20
C_p	1MHz	0/0/1/1	0/0/1/1	0/0/2/2	1/1/18/14	18/14/20/20	20/20/20/20
C_p	10MHz	0/0/1/1	0/0/1/1	0/0/6/5	5/5/20/20	20/20/20/20	20/20/20/20
C_p	100MHz	0/0/1/1	0/0/2/2	2/1/20/17	20/19/20/20	20/20/20/20	20/20/20/20
C_p	200MHz	0/0/2/2	0/0/3/3	3/3/20/20	20/20/20/20	11/6/20/20	20/20/20/20
α/f^2	0.1MHz	20/20/20/20	20/20/20/20	20/20/20/20	20/20/20/20	20/20/20/20	20/20/20/20
α/f^2	1MHz	20/20/20/20	20/20/20/20	20/20/20/20	20/20/20/20	20/20/20/20	20/20/20/20
α/f^2	10MHz	20/20/20/20	20/20/20/20	20/20/20/20	20/20/20/20	20/20/20/20	4/4/20/20
α/f^2	100MHz	20/20/20/20	6/6/20/20	20/20/20/20	4/4/20/20	0/0/4/4	0/0/0/1
α/f^2	200MHz	20/20/20/20	3/3/20/20	20/20/20/20	1/1/12/12	0/0/0/0	2/0/2/0
β	0.1MHz	0/0/1/1	0/0/1/1	0/0/1/1	0/0/6/6	6/6/20/20	20/20/20/20
β	1MHz	0/0/0/0	0/0/0/0	0/0/2/2	1/1/17/16	17/16/20/20	20/20/20/20
β	10MHz	0/0/0/0	0/0/0/0	0/0/5/4	4/4/20/20	20/20/20/20	20/20/20/20
β	100MHz	0/0/0/0	0/0/1/1	1/1/13/12	16/15/20/20	20/20/20/20	20/20/20/20
β	200MHz	0/0/0/0	0/0/1/1	1/1/17/16	20/20/20/20	4/4/20/20	20/20/20/20

Table D2.5 10% v/v aqueous silica - dispersed phase at 25ºC (permissible + & - % variation in input property for 0.01% and 0.1% variation in output phase velocity)

property	frequency	10nm	100nm	1μm	10μm	100μm	1mm
c'	0.1MHz	0/0/0/0	0/0/0/0	0/0/0/0	0/0/0/0	0/0/0/0	0/0/0/0
c'	1MHz	0/0/0/0	0/0/0/0	0/0/0/0	0/0/0/0	0/0/0/0	0/0/0/0
c'	10MHz	0/0/0/0	0/0/0/0	0/0/0/0	0/0/0/0	0/0/0/0	0/0/0/0
c'	100MHz	0/0/0/0	0/0/0/0	0/0/0/0	0/0/0/0	0/0/0/0	0/0/0/0
c'	200MHz	0/0/0/0	0/0/1/1	0/0/1/1	0/0/1/1	0/0/0/0	0/0/0/0
ρ'	0.1MHz	0/0/0/0	0/0/0/0	0/0/0/0	0/0/0/0	0/0/0/0	0/0/0/0
ρ'	1MHz	0/0/0/0	0/0/0/0	0/0/0/0	0/0/0/0	0/0/0/0	0/0/0/0
ρ'	10MHz	0/0/0/0	0/0/0/0	0/0/0/0	0/0/0/0	0/0/1/6	0/0/0/0
ρ'	100MHz	0/0/0/0	0/0/0/0	0/0/0/0	0/0/0/0	0/0/0/0	0/0/0/0
ρ'	200MHz	0/0/0/0	0/0/0/0	0/0/0/0	0/0/0/0	0/0/0/0	0/0/0/0
μ'	0.1MHz	0/0/0/0	0/0/0/0	0/0/0/0	0/0/0/0	0/0/0/0	0/0/0/0
μ'	1MHz	0/0/0/0	0/0/0/0	0/0/0/0	0/0/0/0	0/0/0/0	0/0/0/0
μ'	10MHz	0/0/0/0	0/0/0/0	0/0/0/0	0/0/0/0	0/0/0/0	0/0/0/0
μ'	100MHz	0/0/0/0	0/0/0/0	0/0/0/0	0/0/0/0	0/0/0/0	0/0/0/0
μ'	200MHz	0/0/0/0	0/0/0/0	0/0/0/0	0/0/0/0	0/0/0/0	0/0/0/0
κ'	0.1MHz	20/20/20/20	20/20/20/20	0/0/7/6	0/0/9/9	17/14/20/20	20/20/20/20
κ'	1MHz	20/20/20/20	20/8/20/20	0/0/5/4	4/4/20/20	20/20/20/20	20/20/20/20
κ'	10MHz	20/20/20/20	0/1/12/9	0/0/8/8	15/13/20/20	20/20/20/20	20/20/20/20
κ'	100MHz	9/5/20/20	0/0/7/6	4/4/20/20	20/20/20/20	20/20/20/20	20/20/20/20
κ'	200MHz	4/0/20/15	0/0/7/6	5/4/20/20	20/20/20/20	20/20/20/20	20/20/20/20
C_p'	0.1MHz	0/0/0/0	0/0/0/0	0/0/0/0	0/0/1/1	1/1/20/14	20/13/20/20
C_p'	1MHz	0/0/0/0	0/0/0/0	0/0/0/0	0/0/8/6	9/7/20/20	20/20/20/20
C_p'	10MHz	0/0/0/0	0/0/0/0	0/0/2/2	4/3/20/20	20/20/20/20	20/20/20/20
C_p'	100MHz	0/0/0/0	0/0/0/0	1/1/20/13	20/18/20/20	20/20/20/20	20/20/20/20
C_p'	200MHz	0/0/0/0	0/0/2/1	4/3/20/20	20/20/20/20	20/20/20/20	20/20/20/20
α'/f^2	0.1MHz	20/20/20/20	20/20/20/20	20/20/20/20	20/20/20/20	20/20/20/20	20/20/20/20
α'/f^2	1MHz	20/20/20/20	20/20/20/20	20/20/20/20	20/20/20/20	20/20/20/20	20/20/20/20
α'/f^2	10MHz	20/20/20/20	20/20/20/20	20/20/20/20	20/20/20/20	20/20/20/20	20/20/20/20
α'/f^2	100MHz	0/11/20/20	15/15/20/20	20/20/20/20	20/20/20/20	20/20/20/20	20/17/20/20
α'/f^2	200MHz	2/0/13/11	8/8/20/20	20/20/20/20	18/17/20/20	20/20/20/20	20/20/20/20
β'	0.1MHz	0/0/0/0	0/0/0/0	0/0/0/0	0/0/1/1	1/1/15/18	15/18/20/20
β'	1MHz	0/0/0/0	0/0/0/0	0/0/0/0	0/0/3/3	3/3/20/20	20/20/20/20
β'	10MHz	0/0/0/0	0/0/0/0	0/0/0/0	0/0/7/8	10/11/20/20	20/20/20/20
β'	100MHz	0/0/0/0	0/0/0/0	0/0/1/1	2/2/20/20	20/20/20/20	9/2/20/20
β'	200MHz	0/0/0/0	0/0/0/0	0/0/1/1	2/2/20/20	6/5/20/20	8/20/8/20

Table D2.6 10% v/v aqueous silica - continuous phase at 25ºC (permissible + & - % variation in input property for 0.01% and 0.1% variation in output phase velocity)

property	frequency	10nm	100nm	1μm	10μm	100μm	1mm
c	0.1MHz	0/0/0/0	0/0/0/0	0/0/0/0	0/0/0/0	0/0/0/0	0/0/0/0
c	1MHz	0/0/0/0	0/0/0/0	0/0/0/0	0/0/0/0	0/0/0/0	0/0/0/0
c	10MHz	0/0/0/0	0/0/0/0	0/0/0/0	0/0/0/0	0/0/0/0	0/0/0/0
c	100MHz	0/0/0/0	0/0/0/0	0/0/0/0	0/0/0/0	0/0/0/0	0/0/0/0
c	200MHz	0/0/0/0	0/0/0/0	0/0/0/0	0/0/0/0	0/0/0/0	0/0/0/0
ρ	0.1MHz	0/0/0/0	0/0/0/0	0/0/0/0	0/0/0/0	0/0/0/0	0/0/0/0
ρ	1MHz	0/0/0/0	0/0/0/0	0/0/0/0	0/0/0/0	0/0/0/0	0/0/0/0
ρ	10MHz	0/0/0/0	0/0/0/0	0/0/0/0	0/0/0/0	0/0/0/0	0/0/0/0
ρ	100MHz	0/0/0/0	0/0/0/0	0/0/0/0	0/0/0/0	0/0/0/0	0/0/0/0
ρ	200MHz	0/0/0/0	0/0/1/0	0/0/0/0	0/0/0/0	0/0/0/0	0/0/0/0
η	0.1MHz	20/20/20/20	0/1/19/13	0/0/0/0	0/0/0/0	0/0/5/5	5/4/20/20
η	1MHz	20/20/20/20	0/0/0/0	0/0/0/0	0/0/1/1	1/1/14/13	6/6/20/20
η	10MHz	2/1/20/20	0/0/0/0	0/0/0/0	0/0/4/3	1/1/20/18	1/1/18/17
η	100MHz	0/0/1/1	0/0/0/0	0/0/1/1	0/0/6/6	0/0/4/4	0/0/0/0
η	200MHz	0/0/0/0	0/0/0/0	0/0/0/0	3/3/20/20	0/0/1/1	0/0/0/0
κ	0.1MHz	20/20/20/20	2/4/20/20	0/0/0/0	1/1/14/12	20/19/20/20	20/20/20/20
κ	1MHz	20/20/20/20	0/0/2/2	0/0/2/2	6/6/20/20	20/20/20/20	20/20/20/20
κ	10MHz	5/5/20/20	0/0/0/0	1/1/15/13	20/18/20/20	20/20/20/20	20/20/20/20
κ	100MHz	0/0/3/3	0/0/2/2	6/6/20/20	20/20/20/20	20/20/20/20	20/20/20/20
κ	200MHz	0/0/1/1	0/0/3/3	7/7/20/20	20/20/20/20	20/20/20/20	20/20/20/20
C_p	0.1MHz	0/0/0/0	0/0/0/0	0/0/0/0	0/0/2/2	3/3/20/20	20/20/20/20
C_p	1MHz	0/0/0/0	0/0/0/0	0/0/0/0	1/1/12/10	13/11/20/20	20/20/20/20
C_p	10MHz	0/0/0/0	0/0/0/0	0/0/2/2	4/3/20/20	20/20/20/20	20/20/20/20
C_p	100MHz	0/0/0/0	0/0/0/0	1/1/13/11	20/18/20/20	20/20/20/20	20/17/20/20
C_p	200MHz	0/0/0/0	0/0/0/0	1/1/16/13	20/20/20/20	20/20/20/20	20/7/20/7
α/f^2	0.1MHz	20/20/20/20	20/20/20/20	20/20/20/20	20/20/20/20	20/20/20/20	20/20/20/20
α/f^2	1MHz	20/20/20/20	20/20/20/20	20/20/20/20	20/20/20/20	20/20/20/20	20/20/20/20
α/f^2	10MHz	20/20/20/20	3/3/20/20	20/20/20/20	20/20/20/20	20/20/20/20	20/20/20/20
α/f^2	100MHz	0/0/9/8	1/2/19/19	20/20/20/20	7/7/20/20	20/20/20/20	0/0/2/2
α/f^2	200MHz	0/0/1/1	1/1/13/13	7/7/20/20	20/20/20/20	16/18/20/20	1/2/1/2
β	0.1MHz	0/0/0/0	0/0/0/0	0/0/0/0	0/0/3/3	4/4/20/20	20/20/20/20
β	1MHz	0/0/0/0	0/0/0/0	0/0/0/0	1/1/13/12	13/12/20/20	20/20/20/20
β	10MHz	0/0/0/0	0/0/0/0	0/0/2/2	4/3/20/20	20/20/20/20	20/20/20/20
β	100MHz	0/0/0/0	0/0/0/0	1/1/12/11	20/18/20/20	20/20/20/20	17/20/20/20
β	200MHz	0/0/0/0	0/0/0/0	1/1/18/13	20/20/20/20	14/20/20/20	6/20/6/20

Table D2.7 10% v/v aqueous titanium dioxide - dispersed phase at 25ºC (permissible + & - % variation in input property for 0.01% and 0.1% variation in output phase velocity)

property	frequency	10nm	100nm	1μm	10μm	100μm	1mm
c'	0.1MHz	1/1/13/8	1/1/13/8	1/1/12/8	0/0/1/1	0/0/0/0	0/0/0/0
c'	1MHz	1/1/20/13	1/1/20/13	0/0/11/7	0/0/1/0	0/0/0/0	0/0/2/2
c'	10MHz	2/2/20/18	2/2/20/18	0/0/4/4	0/0/0/0	0/0/4/3	0/0/2/1
c'	100MHz	4/3/20/20	2/2/20/16	0/0/2/2	0/0/7/6	0/0/4/3	0/0/0/3
c'	200MHz	6/5/20/20	2/2/20/17	0/0/4/4	0/0/8/6	0/0/1/1	0/0/0/0
ρ'	0.1MHz	0/0/0/0	0/0/0/0	0/0/0/0	0/0/0/0	0/0/0/0	0/0/0/0
ρ'	1MHz	0/0/0/0	0/0/0/0	0/0/0/0	0/0/0/0	0/0/0/0	0/0/0/0
ρ'	10MHz	0/0/0/0	0/0/0/0	0/0/0/0	0/0/0/0	0/0/0/0	0/0/0/0
ρ'	100MHz	0/0/0/0	0/0/0/0	0/0/0/0	0/0/0/0	0/0/0/0	0/0/0/0
ρ'	200MHz	0/0/0/0	0/0/0/0	0/0/0/0	0/0/0/0	0/0/0/0	0/0/0/0
μ'	0.1MHz	11/12/20/20	11/12/20/20	11/11/20/20	1/1/18/20	0/0/3/3	0/0/2/2
μ'	1MHz	9/9/20/20	9/9/20/20	4/4/20/20	0/0/5/5	0/0/2/2	0/0/0/0
μ'	10MHz	6/7/20/20	6/6/20/20	1/1/10/11	0/0/2/2	0/0/0/0	0/0/0/0
μ'	100MHz	4/5/20/20	2/2/20/20	0/0/3/3	0/0/1/1	0/0/0/0	0/0/0/0
μ'	200MHz	3/3/20/20	1/1/12/13	0/0/2/2	0/0/0/0	0/0/0/0	0/0/0/0
κ'	0.1MHz	20/20/20/20	20/20/20/20	20/20/20/20	17/14/20/20	20/20/20/20	20/20/20/20
κ'	1MHz	20/20/20/20	20/20/20/20	20/20/20/20	20/20/20/20	20/20/20/20	20/20/20/20
κ'	10MHz	20/20/20/20	20/20/20/20	20/15/20/20	20/20/20/20	20/20/20/20	20/20/20/20
κ'	100MHz	20/20/20/20	20/20/20/20	20/20/20/20	20/20/20/20	20/20/20/20	20/20/20/20
κ'	200MHz	20/20/20/20	20/20/20/20	20/20/20/20	20/20/20/20	20/20/20/20	20/20/20/20
C_p'	0.1MHz	2/2/20/20	2/2/20/20	3/3/20/20	20/16/20/20	20/20/20/20	20/20/20/20
C_p'	1MHz	2/2/20/20	2/2/20/20	7/6/20/20	20/15/20/20	20/20/20/20	20/20/20/20
C_p'	10MHz	1/1/18/18	2/2/20/20	20/17/20/20	20/20/20/20	20/20/20/20	20/20/20/20
C_p'	100MHz	1/1/15/15	9/7/20/20	20/18/20/20	20/20/20/20	20/20/20/20	20/20/20/20
C_p'	200MHz	1/1/13/13	18/12/20/20	20/20/20/20	20/20/20/20	20/20/20/20	20/20/20/20
α'/f^2	0.1MHz	20/20/20/20	20/20/20/20	20/20/20/20	20/20/20/20	20/20/20/20	20/20/20/20
α'/f^2	1MHz	20/20/20/20	20/20/20/20	20/20/20/20	20/20/20/20	20/20/20/20	20/20/20/20
α'/f^2	10MHz	20/20/20/20	20/20/20/20	20/20/20/20	20/20/20/20	20/20/20/20	20/20/20/20
α'/f^2	100MHz	20/20/20/20	20/20/20/20	20/20/20/20	20/20/20/20	20/20/20/20	20/20/20/20
α'/f^2	200MHz	20/20/20/20	20/20/20/20	20/20/20/20	20/20/20/20	20/20/20/20	8/20/20/20
β'	0.1MHz	20/20/20/20	20/20/20/20	20/20/20/20	20/20/20/20	20/20/20/20	20/20/20/20
β'	1MHz	20/20/20/20	20/20/20/20	20/20/20/20	20/20/20/20	20/20/20/20	20/20/20/20
β'	10MHz	20/20/20/20	20/20/20/20	20/20/20/20	20/20/20/20	20/20/20/20	20/20/20/20
β'	100MHz	20/20/20/20	20/20/20/20	20/20/20/20	20/20/20/20	20/20/20/20	20/20/20/20
β'	200MHz	20/19/20/20	17/17/20/20	20/20/20/20	20/20/20/20	20/20/20/20	20/20/20/20

Table D2.8 10% v/v aqueous titanium dioxide - continuous phase at 25ºC (permissible + & - % variation in input property for 0.01% and 0.1% variation in output phase velocity)

property	frequency	10nm	100nm	1μm	10μm	100μm	1mm
c	0.1MHz	0/0/0/0	0/0/0/0	0/0/0/0	0/0/0/0	0/0/0/0	0/0/0/0
c	1MHz	0/0/0/0	0/0/0/0	0/0/0/0	0/0/0/0	0/0/0/0	0/0/0/0
c	10MHz	0/0/0/0	0/0/0/0	0/0/0/0	0/0/0/0	0/0/0/0	0/0/0/0
c	100MHz	0/0/0/0	0/0/0/0	0/0/0/0	0/0/0/0	0/0/0/0	0/0/0/0
c	200MHz	0/0/0/0	0/0/0/0	0/0/0/0	0/0/0/0	0/0/0/0	0/0/0/0
ρ	0.1MHz	0/0/0/0	0/0/0/0	0/0/0/0	0/0/0/0	0/0/0/0	0/0/0/0
ρ	1MHz	0/0/0/0	0/0/0/0	0/0/0/0	0/0/0/0	0/0/0/0	0/0/0/0
ρ	10MHz	0/0/0/0	0/0/0/0	0/0/0/0	0/0/0/0	0/0/0/0	0/0/0/0
ρ	100MHz	0/0/0/0	0/0/0/0	0/0/0/0	0/0/0/0	0/0/0/0	0/0/2/1
ρ	200MHz	0/0/0/0	0/0/0/0	0/0/0/0	0/0/0/0	0/0/2/2	0/0/0/0
η	0.1MHz	20/20/20/20	20/20/20/20	0/0/1/1	0/0/0/0	0/0/0/0	0/0/3/3
η	1MHz	20/20/20/20	6/5/20/20	0/0/0/0	0/0/0/0	0/0/1/1	3/2/20/20
η	10MHz	20/20/20/20	0/0/3/2	0/0/0/0	0/0/0/0	0/0/9/8	5/5/20/20
η	100MHz	11/9/20/20	0/0/0/0	0/0/0/0	0/0/2/2	20/9/20/20	0/0/1/1
η	200MHz	5/4/20/20	0/0/0/0	0/0/0/0	0/0/4/4	0/0/4/4	0/0/0/0
κ	0.1MHz	20/20/20/20	20/20/20/20	20/20/20/20	7/6/20/20	14/13/20/20	20/20/20/20
κ	1MHz	20/20/20/20	20/20/20/20	8/7/20/20	8/8/20/20	20/20/20/20	20/20/20/20
κ	10MHz	20/20/20/20	20/20/20/20	6/6/20/20	16/14/20/20	20/20/20/20	20/20/20/20
κ	100MHz	20/20/20/20	8/8/20/20	8/7/20/20	20/20/20/20	20/20/20/20	20/20/20/20
κ	200MHz	20/20/20/20	6/5/20/20	11/10/20/20	20/20/20/20	20/20/20/20	20/20/20/20
C_p	0.1MHz	1/1/17/11	1/1/17/11	1/1/18/11	1/1/20/13	3/2/20/20	20/18/20/20
C_p	1MHz	2/1/20/15	2/1/20/15	2/2/20/16	2/2/20/19	13/10/20/20	20/20/20/20
C_p	10MHz	3/2/20/20	3/2/20/20	3/2/20/20	7/6/20/20	20/20/20/20	20/20/20/20
C_p	100MHz	4/3/20/20	4/3/20/20	5/4/20/20	20/20/20/20	20/20/20/20	20/20/20/20
C_p	200MHz	6/5/20/20	5/4/20/20	10/8/20/20	20/20/20/20	20/20/20/20	20/20/20/20
α/f^2	0.1MHz	20/20/20/20	20/20/20/20	20/20/20/20	20/20/20/20	20/20/20/20	20/20/20/20
α/f^2	1MHz	20/20/20/20	20/20/20/20	20/20/20/20	20/20/20/20	20/20/20/20	20/20/20/20
α/f^2	10MHz	20/20/20/20	20/20/20/20	20/20/20/20	20/20/20/20	20/20/20/20	20/20/20/20
α/f^2	100MHz	20/20/20/20	20/20/20/20	20/20/20/20	10/10/20/20	2/2/20/20	0/0/1/2
α/f^2	200MHz	20/20/20/20	20/20/20/20	11/11/20/20	15/15/20/20	0/0/6/6	0/0/1/1
β	0.1MHz	1/1/12/14	1/1/12/14	1/1/13/15	1/1/12/14	2/2/20/20	17/20/20/20
β	1MHz	0/0/9/10	0/0/9/10	0/0/9/9	1/1/10/11	4/4/20/20	20/20/20/20
β	10MHz	0/0/6/6	0/0/6/7	0/0/6/6	1/1/13/15	20/20/20/20	20/20/20/20
β	100MHz	0/0/4/4	0/0/4/4	0/0/5/6	7/8/20/20	20/20/20/20	11/4/20/20
β	200MHz	0/0/3/3	0/0/2/3	0/0/5/6	9/11/20/20	20/20/20/20	4/10/18/20

Table D2.9 10% v/v aqueous metallic iron - dispersed phase at 25ºC (permissible + & - % variation in input property for 0.01% and 0.1% variation in output phase velocity)

property	frequency	10nm	100nm	1μm	10μm	100μm	1mm
c'	0.1MHz	1/1/20/8	1/1/20/8	1/1/17/8	0/0/1/1	0/0/0/0	0/0/0/0
c'	1MHz	2/2/20/16	2/2/20/16	1/0/12/7	0/0/1/1	0/0/1/0	0/0/1/1
c'	10MHz	5/4/20/20	5/4/20/20	0/0/6/5	0/0/2/2	0/0/3/2	0/0/0/0
c'	100MHz	10/7/20/20	3/2/20/20	0/0/5/4	0/0/6/4	0/0/0/0	0/0/0/0
c'	200MHz	18/11/20/20	3/3/20/20	0/0/9/7	0/0/7/6	0/0/2/2	0/0/0/0
ρ'	0.1MHz	0/0/0/0	0/0/0/0	0/0/0/0	0/0/0/0	0/0/0/0	0/0/0/0
ρ'	1MHz	0/0/0/0	0/0/0/0	0/0/0/0	0/0/0/0	0/0/0/0	0/0/0/0
ρ'	10MHz	0/0/0/0	0/0/0/0	0/0/0/0	0/0/0/0	0/0/0/0	0/0/0/0
ρ'	100MHz	0/0/0/0	0/0/0/0	0/0/0/0	0/0/1/1	0/0/0/0	0/0/0/0
ρ'	200MHz	0/0/0/0	0/0/0/0	0/0/0/0	0/0/0/0	0/0/0/0	0/0/0/0
μ'	0.1MHz	5/5/20/20	5/5/20/20	4/5/20/20	0/0/5/6	0/0/2/2	0/0/1/2
μ'	1MHz	3/3/20/20	3/3/20/20	1/1/10/13	0/0/1/1	0/0/1/1	6/1/11/7
μ'	10MHz	1/1/12/20	1/1/11/19	0/0/1/1	0/0/0/0	0/0/1/2	0/0/0/0
μ'	100MHz	0/0/4/6	0/0/2/2	0/0/0/0	0/0/0/0	0/0/0/0	0/0/0/0
μ'	200MHz	0/0/0/0	0/0/1/1	0/0/0/0	0/0/0/0	0/0/0/0	0/0/0/0
κ'	0.1MHz	20/20/20/20	20/20/20/20	20/20/20/20	20/20/20/20	20/20/20/20	20/20/20/20
κ'	1MHz	20/20/20/20	20/20/20/20	20/20/20/20	20/20/20/20	20/20/20/20	20/20/20/20
κ'	10MHz	20/20/20/20	20/20/20/20	20/20/20/20	20/20/20/20	20/20/20/20	20/20/20/20
κ'	100MHz	20/20/20/20	20/20/20/20	20/20/20/20	20/20/20/20	20/20/20/20	20/20/20/20
κ'	200MHz	20/20/20/20	20/20/20/20	20/20/20/20	20/20/20/20	20/20/20/20	20/20/20/20
C_p'	0.1MHz	9/9/20/20	9/9/20/20	9/9/20/20	11/9/20/20	20/20/20/20	20/20/20/20
C_p'	1MHz	7/7/20/20	7/7/20/20	8/7/20/20	20/19/20/20	20/20/20/20	20/20/20/20
C_p'	10MHz	6/6/20/20	7/6/20/20	16/12/20/20	20/20/20/20	20/20/20/20	20/20/20/20
C_p'	100MHz	5/5/20/20	11/9/20/20	20/20/20/20	20/20/20/20	20/20/20/20	20/20/20/20
C_p'	200MHz	4/4/20/20	20/15/20/20	20/20/20/20	20/20/20/20	20/20/20/20	20/20/20/20
α'/f^2	0.1MHz	20/20/20/20	20/20/20/20	20/20/20/20	20/20/20/20	20/20/20/20	20/20/20/20
α'/f^2	1MHz	20/20/20/20	20/20/20/20	20/20/20/20	20/20/20/20	20/20/20/20	20/20/20/20
α'/f^2	10MHz	20/20/20/20	20/20/20/20	20/20/20/20	20/20/20/20	20/20/20/20	20/20/20/20
α'/f^2	100MHz	20/20/20/20	20/20/20/20	20/20/20/20	20/20/20/20	5/5/20/20	1/2/15/12
α'/f^2	200MHz	20/20/20/20	11/11/20/20	12/13/20/20	14/15/20/20	0/0/2/2	1/0/2/2
β'	0.1MHz	20/20/20/20	20/20/20/20	20/20/20/20	13/12/20/20	20/20/20/20	20/20/20/20
β'	1MHz	20/20/20/20	20/20/20/20	15/14/20/20	19/17/20/20	20/20/20/20	20/20/20/20
β'	10MHz	20/20/20/20	20/20/20/20	10/10/20/20	20/20/20/20	20/20/20/20	20/20/20/20
β'	100MHz	20/20/20/20	13/12/20/20	20/20/20/20	20/20/20/20	20/20/20/20	6/20/20/20
β'	200MHz	20/19/20/20	11/10/20/20	20/20/20/20	20/20/20/20	8/12/20/20	20/20/20/20

Table D2.10 10% v/v aqueous metallic iron - continuous phase at 25ºC (permissible + & - % variation in input property for 0.01% and 0.1% variation in output phase velocity)

property	frequency	10nm	100nm	1μm	10μm	100μm	1mm
c	0.1MHz	0/0/0/0	0/0/0/0	0/0/0/0	0/0/0/0	0/0/0/0	0/0/0/0
c	1MHz	0/0/0/0	0/0/0/0	0/0/0/0	0/0/0/0	0/0/0/0	0/0/0/0
c	10MHz	0/0/0/0	0/0/0/0	0/0/0/0	0/0/0/0	0/0/0/0	0/0/0/0
c	100MHz	0/0/0/0	0/0/0/0	0/0/0/0	0/0/0/0	0/0/0/0	0/0/0/0
c	200MHz	0/0/0/0	0/0/0/0	0/0/0/0	0/0/0/0	0/0/0/0	0/0/0/0
ρ	0.1MHz	0/0/0/0	0/0/0/0	0/0/0/0	0/0/0/0	0/0/0/0	0/0/0/0
ρ	1MHz	0/0/0/0	0/0/0/0	0/0/0/0	0/0/0/0	0/0/0/0	0/0/0/0
ρ	10MHz	0/0/0/0	0/0/0/0	0/0/0/0	0/0/0/0	0/0/0/0	0/0/0/0
ρ	100MHz	0/0/0/0	0/0/0/0	0/0/0/0	0/0/0/0	0/0/0/0	0/0/0/0
ρ	200MHz	0/0/0/0	0/0/0/0	0/0/0/0	0/0/0/0	0/0/0/0	0/0/0/0
η	0.1MHz	20/20/20/20	20/20/20/20	0/0/1/1	0/0/0/0	0/0/1/1	1/0/10/9
η	1MHz	20/20/20/20	4/3/20/20	0/0/0/0	0/0/0/0	0/0/3/3	3/3/20/20
η	10MHz	20/20/20/20	0/0/1/1	0/0/0/0	0/0/1/1	0/0/9/8	1/1/16/14
η	100MHz	7/6/20/20	0/0/0/0	0/0/0/0	0/0/2/2	0/0/7/6	0/0/3/4
η	200MHz	3/3/20/20	0/0/0/0	0/0/0/0	0/0/3/3	1/1/13/17	0/0/0/1
κ	0.1MHz	20/20/20/20	20/20/20/20	20/20/20/20	13/12/20/20	20/20/20/20	20/20/20/20
κ	1MHz	20/20/20/20	20/20/20/20	20/20/20/20	19/17/20/20	20/20/20/20	20/20/20/20
κ	10MHz	20/20/20/20	20/20/20/20	11/10/20/20	20/20/20/20	20/20/20/20	20/20/20/20
κ	100MHz	20/20/20/20	20/20/20/20	19/17/20/20	20/20/20/20	20/20/20/20	20/20/20/20
κ	200MHz	20/20/20/20	18/15/20/20	20/20/20/20	20/20/20/20	20/20/20/20	20/20/20/20
C_p	0.1MHz	5/4/20/20	5/4/20/20	5/4/20/20	2/2/20/20	12/9/20/20	20/20/20/20
C_p	1MHz	9/7/20/20	9/7/20/20	5/4/20/20	7/5/20/20	20/20/20/20	20/20/20/20
C_p	10MHz	15/10/20/20	15/9/20/20	6/5/20/20	20/16/20/20	20/20/20/20	20/20/20/20
C_p	100MHz	20/14/20/20	13/9/20/20	19/11/20/20	20/20/20/20	20/20/20/20	20/20/20/20
C_p	200MHz	20/20/20/20	20/12/20/20	20/20/20/20	20/20/20/20	20/20/20/20	20/4/20/20
α/f^2	0.1MHz	20/20/20/20	20/20/20/20	20/20/20/20	20/20/20/20	20/20/20/20	20/20/20/20
α/f^2	1MHz	20/20/20/20	20/20/20/20	20/20/20/20	20/20/20/20	20/20/20/20	20/20/20/20
α/f^2	10MHz	20/20/20/20	20/20/20/20	20/20/20/20	20/20/20/20	20/20/20/20	20/20/20/20
α/f^2	100MHz	20/20/20/20	20/20/20/20	20/20/20/20	13/13/20/20	2/2/20/20	1/1/11/11
α/f^2	200MHz	20/20/20/20	17/17/20/20	20/20/20/20	20/20/20/20	0/0/6/6	0/0/0/0
β	0.1MHz	5/5/20/20	5/5/20/20	5/5/20/20	2/2/20/20	8/9/20/20	20/20/20/20
β	1MHz	3/3/20/20	3/3/20/20	2/2/18/20	2/2/20/20	15/19/20/20	20/20/20/20
β	10MHz	2/2/20/20	2/2/20/20	1/1/10/11	4/4/20/20	20/20/20/20	20/20/20/20
β	100MHz	1/1/15/18	0/0/9/10	1/1/12/14	7/8/20/20	13/15/20/20	4/20/20/20
β	200MHz	1/1/10/12	0/0/5/5	1/1/11/13	7/8/20/20	15/19/20/20	3/14/18/20

Table D2.11 10% v/v aqueous polystyrene - dispersed phase at 25ºC (permissible + & - % variation in input property for 0.01% and 0.1% variation in output attenuation)

property	frequency	10nm	100nm	1μm	10μm	100μm	1mm
c'	0.1MHz	0/0/0/0	1/0/20/5	0/0/1/1	0/0/1/1	0/0/2/2	0/0/0/0
c'	1MHz	0/0/0/0	11/5/20/15	0/0/3/3	0/0/3/2	0/0/0/0	0/0/0/0
c'	10MHz	0/0/0/0	0/0/9/6	0/0/0/0	0/0/0/0	0/0/0/0	0/0/0/0
c'	100MHz	0/0/0/0	0/0/0/0	0/0/0/0	0/0/0/0	0/0/0/0	0/0/1/0
c'	200MHz	0/0/0/0	0/0/0/0	0/0/0/0	0/0/1/1	1/0/2/1	4/0/20/13
ρ'	0.1MHz	0/0/0/0	0/0/0/0	0/0/0/2	0/0/0/0	0/0/0/0	0/0/0/0
ρ'	1MHz	0/0/0/0	0/0/0/0	0/0/0/0	0/0/0/0	0/0/0/0	0/0/0/0
ρ'	10MHz	0/0/0/0	0/0/0/0	0/0/0/0	0/0/0/0	0/0/0/0	0/0/0/0
ρ'	100MHz	0/0/0/0	0/0/0/0	0/0/0/0	0/0/0/0	0/0/0/0	0/0/0/0
ρ'	200MHz	0/0/0/0	0/0/0/0	0/0/0/0	0/0/0/0	0/0/0/0	0/0/0/0
μ'	0.1MHz	0/0/0/0	0/0/3/3	1/1/13/20	0/0/4/4	0/0/10/8	0/0/0/0
μ'	1MHz	0/0/0/0	0/0/2/2	0/0/7/7	0/0/2/2	0/0/0/0	0/0/0/0
μ'	10MHz	0/0/0/0	0/0/0/0	0/0/0/0	0/0/0/0	0/0/0/0	0/0/0/0
μ'	100MHz	0/0/0/0	0/0/0/0	0/0/0/0	0/0/0/0	0/0/0/0	0/0/0/0
μ'	200MHz	0/0/0/0	0/0/0/0	0/0/0/0	0/0/0/0	0/0/0/0	0/0/0/0
κ'	0.1MHz	0/0/1/1	0/0/0/0	0/0/0/0	0/0/0/0	0/0/0/0	0/0/7/7
κ'	1MHz	0/0/1/1	0/0/0/0	0/0/0/0	0/0/0/0	0/0/3/3	20/20/20/20
κ'	10MHz	0/0/2/2	0/0/0/0	0/0/0/0	0/0/2/2	20/20/20/20	20/20/20/20
κ'	100MHz	0/0/2/2	0/0/1/2	0/0/3/3	20/20/20/20	20/20/20/20	20/20/20/20
κ'	200MHz	0/0/2/2	0/0/20/6	1/1/17/15	20/20/20/20	20/20/20/20	20/20/20/20
C_p'	0.1MHz	0/0/0/0	0/0/0/0	0/0/0/0	0/0/0/0	0/0/0/0	0/0/1/1
C_p'	1MHz	0/0/0/0	0/0/0/0	0/0/0/0	0/0/0/0	0/0/0/0	20/20/20/20
C_p'	10MHz	0/0/0/0	0/0/0/0	0/0/0/0	0/0/0/0	20/20/20/20	20/20/20/20
C_p'	100MHz	0/0/0/0	0/0/0/0	0/0/2/2	20/14/20/20	20/20/20/20	20/20/20/20
C_p'	200MHz	0/0/0/0	0/0/2/1	3/2/20/15	20/20/20/20	20/20/20/20	20/20/20/20
α'/f^2	0.1MHz	0/0/0/0	0/0/2/2	14/14/20/20	5/5/20/20	0/0/5/5	1/1/12/12
α'/f^2	1MHz	0/0/0/0	0/0/1/1	1/1/12/12	0/0/1/1	0/0/1/1	20/20/20/20
α'/f^2	10MHz	0/0/0/0	0/0/1/1	0/0/0/0	0/0/0/0	5/5/20/20	4/4/20/20
α'/f^2	100MHz	0/0/0/0	0/0/0/0	0/0/0/0	0/0/7/7	1/1/16/16	5/5/20/20
α'/f^2	200MHz	0/0/0/0	0/0/0/0	0/0/0/0	1/1/12/11	0/0/9/8	20/20/20/20
β'	0.1MHz	0/0/0/0	0/0/0/0	0/0/0/0	0/0/0/0	0/0/0/0	0/0/1/1
β'	1MHz	0/0/0/0	0/0/0/0	0/0/0/0	0/0/0/0	0/0/0/0	20/20/20/20
β'	10MHz	0/0/0/0	0/0/0/0	0/0/0/0	0/0/0/0	6/6/20/20	20/20/20/20
β'	100MHz	0/0/0/0	0/0/0/0	0/0/0/0	1/1/16/19	20/20/20/20	20/20/20/20
β'	200MHz	0/0/0/0	0/0/0/0	0/0/0/0	20/20/20/20	20/20/20/20	20/20/20/20

Table D2.12 10% v/v aqueous polystyrene - continuous phase at 25ºC (permissible + & - % variation in input property for 0.01% and 0.1% variation in output attenuation)

property	frequency	10nm	100nm	1μm	10μm	100μm	1mm
c	0.1MHz	0/0/0/0	0/0/0/0	0/0/0/0	0/0/0/0	0/0/0/0	0/0/0/0
c	1MHz	0/0/0/0	0/0/0/0	0/0/0/0	0/0/0/0	0/0/0/0	0/0/0/0
c	10MHz	0/0/0/0	0/0/0/0	0/0/0/0	0/0/0/0	0/0/0/0	0/0/0/0
c	100MHz	0/0/0/0	0/0/0/0	0/0/0/0	0/0/0/0	0/0/0/0	0/0/0/0
c	200MHz	0/0/0/0	0/0/0/0	0/0/0/0	0/0/0/0	0/0/1/0	1/0/1/0
ρ	0.1MHz	0/0/0/0	0/0/0/0	0/0/0/0	0/0/0/0	0/0/0/0	0/0/0/0
ρ	1MHz	0/0/0/0	0/0/0/0	0/0/0/0	0/0/0/0	0/0/0/0	0/0/0/0
ρ	10MHz	0/0/0/0	0/0/0/0	0/0/0/0	0/0/0/0	0/0/0/0	0/0/5/3
ρ	100MHz	0/0/0/0	0/0/0/0	0/0/0/0	0/0/0/0	0/0/2/2	0/0/6/6
ρ	200MHz	0/0/0/0	0/0/0/0	0/0/0/0	0/0/0/0	0/0/0/0	4/5/20/20
η	0.1MHz	0/0/0/0	2/1/20/11	0/0/4/4	0/0/3/3	0/0/0/0	0/0/1/1
η	1MHz	0/0/0/0	1/1/12/20	0/0/4/4	0/0/0/0	0/0/0/0	0/0/5/5
η	10MHz	0/0/0/0	0/0/3/4	0/0/1/1	0/0/0/0	0/0/1/1	0/0/8/8
η	100MHz	0/0/0/0	0/0/0/0	0/0/0/0	0/0/0/0	2/3/20/20	19/20/20/20
η	200MHz	0/0/0/0	0/0/0/0	0/0/0/0	0/0/9/9	1/1/20/17	6/6/20/20
κ	0.1MHz	0/0/1/1	0/0/0/0	0/0/0/0	0/0/1/1	0/0/1/1	3/3/20/20
κ	1MHz	0/0/1/1	0/0/0/0	0/0/1/1	0/0/1/1	1/1/16/13	20/20/20/20
κ	10MHz	0/0/2/2	0/0/0/0	0/0/2/1	1/1/13/11	20/20/20/20	20/20/20/20
κ	100MHz	0/0/3/3	0/0/8/6	2/2/20/18	20/20/20/20	20/20/20/20	20/20/20/20
κ	200MHz	0/0/4/3	1/1/19/14	12/10/20/20	20/20/20/20	20/20/20/20	20/20/20/20
C_p	0.1MHz	0/0/0/0	0/0/0/0	0/0/0/0	0/0/0/0	0/0/0/0	0/0/3/3
C_p	1MHz	0/0/0/0	0/0/0/0	0/0/0/0	0/0/0/0	0/0/1/1	20/20/20/20
C_p	10MHz	0/0/0/0	0/0/0/0	0/0/0/0	0/0/1/1	20/20/20/20	20/20/20/20
C_p	100MHz	0/0/0/0	0/0/0/0	0/0/2/2	20/20/20/20	20/20/20/20	20/20/20/20
C_p	200MHz	0/0/0/0	0/0/0/0	0/0/10/9	20/20/20/20	20/20/20/20	20/20/20/20
α/f^2	0.1MHz	0/0/8/8	11/11/20/20	20/20/20/20	20/20/20/20	4/4/20/20	9/9/20/20
α/f^2	1MHz	0/0/8/8	10/10/20/20	13/13/20/20	1/1/14/14	1/1/13/13	20/20/20/20
α/f^2	10MHz	0/0/8/8	4/4/20/20	0/0/4/4	0/0/3/3	20/20/20/20	20/20/20/20
α/f^2	100MHz	0/0/7/7	0/0/2/2	0/0/1/1	6/6/20/20	18/18/20/20	8/8/20/20
α/f^2	200MHz	0/0/7/7	0/0/1/1	0/0/1/1	20/20/20/20	17/17/20/20	8/9/20/20
β	0.1MHz	0/0/0/0	0/0/0/0	0/0/0/0	0/0/0/0	0/0/0/0	0/0/3/3
β	1MHz	0/0/0/0	0/0/0/0	0/0/0/0	0/0/0/0	0/0/1/1	20/20/20/20
β	10MHz	0/0/0/0	0/0/0/0	0/0/0/0	0/0/1/0	20/20/20/20	20/20/20/20
β	100MHz	0/0/0/0	0/0/0/0	0/0/1/1	20/17/20/20	20/20/20/20	20/20/20/20
β	200MHz	0/0/0/0	0/0/0/0	0/0/9/7	20/20/20/20	20/20/20/20	20/20/20/20

Table D2.13 10% v/v aqueous 1-bromo-hexadecane - dispersed phase at 25ºC (permissible + & - % variation in input property for 0.01% and 0.1% variation in output attenuation)

property	frequency	10nm	100nm	1μm	10μm	100μm	1mm
c'	0.1MHz	0/0/0/0	0/0/0/0	0/0/0/0	0/0/0/0	0/0/0/0	0/0/0/0
c'	1MHz	0/0/0/0	0/0/0/0	0/0/0/0	0/0/0/0	0/0/0/0	0/0/0/0
c'	10MHz	0/0/0/0	0/0/1/1	0/0/1/1	0/0/0/0	0/0/0/0	0/0/0/0
c'	100MHz	0/0/0/0	0/0/2/2	0/0/0/0	0/0/0/0	0/0/0/0	0/0/0/0
c'	200MHz	0/0/0/0	0/0/6/20	0/0/0/0	0/0/0/0	0/0/1/0	0/0/5/0
ρ'	0.1MHz	0/0/0/0	0/0/0/0	0/0/0/0	0/0/0/0	0/0/0/0	0/0/0/0
ρ'	1MHz	0/0/0/0	0/0/0/0	0/0/0/0	0/0/0/0	0/0/0/0	0/0/0/0
ρ'	10MHz	0/0/0/0	0/0/0/0	0/0/0/0	0/0/0/0	0/0/0/0	0/0/1/2
ρ'	100MHz	0/0/0/0	0/0/0/0	0/0/0/0	0/0/0/0	0/0/1/1	6/20/20/20
ρ'	200MHz	0/0/0/0	0/0/0/0	0/0/0/0	0/0/0/0	0/0/1/1	5/6/20/20
μ'	0.1MHz	0/0/0/0	0/0/9/9	2/2/20/17	1/2/13/20	0/0/1/1	0/0/6/5
μ'	1MHz	0/0/0/0	0/0/7/7	0/0/6/5	0/0/1/1	0/0/3/3	20/20/20/20
μ'	10MHz	0/0/0/0	0/0/5/4	0/0/3/3	2/12/14/20	20/20/20/20	20/20/20/20
μ'	100MHz	0/0/0/0	0/0/0/0	0/0/0/0	1/1/14/15	8/8/20/20	20/20/20/20
μ'	200MHz	0/0/0/0	0/0/0/0	0/0/0/0	20/20/20/20	8/8/20/20	20/20/20/20
κ'	0.1MHz	0/0/0/0	0/0/0/0	0/0/0/0	0/0/0/0	0/0/0/0	0/0/2/2
κ'	1MHz	0/0/0/0	0/0/0/0	0/0/0/0	0/0/0/0	0/0/1/1	20/20/20/20
κ'	10MHz	0/0/0/0	0/0/0/0	0/0/0/0	0/0/0/0	11/10/20/20	20/20/20/20
κ'	100MHz	0/0/0/0	0/0/2/2	0/0/0/0	3/3/20/20	20/20/20/20	20/20/20/20
κ'	200MHz	0/0/0/0	0/0/0/0	0/0/1/1	6/6/20/20	20/20/20/20	20/20/20/20
C_p'	0.1MHz	0/0/0/0	0/0/0/0	0/0/0/0	0/0/0/0	0/0/0/0	0/0/0/0
C_p'	1MHz	0/0/0/0	0/0/0/0	0/0/0/0	0/0/0/0	0/0/0/0	12/9/20/20
C_p'	10MHz	0/0/0/0	0/0/0/0	0/0/0/0	0/0/0/0	4/4/20/20	20/20/20/20
C_p'	100MHz	0/0/0/0	0/0/0/0	0/0/0/0	2/2/20/16	20/20/20/20	20/20/20/20
C_p'	200MHz	0/0/0/0	0/0/0/0	0/0/1/0	6/5/20/20	20/20/20/20	20/20/20/20
α'/f^2	0.1MHz	0/0/0/0	4/4/20/20	20/20/20/20	20/20/20/20	5/5/20/20	2/2/20/20
α'/f^2	1MHz	0/0/0/0	3/3/20/20	10/10/20/20	1/1/13/13	0/0/3/3	16/16/20/20
α'/f^2	10MHz	0/0/0/0	1/1/15/15	0/0/3/3	0/0/0/0	1/1/13/13	3/3/20/20
α'/f^2	100MHz	0/0/0/0	0/0/0/0	0/0/0/0	0/0/1/1	0/0/3/3	2/2/20/20
α'/f^2	200MHz	0/0/0/0	0/0/0/0	0/0/0/0	0/0/1/1	0/0/1/1	20/20/20/20
β'	0.1MHz	0/0/0/0	0/0/0/0	0/0/0/0	0/0/0/0	0/0/0/0	0/0/0/0
β'	1MHz	0/0/0/0	0/0/0/0	0/0/0/0	0/0/0/0	0/0/0/0	4/4/20/20
β'	10MHz	0/0/0/0	0/0/0/0	0/0/0/0	0/0/0/0	0/0/8/9	20/20/20/20
β'	100MHz	0/0/0/0	0/0/0/0	0/0/0/0	0/0/2/2	20/20/20/20	20/20/20/20
β'	200MHz	0/0/0/0	0/0/0/0	0/0/0/0	0/0/2/2	7/8/20/20	20/20/20/20

Table D2.14 10% v/v aqueous 1-bromo-hexadecane - continuous phase at 25ºC (permissible + & - % variation in input property for 0.01% and 0.1% variation in output attenuation)

property	frequency	10nm	100nm	1μm	10μm	100μm	1mm
c	0.1MHz	0/0/0/0	0/0/0/0	0/0/0/0	0/0/2/10	0/0/2/1	0/0/0/0
c	1MHz	0/0/0/0	0/0/0/0	0/0/0/0	0/0/12/2	0/0/0/0	0/0/0/0
c	10MHz	0/0/0/0	0/0/0/0	0/0/2/10	0/0/0/0	0/0/0/0	0/0/0/0
c	100MHz	0/0/0/0	0/0/0/0	0/0/0/0	0/0/0/0	0/0/0/0	0/0/0/0
c	200MHz	0/0/0/0	0/0/0/0	0/0/0/0	0/0/0/0	0/0/0/0	0/0/1/0
ρ	0.1MHz	0/0/0/0	0/0/0/0	0/0/0/0	0/0/0/0	0/0/0/0	0/0/0/0
ρ	1MHz	0/0/0/0	0/0/0/0	0/0/0/0	0/0/0/0	0/0/0/0	0/0/0/0
ρ	10MHz	0/0/0/0	0/0/0/0	0/0/0/0	0/0/0/0	0/0/0/0	0/0/0/0
ρ	100MHz	0/0/0/0	0/0/0/0	0/0/0/0	0/0/0/0	0/0/0/0	8/7/20/20
ρ	200MHz	0/0/0/0	0/0/0/0	0/0/0/0	0/0/0/0	0/0/1/1	20/20/20/20
η	0.1MHz	0/0/0/0	0/0/2/2	0/0/2/2	0/0/1/1	0/0/0/0	0/0/3/3
η	1MHz	0/0/0/0	0/0/2/2	0/0/1/1	0/0/0/0	0/0/1/1	20/20/20/20
η	10MHz	0/0/0/0	0/0/3/3	0/0/1/1	0/0/0/0	12/11/20/20	20/20/20/20
η	100MHz	0/0/0/0	0/0/3/3	0/0/0/0	2/2/20/20	20/20/20/20	20/20/20/20
η	200MHz	0/0/0/0	3/4/20/20	0/0/0/0	8/7/20/20	20/20/20/20	20/20/20/20
κ	0.1MHz	0/0/0/0	0/0/0/0	0/0/0/0	0/0/1/1	0/0/1/1	0/0/7/7
κ	1MHz	0/0/0/0	0/0/0/0	0/0/1/1	0/0/1/1	0/0/3/3	20/20/20/20
κ	10MHz	0/0/0/0	0/0/0/0	0/0/1/1	0/0/2/2	20/20/20/20	20/20/20/20
κ	100MHz	0/0/0/0	0/0/2/2	0/0/2/2	17/14/20/20	20/20/20/20	20/20/20/20
κ	200MHz	0/0/0/0	0/0/2/2	0/0/6/6	20/20/20/20	20/20/20/20	20/20/20/20
C_p	0.1MHz	0/0/0/0	0/0/0/0	0/0/0/0	0/0/0/0	0/0/0/0	0/0/1/1
C_p	1MHz	0/0/0/0	0/0/0/0	0/0/0/0	0/0/0/0	0/0/1/1	20/20/20/20
C_p	10MHz	0/0/0/0	0/0/0/0	0/0/0/0	0/0/0/0	14/11/20/20	20/20/20/20
C_p	100MHz	0/0/3/2	0/0/0/0	0/0/0/0	4/4/20/20	20/20/20/20	20/20/20/20
C_p	200MHz	0/0/7/20	0/0/0/0	0/0/2/2	10/9/20/20	20/20/20/20	20/20/20/20
α/f^2	0.1MHz	0/0/0/0	4/4/20/20	20/20/20/20	20/20/20/20	20/20/20/20	10/10/20/20
α/f^2	1MHz	0/0/0/0	4/4/20/20	20/20/20/20	7/7/20/20	1/1/15/15	20/20/20/20
α/f^2	10MHz	0/0/0/0	3/3/20/20	2/2/20/20	0/0/3/3	8/8/20/20	20/20/20/20
α/f^2	100MHz	0/0/0/0	1/1/10/10	0/0/1/1	0/0/8/8	2/2/20/20	8/9/20/20
α/f^2	200MHz	0/0/0/0	0/0/2/2	0/0/0/0	0/0/8/8	1/1/10/10	19/20/20/20
β	0.1MHz	0/0/0/0	0/0/0/0	0/0/0/0	0/0/0/0	0/0/0/0	0/0/2/2
β	1MHz	0/0/0/0	0/0/0/0	0/0/0/0	0/0/0/0	0/0/1/1	20/20/20/20
β	10MHz	0/0/0/0	0/0/0/0	0/0/0/0	0/0/0/0	10/10/20/20	20/20/20/20
β	100MHz	0/0/0/0	0/0/0/0	0/0/0/0	3/3/20/20	20/20/20/20	20/20/20/20
β	200MHz	0/0/0/0	0/0/0/0	0/0/0/0	5/5/20/20	20/20/20/20	20/20/20/20

Table D2.15 10% v/v aqueous silica - dispersed phase at 25ºC (permissible + & - % variation in input property for 0.01% and 0.1% variation in output attenuation)

property	frequency	10nm	100nm	1μm	10μm	100μm	1mm
c'	0.1MHz	0/0/0/0	0/0/0/0	0/0/0/0	0/0/0/0	0/0/0/0	0/0/0/0
c'	1MHz	0/0/20/3	0/0/2/1	0/0/20/4	0/0/4/5	0/0/0/0	0/0/0/0
c'	10MHz	0/0/5/6	0/0/8/5	0/0/4/4	0/0/1/1	0/0/1/1	0/0/0/0
c'	100MHz	0/0/4/4	1/1/17/15	1/1/20/8	0/0/4/3	0/0/1/1	0/0/1/0
c'	200MHz	0/0/5/4	1/0/11/8	0/0/3/2	0/0/5/4	1/5/3/6	0/0/0/0
ρ'	0.1MHz	0/0/0/0	0/0/0/0	0/0/0/0	0/0/0/0	0/0/0/0	0/0/0/0
ρ'	1MHz	0/0/0/0	0/0/0/0	0/0/0/0	0/0/0/0	0/0/0/0	0/0/0/0
ρ'	10MHz	0/0/0/0	0/0/0/0	0/0/0/0	0/0/0/0	0/0/5/10	0/0/0/0
ρ'	100MHz	0/0/0/0	0/0/0/0	0/0/0/0	0/0/3/3	0/0/0/0	0/0/0/0
ρ'	200MHz	0/0/0/0	0/0/0/0	0/0/0/0	0/0/0/0	0/0/1/0	0/0/0/0
μ'	0.1MHz	0/0/0/0	0/0/0/0	0/0/0/0	0/0/1/1	0/0/1/1	0/0/0/0
μ'	1MHz	0/0/0/0	0/0/0/0	0/0/0/0	0/0/0/0	0/0/0/0	0/0/0/0
μ'	10MHz	0/0/0/0	0/0/0/0	0/0/2/8	0/0/0/0	0/0/0/0	0/0/0/0
μ'	100MHz	0/0/3/9	0/0/0/0	0/0/0/0	0/0/1/1	0/0/4/1	0/0/0/0
μ'	200MHz	0/0/1/1	0/0/0/0	0/0/0/0	0/0/0/0	0/0/0/0	0/0/0/0
κ'	0.1MHz	1/1/14/11	0/0/7/6	0/0/5/5	0/0/5/5	0/0/6/5	1/1/20/17
κ'	1MHz	1/1/17/13	0/0/8/7	0/0/5/4	0/0/5/5	1/1/10/9	20/20/20/20
κ'	10MHz	1/1/20/15	0/0/8/7	0/0/6/6	0/0/7/7	20/20/20/20	20/20/20/20
κ'	100MHz	2/2/20/17	0/0/7/6	0/0/6/6	20/20/20/20	20/20/20/20	20/20/20/20
κ'	200MHz	2/2/20/19	0/0/8/7	1/1/12/10	20/20/20/20	20/20/20/20	20/20/20/20
C_p'	0.1MHz	0/0/0/0	0/0/0/0	0/0/0/0	0/0/0/0	0/0/0/0	0/0/2/2
C_p'	1MHz	0/0/0/0	0/0/0/0	0/0/0/0	0/0/0/0	0/0/1/1	20/20/20/20
C_p'	10MHz	0/0/0/0	0/0/0/0	0/0/1/1	0/0/1/1	20/20/20/20	20/20/20/20
C_p'	100MHz	0/0/0/0	0/0/0/0	0/0/2/2	20/19/20/20	20/20/20/20	20/20/20/20
C_p'	200MHz	0/0/0/0	0/0/1/1	0/0/8/6	20/20/20/20	20/20/20/20	20/20/20/20
α'/f^2	0.1MHz	0/0/9/9	20/20/20/20	20/20/20/20	20/20/20/20	20/20/20/20	20/20/20/20
α'/f^2	1MHz	0/0/7/7	20/20/20/20	20/20/20/20	20/20/20/20	20/20/20/20	20/20/20/20
α'/f^2	10MHz	0/0/6/6	20/20/20/20	20/20/20/20	6/6/20/20	20/20/20/20	20/20/20/20
α'/f^2	100MHz	0/0/4/4	5/5/20/20	1/1/15/15	20/20/20/20	20/20/20/20	20/20/20/20
α'/f^2	200MHz	0/0/3/3	2/2/20/20	0/0/9/9	20/20/20/20	20/20/20/20	20/20/20/20
β'	0.1MHz	0/0/0/0	0/0/0/0	0/0/0/0	0/0/0/0	0/0/0/0	0/0/1/1
β'	1MHz	0/0/0/0	0/0/0/0	0/0/0/0	0/0/0/0	0/0/0/0	20/20/20/20
β'	10MHz	0/0/0/0	0/0/0/0	0/0/0/0	0/0/0/0	10/11/20/20	20/20/20/20
β'	100MHz	0/0/0/0	0/0/0/0	0/0/0/0	2/2/20/20	20/20/20/20	20/20/20/20
β'	200MHz	0/0/0/0	0/0/0/0	0/0/0/0	14/17/20/20	20/20/20/20	20/20/20/20

Table D2.16 10% v/v aqueous silica - continuous phase at 25ºC (permissible + & - % variation in input property for 0.01% and 0.1% variation in output attenuation)

property	frequency	10nm	100nm	1μm	10μm	100μm	1mm
c	0.1MHz	0/0/0/0	0/0/0/0	0/0/0/0	0/0/0/0	0/0/0/0	0/0/0/0
c	1MHz	0/0/0/0	0/0/0/0	0/0/0/0	0/0/0/0	0/0/0/0	0/0/0/0
c	10MHz	0/0/0/0	0/0/0/0	0/0/0/0	0/0/0/0	0/0/0/0	0/0/0/0
c	100MHz	0/0/0/0	0/0/0/0	0/0/0/0	0/0/0/0	0/0/0/0	0/0/0/0
c	200MHz	0/0/0/0	0/0/0/0	0/0/0/0	0/0/0/1	0/0/0/1	0/0/0/0
ρ	0.1MHz	0/0/0/0	0/0/0/0	0/0/0/0	0/0/0/0	0/0/0/0	0/0/0/0
ρ	1MHz	0/0/0/0	0/0/0/0	0/0/0/0	0/0/0/0	0/0/0/0	0/0/0/0
ρ	10MHz	0/0/0/0	0/0/0/0	0/0/0/0	0/0/0/0	0/0/0/0	0/0/0/0
ρ	100MHz	0/0/0/0	0/0/0/0	0/0/0/0	0/0/0/0	0/0/0/0	0/0/1/1
ρ	200MHz	0/0/0/0	0/0/0/0	0/0/0/0	0/0/0/0	0/0/0/0	0/0/3/2
η	0.1MHz	0/0/0/0	0/0/0/0	0/0/0/0	0/0/0/0	0/0/0/0	0/0/0/0
η	1MHz	0/0/2/1	0/0/0/0	0/0/0/0	0/0/0/0	0/0/0/0	1/1/19/17
η	10MHz	0/0/0/0	0/0/0/0	0/0/0/0	0/0/0/0	0/0/5/5	1/1/20/18
η	100MHz	0/0/0/0	0/0/0/0	0/0/0/0	0/0/1/1	0/0/6/6	20/20/20/20
η	200MHz	0/0/0/0	0/0/0/0	0/0/0/0	0/0/1/1	0/0/6/6	1/1/20/18
κ	0.1MHz	0/0/1/1	0/0/0/0	0/0/1/1	0/0/7/6	0/0/8/7	2/2/20/20
κ	1MHz	0/0/1/1	0/0/1/1	1/1/11/10	0/0/7/7	1/1/15/13	20/20/20/20
κ	10MHz	0/0/2/2	0/0/2/2	0/0/7/6	1/1/11/10	20/20/20/20	20/20/20/20
κ	100MHz	0/0/3/3	1/1/11/10	0/0/10/8	20/20/20/20	20/20/20/20	20/20/20/20
κ	200MHz	0/0/4/3	5/4/20/20	1/1/20/16	20/20/20/20	20/20/20/20	20/20/20/20
C_p	0.1MHz	0/0/0/0	0/0/0/0	0/0/1/1	0/0/1/1	0/0/1/1	0/0/4/4
C_p	1MHz	0/0/0/0	0/0/1/1	0/0/1/1	0/0/1/1	0/0/2/2	20/20/20/20
C_p	10MHz	0/0/0/0	0/0/2/2	0/0/1/1	0/0/2/2	20/20/20/20	20/20/20/20
C_p	100MHz	0/0/1/1	0/0/2/2	0/0/1/1	20/16/20/20	20/20/20/20	20/20/20/20
C_p	200MHz	0/0/1/1	0/0/2/2	0/0/4/3	20/20/20/20	20/20/20/20	20/20/20/20
α/f^2	0.1MHz	0/0/0/0	5/5/20/20	20/20/20/20	20/20/20/20	20/20/20/20	20/20/20/20
α/f^2	1MHz	0/0/0/0	4/4/20/20	20/20/20/20	20/20/20/20	7/7/20/20	20/20/20/20
α/f^2	10MHz	0/0/0/0	4/4/20/20	15/15/20/20	1/1/19/19	20/20/20/20	20/20/20/20
α/f^2	100MHz	0/0/0/0	4/4/20/20	0/0/5/5	20/20/20/20	20/20/20/20	18/19/20/20
α/f^2	200MHz	0/0/0/0	20/20/20/20	0/0/4/4	4/4/20/20	20/20/20/20	0/0/7/7
β	0.1MHz	0/0/0/0	0/0/0/0	0/0/1/1	0/0/1/1	0/0/1/1	0/0/5/5
β	1MHz	0/0/0/0	0/0/0/0	0/0/1/1	0/0/1/1	0/0/2/2	20/20/20/20
β	10MHz	0/0/0/0	0/0/0/0	0/0/1/1	0/0/2/1	20/20/20/20	20/20/20/20
β	100MHz	0/0/0/0	0/0/0/0	0/0/1/1	20/17/20/20	20/20/20/20	20/20/20/20
β	200MHz	0/0/0/0	0/0/0/0	0/0/3/3	20/20/20/20	20/20/20/20	20/20/20/20

Table D2.17 10% v/v aqueous titanium dioxide - dispersed phase at 25ºC (permissible + & - % variation in input property for 0.01% and 0.1% variation in output attenuation)

property	frequency	10nm	100nm	1μm	10μm	100μm	1mm
c'	0.1MHz	17/10/20/20	12/8/20/20	12/8/20/20	10/7/20/20	9/6/20/20	0/0/5/4
c'	1MHz	20/15/20/20	20/12/20/20	20/11/20/20	17/10/20/20	1/1/20/12	2/2/20/17
c'	10MHz	20/20/20/20	20/17/20/20	20/15/20/20	5/4/20/20	4/3/20/20	0/0/4/4
c'	100MHz	20/20/20/20	20/20/20/20	19/12/20/20	8/6/20/20	0/0/6/5	0/0/5/5
c'	200MHz	20/20/20/20	20/20/20/20	6/5/20/20	7/5/20/20	9/2/20/9	0/0/6/1
ρ'	0.1MHz	0/0/0/0	0/0/0/0	0/0/0/0	0/0/0/0	0/0/0/0	0/0/0/0
ρ'	1MHz	0/0/0/0	0/0/0/0	0/0/0/0	0/0/0/0	0/0/0/0	0/0/5/4
ρ'	10MHz	0/0/0/0	0/0/0/0	0/0/0/0	0/0/0/0	2/1/20/10	0/0/0/0
ρ'	100MHz	0/0/0/0	0/0/0/0	0/0/0/0	0/0/6/11	0/0/0/0	0/0/0/0
ρ'	200MHz	0/0/0/0	0/0/0/0	0/0/0/0	0/0/0/0	0/0/0/0	0/0/0/0
μ'	0.1MHz	20/20/20/20	20/20/20/20	20/20/20/20	20/20/20/20	20/20/20/20	5/5/20/20
μ'	1MHz	20/20/20/20	20/20/20/20	20/20/20/20	20/20/20/20	7/8/20/20	0/0/2/1
μ'	10MHz	20/20/20/20	20/20/20/20	20/20/20/20	12/13/20/20	0/0/2/2	0/0/0/0
μ'	100MHz	20/20/20/20	20/20/20/20	15/16/20/20	0/0/3/2	0/0/0/0	0/0/0/0
μ'	200MHz	20/20/20/20	20/20/20/20	3/3/20/20	0/0/4/4	0/0/0/0	0/0/0/0
κ'	0.1MHz	20/20/20/20	20/20/20/20	20/20/20/20	20/20/20/20	20/16/20/20	20/20/20/20
κ'	1MHz	20/20/20/20	20/20/20/20	20/20/20/20	20/17/20/20	20/20/20/20	20/20/20/20
κ'	10MHz	20/20/20/20	20/20/20/20	20/20/20/20	20/20/20/20	20/20/20/20	20/20/20/20
κ'	100MHz	20/20/20/20	20/20/20/20	20/20/20/20	20/20/20/20	20/20/20/20	20/20/20/20
κ'	200MHz	20/20/20/20	20/20/20/20	20/20/20/20	20/20/20/20	20/20/20/20	20/20/20/20
C_p'	0.1MHz	1/1/16/12	0/0/6/6	1/1/10/11	7/6/20/20	12/10/20/20	20/20/20/20
C_p'	1MHz	2/1/20/14	0/0/5/5	2/2/20/20	12/10/20/20	20/15/20/20	20/20/20/20
C_p'	10MHz	17/3/20/18	0/0/6/6	9/8/20/20	17/13/20/20	20/20/20/20	20/20/20/20
C_p'	100MHz	14/3/20/17	2/2/20/20	16/13/20/20	20/20/20/20	20/20/20/20	20/20/20/20
C_p'	200MHz	4/9/17/20	4/4/20/20	20/20/20/20	20/20/20/20	20/20/20/20	20/20/20/20
α'/f^2	0.1MHz	20/20/20/20	20/20/20/20	20/20/20/20	20/20/20/20	20/20/20/20	20/20/20/20
α'/f^2	1MHz	20/20/20/20	20/20/20/20	20/20/20/20	20/20/20/20	20/20/20/20	20/20/20/20
α'/f^2	10MHz	20/20/20/20	20/20/20/20	20/20/20/20	20/20/20/20	20/20/20/20	20/20/20/20
α'/f^2	100MHz	19/19/20/20	20/20/20/20	20/20/20/20	20/20/20/20	20/20/20/20	20/20/20/20
α'/f^2	200MHz	16/16/20/20	20/20/20/20	20/20/20/20	20/20/20/20	20/20/20/20	20/20/20/20
β'	0.1MHz	20/20/20/20	19/19/20/20	20/20/20/20	20/20/20/20	20/20/20/20	20/20/20/20
β'	1MHz	20/20/20/20	18/18/20/20	20/20/20/20	20/20/20/20	20/20/20/20	20/20/20/20
β'	10MHz	20/20/20/20	20/20/20/20	20/20/20/20	20/20/20/20	20/20/20/20	20/20/20/20
β'	100MHz	16/18/20/20	20/20/20/20	20/20/20/20	20/20/20/20	20/20/20/20	20/20/20/20
β'	200MHz	10/11/20/20	20/20/20/20	20/20/20/20	20/20/20/20	20/20/20/20	20/20/20/20

Table D2.18 10% v/v aqueous titanium dioxide - continuous phase at 25ºC (permissible + & - % variation in input property for 0.01% and 0.1% variation in output attenuation)

property	frequency	10nm	100nm	1μm	10μm	100μm	1mm
c	0.1MHz	0/0/0/0	0/0/0/0	0/0/0/0	0/0/0/0	0/0/0/0	0/0/0/0
c	1MHz	0/0/0/0	0/0/0/0	0/0/0/0	0/0/0/0	0/0/0/0	0/0/0/0
c	10MHz	0/0/0/0	0/0/0/0	0/0/0/0	0/0/0/0	0/0/0/0	0/0/0/0
c	100MHz	0/0/0/0	0/0/0/0	0/0/0/0	0/0/0/0	0/0/0/0	0/0/0/0
c	200MHz	0/0/0/0	0/0/0/0	0/0/0/0	0/0/0/0	0/0/0/0	0/0/0/0
ρ	0.1MHz	0/0/0/0	0/0/0/0	0/0/0/0	0/0/0/0	0/0/0/0	0/0/0/0
ρ	1MHz	0/0/0/0	0/0/0/0	0/0/0/0	0/0/0/0	0/0/0/0	0/0/0/0
ρ	10MHz	0/0/0/0	0/0/0/0	0/0/0/0	0/0/0/0	0/0/0/0	0/0/1/1
ρ	100MHz	0/0/0/0	0/0/0/0	0/0/0/0	0/0/0/0	0/0/1/1	0/0/1/1
ρ	200MHz	0/0/0/0	0/0/0/0	0/0/0/0	0/0/0/0	0/0/1/1	0/0/2/2
η	0.1MHz	0/0/0/0	0/0/0/0	0/0/0/0	0/0/0/0	0/0/0/0	0/0/0/0
η	1MHz	0/0/0/0	0/0/0/0	0/0/1/2	0/0/0/0	0/0/0/0	2/2/20/20
η	10MHz	0/0/0/0	0/0/0/0	0/0/0/0	0/0/0/0	0/0/6/6	1/1/19/17
η	100MHz	0/0/0/0	0/0/0/0	0/0/0/0	0/0/1/1	0/0/5/5	1/1/12/11
η	200MHz	0/0/0/0	1/0/11/5	0/0/0/0	0/0/1/1	0/0/4/4	1/1/15/13
κ	0.1MHz	1/1/15/11	1/1/16/12	4/3/20/20	7/6/20/20	6/6/20/20	15/13/20/20
κ	1MHz	1/1/19/14	2/1/20/17	20/20/20/20	6/6/20/20	9/8/20/20	20/20/20/20
κ	10MHz	2/2/20/17	4/4/20/20	6/6/20/20	7/6/20/20	20/20/20/20	20/20/20/20
κ	100MHz	2/2/20/20	20/20/20/20	7/7/20/20	20/20/20/20	20/20/20/20	20/20/20/20
κ	200MHz	3/3/20/20	20/20/20/20	12/11/20/20	20/20/20/20	20/20/20/20	20/20/20/20
C_p	0.1MHz	1/1/13/13	0/0/7/6	0/0/10/8	1/1/16/11	1/1/17/12	3/2/20/20
C_p	1MHz	1/1/12/11	1/1/12/9	2/1/20/15	1/1/20/15	2/2/20/20	20/20/20/20
C_p	10MHz	1/1/11/10	2/2/20/16	2/2/20/19	3/2/20/20	20/20/20/20	20/20/20/20
C_p	100MHz	0/0/10/9	5/4/20/20	4/3/20/20	20/20/20/20	20/20/20/20	20/20/20/20
C_p	200MHz	1/1/11/9	10/7/20/20	11/8/20/20	20/20/20/20	20/20/20/20	20/20/20/20
α/f^2	0.1MHz	1/1/15/15	20/20/20/20	20/20/20/20	20/20/20/20	20/20/20/20	20/20/20/20
α/f^2	1MHz	1/1/15/15	20/20/20/20	20/20/20/20	20/20/20/20	20/20/20/20	20/20/20/20
α/f^2	10MHz	1/1/14/14	20/20/20/20	20/20/20/20	20/20/20/20	20/20/20/20	20/20/20/20
α/f^2	100MHz	1/1/13/13	20/20/20/20	20/20/20/20	20/20/20/20	12/12/20/20	20/20/20/20
α/f^2	200MHz	1/1/13/13	20/20/20/20	5/5/20/20	5/5/20/20	14/14/20/20	2/2/20/20
β	0.1MHz	0/0/6/7	0/0/6/6	1/1/10/11	1/1/11/12	1/1/11/12	2/2/20/20
β	1MHz	0/0/4/4	0/0/5/5	0/0/9/10	0/0/7/8	1/1/10/12	20/20/20/20
β	10MHz	0/0/3/3	0/0/4/5	0/0/5/5	0/0/6/6	20/20/20/20	20/20/20/20
β	100MHz	0/0/2/2	0/0/4/4	0/0/4/4	9/10/20/20	18/20/20/20	20/20/20/20
β	200MHz	0/0/1/1	0/0/3/3	0/0/4/4	4/4/20/20	11/12/20/20	20/20/20/20

Table D2.19 10% v/v aqueous metallic iron - dispersed phase at 25ºC (permissible + & - % variation in input property for 0.01% and 0.1% variation in output attenuation)

property	frequency	10nm	100nm	1μm	10μm	100μm	1mm
c'	0.1MHz	0/0/2/2	8/5/20/20	6/4/20/20	4/3/20/17	4/3/20/17	0/0/2/2
c'	1MHz	0/0/8/5	20/11/20/20	12/7/20/20	10/6/20/20	1/1/16/9	1/1/19/9
c'	10MHz	1/1/19/10	20/18/20/20	20/13/20/20	6/5/20/20	2/2/20/17	0/0/0/0
c'	100MHz	2/2/20/15	20/20/20/20	20/20/20/20	6/5/20/20	0/0/0/0	0/0/3/2
c'	200MHz	3/3/20/20	20/20/20/20	20/19/20/20	11/8/20/20	0/0/7/4	0/0/2/5
ρ'	0.1MHz	0/0/0/0	0/0/0/0	0/0/0/0	0/0/0/0	0/0/0/0	0/0/0/0
ρ'	1MHz	0/0/0/0	0/0/0/0	0/0/0/0	0/0/0/0	0/0/0/0	1/1/20/13
ρ'	10MHz	0/0/0/0	0/0/0/0	0/0/0/0	0/0/0/0	5/3/20/20	0/0/0/0
ρ'	100MHz	0/0/0/0	0/0/0/0	0/0/0/0	3/4/20/20	0/0/0/0	0/0/0/0
ρ'	200MHz	0/0/0/0	0/0/0/0	0/0/0/0	0/0/0/0	0/0/0/0	0/0/0/0
μ'	0.1MHz	0/0/5/6	20/20/20/20	19/20/20/20	14/19/20/20	14/18/20/20	1/1/10/13
μ'	1MHz	0/0/2/3	20/20/20/20	10/13/20/20	9/11/20/20	1/1/12/17	0/0/3/3
μ'	10MHz	0/0/1/1	20/20/20/20	8/10/20/20	6/5/20/20	0/0/2/3	0/0/1/0
μ'	100MHz	0/0/0/0	0/0/3/5	0/0/1/1	0/0/1/2	0/0/1/1	0/0/0/0
μ'	200MHz	0/0/0/0	0/0/0/0	0/0/0/0	0/0/0/0	0/0/0/3	0/0/1/0
κ'	0.1MHz	20/20/20/20	20/20/20/20	20/20/20/20	20/20/20/20	20/20/20/20	20/20/20/20
κ'	1MHz	20/20/20/20	20/20/20/20	20/20/20/20	20/20/20/20	20/20/20/20	20/20/20/20
κ'	10MHz	20/20/20/20	20/20/20/20	20/20/20/20	20/20/20/20	20/20/20/20	20/20/20/20
κ'	100MHz	20/20/20/20	20/20/20/20	20/20/20/20	20/20/20/20	20/20/20/20	20/20/20/20
κ'	200MHz	20/20/20/20	20/20/20/20	20/20/20/20	20/20/20/20	20/20/20/20	20/20/20/20
C_p'	0.1MHz	1/1/13/13	4/4/20/20	7/7/20/20	6/5/20/20	8/7/20/20	17/13/20/20
C_p'	1MHz	1/1/10/10	3/3/20/20	6/6/20/20	8/7/20/20	12/10/20/20	20/20/20/20
C_p'	10MHz	0/0/7/8	3/3/20/20	6/6/20/20	12/10/20/20	20/20/20/20	20/20/20/20
C_p'	100MHz	0/0/6/6	4/4/20/20	11/9/20/20	20/20/20/20	20/20/20/20	20/20/20/20
C_p'	200MHz	0/0/4/5	5/4/20/20	19/14/20/20	20/20/20/20	20/20/20/20	20/20/20/20
α'/f^2	0.1MHz	0/0/9/9	20/20/20/20	20/20/20/20	20/20/20/20	20/20/20/20	20/20/20/20
α'/f^2	1MHz	0/0/7/7	20/20/20/20	20/20/20/20	20/20/20/20	20/20/20/20	20/20/20/20
α'/f^2	10MHz	0/0/6/6	20/20/20/20	20/20/20/20	11/11/20/20	20/20/20/20	20/20/20/20
α'/f^2	100MHz	0/0/5/5	7/7/20/20	2/2/20/20	9/9/20/20	5/5/20/20	20/20/20/20
α'/f^2	200MHz	0/0/4/4	2/2/20/20	1/1/10/10	3/3/20/20	1/1/14/13	20/19/20/20
β'	0.1MHz	0/0/10/8	20/20/20/20	20/20/20/20	13/13/20/20	8/8/20/20	16/16/20/20
β'	1MHz	1/1/13/10	20/20/20/20	20/20/20/20	8/8/20/20	10/9/20/20	20/20/20/20
β'	10MHz	1/1/18/12	20/20/20/20	10/9/20/20	7/7/20/20	20/20/20/20	20/20/20/20
β'	100MHz	1/1/20/14	14/12/20/20	6/5/20/20	20/20/20/20	20/20/20/20	20/20/20/20
β'	200MHz	2/2/20/18	9/8/20/20	8/7/20/20	20/20/20/20	20/20/20/20	20/20/20/20

Table D2.20 10% v/v aqueous metallic iron - continuous phase at 25ºC (permissible + & - % variation in input property for 0.01% and 0.1% variation in output attenuation)

property	frequency	10nm	100nm	1μm	10μm	100μm	1mm
c	0.1MHz	0/0/0/0	0/0/0/0	0/0/0/0	0/0/0/0	0/0/0/0	0/0/0/0
c	1MHz	0/0/0/0	0/0/0/0	0/0/0/0	0/0/0/0	0/0/0/0	0/0/0/0
c	10MHz	0/0/0/0	0/0/0/0	0/0/0/0	0/0/0/0	0/0/0/0	0/0/0/0
c	100MHz	0/0/0/0	0/0/0/0	0/0/0/0	0/0/0/0	0/0/0/0	0/0/0/0
c	200MHz	0/0/0/0	0/0/0/0	0/0/0/0	0/0/0/0	0/0/0/0	0/0/0/0
ρ	0.1MHz	0/0/0/0	0/0/0/0	0/0/0/0	0/0/0/0	0/0/0/0	0/0/0/0
ρ	1MHz	0/0/0/0	0/0/0/0	0/0/0/0	0/0/0/0	0/0/0/0	0/0/2/2
ρ	10MHz	0/0/0/0	0/0/0/0	0/0/0/0	0/0/0/0	0/0/2/2	2/3/11/20
ρ	100MHz	0/0/0/0	0/0/0/0	0/0/0/0	0/0/2/2	0/0/5/11	0/0/2/2
ρ	200MHz	0/0/0/0	0/0/0/0	0/0/0/0	0/0/5/4	0/0/4/4	0/0/2/2
η	0.1MHz	0/0/0/0	0/0/0/0	0/0/0/0	0/0/0/0	0/0/0/0	0/0/0/0
η	1MHz	0/0/0/0	0/0/0/0	0/0/0/0	0/0/0/0	0/0/0/0	2/2/20/19
η	10MHz	0/0/0/0	0/0/0/0	0/0/0/0	0/0/0/0	0/0/6/6	1/1/17/16
η	100MHz	0/0/0/0	0/0/17/2	0/0/0/0	0/0/1/1	0/0/5/5	1/1/12/11
η	200MHz	0/0/0/0	0/0/0/0	0/0/0/0	0/0/1/1	0/0/4/4	1/1/12/11
κ	0.1MHz	11/9/20/20	11/9/20/20	20/20/20/20	20/17/20/20	8/8/20/20	16/15/20/20
κ	1MHz	14/11/20/20	17/13/20/20	20/20/20/20	9/8/20/20	10/9/20/20	20/20/20/20
κ	10MHz	19/14/20/20	20/20/20/20	20/16/20/20	8/7/20/20	20/20/20/20	20/20/20/20
κ	100MHz	20/19/20/20	20/20/20/20	7/6/20/20	20/20/20/20	20/20/20/20	20/20/20/20
κ	200MHz	20/20/20/20	20/20/20/20	7/7/20/20	20/20/20/20	20/20/20/20	20/20/20/20
C_p	0.1MHz	1/1/17/12	5/4/20/20	7/6/20/20	2/2/20/18	1/1/20/15	3/3/20/20
C_p	1MHz	1/1/20/14	9/7/20/20	8/6/20/20	2/2/20/20	3/3/20/20	20/20/20/20
C_p	10MHz	2/2/20/17	20/12/20/20	5/4/20/20	4/3/20/20	20/20/20/20	20/20/20/20
C_p	100MHz	2/2/20/20	18/11/20/20	5/4/20/20	20/20/20/20	20/20/20/20	20/20/20/20
C_p	200MHz	3/2/20/20	15/10/20/20	9/7/20/20	20/20/20/20	20/20/20/20	20/20/20/20
α/f^2	0.1MHz	0/0/6/6	20/20/20/20	20/20/20/20	20/20/20/20	20/20/20/20	20/20/20/20
α/f^2	1MHz	0/0/6/6	20/20/20/20	20/20/20/20	20/20/20/20	20/20/20/20	20/20/20/20
α/f^2	10MHz	0/0/6/6	20/20/20/20	20/20/20/20	20/20/20/20	20/20/20/20	20/20/20/20
α/f^2	100MHz	0/0/6/6	19/19/20/20	10/10/20/20	20/20/20/20	9/9/20/20	20/20/20/20
α/f^2	200MHz	0/0/5/5	12/12/20/20	3/3/20/20	13/13/20/20	4/4/20/20	4/4/20/20
β	0.1MHz	0/0/8/9	4/5/20/20	7/8/20/20	2/2/20/20	1/1/14/17	2/3/20/20
β	1MHz	0/0/6/7	3/3/20/20	3/3/20/20	1/1/10/12	1/1/12/15	20/20/20/20
β	10MHz	0/0/5/5	3/3/20/20	1/1/9/11	0/0/7/8	20/20/20/20	20/20/20/20
β	100MHz	0/0/4/4	1/1/13/14	0/0/5/5	7/8/20/20	14/17/20/20	20/20/20/20
β	200MHz	0/0/3/3	0/0/6/7	0/0/4/4	4/4/20/20	10/11/20/20	20/20/20/20

D3 Key to tables in Appendix D3

The tables that follow are an abbreviated version of the tables upon which the analysis in Appendix D1 and the tables of Appendix D2 are based. Nevertheless, they provide a detailed insight into the behaviour of the ECAH model when its input physical property values are varied from a central value. Each table is labelled simply with the name of the material that constitutes the dispersed phase in a 10% v/v concentration aqueous dispersion at a temperature of 25ºC. The name of the dispersed phase material is followed by the name of the physical property being varied, using the following convention:

Compression wavespeed	***c***
Mass density	***rho***
Shear modulus	***mu***
Thermal conductivity	***kappa***
Specific heat capacity at constant pressure	***Cp***
Compression wave attenuation (α / f^2)	***alpha***
Coefficient of thermal expansion	***beta***
Shear viscosity	***eta***

Following the usual convention, primed variables denote properties of the dispersed phase and unprimed variables denote properties of the continuous phase. In the column headings:

MHz denotes frequency in megahertz

% denotes percentage variation of the physical property in question

c 10nm (etc up to **1mm**) denotes phase velocity variation for a 10nm diameter particle

a 10nm (etc up to **1mm**) denotes attenuation (in terms of alpha) variation for a 10nm diameter particle

Table D3.1 aqueous polystyrene: effect of change in *c'*

MHz	%	c 10nm	c 100nm	c 1um	c 10um	c 100um	c 1mm	a 10nm	a 100nm	a 1um	a 10um	a 100um	a 1mm
0.1	-20	-1.54E+00	-1.54E+00	-1.54E+00	-1.48E+00	-1.47E+00	-1.51E+00	6.07E-01	1.35E-02	-3.01E-02	-2.25E-02	-7.37E-03	-7.44E-01
0.1	-10	-5.61E-01	-5.61E-01	-5.60E-01	-5.37E-01	-5.33E-01	-5.44E-01	1.90E-01	2.60E-03	-1.11E-02	-8.00E-03	-3.87E-03	-5.86E-01
0.1	-5	-2.46E-01	-2.46E-01	-2.46E-01	-2.36E-01	-2.34E-01	-2.38E-01	7.94E-02	8.39E-04	-4.90E-03	-3.48E-03	-1.84E-03	-2.99E-01
0.1	5	1.97E-01	1.97E-01	1.97E-01	1.89E-01	1.87E-01	1.90E-01	-5.94E-02	-3.51E-04	3.95E-03	2.74E-03	1.62E-03	2.84E-01
0.1	10	3.58E-01	3.58E-01	3.57E-01	3.43E-01	3.40E-01	3.45E-01	-1.05E-01	-4.37E-04	7.20E-03	4.95E-03	3.03E-03	5.44E-01
0.1	20	6.03E-01	6.03E-01	6.02E-01	5.77E-01	5.73E-01	5.81E-01	-1.71E-01	-2.52E-04	1.22E-02	8.24E-03	5.31E-03	9.89E-01
1	-20	-4.96E-01	-4.96E-01	-4.88E-01	-4.81E-01	-4.85E-01	-6.28E+00	2.82E-01	2.34E-03	-1.01E-02	1.18E-02	-5.02E-01	7.88E-02
1	-10	-1.91E-01	-1.91E-01	-1.87E-01	-1.85E-01	-1.86E-01	-1.86E+00	1.01E-01	3.58E-04	-3.87E-03	4.08E-03	-2.24E-01	2.00E-01
1	-5	-8.53E-02	-8.53E-02	-8.38E-02	-8.27E-02	-8.31E-02	-6.38E-01	4.39E-02	8.46E-05	-1.73E-03	1.77E-03	-1.05E-01	1.03E-01
1	5	7.02E-02	7.02E-02	6.90E-02	6.80E-02	6.82E-02	3.11E-01	-3.50E-02	1.25E-05	1.41E-03	-1.40E-03	9.18E-02	-8.75E-02
1	10	1.29E-01	1.29E-01	1.26E-01	1.25E-01	1.25E-01	4.51E-01	-6.36E-02	7.21E-05	2.59E-03	-2.55E-03	1.72E-01	-1.57E-01
1	20	2.20E-01	2.20E-01	2.16E-01	2.14E-01	2.14E-01	5.06E-01	-1.08E-01	2.35E-04	4.41E-03	-4.32E-03	3.05E-01	-2.56E-01
10	-20	-2.35E-01	-2.35E-01	-2.30E-01	-2.30E-01	-1.17E+00	-5.44E-01	1.60E-01	4.32E-03	3.40E-02	-1.68E-01	3.71E-01	-3.17E-02
10	-10	-9.33E-02	-9.31E-02	-9.12E-02	-9.10E-02	-2.16E-01	-1.90E-02	6.16E-02	1.56E-03	1.32E-02	-7.18E-02	1.47E-01	-7.50E-02
10	-5	-4.21E-02	-4.21E-02	-4.12E-02	-4.11E-02	-6.58E-02	2.30E-01	2.77E-02	6.90E-04	5.96E-03	-3.33E-02	6.43E-02	-3.44E-02
10	5	3.52E-02	3.52E-02	3.44E-02	3.43E-02	2.25E-02	-4.91E-01	-2.30E-02	-5.66E-04	-4.99E-03	2.88E-02	-5.04E-02	-6.93E-03
10	10	6.50E-02	6.49E-02	6.36E-02	6.33E-02	2.25E-02	-6.19E-01	-4.25E-02	-1.04E-03	-9.23E-03	5.39E-02	-9.04E-02	-3.22E-02
10	20	1.12E-01	1.12E-01	1.10E-01	1.09E-01	-5.74E-03	-2.20E-01	-7.38E-02	-1.83E-03	-1.61E-02	9.49E-02	-1.49E-01	-6.93E-02
100	-20	-1.31E-01	-1.29E-01	-1.28E-01	-7.86E+00	3.85E-01	5.89E-03	1.05E-01	6.46E-02	3.73E-02	1.48E-01	4.28E-02	-2.66E-03
100	-10	-5.27E-02	-5.22E-02	-5.16E-02	-2.34E+00	-3.15E-01	9.69E-02	4.27E-02	2.63E-02	1.45E-02	5.98E-02	4.69E-02	1.60E-03
100	-5	-2.40E-02	-2.37E-02	-2.35E-02	-9.37E-01	-3.19E-01	2.21E-01	1.95E-02	1.20E-02	6.58E-03	2.70E-02	1.32E-02	3.49E-03
100	5	2.02E-02	2.00E-02	1.98E-02	6.41E-01	1.58E-01	1.90E-01	-1.67E-02	-1.03E-02	-5.61E-03	-2.24E-02	1.38E-02	3.24E-03
100	10	3.75E-02	3.71E-02	3.66E-02	1.09E+00	2.36E-01	5.09E-02	-3.13E-02	-1.93E-02	-1.05E-02	-4.11E-02	2.65E-02	3.67E-03
100	20	6.52E-02	6.45E-02	6.37E-02	1.63E+00	3.63E-02	6.26E-02	-5.53E-02	-3.41E-02	-1.87E-02	-7.04E-02	5.01E-02	-8.71E-04
200	-20	-7.89E-02	-7.80E-02	-7.77E-02	-4.38E-04	6.92E-02	-6.19E-02	7.63E-02	9.47E-02	-4.07E-02	-2.30E-02	-1.58E-03	8.36E-04
200	-10	-3.22E-02	-3.18E-02	-3.16E-02	-4.97E-04	-8.44E-02	-2.06E-02	3.20E-02	3.97E-02	-1.68E-02	-1.02E-02	1.39E-03	8.07E-04
200	-5	-1.47E-02	-1.45E-02	-1.44E-02	-2.73E-04	-5.55E-02	-6.45E-03	1.48E-02	1.84E-02	-7.69E-03	-4.80E-03	-6.52E-03	4.16E-04
200	5	1.25E-02	1.23E-02	1.22E-02	2.88E-04	-2.09E-02	2.58E-03	-1.30E-02	-1.60E-02	6.51E-03	4.27E-03	-2.17E-03	-1.80E-04
200	10	2.32E-02	2.29E-02	2.27E-02	5.72E-04	2.18E-02	1.94E-02	-2.44E-02	-3.01E-02	1.20E-02	8.07E-03	-2.79E-03	-4.78E-04
200	20	4.05E-02	4.00E-02	3.96E-02	1.10E-03	-9.56E-03	3.87E-02	-4.37E-02	-5.39E-02	2.08E-02	1.45E-02	4.33E-03	-8.43E-04

Table D3.2 aqueous polystyrene: effect of change in *rho'*

MHz	%	c 10nm	c 100nm	c 1um	c 10um	c 100um	c 1mm	a 10nm	a 100nm	a 1um	a 10um	a 100um	a 1mm
0.1	-20	-4.91E-02	-4.91E-02	-4.84E-02	-6.92E-03	1.49E-02	1.88E-02	1.75E-01	3.49E-01	3.96E-01	2.00E+00	2.94E+00	-4.14E-01
0.1	-10	2.75E-02	2.75E-02	2.75E-02	3.40E-02	3.51E-02	3.68E-02	5.96E-02	7.71E-02	9.08E-02	1.95E-01	1.67E-01	-2.90E-01
0.1	-5	2.38E-02	2.38E-02	2.37E-02	2.37E-02	2.22E-02	2.30E-02	2.37E-02	1.42E-02	1.85E-02	-8.04E-02	-1.80E-01	-1.59E-01
0.1	5	-3.99E-02	-3.99E-02	-3.97E-02	-3.35E-02	-2.86E-02	-2.92E-02	-1.27E-02	3.44E-02	3.51E-02	3.95E-01	6.11E-01	1.79E-01
0.1	10	-9.29E-02	-9.29E-02	-9.22E-02	-7.43E-02	-6.17E-02	-6.27E-02	-1.53E-02	1.17E-01	1.24E-01	1.07E+00	1.57E+00	3.71E-01
0.1	20	-2.29E-01	-2.29E-01	-2.27E-01	-1.70E-01	-1.35E-01	-1.37E-01	7.30E-03	4.28E-01	4.60E-01	3.12E+00	4.30E+00	7.82E-01
1	-20	3.23E-01	3.23E-01	2.94E-01	1.91E-01	1.82E-01	-7.85E-01	1.11E-02	-2.96E-01	-4.79E-01	-8.24E-01	-5.12E-01	2.68E+00
1	-10	2.05E-01	2.05E-01	1.83E-01	1.10E-01	1.03E-01	1.79E-01	-2.23E-02	-2.46E-01	-4.03E-01	-5.86E-01	-3.06E-01	1.44E+00
1	-5	1.11E-01	1.11E-01	9.81E-02	5.70E-02	5.30E-02	1.51E-01	-1.76E-02	-1.47E-01	-2.40E-01	-3.27E-01	-1.62E-01	5.34E-01
1	5	-1.25E-01	-1.25E-01	-1.08E-01	-5.95E-02	-5.47E-02	-1.49E-01	2.98E-02	1.96E-01	3.14E-01	3.82E-01	1.75E-01	-2.92E-01
1	10	-2.60E-01	-2.60E-01	-2.24E-01	-1.20E-01	-1.10E-01	-2.73E-01	7.13E-02	4.39E-01	6.97E-01	8.06E-01	3.59E-01	-4.57E-01
1	20	-5.56E-01	-5.56E-01	-4.71E-01	-2.41E-01	-2.19E-01	-4.55E-01	1.88E-01	1.07E+00	1.66E+00	1.75E+00	7.44E-01	-6.16E-01
10	-20	1.46E+00	1.41E+00	5.47E-01	3.51E-01	1.00E+00	1.20E+00	-1.68E-01	-5.74E-01	-7.31E-01	-5.31E-01	2.50E+00	-2.07E-02
10	-10	7.92E-01	7.66E-01	2.82E-01	1.76E-01	4.07E-01	3.04E+00	-1.11E-01	-3.54E-01	-4.17E-01	-2.89E-01	5.51E-01	6.09E-02
10	-5	4.08E-01	3.95E-01	1.42E-01	8.77E-02	1.81E-01	2.46E+00	-6.23E-02	-1.93E-01	-2.19E-01	-1.48E-01	1.99E-01	1.21E-01
10	5	-4.27E-01	-4.12E-01	-1.41E-01	-8.58E-02	-1.52E-01	2.64E+00	7.50E-02	2.26E-01	2.36E-01	1.53E-01	-1.20E-01	-2.91E-02
10	10	-8.69E-01	-8.39E-01	-2.81E-01	-1.69E-01	-2.94E-01	4.01E+00	1.62E-01	4.84E-01	4.87E-01	3.10E-01	-1.95E-01	1.41E-01
10	20	-1.78E+00	-1.72E+00	-5.53E-01	-3.27E-01	-1.07E-01	2.16E+00	3.73E-01	1.09E+00	1.02E+00	6.26E-01	1.26E+00	2.34E-03
100	-20	-2.70E+00	-7.40E+00	7.56E-01	4.77E-01	4.96E-01	2.23E-02	-2.98E-01	-6.00E-01	-4.42E-01	-2.21E-01	-1.15E-03	-3.49E-03
100	-10	-1.40E+00	-3.76E+00	3.66E-01	-1.17E-03	-4.33E-01	1.91E-01	-1.74E-01	-3.37E-01	-2.29E-01	-4.27E-01	9.13E-02	1.82E-03
100	-5	-7.07E-01	-1.88E+00	1.79E-01	-2.70E-01	-8.27E-03	9.80E-02	-9.30E-02	-1.77E-01	-1.16E-01	-3.89E-01	-8.30E-03	4.98E-03
100	5	7.20E-01	1.88E+00	-1.72E-01	-1.76E-01	-1.72E-02	1.00E+00	1.05E-01	1.92E-01	1.17E-01	-4.10E-01	5.52E-02	7.02E-03
100	10	1.45E+00	3.74E+00	-3.36E-01	-3.14E-01	4.17E-01	5.48E-01	2.21E-01	3.98E-01	2.34E-01	-4.63E-01	-1.01E-01	6.09E-03
100	20	2.92E+00	7.40E+00	-6.42E-01	-5.06E-01	3.72E-01	-1.04E+00	4.88E-01	8.47E-01	4.65E-01	-4.80E-01	1.29E-01	-4.82E-03
200	-20	-8.90E-01	-1.27E+00	4.33E+00	-1.98E-02	-8.21E-03	-1.95E-01	-3.72E-01	-5.05E-01	-2.68E-01	-5.26E-01	5.13E-02	-6.83E-04
200	-10	-4.50E-01	-6.18E-01	2.04E+00	-5.55E-01	-8.06E-01	-2.01E-01	-2.08E-01	-2.68E-01	-1.33E-01	-3.78E-01	8.49E-02	8.88E-03
200	-5	-2.26E-01	-3.05E-01	9.92E-01	-7.76E-01	-3.79E-01	-7.21E-01	-1.09E-01	-1.37E-01	-6.57E-02	-1.94E-01	-2.69E-02	-8.27E-03
200	5	2.26E-01	2.95E-01	-9.35E-01	3.09E-01	-8.41E-01	-5.81E-01	1.20E-01	1.42E-01	6.42E-02	-3.10E-01	4.45E-02	-1.17E-02
200	10	4.53E-01	5.80E-01	-1.82E+00	3.63E-02	1.12E-01	-6.17E-01	2.50E-01	2.89E-01	1.27E-01	-4.47E-01	3.54E-02	-6.67E-03
200	20	9.03E-01	1.12E+00	-3.43E+00	-4.03E-01	-8.71E-01	-4.58E-01	5.40E-01	5.91E-01	2.46E-01	-5.05E-01	-5.46E-02	4.01E-03

Table D3.3 aqueous polystyrene: effect of change in *mu'*

MHz	%	c 10nm	c 100nm	c 1um	c 10um	c 100um	c 1mm	a 10nm	a 100nm	a 1um	a 10um	a 100um	a 1mm
0.1	-20	1.20E-01	1.20E-01	1.20E-01	1.15E-01	1.14E-01	1.16E-01	-8.30E-02	-5.07E-03	9.83E-04	4.40E-03	2.57E-03	1.69E-01
0.1	-10	6.23E-02	6.23E-02	6.22E-02	5.97E-02	5.93E-02	6.02E-02	-4.40E-02	-2.63E-03	5.70E-04	2.16E-03	1.18E-03	8.57E-02
0.1	-5	3.18E-02	3.18E-02	3.17E-02	3.04E-02	3.02E-02	3.07E-02	-2.27E-02	-1.34E-03	3.05E-04	1.07E-03	5.60E-04	4.32E-02
0.1	5	-3.31E-02	-3.31E-02	-3.30E-02	-3.17E-02	-3.15E-02	-3.20E-02	2.42E-02	1.40E-03	-3.47E-04	-1.05E-03	-5.01E-04	-4.38E-02
0.1	10	-6.76E-02	-6.76E-02	-6.74E-02	-6.47E-02	-6.43E-02	-6.53E-02	4.99E-02	2.87E-03	-7.37E-04	-2.08E-03	-9.41E-04	-8.82E-02
0.1	20	-1.41E-01	-1.41E-01	-1.41E-01	-1.35E-01	-1.34E-01	-1.36E-01	1.07E-01	6.04E-03	-1.65E-03	-4.08E-03	-1.63E-03	-1.79E-01
1	-20	1.94E-01	1.94E-01	1.88E-01	1.83E-01	1.87E-01	-3.48E+01	-1.13E-01	-7.79E-03	2.90E-03	-6.44E-03	1.59E-01	1.81E+00
1	-10	1.02E-01	1.02E-01	9.86E-02	9.62E-02	9.81E-02	7.55E+00	-6.10E-02	-4.13E-03	1.41E-03	-3.71E-03	8.05E-02	1.30E+00
1	-5	5.22E-02	5.22E-02	5.06E-02	4.94E-02	5.03E-02	3.63E+00	-3.17E-02	-2.13E-03	6.93E-04	-1.99E-03	4.04E-02	3.35E-01
1	5	-5.50E-02	-5.50E-02	-5.33E-02	-5.20E-02	-5.31E-02	-2.61E+00	3.45E-02	2.29E-03	-6.70E-04	2.28E-03	-4.06E-02	-1.29E-01
1	10	-1.13E-01	-1.13E-01	-1.10E-01	-1.07E-01	-1.09E-01	-4.55E+00	7.20E-02	4.76E-03	-1.32E-03	4.88E-03	-8.11E-02	-1.73E-01
1	20	-2.40E-01	-2.40E-01	-2.32E-01	-2.26E-01	-2.31E-01	-7.21E+00	1.58E-01	1.04E-02	-2.54E-03	1.12E-02	-1.61E-01	-1.46E-01
10	-20	3.70E-01	3.69E-01	3.47E-01	3.55E-01	-1.61E+00	-5.82E+00	-1.59E-01	-1.81E-02	-4.86E-02	-1.68E-03	5.13E-01	5.38E-01
10	-10	1.97E-01	1.97E-01	1.85E-01	1.89E-01	-5.51E-01	-9.51E-01	-8.76E-02	-9.96E-03	-2.70E-02	-5.22E-03	-2.07E-03	5.99E-01
10	-5	1.02E-01	1.02E-01	9.56E-02	9.78E-02	-2.36E-01	1.80E+00	-4.61E-02	-5.24E-03	-1.43E-02	-3.93E-03	-2.72E-02	4.36E-01
10	5	-1.10E-01	-1.09E-01	-1.03E-01	-1.05E-01	1.78E-01	-6.86E+00	5.15E-02	5.85E-03	1.61E-02	7.15E-03	6.00E-02	-1.75E-01
10	10	-2.27E-01	-2.27E-01	-2.13E-01	-2.18E-01	3.07E-01	-1.50E+01	1.09E-01	1.24E-02	3.43E-02	1.82E-02	1.44E-01	-1.85E-01
10	20	-4.92E-01	-4.90E-01	-4.61E-01	-4.73E-01	4.28E-01	-2.05E+01	2.48E-01	2.83E-02	7.84E-02	5.61E-02	3.59E-01	6.20E-01
100	-20	1.13E+00	1.07E+00	1.07E+00	-4.33E-01	-1.17E+00	2.49E-01	-2.31E-01	-1.73E-01	-2.23E-01	-2.35E-01	-1.48E-01	-3.76E-02
100	-10	6.17E-01	5.82E-01	5.82E-01	-1.15E-01	-5.08E-01	-3.78E-01	-1.32E-01	-9.89E-02	-1.29E-01	-1.65E-01	-5.07E-01	-4.28E-02
100	-5	3.23E-01	3.05E-01	3.05E-01	-3.36E-02	-3.57E-02	-3.52E-01	-7.07E-02	-5.31E-02	-6.95E-02	-9.07E-02	-3.19E-01	-4.19E-02
100	5	-3.56E-01	-3.36E-01	-3.37E-01	-1.50E-02	-1.70E-01	-2.77E+00	8.26E-02	6.21E-02	8.24E-02	1.01E-01	2.60E-01	-5.73E-01
100	10	-7.51E-01	-7.09E-01	-7.11E-01	-7.91E-02	-5.68E-01	-3.85E-01	1.80E-01	1.35E-01	1.81E-01	2.08E-01	3.35E-01	-4.45E-01
100	20	-1.69E+00	-1.59E+00	-1.60E+00	-3.49E-01	-9.71E-01	-3.08E-01	4.35E-01	3.27E-01	4.45E-01	4.27E-01	3.38E-02	-3.92E-02
200	-20	-2.82E+00	-3.12E+00	-2.13E+00	-5.16E-03	-8.81E-01	6.92E-01	-3.45E-01	-3.51E-01	-3.26E-01	-2.15E-01	-2.88E-01	8.52E-03
200	-10	-1.59E+00	-1.76E+00	-1.21E+00	3.93E-02	5.31E-01	-4.37E+01	-2.07E-01	-2.11E-01	-2.06E-01	-9.14E-02	1.22E+00	4.01E-01
200	-5	-8.49E-01	-9.40E-01	-6.49E-01	2.82E-02	-2.94E+00	-7.73E-01	-1.15E-01	-1.17E-01	-1.17E-01	-3.88E-02	5.37E-01	-8.50E-03
200	5	9.85E-01	1.09E+00	7.60E-01	-4.19E-02	1.96E+00	1.57E+00	1.45E-01	1.48E-01	1.58E-01	2.23E-02	4.90E-01	-2.37E-03
200	10	2.14E+00	2.37E+00	1.66E+00	-9.70E-02	3.31E-01	3.44E-01	3.33E-01	3.40E-01	3.76E-01	2.94E-02	8.49E-01	3.42E-02
200	20	5.17E+00	5.74E+00	4.08E+00	-2.37E-01	-6.57E-01	1.70E+00	9.18E-01	9.39E-01	1.13E+00	3.61E-02	3.42E-01	3.93E-02

Table D3.4 aqueous polystyrene: effect of change in *kappa'*

MHz	%	c 10nm	c 100nm	c 1um	c 10um	c 100um	c 1mm	a 10nm	a 100nm	a 1um	a 10um	a 100um	a 1mm
0.1	-20	0.00E+00	0.00E+00	5.99E-04	5.47E-04	5.35E-05	5.50E-06	1.71E-02	1.20E-01	1.45E-01	-6.61E-02	-5.92E-02	-2.80E-03
0.1	-10	0.00E+00	0.00E+00	2.56E-04	2.63E-04	2.56E-05	2.75E-06	7.62E-03	5.35E-02	6.56E-02	-3.17E-02	-2.84E-02	-1.35E-03
0.1	-5	0.00E+00	0.00E+00	1.19E-04	1.29E-04	1.26E-05	1.37E-06	3.61E-03	2.53E-02	3.13E-02	-1.55E-02	-1.40E-02	-6.62E-04
0.1	5	0.00E+00	-3.51E-07	-1.05E-04	-1.25E-04	-1.23E-05	-1.03E-06	-3.27E-03	-2.29E-02	-2.86E-02	1.49E-02	1.35E-02	6.39E-04
0.1	10	0.00E+00	-3.51E-07	-1.97E-04	-2.46E-04	-2.43E-05	-2.40E-06	-6.23E-03	-4.38E-02	-5.49E-02	2.94E-02	2.65E-02	1.26E-03
0.1	20	0.00E+00	-3.51E-07	-3.52E-04	-4.77E-04	-4.69E-05	-4.47E-06	-1.14E-02	-8.02E-02	-1.01E-01	5.67E-02	5.14E-02	2.44E-03
1	-20	0.00E+00	5.61E-06	2.24E-03	1.80E-04	1.82E-05	-1.27E-05	1.45E-02	1.18E-01	-4.65E-02	-5.85E-02	-6.53E-03	8.61E-06
1	-10	0.00E+00	2.45E-06	1.09E-03	8.66E-05	8.60E-06	-6.01E-06	6.43E-03	5.23E-02	-2.05E-02	-2.81E-02	-3.14E-03	4.14E-06
1	-5	0.00E+00	1.05E-06	5.37E-04	4.26E-05	4.13E-06	-2.94E-06	3.05E-03	2.48E-02	-9.60E-03	-1.38E-02	-1.54E-03	2.03E-06
1	5	0.00E+00	-1.05E-06	-5.21E-04	-4.10E-05	-4.47E-06	2.94E-06	-2.76E-03	-2.24E-02	8.37E-03	1.33E-02	1.49E-03	-1.96E-06
1	10	0.00E+00	-1.75E-06	-1.03E-03	-8.09E-05	-8.25E-06	5.73E-06	-5.26E-03	-4.28E-02	1.56E-02	2.61E-02	2.92E-03	-3.85E-06
1	20	0.00E+00	-3.51E-06	-1.99E-03	-1.57E-04	-1.62E-05	1.10E-05	-9.64E-03	-7.85E-02	2.69E-02	5.05E-02	5.66E-03	-7.46E-06
10	-20	0.00E+00	3.16E-04	6.23E-04	6.27E-05	-2.86E-05	1.48E-05	1.22E-02	1.20E-01	-5.26E-02	-9.23E-03	2.73E-05	-6.09E-06
10	-10	0.00E+00	1.35E-04	2.99E-04	3.00E-05	-1.37E-05	0.00E+00	5.43E-03	5.39E-02	-2.51E-02	-4.43E-03	1.31E-05	-2.92E-06
10	-5	0.00E+00	6.30E-05	1.47E-04	1.48E-05	-6.78E-06	0.00E+00	2.57E-03	2.56E-02	-1.23E-02	-2.17E-03	6.42E-06	-1.43E-06
10	5	0.00E+00	-5.49E-05	-1.42E-04	-1.41E-05	6.39E-06	0.00E+00	-2.33E-03	-2.33E-02	1.18E-02	2.09E-03	-6.19E-06	1.38E-06
10	10	3.51E-07	-1.03E-04	-2.79E-04	-2.79E-05	1.27E-05	-1.48E-05	-4.44E-03	-4.46E-02	2.32E-02	4.12E-03	-1.22E-05	2.72E-06
10	20	3.51E-07	-1.85E-04	-5.40E-04	-5.41E-05	2.46E-05	-1.48E-05	-8.14E-03	-8.21E-02	4.47E-02	7.97E-03	-2.36E-05	5.26E-06
100	-20	-1.23E-05	2.61E-03	2.42E-04	-4.53E-05	-2.44E-05	0.00E+00	1.04E-02	4.76E-03	-5.82E-03	7.20E-05	-3.76E-06	2.00E-07
100	-10	-5.61E-06	1.23E-03	1.16E-04	-2.17E-05	-1.22E-05	0.00E+00	4.61E-03	3.93E-03	-2.79E-03	3.45E-05	-1.80E-06	9.59E-08
100	-5	-2.81E-06	6.00E-04	5.69E-05	-1.06E-05	-1.22E-05	0.00E+00	2.19E-03	2.30E-03	-1.37E-03	1.69E-05	-8.84E-07	4.71E-08
100	5	2.45E-06	-5.66E-04	-5.45E-05	1.03E-05	0.00E+00	0.00E+00	-1.98E-03	-2.86E-03	1.31E-03	-1.63E-05	8.51E-07	-4.53E-08
100	10	4.56E-06	-1.10E-03	-1.08E-04	2.02E-05	1.22E-05	0.00E+00	-3.77E-03	-6.19E-03	2.58E-03	-3.21E-05	1.67E-06	-8.90E-08
100	20	8.42E-06	-2.08E-03	-2.08E-04	3.90E-05	1.22E-05	0.00E+00	-6.92E-03	-1.40E-02	4.99E-03	-6.21E-05	3.24E-06	-1.72E-07
200	-20	-4.28E-05	2.13E-03	2.30E-04	9.47E-06	0.00E+00	0.00E+00	8.85E-03	-4.69E-03	-1.30E-03	4.96E-06	-4.59E-07	3.97E-08
200	-10	-1.89E-05	1.02E-03	1.10E-04	4.59E-06	0.00E+00	0.00E+00	3.93E-03	-1.71E-03	-6.23E-04	2.37E-06	-2.20E-07	1.90E-08
200	-5	-9.12E-06	5.04E-04	5.37E-05	2.29E-06	0.00E+00	0.00E+00	1.86E-03	-7.01E-04	-3.05E-04	1.16E-06	-1.08E-07	9.28E-09
200	5	8.42E-06	-4.86E-04	-5.18E-05	-2.29E-06	0.00E+00	0.00E+00	-1.68E-03	4.10E-04	2.94E-04	-1.12E-06	1.04E-07	-8.95E-09
200	10	1.58E-05	-9.55E-04	-1.02E-04	-4.30E-06	0.00E+00	0.00E+00	-3.21E-03	5.45E-04	5.76E-04	-2.20E-06	2.04E-07	-1.76E-08
200	20	2.91E-05	-1.85E-03	-1.97E-04	-8.03E-06	0.00E+00	0.00E+00	-5.89E-03	5.91E-05	1.11E-03	-4.24E-06	3.94E-07	-3.40E-08

Table D3.5 aqueous polystyrene: effect of change in *Cp'*

MHz	%	c 10nm	c 100nm	c 1um	c 10um	c 100um	c 1mm	a 10nm	a 100nm	a 1um	a 10um	a 100um	a 1mm
0.1	-20	-2.37E-02	-2.37E-02	-2.35E-02	-4.17E-03	-4.12E-04	-4.19E-05	-6.61E-02	1.57E-01	2.00E-01	5.23E-01	4.55E-01	2.15E-02
0.1	-10	-1.04E-02	-1.04E-02	-1.03E-02	-1.76E-03	-1.74E-04	-1.75E-05	-3.33E-02	7.64E-02	9.70E-02	2.22E-01	1.92E-01	9.07E-03
0.1	-5	-4.93E-03	-4.93E-03	-4.86E-03	-8.13E-04	-8.04E-05	-7.90E-06	-1.67E-02	3.77E-02	4.78E-02	1.03E-01	8.88E-02	4.19E-03
0.1	5	4.42E-03	4.42E-03	4.35E-03	7.03E-04	6.95E-05	7.21E-06	1.69E-02	-3.68E-02	-4.64E-02	-8.92E-02	-7.68E-02	-3.63E-03
0.1	10	8.39E-03	8.39E-03	8.26E-03	1.31E-03	1.30E-04	1.34E-05	3.38E-02	-7.27E-02	-9.15E-02	-1.67E-01	-1.44E-01	-6.78E-03
0.1	20	1.52E-02	1.52E-02	1.50E-02	2.32E-03	2.29E-04	2.37E-05	6.82E-02	-1.42E-01	-1.78E-01	-2.96E-01	-2.53E-01	-1.20E-02
1	-20	-1.88E-02	-1.88E-02	-9.94E-03	-9.26E-04	-9.49E-05	5.79E-05	-7.66E-02	1.99E-01	5.92E-01	4.29E-01	3.48E-02	-3.93E-05
1	-10	-8.26E-03	-8.25E-03	-4.14E-03	-3.88E-04	-3.99E-05	2.45E-05	-3.86E-02	9.65E-02	2.54E-01	1.80E-01	1.46E-02	-1.66E-05
1	-5	-3.89E-03	-3.88E-03	-1.90E-03	-1.79E-04	-1.86E-05	1.13E-05	-1.94E-02	4.75E-02	1.18E-01	8.29E-02	6.71E-03	-7.69E-06
1	5	3.47E-03	3.46E-03	1.63E-03	1.53E-04	1.55E-05	-9.78E-06	1.96E-02	-4.60E-02	-1.03E-01	-7.13E-02	-5.77E-03	6.67E-06
1	10	6.57E-03	6.57E-03	3.04E-03	2.86E-04	2.92E-05	-1.83E-05	3.93E-02	-9.06E-02	-1.94E-01	-1.33E-01	-1.07E-02	1.25E-05
1	20	1.19E-02	1.19E-02	5.31E-03	5.01E-04	5.12E-05	-3.26E-05	7.92E-02	-1.75E-01	-3.44E-01	-2.33E-01	-1.88E-02	2.21E-05
10	-20	-1.48E-02	-1.43E-02	-2.06E-03	-2.10E-04	8.65E-05	-4.43E-05	-8.86E-02	2.80E-01	3.59E-01	3.42E-02	-8.48E-05	1.55E-05
10	-10	-6.43E-03	-6.21E-03	-8.56E-04	-8.71E-05	3.65E-05	-1.48E-05	-4.47E-02	1.33E-01	1.49E-01	1.42E-02	-3.56E-05	6.68E-06
10	-5	-3.01E-03	-2.90E-03	-3.93E-04	-4.00E-05	1.69E-05	0.00E+00	-2.25E-02	6.48E-02	6.86E-02	6.49E-03	-1.64E-05	3.12E-06
10	5	2.67E-03	2.56E-03	3.34E-04	3.41E-05	-1.47E-05	1.48E-05	2.27E-02	-6.14E-02	-5.85E-02	-5.52E-03	1.42E-05	-2.74E-06
10	10	5.04E-03	4.81E-03	6.21E-04	6.34E-05	-2.74E-05	1.48E-05	4.55E-02	-1.19E-01	-1.09E-01	-1.02E-02	2.65E-05	-5.18E-06
10	20	9.03E-03	8.57E-03	1.08E-03	1.10E-04	-4.82E-05	2.95E-05	9.19E-02	-2.26E-01	-1.89E-01	-1.78E-02	4.66E-05	-9.28E-06
100	-20	-1.13E-02	-5.02E-03	-5.11E-04	8.28E-05	3.66E-05	0.00E+00	-1.03E-01	1.47E-01	1.43E-02	-1.51E-04	7.26E-06	-4.94E-07
100	-10	-4.86E-03	-2.08E-03	-2.12E-04	3.62E-05	1.22E-05	0.00E+00	-5.19E-02	5.92E-02	5.70E-03	-6.27E-05	3.17E-06	-2.05E-07
100	-5	-2.26E-03	-9.53E-04	-9.77E-05	1.70E-05	1.22E-05	0.00E+00	-2.61E-02	2.67E-02	2.56E-03	-2.88E-05	1.49E-06	-9.41E-08
100	5	1.98E-03	8.13E-04	8.35E-05	-1.52E-05	0.00E+00	0.00E+00	2.63E-02	-2.20E-02	-2.09E-03	2.46E-05	-1.34E-06	8.03E-08
100	10	3.71E-03	1.51E-03	1.55E-04	-2.90E-05	-1.22E-05	0.00E+00	5.28E-02	-4.00E-02	-3.80E-03	4.58E-05	-2.54E-06	1.49E-07
100	20	6.56E-03	2.63E-03	2.70E-04	-5.27E-05	-1.22E-05	0.00E+00	1.07E-01	-6.67E-02	-6.30E-03	7.98E-05	-4.62E-06	2.60E-07
200	-20	-8.30E-03	-2.79E-03	-3.24E-04	-1.06E-05	0.00E+00	0.00E+00	-1.16E-01	2.47E-02	1.49E-03	-6.46E-06	-1.27E-07	5.27E-08
200	-10	-3.51E-03	-1.17E-03	-1.36E-04	-4.30E-06	0.00E+00	0.00E+00	-5.85E-02	8.29E-03	5.06E-04	-2.76E-06	-8.91E-08	2.38E-08
200	-5	-1.62E-03	-5.38E-04	-6.27E-05	-2.01E-06	0.00E+00	0.00E+00	-2.94E-02	3.35E-03	2.06E-04	-1.28E-06	-4.93E-08	1.14E-08
200	5	1.39E-03	4.63E-04	5.36E-05	1.43E-06	0.00E+00	0.00E+00	2.96E-02	-2.07E-03	-1.32E-04	1.12E-06	5.65E-08	-1.06E-08
200	10	2.58E-03	8.64E-04	1.00E-04	2.58E-06	6.20E-05	0.00E+00	5.95E-02	-3.11E-03	-2.04E-04	2.12E-06	1.18E-07	-2.05E-08
200	20	4.47E-03	1.52E-03	1.76E-04	4.59E-06	6.20E-05	0.00E+00	1.20E-01	-2.83E-03	-2.15E-04	3.78E-06	2.53E-07	-3.83E-08

Table D3.6 aqueous polystyrene: effect of change in *alpha'*

MHz	%	c 10nm	c 100nm	c 1um	c 10um	c 100um	c 1mm	a 10nm	a 100nm	a 1um	a 10um	a 100um	a 1mm
0.1	-20	0.00E+00	0.00E+00	3.50E-07	0.00E+00	0.00E+00	0.00E+00	-1.14E-01	-8.01E-03	-1.35E-04	-3.94E-04	-3.41E-03	-1.61E-03
0.1	-10	0.00E+00	0.00E+00	0.00E+00	0.00E+00	0.00E+00	0.00E+00	-5.71E-02	-4.01E-03	-6.75E-05	-1.97E-04	-1.71E-03	-8.06E-04
0.1	-5	0.00E+00	0.00E+00	0.00E+00	0.00E+00	0.00E+00	0.00E+00	-2.85E-02	-2.00E-03	-3.37E-05	-9.85E-05	-8.53E-04	-4.03E-04
0.1	5	0.00E+00	0.00E+00	0.00E+00	-3.35E-07	0.00E+00	0.00E+00	2.85E-02	2.00E-03	3.37E-05	9.85E-05	8.53E-04	4.03E-04
0.1	10	0.00E+00	0.00E+00	-3.50E-07	-3.35E-07	0.00E+00	0.00E+00	5.71E-02	4.01E-03	6.75E-05	1.97E-04	1.71E-03	8.06E-04
0.1	20	0.00E+00	0.00E+00	-3.50E-07	-3.35E-07	0.00E+00	0.00E+00	1.14E-01	8.01E-03	1.35E-04	3.94E-04	3.41E-03	1.61E-03
1	-20	0.00E+00	3.51E-07	8.51E-06	9.99E-07	3.44E-07	3.77E-05	-1.23E-01	-1.03E-02	-1.60E-03	-1.27E-02	-1.34E-02	3.59E-05
1	-10	0.00E+00	0.00E+00	4.43E-06	3.33E-07	0.00E+00	1.89E-05	-6.15E-02	-5.16E-03	-8.00E-04	-6.35E-03	-6.71E-03	1.79E-05
1	-5	0.00E+00	0.00E+00	2.04E-06	0.00E+00	0.00E+00	9.50E-06	-3.08E-02	-2.58E-03	-4.00E-04	-3.18E-03	-3.35E-03	8.97E-06
1	5	0.00E+00	-3.51E-07	-2.04E-06	-3.33E-07	0.00E+00	-9.36E-06	3.08E-02	2.58E-03	4.00E-04	3.18E-03	3.35E-03	-8.97E-06
1	10	0.00E+00	-3.51E-07	-4.08E-06	-6.66E-07	0.00E+00	-1.89E-05	6.15E-02	5.16E-03	8.00E-04	6.35E-03	6.71E-03	-1.79E-05
1	20	0.00E+00	-7.01E-07	-8.17E-06	-9.99E-07	0.00E+00	-3.77E-05	1.23E-01	1.03E-02	1.60E-03	1.27E-02	1.34E-02	-3.59E-05
10	-20	7.01E-07	5.18E-05	3.68E-05	4.48E-06	4.55E-04	-3.39E-04	-1.32E-01	-1.73E-02	-4.32E-02	-6.41E-02	3.76E-04	-4.98E-04
10	-10	3.51E-07	2.59E-05	1.84E-05	2.41E-06	2.27E-04	-1.62E-04	-6.59E-02	-8.63E-03	-2.16E-02	-3.21E-02	1.88E-04	-2.48E-04
10	-5	0.00E+00	1.29E-05	9.38E-06	1.03E-06	1.14E-04	-7.37E-05	-3.30E-02	-4.32E-03	-1.08E-02	-1.60E-02	9.40E-05	-1.24E-04
10	5	-3.51E-07	-1.29E-05	-9.04E-06	-1.03E-06	-1.14E-04	8.85E-05	3.30E-02	4.32E-03	1.08E-02	1.60E-02	-9.40E-05	1.23E-04
10	10	-3.51E-07	-2.59E-05	-1.81E-05	-2.41E-06	-2.27E-04	1.77E-04	6.59E-02	8.63E-03	2.16E-02	3.21E-02	-1.88E-04	2.46E-04
10	20	-7.01E-07	-5.18E-05	-3.65E-05	-4.48E-06	-4.54E-04	3.39E-04	1.32E-01	1.73E-02	4.32E-02	6.41E-02	-3.76E-04	4.90E-04
100	-20	7.05E-05	1.17E-03	8.71E-05	4.58E-03	6.52E-03	5.09E-04	-1.41E-01	-1.04E-01	-1.40E-01	2.81E-03	-1.22E-03	3.70E-04
100	-10	3.51E-05	5.82E-04	4.13E-05	2.28E-03	3.28E-03	0.00E+00	-7.06E-02	-5.18E-02	-6.98E-02	1.40E-03	-6.11E-04	1.81E-04
100	-5	1.75E-05	2.90E-04	2.01E-05	1.14E-03	1.65E-03	0.00E+00	-3.53E-02	-2.59E-02	-3.49E-02	7.00E-04	-3.06E-04	8.92E-05
100	5	-1.72E-05	-2.90E-04	-1.91E-05	-1.14E-03	-1.65E-03	5.09E-04	3.53E-02	2.59E-02	3.49E-02	-6.97E-04	3.05E-04	-8.68E-05
100	10	-3.44E-05	-5.79E-04	-3.71E-05	-2.27E-03	-3.32E-03	5.09E-04	7.06E-02	5.18E-02	6.98E-02	-1.39E-03	6.11E-04	-1.71E-04
100	20	-6.84E-05	-1.16E-03	-6.94E-05	-4.54E-03	-6.68E-03	1.02E-03	1.41E-01	1.04E-01	1.40E-01	-2.78E-03	1.22E-03	-3.32E-04
200	-20	3.10E-04	1.92E-03	4.19E-05	3.36E-03	-1.07E-02	-3.69E-03	-1.49E-01	-1.53E-01	-1.25E-01	1.68E-03	2.41E-03	-2.14E-05
200	-10	1.53E-04	9.53E-04	6.32E-06	1.67E-03	-5.45E-03	-1.23E-03	-7.47E-02	-7.67E-02	-6.26E-02	8.34E-04	1.14E-03	-6.55E-06
200	-5	7.62E-05	4.74E-04	-7.90E-07	8.36E-04	-2.78E-03	-1.23E-03	-3.74E-02	-3.84E-02	-3.13E-02	4.15E-04	5.57E-04	-2.46E-06
200	5	-7.58E-05	-4.70E-04	7.90E-06	-8.34E-04	2.78E-03	0.00E+00	3.74E-02	3.84E-02	3.13E-02	-4.11E-04	-5.29E-04	1.16E-06
200	10	-1.51E-04	-9.35E-04	2.33E-05	-1.66E-03	5.57E-03	1.23E-03	7.47E-02	7.68E-02	6.26E-02	-8.18E-04	-1.03E-03	1.31E-06
200	20	-2.98E-04	-1.85E-03	7.66E-05	-3.32E-03	1.13E-02	1.23E-03	1.50E-01	1.54E-01	1.25E-01	-1.62E-03	-1.96E-03	-5.98E-07

Table D3.7 aqueous polystyrene: effect of change in *beta'*

MHz	%	c 10nm	c 100nm	c 1um	c 10um	c 100um	c 1mm	a 10nm	a 100nm	a 1um	a 10um	a 100um	a 1mm
0.1	-20	2.47E-02	2.47E-02	2.33E-02	3.01E-03	2.98E-04	3.06E-05	2.91E-04	-4.41E-01	-4.73E-01	-3.92E-01	-3.30E-01	-1.56E-02
0.1	-10	1.33E-02	1.33E-02	1.26E-02	1.63E-03	1.61E-04	1.65E-05	-1.03E-02	-2.40E-01	-2.57E-01	-2.12E-01	-1.78E-01	-8.40E-03
0.1	-5	6.93E-03	6.93E-03	6.53E-03	8.42E-04	8.31E-05	8.59E-06	-7.44E-03	-1.25E-01	-1.33E-01	-1.10E-01	-9.23E-02	-4.35E-03
0.1	5	-7.43E-03	-7.43E-03	-7.00E-03	-9.01E-04	-8.91E-05	-8.93E-06	1.16E-02	1.35E-01	1.44E-01	1.17E-01	9.87E-02	4.65E-03
0.1	10	-1.54E-02	-1.54E-02	-1.45E-02	-1.86E-03	-1.84E-04	-1.86E-05	2.70E-02	2.79E-01	2.97E-01	2.43E-01	2.04E-01	9.60E-03
0.1	20	-3.27E-02	-3.27E-02	-3.08E-02	-3.94E-03	-3.90E-04	-3.99E-05	6.81E-02	5.99E-01	6.36E-01	5.15E-01	4.32E-01	2.04E-02
1	-20	3.96E-02	3.95E-02	1.57E-02	1.45E-03	1.48E-04	-9.03E-05	-6.90E-02	-4.36E-01	-4.38E-01	-3.53E-01	-5.07E-02	6.15E-05
1	-10	2.13E-02	2.12E-02	8.43E-03	7.76E-04	7.94E-05	-4.79E-05	-4.43E-02	-2.36E-01	-2.35E-01	-1.89E-01	-2.72E-02	3.27E-05
1	-5	1.10E-02	1.10E-02	4.35E-03	4.01E-04	4.09E-05	-2.47E-05	-2.44E-02	-1.22E-01	-1.22E-01	-9.78E-02	-1.40E-02	1.68E-05
1	5	-1.18E-02	-1.17E-02	-4.63E-03	-4.26E-04	-4.33E-05	2.60E-05	2.85E-02	1.31E-01	1.30E-01	1.04E-01	1.49E-02	-1.78E-05
1	10	-2.42E-02	-2.42E-02	-9.52E-03	-8.76E-04	-8.94E-05	5.35E-05	6.07E-02	2.72E-01	2.68E-01	2.14E-01	3.07E-02	-3.65E-05
1	20	-5.14E-02	-5.13E-02	-2.01E-02	-1.85E-03	-1.89E-04	1.12E-04	1.36E-01	5.81E-01	5.68E-01	4.52E-01	6.47E-02	-7.67E-05
10	-20	6.36E-02	5.95E-02	7.00E-03	7.03E-04	-2.69E-04	1.18E-04	-1.35E-01	-4.25E-01	-3.61E-01	-9.52E-02	2.73E-04	-4.59E-05
10	-10	3.40E-02	3.18E-02	3.72E-03	3.74E-04	-1.42E-04	5.90E-05	-7.68E-02	-2.29E-01	-1.93E-01	-5.07E-02	1.45E-04	-2.40E-05
10	-5	1.76E-02	1.64E-02	1.92E-03	1.93E-04	-7.31E-05	2.95E-05	-4.06E-02	-1.19E-01	-9.93E-02	-2.61E-02	7.43E-05	-1.23E-05
10	5	-1.87E-02	-1.75E-02	-2.02E-03	-2.03E-04	7.68E-05	-4.43E-05	4.47E-02	1.27E-01	1.05E-01	2.76E-02	-7.82E-05	1.28E-05
10	10	-3.85E-02	-3.59E-02	-4.15E-03	-4.17E-04	1.57E-04	-7.38E-05	9.33E-02	2.62E-01	2.16E-01	5.66E-02	-1.60E-04	2.61E-05
10	20	-8.13E-02	-7.59E-02	-8.72E-03	-8.76E-04	3.29E-04	-1.48E-04	2.02E-01	5.59E-01	4.54E-01	1.19E-01	-3.35E-04	5.42E-05
100	-20	1.04E-01	3.66E-02	3.27E-03	-2.86E-04	-2.44E-04	0.00E+00	-1.88E-01	-3.47E-01	-9.90E-02	1.02E-03	-3.23E-05	3.35E-06
100	-10	5.53E-02	1.94E-02	1.73E-03	-1.50E-04	-1.34E-04	0.00E+00	-1.03E-01	-1.85E-01	-5.24E-02	5.36E-04	-1.68E-05	1.77E-06
100	-5	2.85E-02	9.94E-03	8.88E-04	-7.65E-05	-6.09E-05	0.00E+00	-5.36E-02	-9.55E-02	-2.69E-02	2.75E-04	-8.56E-06	9.07E-07
100	5	-3.02E-02	-1.05E-02	-9.32E-04	7.97E-05	7.31E-05	0.00E+00	5.79E-02	1.01E-01	2.83E-02	-2.87E-04	8.86E-06	-9.51E-07
100	10	-6.21E-02	-2.14E-02	-1.91E-03	1.62E-04	1.34E-04	0.00E+00	1.20E-01	2.08E-01	5.79E-02	-5.87E-04	1.80E-05	-1.95E-06
100	20	-1.31E-01	-4.47E-02	-3.98E-03	3.36E-04	2.92E-04	0.00E+00	2.56E-01	4.37E-01	1.21E-01	-1.22E-03	3.71E-05	-4.05E-06
200	-20	1.76E-01	3.59E-02	3.68E-03	1.75E-04	2.48E-04	0.00E+00	-2.34E-01	-2.91E-01	-4.37E-02	4.56E-05	-7.30E-06	-1.47E-07
200	-10	9.36E-02	1.89E-02	1.93E-03	9.15E-05	1.24E-04	0.00E+00	-1.26E-01	-1.54E-01	-2.30E-02	2.42E-05	-3.83E-06	-8.24E-08
200	-5	4.82E-02	9.67E-03	9.90E-04	4.68E-05	6.21E-05	0.00E+00	-6.53E-02	-7.90E-02	-1.18E-02	1.25E-05	-1.96E-06	-4.34E-08
200	5	-5.09E-02	-1.01E-02	-1.03E-03	-4.88E-05	-6.21E-05	0.00E+00	6.98E-02	8.30E-02	1.23E-02	-1.31E-05	2.04E-06	4.74E-08
200	10	-1.05E-01	-2.06E-02	-2.11E-03	-9.93E-05	-1.86E-04	0.00E+00	1.44E-01	1.70E-01	2.50E-02	-2.69E-05	4.15E-06	9.87E-08
200	20	-2.20E-01	-4.27E-02	-4.36E-03	-2.05E-04	-3.10E-04	0.00E+00	3.07E-01	3.55E-01	5.19E-02	-5.62E-05	8.58E-06	2.12E-07

Table D3.8 aqueous polystyrene: effect of change in *c*

MHz	%	c 10nm	c 100nm	c 1um	c 10um	c 100um	c 1mm	a 10nm	a 100nm	a 1um	a 10um	a 100um	a 1mm
0.1	-20	2.66E-01	2.66E-01	2.64E-01	2.34E-01	2.29E-01	2.14E-01	1.56E-01	-1.55E-01	-1.77E-01	-1.07E-01	-3.00E-02	3.44E+00
0.1	-10	1.75E-01	1.75E-01	1.73E-01	1.56E-01	1.53E-01	1.48E-01	5.07E-02	-7.90E-02	-8.84E-02	-5.55E-02	-2.25E-02	1.13E+00
0.1	-5	9.81E-02	9.81E-02	9.75E-02	8.78E-02	8.63E-02	8.47E-02	2.03E-02	-3.97E-02	-4.41E-02	-2.82E-02	-1.27E-02	4.66E-01
0.1	5	-1.21E-01	-1.21E-01	-1.20E-01	-1.09E-01	-1.07E-01	-1.07E-01	-1.27E-02	4.00E-02	4.39E-02	2.88E-02	1.49E-02	-3.24E-01
0.1	10	-2.64E-01	-2.64E-01	-2.63E-01	-2.39E-01	-2.36E-01	-2.36E-01	-1.96E-02	8.02E-02	8.74E-02	5.81E-02	3.16E-02	-5.46E-01
0.1	20	-6.25E-01	-6.25E-01	-6.21E-01	-5.68E-01	-5.59E-01	-5.66E-01	-2.10E-02	1.60E-01	1.74E-01	1.18E-01	6.88E-02	-7.92E-01
1	-20	2.66E-01	2.66E-01	2.45E-01	2.30E-01	2.14E-01	-1.44E-01	1.57E-01	-1.53E-01	-1.61E-01	-4.63E-02	2.59E+00	-3.10E-01
1	-10	1.75E-01	1.75E-01	1.62E-01	1.53E-01	1.48E-01	2.64E-01	5.08E-02	-7.82E-02	-8.09E-02	-2.96E-02	8.58E-01	-2.44E-01
1	-5	9.81E-02	9.81E-02	9.14E-02	8.67E-02	8.47E-02	3.17E-01	2.04E-02	-3.94E-02	-4.05E-02	-1.61E-02	3.55E-01	-1.42E-01
1	5	-1.21E-01	-1.21E-01	-1.13E-01	-1.07E-01	-1.07E-01	-9.61E-01	-1.28E-02	3.97E-02	4.05E-02	1.80E-02	-2.49E-01	3.30E-02
1	10	-2.64E-01	-2.64E-01	-2.48E-01	-2.36E-01	-2.36E-01	-1.95E+00	-1.97E-02	7.96E-02	8.09E-02	3.75E-02	-4.23E-01	-2.49E-01
1	20	-6.25E-01	-6.24E-01	-5.87E-01	-5.62E-01	-5.66E-01	-2.01E+00	-2.12E-02	1.59E-01	1.61E-01	8.00E-02	-6.20E-01	-7.99E-01
10	-20	2.66E-01	2.64E-01	2.33E-01	2.14E-01	-2.23E-01	-5.43E-01	1.58E-01	-1.46E-01	-7.31E-02	1.35E+00	-2.72E-01	-4.88E-01
10	-10	1.75E-01	1.73E-01	1.56E-01	1.48E-01	1.45E-01	-3.45E-01	5.13E-02	-7.53E-02	-4.28E-02	4.55E-01	-2.19E-01	-3.48E-02
10	-5	9.81E-02	9.75E-02	8.79E-02	8.49E-02	2.09E-01	-1.26E-01	2.06E-02	-3.80E-02	-2.25E-02	1.90E-01	-1.30E-01	2.47E-02
10	5	-1.21E-01	-1.20E-01	-1.09E-01	-1.07E-01	-7.13E-01	-1.81E+00	-1.29E-02	3.85E-02	2.43E-02	-1.35E-01	5.98E-02	1.01E-02
10	10	-2.64E-01	-2.63E-01	-2.39E-01	-2.37E-01	-1.61E+00	-1.91E-01	-2.01E-02	7.74E-02	5.00E-02	-2.30E-01	-1.51E-01	1.58E-01
10	20	-6.25E-01	-6.21E-01	-5.68E-01	-5.67E-01	-1.92E+00	2.78E+00	-2.19E-02	1.55E-01	1.04E-01	-3.40E-01	-7.33E-01	-1.27E-01
100	-20	2.66E-01	2.47E-01	2.15E-01	-3.25E-01	-7.65E-01	-3.39E-01	1.61E-01	-7.37E-02	4.52E-01	-1.44E-01	-5.05E-01	-7.42E-03
100	-10	1.75E-01	1.63E-01	1.49E-01	-1.84E-02	-3.58E-01	-7.56E-02	5.24E-02	-4.57E-02	1.48E-01	-1.37E-01	-7.20E-02	-1.45E-02
100	-5	9.82E-02	9.21E-02	8.54E-02	5.78E-02	-4.43E-01	2.54E-02	2.11E-02	-2.44E-02	6.05E-02	-8.47E-02	-6.94E-03	-5.23E-03
100	5	-1.21E-01	-1.14E-01	-1.08E-01	-3.02E-01	-9.89E-01	-5.87E-01	-1.34E-02	2.68E-02	-4.04E-02	7.25E-02	7.80E-03	-5.06E-03
100	10	-2.64E-01	-2.50E-01	-2.38E-01	-8.52E-01	-2.16E-01	8.59E-01	-2.09E-02	5.53E-02	-6.59E-02	2.11E-02	8.69E-02	3.59E-03
100	20	-6.25E-01	-5.91E-01	-5.72E-01	-1.59E+00	1.54E+00	5.39E-01	-2.34E-02	1.16E-01	-8.59E-02	-4.75E-01	-1.29E-01	2.25E-02
200	-20	2.66E-01	2.42E-01	1.76E-01	-6.06E-01	-1.43E-01	-1.39E+00	1.61E-01	-2.31E-02	9.30E-01	1.14E+00	3.41E-02	-2.67E-01
200	-10	1.75E-01	1.61E-01	1.39E-01	-2.64E-01	1.68E-01	-9.17E-01	5.26E-02	-2.54E-02	3.20E-01	3.76E-01	-1.73E-02	-8.02E-02
200	-5	9.82E-02	9.08E-02	8.23E-02	-1.16E-01	2.89E-01	-2.29E-01	2.12E-02	-1.52E-02	1.34E-01	1.85E-01	1.55E-03	-5.21E-03
200	5	-1.21E-01	-1.12E-01	-1.09E-01	8.26E-02	-9.84E-02	8.92E-03	-1.35E-02	1.90E-02	-9.50E-02	-1.82E-01	-1.02E-02	-4.20E-04
200	10	-2.65E-01	-2.47E-01	-2.46E-01	1.29E-01	1.12E+00	4.46E-02	-2.10E-02	4.08E-02	-1.61E-01	-3.56E-01	-1.68E-02	1.29E-03
200	20	-6.25E-01	-5.85E-01	-6.07E-01	1.02E-01	4.91E+00	6.75E-01	-2.36E-02	9.04E-02	-2.33E-01	-6.51E-01	7.70E-03	-1.20E-02

Table D3.9 aqueous polystyrene: effect of change in *rho*

MHz	%	c 10nm	c 100nm	c 1um	c 10um	c 100um	c 1mm	a 10nm	a 100nm	a 1um	a 10um	a 100um	a 1mm
0.1	-20	-4.02E-01	-4.02E-01	-4.00E-01	-3.19E-01	-2.65E-01	-2.67E-01	1.39E-01	3.48E-01	4.26E-01	4.69E+00	6.73E+00	8.82E-01
0.1	-10	-1.62E-01	-1.62E-01	-1.61E-01	-1.39E-01	-1.23E-01	-1.24E-01	4.60E-02	4.04E-02	5.84E-02	1.31E+00	1.97E+00	3.43E-01
0.1	-5	-7.25E-02	-7.25E-02	-7.23E-02	-6.46E-02	-5.89E-02	-6.00E-02	1.81E-02	-8.08E-03	-2.81E-03	4.46E-01	6.93E-01	1.50E-01
0.1	5	5.80E-02	5.80E-02	5.80E-02	5.64E-02	5.45E-02	5.58E-02	-9.56E-03	5.66E-02	5.67E-02	-1.04E-01	-2.01E-01	-1.13E-01
0.1	10	1.03E-01	1.03E-01	1.04E-01	1.05E-01	1.05E-01	1.08E-01	-1.17E-02	1.55E-01	1.59E-01	7.35E-02	1.31E-02	-1.92E-01
0.1	20	1.62E-01	1.62E-01	1.63E-01	1.84E-01	1.93E-01	2.00E-01	2.37E-03	4.57E-01	4.74E-01	1.08E+00	1.44E+00	-2.66E-01
1	-20	-1.88E-01	-1.88E-01	-1.94E-01	-2.01E-01	-2.06E-01	-9.67E-01	1.20E-02	-3.15E-01	-3.42E-01	-3.70E-01	2.14E-01	2.38E+00
1	-10	-6.51E-02	-6.51E-02	-7.18E-02	-8.84E-02	-9.34E-02	1.25E-01	-1.36E-02	-2.35E-01	-3.25E-01	-6.02E-01	-5.06E-02	1.15E+00
1	-5	-2.64E-02	-2.64E-02	-3.05E-02	-4.15E-02	-4.44E-02	9.18E-02	-1.09E-02	-1.33E-01	-1.93E-01	-3.84E-01	-5.82E-02	3.99E-01
1	5	1.57E-02	1.57E-02	2.12E-02	3.65E-02	4.01E-02	-8.19E-02	1.80E-02	1.61E-01	2.41E-01	5.20E-01	1.14E-01	-2.22E-01
1	10	2.22E-02	2.23E-02	3.44E-02	6.82E-02	7.61E-02	-1.47E-01	4.21E-02	3.45E-01	5.20E-01	1.15E+00	2.75E-01	-3.56E-01
1	20	1.22E-02	1.23E-02	4.04E-02	1.19E-01	1.36E-01	-2.38E-01	1.05E-01	7.69E-01	1.16E+00	2.65E+00	7.10E-01	-5.03E-01
10	-20	-3.19E-02	-3.47E-02	-1.07E-01	-1.48E-01	3.79E-01	-2.04E-01	-9.97E-02	-4.86E-01	-7.50E-01	-5.21E-01	1.52E+00	1.53E-03
10	-10	8.38E-03	6.64E-03	-3.85E-02	-6.33E-02	1.45E-01	-6.66E-02	-6.44E-02	-2.76E-01	-4.40E-01	-3.19E-01	3.79E-01	2.73E-03
10	-5	9.32E-03	8.37E-03	-1.59E-02	-2.92E-02	6.33E-02	-2.59E-02	-3.52E-02	-1.44E-01	-2.32E-01	-1.71E-01	1.47E-01	1.39E-03
10	5	-1.81E-02	-1.70E-02	9.88E-03	2.45E-02	-5.04E-02	1.47E-02	4.03E-02	1.55E-01	2.50E-01	1.89E-01	-9.88E-02	-9.85E-04
10	10	-4.37E-02	-4.15E-02	1.44E-02	4.46E-02	-9.19E-02	2.14E-02	8.51E-02	3.18E-01	5.13E-01	3.92E-01	-1.68E-01	-1.38E-03
10	20	-1.14E-01	-1.09E-01	9.25E-03	7.26E-02	-1.58E-01	1.97E-02	1.85E-01	6.63E-01	1.06E+00	8.28E-01	-2.54E-01	-3.97E-04
100	-20	1.37E-01	7.14E-02	-7.16E-02	2.29E-01	-4.38E-02	0.00E+00	-1.65E-01	-4.80E-01	-4.51E-01	4.47E-01	-5.72E-03	-3.30E-03
100	-10	9.14E-02	5.48E-02	-2.34E-02	9.40E-02	-9.41E-03	-2.04E-03	-9.17E-02	-2.51E-01	-2.38E-01	1.35E-01	-3.59E-03	-1.60E-03
100	-5	5.04E-02	3.14E-02	-8.83E-03	4.37E-02	-2.67E-03	-2.04E-03	-4.77E-02	-1.27E-01	-1.21E-01	5.39E-02	-1.97E-03	-7.84E-04
100	5	-5.85E-02	-3.83E-02	3.60E-03	-3.94E-02	2.47E-05	3.07E-03	5.07E-02	1.29E-01	1.24E-01	-3.45E-02	2.25E-03	7.47E-04
100	10	-1.24E-01	-8.25E-02	2.38E-03	-7.64E-02	-1.58E-03	7.15E-03	1.04E-01	2.60E-01	2.50E-01	-5.39E-02	4.71E-03	1.46E-03
100	20	-2.71E-01	-1.86E-01	-1.31E-02	-1.50E-01	-7.19E-03	1.84E-02	2.17E-01	5.21E-01	5.02E-01	-5.35E-02	9.93E-03	2.75E-03
200	-20	4.28E-01	2.02E-01	1.02E-02	1.00E-02	-4.32E-02	-1.04E-01	-2.00E-01	-3.97E-01	-3.22E-01	-4.50E-02	2.91E-02	2.97E-04
200	-10	2.39E-01	1.19E-01	2.03E-02	6.53E-03	-3.15E-03	-4.72E-02	-1.05E-01	-1.99E-01	-1.68E-01	-2.56E-02	1.28E-02	1.76E-04
200	-5	1.24E-01	6.32E-02	1.37E-02	4.36E-03	4.60E-04	-2.24E-02	-5.35E-02	-9.93E-02	-8.54E-02	-1.54E-02	5.83E-03	9.41E-05
200	5	-1.33E-01	-6.97E-02	-2.01E-02	1.76E-02	-2.05E-03	1.99E-02	5.50E-02	9.83E-02	8.78E-02	1.79E-02	-4.91E-03	-1.04E-04
200	10	-2.73E-01	-1.45E-01	-4.62E-02	1.53E-02	-4.64E-03	3.73E-02	1.11E-01	1.95E-01	1.78E-01	8.76E-03	-9.04E-03	-2.17E-04
200	20	-5.70E-01	-3.10E-01	-1.14E-01	7.16E-03	-9.66E-03	6.79E-02	2.26E-01	3.84E-01	3.63E-01	1.79E-02	-1.54E-02	-4.60E-04

Table D3.10 aqueous polystyrene: effect of change in *eta*

MHz	%	c 10nm	c 100nm	c 1um	c 10um	c 100um	c 1mm	a 10nm	a 100nm	a 1um	a 10um	a 100um	a 1mm
0.1	-20	0.00E+00	0.00E+00	2.24E-05	2.06E-04	2.96E-05	2.68E-05	-5.96E-02	2.37E-03	5.82E-03	-6.90E-03	-3.00E-02	-1.39E-02
0.1	-10	0.00E+00	0.00E+00	9.79E-06	9.88E-05	1.43E-05	1.31E-05	-2.99E-02	8.21E-04	2.63E-03	-3.10E-03	-1.45E-02	-6.78E-03
0.1	-5	0.00E+00	0.00E+00	4.55E-06	4.82E-05	6.98E-06	6.53E-06	-1.50E-02	3.34E-04	1.26E-03	-1.47E-03	-7.16E-03	-3.34E-03
0.1	5	0.00E+00	0.00E+00	-4.20E-06	-4.69E-05	-6.98E-06	-6.18E-06	1.50E-02	-2.02E-04	-1.15E-03	1.33E-03	6.97E-03	3.26E-03
0.1	10	0.00E+00	-3.51E-07	-7.69E-06	-9.17E-05	-1.40E-05	-1.24E-05	2.99E-02	-2.90E-04	-2.22E-03	2.54E-03	1.38E-02	6.45E-03
0.1	20	0.00E+00	-3.51E-07	-1.43E-05	-1.77E-04	-2.69E-05	-2.40E-05	6.00E-02	-1.82E-04	-4.11E-03	4.62E-03	2.68E-02	1.26E-02
1	-20	0.00E+00	7.01E-07	1.55E-04	9.92E-05	9.28E-05	-5.87E-03	-6.79E-02	-1.02E-04	5.38E-03	-2.52E-02	-3.40E-02	3.82E-03
1	-10	0.00E+00	3.51E-07	7.05E-05	4.83E-05	4.50E-05	-2.84E-03	-3.40E-02	-3.40E-04	2.56E-03	-1.21E-02	-1.66E-02	1.86E-03
1	-5	0.00E+00	0.00E+00	3.40E-05	2.40E-05	2.23E-05	-1.40E-03	-1.70E-02	-2.31E-04	1.25E-03	-5.94E-03	-8.18E-03	9.16E-04
1	5	0.00E+00	0.00E+00	-3.10E-05	-2.30E-05	-2.17E-05	1.36E-03	1.70E-02	3.36E-04	-1.19E-03	5.74E-03	7.99E-03	-8.92E-04
1	10	0.00E+00	-3.51E-07	-5.96E-05	-4.53E-05	-4.30E-05	2.68E-03	3.41E-02	7.64E-04	-2.32E-03	1.13E-02	1.58E-02	-1.76E-03
1	20	0.00E+00	-3.51E-07	-1.11E-04	-8.89E-05	-8.39E-05	5.22E-03	6.82E-02	1.85E-03	-4.44E-03	2.19E-02	3.09E-02	-3.44E-03
10	-20	0.00E+00	1.47E-05	2.47E-04	3.22E-04	-1.23E-02	-5.70E-03	-7.68E-02	-4.17E-03	-1.28E-02	-5.41E-02	1.29E-02	-2.67E-03
10	-10	0.00E+00	6.65E-06	1.18E-04	1.57E-04	-5.89E-03	-3.24E-03	-3.84E-02	-2.28E-03	-6.10E-03	-2.64E-02	6.25E-03	-1.26E-03
10	-5	0.00E+00	3.15E-06	5.76E-05	7.72E-05	-2.88E-03	-1.70E-03	-1.92E-02	-1.19E-03	-2.98E-03	-1.30E-02	3.08E-03	-6.12E-04
10	5	0.00E+00	-2.45E-06	-5.50E-05	-7.51E-05	2.77E-03	1.83E-03	1.92E-02	1.26E-03	2.86E-03	1.28E-02	-2.99E-03	5.79E-04
10	10	0.00E+00	-4.90E-06	-1.08E-04	-1.49E-04	5.43E-03	3.76E-03	3.85E-02	2.59E-03	5.61E-03	2.53E-02	-5.89E-03	1.13E-03
10	20	0.00E+00	-9.09E-06	-2.08E-04	-2.90E-04	1.05E-02	7.91E-03	7.70E-02	5.40E-03	1.08E-02	4.96E-02	-1.15E-02	2.15E-03
100	-20	-4.56E-06	1.58E-04	1.08E-03	-7.03E-03	-2.83E-02	-7.96E-03	-8.64E-02	-2.52E-02	-5.75E-02	3.71E-02	6.07E-04	9.78E-05
100	-10	-2.45E-06	7.21E-05	5.26E-04	-3.10E-03	-1.35E-02	-3.98E-03	-4.32E-02	-1.27E-02	-2.83E-02	1.77E-02	3.22E-04	5.04E-05
100	-5	-1.05E-06	3.45E-05	2.59E-04	-1.46E-03	-6.58E-03	-1.99E-03	-2.16E-02	-6.36E-03	-1.40E-02	8.66E-03	1.65E-04	2.54E-05
100	5	1.40E-06	-3.18E-05	-2.52E-04	1.30E-03	6.30E-03	1.49E-03	2.16E-02	6.40E-03	1.38E-02	-8.31E-03	-1.70E-04	-2.58E-05
100	10	2.81E-06	-6.08E-05	-4.98E-04	2.45E-03	1.23E-02	3.48E-03	4.32E-02	1.28E-02	2.74E-02	-1.63E-02	-3.45E-04	-5.19E-05
100	20	5.61E-06	-1.13E-04	-9.72E-04	4.37E-03	2.37E-02	6.46E-03	8.65E-02	2.58E-02	5.42E-02	-3.14E-02	-7.04E-04	-1.04E-04
200	-20	-2.60E-05	2.99E-04	3.78E-03	2.57E-03	-3.24E-02	2.56E-03	-9.56E-02	-4.35E-02	-6.63E-02	-2.20E-03	-1.14E-03	3.35E-04
200	-10	-1.37E-05	1.38E-04	1.83E-03	1.25E-03	-1.52E-02	1.28E-03	-4.78E-02	-2.18E-02	-3.26E-02	-1.08E-03	-5.35E-04	1.60E-04
200	-5	-7.02E-06	6.61E-05	9.03E-04	6.16E-04	-7.37E-03	1.28E-03	-2.39E-02	-1.09E-02	-1.62E-02	-5.39E-04	-2.60E-04	7.80E-05
200	5	7.02E-06	-6.13E-05	-8.78E-04	-6.01E-04	6.93E-03	0.00E+00	2.39E-02	1.09E-02	1.59E-02	5.32E-04	2.46E-04	-7.46E-05
200	10	1.47E-05	-1.19E-04	-1.73E-03	-1.19E-03	1.35E-02	-1.28E-03	4.79E-02	2.18E-02	3.16E-02	1.06E-03	4.81E-04	-1.46E-04
200	20	3.05E-05	-2.22E-04	-3.38E-03	-2.32E-03	2.57E-02	-2.56E-03	9.57E-02	4.36E-02	6.24E-02	2.10E-03	9.22E-04	-2.80E-04

Table D3.11 aqueous polystyrene: effect of change in *kappa*

MHz	%	c 10nm	c 100nm	c 1um	c 10um	c 100um	c 1mm	a 10nm	a 100nm	a 1um	a 10um	a 100um	a 1mm
0.1	-20	0.00E+00	1.40E-06	3.85E-04	1.41E-04	1.36E-05	1.72E-06	1.64E-02	1.03E-01	3.80E-02	-1.70E-02	-1.53E-02	-7.25E-04
0.1	-10	0.00E+00	3.51E-07	1.74E-04	6.56E-05	6.31E-06	6.87E-07	7.29E-03	4.59E-02	1.76E-02	-7.86E-03	-7.09E-03	-3.36E-04
0.1	-5	0.00E+00	0.00E+00	8.32E-05	3.15E-05	2.99E-06	3.44E-07	3.45E-03	2.18E-02	8.46E-03	-3.79E-03	-3.42E-03	-1.62E-04
0.1	5	0.00E+00	-3.51E-07	-7.62E-05	-2.98E-05	-2.99E-06	0.00E+00	-3.12E-03	-1.98E-02	-7.90E-03	3.55E-03	3.21E-03	1.52E-04
0.1	10	0.00E+00	-7.01E-07	-1.46E-04	-5.79E-05	-5.65E-06	-3.44E-07	-5.97E-03	-3.78E-02	-1.53E-02	6.88E-03	6.22E-03	2.95E-04
0.1	20	0.00E+00	-1.05E-06	-2.71E-04	-1.09E-04	-1.06E-05	-1.03E-06	-1.09E-02	-6.94E-02	-2.88E-02	1.30E-02	1.17E-02	5.57E-04
1	-20	0.00E+00	2.56E-05	4.54E-04	4.20E-05	4.13E-06	-2.94E-06	1.35E-02	7.58E-02	-1.23E-02	-1.40E-02	-1.52E-03	2.00E-06
1	-10	0.00E+00	1.12E-05	2.10E-04	1.96E-05	1.72E-06	-1.26E-06	6.01E-03	3.41E-02	-5.63E-03	-6.51E-03	-7.02E-04	9.29E-07
1	-5	0.00E+00	5.26E-06	1.01E-04	9.32E-06	6.88E-07	-5.59E-07	2.85E-03	1.62E-02	-2.70E-03	-3.14E-03	-3.39E-04	4.48E-07
1	5	0.00E+00	-4.56E-06	-9.50E-05	-8.66E-06	-1.03E-06	6.99E-07	-2.58E-03	-1.48E-02	2.50E-03	2.94E-03	3.17E-04	-4.20E-07
1	10	0.00E+00	-8.77E-06	-1.84E-04	-1.66E-05	-1.72E-06	1.26E-06	-4.93E-03	-2.84E-02	4.81E-03	5.70E-03	6.15E-04	-8.15E-07
1	20	0.00E+00	-1.61E-05	-3.47E-04	-3.20E-05	-3.44E-06	2.38E-06	-9.04E-03	-5.25E-02	8.99E-03	1.08E-02	1.16E-03	-1.54E-06
10	-20	7.01E-07	2.88E-04	1.28E-04	1.27E-05	-5.76E-06	0.00E+00	1.07E-02	3.23E-02	-1.18E-02	-1.93E-03	5.77E-06	-1.26E-06
10	-10	3.51E-07	1.30E-04	5.93E-05	5.86E-06	-2.69E-06	0.00E+00	4.75E-03	1.49E-02	-5.43E-03	-8.94E-04	2.68E-06	-5.82E-07
10	-5	0.00E+00	6.19E-05	2.85E-05	2.76E-06	-1.28E-06	0.00E+00	2.25E-03	7.15E-03	-2.62E-03	-4.31E-04	1.29E-06	-2.81E-07
10	5	0.00E+00	-5.63E-05	-2.71E-05	-2.76E-06	1.28E-06	0.00E+00	-2.04E-03	-6.64E-03	2.45E-03	4.03E-04	-1.21E-06	2.63E-07
10	10	-3.51E-07	-1.08E-04	-5.23E-05	-5.17E-06	2.30E-06	0.00E+00	-3.91E-03	-1.28E-02	4.74E-03	7.82E-04	-2.35E-06	5.09E-07
10	20	-3.51E-07	-1.99E-04	-9.85E-05	-9.99E-06	4.35E-06	0.00E+00	-7.18E-03	-2.41E-02	8.92E-03	1.47E-03	-4.44E-06	9.59E-07
100	-20	5.26E-06	4.35E-04	4.48E-05	-7.19E-06	0.00E+00	0.00E+00	7.62E-03	-3.28E-03	-1.09E-03	1.46E-05	-6.71E-07	3.79E-08
100	-10	2.10E-06	2.01E-04	2.08E-05	-3.31E-06	0.00E+00	0.00E+00	3.42E-03	-1.48E-03	-5.03E-04	6.78E-06	-3.09E-07	1.76E-08
100	-5	1.05E-06	9.68E-05	1.01E-05	-1.60E-06	0.00E+00	0.00E+00	1.62E-03	-7.02E-04	-2.42E-04	3.28E-06	-1.49E-07	8.50E-09
100	5	-7.01E-07	-9.06E-05	-9.37E-06	1.48E-06	1.22E-05	0.00E+00	-1.48E-03	6.40E-04	2.26E-04	-3.09E-06	1.39E-07	-7.92E-09
100	10	-1.40E-06	-1.75E-04	-1.80E-05	2.85E-06	1.22E-05	0.00E+00	-2.83E-03	1.23E-03	4.39E-04	-6.00E-06	2.68E-07	-1.54E-08
100	20	-2.81E-06	-3.29E-04	-3.40E-05	5.36E-06	1.22E-05	0.00E+00	-5.22E-03	2.26E-03	8.26E-04	-1.14E-05	5.04E-07	-2.90E-08
200	-20	-7.02E-07	3.21E-04	3.79E-05	1.72E-06	0.00E+00	0.00E+00	6.22E-03	-1.48E-03	-2.10E-04	6.92E-07	-5.02E-08	1.23E-08
200	-10	-7.02E-07	1.48E-04	1.74E-05	8.60E-07	0.00E+00	0.00E+00	2.79E-03	-6.71E-04	-9.68E-05	3.15E-07	-2.22E-08	5.95E-09
200	-5	-3.51E-07	7.12E-05	8.29E-06	2.87E-07	0.00E+00	0.00E+00	1.33E-03	-3.20E-04	-4.66E-05	1.51E-07	-1.04E-08	2.87E-09
200	5	7.02E-07	-6.68E-05	-7.90E-06	-2.87E-07	0.00E+00	0.00E+00	-1.21E-03	2.93E-04	4.34E-05	-1.39E-07	9.29E-09	-2.87E-09
200	10	1.05E-06	-1.29E-04	-1.54E-05	-5.74E-07	0.00E+00	0.00E+00	-2.32E-03	5.62E-04	8.40E-05	-2.68E-07	1.75E-08	-5.62E-09
200	20	2.46E-06	-2.43E-04	-2.88E-05	-1.15E-06	0.00E+00	0.00E+00	-4.28E-03	1.04E-03	1.58E-04	-4.97E-07	3.15E-08	-1.08E-08

Table D3.12 aqueous polystyrene: effect of change in *Cp*

MHz	%	c 10nm	c 100nm	c 1um	c 10um	c 100um	c 1mm	a 10nm	a 100nm	a 1um	a 10um	a 100um	a 1mm
0.1	-20	1.01E-02	1.01E-02	9.60E-03	1.36E-03	1.34E-04	1.37E-05	8.93E-02	-1.71E-01	-1.77E-01	-1.72E-01	-1.49E-01	-7.02E-03
0.1	-10	4.64E-03	4.64E-03	4.40E-03	6.28E-04	6.21E-05	6.53E-06	3.94E-02	-7.81E-02	-8.00E-02	-7.96E-02	-6.89E-02	-3.25E-03
0.1	-5	2.23E-03	2.23E-03	2.11E-03	3.03E-04	2.99E-05	3.09E-06	1.86E-02	-3.74E-02	-3.81E-02	-3.83E-02	-3.32E-02	-1.57E-03
0.1	5	-2.06E-03	-2.06E-03	-1.95E-03	-2.83E-04	-2.82E-05	-2.75E-06	-1.67E-02	3.45E-02	3.47E-02	3.57E-02	3.10E-02	1.47E-03
0.1	10	-3.96E-03	-3.96E-03	-3.76E-03	-5.47E-04	-5.45E-05	-5.50E-06	-3.18E-02	6.64E-02	6.65E-02	6.90E-02	6.00E-02	2.84E-03
0.1	20	-7.38E-03	-7.38E-03	-7.02E-03	-1.03E-03	-1.02E-04	-1.03E-05	-5.81E-02	1.23E-01	1.22E-01	1.29E-01	1.13E-01	5.33E-03
1	-20	9.21E-03	9.19E-03	4.15E-03	3.99E-04	4.06E-05	-1.89E-05	7.77E-02	-1.29E-01	-1.50E-01	-1.24E-01	-1.44E-02	1.30E-05
1	-10	4.19E-03	4.18E-03	1.91E-03	1.84E-04	1.86E-05	-8.67E-06	3.43E-02	-5.78E-02	-6.84E-02	-5.69E-02	-6.63E-03	5.93E-06
1	-5	2.00E-03	2.00E-03	9.17E-04	8.86E-05	8.94E-06	-4.19E-06	1.62E-02	-2.75E-02	-3.27E-02	-2.74E-02	-3.19E-03	2.85E-06
1	5	-1.84E-03	-1.84E-03	-8.50E-04	-8.23E-05	-8.60E-06	3.77E-06	-1.46E-02	2.50E-02	3.02E-02	2.54E-02	2.96E-03	-2.63E-06
1	10	-3.54E-03	-3.53E-03	-1.64E-03	-1.59E-04	-1.65E-05	7.27E-06	-2.78E-02	4.79E-02	5.81E-02	4.91E-02	5.72E-03	-5.08E-06
1	20	-6.58E-03	-6.56E-03	-3.07E-03	-2.97E-04	-3.06E-05	1.37E-05	-5.09E-02	8.79E-02	1.08E-01	9.18E-02	1.07E-02	-9.47E-06
10	-20	8.22E-03	7.85E-03	1.18E-03	1.20E-04	-3.54E-05	0.00E+00	6.87E-02	-9.18E-02	-9.80E-02	-1.78E-02	3.53E-05	-1.60E-06
10	-10	3.72E-03	3.56E-03	5.40E-04	5.48E-05	-1.61E-05	0.00E+00	3.04E-02	-4.07E-02	-4.48E-02	-8.14E-03	1.61E-05	-7.25E-07
10	-5	1.78E-03	1.70E-03	2.59E-04	2.62E-05	-7.80E-06	0.00E+00	1.44E-02	-1.93E-02	-2.15E-02	-3.91E-03	7.72E-06	-3.46E-07
10	5	-1.63E-03	-1.56E-03	-2.40E-04	-2.45E-05	7.16E-06	0.00E+00	-1.30E-02	1.73E-02	1.98E-02	3.62E-03	-7.13E-06	3.19E-07
10	10	-3.12E-03	-2.99E-03	-4.62E-04	-4.72E-05	1.37E-05	0.00E+00	-2.48E-02	3.30E-02	3.82E-02	6.97E-03	-1.37E-05	6.13E-07
10	20	-5.78E-03	-5.55E-03	-8.63E-04	-8.79E-05	2.56E-05	0.00E+00	-4.54E-02	6.01E-02	7.13E-02	1.30E-02	-2.56E-05	1.14E-06
100	-20	7.22E-03	3.65E-03	3.73E-04	-3.70E-05	0.00E+00	0.00E+00	6.38E-02	-5.64E-02	-1.08E-02	8.05E-05	-7.92E-07	3.43E-07
100	-10	3.26E-03	1.66E-03	1.70E-04	-1.68E-05	0.00E+00	0.00E+00	2.84E-02	-2.56E-02	-4.92E-03	3.67E-05	-3.37E-07	1.56E-07
100	-5	1.55E-03	7.97E-04	8.16E-05	-7.99E-06	0.00E+00	0.00E+00	1.35E-02	-1.22E-02	-2.36E-03	1.76E-05	-1.57E-07	7.44E-08
100	5	-1.42E-03	-7.34E-04	-7.54E-05	7.42E-06	0.00E+00	0.00E+00	-1.22E-02	1.12E-02	2.17E-03	-1.62E-05	1.38E-07	-6.84E-08
100	10	-2.72E-03	-1.41E-03	-1.45E-04	1.43E-05	0.00E+00	0.00E+00	-2.33E-02	2.15E-02	4.19E-03	-3.12E-05	2.60E-07	-1.32E-07
100	20	-5.02E-03	-2.63E-03	-2.70E-04	2.64E-05	0.00E+00	0.00E+00	-4.29E-02	3.98E-02	7.81E-03	-5.81E-05	4.67E-07	-2.44E-07
200	-20	6.28E-03	2.45E-03	2.85E-04	7.74E-06	0.00E+00	0.00E+00	5.75E-02	-2.67E-02	-2.44E-03	8.46E-06	1.94E-07	-1.39E-07
200	-10	2.82E-03	1.11E-03	1.30E-04	3.73E-06	0.00E+00	0.00E+00	2.57E-02	-1.21E-02	-1.11E-03	3.85E-06	7.69E-08	-6.10E-08
200	-5	1.34E-03	5.32E-04	6.21E-05	1.72E-06	0.00E+00	0.00E+00	1.22E-02	-5.78E-03	-5.31E-04	1.84E-06	3.45E-08	-2.87E-08
200	5	-1.23E-03	-4.89E-04	-5.69E-05	-1.72E-06	0.00E+00	0.00E+00	-1.11E-02	5.30E-03	4.90E-04	-1.70E-06	-2.83E-08	2.57E-08
200	10	-2.35E-03	-9.41E-04	-1.10E-04	-3.16E-06	0.00E+00	0.00E+00	-2.12E-02	1.02E-02	9.43E-04	-3.27E-06	-5.15E-08	4.89E-08
200	20	-4.33E-03	-1.75E-03	-2.04E-04	-5.74E-06	0.00E+00	0.00E+00	-3.91E-02	1.89E-02	1.75E-03	-6.08E-06	-8.63E-08	8.89E-08

Table D3.13 aqueous polystyrene: effect of change in *alpha*

MHz	%	c 10nm	c 100nm	c 1um	c 10um	c 100um	c 1mm	a 10nm	a 100nm	a 1um	a 10um	a 100um	a 1mm
0.1	-20	0.00E+00	0.00E+00	0.00E+00	-3.35E-07	0.00E+00	0.00E+00	2.45E-03	1.72E-04	5.29E-06	5.09E-05	4.56E-04	2.11E-04
0.1	-10	0.00E+00	0.00E+00	0.00E+00	-3.35E-07	0.00E+00	0.00E+00	1.22E-03	8.60E-05	2.65E-06	2.54E-05	2.28E-04	1.06E-04
0.1	-5	0.00E+00	0.00E+00	0.00E+00	-3.35E-07	0.00E+00	0.00E+00	6.04E-04	4.30E-05	1.32E-06	1.27E-05	1.14E-04	5.28E-05
0.1	5	0.00E+00	0.00E+00	0.00E+00	0.00E+00	0.00E+00	0.00E+00	-6.12E-04	-4.30E-05	-1.32E-06	-1.27E-05	-1.14E-04	-5.28E-05
0.1	10	0.00E+00	0.00E+00	0.00E+00	0.00E+00	0.00E+00	0.00E+00	-1.23E-03	-8.60E-05	-2.65E-06	-2.54E-05	-2.28E-04	-1.06E-04
0.1	20	0.00E+00	0.00E+00	0.00E+00	0.00E+00	0.00E+00	0.00E+00	-2.45E-03	-1.72E-04	-5.29E-06	-5.09E-05	-4.56E-04	-2.11E-04
1	-20	0.00E+00	0.00E+00	-1.36E-06	0.00E+00	0.00E+00	7.69E-06	2.45E-03	1.93E-04	1.51E-04	1.42E-03	1.48E-03	5.50E-06
1	-10	0.00E+00	0.00E+00	-6.81E-07	0.00E+00	0.00E+00	3.91E-06	1.22E-03	9.64E-05	7.54E-05	7.09E-04	7.41E-04	2.75E-06
1	-5	0.00E+00	0.00E+00	-3.40E-07	0.00E+00	0.00E+00	1.96E-06	6.12E-04	4.82E-05	3.77E-05	3.55E-04	3.70E-04	1.38E-06
1	5	0.00E+00	0.00E+00	3.40E-07	0.00E+00	0.00E+00	-1.82E-06	-6.12E-04	-4.82E-05	-3.77E-05	-3.55E-04	-3.70E-04	-1.38E-06
1	10	0.00E+00	0.00E+00	6.81E-07	0.00E+00	0.00E+00	-3.77E-06	-1.22E-03	-9.64E-05	-7.54E-05	-7.09E-04	-7.41E-04	-2.75E-06
1	20	0.00E+00	0.00E+00	1.02E-06	3.33E-07	0.00E+00	-7.55E-06	-2.45E-03	-1.93E-04	-1.51E-04	-1.42E-03	-1.48E-03	-5.50E-06
10	-20	-3.51E-07	-6.64E-06	-4.69E-06	-6.89E-07	6.45E-05	-8.85E-05	2.46E-03	4.83E-04	4.15E-03	6.44E-03	4.75E-05	3.11E-05
10	-10	0.00E+00	-3.50E-06	-2.34E-06	-3.45E-07	3.22E-05	-4.43E-05	1.23E-03	2.42E-04	2.07E-03	3.22E-03	2.37E-05	1.56E-05
10	-5	0.00E+00	-1.75E-06	-1.00E-06	-3.45E-07	1.61E-05	-2.95E-05	6.15E-04	1.21E-04	1.04E-03	1.61E-03	1.19E-05	7.78E-06
10	5	0.00E+00	1.40E-06	1.34E-06	0.00E+00	-1.61E-05	1.48E-05	-6.15E-04	-1.21E-04	-1.04E-03	-1.61E-03	-1.19E-05	-7.78E-06
10	10	0.00E+00	3.15E-06	2.34E-06	3.45E-07	-3.22E-05	2.95E-05	-1.23E-03	-2.42E-04	-2.07E-03	-3.22E-03	-2.37E-05	-1.56E-05
10	20	0.00E+00	6.30E-06	4.69E-06	6.89E-07	-6.43E-05	7.38E-05	-2.46E-03	-4.83E-04	-4.15E-03	-6.44E-03	-4.75E-05	-3.11E-05
100	-20	-9.12E-06	-1.28E-04	-1.91E-05	3.41E-04	-5.97E-04	3.55E-03	2.58E-03	8.61E-03	1.47E-02	3.21E-04	1.08E-04	-2.22E-04
100	-10	-4.56E-06	-6.39E-05	-9.72E-06	1.70E-04	-3.05E-04	2.03E-03	1.29E-03	4.31E-03	7.37E-03	1.60E-04	5.38E-05	-1.12E-04
100	-5	-2.10E-06	-3.18E-05	-4.86E-06	8.53E-05	-1.58E-04	1.01E-03	6.45E-04	2.15E-03	3.68E-03	8.01E-05	2.69E-05	-5.62E-05
100	5	2.10E-06	3.21E-05	4.86E-06	-8.50E-05	1.46E-04	-1.01E-03	-6.45E-04	-2.15E-03	-3.68E-03	-8.01E-05	-2.69E-05	5.67E-05
100	10	4.56E-06	6.42E-05	9.37E-06	-1.70E-04	2.92E-04	-2.03E-03	-1.29E-03	-4.30E-03	-7.37E-03	-1.60E-04	-5.38E-05	1.14E-04
100	20	9.12E-06	1.28E-04	1.91E-05	-3.40E-04	5.97E-04	-4.06E-03	-2.58E-03	-8.61E-03	-1.47E-02	-3.21E-04	-1.08E-04	2.30E-04
200	-20	-3.47E-05	-1.97E-04	-6.08E-05	-5.76E-04	1.24E-03	-1.27E-02	2.76E-03	1.47E-02	1.05E-02	7.33E-06	1.14E-04	-2.12E-04
200	-10	-1.75E-05	-9.87E-05	-3.04E-05	-2.88E-04	6.21E-04	-6.37E-03	1.38E-03	7.33E-03	5.27E-03	3.63E-06	5.67E-05	-1.10E-04
200	-5	-8.77E-06	-4.94E-05	-1.54E-05	-1.44E-04	3.10E-04	-3.82E-03	6.89E-04	3.67E-03	2.63E-03	1.81E-06	2.83E-05	-5.61E-05
200	5	8.77E-06	4.94E-05	1.50E-05	1.44E-04	-3.10E-04	3.82E-03	-6.89E-04	-3.67E-03	-2.63E-03	-1.79E-06	-2.81E-05	5.84E-05
200	10	1.72E-05	9.84E-05	3.04E-05	2.88E-04	-6.83E-04	6.37E-03	-1.38E-03	-7.33E-03	-5.27E-03	-3.56E-06	-5.59E-05	1.19E-04
200	20	3.47E-05	1.97E-04	6.08E-05	5.77E-04	-1.30E-03	1.40E-02	-2.76E-03	-1.47E-02	-1.05E-02	-7.05E-06	-1.11E-04	2.48E-04

Table D3.14 aqueous polystyrene: effect of change in *beta*

MHz	%	c 10nm	c 100nm	c 1um	c 10um	c 100um	c 1mm	a 10nm	a 100nm	a 1um	a 10um	a 100um	a 1mm
0.1	-20	-8.91E-03	-8.91E-03	-8.41E-03	-1.10E-03	-1.09E-04	-1.10E-05	-3.58E-03	1.58E-01	1.70E-01	1.43E-01	1.20E-01	5.67E-03
0.1	-10	-4.37E-03	-4.37E-03	-4.12E-03	-5.38E-04	-5.32E-05	-5.15E-06	-6.81E-03	7.71E-02	8.32E-02	6.99E-02	5.89E-02	2.78E-03
0.1	-5	-2.16E-03	-2.16E-03	-2.04E-03	-2.66E-04	-2.63E-05	-2.40E-06	-4.47E-03	3.81E-02	4.12E-02	3.46E-02	2.91E-02	1.37E-03
0.1	5	2.12E-03	2.12E-03	2.00E-03	2.60E-04	2.56E-05	2.75E-06	6.31E-03	-3.71E-02	-4.03E-02	-3.38E-02	-2.85E-02	-1.34E-03
0.1	10	4.19E-03	4.19E-03	3.95E-03	5.15E-04	5.08E-05	5.50E-06	1.42E-02	-7.34E-02	-7.98E-02	-6.70E-02	-5.65E-02	-2.66E-03
0.1	20	8.20E-03	8.20E-03	7.73E-03	1.01E-03	9.97E-05	1.03E-05	3.41E-02	-1.43E-01	-1.56E-01	-1.31E-01	-1.10E-01	-5.21E-03
1	-20	-9.84E-03	-9.82E-03	-4.07E-03	-3.83E-04	-3.92E-05	1.75E-05	-3.68E-02	2.01E-01	2.13E-01	1.50E-01	1.42E-02	-1.20E-05
1	-10	-4.79E-03	-4.78E-03	-1.98E-03	-1.86E-04	-1.93E-05	8.53E-06	-2.26E-02	9.73E-02	1.04E-01	7.30E-02	6.89E-03	-5.90E-06
1	-5	-2.36E-03	-2.36E-03	-9.78E-04	-9.19E-05	-9.63E-06	4.33E-06	-1.22E-02	4.79E-02	5.12E-02	3.60E-02	3.40E-03	-2.92E-06
1	5	2.30E-03	2.30E-03	9.52E-04	8.92E-05	8.94E-06	-4.19E-06	1.37E-02	-4.64E-02	-4.98E-02	-3.50E-02	-3.31E-03	2.87E-06
1	10	4.54E-03	4.53E-03	1.88E-03	1.76E-04	1.79E-05	-8.25E-06	2.88E-02	-9.14E-02	-9.83E-02	-6.91E-02	-6.52E-03	5.70E-06
1	20	8.82E-03	8.80E-03	3.65E-03	3.43E-04	3.47E-05	-1.64E-05	6.24E-02	-1.77E-01	-1.91E-01	-1.34E-01	-1.27E-02	1.12E-05
10	-20	-1.06E-02	-1.00E-02	-1.34E-03	-1.36E-04	4.08E-05	-1.48E-05	-6.88E-02	2.49E-01	1.79E-01	2.16E-02	-4.07E-05	1.02E-06
10	-10	-5.12E-03	-4.84E-03	-6.45E-04	-6.58E-05	2.01E-05	-1.48E-05	-3.78E-02	1.20E-01	8.64E-02	1.04E-02	-1.99E-05	5.46E-07
10	-5	-2.51E-03	-2.38E-03	-3.17E-04	-3.24E-05	9.98E-06	0.00E+00	-1.97E-02	5.86E-02	4.24E-02	5.11E-03	-9.83E-06	2.81E-07
10	5	2.42E-03	2.29E-03	3.06E-04	3.10E-05	-9.72E-06	0.00E+00	2.09E-02	-5.62E-02	-4.08E-02	-4.92E-03	9.61E-06	-2.98E-07
10	10	4.76E-03	4.50E-03	6.00E-04	6.10E-05	-1.92E-05	0.00E+00	4.30E-02	-1.10E-01	-8.01E-02	-9.65E-03	1.90E-05	-6.13E-07
10	20	9.15E-03	8.65E-03	1.15E-03	1.17E-04	-3.77E-05	1.48E-05	9.01E-02	-2.10E-01	-1.54E-01	-1.86E-02	3.71E-05	-1.29E-06
100	-20	-1.11E-02	-5.01E-03	-4.97E-04	5.47E-05	-3.66E-05	0.00E+00	-9.91E-02	1.34E-01	1.51E-02	-1.13E-04	3.66E-06	-5.52E-07
100	-10	-5.27E-03	-2.40E-03	-2.39E-04	2.75E-05	-2.44E-05	0.00E+00	-5.23E-02	6.27E-02	7.09E-03	-5.48E-05	1.99E-06	-2.71E-07
100	-5	-2.57E-03	-1.17E-03	-1.17E-04	1.38E-05	-1.22E-05	0.00E+00	-2.68E-02	3.03E-02	3.44E-03	-2.70E-05	1.04E-06	-1.34E-07
100	5	2.44E-03	1.12E-03	1.12E-04	-1.37E-05	1.22E-05	0.00E+00	2.78E-02	-2.83E-02	-3.22E-03	2.61E-05	-1.12E-06	1.32E-07
100	10	4.75E-03	2.19E-03	2.19E-04	-2.74E-05	1.22E-05	0.00E+00	5.66E-02	-5.46E-02	-6.24E-03	5.13E-05	-2.31E-06	2.62E-07
100	20	8.97E-03	4.17E-03	4.18E-04	-5.48E-05	3.66E-05	0.00E+00	1.17E-01	-1.01E-01	-1.16E-02	9.91E-05	-4.94E-06	5.14E-07
200	-20	-1.10E-02	-3.94E-03	-4.52E-04	-4.88E-06	-1.24E-04	0.00E+00	-1.24E-01	4.97E-02	3.17E-03	-1.24E-05	-3.08E-06	8.72E-07
200	-10	-5.12E-03	-1.87E-03	-2.15E-04	-2.01E-06	-6.20E-05	0.00E+00	-6.43E-02	2.19E-02	1.41E-03	-5.79E-06	-1.65E-06	4.53E-07
200	-5	-2.47E-03	-9.10E-04	-1.05E-04	-8.60E-07	0.00E+00	0.00E+00	-3.27E-02	1.03E-02	6.65E-04	-2.79E-06	-8.50E-07	2.31E-07
200	5	2.28E-03	8.59E-04	9.94E-05	5.74E-07	6.20E-05	0.00E+00	3.36E-02	-8.84E-03	-5.82E-04	2.59E-06	9.03E-07	-2.39E-07
200	10	4.38E-03	1.67E-03	1.93E-04	5.74E-07	1.24E-04	0.00E+00	6.80E-02	-1.63E-02	-1.08E-03	4.98E-06	1.86E-06	-4.87E-07
200	20	8.02E-03	3.13E-03	3.62E-04	2.87E-07	1.86E-04	0.00E+00	1.39E-01	-2.70E-02	-1.84E-03	9.12E-06	3.93E-06	-1.01E-06

Table D3.15 aqueous 1-bromo-hexadecane: effect of change in *c'*

MHz	%	c 10nm	c 100nm	c 1um	c 10um	c 100um	c 1mm	a 10nm	a 100nm	a 1um	a 10um	a 100um	a 1mm
0.1	-20	1.51E+00	1.51E+00	1.54E+00	2.13E+00	2.32E+00	2.38E+00	-8.59E-01	-4.93E-02	-4.09E-02	-4.14E-02	-4.01E-02	3.71E+00
0.1	-10	6.53E-01	6.53E-01	6.66E-01	9.22E-01	1.00E+00	1.02E+00	-3.23E-01	-2.08E-02	-1.77E-02	-1.79E-02	-1.75E-02	1.17E+00
0.1	-5	3.05E-01	3.05E-01	3.11E-01	4.31E-01	4.69E-01	4.76E-01	-1.42E-01	-9.62E-03	-8.25E-03	-8.35E-03	-8.19E-03	4.73E-01
0.1	5	-2.69E-01	-2.69E-01	-2.74E-01	-3.79E-01	-4.13E-01	-4.17E-01	1.13E-01	8.35E-03	7.26E-03	7.36E-03	7.25E-03	-3.15E-01
0.1	10	-5.06E-01	-5.06E-01	-5.16E-01	-7.15E-01	-7.79E-01	-7.85E-01	2.05E-01	1.56E-02	1.37E-02	1.39E-02	1.37E-02	-5.17E-01
0.1	20	-9.05E-01	-9.05E-01	-9.23E-01	-1.28E+00	-1.39E+00	-1.40E+00	3.40E-01	2.77E-02	2.45E-02	2.48E-02	2.45E-02	-7.09E-01
1	-20	1.21E+01	1.22E+01	-1.36E+01	-4.72E+00	-4.47E+00	-3.65E+00	-3.39E-01	-3.47E-02	-3.06E-02	-3.10E-02	1.38E+00	1.86E+01
1	-10	5.19E+00	5.23E+00	-5.81E+00	-2.02E+00	-1.90E+00	-1.55E+00	-1.27E-01	-1.46E-02	-1.31E-02	-1.32E-02	3.35E-01	2.61E+00
1	-5	2.41E+00	2.44E+00	-2.70E+00	-9.42E-01	-8.85E-01	-7.16E-01	-5.59E-02	-6.75E-03	-6.09E-03	-6.13E-03	1.11E-01	2.70E-01
1	5	-2.11E+00	-2.13E+00	2.37E+00	8.25E-01	7.72E-01	6.02E-01	4.44E-02	5.84E-03	5.33E-03	5.34E-03	-3.63E-02	1.10E+00
1	10	-3.97E+00	-4.01E+00	4.45E+00	1.55E+00	1.45E+00	1.10E+00	8.02E-02	1.09E-02	1.00E-02	1.00E-02	-2.31E-02	3.04E+00
1	20	-7.07E+00	-7.13E+00	7.92E+00	2.76E+00	2.57E+00	1.84E+00	1.33E-01	1.93E-02	1.78E-02	1.78E-02	8.85E-02	7.97E+00
10	-20	-1.48E+00	-1.43E+00	-9.80E-01	-9.20E-01	-8.47E-01	4.32E-01	-1.58E-01	-2.47E-02	-2.23E-02	-8.74E-03	-8.74E-01	-7.14E-01
10	-10	-6.28E-01	-6.08E-01	-4.17E-01	-3.89E-01	-3.27E-01	-1.21E+00	-5.92E-02	-1.03E-02	-9.27E-03	-3.88E-02	-6.40E-01	1.55E-02
10	-5	-2.92E-01	-2.82E-01	-1.93E-01	-1.80E-01	-1.44E-01	-4.60E-01	-2.60E-02	-4.76E-03	-4.26E-03	-2.41E-02	-3.37E-01	-2.94E-01
10	5	2.54E-01	2.46E-01	1.69E-01	1.57E-01	1.12E-01	-4.82E-01	2.06E-02	4.10E-03	3.65E-03	2.93E-02	3.36E-01	1.76E-01
10	10	4.77E-01	4.61E-01	3.16E-01	2.94E-01	1.99E-01	-8.40E-01	3.71E-02	7.66E-03	6.79E-03	6.11E-02	6.53E-01	3.46E-02
10	20	8.46E-01	8.19E-01	5.61E-01	5.21E-01	3.22E-01	-3.50E-01	6.12E-02	1.35E-02	1.19E-02	1.26E-01	1.20E+00	-1.05E-01
100	-20	-5.82E-01	-4.99E-01	-4.40E-01	-3.29E-01	1.07E-01	-2.41E-01	-8.00E-02	-1.48E-02	-2.40E-02	-6.55E-01	-1.69E-01	7.27E-03
100	-10	-2.46E-01	-2.11E-01	-1.86E-01	-1.18E-01	-6.04E-01	3.26E-03	-2.97E-02	-5.64E-03	-1.19E-02	-2.99E-01	2.27E-01	-9.35E-03
100	-5	-1.14E-01	-9.78E-02	-8.59E-02	-5.10E-02	-5.63E-01	-5.10E-02	-1.30E-02	-2.49E-03	-5.74E-03	-1.40E-01	5.09E-03	-7.53E-03
100	5	9.90E-02	8.49E-02	7.44E-02	3.92E-02	1.31E-01	1.66E-02	1.02E-02	1.98E-03	5.23E-03	1.22E-01	1.44E-01	-3.60E-03
100	10	1.85E-01	1.59E-01	1.39E-01	6.99E-02	-1.78E-01	-7.18E-02	1.83E-02	3.56E-03	9.92E-03	2.28E-01	2.19E-01	-1.73E-02
100	20	3.28E-01	2.82E-01	2.46E-01	1.14E-01	-4.78E-01	-1.34E-01	2.99E-02	5.83E-03	1.77E-02	3.99E-01	8.70E-02	2.89E-03
200	-20	-3.15E-01	-2.73E-01	-2.44E-01	1.55E-01	4.06E-01	-4.01E-02	-3.93E-02	-2.93E-04	-1.74E-01	-1.51E-01	-4.17E-03	-1.14E-03
200	-10	-1.33E-01	-1.15E-01	-1.02E-01	6.53E-02	3.36E-01	1.18E-02	-1.43E-02	8.57E-04	-8.02E-02	-3.78E-02	2.82E-03	-4.44E-04
200	-5	-6.13E-02	-5.31E-02	-4.70E-02	2.84E-02	-2.85E-02	2.36E-03	-6.21E-03	5.92E-04	-3.82E-02	-1.36E-02	6.93E-02	9.22E-04
200	5	5.30E-02	4.60E-02	4.05E-02	-2.10E-02	3.08E-01	-5.19E-02	4.78E-03	-8.11E-04	3.46E-02	7.77E-03	4.51E-02	3.98E-04
200	10	9.93E-02	8.61E-02	7.57E-02	-3.63E-02	-7.25E-02	-2.24E-02	8.48E-03	-1.77E-03	6.58E-02	1.24E-02	5.42E-02	1.40E-04
200	20	1.75E-01	1.52E-01	1.33E-01	-5.59E-02	2.37E-01	-1.77E-02	1.36E-02	-3.91E-03	1.19E-01	1.74E-02	3.01E-02	3.60E-04

Table D3.16 aqueous 1-bromo-hexadecane: effect of change in *rho'*

MHz	%	c 10nm	c 100nm	c 1um	c 10um	c 100um	c 1mm	a 10nm	a 100nm	a 1um	a 10um	a 100um	a 1mm
0.1	-20	5.19E-01	5.19E-01	5.29E-01	5.22E-01	4.46E-01	4.55E-01	-2.00E-01	1.41E-01	1.84E-01	1.21E+00	1.39E+00	1.70E+00
0.1	-10	2.19E-01	2.19E-01	2.23E-01	2.14E-01	1.84E-01	1.87E-01	-7.89E-02	6.63E-02	8.64E-02	5.02E-01	5.62E-01	6.58E-01
0.1	-5	1.00E-01	1.00E-01	1.02E-01	9.75E-02	8.38E-02	8.51E-02	-3.55E-02	3.19E-02	4.18E-02	2.28E-01	2.53E-01	2.92E-01
0.1	5	-8.51E-02	-8.51E-02	-8.66E-02	-8.12E-02	-7.04E-02	-7.15E-02	2.95E-02	-2.94E-02	-3.87E-02	-1.87E-01	-2.03E-01	-2.32E-01
0.1	10	-1.57E-01	-1.57E-01	-1.59E-01	-1.49E-01	-1.30E-01	-1.32E-01	5.45E-02	-5.61E-02	-7.42E-02	-3.38E-01	-3.64E-01	-4.15E-01
0.1	20	-2.65E-01	-2.65E-01	-2.70E-01	-2.50E-01	-2.21E-01	-2.24E-01	9.57E-02	-1.01E-01	-1.35E-01	-5.43E-01	-5.76E-01	-6.68E-01
1	-20	4.69E-01	4.69E-01	5.10E-01	3.84E-01	3.77E-01	3.99E-02	-1.14E-01	1.44E-01	7.26E-01	1.76E+00	2.32E+00	7.83E-01
1	-10	1.85E-01	1.85E-01	1.97E-01	1.52E-01	1.50E-01	2.21E-02	-4.70E-02	6.30E-02	2.95E-01	6.19E-01	8.26E-01	3.45E-01
1	-5	8.19E-02	8.20E-02	8.65E-02	6.78E-02	6.70E-02	1.17E-02	-2.19E-02	2.92E-02	1.32E-01	2.54E-01	3.47E-01	1.62E-01
1	5	-6.36E-02	-6.36E-02	-6.57E-02	-5.44E-02	-5.43E-02	-1.28E-02	1.99E-02	-2.43E-02	-1.03E-01	-1.61E-01	-2.39E-01	-1.43E-01
1	10	-1.11E-01	-1.11E-01	-1.14E-01	-9.77E-02	-9.81E-02	-2.66E-02	3.88E-02	-4.38E-02	-1.78E-01	-2.41E-01	-3.91E-01	-2.68E-01
1	20	-1.66E-01	-1.66E-01	-1.66E-01	-1.58E-01	-1.61E-01	-5.67E-02	7.68E-02	-6.76E-02	-2.52E-01	-2.05E-01	-4.89E-01	-4.70E-01
10	-20	2.76E-01	2.84E-01	2.59E-01	2.55E-01	7.01E-02	1.44E-01	-9.10E-02	1.46E-01	4.78E-01	7.43E-01	1.12E+00	5.91E-03
10	-10	8.63E-02	8.93E-02	8.67E-02	9.42E-02	3.78E-02	7.06E-02	-4.38E-02	5.47E-02	-3.51E-03	9.13E-02	4.65E-01	4.06E-03
10	-5	3.22E-02	3.34E-02	3.48E-02	4.05E-02	1.95E-02	3.49E-02	-2.21E-02	2.26E-02	-5.33E-02	-1.06E-02	2.11E-01	2.25E-03
10	5	-1.34E-02	-1.41E-02	-2.11E-02	-2.99E-02	-2.03E-02	-3.40E-02	2.35E-02	-1.31E-02	1.41E-01	1.02E-01	-1.72E-01	-2.61E-03
10	10	-1.06E-02	-1.15E-02	-3.10E-02	-5.13E-02	-4.11E-02	-6.71E-02	4.89E-02	-1.66E-02	3.57E-01	2.79E-01	-3.08E-01	-5.51E-03
10	20	3.57E-02	3.52E-02	-2.54E-02	-7.44E-02	-8.29E-02	-1.31E-01	1.08E-01	5.39E-03	9.70E-01	8.04E-01	-4.84E-01	-1.20E-02
100	-20	-1.11E-02	-2.66E-02	1.00E-01	1.05E-01	1.94E-01	1.04E-01	-1.20E-01	-1.56E-01	-3.49E-01	1.04E+00	1.39E-02	-9.12E-05
100	-10	-4.76E-02	-5.52E-02	2.44E-02	5.32E-02	9.36E-02	5.52E-02	-6.56E-02	-1.63E-01	-2.54E-01	3.59E-01	7.67E-03	-1.79E-05
100	-5	-3.26E-02	-3.61E-02	7.28E-03	2.65E-02	4.59E-02	2.82E-02	-3.46E-02	-1.02E-01	-1.42E-01	1.44E-01	3.97E-03	1.02E-05
100	5	4.77E-02	5.00E-02	4.26E-04	-2.60E-02	-4.43E-02	-2.90E-02	3.88E-02	1.38E-01	1.67E-01	-8.06E-02	-4.16E-03	-6.62E-05
100	10	1.08E-01	1.11E-01	6.89E-03	-5.10E-02	-8.69E-02	-5.80E-02	8.22E-02	3.10E-01	3.54E-01	-1.06E-01	-8.45E-03	-1.95E-04
100	20	2.61E-01	2.60E-01	3.30E-02	-9.72E-02	-1.67E-01	-1.14E-01	1.84E-01	7.48E-01	7.71E-01	-2.13E-02	-1.73E-02	-6.19E-04
200	-20	-2.29E-01	-1.98E-01	-2.30E-02	4.53E-02	-1.37E-01	1.56E-01	-1.80E-01	-5.25E-01	-4.28E-01	1.27E-01	9.87E-03	2.91E-04
200	-10	-1.42E-01	-1.19E-01	-2.68E-02	2.28E-02	-6.15E-02	7.56E-02	-1.01E-01	-3.10E-01	-2.45E-01	3.95E-02	5.23E-03	1.55E-04
200	-5	-7.64E-02	-6.35E-02	-1.62E-02	1.13E-02	-2.91E-02	3.67E-02	-5.38E-02	-1.65E-01	-1.28E-01	1.48E-02	2.67E-03	8.00E-05
200	5	8.59E-02	6.91E-02	2.03E-02	-1.09E-02	2.59E-02	-3.67E-02	6.04E-02	1.83E-01	1.36E-01	-6.36E-03	-2.74E-03	-8.42E-05
200	10	1.80E-01	1.42E-01	4.35E-02	-2.12E-02	4.89E-02	-7.34E-02	1.28E-01	3.82E-01	2.77E-01	-5.75E-03	-5.51E-03	-1.72E-04
200	20	3.86E-01	2.96E-01	9.58E-02	-4.01E-02	8.75E-02	-1.45E-01	2.83E-01	8.20E-01	5.67E-01	1.18E-02	-1.11E-02	-3.60E-04

Table D3.17 aqueous 1-bromo-hexadecane: effect of change in *eta'*

MHz	%	c 10nm	c 100nm	c 1um	c 10um	c 100um	c 1mm	a 10nm	a 100nm	a 1um	a 10um	a 100um	a 1mm
0.1	-20	0.00E+00	0.00E+00	-4.66E-06	-1.75E-03	-1.71E-04	-1.71E-05	1.41E-01	2.27E-03	1.17E-03	1.74E-05	-1.68E-02	-3.72E-03
0.1	-10	0.00E+00	0.00E+00	-2.07E-06	-8.11E-04	-8.01E-05	-7.96E-06	7.11E-02	1.10E-03	5.33E-04	3.01E-04	-7.88E-03	-1.74E-03
0.1	-5	0.00E+00	0.00E+00	-1.04E-06	-3.91E-04	-3.89E-05	-3.79E-06	3.57E-02	5.44E-04	2.55E-04	2.09E-04	-3.83E-03	-8.42E-04
0.1	5	0.00E+00	0.00E+00	7.77E-07	3.65E-04	3.66E-05	3.79E-06	-3.59E-02	-5.33E-04	-2.35E-04	-3.02E-04	3.62E-03	7.93E-04
0.1	10	0.00E+00	0.00E+00	1.55E-06	7.06E-04	7.13E-05	7.58E-06	-7.20E-02	-1.06E-03	-4.52E-04	-6.78E-04	7.04E-03	1.54E-03
0.1	20	0.00E+00	0.00E+00	3.11E-06	1.32E-03	1.36E-04	1.40E-05	-1.45E-01	-2.08E-03	-8.40E-04	-1.60E-03	1.34E-02	2.92E-03
1	-20	0.00E+00	0.00E+00	-2.10E-04	-4.38E-04	-5.37E-05	-1.58E-05	2.05E-01	2.75E-03	3.83E-03	-1.43E-02	-6.29E-03	-1.66E-05
1	-10	0.00E+00	0.00E+00	-9.45E-05	-2.04E-04	-2.53E-05	-7.88E-06	1.03E-01	1.34E-03	1.74E-03	-6.84E-03	-2.89E-03	-7.42E-06
1	-5	0.00E+00	0.00E+00	-4.49E-05	-9.87E-05	-1.21E-05	-3.94E-06	5.17E-02	6.65E-04	8.35E-04	-3.35E-03	-1.39E-03	-3.51E-06
1	5	0.00E+00	0.00E+00	4.10E-05	9.27E-05	1.13E-05	3.45E-06	-5.20E-02	-6.54E-04	-7.70E-04	3.23E-03	1.29E-03	3.17E-06
1	10	0.00E+00	0.00E+00	7.83E-05	1.80E-04	2.23E-05	6.89E-06	-1.04E-01	-1.30E-03	-1.48E-03	6.35E-03	2.49E-03	6.02E-06
1	20	0.00E+00	2.55E-07	1.44E-04	3.42E-04	4.24E-05	1.38E-05	-2.09E-01	-2.56E-03	-2.76E-03	1.23E-02	4.64E-03	1.09E-05
10	-20	0.00E+00	-4.15E-06	-1.52E-03	-1.68E-04	-1.23E-04	-1.24E-05	3.30E-01	4.15E-03	5.81E-03	-7.01E-04	4.38E-05	-1.92E-05
10	-10	0.00E+00	-1.81E-06	-6.95E-04	-7.93E-05	-6.05E-05	-6.19E-06	1.66E-01	2.04E-03	3.01E-03	4.46E-06	2.48E-05	-9.57E-06
10	-5	0.00E+00	-7.77E-07	-3.33E-04	-3.87E-05	-3.00E-05	-6.19E-06	8.31E-02	1.01E-03	1.52E-03	8.15E-05	1.30E-05	-4.78E-06
10	5	0.00E+00	7.77E-07	3.07E-04	3.61E-05	3.05E-05	0.00E+00	-8.34E-02	-9.99E-04	-1.55E-03	-2.25E-04	-1.42E-05	4.77E-06
10	10	0.00E+00	1.55E-06	5.93E-04	7.10E-05	6.01E-05	6.19E-06	-1.67E-01	-1.99E-03	-3.10E-03	-5.79E-04	-2.95E-05	9.53E-06
10	20	0.00E+00	2.85E-06	1.10E-03	1.35E-04	1.19E-04	6.19E-06	-3.35E-01	-3.94E-03	-6.22E-03	-1.63E-03	-6.28E-05	1.90E-05
100	-20	7.39E-06	-1.99E-04	-7.31E-04	-1.35E-03	6.60E-06	0.00E+00	7.43E-01	2.30E-02	3.81E-02	1.30E-03	-2.23E-04	-2.11E-05
100	-10	4.08E-06	-8.91E-05	-3.60E-04	-6.75E-04	6.60E-06	0.00E+00	3.73E-01	1.14E-02	1.95E-02	6.62E-04	-1.11E-04	-1.05E-05
100	-5	2.04E-06	-4.24E-05	-1.79E-04	-3.37E-04	0.00E+00	0.00E+00	1.87E-01	5.68E-03	9.86E-03	3.34E-04	-5.58E-05	-5.25E-06
100	5	-2.55E-06	3.84E-05	1.77E-04	3.38E-04	0.00E+00	0.00E+00	-1.87E-01	-5.65E-03	-1.01E-02	-3.40E-04	5.59E-05	5.24E-06
100	10	-4.84E-06	7.35E-05	3.54E-04	6.76E-04	0.00E+00	0.00E+00	-3.75E-01	-1.13E-02	-2.03E-02	-6.85E-04	1.12E-04	1.05E-05
100	20	-1.04E-05	1.34E-04	7.06E-04	1.35E-03	-6.60E-06	0.00E+00	-7.52E-01	-2.24E-02	-4.14E-02	-1.39E-03	2.24E-04	2.09E-05
200	-20	4.84E-05	-4.84E-04	-1.11E-03	-2.23E-03	-1.74E-03	0.00E+00	7.30E+00	6.52E-02	7.87E-02	-7.76E-05	-2.39E-04	-2.74E-05
200	-10	2.63E-05	-2.16E-04	-5.53E-04	-1.12E-03	-8.70E-04	0.00E+00	3.66E+00	3.25E-02	3.98E-02	-3.23E-05	-1.19E-04	-1.37E-05
200	-5	1.35E-05	-1.02E-04	-2.76E-04	-5.60E-04	-4.35E-04	0.00E+00	1.83E+00	1.62E-02	2.00E-02	-1.47E-05	-5.95E-05	-6.85E-06
200	5	-1.45E-05	9.21E-05	2.76E-04	5.62E-04	4.35E-04	0.00E+00	-1.84E+00	-1.62E-02	-2.02E-02	1.20E-05	5.95E-05	6.85E-06
200	10	-3.01E-05	1.75E-04	5.51E-04	1.13E-03	8.70E-04	0.00E+00	-3.68E+00	-3.24E-02	-4.05E-02	2.14E-05	1.19E-04	1.37E-05
200	20	-6.40E-05	3.17E-04	1.10E-03	2.26E-03	1.80E-03	0.00E+00	-7.37E+00	-6.46E-02	-8.16E-02	3.34E-05	2.38E-04	2.74E-05

Table D3.18 aqueous 1-bromo-hexadecane: effect of change in *kappa'*

MHz	%	c 10nm	c 100nm	c 1um	c 10um	c 100um	c 1mm	a 10nm	a 100nm	a 1um	a 10um	a 100um	a 1mm
0.1	-20	0.00E+00	-5.09E-07	-3.42E-03	-3.79E-03	-4.07E-04	-4.05E-05	1.08E-01	1.13E-01	1.29E-01	-4.66E-02	-4.55E-02	-9.49E-03
0.1	-10	0.00E+00	-2.55E-07	-1.47E-03	-1.82E-03	-1.95E-04	-1.93E-05	4.82E-02	5.02E-02	5.84E-02	-2.23E-02	-2.18E-02	-4.56E-03
0.1	-5	0.00E+00	-2.55E-07	-6.84E-04	-8.92E-04	-9.57E-05	-9.47E-06	2.28E-02	2.38E-02	2.79E-02	-1.09E-02	-1.07E-02	-2.23E-03
0.1	5	0.00E+00	0.00E+00	6.02E-04	8.60E-04	9.23E-05	9.47E-06	-2.06E-02	-2.15E-02	-2.55E-02	1.05E-02	1.03E-02	2.15E-03
0.1	10	0.00E+00	0.00E+00	1.13E-03	1.69E-03	1.81E-04	1.86E-05	-3.94E-02	-4.11E-02	-4.89E-02	2.06E-02	2.03E-02	4.23E-03
0.1	20	0.00E+00	2.55E-07	2.03E-03	3.27E-03	3.51E-04	3.56E-05	-7.22E-02	-7.53E-02	-9.05E-02	3.97E-02	3.92E-02	8.19E-03
1	-20	0.00E+00	-3.52E-05	-1.29E-02	-1.33E-03	-1.35E-04	-1.08E-05	9.82E-02	1.11E-01	-4.44E-02	-4.61E-02	-2.11E-02	-5.97E-05
1	-10	0.00E+00	-1.50E-05	-6.26E-03	-6.36E-04	-6.50E-05	-5.42E-06	4.37E-02	4.95E-02	-1.99E-02	-2.21E-02	-1.01E-02	-2.86E-05
1	-5	0.00E+00	-6.88E-06	-3.09E-03	-3.12E-04	-3.18E-05	-2.46E-06	2.07E-02	2.34E-02	-9.39E-03	-1.08E-02	-4.95E-03	-1.40E-05
1	5	0.00E+00	6.37E-06	3.00E-03	3.00E-04	3.06E-05	2.46E-06	-1.87E-02	-2.12E-02	8.36E-03	1.04E-02	4.77E-03	1.35E-05
1	10	0.00E+00	1.17E-05	5.91E-03	5.90E-04	6.01E-05	4.92E-06	-3.57E-02	-4.05E-02	1.57E-02	2.05E-02	9.36E-03	2.66E-05
1	20	0.00E+00	2.09E-05	1.15E-02	1.14E-03	1.16E-04	9.85E-06	-6.55E-02	-7.43E-02	2.78E-02	3.96E-02	1.81E-02	5.14E-05
10	-20	-2.55E-07	-1.92E-03	-4.16E-03	-4.46E-04	-3.69E-05	-1.86E-05	9.04E-02	1.17E-01	-4.59E-02	-3.20E-02	-1.96E-04	1.95E-06
10	-10	0.00E+00	-8.23E-04	-1.99E-03	-2.14E-04	-1.77E-05	-6.19E-06	4.02E-02	5.23E-02	-2.19E-02	-1.53E-02	-9.40E-05	9.34E-07
10	-5	0.00E+00	-3.84E-04	-9.78E-04	-1.05E-04	-8.86E-06	0.00E+00	1.90E-02	2.49E-02	-1.07E-02	-7.50E-03	-4.60E-05	4.58E-07
10	5	0.00E+00	3.37E-04	9.42E-04	1.01E-04	8.37E-06	6.19E-06	-1.72E-02	-2.26E-02	1.03E-02	7.22E-03	4.43E-05	-4.41E-07
10	10	0.00E+00	6.36E-04	1.85E-03	1.98E-04	1.62E-05	1.24E-05	-3.29E-02	-4.33E-02	2.01E-02	1.42E-02	8.70E-05	-8.65E-07
10	20	0.00E+00	1.14E-03	3.58E-03	3.83E-04	3.15E-05	1.86E-05	-6.03E-02	-7.98E-02	3.88E-02	2.74E-02	1.68E-04	-1.67E-06
100	-20	-1.15E-05	-1.43E-02	-1.47E-03	-1.24E-04	-7.92E-05	0.00E+00	8.87E-02	-1.86E-02	-3.27E-02	-6.14E-04	5.20E-06	-9.40E-07
100	-10	-4.84E-06	-6.81E-03	-7.02E-04	-5.97E-05	-3.96E-05	0.00E+00	3.94E-02	-6.70E-03	-1.56E-02	-2.94E-04	2.49E-06	-4.50E-07
100	-5	-2.29E-06	-3.32E-03	-3.43E-04	-2.91E-05	-1.98E-05	0.00E+00	1.87E-02	-2.77E-03	-7.65E-03	-1.44E-04	1.22E-06	-2.20E-07
100	5	1.78E-06	3.16E-03	3.30E-04	2.81E-05	1.32E-05	0.00E+00	-1.69E-02	1.75E-03	7.35E-03	1.38E-04	-1.17E-06	2.12E-07
100	10	3.57E-06	6.17E-03	6.49E-04	5.52E-05	3.30E-05	0.00E+00	-3.23E-02	2.60E-03	1.44E-02	2.72E-04	-2.30E-06	4.16E-07
100	20	6.37E-06	1.17E-02	1.25E-03	1.06E-04	6.60E-05	0.00E+00	-5.92E-02	2.07E-03	2.78E-02	5.24E-04	-4.44E-06	8.03E-07
200	-20	-2.93E-05	-1.05E-02	-1.08E-03	-4.94E-05	3.75E-04	0.00E+00	8.33E-02	-3.93E-02	-1.57E-02	-3.44E-04	-1.30E-05	-5.96E-07
200	-10	-1.22E-05	-5.10E-03	-5.17E-04	-2.32E-05	1.88E-04	0.00E+00	3.70E-02	-1.80E-02	-7.52E-03	-1.64E-04	-6.22E-06	-2.85E-07
200	-5	-5.61E-06	-2.51E-03	-2.53E-04	-1.16E-05	1.25E-04	0.00E+00	1.75E-02	-8.64E-03	-3.68E-03	-8.05E-05	-3.05E-06	-1.39E-07
200	5	4.84E-06	2.44E-03	2.43E-04	1.10E-05	-6.25E-05	0.00E+00	-1.59E-02	7.91E-03	3.53E-03	7.73E-05	2.93E-06	1.34E-07
200	10	9.18E-06	4.82E-03	4.77E-04	2.21E-05	-1.25E-04	0.00E+00	-3.03E-02	1.51E-02	6.93E-03	1.52E-04	5.74E-06	2.63E-07
200	20	1.61E-05	9.37E-03	9.20E-04	4.24E-05	-3.13E-04	0.00E+00	-5.56E-02	2.76E-02	1.34E-02	2.93E-04	1.11E-05	5.08E-07

Table D3.19 aqueous 1-bromo-hexadecane: effect of change in *Cp'*

MHz	%	c 10nm	c 100nm	c 1um	c 10um	c 100um	c 1mm	a 10nm	a 100nm	a 1um	a 10um	a 100um	a 1mm
0.1	-20	8.73E-02	8.73E-02	8.96E-02	2.39E-02	2.59E-03	2.60E-04	4.67E-02	6.10E-02	8.90E-02	3.00E-01	2.89E-01	6.04E-02
0.1	-10	3.88E-02	3.88E-02	3.98E-02	1.02E-02	1.10E-03	1.11E-04	2.27E-02	3.04E-02	4.43E-02	1.28E-01	1.23E-01	2.57E-02
0.1	-5	1.84E-02	1.84E-02	1.88E-02	4.72E-03	5.11E-04	5.15E-05	1.12E-02	1.52E-02	2.21E-02	5.98E-02	5.72E-02	1.19E-02
0.1	5	-1.66E-02	-1.66E-02	-1.70E-02	-4.12E-03	-4.46E-04	-4.47E-05	-1.09E-02	-1.51E-02	-2.19E-02	-5.24E-02	-4.99E-02	-1.04E-02
0.1	10	-3.17E-02	-3.17E-02	-3.25E-02	-7.73E-03	-8.37E-04	-8.41E-05	-2.17E-02	-3.01E-02	-4.36E-02	-9.86E-02	-9.37E-02	-1.95E-02
0.1	20	-5.80E-02	-5.80E-02	-5.94E-02	-1.38E-02	-1.49E-03	-1.49E-04	-4.24E-02	-6.00E-02	-8.64E-02	-1.76E-01	-1.67E-01	-3.48E-02
1	-20	7.70E-02	7.71E-02	5.23E-02	5.90E-03	6.00E-04	4.92E-05	5.34E-02	7.79E-02	3.80E-01	2.58E-01	1.03E-01	2.65E-04
1	-10	3.42E-02	3.42E-02	2.21E-02	2.50E-03	2.55E-04	2.12E-05	2.60E-02	3.87E-02	1.66E-01	1.10E-01	4.35E-02	1.12E-04
1	-5	1.62E-02	1.62E-02	1.02E-02	1.16E-03	1.18E-04	9.85E-06	1.28E-02	1.93E-02	7.77E-02	5.09E-02	2.02E-02	5.20E-05
1	5	-1.46E-02	-1.46E-02	-8.89E-03	-1.01E-03	-1.03E-04	-8.37E-06	-1.25E-02	-1.91E-02	-6.89E-02	-4.43E-02	-1.76E-02	-4.53E-05
1	10	-2.79E-02	-2.79E-02	-1.67E-02	-1.89E-03	-1.93E-04	-1.58E-05	-2.48E-02	-3.81E-02	-1.30E-01	-8.32E-02	-3.30E-02	-8.50E-05
1	20	-5.10E-02	-5.10E-02	-2.95E-02	-3.36E-03	-3.42E-04	-2.81E-05	-4.84E-02	-7.54E-02	-2.34E-01	-1.48E-01	-5.85E-02	-1.51E-04
10	-20	6.72E-02	6.87E-02	1.30E-02	1.37E-03	1.13E-04	6.81E-05	6.07E-02	1.45E-01	2.33E-01	1.29E-01	6.03E-04	-5.99E-06
10	-10	2.98E-02	3.04E-02	5.50E-03	5.80E-04	4.78E-05	3.10E-05	2.95E-02	7.12E-02	9.91E-02	5.46E-02	2.55E-04	-2.53E-06
10	-5	1.41E-02	1.43E-02	2.55E-03	2.69E-04	2.22E-05	1.24E-05	1.45E-02	3.52E-02	4.60E-02	2.53E-02	1.18E-04	-1.17E-06
10	5	-1.27E-02	-1.29E-02	-2.21E-03	-2.33E-04	-1.92E-05	-1.24E-05	-1.41E-02	-3.45E-02	-4.01E-02	-2.20E-02	-1.02E-04	1.02E-06
10	10	-2.42E-02	-2.45E-02	-4.14E-03	-4.37E-04	-3.59E-05	-1.86E-05	-2.79E-02	-6.83E-02	-7.53E-02	-4.12E-02	-1.92E-04	1.91E-06
10	20	-4.42E-02	-4.46E-02	-7.33E-03	-7.74E-04	-6.40E-05	-3.72E-05	-5.43E-02	-1.33E-01	-1.34E-01	-7.29E-02	-3.40E-04	3.38E-06
100	-20	5.79E-02	2.85E-02	3.12E-03	2.61E-04	1.65E-04	0.00E+00	6.57E-02	3.44E-01	1.04E-01	1.31E-03	-1.11E-05	1.99E-06
100	-10	2.56E-02	1.20E-02	1.31E-03	1.10E-04	7.26E-05	0.00E+00	3.17E-02	1.47E-01	4.39E-02	5.51E-04	-4.68E-06	8.39E-07
100	-5	1.21E-02	5.55E-03	6.08E-04	5.08E-05	3.30E-05	0.00E+00	1.55E-02	6.84E-02	2.03E-02	2.55E-04	-2.16E-06	3.88E-07
100	5	-1.09E-02	-4.80E-03	-5.26E-04	-4.39E-05	-2.64E-05	0.00E+00	-1.50E-02	-5.99E-02	-1.76E-02	-2.20E-04	1.86E-06	-3.36E-07
100	10	-2.07E-02	-8.99E-03	-9.85E-04	-8.24E-05	-4.62E-05	0.00E+00	-2.94E-02	-1.13E-01	-3.28E-02	-4.12E-04	3.48E-06	-6.29E-07
100	20	-3.77E-02	-1.59E-02	-1.74E-03	-1.46E-04	-8.58E-05	0.00E+00	-5.68E-02	-2.00E-01	-5.79E-02	-7.26E-04	6.12E-06	-1.11E-06
200	-20	4.90E-02	1.48E-02	1.57E-03	7.03E-05	-5.60E-04	0.00E+00	6.98E-02	2.13E-01	2.82E-02	4.98E-04	1.88E-05	8.56E-07
200	-10	2.16E-02	6.23E-03	6.59E-04	3.02E-05	-2.49E-04	0.00E+00	3.32E-02	8.98E-02	1.18E-02	2.08E-04	7.92E-06	3.60E-07
200	-5	1.02E-02	2.88E-03	3.04E-04	1.39E-05	-1.24E-04	0.00E+00	1.62E-02	4.15E-02	5.43E-03	9.60E-05	3.66E-06	1.66E-07
200	5	-9.12E-03	-2.48E-03	-2.63E-04	-1.22E-05	6.22E-05	0.00E+00	-1.53E-02	-3.59E-02	-4.67E-03	-8.26E-05	-3.17E-06	-1.44E-07
200	10	-1.73E-02	-4.64E-03	-4.91E-04	-2.27E-05	1.87E-04	0.00E+00	-2.99E-02	-6.71E-02	-8.70E-03	-1.54E-04	-5.92E-06	-2.68E-07
200	20	-3.14E-02	-8.18E-03	-8.66E-04	-4.01E-05	3.11E-04	0.00E+00	-5.66E-02	-1.18E-01	-1.52E-02	-2.71E-04	-1.05E-05	-4.73E-07

Table D3.20 aqueous 1-bromo-hexadecane: effect of change in *alpha'*

MHz	%	c 10nm	c 100nm	c 1um	c 10um	c 100um	c 1mm	a 10nm	a 100nm	a 1um	a 10um	a 100um	a 1mm
0.1	-20	0.00E+00	0.00E+00	-5.18E-07	0.00E+00	0.00E+00	3.79E-07	-4.27E-02	-4.46E-04	-9.12E-06	-3.88E-05	-3.76E-04	-7.85E-04
0.1	-10	0.00E+00	0.00E+00	-2.59E-07	0.00E+00	0.00E+00	0.00E+00	-2.14E-02	-2.23E-04	-4.56E-06	-1.94E-05	-1.88E-04	-3.92E-04
0.1	-5	0.00E+00	0.00E+00	-2.59E-07	0.00E+00	0.00E+00	0.00E+00	-1.07E-02	-1.12E-04	-2.28E-06	-9.70E-06	-9.40E-05	-1.96E-04
0.1	5	0.00E+00	0.00E+00	0.00E+00	3.52E-07	0.00E+00	0.00E+00	1.07E-02	1.12E-04	2.28E-06	9.70E-06	9.40E-05	1.96E-04
0.1	10	0.00E+00	0.00E+00	0.00E+00	3.52E-07	0.00E+00	0.00E+00	2.14E-02	2.23E-04	4.56E-06	1.94E-05	1.88E-04	3.92E-04
0.1	20	0.00E+00	0.00E+00	2.59E-07	3.52E-07	0.00E+00	0.00E+00	4.27E-02	4.46E-04	9.12E-06	3.88E-05	3.76E-04	7.85E-04
1	-20	0.00E+00	-5.09E-07	-8.56E-06	-1.50E-06	3.78E-07	2.17E-05	-4.96E-02	-5.93E-04	-1.83E-04	-1.43E-03	-6.37E-03	-1.23E-04
1	-10	0.00E+00	-2.55E-07	-4.28E-06	-7.48E-07	3.78E-07	1.08E-05	-2.48E-02	-2.97E-04	-9.14E-05	-7.17E-04	-3.18E-03	-6.13E-05
1	-5	0.00E+00	-2.55E-07	-2.14E-06	-3.74E-07	0.00E+00	5.42E-06	-1.24E-02	-1.48E-04	-4.57E-05	-3.59E-04	-1.59E-03	-3.06E-05
1	5	0.00E+00	0.00E+00	1.83E-06	3.74E-07	0.00E+00	-5.42E-06	1.24E-02	1.48E-04	4.57E-05	3.59E-04	1.59E-03	3.06E-05
1	10	0.00E+00	2.55E-07	3.98E-06	3.74E-07	0.00E+00	-1.08E-05	2.48E-02	2.97E-04	9.14E-05	7.17E-04	3.18E-03	6.13E-05
1	20	0.00E+00	5.09E-07	8.26E-06	1.12E-06	0.00E+00	-2.22E-05	4.96E-02	5.93E-04	1.83E-04	1.43E-03	6.37E-03	1.23E-04
10	-20	-7.64E-07	-4.69E-05	-4.43E-05	-3.01E-06	2.62E-04	2.72E-03	-5.81E-02	-1.31E-03	-5.49E-03	-3.47E-02	-1.46E-03	5.44E-04
10	-10	-5.09E-07	-2.36E-05	-2.21E-05	-1.50E-06	1.31E-04	1.36E-03	-2.91E-02	-6.54E-04	-2.74E-03	-1.73E-02	-7.28E-04	2.72E-04
10	-5	-2.55E-07	-1.17E-05	-1.09E-05	-7.52E-07	6.55E-05	6.78E-04	-1.45E-02	-3.27E-04	-1.37E-03	-8.66E-03	-3.64E-04	1.36E-04
10	5	0.00E+00	1.17E-05	1.12E-05	1.13E-06	-6.55E-05	-6.78E-04	1.45E-02	3.27E-04	1.37E-03	8.66E-03	3.64E-04	-1.36E-04
10	10	2.55E-07	2.36E-05	2.21E-05	1.88E-06	-1.31E-04	-1.36E-03	2.91E-02	6.55E-04	2.74E-03	1.73E-02	7.28E-04	-2.72E-04
10	20	5.09E-07	4.69E-05	4.46E-05	3.38E-06	-2.62E-04	-2.71E-03	5.81E-02	1.31E-03	5.49E-03	3.47E-02	1.46E-03	-5.43E-04
100	-20	-7.54E-05	-1.21E-03	-1.68E-04	3.15E-03	3.32E-02	8.68E-02	-7.19E-02	-2.42E-02	-1.10E-01	-1.61E-02	6.22E-03	-9.84E-04
100	-10	-3.77E-05	-6.06E-04	-8.37E-05	1.58E-03	1.65E-02	4.05E-02	-3.59E-02	-1.21E-02	-5.50E-02	-8.04E-03	3.09E-03	-4.45E-04
100	-5	-1.88E-05	-3.03E-04	-4.20E-05	7.89E-04	8.19E-03	1.96E-02	-1.80E-02	-6.05E-03	-2.75E-02	-4.02E-03	1.54E-03	-2.12E-04
100	5	1.86E-05	3.03E-04	4.13E-05	-7.89E-04	-8.13E-03	-1.80E-02	1.80E-02	6.05E-03	2.75E-02	4.02E-03	-1.54E-03	1.93E-04
100	10	3.74E-05	6.05E-04	8.25E-05	-1.58E-03	-1.62E-02	-3.47E-02	3.59E-02	1.21E-02	5.50E-02	8.03E-03	-3.06E-03	3.68E-04
100	20	7.49E-05	1.21E-03	1.64E-04	-3.16E-03	-3.21E-02	-6.43E-02	7.19E-02	2.42E-02	1.10E-01	1.60E-02	-6.09E-03	6.72E-04
200	-20	-3.41E-04	-2.34E-03	1.08E-04	1.35E-02	5.63E-01	4.80E-03	-8.54E-02	-6.58E-02	-1.39E-01	-1.92E-02	1.16E-02	1.89E-05
200	-10	-1.70E-04	-1.17E-03	5.74E-05	6.73E-03	2.71E-01	1.60E-03	-4.27E-02	-3.29E-02	-6.96E-02	-9.58E-03	5.58E-03	1.69E-05
200	-5	-8.51E-05	-5.85E-04	2.94E-05	3.36E-03	1.33E-01	0.00E+00	-2.14E-02	-1.65E-02	-3.48E-02	-4.78E-03	2.74E-03	9.69E-06
200	5	8.48E-05	5.84E-04	-3.12E-05	-3.35E-03	-1.28E-01	0.00E+00	2.14E-02	1.65E-02	3.48E-02	4.77E-03	-2.64E-03	-1.14E-05
200	10	1.70E-04	1.17E-03	-6.42E-05	-6.70E-03	-2.52E-01	0.00E+00	4.27E-02	3.29E-02	6.96E-02	9.52E-03	-5.20E-03	-2.39E-05
200	20	3.39E-04	2.33E-03	-1.35E-04	-1.34E-02	-4.85E-01	-1.60E-03	8.54E-02	6.58E-02	1.39E-01	1.90E-02	-1.00E-02	-5.11E-05

Table D3.21 aqueous 1-bromo-hexadecane: effect of change in *beta'*

MHz	%	c 10nm	c 100nm	c 1um	c 10um	c 100um	c 1mm	a 10nm	a 100nm	a 1um	a 10um	a 100um	a 1mm
0.1	-20	-1.08E-01	-1.08E-01	-1.03E-01	-1.86E-02	-2.02E-03	-2.02E-04	-4.82E-01	-3.89E-01	-3.86E-01	-2.45E-01	-2.26E-01	-4.71E-02
0.1	-10	-5.77E-02	-5.77E-02	-5.50E-02	-9.92E-03	-1.07E-03	-1.08E-04	-2.57E-01	-2.07E-01	-2.05E-01	-1.31E-01	-1.21E-01	-2.51E-02
0.1	-5	-2.97E-02	-2.97E-02	-2.83E-02	-5.11E-03	-5.54E-04	-5.53E-05	-1.32E-01	-1.07E-01	-1.06E-01	-6.73E-02	-6.22E-02	-1.29E-02
0.1	5	3.14E-02	3.14E-02	2.99E-02	5.42E-03	5.87E-04	5.91E-05	1.40E-01	1.13E-01	1.12E-01	7.13E-02	6.59E-02	1.37E-02
0.1	10	6.45E-02	6.45E-02	6.15E-02	1.11E-02	1.21E-03	1.22E-04	2.87E-01	2.32E-01	2.30E-01	1.47E-01	1.36E-01	2.82E-02
0.1	20	1.36E-01	1.36E-01	1.29E-01	2.35E-02	2.55E-03	2.56E-04	6.02E-01	4.88E-01	4.84E-01	3.09E-01	2.86E-01	5.95E-02
1	-20	-1.41E-01	-1.40E-01	-7.34E-02	-9.21E-03	-9.49E-04	-7.78E-05	-4.43E-01	-3.85E-01	-3.60E-01	-2.65E-01	-1.33E-01	-4.18E-04
1	-10	-7.45E-02	-7.44E-02	-3.90E-02	-4.90E-03	-5.05E-04	-4.14E-05	-2.34E-01	-2.05E-01	-1.91E-01	-1.41E-01	-7.09E-02	-2.23E-04
1	-5	-3.83E-02	-3.83E-02	-2.01E-02	-2.52E-03	-2.60E-04	-2.12E-05	-1.20E-01	-1.05E-01	-9.85E-02	-7.26E-02	-3.65E-02	-1.15E-04
1	5	4.04E-02	4.03E-02	2.12E-02	2.67E-03	2.75E-04	2.27E-05	1.26E-01	1.11E-01	1.04E-01	7.68E-02	3.87E-02	1.21E-04
1	10	8.29E-02	8.27E-02	4.36E-02	5.49E-03	5.65E-04	4.63E-05	2.59E-01	2.28E-01	2.14E-01	1.58E-01	7.94E-02	2.49E-04
1	20	1.74E-01	1.74E-01	9.18E-02	1.16E-02	1.19E-03	9.80E-05	5.42E-01	4.79E-01	4.50E-01	3.33E-01	1.67E-01	5.25E-04
10	-20	-1.74E-01	-1.68E-01	-3.85E-02	-4.37E-03	-3.62E-04	-2.17E-04	-4.15E-01	-3.81E-01	-3.02E-01	-2.27E-01	-1.94E-03	1.94E-05
10	-10	-9.22E-02	-8.91E-02	-2.04E-02	-2.32E-03	-1.92E-04	-1.18E-04	-2.19E-01	-2.02E-01	-1.60E-01	-1.21E-01	-1.03E-03	1.03E-05
10	-5	-4.74E-02	-4.57E-02	-1.05E-02	-1.20E-03	-9.89E-05	-6.19E-05	-1.12E-01	-1.04E-01	-8.25E-02	-6.21E-02	-5.29E-04	5.29E-06
10	5	4.98E-02	4.81E-02	1.11E-02	1.26E-03	1.04E-04	6.19E-05	1.18E-01	1.09E-01	8.72E-02	6.56E-02	5.60E-04	-5.60E-06
10	10	1.02E-01	9.86E-02	2.28E-02	2.60E-03	2.15E-04	1.24E-04	2.40E-01	2.24E-01	1.79E-01	1.35E-01	1.15E-03	-1.15E-05
10	20	2.13E-01	2.06E-01	4.80E-02	5.46E-03	4.52E-04	2.66E-04	5.02E-01	4.69E-01	3.77E-01	2.84E-01	2.42E-03	-2.42E-05
100	-20	-2.07E-01	-1.28E-01	-1.92E-02	-1.64E-03	-1.04E-03	-3.43E-04	-3.95E-01	-3.64E-01	-2.66E-01	-8.54E-03	7.71E-05	-1.28E-05
100	-10	-1.09E-01	-6.78E-02	-1.02E-02	-8.70E-04	-5.53E-04	0.00E+00	-2.08E-01	-1.93E-01	-1.41E-01	-4.53E-03	4.09E-05	-6.77E-06
100	-5	-5.59E-02	-3.48E-02	-5.25E-03	-4.47E-04	-2.83E-04	0.00E+00	-1.06E-01	-9.91E-02	-7.27E-02	-2.33E-03	2.10E-05	-3.48E-06
100	5	5.86E-02	3.67E-02	5.54E-03	4.73E-04	3.03E-04	0.00E+00	1.11E-01	1.04E-01	7.67E-02	2.46E-03	-2.22E-05	3.66E-06
100	10	1.20E-01	7.52E-02	1.14E-02	9.69E-04	6.19E-04	0.00E+00	2.27E-01	2.14E-01	1.58E-01	5.05E-03	-4.56E-05	7.51E-06
100	20	2.50E-01	1.58E-01	2.39E-02	2.04E-03	1.30E-03	0.00E+00	4.73E-01	4.49E-01	3.31E-01	1.06E-02	-9.60E-05	1.57E-05
200	-20	-2.36E-01	-1.29E-01	-1.93E-02	-7.55E-04	7.68E-03	0.00E+00	-3.79E-01	-3.53E-01	-2.01E-01	-6.71E-03	-2.29E-04	-1.10E-05
200	-10	-1.24E-01	-6.82E-02	-1.02E-02	-3.99E-04	4.06E-03	0.00E+00	-1.99E-01	-1.87E-01	-1.06E-01	-3.56E-03	-1.21E-04	-5.81E-06
200	-5	-6.33E-02	-3.50E-02	-5.26E-03	-2.05E-04	2.09E-03	0.00E+00	-1.02E-01	-9.59E-02	-5.47E-02	-1.83E-03	-6.19E-05	-2.98E-06
200	5	6.61E-02	3.69E-02	5.54E-03	2.15E-04	-2.22E-03	1.52E-03	1.06E-01	1.01E-01	5.78E-02	1.93E-03	6.49E-05	3.14E-06
200	10	1.35E-01	7.56E-02	1.14E-02	4.40E-04	-4.57E-03	1.52E-03	2.17E-01	2.07E-01	1.19E-01	3.96E-03	1.33E-04	6.44E-06
200	20	2.80E-01	1.58E-01	2.39E-02	9.20E-04	-9.64E-03	1.52E-03	4.51E-01	4.34E-01	2.49E-01	8.32E-03	2.77E-04	1.35E-05

Table D3.22 aqueous 1-bromo-hexadecane: effect of change in *c*

MHz	%	c 10nm	c 100nm	c 1um	c 10um	c 100um	c 1mm	a 10nm	a 100nm	a 1um	a 10um	a 100um	a 1mm
0.1	-20	-1.14E+00	-1.14E+00	-1.15E+00	-1.43E+00	-1.52E+00	-1.52E+00	9.89E-02	-1.47E-01	-1.47E-01	1.13E-02	3.17E-02	-6.66E-01
0.1	-10	-6.47E-01	-6.47E-01	-6.54E-01	-8.14E-01	-8.70E-01	-8.74E-01	3.96E-02	-7.26E-02	-7.25E-02	5.55E-04	9.91E-03	-4.29E-01
0.1	-5	-3.43E-01	-3.43E-01	-3.47E-01	-4.33E-01	-4.62E-01	-4.65E-01	1.81E-02	-3.60E-02	-3.60E-02	-7.45E-04	3.76E-03	-2.24E-01
0.1	5	3.82E-01	3.82E-01	3.86E-01	4.84E-01	5.18E-01	5.22E-01	-1.57E-02	3.53E-02	3.53E-02	2.42E-03	-1.79E-03	2.28E-01
0.1	10	8.02E-01	8.02E-01	8.12E-01	1.02E+00	1.09E+00	1.10E+00	-2.96E-02	7.00E-02	6.99E-02	6.19E-03	-1.94E-03	4.50E-01
0.1	20	1.76E+00	1.76E+00	1.78E+00	2.25E+00	2.41E+00	2.43E+00	-5.44E-02	1.37E-01	1.37E-01	1.69E-02	1.54E-03	8.60E-01
1	-20	-1.14E+00	-1.14E+00	-1.29E+00	-1.50E+00	-1.52E+00	-1.62E+00	1.01E-01	-1.46E-01	-1.07E-01	2.70E-02	-4.45E-01	-7.29E-01
1	-10	-6.47E-01	-6.47E-01	-7.32E-01	-8.57E-01	-8.72E-01	-9.43E-01	4.06E-02	-7.22E-02	-5.42E-02	7.76E-03	-2.90E-01	-8.54E-01
1	-5	-3.43E-01	-3.43E-01	-3.88E-01	-4.55E-01	-4.64E-01	-4.98E-01	1.86E-02	-3.58E-02	-2.72E-02	2.72E-03	-1.52E-01	-5.23E-01
1	5	3.82E-01	3.82E-01	4.34E-01	5.10E-01	5.21E-01	5.38E-01	-1.61E-02	3.52E-02	2.71E-02	-8.08E-04	1.55E-01	6.66E-01
1	10	8.02E-01	8.03E-01	9.13E-01	1.07E+00	1.10E+00	1.11E+00	-3.05E-02	6.96E-02	5.41E-02	-4.48E-05	3.07E-01	1.43E+00
1	20	1.76E+00	1.76E+00	2.01E+00	2.37E+00	2.43E+00	2.30E+00	-5.62E-02	1.36E-01	1.07E-01	5.14E-03	5.88E-01	3.10E+00
10	-20	-1.14E+00	-1.15E+00	-1.43E+00	-1.52E+00	-1.62E+00	-1.28E+00	1.08E-01	-1.43E-01	1.25E-02	-1.95E-01	-7.26E-01	-2.71E-01
10	-10	-6.47E-01	-6.54E-01	-8.14E-01	-8.68E-01	-9.43E-01	-1.67E+00	4.38E-02	-7.08E-02	9.95E-04	-1.34E-01	-8.50E-01	-9.57E-01
10	-5	-3.43E-01	-3.47E-01	-4.32E-01	-4.62E-01	-4.98E-01	-3.19E+00	2.01E-02	-3.52E-02	-5.57E-04	-7.10E-02	-5.20E-01	-1.24E-01
10	5	3.82E-01	3.86E-01	4.84E-01	5.19E-01	5.38E-01	8.03E-02	-1.76E-02	3.46E-02	2.27E-03	7.38E-02	6.62E-01	-4.00E-01
10	10	8.02E-01	8.12E-01	1.02E+00	1.09E+00	1.11E+00	-1.61E+00	-3.34E-02	6.85E-02	5.93E-03	1.47E-01	1.42E+00	-2.83E-01
10	20	1.76E+00	1.78E+00	2.25E+00	2.42E+00	2.30E+00	6.32E-01	-6.17E-02	1.34E-01	1.64E-02	2.85E-01	3.09E+00	-2.46E-01
100	-20	-1.14E+00	-1.29E+00	-1.49E+00	-1.62E+00	-1.26E+00	-4.91E-01	1.32E-01	-9.57E-02	-2.53E-02	-7.04E-01	-2.66E-01	5.37E-03
100	-10	-6.47E-01	-7.31E-01	-8.54E-01	-9.41E-01	-1.68E+00	-4.50E+00	5.45E-02	-4.92E-02	-3.28E-02	-8.18E-01	-9.32E-01	2.97E-01
100	-5	-3.43E-01	-3.88E-01	-4.55E-01	-4.97E-01	-3.24E+00	-1.15E+00	2.53E-02	-2.48E-02	-1.92E-02	-5.01E-01	-1.25E-01	1.09E-02
100	5	3.82E-01	4.33E-01	5.10E-01	5.37E-01	1.16E-01	-1.61E-01	-2.24E-02	2.50E-02	2.24E-02	6.36E-01	-3.86E-01	-9.58E-03
100	10	8.03E-01	9.12E-01	1.08E+00	1.10E+00	-1.55E+00	1.28E-01	-4.28E-02	4.99E-02	4.63E-02	1.37E+00	-2.81E-01	-9.89E-04
100	20	1.76E+00	2.01E+00	2.38E+00	2.30E+00	6.56E-01	3.21E-01	-7.98E-02	9.94E-02	9.49E-02	2.97E+00	-2.32E-01	-9.75E-04
200	-20	-1.14E+00	-1.33E+00	-1.48E+00	-1.63E+00	-2.73E+00	-9.74E-01	1.46E-01	-4.91E-02	-3.24E-01	-4.13E-01	-8.28E-02	-2.71E-01
200	-10	-6.47E-01	-7.57E-01	-8.56E-01	-9.32E-01	4.27E+00	-1.82E-01	6.08E-02	-2.83E-02	-2.26E-01	-8.80E-01	-7.47E-01	-6.48E-02
200	-5	-3.43E-01	-4.02E-01	-4.57E-01	-4.61E-01	-5.36E+00	-2.02E-01	2.83E-02	-1.48E-02	-1.21E-01	-5.65E-01	3.89E-02	-5.77E-04
200	5	3.82E-01	4.49E-01	5.17E-01	4.02E-01	-2.59E+00	9.71E-02	-2.53E-02	1.58E-02	1.29E-01	7.07E-01	-2.03E-01	6.44E-04
200	10	8.03E-01	9.46E-01	1.09E+00	7.11E-01	-4.02E+00	3.41E-01	-4.85E-02	3.22E-02	2.58E-01	1.46E+00	-1.31E-02	7.39E-04
200	20	1.76E+00	2.08E+00	2.42E+00	9.83E-01	-4.51E+00	7.24E-01	-9.05E-02	6.60E-02	5.07E-01	2.86E+00	-3.80E-02	2.07E-03

Table D3.23 aqueous 1-bromo-hexadecane: effect of change in *rho*

MHz	%	c 10nm	c 100nm	c 1um	c 10um	c 100um	c 1mm	a 10nm	a 100nm	a 1um	a 10um	a 100um	a 1mm
0.1	-20	-3.05E-01	-3.05E-01	-3.06E-01	-2.84E-01	-2.56E-01	-2.60E-01	-1.20E-01	-2.93E-01	-2.86E-01	-5.60E-01	-5.94E-01	-7.43E-01
0.1	-10	-1.71E-01	-1.71E-01	-1.72E-01	-1.59E-01	-1.41E-01	-1.43E-01	-6.93E-02	-1.54E-01	-1.51E-01	-3.39E-01	-3.62E-01	-4.43E-01
0.1	-5	-8.92E-02	-8.92E-02	-8.96E-02	-8.33E-02	-7.36E-02	-7.49E-02	-3.66E-02	-7.85E-02	-7.68E-02	-1.80E-01	-1.93E-01	-2.38E-01
0.1	5	9.53E-02	9.53E-02	9.58E-02	8.98E-02	7.92E-02	8.07E-02	3.99E-02	8.11E-02	7.91E-02	1.97E-01	2.10E-01	2.70E-01
0.1	10	1.96E-01	1.96E-01	1.97E-01	1.85E-01	1.64E-01	1.67E-01	8.27E-02	1.64E-01	1.60E-01	4.06E-01	4.33E-01	5.71E-01
0.1	20	4.08E-01	4.08E-01	4.11E-01	3.90E-01	3.46E-01	3.54E-01	1.75E-01	3.35E-01	3.25E-01	8.50E-01	9.01E-01	1.26E+00
1	-20	-3.41E-01	-3.41E-01	-3.52E-01	-3.08E-01	-3.07E-01	-2.65E-02	-1.72E-01	-2.93E-01	-3.81E-01	-5.50E-01	-6.16E-01	-3.79E-01
1	-10	-1.80E-01	-1.80E-01	-1.87E-01	-1.64E-01	-1.64E-01	-1.12E-02	-9.23E-02	-1.50E-01	-1.98E-01	-2.91E-01	-3.40E-01	-1.89E-01
1	-5	-9.18E-02	-9.18E-02	-9.58E-02	-8.45E-02	-8.48E-02	-5.36E-03	-4.74E-02	-7.58E-02	-1.00E-01	-1.48E-01	-1.77E-01	-9.40E-02
1	5	9.47E-02	9.47E-02	9.93E-02	8.87E-02	8.94E-02	5.18E-03	4.95E-02	7.67E-02	1.02E-01	1.50E-01	1.90E-01	9.34E-02
1	10	1.92E-01	1.92E-01	2.01E-01	1.81E-01	1.83E-01	1.04E-02	1.01E-01	1.54E-01	2.05E-01	3.00E-01	3.93E-01	1.86E-01
1	20	3.91E-01	3.91E-01	4.12E-01	3.76E-01	3.82E-01	2.17E-02	2.07E-01	3.10E-01	4.13E-01	5.98E-01	8.32E-01	3.72E-01
10	-20	-3.34E-01	-3.35E-01	-3.35E-01	-3.27E-01	-2.59E-02	-6.01E-02	-1.97E-01	-2.79E-01	-4.47E-01	-4.88E-01	-3.27E-01	2.06E-02
10	-10	-1.71E-01	-1.72E-01	-1.74E-01	-1.72E-01	-1.33E-02	-2.45E-02	-1.02E-01	-1.40E-01	-2.25E-01	-2.54E-01	-1.63E-01	1.13E-02
10	-5	-8.63E-02	-8.67E-02	-8.82E-02	-8.77E-02	-6.86E-03	-1.10E-02	-5.18E-02	-7.01E-02	-1.13E-01	-1.29E-01	-8.13E-02	5.81E-03
10	5	8.73E-02	8.77E-02	9.04E-02	9.11E-02	7.36E-03	8.63E-03	5.29E-02	6.99E-02	1.11E-01	1.33E-01	8.15E-02	-6.07E-03
10	10	1.75E-01	1.76E-01	1.82E-01	1.85E-01	1.52E-02	1.51E-02	1.07E-01	1.39E-01	2.21E-01	2.69E-01	1.63E-01	-1.23E-02
10	20	3.52E-01	3.54E-01	3.71E-01	3.81E-01	3.23E-02	2.22E-02	2.16E-01	2.77E-01	4.33E-01	5.50E-01	3.29E-01	-2.51E-02
100	-20	-3.12E-01	-3.23E-01	-3.27E-01	-3.47E-02	-3.68E-02	-1.33E-02	-1.94E-01	-3.07E-01	-3.70E-01	-2.97E-01	2.71E-02	-3.70E-04
100	-10	-1.57E-01	-1.63E-01	-1.69E-01	-1.82E-02	-1.26E-02	-4.55E-03	-9.85E-02	-1.52E-01	-1.85E-01	-1.50E-01	1.39E-02	-1.47E-04
100	-5	-7.85E-02	-8.20E-02	-8.55E-02	-9.28E-03	-5.04E-03	-1.62E-03	-4.94E-02	-7.54E-02	-9.21E-02	-7.52E-02	6.97E-03	-6.73E-05
100	5	7.84E-02	8.22E-02	8.75E-02	9.45E-03	2.80E-03	9.74E-04	4.96E-02	7.43E-02	9.14E-02	7.61E-02	-6.95E-03	5.96E-05
100	10	1.57E-01	1.64E-01	1.77E-01	1.89E-02	3.64E-03	1.62E-03	9.93E-02	1.47E-01	1.82E-01	1.53E-01	-1.38E-02	1.15E-04
100	20	3.11E-01	3.28E-01	3.59E-01	3.67E-02	5.47E-04	9.74E-04	1.98E-01	2.89E-01	3.61E-01	3.10E-01	-2.71E-02	2.19E-04
200	-20	-2.85E-01	-2.99E-01	-3.34E-01	9.13E-02	-1.38E+00	-2.78E-02	-1.89E-01	-2.83E-01	-4.47E-01	-1.56E-01	1.37E-02	-1.16E-05
200	-10	-1.42E-01	-1.50E-01	-1.72E-01	4.41E-02	-6.18E-01	-1.19E-02	-9.44E-02	-1.38E-01	-2.41E-01	-7.51E-02	7.15E-03	-5.32E-06
200	-5	-7.07E-02	-7.47E-02	-8.71E-02	2.17E-02	-2.92E-01	-5.30E-03	-4.70E-02	-6.78E-02	-1.25E-01	-3.70E-02	3.60E-03	-2.58E-06
200	5	7.00E-02	7.44E-02	8.90E-02	-2.12E-02	2.60E-01	6.62E-03	4.66E-02	6.58E-02	1.34E-01	3.59E-02	-3.56E-03	2.47E-06
200	10	1.39E-01	1.48E-01	1.80E-01	-4.19E-02	4.91E-01	1.06E-02	9.27E-02	1.30E-01	2.78E-01	7.09E-02	-7.01E-03	4.86E-06
200	20	2.75E-01	2.94E-01	3.65E-01	-8.23E-02	8.83E-01	1.85E-02	1.83E-01	2.52E-01	5.95E-01	1.38E-01	-1.35E-02	9.47E-06

Table D3.24 aqueous 1-bromo-hexadecane: effect of change in *eta*

MHz	%	c 10nm	c 100nm	c 1um	c 10um	c 100um	c 1mm	a 10nm	a 100nm	a 1um	a 10um	a 100um	a 1mm
0.1	-20	0.00E+00	-5.09E-07	-2.33E-04	-3.16E-03	-2.84E-04	-2.80E-05	-4.82E-02	1.17E-02	1.09E-02	-1.84E-02	-3.10E-02	-6.55E-03
0.1	-10	0.00E+00	-2.55E-07	-1.03E-04	-1.52E-03	-1.35E-04	-1.33E-05	-2.43E-02	5.18E-03	4.95E-03	-8.52E-03	-1.48E-02	-3.12E-03
0.1	-5	0.00E+00	-2.55E-07	-4.85E-05	-7.44E-04	-6.59E-05	-6.44E-06	-1.21E-02	2.45E-03	2.36E-03	-4.10E-03	-7.26E-03	-1.53E-03
0.1	5	0.00E+00	0.00E+00	4.33E-05	7.18E-04	6.33E-05	6.44E-06	1.21E-02	-2.21E-03	-2.17E-03	3.83E-03	6.97E-03	1.46E-03
0.1	10	0.00E+00	0.00E+00	8.22E-05	1.41E-03	1.24E-04	1.25E-05	2.43E-02	-4.21E-03	-4.18E-03	7.40E-03	1.37E-02	2.86E-03
0.1	20	0.00E+00	2.55E-07	1.50E-04	2.73E-03	2.38E-04	2.39E-05	4.84E-02	-7.69E-03	-7.76E-03	1.39E-02	2.64E-02	5.51E-03
1	-20	0.00E+00	-8.66E-06	-2.12E-03	-9.06E-04	-9.11E-05	-9.85E-06	-5.60E-02	9.53E-03	1.23E-02	-3.13E-02	-1.46E-02	-4.91E-05
1	-10	0.00E+00	-3.82E-06	-9.65E-04	-4.33E-04	-4.35E-05	-4.43E-06	-2.79E-02	4.23E-03	5.85E-03	-1.50E-02	-6.94E-03	-2.34E-05
1	-5	0.00E+00	-1.78E-06	-4.62E-04	-2.12E-04	-2.12E-05	-2.46E-06	-1.39E-02	2.00E-03	2.86E-03	-7.38E-03	-3.39E-03	-1.14E-05
1	5	0.00E+00	1.53E-06	4.26E-04	2.04E-04	2.04E-05	1.97E-06	1.38E-02	-1.80E-03	-2.73E-03	7.13E-03	3.26E-03	1.10E-05
1	10	0.00E+00	2.80E-06	8.21E-04	4.01E-04	3.97E-05	3.94E-06	2.75E-02	-3.44E-03	-5.34E-03	1.40E-02	6.39E-03	2.15E-05
1	20	0.00E+00	5.09E-06	1.53E-03	7.74E-04	7.64E-05	7.88E-06	5.46E-02	-6.29E-03	-1.02E-02	2.73E-02	1.23E-02	4.14E-05
10	-20	-2.55E-07	-1.48E-04	-3.46E-03	-2.91E-04	-1.13E-05	-3.10E-05	-6.40E-02	7.42E-03	-1.56E-02	-2.39E-02	-1.83E-04	2.59E-06
10	-10	0.00E+00	-6.48E-05	-1.66E-03	-1.38E-04	-4.92E-06	-1.24E-05	-3.17E-02	3.31E-03	-7.11E-03	-1.15E-02	-8.75E-05	1.34E-06
10	-5	0.00E+00	-3.06E-05	-8.15E-04	-6.73E-05	-2.46E-06	-6.19E-06	-1.58E-02	1.57E-03	-3.40E-03	-5.63E-03	-4.28E-05	6.81E-07
10	5	0.00E+00	2.72E-05	7.85E-04	6.46E-05	1.48E-06	6.19E-06	1.56E-02	-1.42E-03	3.11E-03	5.44E-03	4.12E-05	-6.99E-07
10	10	0.00E+00	5.16E-05	1.54E-03	1.27E-04	2.95E-06	1.86E-05	3.10E-02	-2.72E-03	5.97E-03	1.07E-02	8.10E-05	-1.42E-06
10	20	0.00E+00	9.35E-05	2.99E-03	2.43E-04	4.92E-06	3.10E-05	6.12E-02	-4.98E-03	1.10E-02	2.07E-02	1.57E-04	-2.89E-06
100	-20	-2.29E-06	-1.58E-03	-9.09E-04	2.17E-04	-1.19E-04	0.00E+00	-7.51E-02	6.58E-03	-3.36E-02	-8.51E-04	4.99E-05	3.82E-06
100	-10	-7.64E-07	-7.14E-04	-4.35E-04	1.11E-04	-5.94E-05	0.00E+00	-3.70E-02	3.00E-03	-1.64E-02	-4.11E-04	2.50E-05	1.94E-06
100	-5	-2.55E-07	-3.40E-04	-2.13E-04	5.58E-05	-2.64E-05	0.00E+00	-1.84E-02	1.44E-03	-8.09E-03	-2.03E-04	1.25E-05	9.78E-07
100	5	2.55E-07	3.11E-04	2.06E-04	-5.67E-05	2.64E-05	3.43E-04	1.81E-02	-1.32E-03	7.92E-03	1.97E-04	-1.25E-05	-9.91E-07
100	10	5.09E-07	5.96E-04	4.04E-04	-1.14E-04	5.28E-05	3.43E-04	3.59E-02	-2.52E-03	1.57E-02	3.89E-04	-2.51E-05	-1.99E-06
100	20	5.09E-07	1.10E-03	7.83E-04	-2.32E-04	1.06E-04	3.43E-04	7.08E-02	-4.65E-03	3.08E-02	7.58E-04	-5.02E-05	-4.03E-06
200	-20	1.53E-06	-2.31E-03	-5.09E-04	4.98E-04	7.51E-04	0.00E+00	-8.30E-02	-1.98E-04	-2.64E-02	-2.80E-04	4.62E-05	6.56E-06
200	-10	1.53E-06	-1.06E-03	-2.41E-04	2.49E-04	3.75E-04	0.00E+00	-4.08E-02	-1.79E-04	-1.30E-02	-1.32E-04	2.34E-05	3.28E-06
200	-5	7.65E-07	-5.06E-04	-1.17E-04	1.24E-04	1.88E-04	0.00E+00	-2.02E-02	-1.10E-04	-6.45E-03	-6.45E-05	1.18E-05	1.64E-06
200	5	-1.27E-06	4.68E-04	1.12E-04	-1.24E-04	-1.88E-04	0.00E+00	1.99E-02	1.52E-04	6.36E-03	6.14E-05	-1.19E-05	-1.64E-06
200	10	-2.80E-06	9.01E-04	2.19E-04	-2.50E-04	-3.13E-04	0.00E+00	3.94E-02	3.45E-04	1.26E-02	1.20E-04	-2.39E-05	-3.29E-06
200	20	-6.12E-06	1.68E-03	4.19E-04	-4.99E-04	-6.88E-04	0.00E+00	7.76E-02	8.52E-04	2.50E-02	2.29E-04	-4.82E-05	-6.58E-06

Table D3.25 aqueous 1-bromo-hexadecane: effect of change in *kappa*

MHz	%	c 10nm	c 100nm	c 1um	c 10um	c 100um	c 1mm	a 10nm	a 100nm	a 1um	a 10um	a 100um	a 1mm
0.1	-20	0.00E+00	-9.42E-06	-2.57E-03	-1.21E-03	-1.31E-04	-1.29E-05	1.26E-01	1.18E-01	4.03E-02	-1.48E-02	-1.46E-02	-3.05E-03
0.1	-10	0.00E+00	-4.07E-06	-1.16E-03	-5.65E-04	-6.06E-05	-6.06E-06	5.61E-02	5.26E-02	1.87E-02	-6.89E-03	-6.78E-03	-1.42E-03
0.1	-5	0.00E+00	-2.04E-06	-5.55E-04	-2.73E-04	-2.94E-05	-2.65E-06	2.66E-02	2.50E-02	9.01E-03	-3.33E-03	-3.28E-03	-6.84E-04
0.1	5	0.00E+00	1.53E-06	5.09E-04	2.57E-04	2.74E-05	3.03E-06	-2.41E-02	-2.26E-02	-8.43E-03	3.12E-03	3.07E-03	6.42E-04
0.1	10	0.00E+00	3.05E-06	9.78E-04	4.98E-04	5.34E-05	5.68E-06	-4.59E-02	-4.33E-02	-1.63E-02	6.05E-03	5.97E-03	1.25E-03
0.1	20	0.00E+00	5.60E-06	1.81E-03	9.42E-04	1.01E-04	1.02E-05	-8.43E-02	-7.95E-02	-3.08E-02	1.14E-02	1.13E-02	2.36E-03
1	-20	-2.55E-07	-1.68E-04	-3.34E-03	-3.86E-04	-3.93E-05	-2.95E-06	1.13E-01	8.87E-02	-1.40E-02	-1.38E-02	-6.20E-03	-1.74E-05
1	-10	0.00E+00	-7.39E-05	-1.55E-03	-1.79E-04	-1.82E-05	-1.48E-06	5.03E-02	3.99E-02	-6.41E-03	-6.41E-03	-2.88E-03	-8.07E-06
1	-5	0.00E+00	-3.49E-05	-7.48E-04	-8.67E-05	-8.70E-06	-4.92E-07	2.38E-02	1.90E-02	-3.08E-03	-3.10E-03	-1.39E-03	-3.90E-06
1	5	2.55E-07	3.11E-05	7.01E-04	8.11E-05	8.32E-06	4.92E-07	-2.16E-02	-1.74E-02	2.85E-03	2.90E-03	1.31E-03	3.66E-06
1	10	2.55E-07	5.91E-05	1.36E-03	1.57E-04	1.63E-05	1.48E-06	-4.12E-02	-3.33E-02	5.50E-03	5.63E-03	2.53E-03	7.10E-06
1	20	2.55E-07	1.07E-04	2.57E-03	2.98E-04	3.06E-05	2.46E-06	-7.56E-02	-6.15E-02	1.03E-02	1.06E-02	4.79E-03	1.34E-05
10	-20	-5.60E-06	-1.95E-03	-1.10E-03	-1.18E-04	-9.35E-06	-6.19E-06	9.71E-02	3.78E-02	-1.29E-02	-8.78E-03	-5.18E-05	5.18E-07
10	-10	-2.55E-06	-8.78E-04	-5.12E-04	-5.45E-05	-4.43E-06	0.00E+00	4.33E-02	1.74E-02	-5.96E-03	-4.07E-03	-2.40E-05	2.40E-07
10	-5	-1.27E-06	-4.18E-04	-2.47E-04	-2.63E-05	-1.97E-06	0.00E+00	2.05E-02	8.38E-03	-2.88E-03	-1.97E-03	-1.16E-05	1.16E-07
10	5	7.64E-07	3.83E-04	2.32E-04	2.48E-05	1.97E-06	0.00E+00	-1.86E-02	-7.81E-03	2.69E-03	1.84E-03	1.09E-05	-1.09E-07
10	10	1.78E-06	7.34E-04	4.49E-04	4.81E-05	3.94E-06	6.19E-06	-3.56E-02	-1.51E-02	5.22E-03	3.58E-03	2.11E-05	-2.11E-07
10	20	3.31E-06	1.36E-03	8.49E-04	9.06E-05	7.38E-06	6.19E-06	-6.54E-02	-2.83E-02	9.84E-03	6.75E-03	3.99E-05	-3.99E-07
100	-20	-1.00E-04	-2.99E-03	-3.52E-04	-2.96E-05	-1.98E-05	0.00E+00	7.38E-02	-1.05E-02	-8.36E-03	-1.48E-04	1.28E-06	-2.22E-07
100	-10	-4.38E-05	-1.39E-03	-1.64E-04	-1.38E-05	-1.32E-05	0.00E+00	3.31E-02	-4.78E-03	-3.87E-03	-6.84E-05	5.96E-07	-1.03E-07
100	-5	-2.06E-05	-6.69E-04	-7.88E-05	-6.41E-06	-6.60E-06	0.00E+00	1.58E-02	-2.29E-03	-1.87E-03	-3.30E-05	2.88E-07	-4.95E-08
100	5	1.83E-05	6.25E-04	7.37E-05	6.41E-06	0.00E+00	0.00E+00	-1.44E-02	2.11E-03	1.75E-03	3.09E-05	-2.70E-07	4.64E-08
100	10	3.49E-05	1.21E-03	1.43E-04	1.18E-05	6.60E-06	0.00E+00	-2.75E-02	4.06E-03	3.40E-03	6.00E-05	-5.24E-07	8.99E-08
100	20	6.31E-05	2.28E-03	2.70E-04	2.27E-05	1.32E-05	0.00E+00	-5.07E-02	7.56E-03	6.40E-03	1.13E-04	-9.89E-07	1.70E-07
200	-20	-1.93E-04	-2.10E-03	-2.36E-04	-1.05E-05	6.25E-05	0.00E+00	6.02E-02	-1.02E-02	-3.59E-03	-7.48E-05	-2.77E-06	-1.23E-07
200	-10	-8.46E-05	-9.72E-04	-1.09E-04	-4.65E-06	6.25E-05	0.00E+00	2.71E-02	-4.69E-03	-1.67E-03	-3.47E-05	-1.28E-06	-5.69E-08
200	-5	-3.97E-05	-4.69E-04	-5.27E-05	-2.32E-06	0.00E+00	0.00E+00	1.29E-02	-2.25E-03	-8.04E-04	-1.67E-05	-6.18E-07	-2.74E-08
200	5	3.57E-05	4.39E-04	4.94E-05	1.74E-06	0.00E+00	0.00E+00	-1.18E-02	2.09E-03	7.52E-04	1.57E-05	5.77E-07	2.56E-08
200	10	6.75E-05	8.51E-04	9.57E-05	4.07E-06	0.00E+00	0.00E+00	-2.26E-02	4.04E-03	1.46E-03	3.03E-05	1.12E-06	4.95E-08
200	20	1.23E-04	1.60E-03	1.81E-04	7.55E-06	-6.25E-05	0.00E+00	-4.18E-02	7.56E-03	2.75E-03	5.72E-05	2.11E-06	9.30E-08

Table D3.26 aqueous 1-bromo-hexadecane: effect of change in *Cp*

MHz	%	c 10nm	c 100nm	c 1um	c 10um	c 100um	c 1mm	a 10nm	a 100nm	a 1um	a 10um	a 100um	a 1mm
0.1	-20	-2.12E-02	-2.12E-02	-2.06E-02	-4.73E-03	-5.17E-04	-5.15E-05	-4.74E-02	-7.21E-02	-5.58E-02	-5.83E-02	-5.75E-02	-1.20E-02
0.1	-10	-9.55E-03	-9.55E-03	-9.29E-03	-2.17E-03	-2.37E-04	-2.35E-05	-2.14E-02	-3.22E-02	-2.42E-02	-2.66E-02	-2.64E-02	-5.52E-03
0.1	-5	-4.54E-03	-4.54E-03	-4.42E-03	-1.04E-03	-1.14E-04	-1.14E-05	-1.02E-02	-1.53E-02	-1.13E-02	-1.28E-02	-1.27E-02	-2.65E-03
0.1	5	4.14E-03	4.14E-03	4.04E-03	9.65E-04	1.05E-04	1.06E-05	9.36E-03	1.38E-02	1.00E-02	1.18E-02	1.17E-02	2.46E-03
0.1	10	7.94E-03	7.94E-03	7.75E-03	1.86E-03	2.03E-04	2.05E-05	1.80E-02	2.64E-02	1.89E-02	2.27E-02	2.26E-02	4.74E-03
0.1	20	1.46E-02	1.46E-02	1.43E-02	3.48E-03	3.80E-04	3.83E-05	3.32E-02	4.84E-02	3.38E-02	4.24E-02	4.23E-02	8.87E-03
1	-20	-1.80E-02	-1.79E-02	-1.14E-02	-1.46E-03	-1.49E-04	-1.23E-05	-3.89E-02	-4.94E-02	-6.00E-02	-5.02E-02	-2.31E-02	-6.57E-05
1	-10	-8.06E-03	-8.03E-03	-5.21E-03	-6.66E-04	-6.81E-05	-5.91E-06	-1.75E-02	-2.15E-02	-2.71E-02	-2.29E-02	-1.06E-02	-3.01E-05
1	-5	-3.83E-03	-3.82E-03	-2.50E-03	-3.19E-04	-3.25E-05	-2.95E-06	-8.30E-03	-1.01E-02	-1.29E-02	-1.10E-02	-5.08E-03	-1.44E-05
1	5	3.49E-03	3.48E-03	2.31E-03	2.96E-04	3.06E-05	2.46E-06	7.56E-03	8.95E-03	1.18E-02	1.02E-02	4.70E-03	1.34E-05
1	10	6.68E-03	6.66E-03	4.44E-03	5.71E-04	5.86E-05	4.92E-06	1.45E-02	1.69E-02	2.27E-02	1.96E-02	9.06E-03	2.58E-05
1	20	1.23E-02	1.23E-02	8.29E-03	1.07E-03	1.09E-04	8.86E-06	2.66E-02	3.03E-02	4.21E-02	3.66E-02	1.69E-02	4.81E-05
10	-20	-1.52E-02	-1.50E-02	-3.88E-03	-4.25E-04	-3.54E-05	-1.86E-05	-2.85E-02	-2.96E-02	-4.31E-02	-3.04E-02	-1.87E-04	1.86E-06
10	-10	-6.79E-03	-6.72E-03	-1.77E-03	-1.94E-04	-1.62E-05	-6.19E-06	-1.26E-02	-1.25E-02	-1.96E-02	-1.39E-02	-8.54E-05	8.49E-07
10	-5	-3.22E-03	-3.20E-03	-8.49E-04	-9.32E-05	-7.88E-06	0.00E+00	-5.92E-03	-5.78E-03	-9.40E-03	-6.65E-03	-4.09E-05	4.07E-07
10	5	2.93E-03	2.92E-03	7.84E-04	8.60E-05	6.89E-06	6.19E-06	5.31E-03	4.98E-03	8.67E-03	6.15E-03	3.79E-05	-3.76E-07
10	10	5.61E-03	5.59E-03	1.51E-03	1.66E-04	1.33E-05	1.24E-05	1.01E-02	9.29E-03	1.67E-02	1.19E-02	7.30E-05	-7.26E-07
10	20	1.03E-02	1.03E-02	2.82E-03	3.10E-04	2.56E-05	1.86E-05	1.83E-02	1.62E-02	3.11E-02	2.21E-02	1.36E-04	-1.35E-06
100	-20	-1.27E-02	-9.09E-03	-1.20E-03	-1.02E-04	-5.94E-05	0.00E+00	-1.10E-02	-4.03E-02	-2.70E-02	-5.07E-04	4.35E-06	-7.73E-07
100	-10	-5.68E-03	-4.14E-03	-5.46E-04	-4.63E-05	-2.64E-05	0.00E+00	-4.31E-03	-1.82E-02	-1.23E-02	-2.31E-04	1.99E-06	-3.53E-07
100	-5	-2.70E-03	-1.98E-03	-2.62E-04	-2.22E-05	-1.32E-05	0.00E+00	-1.90E-03	-8.67E-03	-5.89E-03	-1.11E-04	9.51E-07	-1.69E-07
100	5	2.45E-03	1.83E-03	2.42E-04	2.02E-05	1.32E-05	0.00E+00	1.47E-03	7.93E-03	5.44E-03	1.02E-04	-8.79E-07	1.56E-07
100	10	4.68E-03	3.52E-03	4.66E-04	3.94E-05	2.64E-05	0.00E+00	2.59E-03	1.52E-02	1.05E-02	1.97E-04	-1.69E-06	3.01E-07
100	20	8.61E-03	6.56E-03	8.69E-04	7.35E-05	4.62E-05	0.00E+00	3.93E-03	2.82E-02	1.95E-02	3.68E-04	-3.16E-06	5.61E-07
200	-20	-1.06E-02	-6.21E-03	-7.58E-04	-3.37E-05	3.13E-04	0.00E+00	-5.99E-04	-3.24E-02	-1.13E-02	-2.46E-04	-9.11E-06	-4.20E-07
200	-10	-4.74E-03	-2.83E-03	-3.45E-04	-1.51E-05	1.25E-04	0.00E+00	4.95E-04	-1.47E-02	-5.17E-03	-1.12E-04	-4.15E-06	-1.91E-07
200	-5	-2.25E-03	-1.35E-03	-1.66E-04	-7.55E-06	6.25E-05	0.00E+00	4.07E-04	-7.01E-03	-2.48E-03	-5.36E-05	-1.99E-06	-9.16E-08
200	5	2.04E-03	1.25E-03	1.53E-04	6.39E-06	-6.25E-05	0.00E+00	-6.66E-04	6.44E-03	2.28E-03	4.95E-05	1.84E-06	8.46E-08
200	10	3.91E-03	2.41E-03	2.95E-04	1.28E-05	-6.25E-05	0.00E+00	-1.54E-03	1.24E-02	4.40E-03	9.54E-05	3.54E-06	1.63E-07
200	20	7.19E-03	4.48E-03	5.50E-04	2.44E-05	-1.88E-04	0.00E+00	-3.79E-03	2.30E-02	8.20E-03	1.78E-04	6.59E-06	3.04E-07

Table D3.27 aqueous 1-bromo-hexadecane: effect of change in *alpha*

MHz	%	c 10nm	c 100nm	c 1um	c 10um	c 100um	c 1mm	a 10nm	a 100nm	a 1um	a 10um	a 100um	a 1mm
0.1	-20	0.00E+00	0.00E+00	0.00E+00	3.52E-07	0.00E+00	0.00E+00	-4.27E-02	-4.46E-04	-5.39E-06	8.47E-06	9.07E-05	1.90E-04
0.1	-10	0.00E+00	0.00E+00	0.00E+00	3.52E-07	0.00E+00	0.00E+00	-2.13E-02	-2.23E-04	-2.70E-06	4.23E-06	4.54E-05	9.52E-05
0.1	-5	0.00E+00	0.00E+00	0.00E+00	3.52E-07	0.00E+00	0.00E+00	-1.07E-02	-1.11E-04	-1.35E-06	2.12E-06	2.27E-05	4.76E-05
0.1	5	0.00E+00	0.00E+00	0.00E+00	0.00E+00	0.00E+00	0.00E+00	1.07E-02	1.11E-04	1.35E-06	-2.12E-06	-2.27E-05	-4.76E-05
0.1	10	0.00E+00	0.00E+00	-2.59E-07	0.00E+00	0.00E+00	0.00E+00	2.14E-02	2.23E-04	2.70E-06	-4.23E-06	-4.54E-05	-9.52E-05
0.1	20	0.00E+00	0.00E+00	-2.59E-07	0.00E+00	0.00E+00	0.00E+00	4.27E-02	4.46E-04	5.39E-06	-8.47E-06	-9.07E-05	-1.90E-04
1	-20	0.00E+00	2.55E-07	3.06E-06	3.74E-07	0.00E+00	-4.92E-06	-4.31E-02	-4.83E-04	2.02E-05	2.83E-04	1.29E-03	2.43E-05
1	-10	0.00E+00	2.55E-07	1.53E-06	0.00E+00	0.00E+00	-2.46E-06	-2.15E-02	-2.42E-04	1.01E-05	1.41E-04	6.45E-04	1.21E-05
1	-5	0.00E+00	0.00E+00	6.12E-07	0.00E+00	0.00E+00	-1.48E-06	-1.08E-02	-1.21E-04	5.06E-06	7.07E-05	3.23E-04	6.07E-06
1	5	0.00E+00	0.00E+00	-9.17E-07	-3.74E-07	-3.78E-07	9.85E-07	1.08E-02	1.21E-04	-5.06E-06	-7.07E-05	-3.23E-04	-6.07E-06
1	10	0.00E+00	0.00E+00	-1.83E-06	-3.74E-07	-3.78E-07	1.97E-06	2.15E-02	2.42E-04	-1.01E-05	-1.41E-04	-6.45E-04	-1.21E-05
1	20	0.00E+00	-2.55E-07	-3.36E-06	-7.48E-07	-3.78E-07	4.43E-06	4.31E-02	4.83E-04	-2.02E-05	-2.83E-04	-1.29E-03	-2.43E-05
10	-20	2.55E-07	1.45E-05	1.41E-05	1.50E-06	-4.53E-05	-4.52E-04	-4.42E-02	-5.39E-04	8.39E-04	6.11E-03	2.41E-04	-9.30E-05
10	-10	2.55E-07	7.26E-06	7.03E-06	7.52E-07	-2.26E-05	-2.29E-04	-2.21E-02	-2.69E-04	4.19E-04	3.06E-03	1.20E-04	-4.65E-05
10	-5	2.55E-07	3.63E-06	3.52E-06	3.76E-07	-1.13E-05	-1.11E-04	-1.11E-02	-1.35E-04	2.10E-04	1.53E-03	6.03E-05	-2.32E-05
10	5	0.00E+00	-3.63E-06	-3.52E-06	-3.76E-07	1.18E-05	1.11E-04	1.11E-02	1.35E-04	-2.10E-04	-1.53E-03	-6.03E-05	2.32E-05
10	10	0.00E+00	-7.26E-06	-6.68E-06	-7.52E-07	2.31E-05	2.23E-04	2.21E-02	2.69E-04	-4.19E-04	-3.06E-03	-1.21E-04	4.65E-05
10	20	0.00E+00	-1.45E-05	-1.37E-05	-1.50E-06	4.58E-05	4.46E-04	4.42E-02	5.39E-04	-8.39E-04	-6.11E-03	-2.41E-04	9.30E-05
100	-20	1.99E-05	3.13E-04	4.76E-05	-4.52E-04	-4.49E-03	-1.65E-02	-4.79E-02	1.96E-03	1.95E-02	2.30E-03	-9.03E-04	2.17E-04
100	-10	9.93E-06	1.57E-04	2.36E-05	-2.26E-04	-2.25E-03	-8.24E-03	-2.39E-02	9.82E-04	9.75E-03	1.15E-03	-4.52E-04	1.10E-04
100	-5	5.09E-06	7.81E-05	1.18E-05	-1.13E-04	-1.13E-03	-4.12E-03	-1.20E-02	4.91E-04	4.87E-03	5.75E-04	-2.26E-04	5.54E-05
100	5	-4.84E-06	-7.84E-05	-1.18E-05	1.13E-04	1.12E-03	4.46E-03	1.20E-02	-4.91E-04	-4.87E-03	-5.75E-04	2.26E-04	-5.61E-05
100	10	-9.93E-06	-1.57E-04	-2.40E-05	2.26E-04	2.25E-03	8.58E-03	2.39E-02	-9.82E-04	-9.75E-03	-1.15E-03	4.52E-04	-1.13E-04
100	20	-1.99E-05	-3.13E-04	-4.76E-05	4.52E-04	4.51E-03	1.75E-02	4.79E-02	-1.96E-03	-1.95E-02	-2.30E-03	9.05E-04	-2.29E-04
200	-20	7.55E-05	5.09E-04	3.91E-05	-1.58E-03	-3.03E-02	-9.10E-03	-4.97E-02	6.78E-03	2.48E-02	2.44E-03	-1.81E-03	8.65E-05
200	-10	3.77E-05	2.54E-04	1.94E-05	-7.89E-04	-1.52E-02	-4.55E-03	-2.48E-02	3.39E-03	1.24E-02	1.22E-03	-9.10E-04	4.54E-05
200	-5	1.89E-05	1.27E-04	9.68E-06	-3.94E-04	-7.62E-03	-3.03E-03	-1.24E-02	1.69E-03	6.21E-03	6.10E-04	-4.56E-04	2.33E-05
200	5	-1.89E-05	-1.27E-04	-1.00E-05	3.95E-04	7.62E-03	1.52E-03	1.24E-02	-1.69E-03	-6.21E-03	-6.10E-04	4.58E-04	-2.45E-05
200	10	-3.77E-05	-2.55E-04	-1.97E-05	7.90E-04	1.53E-02	4.55E-03	2.48E-02	-3.39E-03	-1.24E-02	-1.22E-03	9.18E-04	-5.02E-05
200	20	-7.55E-05	-5.09E-04	-3.94E-05	1.58E-03	3.08E-02	9.10E-03	4.97E-02	-6.78E-03	-2.48E-02	-2.44E-03	1.84E-03	-1.06E-04

Table D3.28 aqueous 1-bromo-hexadecane: effect of change in *beta*

MHz	%	c 10nm	c 100nm	c 1um	c 10um	c 100um	c 1mm	a 10nm	a 100nm	a 1um	a 10um	a 100um	a 1mm
0.1	-20	1.76E-02	1.76E-02	1.68E-02	3.04E-03	3.29E-04	3.33E-05	1.94E-01	6.45E-02	6.28E-02	4.00E-02	3.70E-02	7.69E-03
0.1	-10	8.74E-03	8.74E-03	8.33E-03	1.51E-03	1.63E-04	1.67E-05	8.70E-02	3.19E-02	3.11E-02	1.98E-02	1.83E-02	3.81E-03
0.1	-5	4.35E-03	4.35E-03	4.15E-03	7.51E-04	8.12E-05	8.34E-06	4.14E-02	1.59E-02	1.55E-02	9.87E-03	9.13E-03	1.90E-03
0.1	5	-4.32E-03	-4.32E-03	-4.12E-03	-7.44E-04	-8.08E-05	-7.96E-06	-3.78E-02	-1.57E-02	-1.54E-02	-9.79E-03	-9.05E-03	-1.88E-03
0.1	10	-8.60E-03	-8.60E-03	-8.20E-03	-1.48E-03	-1.60E-04	-1.59E-05	-7.26E-02	-3.13E-02	-3.06E-02	-1.95E-02	-1.80E-02	-3.75E-03
0.1	20	-1.71E-02	-1.71E-02	-1.63E-02	-2.94E-03	-3.19E-04	-3.18E-05	-1.34E-01	-6.19E-02	-6.08E-02	-3.87E-02	-3.58E-02	-7.44E-03
1	-20	2.09E-02	2.09E-02	1.01E-02	1.19E-03	1.21E-04	9.85E-06	1.94E-01	7.95E-02	7.05E-02	4.55E-02	1.96E-02	5.36E-05
1	-10	1.04E-02	1.03E-02	5.02E-03	5.89E-04	6.01E-05	4.92E-06	8.72E-02	3.93E-02	3.49E-02	2.25E-02	9.69E-03	2.65E-05
1	-5	5.15E-03	5.14E-03	2.50E-03	2.93E-04	2.99E-05	2.46E-06	4.16E-02	1.95E-02	1.74E-02	1.12E-02	4.82E-03	1.32E-05
1	5	-5.10E-03	-5.09E-03	-2.47E-03	-2.90E-04	-2.99E-05	-2.46E-06	-3.80E-02	-1.93E-02	-1.72E-02	-1.11E-02	-4.77E-03	-1.31E-05
1	10	-1.01E-02	-1.01E-02	-4.92E-03	-5.77E-04	-5.90E-05	-4.92E-06	-7.29E-02	-3.84E-02	-3.42E-02	-2.21E-02	-9.49E-03	-2.60E-05
1	20	-2.01E-02	-2.01E-02	-9.73E-03	-1.14E-03	-1.17E-04	-9.36E-06	-1.35E-01	-7.58E-02	-6.77E-02	-4.37E-02	-1.88E-02	-5.15E-05
10	-20	2.47E-02	2.35E-02	4.11E-03	4.42E-04	3.64E-05	2.48E-05	1.97E-01	9.86E-02	5.83E-02	3.56E-02	1.95E-04	-1.94E-06
10	-10	1.22E-02	1.16E-02	2.03E-03	2.18E-04	1.82E-05	1.24E-05	8.84E-02	4.86E-02	2.88E-02	1.76E-02	9.63E-05	-9.59E-07
10	-5	6.06E-03	5.77E-03	1.01E-03	1.08E-04	8.86E-06	6.19E-06	4.21E-02	2.41E-02	1.43E-02	8.73E-03	4.78E-05	-4.76E-07
10	5	-5.99E-03	-5.70E-03	-9.98E-04	-1.07E-04	-8.86E-06	-6.19E-06	-3.84E-02	-2.38E-02	-1.41E-02	-8.62E-03	-4.72E-05	4.70E-07
10	10	-1.19E-02	-1.13E-02	-1.98E-03	-2.13E-04	-1.72E-05	-6.19E-06	-7.36E-02	-4.72E-02	-2.80E-02	-1.71E-02	-9.38E-05	9.34E-07
10	20	-2.35E-02	-2.24E-02	-3.91E-03	-4.20E-04	-3.45E-05	-1.86E-05	-1.36E-01	-9.31E-02	-5.53E-02	-3.38E-02	-1.85E-04	1.84E-06
100	-20	2.90E-02	1.36E-02	1.56E-03	1.29E-04	7.92E-05	0.00E+00	2.02E-01	1.07E-01	4.45E-02	6.80E-04	-6.00E-06	1.02E-06
100	-10	1.43E-02	6.72E-03	7.72E-04	6.41E-05	3.96E-05	0.00E+00	9.01E-02	5.23E-02	2.18E-02	3.34E-04	-2.93E-06	5.03E-07
100	-5	7.08E-03	3.34E-03	3.83E-04	3.16E-05	1.98E-05	0.00E+00	4.27E-02	2.59E-02	1.08E-02	1.66E-04	-1.45E-06	2.50E-07
100	5	-6.97E-03	-3.29E-03	-3.78E-04	-3.16E-05	-1.98E-05	0.00E+00	-3.85E-02	-2.54E-02	-1.06E-02	-1.63E-04	1.42E-06	-2.46E-07
100	10	-1.38E-02	-6.53E-03	-7.51E-04	-6.27E-05	-3.96E-05	0.00E+00	-7.34E-02	-5.04E-02	-2.10E-02	-3.23E-04	2.80E-06	-4.88E-07
100	20	-2.72E-02	-1.29E-02	-1.48E-03	-1.24E-04	-7.92E-05	0.00E+00	-1.34E-01	-9.89E-02	-4.13E-02	-6.34E-04	5.49E-06	-9.61E-07
200	-20	3.37E-02	1.13E-02	1.24E-03	5.11E-05	-4.36E-04	0.00E+00	1.94E-01	1.08E-01	2.19E-02	4.12E-04	1.48E-05	6.92E-07
200	-10	1.65E-02	5.56E-03	6.11E-04	2.56E-05	-2.49E-04	0.00E+00	8.49E-02	5.25E-02	1.07E-02	2.02E-04	7.32E-06	3.41E-07
200	-5	8.17E-03	2.76E-03	3.03E-04	1.28E-05	-1.25E-04	0.00E+00	3.98E-02	2.59E-02	5.27E-03	9.98E-05	3.63E-06	1.69E-07
200	5	-8.01E-03	-2.71E-03	-2.98E-04	-1.22E-05	1.25E-04	0.00E+00	-3.52E-02	-2.53E-02	-5.15E-03	-9.77E-05	-3.58E-06	-1.66E-07
200	10	-1.59E-02	-5.37E-03	-5.91E-04	-2.50E-05	1.87E-04	0.00E+00	-6.63E-02	-5.00E-02	-1.02E-02	-1.93E-04	-7.10E-06	-3.30E-07
200	20	-3.10E-02	-1.05E-02	-1.16E-03	-5.00E-05	4.36E-04	0.00E+00	-1.18E-01	-9.75E-02	-1.98E-02	-3.78E-04	-1.40E-05	-6.48E-07

Table D3.29 aqueous silica:: effect of change in *c'*

MHz	%	c 10nm	c 100nm	c 1um	c 10um	c 100um	c 1mm	a 10nm	a 100nm	a 1um	a 10um	a 100um	a 1mm
0.1	-20	-6.26E+02	-6.30E+02	2.54E+02	5.10E+00	3.51E+00	3.52E+00	1.44E-01	1.25E-02	1.65E-02	5.52E-02	6.46E-02	1.66E+00
0.1	-10	-1.50E+03	-1.51E+03	6.11E+02	1.23E+01	8.42E+00	8.31E+00	4.97E-01	7.56E-02	7.08E-02	8.70E-02	9.17E-02	5.28E+00
0.1	-5	8.37E+02	8.42E+02	-3.40E+02	-6.81E+00	-4.67E+00	-4.83E+00	6.52E-02	-4.37E-02	-4.46E-02	-3.91E-02	-3.90E-02	-4.60E-01
0.1	5	-1.60E+02	-1.61E+02	6.51E+01	1.30E+00	8.92E-01	9.04E-01	1.51E-02	1.08E-02	9.87E-03	4.84E-03	4.73E-03	3.27E-01
0.1	10	-2.28E+02	-2.29E+02	9.26E+01	1.85E+00	1.27E+00	1.28E+00	2.23E-02	1.64E-02	1.47E-02	5.47E-03	5.32E-03	4.84E-01
0.1	20	-2.89E+02	-2.91E+02	1.18E+02	2.35E+00	1.61E+00	1.63E+00	2.72E-02	2.25E-02	1.97E-02	4.08E-03	4.04E-03	6.34E-01
1	-20	-2.64E+00	-2.64E+00	-2.31E+00	-1.67E+00	-1.65E+00	4.03E+00	-2.41E-02	-4.65E-02	-3.72E-02	-2.46E-02	-5.01E-01	-2.11E-01
1	-10	-2.88E-01	-2.88E-01	-2.53E-01	-1.82E-01	-1.77E-01	2.44E-01	-6.97E-03	-7.54E-03	-3.37E-03	1.33E-03	-8.44E-02	-3.97E-02
1	-5	-1.04E-01	-1.03E-01	-9.09E-02	-6.53E-02	-6.34E-02	8.58E-02	-1.96E-03	-2.96E-03	-1.06E-03	9.72E-04	-3.08E-02	-1.34E-02
1	5	6.61E-02	6.60E-02	5.80E-02	4.16E-02	4.03E-02	-5.38E-02	5.66E-04	2.09E-03	4.88E-04	-1.08E-03	1.99E-02	8.02E-03
1	10	1.12E-01	1.12E-01	9.82E-02	7.03E-02	6.81E-02	-9.07E-02	4.42E-04	3.63E-03	6.80E-04	-2.12E-03	3.37E-02	1.33E-02
1	20	1.71E-01	1.71E-01	1.50E-01	1.07E-01	1.04E-01	-1.38E-01	-6.84E-04	5.76E-03	6.41E-04	-3.93E-03	5.15E-02	1.99E-02
10	-20	-2.13E-01	-2.11E-01	-1.55E-01	-1.39E-01	2.30E-01	9.17E-02	-5.39E-04	-6.35E-03	5.10E-03	-3.58E-02	-2.86E-02	1.07E-01
10	-10	-6.45E-02	-6.39E-02	-4.68E-02	-4.18E-02	6.84E-02	4.88E-02	1.32E-03	-2.02E-03	2.45E-03	-1.06E-02	-8.10E-03	2.77E-02
10	-5	-2.69E-02	-2.66E-02	-1.95E-02	-1.74E-02	2.84E-02	2.18E-02	8.04E-04	-8.47E-04	1.16E-03	-4.36E-03	-3.32E-03	1.16E-02
10	5	2.01E-02	1.99E-02	1.46E-02	1.30E-02	-2.11E-02	-1.80E-02	-9.15E-04	6.28E-04	-1.02E-03	3.20E-03	2.43E-03	-8.59E-03
10	10	3.57E-02	3.54E-02	2.58E-02	2.30E-02	-3.74E-02	-3.29E-02	-1.85E-03	1.10E-03	-1.93E-03	5.64E-03	4.27E-03	-1.52E-02
10	20	5.82E-02	5.76E-02	4.20E-02	3.74E-02	-6.07E-02	-5.60E-02	-3.64E-03	1.76E-03	-3.42E-03	9.07E-03	6.88E-03	-2.44E-02
100	-20	-7.47E-02	-6.72E-02	-5.06E-02	8.22E-02	7.38E-02	-1.40E-02	4.83E-03	1.25E-03	-3.82E-03	-8.63E-03	3.41E-02	1.49E-02
100	-10	-2.67E-02	-2.40E-02	-1.80E-02	2.92E-02	2.91E-02	7.30E-02	2.39E-03	6.76E-04	-1.19E-03	-3.00E-03	1.19E-02	6.95E-03
100	-5	-1.17E-02	-1.05E-02	-7.86E-03	1.27E-02	1.31E-02	7.14E-02	1.16E-03	3.36E-04	-4.93E-04	-1.30E-03	5.15E-03	3.48E-03
100	5	9.28E-03	8.35E-03	6.24E-03	-1.01E-02	-1.07E-02	2.37E-03	-1.06E-03	-3.20E-04	3.58E-04	1.02E-03	-3.94E-03	-2.60E-03
100	10	1.68E-02	1.51E-02	1.13E-02	-1.82E-02	-1.93E-02	-1.90E-02	-2.04E-03	-6.18E-04	6.24E-04	1.84E-03	-6.82E-03	-3.13E-04
100	20	2.83E-02	2.54E-02	1.89E-02	-3.06E-02	-1.91E-02	-1.11E-02	-3.72E-03	-1.15E-03	9.82E-04	3.07E-03	-1.19E-02	-2.74E-03
200	-20	-3.63E-02	-3.08E-02	-2.52E-02	2.64E-02	1.39E-01	-1.43E-01	4.90E-03	2.63E-03	-1.10E-02	7.31E-03	-5.04E-04	2.65E-02
200	-10	-1.39E-02	-1.18E-02	-9.59E-03	1.01E-02	3.79E-02	-9.20E-02	2.17E-03	1.14E-03	-4.19E-03	2.75E-03	-2.72E-03	2.54E-02
200	-5	-6.19E-03	-5.24E-03	-4.27E-03	4.52E-03	1.52E-02	-2.31E-01	1.02E-03	5.31E-04	-1.86E-03	1.22E-03	5.52E-07	1.94E-02
200	5	5.08E-03	4.30E-03	3.50E-03	-3.71E-03	-3.70E-02	-3.91E-01	-9.04E-04	-4.65E-04	1.52E-03	-9.91E-04	3.12E-03	-5.47E-03
200	10	9.31E-03	7.87E-03	6.40E-03	-6.80E-03	-3.89E-03	-2.53E-01	-1.71E-03	-8.75E-04	2.78E-03	-1.81E-03	4.21E-03	-3.12E-03
200	20	1.59E-02	1.34E-02	1.09E-02	-1.16E-02	-2.38E-02	-3.41E-01	-3.06E-03	-1.56E-03	4.75E-03	-3.08E-03	3.49E-03	-4.97E-03

Table D3.30 aqueous silica: effect of change in *rho'*

MHz	%	c 10nm	c 100nm	c 1um	c 10um	c 100um	c 1mm	a 10nm	a 100nm	a 1um	a 10um	a 100um	a 1mm
0.1	-20	-1.70E+03	-1.71E+03	6.88E+02	1.30E+01	8.67E+00	8.59E+00	-2.41E-02	-6.24E-01	-6.60E-01	-5.67E-01	-5.51E-01	4.16E+00
0.1	-10	7.74E+02	7.79E+02	-3.15E+02	-6.63E+00	-4.64E+00	-4.81E+00	-1.43E-01	-4.09E-01	-4.27E-01	-3.68E-01	-3.51E-01	-5.11E-01
0.1	-5	1.32E+02	1.32E+02	-5.38E+01	-1.27E+00	-9.25E-01	-9.47E-01	-1.33E-01	-2.14E-01	-2.22E-01	-1.85E-01	-1.73E-01	-3.88E-01
0.1	5	-2.08E+01	-2.09E+01	8.78E+00	3.97E-01	3.29E-01	3.37E-01	1.51E-01	2.39E-01	2.49E-01	1.95E-01	1.75E-01	2.65E-01
0.1	10	1.15E-01	1.14E-01	6.88E-01	4.75E-01	4.43E-01	4.55E-01	3.16E-01	5.06E-01	5.25E-01	3.98E-01	3.52E-01	4.61E-01
0.1	20	9.23E+01	9.28E+01	-3.59E+01	2.73E-01	4.23E-01	4.41E-01	6.90E-01	1.12E+00	1.16E+00	8.24E-01	7.06E-01	7.54E-01
1	-20	-3.97E-02	-3.79E-02	1.10E+01	-7.80E-01	-7.70E-01	8.90E-01	-4.72E-01	-6.13E-01	-5.96E-01	-5.05E-01	-5.43E-01	-2.27E-01
1	-10	-1.11E+00	-1.11E+00	-1.55E+01	1.88E-02	-9.60E-03	1.28E-01	-2.61E-01	-3.44E-01	-3.26E-01	-2.57E-01	-2.18E-01	-3.32E-02
1	-5	-6.50E-01	-6.52E-01	-9.48E+00	4.16E-02	2.46E-02	4.31E-02	-1.37E-01	-1.81E-01	-1.70E-01	-1.29E-01	-1.03E-01	-1.06E-02
1	5	7.49E-01	7.51E-01	1.11E+01	-7.17E-02	-5.22E-02	-2.24E-02	1.50E-01	2.00E-01	1.82E-01	1.28E-01	9.43E-02	5.07E-03
1	10	1.55E+00	1.56E+00	2.31E+01	-1.58E-01	-1.18E-01	-3.32E-02	3.13E-01	4.18E-01	3.76E-01	2.55E-01	1.83E-01	7.26E-03
1	20	3.24E+00	3.25E+00	4.78E+01	-3.44E-01	-2.63E-01	-3.67E-02	6.78E-01	9.09E-01	7.92E-01	5.04E-01	3.45E-01	7.63E-03
10	-20	-8.90E-01	-9.02E-01	3.43E+00	4.40E-01	6.95E-02	8.07E-02	-4.69E-01	-5.53E-01	-4.41E-01	-3.51E-01	-1.50E-02	1.07E-01
10	-10	-4.75E-01	-4.82E-01	1.89E+00	2.62E-01	6.60E-03	-3.27E-02	-2.57E-01	-3.03E-01	-2.23E-01	-1.68E-01	-9.67E-04	5.97E-02
10	-5	-2.41E-01	-2.44E-01	9.52E-01	1.34E-01	-1.98E-04	-4.20E-02	-1.34E-01	-1.58E-01	-1.11E-01	-8.24E-02	2.11E-04	3.15E-02
10	5	2.44E-01	2.47E-01	-9.38E-01	-1.34E-01	4.29E-03	4.78E-02	1.45E-01	1.71E-01	1.11E-01	7.92E-02	-9.07E-04	-2.21E-02
10	10	4.90E-01	4.95E-01	-1.85E+00	-2.64E-01	1.10E-02	2.01E-01	3.01E-01	3.55E-01	2.21E-01	1.55E-01	-2.15E-03	-3.72E-02
10	20	9.79E-01	9.88E-01	-3.56E+00	-5.09E-01	2.83E-02	4.54E-01	6.44E-01	7.59E-01	4.36E-01	2.98E-01	-4.93E-03	6.45E-03
100	-20	-5.93E-01	-6.53E-01	3.39E+00	-2.93E-02	-3.47E-01	5.49E-01	-4.55E-01	-4.54E-01	-3.06E-01	4.65E-03	1.84E-02	1.70E-02
100	-10	-2.97E-01	-3.19E-01	1.63E+00	-1.99E-02	-2.23E-01	3.37E-01	-2.46E-01	-2.37E-01	-1.47E-01	2.95E-03	-4.14E-02	1.07E-02
100	-5	-1.48E-01	-1.57E-01	7.95E-01	-1.05E-02	-9.15E-02	1.87E-01	-1.28E-01	-1.21E-01	-7.20E-02	1.49E-03	-3.48E-02	-9.38E-03
100	5	1.47E-01	1.51E-01	-7.50E-01	1.11E-02	2.39E-02	3.36E-01	1.37E-01	1.24E-01	6.90E-02	-1.43E-03	4.58E-02	1.83E-02
100	10	2.92E-01	2.97E-01	-1.46E+00	2.24E-02	-2.88E-03	5.38E-01	2.82E-01	2.51E-01	1.35E-01	-2.76E-03	8.65E-02	1.83E-02
100	20	5.77E-01	5.71E-01	-2.74E+00	4.48E-02	-1.85E-01	5.95E-01	5.99E-01	5.13E-01	2.59E-01	-5.01E-03	1.52E-01	-2.32E-03
200	-20	-4.41E-01	-4.69E-01	-1.45E+00	-3.44E-02	-3.45E-02	-6.11E-01	-4.37E-01	-3.67E-01	-1.97E-01	4.25E-02	-2.37E-02	-1.46E-02
200	-10	-2.17E-01	-2.21E-01	-6.70E-01	-2.79E-02	1.04E-01	-1.09E+00	-2.34E-01	-1.84E-01	-9.25E-02	2.04E-02	5.96E-03	-3.93E-02
200	-5	-1.08E-01	-1.07E-01	-3.23E-01	-1.68E-02	1.75E-01	1.64E-01	-1.21E-01	-9.21E-02	-4.49E-02	1.01E-02	1.64E-02	-3.39E-02
200	5	1.06E-01	1.00E-01	2.99E-01	2.37E-02	-9.83E-02	2.21E+00	1.29E-01	9.16E-02	4.24E-02	-9.38E-03	-5.01E-02	-7.58E-03
200	10	2.10E-01	1.95E-01	5.78E-01	5.60E-02	1.25E-02	2.48E+00	2.64E-01	1.82E-01	8.25E-02	-1.71E-02	-3.45E-02	-5.16E-02
200	20	4.12E-01	3.67E-01	1.08E+00	1.58E-01	1.69E-01	1.69E+00	5.58E-01	3.60E-01	1.56E-01	-1.61E-02	-6.93E-03	8.24E-03

Table D3.31 aqueous silica: effect of change in *mu'*

MHz	%	c 10nm	c 100nm	c 1um	c 10um	c 100um	c 1mm	a 10nm	a 100nm	a 1um	a 10um	a 100um	a 1mm
0.1	-20	-2.09E+02	-2.11E+02	8.51E+01	1.70E+00	1.17E+00	1.18E+00	2.05E-02	1.43E-02	1.30E-02	6.12E-03	6.00E-03	4.40E-01
0.1	-10	-1.44E+02	-1.45E+02	5.86E+01	1.17E+00	8.04E-01	8.15E-01	1.30E-02	9.49E-03	8.73E-03	4.71E-03	4.63E-03	2.91E-01
0.1	-5	-8.89E+01	-8.94E+01	3.61E+01	7.23E-01	4.96E-01	5.03E-01	7.37E-03	5.68E-03	5.28E-03	3.12E-03	3.07E-03	1.73E-01
0.1	5	1.66E+02	1.67E+02	-6.76E+01	-1.35E+00	-9.28E-01	-9.46E-01	-6.80E-03	-9.71E-03	-9.33E-03	-6.91E-03	-6.87E-03	-2.67E-01
0.1	10	5.90E+02	5.94E+02	-2.40E+02	-4.80E+00	-3.29E+00	-3.39E+00	2.54E-02	-3.17E-02	-3.18E-02	-2.69E-02	-2.68E-02	-5.68E-01
0.1	20	-2.15E+03	-2.17E+03	8.75E+02	1.76E+01	1.21E+01	1.17E+01	9.23E-01	1.16E-01	1.04E-01	1.20E-01	1.26E-01	8.69E+00
1	-20	-9.66E-01	-9.66E-01	-9.48E-01	-8.97E-01	-8.89E-01	-1.29E+00	-4.78E-01	-1.01E-01	-9.54E-02	-1.09E-01	-8.20E-01	-6.87E-01
1	-10	-1.17E+00	-1.17E+00	-1.15E+00	-1.08E+00	-1.08E+00	-1.68E+00	-4.82E-01	-1.23E-01	-1.15E-01	-1.25E-01	-8.80E-01	-7.73E-01
1	-5	-2.01E+00	-2.01E+00	-1.97E+00	-1.86E+00	-1.93E+00	-1.47E+00	3.10E-02	-1.89E-01	-1.98E-01	-2.03E-01	-3.60E-01	2.52E-01
1	5	-5.19E-01	-5.19E-01	-5.10E-01	-4.82E-01	-4.69E-01	-3.95E-01	-3.31E-01	-6.27E-02	-5.22E-02	-5.03E-02	-5.27E-01	-5.52E-01
1	10	-6.37E-01	-6.37E-01	-6.25E-01	-5.92E-01	-5.78E-01	-8.79E-01	-3.82E-01	-7.84E-02	-6.46E-02	-5.83E-02	-6.21E-01	-6.11E-01
1	20	-7.19E-01	-7.19E-01	-7.06E-01	-6.67E-01	-6.54E-01	-9.95E-01	-4.08E-01	-9.38E-02	-7.51E-02	-5.62E-02	-6.78E-01	-6.20E-01
10	-20	-8.74E+00	-8.69E+00	-7.23E+00	-7.46E+00	-2.85E+02	-2.61E+00	6.12E+00	-7.18E-02	-2.00E-01	1.02E+01	2.12E+00	5.22E-02
10	-10	4.14E-01	4.11E-01	3.44E-01	3.15E-01	6.78E+01	-2.21E+00	6.81E-02	2.07E-02	3.79E-03	1.53E-01	3.73E-02	3.51E-01
10	-5	1.34E-01	1.33E-01	1.11E-01	1.02E-01	2.72E+01	-3.67E-01	1.88E-02	8.09E-03	-6.58E-04	4.52E-02	1.22E-02	3.53E-01
10	5	-7.88E-02	-7.84E-02	-6.56E-02	-5.99E-02	-1.42E+01	-5.04E-01	-8.57E-03	-6.89E-03	2.84E-03	-2.26E-02	-9.14E-03	-1.61E-01
10	10	-1.31E-01	-1.30E-01	-1.09E-01	-9.94E-02	-2.29E+01	-8.28E-01	-1.26E-02	-1.37E-02	6.86E-03	-3.37E-02	-1.63E-02	-2.15E-01
10	20	-1.96E-01	-1.95E-01	-1.65E-01	-1.48E-01	-3.29E+01	-1.22E+00	-1.44E-02	-2.87E-02	1.58E-02	-3.45E-02	-2.67E-02	-2.24E-01
100	-20	3.68E-01	3.44E-01	2.72E-01	-1.41E+00	-5.63E+00	2.64E+00	2.64E-02	2.55E-02	1.61E-02	3.34E-02	6.52E-01	8.49E-02
100	-10	1.04E-01	9.79E-02	7.71E-02	-3.48E-01	-1.87E+00	1.40E+00	1.49E-03	1.29E-02	-1.07E-02	1.23E-02	1.68E-02	2.98E-02
100	-5	4.29E-02	4.05E-02	3.19E-02	-1.38E-01	-7.57E-01	1.38E+00	-4.62E-04	7.02E-03	-8.66E-03	5.42E-03	-1.94E-03	1.51E-02
100	5	-3.21E-02	-3.06E-02	-2.42E-02	9.77E-02	5.97E-01	-7.00E-01	1.75E-03	-8.98E-03	1.60E-02	-4.29E-03	-1.17E-03	5.20E-03
100	10	-5.71E-02	-5.48E-02	-4.41E-02	1.71E-01	9.34E-01	-1.21E+00	4.14E-03	-2.07E-02	4.13E-02	-7.57E-03	-2.71E-02	-7.48E-03
100	20	-9.43E-02	-9.15E-02	-8.76E-02	3.19E-01	8.65E-01	-2.00E+00	9.30E-03	-5.55E-02	6.02E-02	-8.56E-03	-6.03E-03	-1.69E-03
200	-20	1.41E-01	1.33E-01	1.22E-01	-2.20E-01	-1.28E+00	-2.89E+00	-1.35E-02	6.63E-02	-1.28E-02	-3.90E-02	-3.52E-02	6.53E-03
200	-10	5.14E-02	5.05E-02	5.53E-02	-8.47E-02	-4.62E-01	-2.29E+00	-8.29E-03	4.80E-02	-2.38E-02	-2.21E-02	-2.74E-02	-2.38E-02
200	-5	2.28E-02	2.28E-02	3.13E-02	-4.64E-02	-3.05E-01	-9.03E-01	-4.20E-03	2.93E-02	-1.10E-02	-1.44E-02	-1.55E-02	-8.15E-03
200	5	-1.89E-02	-1.93E-02	9.98E-04	-1.83E-02	6.76E-03	-6.23E-02	3.88E-03	-4.37E-02	-5.72E-01	-3.89E-02	-2.01E-02	-2.22E-02
200	10	-3.50E-02	-3.56E-02	1.24E-02	-3.36E-03	3.46E-01	-2.02E-01	7.05E-03	-1.05E-01	-2.84E-01	-2.02E-02	-4.50E-03	-8.90E-03
200	20	-6.17E-02	-5.76E-02	-5.18E-03	1.77E-02	3.39E-01	-3.83E-01	9.83E-03	-2.77E-01	-1.83E-01	-1.16E-02	-1.39E-02	-1.67E-02

Table D3.32 aqueous silica: effect of change in *kappa'*

MHz	%	c 10nm	c 100nm	c 1um	c 10um	c 100um	c 1mm	a 10nm	a 100nm	a 1um	a 10um	a 100um	a 1mm
0.1	-20	0.00E+00	0.00E+00	3.59E-03	2.30E-03	1.37E-04	1.41E-05	1.97E-03	3.52E-03	4.67E-03	-4.33E-03	-3.77E-03	-1.18E-03
0.1	-10	0.00E+00	0.00E+00	1.55E-03	1.10E-03	6.51E-05	6.66E-06	8.73E-04	1.57E-03	2.07E-03	-2.03E-03	-1.79E-03	-5.60E-04
0.1	-5	0.00E+00	0.00E+00	7.49E-04	5.44E-04	3.15E-05	3.70E-06	4.14E-04	7.41E-04	9.83E-04	-9.84E-04	-8.72E-04	-2.73E-04
0.1	5	0.00E+00	0.00E+00	-6.42E-04	-5.27E-04	-3.08E-05	-2.96E-06	-3.74E-04	-6.71E-04	-8.90E-04	9.25E-04	8.32E-04	2.61E-04
0.1	10	0.00E+00	0.00E+00	-1.23E-03	-1.04E-03	-5.94E-05	-5.92E-06	-7.14E-04	-1.28E-03	-1.70E-03	1.79E-03	1.63E-03	5.10E-04
0.1	20	0.00E+00	0.00E+00	-2.25E-03	-2.02E-03	-1.14E-04	-1.18E-05	-1.31E-03	-2.35E-03	-3.12E-03	3.37E-03	3.12E-03	9.79E-04
1	-20	0.00E+00	-1.56E-04	5.17E-03	4.82E-04	4.56E-05	-3.20E-06	1.65E-03	3.17E-03	4.99E-03	-3.94E-03	-2.14E-03	-3.23E-06
1	-10	0.00E+00	-1.56E-04	2.27E-03	2.29E-04	2.17E-05	-1.60E-06	7.31E-04	1.41E-03	2.27E-03	-1.86E-03	-1.01E-03	-1.53E-06
1	-5	0.00E+00	0.00E+00	1.07E-03	1.11E-04	1.12E-05	-8.01E-07	3.46E-04	6.67E-04	1.09E-03	-9.08E-04	-4.93E-04	-7.47E-07
1	5	0.00E+00	0.00E+00	-9.53E-04	-1.07E-04	-9.71E-06	8.01E-07	-3.14E-04	-6.04E-04	-9.99E-04	8.65E-04	4.70E-04	7.13E-07
1	10	0.00E+00	0.00E+00	-1.81E-03	-2.08E-04	-1.94E-05	1.60E-06	-5.99E-04	-1.15E-03	-1.92E-03	1.69E-03	9.20E-04	1.39E-06
1	20	0.00E+00	0.00E+00	-3.29E-03	-3.99E-04	-3.74E-05	2.80E-06	-1.10E-03	-2.11E-03	-3.56E-03	3.23E-03	1.76E-03	2.67E-06
10	-20	0.00E+00	2.31E-03	2.61E-03	1.49E-04	-1.08E-05	-5.60E-06	1.39E-03	3.23E-03	-3.76E-03	-2.89E-03	-1.04E-05	-3.31E-07
10	-10	0.00E+00	1.02E-03	1.25E-03	7.08E-05	-5.18E-06	0.00E+00	6.19E-04	1.44E-03	-1.70E-03	-1.37E-03	-4.93E-06	-1.58E-07
10	-5	0.00E+00	4.83E-04	6.15E-04	3.46E-05	-2.39E-06	0.00E+00	2.93E-04	6.81E-04	-8.07E-04	-6.67E-04	-2.40E-06	-7.71E-08
10	5	0.00E+00	-4.30E-04	-5.92E-04	-3.31E-05	2.39E-06	0.00E+00	-2.66E-04	-6.16E-04	7.29E-04	6.35E-04	2.30E-06	7.39E-08
10	10	0.00E+00	-8.60E-04	-1.16E-03	-6.39E-05	4.78E-06	0.00E+00	-5.07E-04	-1.18E-03	1.39E-03	1.24E-03	4.50E-06	1.45E-07
10	20	0.00E+00	-1.50E-03	-2.24E-03	-1.23E-04	8.76E-06	0.00E+00	-9.31E-04	-2.16E-03	2.51E-03	2.38E-03	8.63E-06	2.79E-07
100	-20	-3.12E-04	3.52E-03	5.16E-04	-3.17E-05	-5.72E-06	0.00E+00	1.21E-03	3.67E-03	-3.41E-03	-3.51E-05	-1.31E-06	3.10E-07
100	-10	-1.56E-04	1.54E-03	2.44E-04	-1.49E-05	-5.72E-06	0.00E+00	5.39E-04	1.66E-03	-1.61E-03	-1.68E-05	-6.33E-07	1.54E-07
100	-5	0.00E+00	7.30E-04	1.19E-04	-7.44E-06	0.00E+00	0.00E+00	2.55E-04	7.90E-04	-7.84E-04	-8.21E-06	-3.11E-07	7.67E-08
100	5	0.00E+00	-6.49E-04	-1.13E-04	6.65E-06	0.00E+00	0.00E+00	-2.31E-04	-7.22E-04	7.45E-04	7.89E-06	3.02E-07	-7.62E-08
100	10	1.56E-04	-1.24E-03	-2.22E-04	1.33E-05	0.00E+00	0.00E+00	-4.42E-04	-1.38E-03	1.46E-03	1.55E-05	5.95E-07	-1.52E-07
100	20	1.56E-04	-2.25E-03	-4.24E-04	2.54E-05	5.72E-06	0.00E+00	-8.12E-04	-2.56E-03	2.78E-03	2.99E-05	1.16E-06	-3.03E-07
200	-20	-1.35E-03	3.66E-03	4.41E-04	-2.86E-05	0.00E+00	0.00E+00	1.03E-03	2.91E-03	-1.92E-03	7.41E-06	-1.58E-06	6.62E-07
200	-10	-6.75E-04	1.62E-03	2.09E-04	-1.33E-05	0.00E+00	0.00E+00	4.61E-04	1.34E-03	-9.09E-04	3.29E-06	-7.53E-07	3.30E-07
200	-5	-4.50E-04	7.67E-04	1.01E-04	-6.66E-06	0.00E+00	0.00E+00	2.19E-04	6.45E-04	-4.43E-04	1.55E-06	-3.68E-07	1.65E-07
200	5	2.25E-04	-6.88E-04	-9.69E-05	6.19E-06	0.00E+00	0.00E+00	-1.98E-04	-5.98E-04	4.22E-04	-1.38E-06	3.54E-07	-1.64E-07
200	10	4.50E-04	-1.31E-03	-1.89E-04	1.19E-05	-1.74E-05	0.00E+00	-3.79E-04	-1.15E-03	8.26E-04	-2.61E-06	6.94E-07	-3.29E-07
200	20	6.75E-04	-2.40E-03	-3.61E-04	2.24E-05	-1.74E-05	0.00E+00	-6.97E-04	-2.16E-03	1.58E-03	-4.65E-06	1.34E-06	-6.56E-07

Table D3.33 aqueous silica: effect of change in *Cp'*

MHz	%	c 10nm	c 100nm	c 1um	c 10um	c 100um	c 1mm	a 10nm	a 100nm	a 1um	a 10um	a 100um	a 1mm
0.1	-20	7.68E+00	7.73E+00	-3.09E+00	-2.42E-02	-1.56E-03	-1.60E-04	3.70E-02	2.78E-02	2.26E-02	5.32E-02	4.30E-02	1.34E-02
0.1	-10	3.38E+00	3.40E+00	-1.35E+00	-1.01E-02	-6.54E-04	-6.74E-05	1.82E-02	1.34E-02	1.08E-02	2.26E-02	1.80E-02	5.62E-03
0.1	-5	1.59E+00	1.60E+00	-6.38E-01	-4.64E-03	-3.02E-04	-3.11E-05	9.06E-03	6.58E-03	5.31E-03	1.05E-02	8.32E-03	2.59E-03
0.1	5	-1.42E+00	-1.43E+00	5.70E-01	3.97E-03	2.60E-04	2.66E-05	-8.94E-03	-6.36E-03	-5.11E-03	-9.09E-03	-7.17E-03	-2.23E-03
0.1	10	-2.70E+00	-2.72E+00	1.08E+00	7.40E-03	4.84E-04	4.96E-05	-1.78E-02	-1.25E-02	-1.00E-02	-1.70E-02	-1.34E-02	-4.16E-03
0.1	20	-4.90E+00	-4.93E+00	1.96E+00	1.30E-02	8.50E-04	8.73E-05	-3.51E-02	-2.42E-02	-1.94E-02	-3.01E-02	-2.35E-02	-7.31E-03
1	-20	-1.58E+00	-1.52E+00	-1.22E-01	-3.73E-03	-3.56E-04	2.56E-05	4.38E-02	2.81E-02	2.91E-02	3.26E-02	1.70E-02	2.59E-05
1	-10	-6.90E-01	-6.64E-01	-5.22E-02	-1.55E-03	-1.48E-04	1.08E-05	2.16E-02	1.35E-02	1.35E-02	1.36E-02	7.05E-03	1.07E-05
1	-5	-3.24E-01	-3.12E-01	-2.43E-02	-7.13E-04	-6.80E-05	4.81E-06	1.07E-02	6.61E-03	6.48E-03	6.24E-03	3.24E-03	4.91E-06
1	5	2.89E-01	2.78E-01	2.12E-02	6.07E-04	5.83E-05	-4.41E-06	-1.06E-02	-6.36E-03	-6.01E-03	-5.34E-03	-2.76E-03	-4.18E-06
1	10	5.46E-01	5.26E-01	3.99E-02	1.13E-03	1.08E-04	-8.01E-06	-2.10E-02	-1.25E-02	-1.16E-02	-9.92E-03	-5.14E-03	-7.75E-06
1	20	9.84E-01	9.47E-01	7.07E-02	1.97E-03	1.88E-04	-1.40E-05	-4.15E-02	-2.40E-02	-2.15E-02	-1.73E-02	-8.95E-03	-1.34E-05
10	-20	-6.25E-01	-4.29E-01	-1.09E-02	-7.83E-04	5.58E-05	1.12E-05	5.21E-02	2.57E-02	2.81E-02	1.58E-02	5.36E-05	2.47E-06
10	-10	-2.71E-01	-1.85E-01	-4.44E-03	-3.21E-04	2.31E-05	5.60E-06	2.56E-02	1.22E-02	1.16E-02	6.48E-03	2.18E-05	7.83E-07
10	-5	-1.27E-01	-8.66E-02	-2.02E-03	-1.47E-04	1.04E-05	0.00E+00	1.27E-02	5.95E-03	5.33E-03	2.96E-03	9.94E-06	3.04E-07
10	5	1.12E-01	7.62E-02	1.70E-03	1.24E-04	-8.76E-06	-5.60E-06	-1.25E-02	-5.65E-03	-4.53E-03	-2.50E-03	-8.33E-06	-1.67E-07
10	10	2.10E-01	1.43E-01	3.14E-03	2.28E-04	-1.63E-05	-5.60E-06	-2.49E-02	-1.10E-02	-8.38E-03	-4.61E-03	-1.53E-05	-2.26E-07
10	20	3.75E-01	2.55E-01	5.40E-03	3.92E-04	-2.83E-05	-1.12E-05	-4.90E-02	-2.09E-02	-1.45E-02	-7.94E-03	-2.62E-05	-1.04E-07
100	-20	-3.41E-01	-5.58E-02	-1.70E-03	1.09E-04	2.86E-05	0.00E+00	6.20E-02	2.57E-02	1.26E-02	1.04E-04	8.24E-07	-8.01E-07
100	-10	-1.45E-01	-2.29E-02	-6.82E-04	4.43E-05	1.72E-05	0.00E+00	3.05E-02	1.15E-02	5.10E-03	4.15E-05	-4.16E-07	-3.67E-07
100	-5	-6.74E-02	-1.05E-02	-3.07E-04	2.00E-05	5.72E-06	0.00E+00	1.51E-02	5.41E-03	2.32E-03	1.87E-05	-3.62E-07	-1.76E-07
100	5	5.85E-02	8.75E-03	2.52E-04	-1.68E-05	-5.72E-06	0.00E+00	-1.49E-02	-4.83E-03	-1.93E-03	-1.54E-05	5.95E-07	1.63E-07
100	10	1.09E-01	1.61E-02	4.60E-04	-3.09E-05	-1.14E-05	0.00E+00	-2.95E-02	-9.14E-03	-3.54E-03	-2.81E-05	1.37E-06	3.15E-07
100	20	1.91E-01	2.73E-02	7.71E-04	-5.21E-05	-1.72E-05	0.00E+00	-5.81E-02	-1.64E-02	-6.02E-03	-4.72E-05	3.28E-06	5.90E-07
200	-20	-2.01E-01	-1.68E-02	-8.49E-04	6.43E-05	1.74E-05	0.00E+00	7.48E-02	2.00E-02	4.16E-03	-4.04E-05	-3.80E-06	8.16E-07
200	-10	-8.32E-02	-6.43E-03	-3.23E-04	2.62E-05	1.74E-05	0.00E+00	3.67E-02	8.35E-03	1.66E-03	-1.97E-05	-2.23E-06	5.00E-07
200	-5	-3.80E-02	-2.82E-03	-1.42E-04	1.19E-05	1.74E-05	0.00E+00	1.82E-02	3.82E-03	7.45E-04	-9.73E-06	-1.17E-06	2.66E-07
200	5	3.18E-02	2.19E-03	1.11E-04	-1.05E-05	0.00E+00	0.00E+00	-1.78E-02	-3.22E-03	-6.09E-04	9.42E-06	1.25E-06	-2.87E-07
200	10	5.82E-02	3.88E-03	1.96E-04	-1.90E-05	0.00E+00	0.00E+00	-3.53E-02	-5.93E-03	-1.11E-03	1.85E-05	2.54E-06	-5.89E-07
200	20	9.78E-02	6.09E-03	3.08E-04	-3.24E-05	0.00E+00	0.00E+00	-6.92E-02	-1.01E-02	-1.85E-03	3.57E-05	5.19E-06	-1.22E-06

Table D3.34 aqueous silica: effect of change in *alpha'*

MHz	%	c 10nm	c 100nm	c 1um	c 10um	c 100um	c 1mm	a 10nm	a 100nm	a 1um	a 10um	a 100um	a 1mm
0.1	-20	0.00E+00	0.00E+00	0.00E+00	0.00E+00	0.00E+00	0.00E+00	-2.21E-03	-3.92E-05	-5.92E-07	-3.42E-07	-2.72E-06	-8.48E-06
0.1	-10	0.00E+00	0.00E+00	0.00E+00	0.00E+00	0.00E+00	0.00E+00	-1.11E-03	-1.96E-05	-2.96E-07	-1.71E-07	-1.36E-06	-4.24E-06
0.1	-5	0.00E+00	0.00E+00	0.00E+00	0.00E+00	0.00E+00	0.00E+00	-5.53E-04	-9.81E-06	-1.48E-07	-8.55E-08	-6.81E-07	-2.12E-06
0.1	5	0.00E+00	0.00E+00	0.00E+00	0.00E+00	0.00E+00	0.00E+00	5.53E-04	9.80E-06	1.48E-07	8.55E-08	6.81E-07	2.12E-06
0.1	10	0.00E+00	0.00E+00	0.00E+00	0.00E+00	0.00E+00	0.00E+00	1.11E-03	1.96E-05	2.96E-07	1.71E-07	1.36E-06	4.24E-06
0.1	20	0.00E+00	0.00E+00	0.00E+00	0.00E+00	0.00E+00	0.00E+00	2.21E-03	3.92E-05	5.92E-07	3.42E-07	2.72E-06	8.48E-06
1	-20	0.00E+00	0.00E+00	3.32E-06	7.78E-07	0.00E+00	-4.01E-07	-2.66E-03	-5.11E-05	-2.50E-06	-1.09E-05	-5.75E-05	-5.38E-07
1	-10	0.00E+00	0.00E+00	3.32E-06	7.78E-07	0.00E+00	-4.01E-07	-1.33E-03	-2.55E-05	-1.25E-06	-5.43E-06	-2.88E-05	-2.69E-07
1	-5	0.00E+00	0.00E+00	3.32E-06	7.78E-07	0.00E+00	-4.01E-07	-6.65E-04	-1.28E-05	-6.24E-07	-2.72E-06	-1.44E-05	-1.35E-07
1	5	0.00E+00	0.00E+00	0.00E+00	0.00E+00	0.00E+00	0.00E+00	6.65E-04	1.28E-05	6.24E-07	2.72E-06	1.44E-05	1.35E-07
1	10	0.00E+00	0.00E+00	0.00E+00	0.00E+00	0.00E+00	0.00E+00	1.33E-03	2.55E-05	1.25E-06	5.43E-06	2.88E-05	2.69E-07
1	20	0.00E+00	0.00E+00	0.00E+00	0.00E+00	0.00E+00	0.00E+00	2.66E-03	5.11E-05	2.50E-06	1.09E-05	5.75E-05	5.38E-07
10	-20	0.00E+00	0.00E+00	3.16E-06	0.00E+00	-1.99E-06	0.00E+00	-3.23E-03	-8.43E-05	-4.91E-05	-2.93E-04	-6.29E-06	-8.12E-07
10	-10	0.00E+00	0.00E+00	2.11E-06	0.00E+00	-7.96E-07	0.00E+00	-1.61E-03	-4.21E-05	-2.46E-05	-1.46E-04	-3.15E-06	-4.06E-07
10	-5	0.00E+00	0.00E+00	1.05E-06	0.00E+00	-3.98E-07	0.00E+00	-8.07E-04	-2.11E-05	-1.23E-05	-7.31E-05	-1.57E-06	-2.03E-07
10	5	0.00E+00	-5.35E-05	0.00E+00	0.00E+00	3.98E-07	0.00E+00	8.07E-04	2.11E-05	1.23E-05	7.31E-05	1.57E-06	2.03E-07
10	10	0.00E+00	-5.35E-05	-1.05E-06	0.00E+00	7.96E-07	0.00E+00	1.61E-03	4.21E-05	2.46E-05	1.46E-04	3.15E-06	4.06E-07
10	20	0.00E+00	-5.35E-05	-2.11E-06	-7.69E-07	1.99E-06	0.00E+00	3.23E-03	8.43E-05	4.91E-05	2.93E-04	6.29E-06	8.12E-07
100	-20	-1.56E-04	1.33E-04	1.02E-05	-2.15E-05	1.14E-05	2.98E-04	-4.05E-03	-3.51E-04	-1.27E-03	-6.97E-05	-9.44E-06	9.43E-06
100	-10	0.00E+00	6.66E-05	5.10E-06	-1.10E-05	5.72E-06	0.00E+00	-2.03E-03	-1.75E-04	-6.35E-04	-3.49E-05	-4.72E-06	4.70E-06
100	-5	0.00E+00	3.33E-05	2.55E-06	-5.48E-06	5.72E-06	0.00E+00	-1.01E-03	-8.76E-05	-3.18E-04	-1.74E-05	-2.36E-06	2.35E-06
100	5	1.56E-04	-3.33E-05	-2.55E-06	5.48E-06	0.00E+00	0.00E+00	1.01E-03	8.76E-05	3.18E-04	1.74E-05	2.36E-06	-2.34E-06
100	10	1.56E-04	-6.66E-05	-5.10E-06	1.10E-05	0.00E+00	0.00E+00	2.03E-03	1.75E-04	6.35E-04	3.49E-05	4.72E-06	-4.68E-06
100	20	3.12E-04	-1.30E-04	-1.02E-05	2.19E-05	-5.72E-06	0.00E+00	4.05E-03	3.51E-04	1.27E-03	6.97E-05	9.43E-06	-9.35E-06
200	-20	-1.58E-03	2.27E-04	3.51E-05	-1.12E-04	5.22E-05	0.00E+00	-5.00E-03	-8.47E-04	-2.20E-03	-3.14E-05	-6.56E-06	-3.23E-05
200	-10	-9.01E-04	1.12E-04	1.70E-05	-5.57E-05	3.48E-05	0.00E+00	-2.50E-03	-4.24E-04	-1.10E-03	-1.57E-05	-3.28E-06	-1.60E-05
200	-5	-4.50E-04	5.72E-05	8.51E-06	-2.81E-05	1.74E-05	0.00E+00	-1.25E-03	-2.12E-04	-5.50E-04	-7.85E-06	-1.64E-06	-8.00E-06
200	5	2.25E-04	-5.72E-05	-9.57E-06	2.76E-05	-1.74E-05	0.00E+00	1.25E-03	2.12E-04	5.50E-04	7.86E-06	1.64E-06	7.95E-06
200	10	6.76E-04	-1.12E-04	-1.81E-05	5.57E-05	-1.74E-05	0.00E+00	2.50E-03	4.24E-04	1.10E-03	1.57E-05	3.28E-06	1.58E-05
200	20	1.58E-03	-2.27E-04	-3.51E-05	1.11E-04	-5.22E-05	0.00E+00	5.00E-03	8.47E-04	2.20E-03	3.15E-05	6.55E-06	3.15E-05

Table D3.35 aqueous silica: effect of change in *beta'*

MHz	%	c 10nm	c 100nm	c 1um	c 10um	c 100um	c 1mm	a 10nm	a 100nm	a 1um	a 10um	a 100um	a 1mm
0.1	-20	-7.73E+00	-7.78E+00	3.04E+00	1.58E-02	1.05E-03	1.08E-04	-1.07E-01	-6.64E-02	-5.03E-02	-3.88E-02	-2.91E-02	-9.01E-03
0.1	-10	-4.19E+00	-4.21E+00	1.65E+00	8.48E-03	5.61E-04	5.77E-05	-5.55E-02	-3.63E-02	-2.75E-02	-2.09E-02	-1.56E-02	-4.83E-03
0.1	-5	-2.17E+00	-2.19E+00	8.55E-01	4.38E-03	2.89E-04	2.96E-05	-2.82E-02	-1.89E-02	-1.44E-02	-1.08E-02	-8.03E-03	-2.49E-03
0.1	5	2.33E+00	2.35E+00	-9.17E-01	-4.64E-03	-3.07E-04	-3.11E-05	2.92E-02	2.06E-02	1.56E-02	1.15E-02	8.51E-03	2.64E-03
0.1	10	4.82E+00	4.85E+00	-1.90E+00	-9.53E-03	-6.30E-04	-6.44E-05	5.93E-02	4.28E-02	3.25E-02	2.38E-02	1.75E-02	5.41E-03
0.1	20	1.03E+01	1.03E+01	-4.04E+00	-2.00E-02	-1.32E-03	-1.35E-04	1.23E-01	9.25E-02	7.03E-02	5.03E-02	3.67E-02	1.14E-02
1	-20	-1.07E+00	-1.08E+00	2.78E-01	5.37E-03	5.10E-04	-3.69E-05	-1.29E-01	-9.22E-02	-6.72E-02	-4.46E-02	-2.35E-02	-3.72E-05
1	-10	-5.74E-01	-5.81E-01	1.49E-01	2.84E-03	2.70E-04	-1.92E-05	-6.71E-02	-5.03E-02	-3.64E-02	-2.37E-02	-1.24E-02	-1.97E-05
1	-5	-2.97E-01	-3.01E-01	7.68E-02	1.46E-03	1.38E-04	-1.00E-05	-3.42E-02	-2.62E-02	-1.89E-02	-1.22E-02	-6.37E-03	-1.01E-05
1	5	3.17E-01	3.21E-01	-8.14E-02	-1.53E-03	-1.45E-04	1.04E-05	3.56E-02	2.85E-02	2.04E-02	1.28E-02	6.68E-03	1.06E-05
1	10	6.53E-01	6.62E-01	-1.67E-01	-3.12E-03	-2.95E-04	2.12E-05	7.25E-02	5.93E-02	4.22E-02	2.61E-02	1.36E-02	2.17E-05
1	20	1.38E+00	1.40E+00	-3.52E-01	-6.47E-03	-6.14E-04	4.41E-05	1.51E-01	1.28E-01	9.04E-02	5.43E-02	2.83E-02	4.51E-05
10	-20	-6.81E-01	-7.84E-01	3.53E-02	2.36E-03	-1.63E-04	-1.68E-05	-1.54E-01	-1.13E-01	-7.71E-02	-4.33E-02	-1.65E-04	-1.42E-05
10	-10	-3.64E-01	-4.19E-01	1.85E-02	1.24E-03	-8.48E-05	-5.60E-06	-8.02E-02	-6.14E-02	-4.08E-02	-2.27E-02	-8.63E-05	-7.66E-06
10	-5	-1.88E-01	-2.16E-01	9.43E-03	6.30E-04	-4.34E-05	-5.60E-06	-4.10E-02	-3.20E-02	-2.09E-02	-1.16E-02	-4.40E-05	-3.96E-06
10	5	2.00E-01	2.29E-01	-9.76E-03	-6.52E-04	4.50E-05	5.60E-06	4.29E-02	3.47E-02	2.19E-02	1.20E-02	4.56E-05	4.19E-06
10	10	4.11E-01	4.72E-01	-1.98E-02	-1.32E-03	9.08E-05	1.12E-05	8.77E-02	7.24E-02	4.48E-02	2.43E-02	9.27E-05	8.59E-06
10	20	8.68E-01	9.95E-01	-4.07E-02	-2.72E-03	1.86E-04	1.68E-05	1.84E-01	1.57E-01	9.30E-02	5.00E-02	1.90E-04	1.79E-05
100	-20	-5.47E-01	4.16E+00	1.14E-02	-6.72E-04	-6.29E-05	5.97E-04	-1.77E-01	-1.34E-01	-6.65E-02	-6.72E-04	-6.34E-05	1.31E-06
100	-10	-2.91E-01	2.19E+00	5.86E-03	-3.46E-04	-2.86E-05	2.98E-04	-9.31E-02	-7.20E-02	-3.44E-02	-3.47E-04	-3.34E-05	6.33E-07
100	-5	-1.50E-01	1.12E+00	2.97E-03	-1.76E-04	-1.72E-05	2.98E-04	-4.77E-02	-3.73E-02	-1.75E-02	-1.76E-04	-1.71E-05	3.11E-07
100	5	1.59E-01	-1.17E+00	-3.04E-03	1.79E-04	1.72E-05	0.00E+00	5.02E-02	3.99E-02	1.79E-02	1.80E-04	1.77E-05	-3.00E-07
100	10	3.26E-01	-2.38E+00	-6.12E-03	3.60E-04	3.43E-05	-2.98E-04	1.03E-01	8.26E-02	3.62E-02	3.63E-04	3.59E-05	-5.89E-07
100	20	6.87E-01	-4.93E+00	-1.24E-02	7.29E-04	6.29E-05	-5.97E-04	2.17E-01	1.76E-01	7.36E-02	7.35E-04	7.36E-05	-1.13E-06
200	-20	-4.80E-01	9.35E-01	1.31E-02	-6.64E-04	3.13E-04	0.00E+00	-2.05E-01	-1.63E-01	-4.55E-02	-1.11E-04	-7.05E-05	1.77E-05
200	-10	-2.55E-01	4.82E-01	6.64E-03	-3.36E-04	1.57E-04	0.00E+00	-1.09E-01	-8.63E-02	-2.32E-02	-6.02E-05	-3.63E-05	9.10E-06
200	-5	-1.31E-01	2.44E-01	3.34E-03	-1.69E-04	8.70E-05	0.00E+00	-5.59E-02	-4.44E-02	-1.17E-02	-3.11E-05	-1.84E-05	4.60E-06
200	5	1.38E-01	-2.49E-01	-3.36E-03	1.70E-04	-6.96E-05	0.00E+00	5.93E-02	4.67E-02	1.18E-02	3.27E-05	1.87E-05	-4.66E-06
200	10	2.83E-01	-5.02E-01	-6.72E-03	3.39E-04	-1.57E-04	-1.14E-02	1.22E-01	9.56E-02	2.36E-02	6.66E-05	3.75E-05	-9.35E-06
200	20	5.93E-01	-1.02E+00	-1.34E-02	6.76E-04	-3.13E-04	-1.14E-02	2.60E-01	2.00E-01	4.71E-02	1.37E-04	7.53E-05	-1.87E-05

Table D3.36 aqueous silica: effect of change in *c*

MHz	%	c 10nm	c 100nm	c 1um	c 10um	c 100um	c 1mm	a 10nm	a 100nm	a 1um	a 10um	a 100um	a 1mm
0.1	-20	-1.12E+02	-1.13E+02	4.54E+01	6.86E-01	4.02E-01	3.72E-01	4.14E-01	2.04E-01	2.14E-01	2.23E-01	2.33E-01	1.64E+00
0.1	-10	-6.64E+01	-6.68E+01	2.68E+01	4.23E-01	2.56E-01	2.45E-01	1.70E-01	8.92E-02	9.41E-02	9.83E-02	1.03E-01	5.78E-01
0.1	-5	-3.59E+01	-3.61E+01	1.45E+01	2.33E-01	1.42E-01	1.38E-01	7.78E-02	4.20E-02	4.44E-02	4.64E-02	4.86E-02	2.47E-01
0.1	5	4.14E+01	4.17E+01	-1.67E+01	-2.77E-01	-1.72E-01	-1.69E-01	-6.68E-02	-3.74E-02	-3.98E-02	-4.17E-02	-4.38E-02	-1.86E-01
0.1	10	8.86E+01	8.92E+01	-3.58E+01	-5.99E-01	-3.75E-01	-3.71E-01	-1.25E-01	-7.09E-02	-7.57E-02	-7.94E-02	-8.34E-02	-3.28E-01
0.1	20	2.01E+02	2.02E+02	-8.14E+01	-1.39E+00	-8.78E-01	-8.79E-01	-2.21E-01	-1.28E-01	-1.37E-01	-1.45E-01	-1.52E-01	-5.19E-01
1	-20	-1.13E+02	-1.33E+02	2.62E+00	4.54E-01	3.77E-01	-3.57E-01	4.15E-01	2.08E-01	2.18E-01	2.31E-01	1.06E+00	5.11E-01
1	-10	-6.65E+01	-7.84E+01	1.56E+00	2.86E-01	2.48E-01	-2.03E-01	1.70E-01	9.13E-02	9.63E-02	1.02E-01	3.85E-01	2.85E-01
1	-5	-3.59E+01	-4.24E+01	8.49E-01	1.59E-01	1.39E-01	-1.07E-01	7.81E-02	4.30E-02	4.55E-02	4.82E-02	1.67E-01	1.47E-01
1	5	4.15E+01	4.89E+01	-9.89E-01	-1.91E-01	-1.71E-01	1.15E-01	-6.70E-02	-3.84E-02	-4.08E-02	-4.34E-02	-1.29E-01	-1.47E-01
1	10	8.87E+01	1.05E+02	-2.12E+00	-4.16E-01	-3.76E-01	2.37E-01	-1.25E-01	-7.28E-02	-7.76E-02	-8.26E-02	-2.30E-01	-2.86E-01
1	20	2.01E+02	2.38E+02	-4.85E+00	-9.72E-01	-8.88E-01	5.11E-01	-2.22E-01	-1.32E-01	-1.41E-01	-1.51E-01	-3.73E-01	-5.22E-01
10	-20	-1.13E+02	4.53E+01	6.86E-01	3.93E-01	-3.56E-01	-4.69E-01	4.19E-01	2.19E-01	2.25E-01	6.38E-01	5.06E-01	-5.13E-02
10	-10	-6.68E+01	2.68E+01	4.23E-01	2.57E-01	-2.03E-01	-2.15E-01	1.72E-01	9.61E-02	9.93E-02	2.42E-01	2.82E-01	-4.35E-02
10	-5	-3.61E+01	1.45E+01	2.33E-01	1.45E-01	-1.07E-01	-1.10E-01	7.88E-02	4.53E-02	4.69E-02	1.07E-01	1.45E-01	6.94E-03
10	5	4.17E+01	-1.67E+01	-2.77E-01	-1.78E-01	1.15E-01	3.05E-01	-6.76E-02	-4.05E-02	-4.21E-02	-8.67E-02	-1.45E-01	1.48E-02
10	10	8.92E+01	-3.58E+01	-5.99E-01	-3.89E-01	2.37E-01	5.71E-01	-1.26E-01	-7.70E-02	-8.01E-02	-1.58E-01	-2.83E-01	8.51E-02
10	20	2.02E+02	-8.14E+01	-1.39E+00	-9.20E-01	5.11E-01	7.74E-01	-2.24E-01	-1.40E-01	-1.46E-01	-2.66E-01	-5.18E-01	1.57E-01
100	-20	-1.33E+02	2.62E+00	4.50E-01	-3.53E-01	-4.65E-01	-3.58E-01	4.31E-01	2.34E-01	4.57E-01	4.92E-01	-4.60E-02	-4.20E-02
100	-10	-7.87E+01	1.57E+00	2.92E-01	-2.02E-01	-2.11E-01	-1.96E-01	1.77E-01	1.02E-01	1.83E-01	2.72E-01	-4.00E-02	-2.55E-02
100	-5	-4.25E+01	8.51E-01	1.64E-01	-1.07E-01	-1.10E-01	-3.04E-01	8.10E-02	4.80E-02	8.27E-02	1.40E-01	8.07E-03	-1.45E-02
100	5	4.91E+01	-9.91E-01	-2.00E-01	1.15E-01	3.06E-01	2.27E-02	-6.95E-02	-4.29E-02	-6.95E-02	-1.41E-01	1.43E-02	1.61E-02
100	10	1.05E+02	-2.13E+00	-4.38E-01	2.38E-01	5.69E-01	-4.07E-01	-1.30E-01	-8.15E-02	-1.29E-01	-2.74E-01	8.21E-02	6.26E-03
100	20	2.39E+02	-4.86E+00	-1.03E+00	5.12E-01	7.63E-01	-1.71E+00	-2.30E-01	-1.48E-01	-2.23E-01	-5.04E-01	1.49E-01	2.90E-02
200	-20	-1.93E+02	1.52E+00	4.32E-01	-5.49E-01	-4.73E-01	-9.66E-01	4.39E-01	2.46E-01	1.02E+00	3.40E-02	-6.14E-02	-2.97E-01
200	-10	-1.14E+02	9.16E-01	3.04E-01	-3.30E-01	-2.36E-01	1.60E+00	1.80E-01	1.07E-01	3.85E-01	1.02E-02	-4.34E-02	-1.07E-01
200	-5	-6.15E+01	4.99E-01	1.75E-01	-1.84E-01	-1.27E-01	4.49E+00	8.25E-02	5.02E-02	1.70E-01	6.05E-04	-2.97E-02	5.15E-03
200	5	7.11E+01	-5.85E-01	-2.23E-01	2.26E-01	2.36E-01	-1.99E+00	-7.07E-02	-4.46E-02	-1.34E-01	1.23E-02	2.49E-02	3.32E-03
200	10	1.52E+02	-1.26E+00	-4.94E-01	4.91E-01	3.22E-01	-3.22E+00	-1.32E-01	-8.45E-02	-2.42E-01	4.53E-02	4.17E-02	4.25E-02
200	20	3.45E+02	-2.89E+00	-1.19E+00	1.13E+00	5.71E-01	-2.27E+01	-2.34E-01	-1.53E-01	-4.00E-01	2.03E-01	1.09E-01	-1.13E-02

Table D3.37 aqueous silica: effect of change in *rho*

MHz	%	c 10nm	c 100nm	c 1um	c 10um	c 100um	c 1mm	a 10nm	a 100nm	a 1um	a 10um	a 100um	a 1mm
0.1	-20	3.09E+02	3.11E+02	-1.24E+02	-1.34E+00	-5.63E-01	-5.46E-01	6.72E-01	9.69E-01	1.09E+00	1.16E+00	1.08E+00	5.67E-01
0.1	-10	1.35E+02	1.36E+02	-5.43E+01	-6.09E-01	-2.68E-01	-2.62E-01	2.85E-01	4.05E-01	4.51E-01	4.79E-01	4.57E-01	2.51E-01
0.1	-5	6.32E+01	6.36E+01	-2.54E+01	-2.91E-01	-1.31E-01	-1.28E-01	1.32E-01	1.86E-01	2.06E-01	2.18E-01	2.10E-01	1.18E-01
0.1	5	-5.57E+01	-5.61E+01	2.24E+01	2.67E-01	1.25E-01	1.23E-01	-1.13E-01	-1.57E-01	-1.73E-01	-1.81E-01	-1.78E-01	-1.05E-01
0.1	10	-1.05E+02	-1.06E+02	4.23E+01	5.13E-01	2.44E-01	2.41E-01	-2.10E-01	-2.88E-01	-3.17E-01	-3.31E-01	-3.29E-01	-1.99E-01
0.1	20	-1.87E+02	-1.88E+02	7.52E+01	9.47E-01	4.66E-01	4.62E-01	-3.62E-01	-4.86E-01	-5.34E-01	-5.54E-01	-5.59E-01	-3.56E-01
1	-20	-1.27E+00	-1.27E+00	-1.02E+00	-4.39E-01	-3.91E-01	-7.82E-02	7.30E-01	1.30E+00	1.63E+00	1.65E+00	9.35E-01	-2.12E-02
1	-10	-5.42E-01	-5.42E-01	-4.38E-01	-2.04E-01	-1.85E-01	-4.11E-02	2.96E-01	5.10E-01	6.24E-01	6.48E-01	3.86E-01	-1.28E-02
1	-5	-2.51E-01	-2.51E-01	-2.04E-01	-9.84E-02	-9.02E-02	-2.11E-02	1.33E-01	2.25E-01	2.73E-01	2.87E-01	1.75E-01	-7.01E-03
1	5	2.16E-01	2.16E-01	1.77E-01	9.18E-02	8.54E-02	2.20E-02	-1.08E-01	-1.74E-01	-2.07E-01	-2.23E-01	-1.44E-01	8.27E-03
1	10	4.01E-01	4.00E-01	3.31E-01	1.77E-01	1.66E-01	4.51E-02	-1.94E-01	-3.05E-01	-3.61E-01	-3.91E-01	-2.62E-01	1.79E-02
1	20	6.92E-01	6.92E-01	5.79E-01	3.31E-01	3.15E-01	9.38E-02	-3.11E-01	-4.56E-01	-5.37E-01	-5.91E-01	-4.27E-01	4.14E-02
10	-20	-5.26E-01	-5.21E-01	-3.61E-01	-3.00E-01	-1.00E-01	-7.64E-02	6.12E-01	1.49E+00	1.63E+00	1.17E+00	-4.36E-02	-8.45E-02
10	-10	-2.14E-01	-2.12E-01	-1.59E-01	-1.39E-01	-5.25E-02	-3.03E-02	2.20E-01	4.77E-01	5.04E-01	4.04E-01	-2.56E-02	-4.27E-02
10	-5	-9.66E-02	-9.58E-02	-7.46E-02	-6.72E-02	-2.69E-02	-1.31E-02	9.20E-02	1.83E-01	1.88E-01	1.64E-01	-1.38E-02	-2.15E-02
10	5	7.85E-02	7.80E-02	6.59E-02	6.23E-02	2.80E-02	9.03E-03	-6.08E-02	-8.91E-02	-8.31E-02	-9.82E-02	1.60E-02	2.16E-02
10	10	1.41E-01	1.41E-01	1.24E-01	1.20E-01	5.72E-02	1.39E-02	-9.46E-02	-9.92E-02	-7.87E-02	-1.40E-01	3.42E-02	4.32E-02
10	20	2.27E-01	2.27E-01	2.19E-01	2.23E-01	1.19E-01	1.09E-02	-9.48E-02	7.17E-02	1.37E-01	-8.56E-02	7.78E-02	8.63E-02
100	-20	-2.47E-01	-2.39E-01	-2.29E-01	-1.22E-01	-1.70E-02	-1.91E+00	2.25E-01	5.93E-02	1.59E-01	-7.72E-02	-9.14E-02	8.28E-03
100	-10	-8.88E-02	-9.08E-02	-1.02E-01	-6.39E-02	3.42E-03	-8.71E-01	3.17E-02	-1.60E-01	-8.79E-02	-4.47E-02	-4.57E-02	6.67E-03
100	-5	-3.71E-02	-3.92E-02	-4.80E-02	-3.26E-02	4.73E-03	-4.17E-01	-1.04E-03	-1.17E-01	-7.81E-02	-2.39E-02	-2.28E-02	3.79E-03
100	5	2.45E-02	2.86E-02	4.26E-02	3.37E-02	-1.08E-02	3.37E-01	2.97E-02	1.77E-01	1.35E-01	2.73E-02	2.25E-02	-5.07E-03
100	10	3.80E-02	4.78E-02	8.01E-02	6.85E-02	-2.76E-02	6.13E-01	8.40E-02	4.01E-01	3.16E-01	5.80E-02	4.45E-02	-9.61E-03
100	20	3.78E-02	6.26E-02	1.41E-01	1.41E-01	-7.86E-02	9.71E-01	2.53E-01	9.55E-01	7.87E-01	1.31E-01	8.67E-02	-2.02E-02
200	-20	-6.42E-02	-1.01E-01	-1.70E-01	-1.06E-01	6.38E-01	-4.64E-02	-1.85E-01	-5.18E-01	-1.44E-01	-2.05E-01	-5.64E-02	1.12E-02
200	-10	-3.96E-03	-2.90E-02	-7.17E-02	-4.56E-02	3.56E-01	4.64E-03	-1.45E-01	-3.18E-01	-1.28E-01	-1.07E-01	-2.47E-02	4.33E-03
200	-5	3.96E-03	-9.92E-03	-3.28E-02	-2.08E-02	1.85E-01	5.57E-03	-8.32E-02	-1.70E-01	-7.57E-02	-5.43E-02	-1.14E-02	1.87E-03
200	5	-1.41E-02	1.89E-03	2.71E-02	1.69E-02	-1.92E-01	-8.35E-03	1.01E-01	1.86E-01	9.54E-02	5.56E-02	9.28E-03	-1.38E-03
200	10	-3.70E-02	-3.27E-03	4.89E-02	3.00E-02	-3.86E-01	-1.76E-02	2.17E-01	3.85E-01	2.08E-01	1.12E-01	1.67E-02	-2.38E-03
200	20	-1.04E-01	-3.16E-02	7.77E-02	4.48E-02	-7.78E-01	-3.25E-02	4.86E-01	8.06E-01	4.73E-01	2.25E-01	2.80E-02	-3.65E-03

Table D3.38 aqueous silica: effect of change in *eta*

MHz	%	c 10nm	c 100nm	c 1um	c 10um	c 100um	c 1mm	a 10nm	a 100nm	a 1um	a 10um	a 100um	a 1mm
0.1	-20	0.00E+00	-1.59E-03	4.03E-01	4.80E-02	3.69E-03	4.23E-04	6.39E-02	2.11E-01	1.75E-01	-5.30E-02	-9.57E-02	-3.56E-02
0.1	-10	0.00E+00	-6.63E-04	1.77E-01	2.31E-02	1.79E-03	2.06E-04	2.50E-02	9.38E-02	7.93E-02	-2.47E-02	-4.64E-02	-1.73E-02
0.1	-5	0.00E+00	-2.65E-04	8.33E-02	1.14E-02	8.84E-04	1.01E-04	1.10E-02	4.45E-02	3.79E-02	-1.19E-02	-2.29E-02	-8.53E-03
0.1	5	0.00E+00	2.65E-04	-7.45E-02	-1.10E-02	-8.62E-04	-9.84E-05	-8.55E-03	-4.03E-02	-3.49E-02	1.11E-02	2.23E-02	8.31E-03
0.1	10	0.00E+00	5.30E-04	-1.42E-01	-2.17E-02	-1.70E-03	-1.95E-04	-1.50E-02	-7.69E-02	-6.71E-02	2.16E-02	4.40E-02	1.64E-02
0.1	20	0.00E+00	1.06E-03	-2.57E-01	-4.21E-02	-3.33E-03	-3.82E-04	-2.24E-02	-1.41E-01	-1.25E-01	4.05E-02	8.58E-02	3.21E-02
1	-20	0.00E+00	-4.07E-02	1.86E-01	1.39E-02	1.48E-03	-3.26E-04	3.08E-02	1.99E-01	7.03E-02	-8.62E-02	-6.53E-02	-1.14E-03
1	-10	0.00E+00	-1.76E-02	8.56E-02	6.75E-03	7.19E-04	-1.59E-04	9.53E-03	8.89E-02	3.43E-02	-4.15E-02	-3.17E-02	-5.53E-04
1	-5	0.00E+00	-8.28E-03	4.11E-02	3.33E-03	3.55E-04	-7.85E-05	3.53E-03	4.22E-02	1.69E-02	-2.04E-02	-1.57E-02	-2.73E-04
1	5	0.00E+00	7.23E-03	-3.81E-02	-3.24E-03	-3.46E-04	7.61E-05	-1.41E-03	-3.83E-02	-1.64E-02	1.97E-02	1.53E-02	2.66E-04
1	10	0.00E+00	1.37E-02	-7.35E-02	-6.41E-03	-6.84E-04	1.51E-04	-9.96E-04	-7.32E-02	-3.24E-02	3.88E-02	3.02E-02	5.26E-04
1	20	0.00E+00	2.47E-02	-1.37E-01	-1.25E-02	-1.34E-03	2.95E-04	4.42E-03	-1.34E-01	-6.29E-02	7.53E-02	5.90E-02	1.03E-03
10	-20	-9.26E-04	4.79E-01	5.96E-02	5.30E-03	-1.09E-03	1.16E-03	-4.20E-03	1.72E-01	-4.29E-02	-8.51E-02	-3.87E-03	-1.07E-03
10	-10	-3.97E-04	2.09E-01	2.86E-02	2.58E-03	-5.29E-04	5.66E-04	-6.85E-03	7.77E-02	-1.96E-02	-4.13E-02	-1.88E-03	-5.18E-04
10	-5	-2.65E-04	9.84E-02	1.41E-02	1.27E-03	-2.61E-04	2.80E-04	-4.43E-03	3.70E-02	-9.36E-03	-2.04E-02	-9.29E-04	-2.56E-04
10	5	1.32E-04	-8.80E-02	-1.36E-02	-1.24E-03	2.54E-04	-2.69E-04	6.15E-03	-3.39E-02	8.59E-03	1.98E-02	9.07E-04	2.49E-04
10	10	2.65E-04	-1.67E-01	-2.67E-02	-2.45E-03	5.02E-04	-5.38E-04	1.38E-02	-6.50E-02	1.65E-02	3.92E-02	1.79E-03	4.93E-04
10	20	5.29E-04	-3.02E-01	-5.16E-02	-4.79E-03	9.82E-04	-1.05E-03	3.28E-02	-1.20E-01	3.04E-02	7.65E-02	3.51E-03	9.63E-04
100	-20	-2.28E-02	2.08E-01	2.07E-02	-3.30E-03	4.83E-03	3.55E-02	-4.20E-02	8.01E-02	-8.80E-02	-1.27E-02	-3.46E-03	7.42E-05
100	-10	-9.86E-03	9.46E-02	1.01E-02	-1.60E-03	2.36E-03	1.71E-02	-2.45E-02	3.81E-02	-4.25E-02	-6.17E-03	-1.68E-03	4.01E-05
100	-5	-4.64E-03	4.52E-02	4.96E-03	-7.85E-04	1.17E-03	8.38E-03	-1.30E-02	1.86E-02	-2.09E-02	-3.05E-03	-8.27E-04	2.07E-05
100	5	3.91E-03	-4.16E-02	-4.83E-03	7.63E-04	-1.14E-03	-8.06E-03	1.43E-02	-1.77E-02	2.03E-02	2.98E-03	8.05E-04	-2.20E-05
100	10	7.54E-03	-8.00E-02	-9.54E-03	1.50E-03	-2.27E-03	-1.61E-02	2.97E-02	-3.45E-02	4.00E-02	5.89E-03	1.59E-03	-4.50E-05
100	20	1.35E-02	-1.48E-01	-1.86E-02	2.93E-03	-4.45E-03	-3.13E-02	6.34E-02	-6.58E-02	7.78E-02	1.15E-02	3.10E-03	-9.42E-05
200	-20	-5.24E-02	1.72E-01	2.67E-02	-6.45E-04	1.72E-02	-1.36E+00	-7.29E-02	3.99E-02	-8.06E-02	-1.17E-02	-3.36E-03	1.09E-03
200	-10	-2.23E-02	7.93E-02	1.30E-02	-3.02E-04	8.39E-03	-6.43E-01	-3.91E-02	1.96E-02	-3.92E-02	-5.68E-03	-1.62E-03	5.31E-04
200	-5	-1.03E-02	3.82E-02	6.39E-03	-1.46E-04	4.14E-03	-3.21E-01	-2.01E-02	9.67E-03	-1.94E-02	-2.80E-03	-7.97E-04	2.61E-04
200	5	9.17E-03	-3.55E-02	-6.23E-03	1.37E-04	-4.05E-03	3.21E-01	2.11E-02	-9.42E-03	1.89E-02	2.74E-03	7.73E-04	-2.54E-04
200	10	1.72E-02	-6.86E-02	-1.23E-02	2.67E-04	-8.01E-03	6.07E-01	4.31E-02	-1.86E-02	3.74E-02	5.41E-03	1.52E-03	-5.02E-04
200	20	3.05E-02	-1.28E-01	-2.41E-02	5.03E-04	-1.57E-02	1.14E+00	8.91E-02	-3.59E-02	7.31E-02	1.06E-02	2.96E-03	-9.78E-04

Table D3.39 aqueous silica: effect of change in *kappa*

MHz	%	c 10nm	c 100nm	c 1um	c 10um	c 100um	c 1mm	a 10nm	a 100nm	a 1um	a 10um	a 100um	a 1mm
0.1	-20	0.00E+00	-5.30E-04	4.71E-02	1.63E-03	1.04E-04	1.11E-05	1.72E-02	2.73E-02	1.19E-02	-3.36E-03	-2.88E-03	-9.02E-04
0.1	-10	0.00E+00	-1.33E-04	2.12E-02	7.65E-04	4.94E-05	5.18E-06	7.65E-03	1.22E-02	5.48E-03	-1.58E-03	-1.36E-03	-4.25E-04
0.1	-5	0.00E+00	-1.33E-04	1.01E-02	3.72E-04	2.36E-05	2.22E-06	3.62E-03	5.79E-03	2.64E-03	-7.64E-04	-6.59E-04	-2.06E-04
0.1	5	0.00E+00	1.33E-04	-9.20E-03	-3.53E-04	-2.29E-05	-2.22E-06	-3.28E-03	-5.25E-03	-2.46E-03	7.22E-04	6.25E-04	1.96E-04
0.1	10	0.00E+00	1.33E-04	-1.77E-02	-6.89E-04	-4.44E-05	-4.44E-06	-6.26E-03	-1.00E-02	-4.75E-03	1.40E-03	1.22E-03	3.81E-04
0.1	20	0.00E+00	2.65E-04	-3.26E-02	-1.31E-03	-8.44E-05	-8.88E-06	-1.15E-02	-1.85E-02	-8.91E-03	2.67E-03	2.32E-03	7.27E-04
1	-20	0.00E+00	-9.88E-03	1.03E-02	3.58E-04	3.44E-05	-2.40E-06	1.42E-02	1.95E-02	1.91E-03	-2.95E-03	-1.59E-03	-2.37E-06
1	-10	0.00E+00	-4.32E-03	4.76E-03	1.69E-04	1.64E-05	-1.20E-06	6.33E-03	8.76E-03	9.35E-04	-1.39E-03	-7.47E-04	-1.12E-06
1	-5	0.00E+00	-2.01E-03	2.30E-03	8.17E-05	8.22E-06	-4.01E-07	3.00E-03	4.17E-03	4.62E-04	-6.73E-04	-3.63E-04	-5.42E-07
1	5	0.00E+00	1.85E-03	-2.15E-03	-7.70E-05	-7.47E-06	8.01E-07	-2.72E-03	-3.81E-03	-4.52E-04	6.37E-04	3.44E-04	5.13E-07
1	10	0.00E+00	3.40E-03	-4.17E-03	-1.50E-04	-1.42E-05	1.20E-06	-5.19E-03	-7.30E-03	-8.93E-04	1.24E-03	6.70E-04	1.00E-06
1	20	0.00E+00	6.17E-03	-7.86E-03	-2.87E-04	-2.69E-05	2.40E-06	-9.51E-03	-1.35E-02	-1.74E-03	2.36E-03	1.28E-03	1.90E-06
10	-20	-2.65E-04	3.71E-02	1.59E-03	1.09E-04	-7.96E-06	-5.60E-06	1.13E-02	1.02E-02	-3.17E-03	-2.09E-03	-7.16E-06	-2.15E-07
10	-10	-1.32E-04	1.66E-02	7.45E-04	5.16E-05	-3.98E-06	-5.60E-06	5.04E-03	4.66E-03	-1.48E-03	-9.82E-04	-3.36E-06	-1.01E-07
10	-5	0.00E+00	7.92E-03	3.62E-04	2.54E-05	-1.99E-06	0.00E+00	2.39E-03	2.24E-03	-7.17E-04	-4.77E-04	-1.63E-06	-4.91E-08
10	5	0.00E+00	-7.18E-03	-3.43E-04	-2.31E-05	1.59E-06	0.00E+00	-2.17E-03	-2.08E-03	6.76E-04	4.51E-04	1.54E-06	4.65E-08
10	10	1.32E-04	-1.38E-02	-6.68E-04	-4.54E-05	3.19E-06	0.00E+00	-4.15E-03	-4.01E-03	1.31E-03	8.78E-04	3.01E-06	9.06E-08
10	20	1.32E-04	-2.53E-02	-1.27E-03	-8.62E-05	6.37E-06	0.00E+00	-7.61E-03	-7.50E-03	2.49E-03	1.67E-03	5.72E-06	1.72E-07
100	-20	-7.03E-03	9.34E-03	3.60E-04	-2.35E-05	-5.72E-06	0.00E+00	7.94E-03	1.91E-03	-2.39E-03	-2.07E-05	-6.49E-07	4.88E-08
100	-10	-3.06E-03	4.31E-03	1.68E-04	-1.10E-05	-5.72E-06	0.00E+00	3.56E-03	9.28E-04	-1.12E-03	-9.72E-06	-3.06E-07	2.34E-08
100	-5	-1.38E-03	2.08E-03	8.16E-05	-5.48E-06	-5.72E-06	0.00E+00	1.69E-03	4.57E-04	-5.43E-04	-4.72E-06	-1.49E-07	1.15E-08
100	5	1.38E-03	-1.94E-03	-7.74E-05	5.09E-06	0.00E+00	0.00E+00	-1.54E-03	-4.44E-04	5.13E-04	4.46E-06	1.41E-07	-1.11E-08
100	10	2.60E-03	-3.75E-03	-1.51E-04	9.79E-06	0.00E+00	0.00E+00	-2.96E-03	-8.74E-04	9.98E-04	8.68E-06	2.75E-07	-2.18E-08
100	20	4.59E-03	-7.05E-03	-2.86E-04	1.88E-05	5.72E-06	0.00E+00	-5.46E-03	-1.70E-03	1.90E-03	1.65E-05	5.25E-07	-4.23E-08
200	-20	-2.00E-02	6.07E-03	2.98E-04	-2.19E-05	0.00E+00	0.00E+00	6.08E-03	-6.27E-04	-1.24E-03	9.53E-06	-9.24E-07	6.57E-08
200	-10	-8.86E-03	2.82E-03	1.39E-04	-9.99E-06	0.00E+00	0.00E+00	2.74E-03	-2.60E-04	-5.81E-04	4.45E-06	-4.33E-07	3.19E-08
200	-5	-4.12E-03	1.37E-03	6.71E-05	-4.76E-06	0.00E+00	0.00E+00	1.30E-03	-1.19E-04	-2.81E-04	2.15E-06	-2.10E-07	1.58E-08
200	5	3.71E-03	-1.28E-03	-6.39E-05	4.76E-06	0.00E+00	0.00E+00	-1.19E-03	9.95E-05	2.65E-04	-2.03E-06	1.98E-07	-1.54E-08
200	10	7.01E-03	-2.49E-03	-1.25E-04	9.52E-06	0.00E+00	0.00E+00	-2.29E-03	1.82E-04	5.16E-04	-3.94E-06	3.86E-07	-3.06E-08
200	20	1.28E-02	-4.71E-03	-2.36E-04	1.76E-05	0.00E+00	0.00E+00	-4.22E-03	3.06E-04	9.80E-04	-7.46E-06	7.34E-07	-5.99E-08

Table D3.40 aqueous silica: effect of change in *Cp*

MHz	%	c 10nm	c 100nm	c 1um	c 10um	c 100um	c 1mm	a 10nm	a 100nm	a 1um	a 10um	a 100um	a 1mm
0.1	-20	-3.54E+00	-3.56E+00	1.40E+00	8.62E-03	5.74E-04	5.92E-05	-4.58E-02	-2.88E-02	-1.83E-02	-1.99E-02	-1.58E-02	-4.93E-03
0.1	-10	-1.63E+00	-1.64E+00	6.43E-01	4.07E-03	2.71E-04	2.81E-05	-2.06E-02	-1.32E-02	-8.07E-03	-9.31E-03	-7.47E-03	-2.33E-03
0.1	-5	-7.82E-01	-7.87E-01	3.09E-01	1.98E-03	1.32E-04	1.33E-05	-9.82E-03	-6.31E-03	-3.80E-03	-4.51E-03	-3.63E-03	-1.13E-03
0.1	5	7.25E-01	7.29E-01	-2.86E-01	-1.87E-03	-1.25E-04	-1.26E-05	8.97E-03	5.81E-03	3.38E-03	4.24E-03	3.43E-03	1.07E-03
0.1	10	1.40E+00	1.41E+00	-5.53E-01	-3.65E-03	-2.43E-04	-2.52E-05	1.72E-02	1.12E-02	6.39E-03	8.23E-03	6.69E-03	2.09E-03
0.1	20	2.61E+00	2.62E+00	-1.03E+00	-6.93E-03	-4.62E-04	-4.74E-05	3.17E-02	2.07E-02	1.15E-02	1.56E-02	1.27E-02	3.97E-03
1	-20	-8.95E-01	-9.34E-01	7.31E-02	1.95E-03	1.85E-04	-1.28E-05	-3.81E-02	-2.13E-02	-1.49E-02	-1.61E-02	-8.65E-03	-1.42E-05
1	-10	-4.09E-01	-4.26E-01	3.38E-02	9.15E-04	8.67E-05	-6.01E-06	-1.71E-02	-9.49E-03	-6.64E-03	-7.54E-03	-4.05E-03	-6.68E-06
1	-5	-1.96E-01	-2.04E-01	1.63E-02	4.44E-04	4.18E-05	-2.80E-06	-8.13E-03	-4.49E-03	-3.14E-03	-3.65E-03	-1.96E-03	-3.24E-06
1	5	1.80E-01	1.88E-01	-1.51E-02	-4.17E-04	-3.96E-05	2.40E-06	7.41E-03	4.05E-03	2.82E-03	3.43E-03	1.85E-03	3.06E-06
1	10	3.47E-01	3.62E-01	-2.93E-02	-8.12E-04	-7.77E-05	5.21E-06	1.42E-02	7.70E-03	5.37E-03	6.66E-03	3.59E-03	5.95E-06
1	20	6.45E-01	6.73E-01	-5.49E-02	-1.54E-03	-1.46E-04	9.61E-06	2.61E-02	1.40E-02	9.77E-03	1.26E-02	6.80E-03	1.13E-05
10	-20	-4.87E-01	-1.20E+00	8.32E-03	5.85E-04	-3.74E-05	5.60E-06	-3.10E-02	-1.09E-02	-1.75E-02	-1.11E-02	-4.27E-05	-6.32E-06
10	-10	-2.21E-01	-5.45E-01	3.87E-03	2.72E-04	-1.75E-05	0.00E+00	-1.38E-02	-4.61E-03	-8.10E-03	-5.16E-03	-1.99E-05	-3.03E-06
10	-5	-1.06E-01	-2.60E-01	1.87E-03	1.32E-04	-8.36E-06	0.00E+00	-6.57E-03	-2.13E-03	-3.90E-03	-2.49E-03	-9.65E-06	-1.48E-06
10	5	9.69E-02	2.39E-01	-1.76E-03	-1.24E-04	8.36E-06	0.00E+00	5.95E-03	1.82E-03	3.64E-03	2.34E-03	9.06E-06	1.41E-06
10	10	1.86E-01	4.60E-01	-3.41E-03	-2.40E-04	1.55E-05	0.00E+00	1.14E-02	3.39E-03	7.03E-03	4.53E-03	1.76E-05	2.76E-06
10	20	3.45E-01	8.53E-01	-6.43E-03	-4.53E-04	2.95E-05	0.00E+00	2.09E-02	5.88E-03	1.32E-02	8.56E-03	3.33E-05	5.27E-06
100	-20	-3.25E-01	6.94E-02	1.92E-03	-1.08E-04	1.72E-05	2.98E-04	-2.34E-02	-1.03E-02	-1.20E-02	-1.21E-04	-1.87E-05	4.41E-07
100	-10	-1.47E-01	3.18E-02	8.88E-04	-5.01E-05	5.72E-06	0.00E+00	-1.03E-02	-4.51E-03	-5.56E-03	-5.62E-05	-8.85E-06	2.00E-07
100	-5	-6.99E-02	1.52E-02	4.28E-04	-2.39E-05	5.72E-06	0.00E+00	-4.86E-03	-2.12E-03	-2.68E-03	-2.71E-05	-4.30E-06	9.57E-08
100	5	6.40E-02	-1.41E-02	-4.02E-04	2.27E-05	-5.72E-06	0.00E+00	4.36E-03	1.88E-03	2.51E-03	2.54E-05	4.07E-06	-8.82E-08
100	10	1.23E-01	-2.72E-02	-7.78E-04	4.38E-05	-5.72E-06	0.00E+00	8.28E-03	3.56E-03	4.85E-03	4.92E-05	7.93E-06	-1.70E-07
100	20	2.27E-01	-5.08E-02	-1.47E-03	8.26E-05	-1.14E-05	0.00E+00	1.50E-02	6.40E-03	9.13E-03	9.28E-05	1.51E-05	-3.16E-07
200	-20	-2.37E-01	3.29E-02	1.56E-03	-5.19E-05	6.96E-05	1.14E-02	-1.78E-02	-1.18E-02	-5.97E-03	-6.76E-05	-1.26E-05	4.83E-06
200	-10	-1.07E-01	1.51E-02	7.22E-04	-2.43E-05	3.48E-05	1.14E-02	-7.77E-03	-5.28E-03	-2.76E-03	-3.14E-05	-5.95E-06	2.27E-06
200	-5	-5.07E-02	7.27E-03	3.48E-04	-1.14E-05	1.74E-05	0.00E+00	-3.65E-03	-2.51E-03	-1.33E-03	-1.52E-05	-2.89E-06	1.10E-06
200	5	4.63E-02	-6.75E-03	-3.24E-04	1.09E-05	-1.74E-05	0.00E+00	3.25E-03	2.27E-03	1.24E-03	1.42E-05	2.73E-06	-1.04E-06
200	10	8.88E-02	-1.30E-02	-6.28E-04	2.09E-05	-3.48E-05	0.00E+00	6.15E-03	4.34E-03	2.40E-03	2.75E-05	5.32E-06	-2.01E-06
200	20	1.64E-01	-2.44E-02	-1.18E-03	3.95E-05	-5.22E-05	0.00E+00	1.11E-02	7.96E-03	4.51E-03	5.17E-05	1.01E-05	-3.81E-06

Table D3.41 aqueous silica: effect of change in *alpha*

MHz	%	c 10nm	c 100nm	c 1um	c 10um	c 100um	c 1mm	a 10nm	a 100nm	a 1um	a 10um	a 100um	a 1mm
0.1	-20	0.00E+00	0.00E+00	0.00E+00	-1.05E-06	0.00E+00	0.00E+00	-2.12E-02	-3.76E-04	-4.94E-06	1.26E-06	1.45E-05	4.47E-05
0.1	-10	0.00E+00	0.00E+00	0.00E+00	-1.05E-06	0.00E+00	0.00E+00	-1.07E-02	-1.88E-04	-2.47E-06	6.29E-07	7.26E-06	2.24E-05
0.1	-5	0.00E+00	0.00E+00	0.00E+00	0.00E+00	0.00E+00	0.00E+00	-5.39E-03	-9.39E-05	-1.23E-06	3.15E-07	3.63E-06	1.12E-05
0.1	5	0.00E+00	0.00E+00	0.00E+00	0.00E+00	0.00E+00	0.00E+00	5.29E-03	9.39E-05	1.23E-06	-3.15E-07	-3.63E-06	-1.12E-05
0.1	10	0.00E+00	0.00E+00	0.00E+00	0.00E+00	0.00E+00	0.00E+00	1.06E-02	1.88E-04	2.47E-06	-6.29E-07	-7.26E-06	-2.24E-05
0.1	20	0.00E+00	0.00E+00	0.00E+00	0.00E+00	0.00E+00	0.00E+00	2.11E-02	3.76E-04	4.94E-06	-1.26E-06	-1.45E-05	-4.47E-05
1	-20	0.00E+00	0.00E+00	-9.96E-06	-7.78E-07	0.00E+00	2.80E-06	-2.13E-02	-4.04E-04	-5.09E-06	4.51E-05	2.51E-04	2.98E-07
1	-10	0.00E+00	0.00E+00	-6.64E-06	-7.78E-07	0.00E+00	1.20E-06	-1.06E-02	-2.02E-04	-2.55E-06	2.26E-05	1.26E-04	1.49E-07
1	-5	0.00E+00	0.00E+00	-3.32E-06	-7.78E-07	0.00E+00	8.01E-07	-5.32E-03	-1.01E-04	-1.27E-06	1.13E-05	6.28E-05	7.46E-08
1	5	0.00E+00	0.00E+00	0.00E+00	0.00E+00	0.00E+00	-4.01E-07	5.32E-03	1.01E-04	1.27E-06	-1.13E-05	-6.28E-05	-7.46E-08
1	10	0.00E+00	0.00E+00	3.32E-06	0.00E+00	0.00E+00	-1.20E-06	1.06E-02	2.02E-04	2.55E-06	-2.26E-05	-1.26E-04	-1.49E-07
1	20	0.00E+00	0.00E+00	9.96E-06	7.78E-07	7.47E-07	-2.40E-06	2.13E-02	4.04E-04	5.09E-06	-4.51E-05	-2.51E-04	-2.98E-07
10	-20	0.00E+00	-4.28E-04	-2.95E-05	-3.08E-06	2.59E-05	1.12E-05	-2.16E-02	-4.89E-04	1.25E-04	1.04E-03	2.84E-06	8.03E-06
10	-10	0.00E+00	-2.14E-04	-1.47E-05	-1.54E-06	1.27E-05	5.60E-06	-1.08E-02	-2.44E-04	6.27E-05	5.21E-04	1.42E-06	4.02E-06
10	-5	0.00E+00	-1.07E-04	-7.37E-06	-7.69E-07	6.37E-06	0.00E+00	-5.40E-03	-1.22E-04	3.13E-05	2.60E-04	7.10E-07	2.01E-06
10	5	0.00E+00	1.07E-04	7.37E-06	7.69E-07	-6.37E-06	0.00E+00	5.40E-03	1.22E-04	-3.13E-05	-2.60E-04	-7.10E-07	-2.01E-06
10	10	0.00E+00	2.14E-04	1.37E-05	1.54E-06	-1.27E-05	-5.60E-06	1.08E-02	2.44E-04	-6.27E-05	-5.21E-04	-1.42E-06	-4.02E-06
10	20	0.00E+00	4.28E-04	2.84E-05	3.08E-06	-2.59E-05	-1.12E-05	2.16E-02	4.89E-04	-1.25E-04	-1.04E-03	-2.84E-06	-8.04E-06
100	-20	2.19E-03	-1.02E-03	-9.34E-05	2.63E-04	9.72E-05	-8.94E-03	-2.25E-02	-5.00E-04	3.49E-03	2.43E-05	7.87E-05	1.02E-04
100	-10	1.09E-03	-5.06E-04	-4.67E-05	1.32E-04	4.58E-05	-4.47E-03	-1.12E-02	-2.50E-04	1.75E-03	1.22E-05	3.94E-05	5.16E-05
100	-5	6.25E-04	-2.53E-04	-2.29E-05	6.58E-05	2.29E-05	-2.39E-03	-5.61E-03	-1.25E-04	8.73E-04	6.07E-06	1.97E-05	2.60E-05
100	5	-6.25E-04	2.56E-04	2.38E-05	-6.58E-05	-2.86E-05	2.39E-03	5.61E-03	1.25E-04	-8.73E-04	-6.07E-06	-1.97E-05	-2.63E-05
100	10	-1.09E-03	5.09E-04	4.67E-05	-1.32E-04	-5.15E-05	4.77E-03	1.12E-02	2.50E-04	-1.75E-03	-1.21E-05	-3.94E-05	-5.29E-05
100	20	-2.19E-03	1.02E-03	9.34E-05	-2.63E-04	-9.72E-05	9.24E-03	2.25E-02	5.00E-04	-3.49E-03	-2.43E-05	-7.89E-05	-1.07E-04
200	-20	1.22E-02	-1.49E-03	-2.74E-04	-1.38E-05	1.04E-04	5.62E-02	-2.29E-02	1.55E-06	4.54E-03	4.80E-04	-9.73E-06	2.48E-03
200	-10	6.11E-03	-7.45E-04	-1.37E-04	-6.66E-06	5.22E-05	3.37E-02	-1.15E-02	7.33E-07	2.27E-03	2.40E-04	-4.98E-06	1.29E-03
200	-5	3.17E-03	-3.73E-04	-6.91E-05	-3.33E-06	1.74E-05	1.12E-02	-5.73E-03	3.56E-07	1.14E-03	1.20E-04	-2.52E-06	6.60E-04
200	5	-2.94E-03	3.73E-04	6.81E-05	2.86E-06	-3.48E-05	-2.25E-02	5.73E-03	-3.36E-07	-1.14E-03	-1.20E-04	2.57E-06	-6.89E-04
200	10	-5.88E-03	7.45E-04	1.37E-04	6.19E-06	-5.22E-05	-3.37E-02	1.15E-02	-6.53E-07	-2.27E-03	-2.40E-04	5.21E-06	-1.41E-03
200	20	-1.20E-02	1.49E-03	2.74E-04	1.29E-05	-1.22E-04	-6.74E-02	2.29E-02	-1.23E-06	-4.54E-03	-4.80E-04	1.06E-05	-2.94E-03

Table D3.42 aqueous silica: effect of change in *beta*

MHz	%	c 10nm	c 100nm	c 1um	c 10um	c 100um	c 1mm	a 10nm	a 100nm	a 1um	a 10um	a 100um	a 1mm
0.1	-20	3.15E+00	3.17E+00	-1.24E+00	-6.63E-03	-4.40E-04	-4.52E-05	1.06E-01	2.75E-02	2.00E-02	1.61E-02	1.22E-02	3.78E-03
0.1	-10	1.54E+00	1.55E+00	-6.07E-01	-3.24E-03	-2.15E-04	-2.22E-05	4.79E-02	1.34E-02	9.79E-03	7.84E-03	5.95E-03	1.85E-03
0.1	-5	7.61E-01	7.66E-01	-3.00E-01	-1.60E-03	-1.07E-04	-1.11E-05	2.28E-02	6.59E-03	4.84E-03	3.88E-03	2.94E-03	9.12E-04
0.1	5	-7.44E-01	-7.48E-01	2.93E-01	1.56E-03	1.04E-04	1.04E-05	-2.08E-02	-6.41E-03	-4.72E-03	-3.78E-03	-2.87E-03	-8.90E-04
0.1	10	-1.47E+00	-1.48E+00	5.79E-01	3.09E-03	2.05E-04	2.15E-05	-4.00E-02	-1.26E-02	-9.33E-03	-7.48E-03	-5.67E-03	-1.76E-03
0.1	20	-2.87E+00	-2.88E+00	1.13E+00	6.02E-03	3.99E-04	4.07E-05	-7.39E-02	-2.46E-02	-1.82E-02	-1.46E-02	-1.11E-02	-3.43E-03
1	-20	-1.86E+00	-1.72E+00	-6.32E-02	-1.66E-03	-1.58E-04	1.04E-05	9.95E-02	2.85E-02	2.02E-02	1.45E-02	7.50E-03	1.23E-05
1	-10	-9.03E-01	-8.35E-01	-3.06E-02	-8.07E-04	-7.69E-05	4.81E-06	4.48E-02	1.38E-02	9.78E-03	7.01E-03	3.64E-03	5.92E-06
1	-5	-4.44E-01	-4.11E-01	-1.51E-02	-3.97E-04	-3.73E-05	2.40E-06	2.13E-02	6.77E-03	4.81E-03	3.45E-03	1.79E-03	2.91E-06
1	5	4.30E-01	3.98E-01	1.46E-02	3.84E-04	3.66E-05	-2.40E-06	-1.95E-02	-6.53E-03	-4.66E-03	-3.34E-03	-1.73E-03	-2.80E-06
1	10	8.47E-01	7.84E-01	2.87E-02	7.56E-04	7.25E-05	-4.81E-06	-3.74E-02	-1.28E-02	-9.17E-03	-6.57E-03	-3.41E-03	-5.49E-06
1	20	1.64E+00	1.52E+00	5.56E-02	1.46E-03	1.40E-04	-9.62E-06	-6.92E-02	-2.48E-02	-1.77E-02	-1.27E-02	-6.60E-03	-1.06E-05
10	-20	-7.54E-01	-4.39E-01	-7.70E-03	-5.49E-04	3.54E-05	-5.60E-06	9.28E-02	2.59E-02	1.96E-02	1.10E-02	3.97E-05	3.87E-06
10	-10	-3.62E-01	-2.11E-01	-3.69E-03	-2.64E-04	1.71E-05	0.00E+00	4.18E-02	1.24E-02	9.38E-03	5.26E-03	1.89E-05	1.57E-06
10	-5	-1.77E-01	-1.03E-01	-1.81E-03	-1.29E-04	8.36E-06	0.00E+00	1.99E-02	6.04E-03	4.59E-03	2.58E-03	9.21E-06	6.91E-07
10	5	1.70E-01	9.88E-02	1.73E-03	1.24E-04	-7.96E-06	0.00E+00	-1.81E-02	-5.76E-03	-4.39E-03	-2.46E-03	-8.73E-06	-5.06E-07
10	10	3.32E-01	1.93E-01	3.39E-03	2.42E-04	-1.59E-05	0.00E+00	-3.47E-02	-1.12E-02	-8.59E-03	-4.82E-03	-1.70E-05	-8.28E-07
10	20	6.33E-01	3.69E-01	6.46E-03	4.62E-04	-3.03E-05	-5.60E-06	-6.40E-02	-2.14E-02	-1.64E-02	-9.19E-03	-3.21E-05	-9.16E-07
100	-20	-4.66E-01	-6.19E-02	-1.90E-03	1.11E-04	5.72E-06	0.00E+00	8.59E-02	2.50E-02	1.37E-02	1.17E-04	3.67E-06	-5.25E-07
100	-10	-2.20E-01	-2.92E-02	-8.99E-04	5.33E-05	5.72E-06	0.00E+00	3.84E-02	1.17E-02	6.44E-03	5.41E-05	2.71E-07	-2.41E-07
100	-5	-1.07E-01	-1.42E-02	-4.36E-04	2.58E-05	0.00E+00	0.00E+00	1.82E-02	5.66E-03	3.12E-03	2.60E-05	-2.57E-07	-1.16E-07
100	5	9.99E-02	1.33E-02	4.10E-04	-2.47E-05	-5.72E-06	0.00E+00	-1.65E-02	-5.29E-03	-2.92E-03	-2.38E-05	1.04E-06	1.10E-07
100	10	1.93E-01	2.57E-02	7.94E-04	-4.78E-05	-1.14E-05	0.00E+00	-3.15E-02	-1.02E-02	-5.65E-03	-4.55E-05	2.87E-06	2.14E-07
100	20	3.60E-01	4.80E-02	1.48E-03	-9.05E-05	-2.86E-05	-2.98E-04	-5.75E-02	-1.90E-02	-1.05E-02	-8.26E-05	8.90E-06	4.12E-07
200	-20	-3.20E-01	-3.03E-02	-1.57E-03	6.66E-05	8.70E-05	0.00E+00	7.66E-02	2.50E-02	6.73E-03	2.02E-05	-1.82E-05	5.69E-06
200	-10	-1.46E-01	-1.39E-02	-7.20E-04	3.28E-05	5.22E-05	0.00E+00	3.39E-02	1.14E-02	3.07E-03	2.45E-06	-1.11E-05	3.58E-06
200	-5	-6.97E-02	-6.62E-03	-3.43E-04	1.62E-05	3.48E-05	0.00E+00	1.60E-02	5.41E-03	1.46E-03	-6.81E-07	-6.03E-06	1.97E-06
200	5	6.29E-02	5.97E-03	3.11E-04	-1.62E-05	-1.74E-05	0.00E+00	-1.43E-02	-4.88E-03	-1.32E-03	4.48E-06	7.02E-06	-2.33E-06
200	10	1.19E-01	1.13E-02	5.88E-04	-3.19E-05	-5.22E-05	-1.12E-02	-2.70E-02	-9.22E-03	-2.49E-03	1.28E-05	1.51E-05	-5.02E-06
200	20	2.11E-01	2.00E-02	1.04E-03	-6.28E-05	-1.39E-04	-1.12E-02	-4.84E-02	-1.63E-02	-4.40E-03	4.07E-05	3.41E-05	-1.15E-05

Table D3.43 aqueous titanium dioxide:: effect of change in *c'*

MHz	%	c 10nm	c 100nm	c 1um	c 10um	c 100um	c 1mm	a 10nm	a 100nm	a 1um	a 10um	a 100um	a 1mm
0.1	-20	2.97E-03	2.97E-03	3.14E-03	1.86E-02	1.06E-01	1.31E-01	-2.44E-04	-3.23E-04	-3.26E-04	-3.81E-04	-3.96E-04	-6.34E-03
0.1	-10	1.15E-03	1.15E-03	1.21E-03	7.19E-03	4.08E-02	5.07E-02	-9.60E-05	-1.25E-04	-1.26E-04	-1.47E-04	-1.53E-04	-2.45E-03
0.1	-5	5.14E-04	5.14E-04	5.42E-04	3.22E-03	1.82E-02	2.27E-02	-4.32E-05	-5.58E-05	-5.64E-05	-6.59E-05	-6.85E-05	-1.10E-03
0.1	5	-4.24E-04	-4.24E-04	-4.47E-04	-2.65E-03	-1.50E-02	-1.87E-02	3.58E-05	4.60E-05	4.65E-05	5.43E-05	5.65E-05	9.06E-04
0.1	10	-7.77E-04	-7.78E-04	-8.20E-04	-4.87E-03	-2.76E-02	-3.43E-02	6.57E-05	8.44E-05	8.53E-05	9.97E-05	1.04E-04	1.66E-03
0.1	20	-1.33E-03	-1.33E-03	-1.40E-03	-8.34E-03	-4.73E-02	-5.89E-02	1.13E-04	1.45E-04	1.46E-04	1.71E-04	1.78E-04	2.85E-03
1	-20	1.74E-03	1.74E-03	3.29E-03	3.06E-02	7.12E-02	1.15E-02	-1.46E-04	-1.88E-04	-2.05E-04	-2.29E-04	-1.95E-03	-1.22E-03
1	-10	6.90E-04	6.91E-04	1.31E-03	1.22E-02	2.83E-02	4.57E-03	-5.81E-05	-7.48E-05	-8.15E-05	-9.10E-05	-7.74E-04	-4.80E-04
1	-5	3.12E-04	3.13E-04	5.92E-04	5.50E-03	1.28E-02	2.07E-03	-2.62E-05	-3.38E-05	-3.69E-05	-4.11E-05	-3.50E-04	-2.17E-04
1	5	-2.61E-04	-2.62E-04	-4.95E-04	-4.60E-03	-1.07E-02	-1.73E-03	2.18E-05	2.83E-05	3.08E-05	3.44E-05	2.93E-04	1.80E-04
1	10	-4.82E-04	-4.83E-04	-9.14E-04	-8.50E-03	-1.98E-02	-3.19E-03	4.02E-05	5.23E-05	5.69E-05	6.35E-05	5.41E-04	3.32E-04
1	20	-8.34E-04	-8.35E-04	-1.58E-03	-1.47E-02	-3.42E-02	-5.52E-03	6.89E-05	9.04E-05	9.85E-05	1.10E-04	9.36E-04	5.73E-04
10	-20	1.08E-03	1.14E-03	6.83E-03	3.24E-02	7.05E-03	8.34E-03	-8.89E-05	-1.18E-04	-1.39E-04	-5.63E-04	-7.16E-04	9.65E-03
10	-10	4.36E-04	4.60E-04	2.76E-03	1.31E-02	2.85E-03	8.22E-03	-3.55E-05	-4.76E-05	-5.60E-05	-2.28E-04	-2.88E-04	7.01E-03
10	-5	1.98E-04	2.09E-04	1.26E-03	5.96E-03	1.29E-03	3.31E-03	-1.61E-05	-2.17E-05	-2.55E-05	-1.04E-04	-1.31E-04	1.03E-03
10	5	-1.68E-04	-1.77E-04	-1.06E-03	-5.03E-03	-1.09E-03	-1.98E-03	1.34E-05	1.83E-05	2.15E-05	8.75E-05	1.10E-04	-1.11E-03
10	10	-3.11E-04	-3.27E-04	-1.97E-03	-9.33E-03	-2.03E-03	-3.56E-03	2.46E-05	3.39E-05	3.99E-05	1.62E-04	2.04E-04	-2.10E-03
10	20	-5.40E-04	-5.70E-04	-3.42E-03	-1.62E-02	-3.52E-03	-6.06E-03	4.22E-05	5.89E-05	6.94E-05	2.82E-04	3.53E-04	-3.70E-03
100	-20	6.98E-04	1.32E-03	1.09E-02	4.32E-03	8.17E-03	-2.66E-02	-5.35E-05	-8.22E-05	-1.96E-04	-4.07E-04	4.56E-03	4.82E-03
100	-10	2.85E-04	5.39E-04	4.44E-03	1.76E-03	2.99E-03	-6.86E-03	-2.13E-05	-3.35E-05	-7.99E-05	-1.66E-04	1.98E-03	3.15E-03
100	-5	1.30E-04	2.46E-04	2.03E-03	8.05E-04	1.37E-03	4.24E-03	-9.60E-06	-1.53E-05	-3.65E-05	-7.55E-05	9.09E-04	4.29E-04
100	5	-1.11E-04	-2.09E-04	-1.72E-03	-6.84E-04	-1.16E-03	8.27E-03	7.95E-06	1.30E-05	3.10E-05	6.40E-05	-7.71E-04	-9.10E-04
100	10	-2.05E-04	-3.89E-04	-3.20E-03	-1.27E-03	-2.16E-03	-4.24E-03	1.46E-05	2.42E-05	5.76E-05	1.19E-04	-1.43E-03	-2.40E-03
100	20	-3.59E-04	-6.79E-04	-5.59E-03	-2.22E-03	-3.78E-03	-1.39E-02	2.48E-05	4.22E-05	1.01E-04	2.07E-04	-2.49E-03	-2.60E-03
200	-20	4.63E-04	1.24E-03	6.44E-03	3.75E-03	-1.23E-02	-5.78E-02	-3.18E-05	-5.66E-05	-4.76E-04	4.60E-04	-4.21E-03	2.23E-03
200	-10	1.90E-04	5.10E-04	2.65E-03	1.54E-03	-1.10E-02	-5.33E-03	-1.25E-05	-2.32E-05	-1.96E-04	1.88E-04	-1.20E-03	2.29E-03
200	-5	8.72E-05	2.34E-04	1.21E-03	7.06E-04	-5.07E-03	3.56E-03	-5.61E-06	-1.06E-05	-8.97E-05	8.61E-05	-3.07E-04	3.28E-04
200	5	-7.43E-05	-1.99E-04	-1.03E-03	-6.02E-04	4.31E-03	2.49E-02	4.59E-06	9.07E-06	7.65E-05	-7.33E-05	2.46E-05	-2.16E-04
200	10	-1.38E-04	-3.71E-04	-1.92E-03	-1.12E-03	7.86E-03	3.29E-02	8.36E-06	1.69E-05	1.42E-04	-1.36E-04	-1.04E-04	-9.92E-04
200	20	-2.42E-04	-6.49E-04	-3.37E-03	-1.96E-03	1.24E-02	2.58E-02	1.41E-05	2.95E-05	2.49E-04	-2.38E-04	-6.34E-04	-1.98E-03

Table D3.44 aqueous titanium dioxide:: effect of change in *rho'*

MHz	%	c 10nm	c 100nm	c 1um	c 10um	c 100um	c 1mm	a 10nm	a 100nm	a 1um	a 10um	a 100um	a 1mm
0.1	-20	-3.37E-01	-3.37E-01	-3.33E-01	-4.11E-01	-1.42E+00	-1.71E+00	-4.28E-01	-4.33E-01	-4.25E-01	-2.39E-01	-1.91E-01	-1.15E-01
0.1	-10	-1.64E-01	-1.64E-01	-1.62E-01	-1.87E-01	-6.41E-01	-7.67E-01	-2.27E-01	-2.30E-01	-2.25E-01	-1.14E-01	-8.85E-02	-5.31E-02
0.1	-5	-8.09E-02	-8.09E-02	-7.96E-02	-8.91E-02	-3.06E-01	-3.65E-01	-1.17E-01	-1.18E-01	-1.15E-01	-5.53E-02	-4.27E-02	-2.56E-02
0.1	5	7.89E-02	7.89E-02	7.72E-02	8.18E-02	2.79E-01	3.33E-01	1.23E-01	1.25E-01	1.21E-01	5.26E-02	3.99E-02	2.38E-02
0.1	10	1.56E-01	1.56E-01	1.52E-01	1.57E-01	5.35E-01	6.39E-01	2.52E-01	2.56E-01	2.47E-01	1.03E-01	7.71E-02	4.61E-02
0.1	20	3.04E-01	3.04E-01	2.96E-01	2.91E-01	9.88E-01	1.18E+00	5.29E-01	5.37E-01	5.14E-01	1.95E-01	1.45E-01	8.64E-02
1	-20	-2.83E-01	-2.82E-01	-2.33E-01	-4.43E-01	-6.39E-01	-6.54E-02	-4.07E-01	-4.11E-01	-3.04E-01	-1.67E-01	-1.26E-01	6.49E-03
1	-10	-1.37E-01	-1.37E-01	-1.07E-01	-1.99E-01	-2.87E-01	-2.98E-02	-2.15E-01	-2.17E-01	-1.50E-01	-7.71E-02	-5.79E-02	2.55E-03
1	-5	-6.75E-02	-6.75E-02	-5.15E-02	-9.49E-02	-1.37E-01	-1.43E-02	-1.10E-01	-1.11E-01	-7.46E-02	-3.71E-02	-2.78E-02	1.13E-03
1	5	6.56E-02	6.55E-02	4.77E-02	8.67E-02	1.25E-01	1.32E-02	1.16E-01	1.17E-01	7.34E-02	3.46E-02	2.58E-02	-8.89E-04
1	10	1.29E-01	1.29E-01	9.18E-02	1.66E-01	2.38E-01	2.56E-02	2.37E-01	2.39E-01	1.45E-01	6.69E-02	4.98E-02	-1.57E-03
1	20	2.52E-01	2.51E-01	1.71E-01	3.07E-01	4.40E-01	4.79E-02	4.94E-01	4.99E-01	2.85E-01	1.26E-01	9.31E-02	-2.43E-03
10	-20	-2.44E-01	-2.37E-01	-2.04E-01	-3.45E-01	-5.61E-02	-2.73E-01	-3.90E-01	-3.80E-01	-1.68E-01	-1.20E-01	2.94E-03	1.80E-01
10	-10	-1.18E-01	-1.14E-01	-9.16E-02	-1.55E-01	-2.57E-02	-3.51E-01	-2.05E-01	-1.98E-01	-7.81E-02	-5.48E-02	9.34E-04	1.03E-02
10	-5	-5.80E-02	-5.56E-02	-4.36E-02	-7.35E-02	-1.24E-02	-4.48E-02	-1.05E-01	-1.01E-01	-3.77E-02	-2.63E-02	3.56E-04	-1.23E-02
10	5	5.61E-02	5.35E-02	3.98E-02	6.70E-02	1.15E-02	3.55E-01	1.10E-01	1.05E-01	3.53E-02	2.43E-02	-1.65E-04	7.16E-02
10	10	1.10E-01	1.05E-01	7.63E-02	1.28E-01	2.23E-02	3.61E-01	2.24E-01	2.13E-01	6.85E-02	4.69E-02	-1.63E-04	1.43E-01
10	20	2.14E-01	2.02E-01	1.41E-01	2.36E-01	4.22E-02	-1.84E-03	4.67E-01	4.38E-01	1.29E-01	8.73E-02	2.65E-04	2.61E-01
100	-20	-2.14E-01	-1.41E-01	-1.99E-01	-4.87E-02	6.47E-02	7.60E-01	-3.75E-01	-2.34E-01	-1.11E-01	-1.02E-03	-2.06E-01	2.90E-02
100	-10	-1.03E-01	-6.33E-02	-8.93E-02	-2.26E-02	3.66E-01	-2.53E-01	-1.96E-01	-1.13E-01	-5.07E-02	-9.19E-04	-1.10E-01	-1.28E-02
100	-5	-5.06E-02	-3.01E-02	-4.24E-02	-1.09E-02	4.03E-01	4.52E-01	-1.00E-01	-5.54E-02	-2.43E-02	-5.48E-04	-3.71E-02	2.14E-03
100	5	4.88E-02	2.74E-02	3.87E-02	1.03E-02	-1.15E-01	3.08E-01	1.05E-01	5.32E-02	2.24E-02	7.08E-04	5.56E-03	6.43E-04
100	10	9.59E-02	5.23E-02	7.40E-02	2.01E-02	-4.33E-01	2.94E-02	2.13E-01	1.04E-01	4.32E-02	1.56E-03	1.28E-02	2.65E-02
100	20	1.85E-01	9.59E-02	1.36E-01	3.84E-02	-4.21E-01	0.00E+00	4.43E-01	2.01E-01	8.05E-02	3.67E-03	-1.31E-01	1.20E-02
200	-20	-1.90E-01	-1.02E-01	-1.42E-01	8.53E-03	1.08E-01	-1.99E-01	-3.61E-01	-1.65E-01	-7.78E-02	1.93E-01	1.21E-01	-8.33E-03
200	-10	-9.08E-02	-4.55E-02	-6.38E-02	-3.61E-02	-3.44E-01	-7.87E-02	-1.88E-01	-7.73E-02	-3.54E-02	4.73E-02	1.60E-01	3.47E-03
200	-5	-4.45E-02	-2.15E-02	-3.03E-02	-2.04E-02	-4.12E-01	1.09E-01	-9.61E-02	-3.74E-02	-1.69E-02	1.74E-02	4.54E-02	2.08E-02
200	5	4.27E-02	1.94E-02	2.76E-02	2.31E-02	3.67E-01	-4.06E-01	9.98E-02	3.51E-02	1.56E-02	-9.30E-03	1.66E-01	8.51E-03
200	10	8.38E-02	3.70E-02	5.28E-02	4.89E-02	1.72E-01	-2.30E-02	2.03E-01	6.82E-02	2.99E-02	-1.26E-02	3.02E-01	4.38E-02
200	20	1.61E-01	6.75E-02	9.72E-02	1.12E-01	-1.01E+00	-9.43E-01	4.20E-01	1.29E-01	5.55E-02	-3.34E-03	1.83E-01	-1.80E-02

Table D3.45 aqueous titanium dioxide: effect of change in *mu'*

MHz	%	c 10nm	c 100nm	c 1um	c 10um	c 100um	c 1mm	a 10nm	a 100nm	a 1um	a 10um	a 100um	a 1mm
0.1	-20	-1.58E-04	-1.58E-04	-1.67E-04	-9.90E-04	-5.62E-03	-6.96E-03	7.44E-07	1.65E-05	1.70E-05	2.02E-05	2.11E-05	3.41E-04
0.1	-10	-8.09E-05	-8.08E-05	-8.52E-05	-5.06E-04	-2.87E-03	-3.56E-03	2.13E-07	8.43E-06	8.70E-06	1.03E-05	1.08E-05	1.74E-04
0.1	-5	-4.08E-05	-4.09E-05	-4.31E-05	-2.56E-04	-1.45E-03	-1.80E-03	1.58E-07	4.26E-06	4.40E-06	5.22E-06	5.45E-06	8.79E-05
0.1	5	4.17E-05	4.17E-05	4.40E-05	2.61E-04	1.48E-03	1.84E-03	-1.18E-07	-4.36E-06	-4.50E-06	-5.34E-06	-5.57E-06	-8.97E-05
0.1	10	8.43E-05	8.44E-05	8.90E-05	5.28E-04	2.99E-03	3.71E-03	-1.67E-07	-8.83E-06	-9.10E-06	-1.08E-05	-1.13E-05	-1.81E-04
0.1	20	1.72E-04	1.73E-04	1.82E-04	1.08E-03	6.12E-03	7.60E-03	9.58E-08	-1.81E-05	-1.86E-05	-2.21E-05	-2.30E-05	-3.71E-04
1	-20	-2.05E-04	-2.06E-04	-3.88E-04	-3.53E-03	-7.91E-03	3.80E-02	-2.88E-07	2.15E-05	2.41E-05	2.73E-05	2.35E-04	1.29E-02
1	-10	-1.05E-04	-1.06E-04	-1.99E-04	-1.81E-03	-4.06E-03	1.64E-02	-3.50E-07	1.11E-05	1.24E-05	1.40E-05	1.20E-04	5.55E-03
1	-5	-5.34E-05	-5.35E-05	-1.01E-04	-9.18E-04	-2.06E-03	7.66E-03	-2.31E-07	5.61E-06	6.28E-06	7.08E-06	6.09E-05	2.60E-03
1	5	5.48E-05	5.49E-05	1.04E-04	9.43E-04	2.12E-03	-6.77E-03	3.53E-07	-5.77E-06	-6.45E-06	-7.27E-06	-6.24E-05	-2.30E-03
1	10	1.11E-04	1.11E-04	2.10E-04	1.91E-03	4.29E-03	-1.28E-02	8.33E-07	-1.17E-05	-1.31E-05	-1.47E-05	-1.26E-04	-4.36E-03
1	20	2.29E-04	2.29E-04	4.33E-04	3.93E-03	8.83E-03	-2.30E-02	2.23E-06	-2.41E-05	-2.69E-05	-3.03E-05	-2.60E-04	-7.88E-03
10	-20	-2.72E-04	-2.86E-04	-1.69E-03	-7.57E-03	2.93E-02	8.89E-01	-3.04E-06	2.90E-05	3.54E-05	1.50E-04	1.02E-02	-9.89E-02
10	-10	-1.40E-04	-1.48E-04	-8.75E-04	-3.91E-03	1.26E-02	4.09E-01	-1.93E-06	1.50E-05	1.82E-05	7.69E-05	4.44E-03	-7.81E-02
10	-5	-7.13E-05	-7.52E-05	-4.45E-04	-1.99E-03	5.90E-03	1.21E-01	-1.08E-06	7.62E-06	9.26E-06	3.89E-05	2.09E-03	-6.81E-02
10	5	7.38E-05	7.78E-05	4.60E-04	2.06E-03	-5.21E-03	2.62E-01	1.32E-06	-7.89E-06	-9.57E-06	-4.01E-05	-1.86E-03	2.37E-02
10	10	1.50E-04	1.58E-04	9.37E-04	4.19E-03	-9.82E-03	3.81E-01	2.92E-06	-1.61E-05	-1.95E-05	-8.13E-05	-3.54E-03	2.10E-02
10	20	3.11E-04	3.28E-04	1.94E-03	8.69E-03	-1.76E-02	5.06E-01	7.02E-06	-3.33E-05	-4.03E-05	-1.68E-04	-6.43E-03	2.60E-02
100	-20	-3.69E-04	-6.96E-04	-5.47E-03	2.18E-02	-3.08E-01	4.44E-02	-1.08E-05	4.37E-05	1.20E-04	8.60E-03	-8.20E-02	8.39E-03
100	-10	-1.92E-04	-3.63E-04	-2.85E-03	9.34E-03	-1.10E-01	9.79E-02	-6.36E-06	2.27E-05	6.13E-05	3.77E-03	1.03E-03	8.62E-03
100	-5	-9.83E-05	-1.85E-04	-1.46E-03	4.35E-03	-4.39E-02	2.00E-01	-3.44E-06	1.15E-05	3.10E-05	1.78E-03	3.58E-03	4.23E-03
100	5	1.03E-04	1.94E-04	1.52E-03	-3.81E-03	2.43E-01	3.49E-01	4.02E-06	-1.20E-05	-3.19E-05	-1.60E-03	-6.31E-03	-4.03E-03
100	10	2.10E-04	3.96E-04	3.12E-03	-7.14E-03	2.29E-01	2.12E-01	8.69E-06	-2.45E-05	-6.48E-05	-3.05E-03	-5.18E-02	1.73E-02
100	20	4.41E-04	8.31E-04	6.54E-03	-1.26E-02	1.32E-01	2.97E-01	2.03E-05	-5.13E-05	-1.34E-04	-5.59E-03	-7.11E-02	-5.83E-04
200	-20	-5.21E-04	-1.39E-03	-6.81E-03	4.08E-02	-8.36E-02	-4.34E-01	-2.58E-05	6.44E-05	5.97E-04	-6.75E-03	7.26E-02	1.29E-02
200	-10	-2.75E-04	-7.31E-04	-3.60E-03	1.70E-02	3.51E-01	-6.51E-02	-1.51E-05	3.36E-05	3.10E-04	-2.69E-03	3.64E-02	3.31E-03
200	-5	-1.41E-04	-3.76E-04	-1.85E-03	7.83E-03	1.69E-01	-2.74E-02	-8.15E-06	1.72E-05	1.58E-04	-1.22E-03	-1.42E-02	3.01E-02
200	5	1.50E-04	3.98E-04	1.97E-03	-6.74E-03	-2.08E-01	-3.04E-01	9.56E-06	-1.81E-05	-1.65E-04	1.03E-03	4.50E-03	1.60E-02
200	10	3.09E-04	8.21E-04	4.05E-03	-1.26E-02	-2.10E-01	1.71E-03	2.07E-05	-3.71E-05	-3.39E-04	1.90E-03	3.78E-02	1.56E-02
200	20	6.58E-04	1.75E-03	8.65E-03	-2.20E-02	-2.25E-02	-8.65E-02	4.91E-05	-7.85E-05	-7.16E-04	3.32E-03	5.48E-02	-1.60E-03

Table D3.46 aqueous titanium dioxide: effect of change in *kappa'*

MHz	%	c 10nm	c 100nm	c 1um	c 10um	c 100um	c 1mm	a 10nm	a 100nm	a 1um	a 10um	a 100um	a 1mm
0.1	-20	0.00E+00	0.00E+00	-2.06E-06	-1.37E-04	-5.93E-05	-6.86E-06	4.34E-05	4.74E-05	5.47E-05	-9.95E-05	-1.22E-04	-5.67E-05
0.1	-10	0.00E+00	0.00E+00	-9.22E-07	-6.49E-05	-2.69E-05	-4.57E-06	1.93E-05	2.11E-05	2.43E-05	-4.45E-05	-5.68E-05	-2.64E-05
0.1	-5	0.00E+00	0.00E+00	-4.26E-07	-3.16E-05	-1.26E-05	-2.29E-06	9.12E-06	9.99E-06	1.15E-05	-2.11E-05	-2.75E-05	-1.28E-05
0.1	5	0.00E+00	0.00E+00	4.26E-07	3.00E-05	1.26E-05	0.00E+00	-8.24E-06	-9.03E-06	-1.04E-05	1.90E-05	2.58E-05	1.20E-05
0.1	10	0.00E+00	0.00E+00	7.80E-07	5.82E-05	2.33E-05	2.29E-06	-1.57E-05	-1.72E-05	-1.99E-05	3.61E-05	5.01E-05	2.33E-05
0.1	20	0.00E+00	0.00E+00	1.42E-06	1.11E-04	4.49E-05	4.57E-06	-2.88E-05	-3.16E-05	-3.65E-05	6.54E-05	9.49E-05	4.42E-05
1	-20	0.00E+00	-6.82E-08	-3.39E-05	-8.83E-05	-2.02E-05	-5.73E-07	3.63E-05	4.19E-05	4.43E-05	-1.14E-04	-8.39E-05	-4.68E-07
1	-10	0.00E+00	-6.82E-08	-1.50E-05	-4.06E-05	-1.01E-05	-5.73E-07	1.61E-05	1.86E-05	2.00E-05	-5.32E-05	-3.91E-05	-2.18E-07
1	-5	0.00E+00	0.00E+00	-7.05E-06	-1.94E-05	-4.04E-06	0.00E+00	7.63E-06	8.82E-06	9.56E-06	-2.57E-05	-1.89E-05	-1.05E-07
1	5	0.00E+00	0.00E+00	6.48E-06	1.85E-05	4.04E-06	0.00E+00	-6.90E-06	-7.98E-06	-8.75E-06	2.41E-05	1.77E-05	9.90E-08
1	10	0.00E+00	0.00E+00	1.23E-05	3.62E-05	8.07E-06	0.00E+00	-1.32E-05	-1.52E-05	-1.68E-05	4.69E-05	3.44E-05	1.92E-07
1	20	0.00E+00	0.00E+00	2.25E-05	6.88E-05	1.41E-05	5.73E-07	-2.41E-05	-2.79E-05	-3.11E-05	8.86E-05	6.51E-05	3.64E-07
10	-20	0.00E+00	-1.35E-06	-1.31E-04	-4.41E-05	-1.70E-06	0.00E+00	3.08E-05	3.82E-05	-6.19E-05	-9.56E-05	-1.39E-06	-6.92E-07
10	-10	0.00E+00	-6.39E-07	-6.12E-05	-2.06E-05	-1.13E-06	0.00E+00	1.37E-05	1.70E-05	-2.64E-05	-4.44E-05	-6.46E-07	-3.22E-07
10	-5	0.00E+00	-2.84E-07	-2.96E-05	-1.03E-05	-5.66E-07	0.00E+00	6.47E-06	8.04E-06	-1.22E-05	-2.15E-05	-3.12E-07	-1.56E-07
10	5	0.00E+00	2.84E-07	2.73E-05	8.82E-06	5.66E-07	0.00E+00	-5.85E-06	-7.28E-06	1.06E-05	2.01E-05	2.93E-07	1.46E-07
10	10	0.00E+00	4.97E-07	5.29E-05	1.76E-05	5.66E-07	0.00E+00	-1.12E-05	-1.39E-05	1.98E-05	3.91E-05	5.69E-07	2.83E-07
10	20	0.00E+00	9.22E-07	9.94E-05	3.38E-05	1.13E-06	0.00E+00	-2.05E-05	-2.55E-05	3.47E-05	7.39E-05	1.08E-06	5.35E-07
100	-20	6.82E-08	-2.16E-05	-7.76E-05	-5.99E-06	0.00E+00	0.00E+00	2.72E-05	3.78E-05	-8.58E-05	-3.74E-06	-2.03E-06	-1.06E-06
100	-10	0.00E+00	-9.55E-06	-3.64E-05	-2.72E-06	0.00E+00	0.00E+00	1.21E-05	1.69E-05	-3.98E-05	-1.74E-06	-9.45E-07	-4.94E-07
100	-5	0.00E+00	-4.55E-06	-1.74E-05	-1.63E-06	0.00E+00	0.00E+00	5.72E-06	8.06E-06	-1.92E-05	-8.41E-07	-4.56E-07	-2.39E-07
100	5	0.00E+00	4.09E-06	1.66E-05	1.09E-06	0.00E+00	0.00E+00	-5.18E-06	-7.34E-06	1.80E-05	7.89E-07	4.28E-07	2.24E-07
100	10	0.00E+00	7.84E-06	3.17E-05	2.18E-06	0.00E+00	0.00E+00	-9.88E-06	-1.41E-05	3.49E-05	1.53E-06	8.31E-07	4.35E-07
100	20	0.00E+00	1.43E-05	6.02E-05	4.36E-06	0.00E+00	0.00E+00	-1.81E-05	-2.59E-05	6.58E-05	2.89E-06	1.57E-06	8.21E-07
200	-20	6.84E-08	-3.58E-05	-5.39E-05	-3.85E-06	0.00E+00	0.00E+00	2.36E-05	3.86E-05	-5.01E-05	-5.97E-06	-2.36E-06	-1.01E-06
200	-10	6.84E-08	-1.60E-05	-2.50E-05	-1.93E-06	0.00E+00	0.00E+00	1.05E-05	1.74E-05	-2.32E-05	-2.77E-06	-1.10E-06	-4.71E-07
200	-5	6.84E-08	-7.53E-06	-1.21E-05	-1.28E-06	0.00E+00	0.00E+00	4.96E-06	8.31E-06	-1.12E-05	-1.34E-06	-5.29E-07	-2.27E-07
200	5	0.00E+00	6.76E-06	1.14E-05	6.42E-07	0.00E+00	0.00E+00	-4.49E-06	-7.60E-06	1.05E-05	1.26E-06	4.96E-07	2.13E-07
200	10	0.00E+00	1.29E-05	2.20E-05	1.28E-06	0.00E+00	0.00E+00	-8.56E-06	-1.46E-05	2.04E-05	2.44E-06	9.63E-07	4.13E-07
200	20	0.00E+00	2.37E-05	4.10E-05	2.57E-06	0.00E+00	0.00E+00	-1.57E-05	-2.70E-05	3.85E-05	4.60E-06	1.82E-06	7.80E-07

Table D3.47 aqueous titanium dioxide: effect of change in *Cp'*

MHz	%	c 10nm	c 100nm	c 1um	c 10um	c 100um	c 1mm	a 10nm	a 100nm	a 1um	a 10um	a 100um	a 1mm
0.1	-20	-7.49E-04	-7.49E-04	-6.59E-04	-1.29E-04	-9.34E-05	-1.14E-05	1.79E-03	-2.67E-03	-1.65E-03	-3.48E-04	-2.04E-04	-9.06E-05
0.1	-10	-3.75E-04	-3.74E-04	-3.25E-04	-5.89E-05	-4.31E-05	-6.86E-06	8.14E-04	-1.42E-03	-8.61E-04	-1.58E-04	-9.40E-05	-4.18E-05
0.1	-5	-1.87E-04	-1.87E-04	-1.61E-04	-2.83E-05	-2.16E-05	-2.29E-06	3.86E-04	-7.29E-04	-4.40E-04	-7.58E-05	-4.53E-05	-2.01E-05
0.1	5	1.87E-04	1.87E-04	1.59E-04	2.63E-05	1.98E-05	2.29E-06	-3.45E-04	7.70E-04	4.57E-04	6.99E-05	4.22E-05	1.87E-05
0.1	10	3.75E-04	3.74E-04	3.16E-04	5.13E-05	3.77E-05	4.57E-06	-6.49E-04	1.58E-03	9.31E-04	1.35E-04	8.17E-05	3.63E-05
0.1	20	7.49E-04	7.49E-04	6.23E-04	9.68E-05	7.00E-05	9.15E-06	-1.13E-03	3.32E-03	1.93E-03	2.51E-04	1.54E-04	6.82E-05
1	-20	-8.98E-04	-8.88E-04	-3.49E-04	-1.32E-04	-3.03E-05	-5.73E-07	1.52E-03	-3.46E-03	-9.20E-04	-2.10E-04	-1.31E-04	-7.52E-07
1	-10	-4.49E-04	-4.44E-04	-1.57E-04	-6.09E-05	-1.41E-05	0.00E+00	6.40E-04	-1.83E-03	-4.45E-04	-9.70E-05	-6.06E-05	-3.46E-07
1	-5	-2.25E-04	-2.22E-04	-7.50E-05	-2.91E-05	-6.05E-06	0.00E+00	2.91E-04	-9.43E-04	-2.19E-04	-4.67E-05	-2.92E-05	-1.67E-07
1	5	2.25E-04	2.22E-04	6.83E-05	2.74E-05	6.05E-06	5.73E-07	-2.32E-04	9.93E-04	2.11E-04	4.35E-05	2.72E-05	1.55E-07
1	10	4.49E-04	4.43E-04	1.31E-04	5.30E-05	1.21E-05	5.73E-07	-4.06E-04	2.04E-03	4.14E-04	8.42E-05	5.26E-05	3.00E-07
1	20	8.98E-04	8.85E-04	2.39E-04	9.88E-05	2.22E-05	1.15E-06	-5.77E-04	4.28E-03	7.99E-04	1.58E-04	9.88E-05	5.64E-07
10	-20	-1.08E-03	-8.49E-04	-1.16E-04	-6.62E-05	-2.83E-06	0.00E+00	1.12E-03	-3.01E-03	-2.78E-04	-1.51E-04	-2.16E-06	-1.13E-06
10	-10	-5.38E-04	-4.15E-04	-5.42E-05	-3.09E-05	-1.13E-06	0.00E+00	3.98E-04	-1.56E-03	-1.27E-04	-6.96E-05	-9.95E-07	-5.19E-07
10	-5	-2.69E-04	-2.05E-04	-2.63E-05	-1.47E-05	-5.66E-07	0.00E+00	1.58E-04	-7.95E-04	-6.08E-05	-3.35E-05	-4.79E-07	-2.50E-07
10	5	2.69E-04	2.01E-04	2.49E-05	1.32E-05	5.66E-07	0.00E+00	-7.60E-05	8.19E-04	5.63E-05	3.12E-05	4.46E-07	2.32E-07
10	10	5.38E-04	3.96E-04	4.82E-05	2.65E-05	1.13E-06	0.00E+00	-7.01E-05	1.66E-03	1.09E-04	6.04E-05	8.63E-07	4.49E-07
10	20	1.08E-03	7.74E-04	9.18E-05	4.85E-05	2.26E-06	0.00E+00	1.87E-04	3.41E-03	2.04E-04	1.13E-04	1.62E-06	8.44E-07
100	-20	-1.28E-03	-2.90E-04	-1.11E-04	-8.17E-06	0.00E+00	0.00E+00	1.29E-03	-9.45E-04	-1.55E-04	-5.69E-06	-3.18E-06	-1.55E-06
100	-10	-6.38E-04	-1.28E-04	-5.14E-05	-3.81E-06	0.00E+00	0.00E+00	4.38E-04	-4.48E-04	-7.14E-05	-2.62E-06	-1.46E-06	-7.12E-07
100	-5	-3.19E-04	-6.03E-05	-2.45E-05	-1.63E-06	0.00E+00	0.00E+00	1.67E-04	-2.18E-04	-3.43E-05	-1.26E-06	-7.04E-07	-3.43E-07
100	5	3.18E-04	5.41E-05	2.30E-05	1.63E-06	0.00E+00	0.00E+00	-6.28E-05	2.07E-04	3.20E-05	1.17E-06	6.55E-07	3.19E-07
100	10	6.36E-04	1.02E-04	4.43E-05	3.27E-06	0.00E+00	0.00E+00	-2.20E-05	4.04E-04	6.18E-05	2.27E-06	1.27E-06	6.17E-07
100	20	1.27E-03	1.85E-04	8.31E-05	5.99E-06	0.00E+00	0.00E+00	3.69E-04	7.68E-04	1.16E-04	4.26E-06	2.38E-06	1.16E-06
200	-20	-1.50E-03	-1.70E-04	-7.51E-05	-5.78E-06	0.00E+00	0.00E+00	8.07E-04	-5.65E-04	-8.57E-05	-8.80E-06	-3.33E-06	-1.37E-06
200	-10	-7.49E-04	-7.43E-05	-3.41E-05	-2.57E-06	0.00E+00	0.00E+00	1.33E-04	-2.60E-04	-3.94E-05	-4.05E-06	-1.53E-06	-6.31E-07
200	-5	-3.74E-04	-3.50E-05	-1.59E-05	-1.28E-06	0.00E+00	0.00E+00	-7.72E-07	-1.25E-04	-1.90E-05	-1.95E-06	-7.37E-07	-3.04E-07
200	5	3.73E-04	3.10E-05	1.59E-05	1.28E-06	0.00E+00	0.00E+00	1.33E-04	1.16E-04	1.76E-05	1.81E-06	6.87E-07	2.83E-07
200	10	7.44E-04	5.88E-05	3.03E-05	2.57E-06	1.80E-05	0.00E+00	3.98E-04	2.23E-04	3.41E-05	3.50E-06	1.33E-06	5.48E-07
200	20	1.48E-03	1.06E-04	5.69E-05	4.49E-06	1.80E-05	0.00E+00	1.32E-03	4.15E-04	6.40E-05	6.58E-06	2.50E-06	1.03E-06

Table D3.48 aqueous titanium dioxide: effect of change in *alpha'*

MHz	%	c 10nm	c 100nm	c 1um	c 10um	c 100um	c 1mm	a 10nm	a 100nm	a 1um	a 10um	a 100um	a 1mm
0.1	-20	0.00E+00	0.00E+00	0.00E+00	0.00E+00	0.00E+00	0.00E+00	-5.30E-05	-5.59E-07	-7.35E-09	-1.31E-09	-3.24E-09	-1.09E-08
0.1	-10	0.00E+00	0.00E+00	0.00E+00	0.00E+00	0.00E+00	0.00E+00	-2.65E-05	-2.80E-07	-3.67E-09	-6.62E-10	-1.61E-09	-5.49E-09
0.1	-5	0.00E+00	0.00E+00	0.00E+00	0.00E+00	0.00E+00	0.00E+00	-1.32E-05	-1.40E-07	-1.83E-09	-3.38E-10	-8.13E-10	-2.78E-09
0.1	5	0.00E+00	0.00E+00	0.00E+00	0.00E+00	0.00E+00	0.00E+00	1.32E-05	1.40E-07	1.83E-09	3.24E-10	8.13E-10	2.71E-09
0.1	10	0.00E+00	0.00E+00	0.00E+00	0.00E+00	0.00E+00	0.00E+00	2.65E-05	2.80E-07	3.67E-09	6.48E-10	1.61E-09	5.43E-09
0.1	20	0.00E+00	0.00E+00	0.00E+00	0.00E+00	0.00E+00	0.00E+00	5.30E-05	5.59E-07	7.35E-09	1.30E-09	3.24E-09	1.09E-08
1	-20	0.00E+00	0.00E+00	0.00E+00	0.00E+00	0.00E+00	0.00E+00	-6.40E-05	-7.16E-07	-2.17E-08	-2.04E-08	-6.98E-08	-1.87E-09
1	-10	0.00E+00	0.00E+00	0.00E+00	0.00E+00	0.00E+00	0.00E+00	-3.20E-05	-3.58E-07	-1.08E-08	-1.02E-08	-3.49E-08	-9.27E-10
1	-5	0.00E+00	0.00E+00	0.00E+00	0.00E+00	0.00E+00	0.00E+00	-1.60E-05	-1.79E-07	-5.41E-09	-5.12E-09	-1.74E-08	-4.71E-10
1	5	0.00E+00	0.00E+00	0.00E+00	0.00E+00	0.00E+00	0.00E+00	1.60E-05	1.79E-07	5.41E-09	5.08E-09	1.74E-08	4.71E-10
1	10	0.00E+00	0.00E+00	0.00E+00	0.00E+00	0.00E+00	0.00E+00	3.20E-05	3.58E-07	1.08E-08	1.02E-08	3.49E-08	9.43E-10
1	20	0.00E+00	0.00E+00	0.00E+00	0.00E+00	0.00E+00	0.00E+00	6.40E-05	7.16E-07	2.16E-08	2.04E-08	6.98E-08	1.89E-09
10	-20	0.00E+00	7.09E-08	0.00E+00	0.00E+00	0.00E+00	0.00E+00	-7.83E-05	-1.06E-06	-1.88E-07	-4.04E-07	-2.33E-08	-5.24E-09
10	-10	0.00E+00	7.09E-08	0.00E+00	0.00E+00	0.00E+00	0.00E+00	-3.92E-05	-5.28E-07	-9.40E-08	-2.02E-07	-1.17E-08	-2.62E-09
10	-5	0.00E+00	7.09E-08	0.00E+00	0.00E+00	0.00E+00	0.00E+00	-1.96E-05	-2.64E-07	-4.70E-08	-1.01E-07	-5.84E-09	-1.31E-09
10	5	0.00E+00	0.00E+00	0.00E+00	0.00E+00	0.00E+00	0.00E+00	1.96E-05	2.64E-07	4.70E-08	1.01E-07	5.82E-09	1.31E-09
10	10	0.00E+00	0.00E+00	0.00E+00	0.00E+00	0.00E+00	0.00E+00	3.92E-05	5.28E-07	9.40E-08	2.02E-07	1.16E-08	2.55E-09
10	20	0.00E+00	0.00E+00	0.00E+00	0.00E+00	0.00E+00	0.00E+00	7.83E-05	1.06E-06	1.88E-07	4.04E-07	2.33E-08	5.17E-09
100	-20	0.00E+00	6.82E-07	7.92E-07	0.00E+00	0.00E+00	0.00E+00	-1.00E-04	-3.11E-06	-2.72E-06	-3.04E-07	-5.54E-08	3.09E-07
100	-10	0.00E+00	3.41E-07	0.00E+00	0.00E+00	0.00E+00	0.00E+00	-5.01E-05	-1.55E-06	-1.36E-06	-1.52E-07	-2.77E-08	1.54E-07
100	-5	0.00E+00	1.14E-07	0.00E+00	0.00E+00	0.00E+00	0.00E+00	-2.50E-05	-7.77E-07	-6.80E-07	-7.59E-08	-1.39E-08	7.69E-08
100	5	0.00E+00	-2.27E-07	0.00E+00	0.00E+00	0.00E+00	0.00E+00	2.50E-05	7.77E-07	6.80E-07	7.59E-08	1.39E-08	-7.67E-08
100	10	0.00E+00	-3.41E-07	-7.92E-07	0.00E+00	0.00E+00	0.00E+00	5.01E-05	1.55E-06	1.36E-06	1.52E-07	2.76E-08	-1.53E-07
100	20	-6.82E-08	-6.82E-07	-7.92E-07	0.00E+00	0.00E+00	0.00E+00	1.00E-04	3.11E-06	2.72E-06	3.04E-07	5.54E-08	-3.05E-07
200	-20	1.37E-07	2.15E-06	1.52E-06	6.42E-07	0.00E+00	0.00E+00	-1.25E-04	-6.28E-06	-5.44E-06	-1.14E-06	2.64E-07	1.90E-06
200	-10	6.84E-08	1.08E-06	7.59E-07	0.00E+00	0.00E+00	0.00E+00	-6.23E-05	-3.14E-06	-2.72E-06	-5.70E-07	1.32E-07	9.17E-07
200	-5	6.84E-08	4.61E-07	0.00E+00	0.00E+00	0.00E+00	0.00E+00	-3.12E-05	-1.57E-06	-1.36E-06	-2.85E-07	6.61E-08	4.51E-07
200	5	-6.84E-08	-6.14E-07	-7.59E-07	0.00E+00	0.00E+00	0.00E+00	3.12E-05	1.57E-06	1.36E-06	2.85E-07	-6.61E-08	-4.36E-07
200	10	-6.84E-08	-1.23E-06	-7.59E-07	0.00E+00	0.00E+00	-8.68E-04	6.23E-05	3.14E-06	2.72E-06	5.70E-07	-1.32E-07	-8.57E-07
200	20	-1.37E-07	-2.30E-06	-1.52E-06	-6.42E-07	-1.80E-05	-8.68E-04	1.25E-04	6.28E-06	5.44E-06	1.14E-06	-2.65E-07	-1.66E-06

Table D3.49 aqueous titanium dioxide: effect of change in *beta'*

MHz	%	c 10nm	c 100nm	c 1um	c 10um	c 100um	c 1mm	a 10nm	a 100nm	a 1um	a 10um	a 100um	a 1mm
0.1	-20	5.09E-05	5.09E-05	4.89E-05	5.32E-05	2.87E-05	2.29E-06	1.08E-05	1.03E-04	6.65E-05	5.91E-05	5.97E-05	2.78E-05
0.1	-10	2.54E-05	2.54E-05	2.44E-05	2.66E-05	1.44E-05	2.29E-06	1.61E-06	5.13E-05	3.32E-05	2.95E-05	2.98E-05	1.39E-05
0.1	-5	1.27E-05	1.27E-05	1.22E-05	1.33E-05	7.18E-06	0.00E+00	5.48E-09	2.56E-05	1.66E-05	1.47E-05	1.49E-05	6.92E-06
0.1	5	-1.27E-05	-1.27E-05	-1.21E-05	-1.33E-05	-7.18E-06	-2.29E-06	1.37E-06	-2.55E-05	-1.65E-05	-1.47E-05	-1.49E-05	-6.91E-06
0.1	10	-2.54E-05	-2.54E-05	-2.43E-05	-2.66E-05	-1.44E-05	-2.29E-06	3.93E-06	-5.10E-05	-3.30E-05	-2.94E-05	-2.97E-05	-1.38E-05
0.1	20	-5.05E-05	-5.05E-05	-4.85E-05	-5.29E-05	-2.87E-05	-4.57E-06	1.20E-05	-1.02E-04	-6.59E-05	-5.86E-05	-5.93E-05	-2.76E-05
1	-20	6.07E-05	6.04E-05	6.16E-05	5.30E-05	1.21E-05	0.00E+00	-1.43E-05	1.09E-04	5.97E-05	7.07E-05	5.11E-05	3.18E-07
1	-10	3.03E-05	3.02E-05	3.07E-05	2.65E-05	6.05E-06	0.00E+00	-1.04E-05	5.44E-05	2.98E-05	3.53E-05	2.55E-05	1.59E-07
1	-5	1.51E-05	1.51E-05	1.53E-05	1.32E-05	2.02E-06	0.00E+00	-5.86E-06	2.72E-05	1.49E-05	1.76E-05	1.27E-05	7.92E-08
1	5	-1.51E-05	-1.50E-05	-1.53E-05	-1.32E-05	-2.02E-06	-5.73E-07	7.03E-06	-2.71E-05	-1.48E-05	-1.76E-05	-1.27E-05	-7.90E-08
1	10	-3.01E-05	-3.00E-05	-3.06E-05	-2.56E-05	-6.05E-06	-5.73E-07	1.51E-05	-5.40E-05	-2.96E-05	-3.51E-05	-2.54E-05	-1.58E-07
1	20	-6.00E-05	-5.98E-05	-6.10E-05	-5.21E-05	-1.21E-05	-5.73E-07	3.37E-05	-1.08E-04	-5.91E-05	-7.00E-05	-5.07E-05	-3.15E-07
10	-20	7.21E-05	6.93E-05	7.58E-05	3.24E-05	1.13E-06	0.00E+00	-4.71E-05	9.14E-05	8.33E-05	7.30E-05	1.17E-06	6.58E-07
10	-10	3.59E-05	3.45E-05	3.79E-05	1.62E-05	5.66E-07	0.00E+00	-2.63E-05	4.55E-05	4.15E-05	3.64E-05	5.82E-07	3.27E-07
10	-5	1.79E-05	1.72E-05	1.90E-05	7.35E-06	0.00E+00	0.00E+00	-1.38E-05	2.27E-05	2.07E-05	1.82E-05	2.90E-07	1.63E-07
10	5	-1.79E-05	-1.72E-05	-1.86E-05	-8.83E-06	-5.66E-07	0.00E+00	1.48E-05	-2.26E-05	-2.07E-05	-1.81E-05	-2.90E-07	-1.63E-07
10	10	-3.57E-05	-3.43E-05	-3.76E-05	-1.62E-05	-1.13E-06	0.00E+00	3.04E-05	-4.51E-05	-4.13E-05	-3.62E-05	-5.78E-07	-3.24E-07
10	20	-7.12E-05	-6.85E-05	-7.48E-05	-3.24E-05	-1.70E-06	0.00E+00	6.40E-05	-8.99E-05	-8.24E-05	-7.21E-05	-1.15E-06	-6.45E-07
100	-20	8.54E-05	8.89E-05	6.89E-05	4.90E-06	0.00E+00	0.00E+00	-1.09E-04	7.63E-05	8.76E-05	3.95E-06	2.35E-06	1.02E-06
100	-10	4.25E-05	4.43E-05	3.48E-05	2.18E-06	0.00E+00	0.00E+00	-5.70E-05	3.79E-05	4.36E-05	1.96E-06	1.17E-06	5.08E-07
100	-5	2.12E-05	2.22E-05	1.74E-05	1.09E-06	0.00E+00	0.00E+00	-2.91E-05	1.89E-05	2.17E-05	9.80E-07	5.83E-07	2.54E-07
100	5	-2.12E-05	-2.21E-05	-1.66E-05	-1.63E-06	0.00E+00	0.00E+00	3.00E-05	-1.88E-05	-2.17E-05	-9.75E-07	-5.79E-07	-2.53E-07
100	10	-4.22E-05	-4.40E-05	-3.40E-05	-2.72E-06	0.00E+00	0.00E+00	6.07E-05	-3.75E-05	-4.32E-05	-1.95E-06	-1.16E-06	-5.05E-07
100	20	-8.41E-05	-8.78E-05	-6.81E-05	-5.44E-06	0.00E+00	0.00E+00	1.24E-04	-7.46E-05	-8.61E-05	-3.87E-06	-2.30E-06	-1.01E-06
200	-20	1.01E-04	1.15E-04	5.77E-05	5.13E-06	0.00E+00	0.00E+00	-1.72E-04	8.83E-05	6.68E-05	7.96E-06	2.70E-06	1.04E-06
200	-10	5.02E-05	5.73E-05	2.88E-05	2.57E-06	0.00E+00	0.00E+00	-8.83E-05	4.38E-05	3.32E-05	3.96E-06	1.34E-06	5.21E-07
200	-5	2.51E-05	2.86E-05	1.44E-05	1.28E-06	0.00E+00	0.00E+00	-4.46E-05	2.18E-05	1.66E-05	1.97E-06	6.68E-07	2.61E-07
200	5	-2.49E-05	-2.84E-05	-1.44E-05	-1.28E-06	0.00E+00	0.00E+00	4.54E-05	-2.17E-05	-1.65E-05	-1.96E-06	-6.63E-07	-2.61E-07
200	10	-4.98E-05	-5.69E-05	-2.88E-05	-2.57E-06	0.00E+00	0.00E+00	9.16E-05	-4.32E-05	-3.28E-05	-3.91E-06	-1.32E-06	-5.21E-07
200	20	-9.91E-05	-1.13E-04	-5.69E-05	-5.13E-06	0.00E+00	0.00E+00	1.86E-04	-8.59E-05	-6.53E-05	-7.78E-06	-2.63E-06	-1.04E-06

Table D3.50 aqueous titanium dioxide: effect of change in *c*

MHz	%	c 10nm	c 100nm	c 1um	c 10um	c 100um	c 1mm	a 10nm	a 100nm	a 1um	a 10um	a 100um	a 1mm
0.1	-20	-2.02E-01	-2.02E-01	-2.02E-01	-2.08E-01	-2.39E-01	-1.34E-01	2.59E-01	2.47E-01	2.48E-01	2.48E-01	2.49E-01	8.46E-01
0.1	-10	-1.01E-01	-1.01E-01	-1.01E-01	-1.05E-01	-1.23E-01	-7.43E-02	1.14E-01	1.10E-01	1.10E-01	1.10E-01	1.10E-01	3.20E-01
0.1	-5	-5.07E-02	-5.07E-02	-5.07E-02	-5.26E-02	-6.25E-02	-3.90E-02	5.38E-02	5.20E-02	5.22E-02	5.23E-02	5.23E-02	1.42E-01
0.1	5	5.08E-02	5.08E-02	5.08E-02	5.30E-02	6.46E-02	4.26E-02	-4.84E-02	-4.70E-02	-4.72E-02	-4.73E-02	-4.73E-02	-1.14E-01
0.1	10	1.02E-01	1.02E-01	1.02E-01	1.06E-01	1.31E-01	8.89E-02	-9.21E-02	-8.96E-02	-9.01E-02	-9.02E-02	-9.03E-02	-2.07E-01
0.1	20	2.04E-01	2.04E-01	2.04E-01	2.15E-01	2.72E-01	1.92E-01	-1.68E-01	-1.64E-01	-1.65E-01	-1.65E-01	-1.65E-01	-3.48E-01
1	-20	-2.02E-01	-2.02E-01	-2.03E-01	-2.19E-01	-1.41E-01	-2.59E-01	2.59E-01	2.47E-01	2.49E-01	2.49E-01	5.48E-01	2.39E-01
1	-10	-1.01E-01	-1.01E-01	-1.02E-01	-1.12E-01	-7.71E-02	-1.27E-01	1.14E-01	1.10E-01	1.10E-01	1.10E-01	2.16E-01	1.32E-01
1	-5	-5.07E-02	-5.07E-02	-5.10E-02	-5.63E-02	-4.02E-02	-6.11E-02	5.38E-02	5.20E-02	5.23E-02	5.23E-02	9.72E-02	6.77E-02
1	5	5.08E-02	5.08E-02	5.12E-02	5.73E-02	4.34E-02	5.42E-02	-4.84E-02	-4.70E-02	-4.73E-02	-4.73E-02	-8.09E-02	-6.80E-02
1	10	1.02E-01	1.02E-01	1.02E-01	1.16E-01	9.00E-02	1.01E-01	-9.21E-02	-8.98E-02	-9.03E-02	-9.03E-02	-1.49E-01	-1.33E-01
1	20	2.04E-01	2.04E-01	2.06E-01	2.36E-01	1.93E-01	1.74E-01	-1.68E-01	-1.65E-01	-1.66E-01	-1.65E-01	-2.57E-01	-2.49E-01
10	-20	-2.02E-01	-2.02E-01	-2.08E-01	-1.56E-01	-2.59E-01	-6.81E-01	2.59E-01	2.48E-01	2.49E-01	3.72E-01	2.39E-01	-7.71E-02
10	-10	-1.01E-01	-1.01E-01	-1.05E-01	-8.27E-02	-1.27E-01	-5.92E-01	1.14E-01	1.10E-01	1.10E-01	1.54E-01	1.32E-01	-3.30E-02
10	-5	-5.07E-02	-5.07E-02	-5.25E-02	-4.26E-02	-6.14E-02	-2.62E-01	5.39E-02	5.22E-02	5.23E-02	7.10E-02	6.76E-02	-1.25E-01
10	5	5.08E-02	5.08E-02	5.29E-02	4.49E-02	5.46E-02	-3.38E-01	-4.84E-02	-4.72E-02	-4.73E-02	-6.13E-02	-6.79E-02	9.13E-03
10	10	1.02E-01	1.02E-01	1.06E-01	9.22E-02	1.02E-01	-2.09E-01	-9.22E-02	-9.02E-02	-9.03E-02	-1.15E-01	-1.33E-01	-1.34E-01
10	20	2.04E-01	2.04E-01	2.14E-01	1.94E-01	1.76E-01	1.07E+00	-1.68E-01	-1.65E-01	-1.65E-01	-2.04E-01	-2.49E-01	1.00E-03
100	-20	-2.02E-01	-2.03E-01	-1.74E-01	-2.59E-01	-6.78E-01	-6.40E-01	2.60E-01	2.50E-01	3.03E-01	2.41E-01	-7.43E-02	-1.54E-02
100	-10	-1.01E-01	-1.02E-01	-8.98E-02	-1.28E-01	-5.91E-01	-3.94E-01	1.15E-01	1.11E-01	1.30E-01	1.31E-01	-3.17E-02	6.06E-03
100	-5	-5.07E-02	-5.10E-02	-4.56E-02	-6.21E-02	-2.61E-01	-3.09E-01	5.41E-02	5.25E-02	6.06E-02	6.73E-02	-1.23E-01	-2.32E-02
100	5	5.08E-02	5.11E-02	4.69E-02	5.59E-02	-3.41E-01	7.42E-02	-4.86E-02	-4.74E-02	-5.36E-02	-6.76E-02	8.72E-03	-1.21E-02
100	10	1.02E-01	1.02E-01	9.50E-02	1.05E-01	-2.15E-01	-9.09E-02	-9.25E-02	-9.05E-02	-1.01E-01	-1.33E-01	-1.34E-01	1.85E-02
100	20	2.04E-01	2.06E-01	1.95E-01	1.82E-01	1.06E+00	7.85E-02	-1.69E-01	-1.66E-01	-1.83E-01	-2.49E-01	-6.48E-04	1.44E-02
200	-20	-2.02E-01	-2.03E-01	-1.13E-01	-6.04E-01	-5.57E-01	-1.14E+00	2.61E-01	2.51E-01	5.25E-01	1.07E-01	7.69E-03	-2.81E-01
200	-10	-1.01E-01	-1.02E-01	-5.76E-02	-3.54E-01	-3.94E-01	-6.30E-01	1.15E-01	1.11E-01	2.12E-01	-5.54E-03	-4.79E-02	-8.76E-02
200	-5	-5.07E-02	-5.12E-02	-2.92E-02	-1.87E-01	-4.83E-01	-6.46E-01	5.42E-02	5.27E-02	9.62E-02	-1.62E-02	-8.10E-03	1.59E-02
200	5	5.08E-02	5.14E-02	3.01E-02	1.99E-01	-3.35E-01	-2.64E-01	-4.87E-02	-4.76E-02	-8.10E-02	3.58E-02	-4.18E-02	4.50E-02
200	10	1.02E-01	1.03E-01	6.13E-02	4.01E-01	4.79E-01	-3.90E-02	-9.27E-02	-9.08E-02	-1.50E-01	8.60E-02	2.12E-02	1.79E-02
200	20	2.04E-01	2.07E-01	1.27E-01	8.03E-01	1.11E+00	1.11E+00	-1.69E-01	-1.66E-01	-2.60E-01	2.14E-01	-6.28E-02	6.10E-03

Table D3.51 aqueous titanium dioxide: effect of change in *rho*

MHz	%	c 10nm	c 100nm	c 1um	c 10um	c 100um	c 1mm	a 10nm	a 100nm	a 1um	a 10um	a 100um	a 1mm
0.1	-20	3.76E-01	3.76E-01	3.82E-01	4.82E-01	1.26E+00	1.43E+00	3.52E-01	3.53E-01	4.01E-01	3.75E-01	3.15E-01	1.71E-01
0.1	-10	1.73E-01	1.73E-01	1.75E-01	2.28E-01	6.19E-01	7.10E-01	1.59E-01	1.59E-01	1.79E-01	1.68E-01	1.44E-01	7.89E-02
0.1	-5	8.30E-02	8.30E-02	8.43E-02	1.12E-01	3.07E-01	3.53E-01	7.57E-02	7.59E-02	8.48E-02	7.99E-02	6.89E-02	3.80E-02
0.1	5	-7.71E-02	-7.71E-02	-7.82E-02	-1.07E-01	-3.03E-01	-3.50E-01	-6.92E-02	-6.93E-02	-7.67E-02	-7.26E-02	-6.36E-02	-3.54E-02
0.1	10	-1.49E-01	-1.49E-01	-1.51E-01	-2.09E-01	-6.02E-01	-6.98E-01	-1.33E-01	-1.33E-01	-1.46E-01	-1.39E-01	-1.23E-01	-6.85E-02
0.1	20	-2.78E-01	-2.78E-01	-2.82E-01	-4.02E-01	-1.19E+00	-1.38E+00	-2.45E-01	-2.45E-01	-2.68E-01	-2.55E-01	-2.28E-01	-1.29E-01
1	-20	4.77E-01	4.78E-01	5.36E-01	2.76E+00	-6.10E+00	3.39E-02	4.04E-01	4.16E-01	4.98E-01	3.83E-01	2.66E-01	-2.30E-02
1	-10	2.19E-01	2.19E-01	2.47E-01	1.34E+00	-3.01E+00	1.65E-02	1.81E-01	1.86E-01	2.18E-01	1.73E-01	1.22E-01	-1.18E-02
1	-5	1.05E-01	1.05E-01	1.19E-01	6.62E-01	-1.50E+00	8.11E-03	8.63E-02	8.83E-02	1.03E-01	8.25E-02	5.83E-02	-5.99E-03
1	5	-9.71E-02	-9.72E-02	-1.11E-01	-6.46E-01	1.48E+00	-7.88E-03	-7.84E-02	-8.00E-02	-9.15E-02	-7.55E-02	-5.38E-02	6.14E-03
1	10	-1.87E-01	-1.87E-01	-2.14E-01	-1.28E+00	2.95E+00	-1.55E-02	-1.50E-01	-1.53E-01	-1.73E-01	-1.45E-01	-1.04E-01	1.24E-02
1	20	-3.49E-01	-3.50E-01	-4.02E-01	-2.50E+00	5.83E+00	-3.01E-02	-2.76E-01	-2.80E-01	-3.13E-01	-2.67E-01	-1.92E-01	2.54E-02
10	-20	6.65E-01	6.83E-01	2.69E+00	-1.24E+00	3.90E-02	-4.31E-02	4.79E-01	5.33E-01	5.00E-01	3.75E-01	-2.76E-02	-2.05E-02
10	-10	3.04E-01	3.11E-01	1.28E+00	-6.12E-01	1.87E-02	-2.02E-02	2.13E-01	2.34E-01	2.22E-01	1.69E-01	-1.43E-02	-9.80E-03
10	-5	1.45E-01	1.49E-01	6.26E-01	-3.03E-01	9.18E-03	-9.82E-03	1.01E-01	1.10E-01	1.05E-01	8.07E-02	-7.26E-03	-4.80E-03
10	5	-1.34E-01	-1.37E-01	-6.00E-01	2.99E-01	-8.82E-03	9.32E-03	-9.14E-02	-9.85E-02	-9.42E-02	-7.38E-02	7.48E-03	4.62E-03
10	10	-2.58E-01	-2.65E-01	-1.18E+00	5.93E-01	-1.73E-02	1.82E-02	-1.74E-01	-1.87E-01	-1.79E-01	-1.41E-01	1.52E-02	9.08E-03
10	20	-4.81E-01	-4.93E-01	-2.27E+00	1.17E+00	-3.32E-02	3.49E-02	-3.18E-01	-3.37E-01	-3.26E-01	-2.60E-01	3.12E-02	1.76E-02
100	-20	1.15E+00	2.03E+00	-8.64E-01	4.54E-02	-3.76E-02	-3.22E-02	6.01E-01	6.84E-01	5.08E-01	-3.07E-02	-1.96E-02	-1.35E-02
100	-10	5.24E-01	9.34E-01	-4.21E-01	2.15E-02	-1.77E-02	-1.08E-02	2.65E-01	2.95E-01	2.26E-01	-1.61E-02	-9.45E-03	-6.95E-03
100	-5	2.50E-01	4.49E-01	-2.08E-01	1.04E-02	-8.59E-03	-4.17E-03	1.25E-01	1.37E-01	1.07E-01	-8.24E-03	-4.65E-03	-3.51E-03
100	5	-2.30E-01	-4.18E-01	2.03E-01	-9.88E-03	8.18E-03	1.52E-03	-1.11E-01	-1.20E-01	-9.64E-02	8.57E-03	4.53E-03	3.58E-03
100	10	-4.43E-01	-8.10E-01	4.01E-01	-1.92E-02	1.60E-02	5.68E-04	-2.11E-01	-2.27E-01	-1.83E-01	1.75E-02	8.97E-03	7.20E-03
100	20	-8.23E-01	-1.52E+00	7.84E-01	-3.62E-02	3.07E-02	-9.09E-03	-3.82E-01	-4.03E-01	-3.33E-01	3.61E-02	1.77E-02	1.46E-02
200	-20	5.89E+00	-1.84E+00	-5.78E-01	-1.24E-01	-1.20E-02	2.97E-01	7.91E-01	8.35E-01	3.47E-01	-3.63E-02	-1.17E-02	-8.55E-03
200	-10	2.67E+00	-8.56E-01	-2.82E-01	-6.16E-02	-5.12E-03	1.65E-01	3.43E-01	3.56E-01	1.53E-01	-2.16E-02	-6.50E-03	-4.35E-03
200	-5	1.27E+00	-4.14E-01	-1.39E-01	-3.07E-02	-2.36E-03	8.65E-02	1.61E-01	1.65E-01	7.21E-02	-1.16E-02	-3.42E-03	-2.17E-03
200	5	-1.17E+00	3.90E-01	1.36E-01	3.04E-02	1.91E-03	-9.42E-02	-1.41E-01	-1.43E-01	-6.44E-02	1.32E-02	3.76E-03	2.13E-03
200	10	-2.25E+00	7.57E-01	2.69E-01	6.05E-02	3.40E-03	-1.96E-01	-2.66E-01	-2.68E-01	-1.22E-01	2.80E-02	7.87E-03	4.17E-03
200	20	-4.16E+00	1.44E+00	5.26E-01	1.19E-01	4.88E-03	-4.18E-01	-4.74E-01	-4.71E-01	-2.19E-01	6.20E-02	1.71E-02	7.85E-03

Table D3.52 aqueous titanium dioxide: effect of change in *eta*

MHz	%	c 10nm	c 100nm	c 1um	c 10um	c 100um	c 1mm	a 10nm	a 100nm	a 1um	a 10um	a 100um	a 1mm
0.1	-20	-6.81E-08	-1.85E-05	-1.38E-02	-9.81E-02	-5.02E-02	-6.50E-03	2.37E-01	2.44E-01	1.76E-01	-9.49E-02	-1.05E-01	-5.08E-02
0.1	-10	0.00E+00	-7.97E-06	-6.09E-03	-4.78E-02	-2.44E-02	-3.16E-03	1.05E-01	1.08E-01	8.07E-02	-4.57E-02	-5.11E-02	-2.47E-02
0.1	-5	0.00E+00	-3.75E-06	-2.87E-03	-2.36E-02	-1.20E-02	-1.56E-03	4.98E-02	5.14E-02	3.88E-02	-2.24E-02	-2.52E-02	-1.22E-02
0.1	5	0.00E+00	3.27E-06	2.57E-03	2.30E-02	1.17E-02	1.52E-03	-4.50E-02	-4.65E-02	-3.60E-02	2.17E-02	2.46E-02	1.19E-02
0.1	10	0.00E+00	6.13E-06	4.88E-03	4.56E-02	2.32E-02	3.00E-03	-8.58E-02	-8.89E-02	-6.94E-02	4.27E-02	4.86E-02	2.35E-02
0.1	20	0.00E+00	1.11E-05	8.86E-03	8.93E-02	4.54E-02	5.87E-03	-1.57E-01	-1.63E-01	-1.30E-01	8.27E-02	9.49E-02	4.59E-02
1	-20	-4.09E-07	-4.34E-04	-8.20E-02	-8.03E-02	-1.95E-02	-7.05E-04	2.32E-01	2.34E-01	2.05E-03	-1.04E-01	-8.04E-02	-9.87E-04
1	-10	-2.04E-07	-1.87E-04	-3.87E-02	-3.91E-02	-9.48E-03	-3.42E-04	1.03E-01	1.04E-01	3.25E-03	-5.05E-02	-3.91E-02	-4.80E-04
1	-5	-6.81E-08	-8.75E-05	-1.88E-02	-1.93E-02	-4.68E-03	-1.69E-04	4.86E-02	4.95E-02	2.10E-03	-2.49E-02	-1.93E-02	-2.37E-04
1	5	6.81E-08	7.73E-05	1.78E-02	1.88E-02	4.56E-03	1.65E-04	-4.39E-02	-4.50E-02	-2.92E-03	2.43E-02	1.88E-02	2.31E-04
1	10	1.36E-07	1.46E-04	3.47E-02	3.72E-02	9.02E-03	3.26E-04	-8.37E-02	-8.60E-02	-6.55E-03	4.79E-02	3.72E-02	4.57E-04
1	20	2.73E-07	2.62E-04	6.60E-02	7.27E-02	1.76E-02	6.37E-04	-1.53E-01	-1.58E-01	-1.55E-02	9.37E-02	7.27E-02	8.93E-04
10	-20	-1.07E-05	-8.73E-03	-1.00E-01	-4.64E-02	-2.36E-03	-3.69E-04	2.23E-01	1.92E-01	-9.05E-02	-9.67E-02	-3.38E-03	-1.15E-03
10	-10	-4.63E-06	-3.81E-03	-4.88E-02	-2.25E-02	-1.15E-03	-1.81E-04	9.90E-02	8.74E-02	-4.34E-02	-4.70E-02	-1.64E-03	-5.60E-04
10	-5	-2.18E-06	-1.79E-03	-2.41E-02	-1.11E-02	-5.66E-04	-8.75E-05	4.68E-02	4.18E-02	-2.12E-02	-2.32E-02	-8.10E-04	-2.76E-04
10	5	1.91E-06	1.60E-03	2.36E-02	1.08E-02	5.52E-04	8.13E-05	-4.22E-02	-3.85E-02	2.04E-02	2.26E-02	7.91E-04	2.69E-04
10	10	3.54E-06	3.03E-03	4.66E-02	2.14E-02	1.09E-03	1.63E-04	-8.04E-02	-7.41E-02	4.01E-02	4.47E-02	1.56E-03	5.32E-04
10	20	6.41E-06	5.48E-03	9.12E-02	4.19E-02	2.13E-03	3.19E-04	-1.47E-01	-1.38E-01	7.74E-02	8.74E-02	3.06E-03	1.04E-03
100	-20	-2.54E-04	-6.94E-02	-7.75E-02	-7.30E-03	-2.60E-04	1.08E-02	2.07E-01	3.34E-02	-1.02E-01	-1.12E-02	-3.84E-03	-1.72E-03
100	-10	-1.09E-04	-3.23E-02	-3.77E-02	-3.54E-03	-1.12E-04	5.30E-03	9.17E-02	1.81E-02	-4.94E-02	-5.45E-03	-1.87E-03	-8.33E-04
100	-5	-5.11E-05	-1.56E-02	-1.86E-02	-1.74E-03	-4.96E-05	2.65E-03	4.34E-02	9.33E-03	-2.44E-02	-2.69E-03	-9.21E-04	-4.10E-04
100	5	4.51E-05	1.46E-02	1.82E-02	1.70E-03	3.72E-05	-2.43E-03	-3.91E-02	-9.76E-03	2.37E-02	2.63E-03	8.98E-04	3.97E-04
100	10	8.53E-05	2.83E-02	3.59E-02	3.35E-03	6.82E-05	-5.08E-03	-7.44E-02	-1.98E-02	4.69E-02	5.20E-03	1.77E-03	7.83E-04
100	20	1.53E-04	5.33E-02	7.02E-02	6.53E-03	9.92E-05	-9.94E-03	-1.36E-01	-4.06E-02	9.16E-02	1.02E-02	3.47E-03	1.52E-03
200	-20	-5.40E-04	-8.63E-02	-5.91E-02	-5.07E-03	4.15E-03	4.28E-02	1.91E-01	-1.07E-02	-8.77E-02	-1.44E-02	-4.69E-03	-1.50E-03
200	-10	-2.33E-04	-4.09E-02	-2.87E-02	-2.44E-03	2.07E-03	2.14E-02	8.47E-02	-2.97E-03	-4.26E-02	-7.02E-03	-2.27E-03	-7.16E-04
200	-5	-1.09E-04	-1.99E-02	-1.42E-02	-1.20E-03	1.04E-03	1.07E-02	4.00E-02	-9.61E-04	-2.10E-02	-3.46E-03	-1.12E-03	-3.50E-04
200	5	9.63E-05	1.90E-02	1.38E-02	1.16E-03	-1.04E-03	-9.73E-03	-3.59E-02	4.40E-05	2.05E-02	3.38E-03	1.09E-03	3.35E-04
200	10	1.82E-04	3.71E-02	2.73E-02	2.29E-03	-2.07E-03	-1.95E-02	-6.84E-02	-7.17E-04	4.06E-02	6.69E-03	2.15E-03	6.57E-04
200	20	3.27E-04	7.08E-02	5.34E-02	4.45E-03	-4.15E-03	-3.89E-02	-1.24E-01	-4.27E-03	7.94E-02	1.31E-02	4.19E-03	1.26E-03

Table D3.53 aqueous titanium dioxide: effect of change in *kappa*

MHz	%	c 10nm	c 100nm	c 1um	c 10um	c 100um	c 1mm	a 10nm	a 100nm	a 1um	a 10um	a 100um	a 1mm
0.1	-20	0.00E+00	-3.41E-07	-7.89E-05	-3.04E-04	-1.56E-04	-2.06E-05	1.85E-03	1.75E-03	5.64E-04	-3.10E-04	-3.26E-04	-1.52E-04
0.1	-10	0.00E+00	-1.36E-07	-3.57E-05	-1.46E-04	-7.54E-05	-9.15E-06	8.23E-04	7.82E-04	2.65E-04	-1.48E-04	-1.56E-04	-7.27E-05
0.1	-5	0.00E+00	-6.82E-08	-1.70E-05	-7.16E-05	-3.59E-05	-4.57E-06	3.90E-04	3.71E-04	1.29E-04	-7.25E-05	-7.66E-05	-3.56E-05
0.1	5	0.00E+00	6.82E-08	1.56E-05	6.89E-05	3.59E-05	4.57E-06	-3.53E-04	-3.37E-04	-1.22E-04	6.96E-05	7.37E-05	3.43E-05
0.1	10	0.00E+00	6.82E-08	2.99E-05	1.35E-04	7.00E-05	9.15E-06	-6.73E-04	-6.44E-04	-2.37E-04	1.37E-04	1.45E-04	6.74E-05
0.1	20	0.00E+00	1.36E-07	5.54E-05	2.62E-04	1.35E-04	1.60E-05	-1.23E-03	-1.18E-03	-4.50E-04	2.63E-04	2.80E-04	1.30E-04
1	-20	0.00E+00	-5.53E-06	-2.68E-04	-2.53E-04	-5.65E-05	-1.72E-06	1.52E-03	1.20E-03	-3.86E-05	-3.36E-04	-2.45E-04	-1.37E-06
1	-10	0.00E+00	-2.39E-06	-1.27E-04	-1.22E-04	-2.62E-05	-1.15E-06	6.75E-04	5.42E-04	-1.43E-05	-1.61E-04	-1.17E-04	-6.53E-07
1	-5	0.00E+00	-1.09E-06	-6.18E-05	-5.91E-05	-1.21E-05	-5.73E-07	3.20E-04	2.58E-04	-6.06E-06	-7.88E-05	-5.74E-05	-3.20E-07
1	5	0.00E+00	1.02E-06	5.90E-05	5.74E-05	1.41E-05	0.00E+00	-2.89E-04	-2.36E-04	4.16E-06	7.58E-05	5.52E-05	3.08E-07
1	10	0.00E+00	1.98E-06	1.15E-04	1.12E-04	2.62E-05	5.73E-07	-5.52E-04	-4.52E-04	6.64E-06	1.49E-04	1.08E-04	6.04E-07
1	20	0.00E+00	3.55E-06	2.20E-04	2.17E-04	5.04E-05	1.15E-06	-1.01E-03	-8.36E-04	7.36E-06	2.87E-04	2.09E-04	1.17E-06
10	-20	-1.36E-07	-5.90E-05	-3.37E-04	-1.38E-04	-5.66E-06	0.00E+00	1.20E-03	5.38E-04	-3.27E-04	-3.04E-04	-4.41E-06	-2.20E-06
10	-10	-6.82E-08	-2.65E-05	-1.61E-04	-6.62E-05	-2.83E-06	0.00E+00	5.37E-04	2.51E-04	-1.56E-04	-1.45E-04	-2.11E-06	-1.05E-06
10	-5	0.00E+00	-1.26E-05	-7.91E-05	-3.24E-05	-1.13E-06	0.00E+00	2.54E-04	1.21E-04	-7.61E-05	-7.12E-05	-1.03E-06	-5.14E-07
10	5	0.00E+00	1.15E-05	7.61E-05	3.09E-05	1.13E-06	0.00E+00	-2.31E-04	-1.13E-04	7.29E-05	6.84E-05	9.91E-07	4.94E-07
10	10	6.82E-08	2.19E-05	1.49E-04	6.18E-05	2.83E-06	0.00E+00	-4.41E-04	-2.20E-04	1.43E-04	1.34E-04	1.95E-06	9.70E-07
10	20	6.82E-08	4.04E-05	2.89E-04	1.19E-04	5.09E-06	0.00E+00	-8.09E-04	-4.15E-04	2.75E-04	2.59E-04	3.75E-06	1.87E-06
100	-20	-2.18E-06	-2.67E-04	-2.67E-04	-1.96E-05	-6.20E-06	0.00E+00	8.85E-04	6.94E-05	-3.01E-04	-1.28E-05	-7.00E-06	-3.68E-06
100	-10	-8.87E-07	-1.26E-04	-1.27E-04	-9.25E-06	-6.20E-06	0.00E+00	3.97E-04	3.70E-05	-1.43E-04	-6.11E-06	-3.34E-06	-1.76E-06
100	-5	-4.09E-07	-6.10E-05	-6.25E-05	-4.36E-06	0.00E+00	0.00E+00	1.89E-04	1.89E-05	-7.02E-05	-2.99E-06	-1.63E-06	-8.59E-07
100	5	4.09E-07	5.78E-05	5.93E-05	4.36E-06	0.00E+00	0.00E+00	-1.72E-04	-1.97E-05	6.73E-05	2.87E-06	1.57E-06	8.25E-07
100	10	7.51E-07	1.13E-04	1.17E-04	8.71E-06	0.00E+00	0.00E+00	-3.29E-04	-3.99E-05	1.32E-04	5.63E-06	3.08E-06	1.62E-06
100	20	1.30E-06	2.14E-04	2.26E-04	1.63E-05	0.00E+00	0.00E+00	-6.06E-04	-8.15E-05	2.54E-04	1.09E-05	5.93E-06	3.12E-06
200	-20	-2.87E-06	-3.65E-04	-2.01E-04	-1.48E-05	0.00E+00	0.00E+00	7.21E-04	5.37E-06	-1.89E-04	-2.22E-05	-8.82E-06	-3.82E-06
200	-10	-1.16E-06	-1.73E-04	-9.63E-05	-7.06E-06	0.00E+00	0.00E+00	3.24E-04	6.17E-06	-9.01E-05	-1.06E-05	-4.21E-06	-1.82E-06
200	-5	-5.47E-07	-8.42E-05	-4.70E-05	-3.85E-06	0.00E+00	0.00E+00	1.54E-04	3.83E-06	-4.41E-05	-5.17E-06	-2.06E-06	-8.92E-07
200	5	4.79E-07	8.01E-05	4.47E-05	3.21E-06	0.00E+00	0.00E+00	-1.41E-04	-5.13E-06	4.22E-05	4.96E-06	1.97E-06	8.55E-07
200	10	9.58E-07	1.57E-04	8.79E-05	6.42E-06	0.00E+00	0.00E+00	-2.69E-04	-1.14E-05	8.28E-05	9.72E-06	3.87E-06	1.68E-06
200	20	1.64E-06	3.00E-04	1.70E-04	1.22E-05	0.00E+00	0.00E+00	-4.97E-04	-2.67E-05	1.59E-04	1.87E-05	7.45E-06	3.23E-06

Table D3.54 aqueous titanium dioxide: effect of change in *Cp*

MHz	%	c 10nm	c 100nm	c 1um	c 10um	c 100um	c 1mm	a 10nm	a 100nm	a 1um	a 10um	a 100um	a 1mm
0.1	-20	2.04E-03	2.04E-03	1.94E-03	1.67E-03	8.94E-04	1.12E-04	-1.39E-03	4.23E-03	3.15E-03	2.00E-03	1.88E-03	8.69E-04
0.1	-10	8.50E-04	8.50E-04	8.09E-04	7.13E-04	3.83E-04	4.80E-05	-7.39E-04	1.76E-03	1.29E-03	8.46E-04	8.03E-04	3.71E-04
0.1	-5	3.91E-04	3.91E-04	3.72E-04	3.31E-04	1.78E-04	2.29E-05	-3.75E-04	8.07E-04	5.89E-04	3.92E-04	3.74E-04	1.73E-04
0.1	5	-3.36E-04	-3.36E-04	-3.20E-04	-2.91E-04	-1.56E-04	-2.06E-05	3.77E-04	-6.91E-04	-5.00E-04	-3.42E-04	-3.27E-04	-1.51E-04
0.1	10	-6.27E-04	-6.27E-04	-5.97E-04	-5.47E-04	-2.93E-04	-3.66E-05	7.50E-04	-1.29E-03	-9.26E-04	-6.42E-04	-6.16E-04	-2.85E-04
0.1	20	-1.10E-03	-1.10E-03	-1.05E-03	-9.77E-04	-5.24E-04	-6.63E-05	1.48E-03	-2.26E-03	-1.61E-03	-1.14E-03	-1.10E-03	-5.09E-04
1	-20	1.41E-03	1.41E-03	1.29E-03	1.03E-03	2.32E-04	7.45E-06	-1.82E-03	2.69E-03	1.45E-03	1.40E-03	9.99E-04	5.58E-06
1	-10	5.87E-04	5.85E-04	5.47E-04	4.39E-04	9.89E-05	3.44E-06	-8.95E-04	1.11E-03	5.99E-04	5.97E-04	4.26E-04	2.38E-06
1	-5	2.70E-04	2.69E-04	2.54E-04	2.04E-04	4.64E-05	1.72E-06	-4.41E-04	5.08E-04	2.75E-04	2.77E-04	1.98E-04	1.11E-06
1	5	-2.32E-04	-2.31E-04	-2.21E-04	-1.79E-04	-4.24E-05	-1.15E-06	4.25E-04	-4.33E-04	-2.35E-04	-2.43E-04	-1.74E-04	-9.71E-07
1	10	-4.33E-04	-4.31E-04	-4.13E-04	-3.37E-04	-7.67E-05	-2.29E-06	8.33E-04	-8.05E-04	-4.38E-04	-4.56E-04	-3.27E-04	-1.83E-06
1	20	-7.60E-04	-7.58E-04	-7.33E-04	-6.02E-04	-1.37E-04	-4.01E-06	1.60E-03	-1.41E-03	-7.67E-04	-8.13E-04	-5.83E-04	-3.26E-06
10	-20	9.74E-04	9.31E-04	9.24E-04	4.00E-04	1.70E-05	6.26E-06	-2.08E-03	1.31E-03	1.05E-03	8.90E-04	1.29E-05	6.42E-06
10	-10	4.05E-04	3.88E-04	3.94E-04	1.71E-04	7.35E-06	0.00E+00	-9.81E-04	5.32E-04	4.43E-04	3.79E-04	5.49E-06	2.73E-06
10	-5	1.86E-04	1.78E-04	1.83E-04	7.95E-05	3.39E-06	0.00E+00	-4.76E-04	2.42E-04	2.05E-04	1.76E-04	2.55E-06	1.27E-06
10	5	-1.60E-04	-1.53E-04	-1.60E-04	-7.07E-05	-2.83E-06	0.00E+00	4.49E-04	-2.04E-04	-1.79E-04	-1.54E-04	-2.23E-06	-1.11E-06
10	10	-2.98E-04	-2.86E-04	-3.02E-04	-1.31E-04	-5.66E-06	0.00E+00	8.72E-04	-3.78E-04	-3.35E-04	-2.90E-04	-4.19E-06	-2.09E-06
10	20	-5.23E-04	-5.02E-04	-5.38E-04	-2.34E-04	-9.62E-06	0.00E+00	1.65E-03	-6.54E-04	-5.95E-04	-5.16E-04	-7.48E-06	-3.73E-06
100	-20	6.69E-04	6.99E-04	5.31E-04	3.87E-05	0.00E+00	0.00E+00	-2.37E-03	5.71E-04	6.56E-04	2.75E-05	1.45E-05	7.46E-06
100	-10	2.78E-04	2.95E-04	2.28E-04	1.63E-05	0.00E+00	0.00E+00	-1.09E-03	2.32E-04	2.78E-04	1.16E-05	6.18E-06	3.18E-06
100	-5	1.28E-04	1.37E-04	1.06E-04	7.62E-06	0.00E+00	0.00E+00	-5.26E-04	1.05E-04	1.29E-04	5.40E-06	2.87E-06	1.48E-06
100	5	-1.10E-04	-1.19E-04	-9.28E-05	-7.08E-06	-6.20E-06	0.00E+00	4.88E-04	-8.87E-05	-1.12E-04	-4.70E-06	-2.51E-06	-1.30E-06
100	10	-2.04E-04	-2.23E-04	-1.74E-04	-1.31E-05	-6.20E-06	0.00E+00	9.42E-04	-1.64E-04	-2.09E-04	-8.81E-06	-4.71E-06	-2.44E-06
100	20	-3.59E-04	-3.96E-04	-3.12E-04	-2.29E-05	-6.20E-06	0.00E+00	1.76E-03	-2.82E-04	-3.71E-04	-1.56E-05	-8.39E-06	-4.36E-06
200	-20	4.61E-04	5.69E-04	2.86E-04	1.99E-05	0.00E+00	0.00E+00	-2.34E-03	3.49E-04	2.97E-04	3.32E-05	1.29E-05	5.44E-06
200	-10	1.91E-04	2.42E-04	1.23E-04	8.34E-06	0.00E+00	0.00E+00	-1.07E-03	1.40E-04	1.24E-04	1.40E-05	5.49E-06	2.33E-06
200	-5	8.79E-05	1.13E-04	5.77E-05	3.85E-06	0.00E+00	0.00E+00	-5.10E-04	6.33E-05	5.73E-05	6.50E-06	2.55E-06	1.09E-06
200	5	-7.54E-05	-9.86E-05	-5.01E-05	-3.85E-06	0.00E+00	0.00E+00	4.70E-04	-5.25E-05	-4.93E-05	-5.65E-06	-2.23E-06	-9.58E-07
200	10	-1.41E-04	-1.85E-04	-9.42E-05	-7.06E-06	0.00E+00	0.00E+00	9.03E-04	-9.63E-05	-9.19E-05	-1.06E-05	-4.19E-06	-1.81E-06
200	20	-2.47E-04	-3.30E-04	-1.69E-04	-1.28E-05	-1.80E-05	0.00E+00	1.68E-03	-1.64E-04	-1.61E-04	-1.88E-05	-7.46E-06	-3.24E-06

Table D3.55 aqueous titanium dioxide: effect of change in *alpha*

MHz	%	c 10nm	c 100nm	c 1um	c 10um	c 100um	c 1mm	a 10nm	a 100nm	a 1um	a 10um	a 100um	a 1mm
0.1	-20	0.00E+00	0.00E+00	0.00E+00	0.00E+00	0.00E+00	0.00E+00	-1.30E-03	-1.37E-05	-2.17E-07	-2.72E-08	-7.52E-08	-9.24E-07
0.1	-10	0.00E+00	0.00E+00	0.00E+00	0.00E+00	0.00E+00	0.00E+00	-6.74E-04	-6.86E-06	-1.08E-07	-1.36E-08	-3.76E-08	-4.62E-07
0.1	-5	0.00E+00	0.00E+00	0.00E+00	0.00E+00	0.00E+00	0.00E+00	-3.57E-04	-3.43E-06	-5.41E-08	-6.81E-09	-1.88E-08	-2.31E-07
0.1	5	0.00E+00	0.00E+00	0.00E+00	0.00E+00	0.00E+00	0.00E+00	3.22E-04	3.43E-06	5.41E-08	6.79E-09	1.88E-08	2.31E-07
0.1	10	0.00E+00	0.00E+00	0.00E+00	0.00E+00	0.00E+00	0.00E+00	6.34E-04	6.86E-06	1.08E-07	1.36E-08	3.76E-08	4.62E-07
0.1	20	0.00E+00	0.00E+00	0.00E+00	0.00E+00	0.00E+00	0.00E+00	1.28E-03	1.37E-05	2.17E-07	2.72E-08	7.52E-08	9.24E-07
1	-20	0.00E+00	0.00E+00	1.14E-07	0.00E+00	0.00E+00	1.72E-06	-1.31E-03	-1.49E-05	-4.74E-07	-3.78E-07	-4.65E-06	-6.59E-07
1	-10	0.00E+00	0.00E+00	1.14E-07	0.00E+00	0.00E+00	1.15E-06	-6.54E-04	-7.45E-06	-2.37E-07	-1.89E-07	-2.32E-06	-3.30E-07
1	-5	0.00E+00	0.00E+00	0.00E+00	0.00E+00	0.00E+00	5.73E-07	-3.27E-04	-3.73E-06	-1.19E-07	-9.44E-08	-1.16E-06	-1.65E-07
1	5	0.00E+00	0.00E+00	0.00E+00	0.00E+00	0.00E+00	-5.73E-07	3.27E-04	3.73E-06	1.19E-07	9.44E-08	1.16E-06	1.65E-07
1	10	0.00E+00	0.00E+00	-1.14E-07	0.00E+00	0.00E+00	-1.15E-06	6.54E-04	7.45E-06	2.37E-07	1.89E-07	2.32E-06	3.30E-07
1	20	0.00E+00	0.00E+00	-1.14E-07	0.00E+00	0.00E+00	-1.72E-06	1.31E-03	1.49E-05	4.74E-07	3.78E-07	4.65E-06	6.59E-07
10	-20	0.00E+00	7.09E-08	1.66E-06	2.94E-06	1.87E-05	-8.76E-05	-1.34E-03	-2.17E-05	-2.74E-06	-1.93E-05	-6.43E-06	-1.62E-05
10	-10	0.00E+00	7.09E-08	6.65E-07	1.47E-06	9.05E-06	-4.38E-05	-6.68E-04	-1.08E-05	-1.37E-06	-9.64E-06	-3.22E-06	-8.09E-06
10	-5	0.00E+00	0.00E+00	3.33E-07	1.47E-06	4.52E-06	-2.50E-05	-3.34E-04	-5.41E-06	-6.85E-07	-4.82E-06	-1.61E-06	-4.05E-06
10	5	0.00E+00	-7.09E-08	-6.65E-07	0.00E+00	-5.09E-06	1.88E-05	3.34E-04	5.41E-06	6.85E-07	4.82E-06	1.61E-06	4.05E-06
10	10	0.00E+00	-7.09E-08	-9.98E-07	-1.47E-06	-9.62E-06	4.38E-05	6.68E-04	1.08E-05	1.37E-06	9.64E-06	3.22E-06	8.09E-06
10	20	0.00E+00	-1.42E-07	-2.00E-06	-2.94E-06	-1.92E-05	8.76E-05	1.34E-03	2.17E-05	2.74E-06	1.93E-05	6.43E-06	1.62E-05
100	-20	-2.73E-07	1.67E-05	2.93E-05	1.87E-04	-8.68E-04	-9.50E-03	-1.45E-03	-4.75E-05	-8.17E-05	-5.95E-05	-1.61E-04	-6.85E-05
100	-10	-1.36E-07	8.30E-06	1.42E-05	9.36E-05	-4.34E-04	-4.75E-03	-7.24E-04	-2.38E-05	-4.09E-05	-2.97E-05	-8.06E-05	-3.46E-05
100	-5	-6.82E-08	4.09E-06	7.12E-06	4.68E-05	-2.17E-04	-2.37E-03	-3.62E-04	-1.19E-05	-2.04E-05	-1.49E-05	-4.03E-05	-1.74E-05
100	5	6.82E-08	-4.20E-06	-7.92E-06	-4.68E-05	2.17E-04	2.59E-03	3.62E-04	1.19E-05	2.04E-05	1.49E-05	4.03E-05	1.76E-05
100	10	1.36E-07	-8.41E-06	-1.50E-05	-9.31E-05	4.34E-04	4.96E-03	7.24E-04	2.38E-05	4.09E-05	2.97E-05	8.07E-05	3.54E-05
100	20	2.73E-07	-1.68E-05	-2.93E-05	-1.87E-04	8.68E-04	1.01E-02	1.45E-03	4.75E-05	8.17E-05	5.95E-05	1.62E-04	7.15E-05
200	-20	-6.16E-07	3.87E-05	1.67E-04	-1.28E-04	-3.15E-03	-1.56E-02	-1.54E-03	-6.59E-05	-3.42E-04	3.91E-04	-1.37E-04	8.45E-04
200	-10	-2.74E-07	1.94E-05	8.34E-05	-6.42E-05	-1.58E-03	-7.81E-03	-7.69E-04	-3.29E-05	-1.71E-04	1.96E-04	-6.86E-05	4.36E-04
200	-5	-1.37E-07	9.68E-06	4.17E-05	-3.21E-05	-7.92E-04	-3.47E-03	-3.84E-04	-1.65E-05	-8.55E-05	9.79E-05	-3.43E-05	2.22E-04
200	5	1.37E-07	-9.83E-06	-4.17E-05	3.14E-05	7.92E-04	4.34E-03	3.84E-04	1.65E-05	8.55E-05	-9.79E-05	3.45E-05	-2.29E-04
200	10	3.42E-07	-1.95E-05	-8.42E-05	6.35E-05	1.60E-03	9.54E-03	7.69E-04	3.29E-05	1.71E-04	-1.96E-04	6.91E-05	-4.65E-04
200	20	6.16E-07	-3.89E-05	-1.68E-04	1.27E-04	3.20E-03	1.91E-02	1.54E-03	6.58E-05	3.42E-04	-3.92E-04	1.39E-04	-9.60E-04

Table D3.56 aqueous titanium dioxide: effect of change in *beta*

MHz	%	c 10nm	c 100nm	c 1um	c 10um	c 100um	c 1mm	a 10nm	a 100nm	a 1um	a 10um	a 100um	a 1mm
0.1	-20	-1.30E-03	-1.30E-03	-1.24E-03	-1.35E-03	-7.26E-04	-9.15E-05	-2.58E-03	-2.66E-03	-1.70E-03	-1.50E-03	-1.51E-03	-7.04E-04
0.1	-10	-6.86E-04	-6.86E-04	-6.58E-04	-7.15E-04	-3.84E-04	-4.80E-05	-1.38E-03	-1.41E-03	-9.00E-04	-7.93E-04	-8.00E-04	-3.72E-04
0.1	-5	-3.53E-04	-3.52E-04	-3.38E-04	-3.67E-04	-1.98E-04	-2.52E-05	-7.13E-04	-7.23E-04	-4.62E-04	-4.08E-04	-4.11E-04	-1.91E-04
0.1	5	3.71E-04	3.71E-04	3.56E-04	3.86E-04	2.07E-04	2.52E-05	7.57E-04	7.62E-04	4.87E-04	4.29E-04	4.33E-04	2.01E-04
0.1	10	7.61E-04	7.61E-04	7.30E-04	7.93E-04	4.26E-04	5.26E-05	1.56E-03	1.56E-03	9.99E-04	8.80E-04	8.88E-04	4.13E-04
0.1	20	1.60E-03	1.60E-03	1.53E-03	1.66E-03	8.93E-04	1.12E-04	3.28E-03	3.28E-03	2.10E-03	1.85E-03	1.86E-03	8.66E-04
1	-20	-1.88E-03	-1.87E-03	-1.90E-03	-1.62E-03	-3.71E-04	-1.15E-05	-3.81E-03	-3.45E-03	-1.85E-03	-2.18E-03	-1.58E-03	-8.83E-06
1	-10	-9.93E-04	-9.89E-04	-1.00E-03	-8.59E-04	-1.96E-04	-6.30E-06	-2.02E-03	-1.82E-03	-9.79E-04	-1.15E-03	-8.33E-04	-4.67E-06
1	-5	-5.10E-04	-5.08E-04	-5.16E-04	-4.41E-04	-1.01E-04	-2.86E-06	-1.04E-03	-9.36E-04	-5.03E-04	-5.91E-04	-4.28E-04	-2.40E-06
1	5	5.37E-04	5.34E-04	5.43E-04	4.64E-04	1.05E-04	3.44E-06	1.10E-03	9.85E-04	5.30E-04	6.22E-04	4.50E-04	2.53E-06
1	10	1.10E-03	1.10E-03	1.11E-03	9.51E-04	2.16E-04	6.88E-06	2.26E-03	2.02E-03	1.09E-03	1.28E-03	9.23E-04	5.18E-06
1	20	2.31E-03	2.30E-03	2.33E-03	2.00E-03	4.54E-04	1.43E-05	4.76E-03	4.24E-03	2.28E-03	2.68E-03	1.94E-03	1.09E-05
10	-20	-2.71E-03	-2.60E-03	-2.82E-03	-1.23E-03	-5.15E-05	-6.26E-06	-5.39E-03	-3.55E-03	-3.13E-03	-2.74E-03	-4.00E-05	-1.99E-05
10	-10	-1.43E-03	-1.37E-03	-1.49E-03	-6.49E-04	-2.71E-05	0.00E+00	-2.86E-03	-1.88E-03	-1.66E-03	-1.45E-03	-2.12E-05	-1.05E-05
10	-5	-7.35E-04	-7.06E-04	-7.66E-04	-3.33E-04	-1.41E-05	0.00E+00	-1.47E-03	-9.64E-04	-8.50E-04	-7.44E-04	-1.09E-05	-5.41E-06
10	5	7.74E-04	7.43E-04	8.06E-04	3.51E-04	1.47E-05	0.00E+00	1.55E-03	1.01E-03	8.95E-04	7.83E-04	1.14E-05	5.69E-06
10	10	1.59E-03	1.52E-03	1.65E-03	7.21E-04	3.00E-05	6.26E-06	3.18E-03	2.08E-03	1.83E-03	1.61E-03	2.35E-05	1.17E-05
10	20	3.33E-03	3.19E-03	3.47E-03	1.51E-03	6.28E-05	6.26E-06	6.68E-03	4.36E-03	3.85E-03	3.37E-03	4.92E-05	2.45E-05
100	-20	-3.89E-03	-3.95E-03	-3.00E-03	-2.19E-04	-6.20E-06	2.16E-04	-7.00E-03	-3.85E-03	-4.20E-03	-1.77E-04	-8.85E-05	-4.38E-05
100	-10	-2.06E-03	-2.09E-03	-1.58E-03	-1.16E-04	-6.20E-06	2.16E-04	-3.71E-03	-2.04E-03	-2.22E-03	-9.35E-05	-4.68E-05	-2.32E-05
100	-5	-1.06E-03	-1.07E-03	-8.13E-04	-5.93E-05	-6.20E-06	2.16E-04	-1.91E-03	-1.05E-03	-1.14E-03	-4.80E-05	-2.40E-05	-1.19E-05
100	5	1.11E-03	1.13E-03	8.57E-04	6.26E-05	0.00E+00	0.00E+00	2.01E-03	1.10E-03	1.20E-03	5.05E-05	2.53E-05	1.25E-05
100	10	2.27E-03	2.31E-03	1.75E-03	1.28E-04	0.00E+00	0.00E+00	4.12E-03	2.26E-03	2.46E-03	1.04E-04	5.19E-05	2.57E-05
100	20	4.77E-03	4.85E-03	3.68E-03	2.69E-04	6.20E-06	-2.16E-04	8.64E-03	4.73E-03	5.15E-03	2.17E-04	1.09E-04	5.38E-05
200	-20	-5.56E-03	-5.97E-03	-2.93E-03	-1.71E-04	7.20E-05	8.69E-04	-9.43E-03	-5.82E-03	-4.22E-03	-4.22E-04	-1.51E-04	-5.70E-05
200	-10	-2.94E-03	-3.16E-03	-1.55E-03	-9.05E-05	3.60E-05	0.00E+00	-4.98E-03	-3.07E-03	-2.23E-03	-2.23E-04	-7.98E-05	-3.01E-05
200	-5	-1.51E-03	-1.62E-03	-7.94E-04	-4.62E-05	1.80E-05	0.00E+00	-2.56E-03	-1.58E-03	-1.15E-03	-1.15E-04	-4.10E-05	-1.54E-05
200	5	1.59E-03	1.70E-03	8.35E-04	4.88E-05	-1.80E-05	-8.69E-04	2.69E-03	1.66E-03	1.20E-03	1.21E-04	4.31E-05	1.62E-05
200	10	3.25E-03	3.49E-03	1.71E-03	1.00E-04	-3.60E-05	-8.69E-04	5.52E-03	3.40E-03	2.47E-03	2.47E-04	8.84E-05	3.33E-05
200	20	6.81E-03	7.32E-03	3.59E-03	2.10E-04	-7.20E-05	-1.74E-03	1.16E-02	7.14E-03	5.18E-03	5.18E-04	1.85E-04	6.97E-05

Table D3.57 aqueous iron:: effect of change in *c'*

MHz	%	c 10nm	c 100nm	c 1um	c 10um	c 100um	c 1mm	a 10nm	a 100nm	a 1um	a 10um	a 100um	a 1mm
0.1	-20	4.13E-03	4.13E-03	4.58E-03	3.75E-02	1.05E-01	1.16E-01	3.27E-02	-6.19E-04	-9.95E-04	-1.37E-03	-1.42E-03	-1.90E-02
0.1	-10	1.17E-03	1.17E-03	1.29E-03	1.06E-02	2.98E-02	3.27E-02	7.04E-03	-1.99E-04	-2.82E-04	-3.89E-04	-4.04E-04	-5.42E-03
0.1	-5	4.77E-04	4.77E-04	5.30E-04	4.34E-03	1.22E-02	1.34E-02	2.68E-03	-8.38E-05	-1.16E-04	-1.59E-04	-1.66E-04	-2.23E-03
0.1	5	-3.49E-04	-3.49E-04	-3.88E-04	-3.18E-03	-8.93E-03	-9.79E-03	-1.78E-03	6.34E-05	8.47E-05	1.17E-04	1.21E-04	1.63E-03
0.1	10	-6.15E-04	-6.15E-04	-6.83E-04	-5.60E-03	-1.57E-02	-1.72E-02	-3.04E-03	1.13E-04	1.49E-04	2.06E-04	2.14E-04	2.88E-03
0.1	20	-9.91E-04	-9.91E-04	-1.10E-03	-9.02E-03	-2.54E-02	-2.78E-02	-4.68E-03	1.84E-04	2.41E-04	3.32E-04	3.45E-04	4.65E-03
1	-20	1.36E-03	1.37E-03	3.80E-03	2.52E-02	3.74E-02	2.29E-02	6.80E-03	-2.44E-04	-3.95E-04	-4.55E-04	-3.11E-03	-3.05E-03
1	-10	4.74E-04	4.76E-04	1.33E-03	8.79E-03	1.31E-02	7.99E-03	2.12E-03	-8.81E-05	-1.38E-04	-1.59E-04	-1.09E-03	-1.02E-03
1	-5	2.05E-04	2.06E-04	5.75E-04	3.81E-03	5.66E-03	3.46E-03	8.86E-04	-3.86E-05	-5.99E-05	-6.92E-05	-4.74E-04	-4.38E-04
1	5	-1.62E-04	-1.62E-04	-4.52E-04	-3.00E-03	-4.45E-03	-2.72E-03	-6.64E-04	3.08E-05	4.72E-05	5.45E-05	3.73E-04	3.39E-04
1	10	-2.92E-04	-2.93E-04	-8.16E-04	-5.41E-03	-8.03E-03	-4.91E-03	-1.18E-03	5.58E-05	8.52E-05	9.84E-05	6.74E-04	6.08E-04
1	20	-4.87E-04	-4.88E-04	-1.36E-03	-9.03E-03	-1.34E-02	-8.19E-03	-1.92E-03	9.37E-05	1.42E-04	1.64E-04	1.13E-03	1.01E-03
10	-20	6.47E-04	7.19E-04	5.95E-03	1.58E-02	1.08E-02	2.93E-01	2.67E-03	-1.16E-04	-1.87E-04	-5.64E-04	-1.29E-03	-3.36E-02
10	-10	2.44E-04	2.71E-04	2.25E-03	5.96E-03	4.07E-03	9.16E-02	9.58E-04	-4.47E-05	-7.10E-05	-2.16E-04	-4.76E-04	-1.74E-02
10	-5	1.08E-04	1.20E-04	9.98E-04	2.65E-03	1.81E-03	3.63E-02	4.19E-04	-1.99E-05	-3.16E-05	-9.62E-05	-2.10E-04	-9.40E-03
10	5	-8.83E-05	-9.80E-05	-8.13E-04	-2.16E-03	-1.47E-03	-1.73E-02	-3.35E-04	1.64E-05	2.59E-05	7.88E-05	1.70E-04	8.97E-03
10	10	-1.61E-04	-1.79E-04	-1.49E-03	-3.94E-03	-2.69E-03	-2.11E-02	-6.09E-04	3.00E-05	4.73E-05	1.44E-04	3.09E-04	1.69E-02
10	20	-2.75E-04	-3.05E-04	-2.53E-03	-6.71E-03	-4.58E-03	-6.27E-03	-1.03E-03	5.11E-05	8.06E-05	2.46E-04	5.23E-04	2.98E-02
100	-20	3.60E-04	9.93E-04	6.26E-03	5.72E-03	3.25E-02	3.65E-02	1.46E-03	-5.90E-06	8.87E-05	-5.50E-04	-3.51E-02	-7.69E-03
100	-10	1.41E-04	3.89E-04	2.46E-03	2.24E-03	-1.47E-02	2.42E-02	5.63E-04	-2.88E-06	3.32E-05	-2.13E-04	-1.50E-02	-4.54E-03
100	-5	6.35E-05	1.75E-04	1.11E-03	1.01E-03	-1.22E-02	-2.15E-02	2.53E-04	-1.34E-06	1.48E-05	-9.56E-05	-6.95E-03	-3.09E-03
100	5	-5.28E-05	-1.46E-04	-9.18E-04	-8.38E-04	2.13E-02	2.92E-02	-2.10E-04	1.11E-06	-1.24E-05	7.89E-05	3.30E-03	1.32E-03
100	10	-9.72E-05	-2.68E-04	-1.69E-03	-1.54E-03	2.99E-02	4.53E-02	-3.88E-04	1.99E-06	-2.30E-05	1.45E-04	7.51E-03	1.77E-03
100	20	-1.67E-04	-4.62E-04	-2.91E-03	-2.66E-03	5.78E-02	8.30E-02	-6.72E-04	3.16E-06	-4.05E-05	2.48E-04	1.33E-02	2.64E-03
200	-20	2.18E-04	8.86E-04	3.65E-03	4.48E-03	8.91E-03	3.34E-01	9.12E-04	6.18E-05	-1.01E-04	3.15E-04	3.14E-03	3.31E-03
200	-10	8.72E-05	3.55E-04	1.46E-03	1.80E-03	1.97E-04	1.01E-01	3.69E-04	2.52E-05	-3.92E-05	1.28E-04	1.24E-03	-3.58E-03
200	-5	3.96E-05	1.61E-04	6.63E-04	8.17E-04	1.23E-03	3.93E-02	1.68E-04	1.16E-05	-1.74E-05	5.82E-05	1.20E-03	-1.82E-04
200	5	-3.33E-05	-1.35E-04	-5.58E-04	-6.87E-04	-2.02E-03	3.10E-03	-1.44E-04	-1.00E-05	1.38E-05	-4.94E-05	-7.34E-04	5.34E-04
200	10	-6.15E-05	-2.50E-04	-1.03E-03	-1.27E-03	-3.23E-03	2.07E-03	-2.68E-04	-1.88E-05	2.47E-05	-9.17E-05	-1.34E-03	1.83E-03
200	20	-1.07E-04	-4.34E-04	-1.79E-03	-2.21E-03	-7.80E-03	-2.69E-02	-4.72E-04	-3.37E-05	3.98E-05	-1.60E-04	-2.64E-03	3.33E-03

Table D3.58 aqueous iron:: effect of change in *rho'*

MHz	%	c 10nm	c 100nm	c 1um	c 10um	c 100um	c 1mm	a 10nm	a 100nm	a 1um	a 10um	a 100um	a 1mm
0.1	-20	-2.16E-01	-2.16E-01	-2.07E-01	-1.47E-01	-2.27E-01	-2.36E-01	-3.66E-01	-3.80E-01	-3.64E-01	-1.44E-01	-1.09E-01	-7.77E-02
0.1	-10	-1.04E-01	-1.04E-01	-9.89E-02	-6.67E-02	-1.04E-01	-1.07E-01	-1.93E-01	-1.99E-01	-1.89E-01	-6.68E-02	-4.97E-02	-3.50E-02
0.1	-5	-5.12E-02	-5.12E-02	-4.84E-02	-3.18E-02	-4.96E-02	-5.14E-02	-9.87E-02	-1.02E-01	-9.60E-02	-3.22E-02	-2.38E-02	-1.67E-02
0.1	5	4.95E-02	4.95E-02	4.64E-02	2.92E-02	4.56E-02	4.72E-02	1.03E-01	1.06E-01	9.90E-02	3.00E-02	2.19E-02	1.53E-02
0.1	10	9.73E-02	9.73E-02	9.08E-02	5.59E-02	8.75E-02	9.07E-02	2.11E-01	2.17E-01	2.01E-01	5.79E-02	4.22E-02	2.93E-02
0.1	20	1.88E-01	1.88E-01	1.74E-01	1.03E-01	1.62E-01	1.68E-01	4.38E-01	4.51E-01	4.12E-01	1.09E-01	7.84E-02	5.42E-02
1	-20	-1.93E-01	-1.92E-01	-1.11E-01	-1.49E-01	-1.75E-01	-2.91E-02	-3.60E-01	-3.67E-01	-2.08E-01	-9.74E-02	-7.67E-02	1.63E-03
1	-10	-9.25E-02	-9.23E-02	-4.96E-02	-6.73E-02	-7.90E-02	-1.35E-02	-1.88E-01	-1.92E-01	-9.90E-02	-4.43E-02	-3.47E-02	7.06E-04
1	-5	-4.53E-02	-4.52E-02	-2.35E-02	-3.21E-02	-3.76E-02	-6.54E-03	-9.62E-02	-9.78E-02	-4.83E-02	-2.12E-02	-1.66E-02	3.26E-04
1	5	4.36E-02	4.35E-02	2.12E-02	2.93E-02	3.44E-02	6.10E-03	1.00E-01	1.02E-01	4.61E-02	1.95E-02	1.52E-02	-2.76E-04
1	10	8.56E-02	8.54E-02	4.05E-02	5.62E-02	6.59E-02	1.18E-02	2.04E-01	2.07E-01	8.99E-02	3.75E-02	2.92E-02	-5.06E-04
1	20	1.65E-01	1.65E-01	7.38E-02	1.04E-01	1.22E-01	2.21E-02	4.23E-01	4.29E-01	1.72E-01	6.97E-02	5.40E-02	-8.47E-04
10	-20	-1.73E-01	-1.59E-01	-9.27E-02	-1.28E-01	-2.66E-02	-5.36E-02	-3.51E-01	-3.29E-01	-1.01E-01	-7.08E-02	9.16E-04	-1.94E-01
10	-10	-8.25E-02	-7.47E-02	-4.16E-02	-5.75E-02	-1.22E-02	1.11E-01	-1.83E-01	-1.69E-01	-4.63E-02	-3.20E-02	3.41E-04	-9.42E-02
10	-5	-4.04E-02	-3.63E-02	-1.98E-02	-2.74E-02	-5.87E-03	1.50E-01	-9.35E-02	-8.53E-02	-2.22E-02	-1.53E-02	1.45E-04	-8.15E-02
10	5	3.87E-02	3.43E-02	1.80E-02	2.49E-02	5.44E-03	-3.67E-01	9.70E-02	8.69E-02	2.05E-02	1.40E-02	-9.97E-05	-6.82E-02
10	10	7.59E-02	6.68E-02	3.44E-02	4.77E-02	1.05E-02	-1.87E-01	1.98E-01	1.75E-01	3.94E-02	2.69E-02	-1.60E-04	-7.54E-02
10	20	1.46E-01	1.27E-01	6.33E-02	8.79E-02	1.97E-02	-5.50E-01	4.09E-01	3.55E-01	7.34E-02	4.97E-02	-1.78E-04	-1.49E-01
100	-20	-1.55E-01	-6.57E-02	-8.98E-02	-2.34E-02	1.53E+00	6.62E-02	-3.42E-01	-1.53E-01	-6.55E-02	-1.48E-04	8.79E-02	-9.86E-03
100	-10	-7.37E-02	-2.87E-02	-4.02E-02	-1.07E-02	8.34E-01	4.16E-01	-1.78E-01	-7.16E-02	-2.96E-02	-1.67E-04	8.29E-02	-3.27E-03
100	-5	-3.60E-02	-1.35E-02	-1.91E-02	-5.15E-03	6.23E-01	3.64E-01	-9.05E-02	-3.46E-02	-1.41E-02	-1.03E-04	1.07E-01	-3.90E-03
100	5	3.43E-02	1.20E-02	1.74E-02	4.78E-03	7.84E-01	1.91E-01	9.37E-02	3.24E-02	1.29E-02	1.37E-04	-1.30E-02	4.11E-03
100	10	6.72E-02	2.27E-02	3.33E-02	9.25E-03	9.46E-01	3.76E-01	1.90E-01	6.29E-02	2.48E-02	3.05E-04	-1.92E-02	2.70E-02
100	20	1.29E-01	4.08E-02	6.13E-02	1.74E-02	1.78E+00	1.09E-01	3.93E-01	1.18E-01	4.59E-02	7.19E-04	3.17E-02	-8.38E-03
200	-20	-1.38E-01	-4.86E-02	-6.92E-02	-3.84E-01	5.35E-01	3.01E-03	-3.31E-01	-1.02E-01	-4.68E-02	-4.32E-01	2.32E-02	5.52E-02
200	-10	-6.54E-02	-2.13E-02	-3.09E-02	-2.73E-01	4.42E-01	-3.25E-01	-1.71E-01	-4.68E-02	-2.11E-02	-4.76E-01	9.45E-02	4.58E-02
200	-5	-3.18E-02	-1.00E-02	-1.47E-02	-4.62E-02	1.20E-01	-3.58E-01	-8.71E-02	-2.24E-02	-1.01E-02	-4.71E-01	4.89E-02	2.96E-02
200	5	3.03E-02	8.97E-03	1.34E-02	-4.69E-01	4.15E-01	-3.93E-01	8.98E-02	2.07E-02	9.19E-03	-1.02E-01	-1.18E-02	5.28E-02
200	10	5.91E-02	1.70E-02	2.55E-02	-5.10E-01	7.54E-01	-1.27E-01	1.82E-01	3.99E-02	1.76E-02	-2.11E-01	6.33E-02	5.92E-02
200	20	1.13E-01	3.09E-02	4.70E-02	-4.99E-01	2.80E-01	-4.62E-01	3.74E-01	7.44E-02	3.25E-02	-2.82E-01	1.06E-01	7.06E-02

Table D3.59 aqueous iron: effect of change in *mu'*

MHz	%	c 10nm	c 100nm	c 1um	c 10um	c 100um	c 1mm	a 10nm	a 100nm	a 1um	a 10um	a 100um	a 1mm
0.1	-20	-3.10E-04	-3.10E-04	-3.45E-04	-2.82E-03	-7.92E-03	-8.67E-03	-2.62E-03	4.31E-05	7.37E-05	1.02E-04	1.06E-04	1.44E-03
0.1	-10	-1.67E-04	-1.67E-04	-1.85E-04	-1.51E-03	-4.25E-03	-4.66E-03	-1.46E-03	2.27E-05	3.96E-05	5.49E-05	5.70E-05	7.75E-04
0.1	-5	-8.64E-05	-8.65E-05	-9.60E-05	-7.85E-04	-2.21E-03	-2.42E-03	-7.73E-04	1.17E-05	2.06E-05	2.85E-05	2.96E-05	4.02E-04
0.1	5	9.37E-05	9.37E-05	1.04E-04	8.50E-04	2.39E-03	2.62E-03	8.74E-04	-1.23E-05	-2.24E-05	-3.10E-05	-3.21E-05	-4.36E-04
0.1	10	1.96E-04	1.95E-04	2.17E-04	1.77E-03	4.99E-03	5.47E-03	1.87E-03	-2.54E-05	-4.67E-05	-6.46E-05	-6.69E-05	-9.09E-04
0.1	20	4.28E-04	4.28E-04	4.75E-04	3.89E-03	1.09E-02	1.20E-02	4.31E-03	-5.36E-05	-1.02E-04	-1.42E-04	-1.47E-04	-1.99E-03
1	-20	-4.97E-04	-4.99E-04	-1.39E-03	-8.98E-03	-1.32E-02	5.76E-03	-4.94E-03	5.93E-05	1.41E-04	1.59E-04	1.10E-03	6.00E-03
1	-10	-2.74E-04	-2.75E-04	-7.64E-04	-4.95E-03	-7.26E-03	1.64E-03	-2.86E-03	3.13E-05	7.80E-05	8.77E-05	6.05E-04	2.78E-03
1	-5	-1.44E-04	-1.45E-04	-4.03E-04	-2.61E-03	-3.83E-03	5.33E-04	-1.55E-03	1.61E-05	4.11E-05	4.61E-05	3.18E-04	1.35E-03
1	5	1.62E-04	1.63E-04	4.51E-04	2.92E-03	4.29E-03	2.67E-05	1.84E-03	-1.69E-05	-4.61E-05	-5.15E-05	-3.55E-04	-1.31E-03
1	10	3.45E-04	3.46E-04	9.61E-04	6.23E-03	9.14E-03	6.20E-04	4.06E-03	-3.45E-05	-9.80E-05	-1.09E-04	-7.53E-04	-2.60E-03
1	20	7.92E-04	7.95E-04	2.21E-03	1.43E-02	2.10E-02	3.65E-03	1.01E-02	-7.07E-05	-2.25E-04	-2.49E-04	-1.72E-03	-5.26E-03
10	-20	-9.08E-04	-1.01E-03	-8.14E-03	-2.08E-02	-3.16E-03	-2.24E-01	-1.15E-02	4.34E-05	1.73E-04	3.48E-04	6.32E-03	-2.92E-02
10	-10	-5.22E-04	-5.79E-04	-4.68E-03	-1.20E-02	-3.25E-03	-1.47E-01	-7.04E-03	1.84E-05	9.45E-05	1.75E-04	3.15E-03	-2.85E-02
10	-5	-2.83E-04	-3.13E-04	-2.53E-03	-6.48E-03	-2.07E-03	-1.14E-01	-3.96E-03	7.71E-06	4.95E-05	8.61E-05	1.60E-03	-1.49E-02
10	5	3.38E-04	3.74E-04	3.02E-03	7.75E-03	3.11E-03	1.46E-01	5.19E-03	-2.27E-06	-5.40E-05	-7.67E-05	-1.71E-03	-1.68E-02
10	10	7.49E-04	8.29E-04	6.70E-03	1.72E-02	7.49E-03	1.92E-01	1.22E-02	5.19E-06	-1.12E-04	-1.32E-04	-3.61E-03	-3.53E-02
10	20	1.91E-03	2.12E-03	1.71E-02	4.38E-02	2.17E-02	2.19E-01	3.60E-02	8.72E-05	-2.32E-04	-5.91E-05	-8.58E-03	-4.08E-02
100	-20	-2.13E-03	-5.51E-03	-3.37E-02	-2.20E-02	-2.25E-01	-9.23E-02	-4.04E-02	-2.20E-03	-7.31E-03	7.76E-03	3.00E-02	8.12E-03
100	-10	-1.33E-03	-3.41E-03	-2.10E-02	-1.52E-02	-2.01E-02	-1.14E-01	-2.76E-02	-1.54E-03	-5.07E-03	4.30E-03	1.23E-02	6.46E-03
100	-5	-7.58E-04	-1.94E-03	-1.20E-02	-9.01E-03	-1.26E-02	-8.49E-02	-1.68E-02	-9.51E-04	-3.10E-03	2.33E-03	-4.98E-04	2.40E-03
100	5	1.06E-03	2.65E-03	1.66E-02	1.34E-02	1.67E-02	-9.39E-02	2.79E-02	1.64E-03	5.24E-03	-3.00E-03	2.98E-03	3.63E-03
100	10	2.64E-03	6.50E-03	4.11E-02	3.45E-02	-6.73E-02	-8.59E-02	7.92E-02	4.76E-03	1.50E-02	-7.28E-03	1.22E-02	2.59E-03
100	20	1.04E-02	2.31E-02	1.56E-01	1.51E-01	-2.67E-01	-3.39E-02	5.05E-01	3.23E-02	9.73E-02	-2.61E-02	1.19E-02	7.28E-03
200	-20	-1.05E-02	-2.11E-02	-1.30E-01	5.25E-04	2.30E-01	-1.18E-01	-3.56E-01	-6.87E-02	-1.52E-01	6.72E-02	-1.34E-02	-4.53E-03
200	-10	-8.02E-03	-1.33E-02	-9.64E-02	1.01E-02	1.68E-01	-2.21E-01	-3.09E-01	-5.99E-02	-1.32E-01	7.32E-02	-2.15E-02	-4.77E-03
200	-5	-5.46E-03	-6.78E-03	-6.32E-02	8.35E-03	1.01E-01	2.15E-02	-2.37E-01	-4.60E-02	-1.01E-01	7.67E-02	-2.42E-03	2.32E-04
200	5	2.05E-02	-1.26E-01	8.20E-02	2.80E-01	-4.49E-02	1.74E-02	2.00E+00	3.48E-01	6.15E-01	5.10E-02	-1.50E-02	-9.02E-04
200	10	-5.81E-02	-9.50E-02	-5.17E-01	4.99E-01	1.49E-01	1.13E-02	1.05E+01	1.44E+00	2.20E+00	3.60E-01	-1.44E-02	6.40E-03
200	20	-2.72E-02	-9.19E-02	-3.50E-01	-4.84E-01	1.96E-01	5.42E-02	-1.77E-01	-2.96E-02	-3.74E-02	4.46E-01	5.58E-03	1.36E-02

Table D3.60 aqueous iron: effect of change in *kappa'*

MHz	%	c 10nm	c 100nm	c 1um	c 10um	c 100um	c 1mm	a 10nm	a 100nm	a 1um	a 10um	a 100um	a 1mm
0.1	-20	0.00E+00	0.00E+00	0.00E+00	-6.24E-06	-4.97E-06	-5.55E-07	1.12E-06	3.96E-07	5.07E-07	2.85E-06	-2.64E-05	-1.44E-05
0.1	-10	0.00E+00	0.00E+00	0.00E+00	-2.84E-06	-1.99E-06	-5.55E-07	5.41E-07	1.77E-07	2.25E-07	1.28E-06	-1.22E-05	-6.64E-06
0.1	-5	0.00E+00	0.00E+00	0.00E+00	-1.32E-06	-9.94E-07	-5.55E-07	2.67E-07	8.38E-08	1.07E-07	6.12E-07	-5.85E-06	-3.20E-06
0.1	5	0.00E+00	0.00E+00	0.00E+00	1.32E-06	9.94E-07	0.00E+00	-2.60E-07	-7.60E-08	-9.65E-08	-5.59E-07	5.45E-06	2.98E-06
0.1	10	0.00E+00	0.00E+00	0.00E+00	2.27E-06	1.99E-06	0.00E+00	-5.15E-07	-1.45E-07	-1.84E-07	-1.07E-06	1.05E-05	5.77E-06
0.1	20	0.00E+00	0.00E+00	0.00E+00	4.35E-06	3.98E-06	0.00E+00	-1.01E-06	-2.67E-07	-3.38E-07	-1.98E-06	1.98E-05	1.09E-05
1	-20	0.00E+00	0.00E+00	-5.64E-07	-1.26E-05	-1.60E-06	0.00E+00	1.23E-06	3.55E-07	1.04E-06	-7.58E-06	-1.99E-05	-1.78E-07
1	-10	0.00E+00	0.00E+00	-2.12E-07	-5.75E-06	-5.32E-07	0.00E+00	6.01E-07	1.58E-07	4.61E-07	-3.14E-06	-9.17E-06	-8.33E-08
1	-5	0.00E+00	0.00E+00	-1.41E-07	-2.88E-06	0.00E+00	0.00E+00	2.97E-07	7.52E-08	2.18E-07	-1.44E-06	-4.42E-06	-4.03E-08
1	5	0.00E+00	0.00E+00	7.05E-08	2.16E-06	5.32E-07	0.00E+00	-2.92E-07	-6.83E-08	-1.98E-07	1.23E-06	4.12E-06	3.81E-08
1	10	0.00E+00	0.00E+00	2.12E-07	4.67E-06	5.32E-07	0.00E+00	-5.79E-07	-1.31E-07	-3.78E-07	2.28E-06	7.99E-06	7.41E-08
1	20	0.00E+00	0.00E+00	3.53E-07	8.63E-06	1.06E-06	0.00E+00	-1.14E-06	-2.40E-07	-6.92E-07	3.95E-06	1.50E-05	1.41E-07
10	-20	0.00E+00	0.00E+00	-4.54E-06	-3.77E-06	-5.35E-07	0.00E+00	1.41E-06	3.68E-07	2.04E-06	-2.28E-05	-7.99E-07	-4.09E-07
10	-10	0.00E+00	0.00E+00	-2.08E-06	-1.88E-06	0.00E+00	0.00E+00	6.91E-07	1.65E-07	9.16E-07	-1.06E-05	-3.81E-07	-1.93E-07
10	-5	0.00E+00	0.00E+00	-9.46E-07	-4.71E-07	0.00E+00	0.00E+00	3.43E-07	7.82E-08	4.36E-07	-5.11E-06	-1.87E-07	-9.43E-08
10	5	0.00E+00	0.00E+00	7.57E-07	9.41E-07	0.00E+00	0.00E+00	-3.38E-07	-7.12E-08	-3.97E-07	4.79E-06	1.79E-07	9.01E-08
10	10	0.00E+00	0.00E+00	1.70E-06	1.88E-06	0.00E+00	0.00E+00	-6.72E-07	-1.36E-07	-7.61E-07	9.30E-06	3.52E-07	1.76E-07
10	20	0.00E+00	0.00E+00	3.03E-06	3.30E-06	5.35E-07	0.00E+00	-1.33E-06	-2.51E-07	-1.40E-06	1.76E-05	6.82E-07	3.39E-07
100	-20	3.52E-08	-4.23E-07	-1.17E-05	-4.64E-06	-1.04E-05	0.00E+00	1.75E-06	7.67E-07	-5.80E-06	-5.90E-06	-2.76E-06	-4.54E-07
100	-10	3.52E-08	-1.41E-07	-5.17E-06	-2.06E-06	-1.04E-05	0.00E+00	8.66E-07	3.48E-07	-2.26E-06	-2.87E-06	-1.34E-06	-2.14E-07
100	-5	0.00E+00	-7.05E-08	-2.41E-06	-1.03E-06	0.00E+00	0.00E+00	4.31E-07	1.67E-07	-9.95E-07	-1.42E-06	-6.63E-07	-1.04E-07
100	5	0.00E+00	7.05E-08	2.41E-06	1.55E-06	0.00E+00	0.00E+00	-4.27E-07	-1.54E-07	7.74E-07	1.39E-06	6.48E-07	9.86E-08
100	10	0.00E+00	1.41E-07	4.48E-06	2.58E-06	0.00E+00	0.00E+00	-8.50E-07	-2.97E-07	1.36E-06	2.74E-06	1.28E-06	1.92E-07
100	20	-3.52E-08	2.12E-07	8.62E-06	4.64E-06	0.00E+00	0.00E+00	-1.69E-06	-5.55E-07	2.10E-06	5.37E-06	2.51E-06	3.67E-07
200	-20	1.77E-07	-5.82E-07	-2.05E-05	-1.67E-05	2.12E-05	0.00E+00	2.27E-06	1.05E-06	-2.51E-06	-1.03E-05	-6.48E-06	-3.19E-06
200	-10	1.06E-07	-2.91E-07	-9.53E-06	-8.33E-06	0.00E+00	0.00E+00	1.12E-06	4.93E-07	1.20E-07	-5.00E-06	-3.19E-06	-1.57E-06
200	-5	3.54E-08	-9.71E-08	-4.59E-06	-4.16E-06	0.00E+00	0.00E+00	5.60E-07	2.40E-07	3.58E-07	-2.47E-06	-1.58E-06	-7.81E-07
200	5	-3.54E-08	9.71E-08	4.24E-06	4.16E-06	-2.12E-05	0.00E+00	-5.57E-07	-2.28E-07	-8.77E-07	2.41E-06	1.56E-06	7.72E-07
200	10	-7.07E-08	9.71E-08	8.47E-06	8.33E-06	-2.12E-05	0.00E+00	-1.11E-06	-4.46E-07	-2.20E-06	4.75E-06	3.10E-06	1.53E-06
200	20	-1.41E-07	1.94E-07	1.62E-05	1.67E-05	-4.24E-05	0.00E+00	-2.21E-06	-8.56E-07	-5.98E-06	9.30E-06	6.12E-06	3.04E-06

Table D3.61 aqueous iron: effect of change in *Cp'*

MHz	%	c 10nm	c 100nm	c 1um	c 10um	c 100um	c 1mm	a 10nm	a 100nm	a 1um	a 10um	a 100um	a 1mm
0.1	-20	-2.17E-04	-2.17E-04	-2.16E-04	-2.36E-04	-5.42E-05	-6.11E-06	-1.42E-03	-3.76E-04	-2.35E-04	-3.66E-04	-3.11E-04	-1.60E-04
0.1	-10	-1.09E-04	-1.09E-04	-1.07E-04	-1.07E-04	-2.44E-05	-2.78E-06	-7.26E-04	-2.02E-04	-1.26E-04	-1.73E-04	-1.42E-04	-7.29E-05
0.1	-5	-5.46E-05	-5.46E-05	-5.36E-05	-5.11E-05	-1.14E-05	-1.67E-06	-3.67E-04	-1.05E-04	-6.49E-05	-8.41E-05	-6.79E-05	-3.49E-05
0.1	5	5.48E-05	5.47E-05	5.33E-05	4.69E-05	1.09E-05	1.11E-06	3.74E-04	1.12E-04	6.88E-05	7.97E-05	6.25E-05	3.21E-05
0.1	10	1.10E-04	1.10E-04	1.06E-04	9.01E-05	2.09E-05	2.22E-06	7.55E-04	2.31E-04	1.41E-04	1.55E-04	1.20E-04	6.18E-05
0.1	20	2.20E-04	2.20E-04	2.11E-04	1.66E-04	3.88E-05	3.89E-06	1.54E-03	4.90E-04	2.98E-04	2.95E-04	2.24E-04	1.15E-04
1	-20	-2.64E-04	-2.62E-04	-2.87E-04	-1.05E-04	-1.65E-05	-2.17E-06	-1.83E-03	-5.10E-04	-3.28E-04	-3.05E-04	-2.08E-04	-1.66E-06
1	-10	-1.32E-04	-1.31E-04	-1.35E-04	-4.71E-05	-7.45E-06	-1.08E-06	-9.36E-04	-2.73E-04	-1.64E-04	-1.39E-04	-9.45E-05	-7.53E-07
1	-5	-6.62E-05	-6.58E-05	-6.54E-05	-2.26E-05	-3.73E-06	-5.42E-07	-4.73E-04	-1.41E-04	-8.16E-05	-6.63E-05	-4.51E-05	-3.60E-07
1	5	6.63E-05	6.59E-05	6.16E-05	2.05E-05	3.19E-06	0.00E+00	4.83E-04	1.50E-04	8.09E-05	6.10E-05	4.15E-05	3.32E-07
1	10	1.33E-04	1.32E-04	1.20E-04	3.95E-05	5.86E-06	5.42E-07	9.77E-04	3.09E-04	1.61E-04	1.17E-04	7.97E-05	6.38E-07
1	20	2.66E-04	2.64E-04	2.26E-04	7.33E-05	1.12E-05	1.08E-06	2.00E-03	6.55E-04	3.18E-04	2.18E-04	1.48E-04	1.18E-06
10	-20	-3.19E-04	-2.93E-04	-1.75E-04	-3.95E-05	-5.35E-06	0.00E+00	-2.37E-03	-5.28E-04	-3.48E-04	-2.17E-04	-4.35E-06	-1.06E-06
10	-10	-1.60E-04	-1.45E-04	-7.83E-05	-1.79E-05	-2.68E-06	0.00E+00	-1.21E-03	-2.78E-04	-1.62E-04	-9.85E-05	-1.98E-06	-4.95E-07
10	-5	-7.99E-05	-7.19E-05	-3.71E-05	-8.47E-06	-1.07E-06	0.00E+00	-6.14E-04	-1.42E-04	-7.79E-05	-4.70E-05	-9.47E-07	-2.39E-07
10	5	8.01E-05	7.09E-05	3.38E-05	8.00E-06	1.07E-06	0.00E+00	6.28E-04	1.49E-04	7.27E-05	4.32E-05	8.72E-07	2.24E-07
10	10	1.60E-04	1.41E-04	6.47E-05	1.51E-05	2.14E-06	0.00E+00	1.27E-03	3.03E-04	1.41E-04	8.30E-05	1.68E-06	4.35E-07
10	20	3.21E-04	2.78E-04	1.19E-04	2.78E-05	3.75E-06	0.00E+00	2.60E-03	6.30E-04	2.64E-04	1.54E-04	3.12E-06	8.19E-07
100	-20	-3.78E-04	-2.31E-04	-6.62E-05	-1.13E-05	0.00E+00	0.00E+00	-3.04E-03	-4.71E-04	-2.28E-04	-1.04E-05	-2.66E-06	-3.48E-06
100	-10	-1.89E-04	-1.05E-04	-2.97E-05	-5.15E-06	0.00E+00	0.00E+00	-1.56E-03	-2.28E-04	-1.03E-04	-4.75E-06	-1.25E-06	-1.55E-06
100	-5	-9.45E-05	-5.03E-05	-1.41E-05	-2.58E-06	0.00E+00	0.00E+00	-7.87E-04	-1.12E-04	-4.91E-05	-2.28E-06	-6.06E-07	-7.38E-07
100	5	9.45E-05	4.60E-05	1.31E-05	2.06E-06	0.00E+00	0.00E+00	8.04E-04	1.08E-04	4.50E-05	2.11E-06	5.70E-07	6.70E-07
100	10	1.89E-04	8.82E-05	2.52E-05	4.12E-06	0.00E+00	0.00E+00	1.63E-03	2.12E-04	8.63E-05	4.07E-06	1.11E-06	1.28E-06
100	20	3.77E-04	1.63E-04	4.65E-05	7.73E-06	0.00E+00	0.00E+00	3.32E-03	4.10E-04	1.60E-04	7.59E-06	2.09E-06	2.36E-06
200	-20	-4.33E-04	-1.34E-04	-3.67E-05	-3.33E-06	-2.12E-05	0.00E+00	-3.85E-03	-4.46E-04	-1.44E-04	-1.08E-05	1.64E-07	-5.40E-07
200	-10	-2.16E-04	-5.83E-05	-1.66E-05	-1.67E-06	0.00E+00	0.00E+00	-1.96E-03	-2.08E-04	-6.51E-05	-4.95E-06	6.57E-08	-2.59E-07
200	-5	-1.08E-04	-2.73E-05	-7.77E-06	-8.33E-07	0.00E+00	0.00E+00	-9.92E-04	-1.01E-04	-3.11E-05	-2.37E-06	2.96E-08	-1.27E-07
200	5	1.07E-04	2.41E-05	7.41E-06	8.33E-07	2.12E-05	0.00E+00	1.01E-03	9.47E-05	2.85E-05	2.19E-06	-2.40E-08	1.21E-07
200	10	2.14E-04	4.55E-05	1.41E-05	1.67E-06	2.12E-05	0.00E+00	2.04E-03	1.84E-04	5.48E-05	4.22E-06	-4.34E-08	2.36E-07
200	20	4.25E-04	8.13E-05	2.58E-05	2.50E-06	2.12E-05	0.00E+00	4.16E-03	3.46E-04	1.02E-04	7.85E-06	-7.11E-08	4.50E-07

Table D3.62 aqueous iron: effect of change in *alpha'*

MHz	%	c 10nm	c 100nm	c 1um	c 10um	c 100um	c 1mm	a 10nm	a 100nm	a 1um	a 10um	a 100um	a 1mm
0.1	-20	0.00E+00	0.00E+00	0.00E+00	0.00E+00	0.00E+00	0.00E+00	-2.11E-03	-2.24E-05	-3.24E-07	-2.42E-07	-1.37E-06	-6.56E-06
0.1	-10	0.00E+00	0.00E+00	0.00E+00	0.00E+00	0.00E+00	0.00E+00	-1.06E-03	-1.12E-05	-1.62E-07	-1.21E-07	-6.84E-07	-3.28E-06
0.1	-5	0.00E+00	0.00E+00	0.00E+00	0.00E+00	0.00E+00	0.00E+00	-5.29E-04	-5.60E-06	-8.10E-08	-6.05E-08	-3.42E-07	-1.64E-06
0.1	5	0.00E+00	0.00E+00	0.00E+00	0.00E+00	0.00E+00	0.00E+00	5.29E-04	5.61E-06	8.11E-08	6.06E-08	3.42E-07	1.64E-06
0.1	10	0.00E+00	0.00E+00	0.00E+00	0.00E+00	0.00E+00	0.00E+00	1.06E-03	1.12E-05	1.62E-07	1.21E-07	6.84E-07	3.28E-06
0.1	20	0.00E+00	0.00E+00	0.00E+00	0.00E+00	0.00E+00	0.00E+00	2.11E-03	2.24E-05	3.24E-07	2.42E-07	1.37E-06	6.56E-06
1	-20	0.00E+00	0.00E+00	2.82E-07	7.19E-07	0.00E+00	0.00E+00	-2.55E-03	-2.88E-05	-1.84E-06	-6.17E-06	-3.71E-05	-1.47E-06
1	-10	0.00E+00	0.00E+00	1.41E-07	3.59E-07	0.00E+00	0.00E+00	-1.27E-03	-1.44E-05	-9.20E-07	-3.09E-06	-1.85E-05	-7.34E-07
1	-5	0.00E+00	0.00E+00	7.05E-08	3.59E-07	0.00E+00	0.00E+00	-6.37E-04	-7.20E-06	-4.60E-07	-1.54E-06	-9.27E-06	-3.67E-07
1	5	0.00E+00	0.00E+00	-7.05E-08	0.00E+00	0.00E+00	0.00E+00	6.37E-04	7.20E-06	4.60E-07	1.54E-06	9.27E-06	3.67E-07
1	10	0.00E+00	0.00E+00	-1.41E-07	-3.59E-07	0.00E+00	5.42E-07	1.27E-03	1.44E-05	9.21E-07	3.09E-06	1.85E-05	7.34E-07
1	20	0.00E+00	0.00E+00	-2.12E-07	-3.59E-07	0.00E+00	5.42E-07	2.55E-03	2.88E-05	1.84E-06	6.17E-06	3.71E-05	1.47E-06
10	-20	0.00E+00	4.87E-07	8.32E-06	2.82E-06	-2.68E-06	3.16E-05	-3.11E-03	-4.67E-05	-3.49E-05	-1.75E-04	-1.75E-05	-2.91E-05
10	-10	0.00E+00	2.25E-07	4.16E-06	1.41E-06	-1.61E-06	2.11E-05	-1.56E-03	-2.33E-05	-1.74E-05	-8.72E-05	-8.74E-06	-1.45E-05
10	-5	0.00E+00	1.12E-07	2.08E-06	4.71E-07	-5.35E-07	1.05E-05	-7.78E-04	-1.17E-05	-8.72E-06	-4.36E-05	-4.37E-06	-7.27E-06
10	5	0.00E+00	-1.50E-07	-2.08E-06	-9.41E-07	5.35E-07	-1.05E-05	7.78E-04	1.17E-05	8.72E-06	4.36E-05	4.37E-06	7.27E-06
10	10	0.00E+00	-2.62E-07	-4.16E-06	-1.88E-06	1.61E-06	-1.05E-05	1.56E-03	2.33E-05	1.74E-05	8.72E-05	8.74E-06	1.45E-05
10	20	-3.52E-08	-4.87E-07	-8.32E-06	-3.30E-06	2.68E-06	-3.16E-05	3.11E-03	4.67E-05	3.49E-05	1.74E-04	1.75E-05	2.91E-05
100	-20	2.04E-06	3.89E-05	8.59E-05	-1.70E-05	3.52E-04	-1.90E-03	-3.98E-03	-2.64E-04	-8.20E-04	-2.05E-04	-3.41E-04	2.03E-05
100	-10	1.06E-06	1.95E-05	4.31E-05	-8.25E-06	1.76E-04	-9.52E-04	-1.99E-03	-1.32E-04	-4.10E-04	-1.03E-04	-1.70E-04	6.49E-06
100	-5	5.29E-07	9.80E-06	2.17E-05	-4.12E-06	8.29E-05	-3.17E-04	-9.94E-04	-6.61E-05	-2.05E-04	-5.14E-05	-8.51E-05	2.46E-06
100	5	-5.29E-07	-9.80E-06	-2.21E-05	3.61E-06	-9.33E-05	3.17E-04	9.94E-04	6.61E-05	2.05E-04	5.14E-05	8.51E-05	-1.08E-06
100	10	-1.06E-06	-1.97E-05	-4.41E-05	7.73E-06	-1.87E-04	6.35E-04	1.99E-03	1.32E-04	4.09E-04	1.03E-04	1.70E-04	-9.28E-07
100	20	-2.18E-06	-3.96E-05	-8.90E-05	1.49E-05	-3.52E-04	1.27E-03	3.98E-03	2.65E-04	8.18E-04	2.06E-04	3.40E-04	2.60E-06
200	-20	9.94E-06	1.66E-04	1.49E-04	1.32E-04	8.49E-03	8.74E-03	-4.97E-03	-6.85E-04	-1.90E-03	-5.03E-04	1.48E-03	1.04E-04
200	-10	5.09E-06	8.38E-05	7.63E-05	6.75E-05	4.13E-03	4.70E-03	-2.49E-03	-3.42E-04	-9.50E-04	-2.51E-04	7.21E-04	4.71E-05
200	-5	2.58E-06	4.20E-05	3.85E-05	3.42E-05	2.04E-03	2.02E-03	-1.24E-03	-1.71E-04	-4.75E-04	-1.26E-04	3.56E-04	2.24E-05
200	5	-2.62E-06	-4.25E-05	-3.92E-05	-3.50E-05	-1.98E-03	-2.02E-03	1.24E-03	1.71E-04	4.75E-04	1.25E-04	-3.47E-04	-2.03E-05
200	10	-5.31E-06	-8.55E-05	-7.95E-05	-7.08E-05	-3.91E-03	-4.03E-03	2.49E-03	3.42E-04	9.49E-04	2.51E-04	-6.85E-04	-3.88E-05
200	20	-1.08E-05	-1.72E-04	-1.62E-04	-1.44E-04	-7.67E-03	-8.06E-03	4.97E-03	6.84E-04	1.90E-03	5.01E-04	-1.34E-03	-7.05E-05

Table D3.63 aqueous iron: effect of change in *beta'*

MHz	%	c 10nm	c 100nm	c 1um	c 10um	c 100um	c 1mm	a 10nm	a 100nm	a 1um	a 10um	a 100um	a 1mm
0.1	-20	6.67E-05	6.67E-05	6.93E-05	1.56E-04	4.23E-05	4.44E-06	2.58E-03	9.34E-05	4.37E-05	1.55E-04	2.33E-04	1.24E-04
0.1	-10	3.29E-05	3.29E-05	3.42E-05	7.70E-05	2.09E-05	2.22E-06	1.14E-03	4.47E-05	2.15E-05	7.64E-05	1.15E-04	6.11E-05
0.1	-5	1.63E-05	1.64E-05	1.70E-05	3.82E-05	1.04E-05	1.11E-06	5.37E-04	2.19E-05	1.07E-05	3.80E-05	5.72E-05	3.04E-05
0.1	5	-1.62E-05	-1.62E-05	-1.68E-05	-3.78E-05	-9.94E-06	-1.67E-06	-4.83E-04	-2.11E-05	-1.05E-05	-3.75E-05	-5.65E-05	-3.00E-05
0.1	10	-3.21E-05	-3.21E-05	-3.34E-05	-7.51E-05	-2.04E-05	-2.78E-06	-9.18E-04	-4.15E-05	-2.09E-05	-7.45E-05	-1.12E-04	-5.97E-05
0.1	20	-6.34E-05	-6.34E-05	-6.59E-05	-1.49E-04	-3.98E-05	-4.44E-06	-1.67E-03	-8.03E-05	-4.13E-05	-1.47E-04	-2.22E-04	-1.18E-04
1	-20	7.65E-05	7.64E-05	1.36E-04	1.12E-04	1.60E-05	1.63E-06	2.11E-03	8.99E-05	7.70E-05	2.52E-04	2.07E-04	1.67E-06
1	-10	3.77E-05	3.76E-05	6.70E-05	5.54E-05	7.99E-06	1.08E-06	9.29E-04	4.30E-05	3.78E-05	1.24E-04	1.02E-04	8.17E-07
1	-5	1.87E-05	1.87E-05	3.33E-05	2.77E-05	3.73E-06	5.42E-07	4.38E-04	2.11E-05	1.88E-05	6.15E-05	5.05E-05	4.05E-07
1	5	-1.84E-05	-1.84E-05	-3.27E-05	-2.70E-05	-4.26E-06	-5.42E-07	-3.92E-04	-2.03E-05	-1.84E-05	-6.05E-05	-4.97E-05	-3.97E-07
1	10	-3.65E-05	-3.65E-05	-6.49E-05	-5.32E-05	-7.99E-06	-1.08E-06	-7.45E-04	-3.98E-05	-3.66E-05	-1.20E-04	-9.86E-05	-7.86E-07
1	20	-7.18E-05	-7.17E-05	-1.28E-04	-1.05E-04	-1.54E-05	-1.63E-06	-1.35E-03	-7.71E-05	-7.19E-05	-2.36E-04	-1.94E-04	-1.54E-06
10	-20	8.68E-05	8.98E-05	1.98E-04	4.94E-05	6.96E-06	1.05E-05	1.73E-03	8.01E-05	2.13E-04	2.76E-04	5.47E-06	6.33E-07
10	-10	4.26E-05	4.41E-05	9.72E-05	2.45E-05	3.75E-06	1.05E-05	7.57E-04	3.79E-05	1.04E-04	1.35E-04	2.65E-06	2.68E-07
10	-5	2.11E-05	2.18E-05	4.82E-05	1.22E-05	1.61E-06	1.05E-05	3.56E-04	1.85E-05	5.12E-05	6.65E-05	1.30E-06	1.22E-07
10	5	-2.06E-05	-2.14E-05	-4.75E-05	-1.18E-05	-1.61E-06	0.00E+00	-3.17E-04	-1.77E-05	-5.00E-05	-6.49E-05	-1.26E-06	-9.88E-08
10	10	-4.09E-05	-4.24E-05	-9.40E-05	-2.35E-05	-3.21E-06	0.00E+00	-6.00E-04	-3.46E-05	-9.89E-05	-1.28E-04	-2.47E-06	-1.74E-07
10	20	-8.02E-05	-8.32E-05	-1.85E-04	-4.66E-05	-5.89E-06	0.00E+00	-1.08E-03	-6.65E-05	-1.93E-04	-2.51E-04	-4.78E-06	-2.57E-07
100	-20	9.64E-05	1.57E-04	9.86E-05	1.91E-05	0.00E+00	0.00E+00	1.44E-03	1.76E-04	3.70E-04	1.57E-05	-9.19E-07	6.98E-06
100	-10	4.71E-05	7.75E-05	4.97E-05	9.79E-06	0.00E+00	0.00E+00	6.24E-04	8.14E-05	1.75E-04	7.03E-06	-7.55E-07	3.51E-06
100	-5	2.33E-05	3.84E-05	2.48E-05	4.64E-06	0.00E+00	0.00E+00	2.92E-04	3.92E-05	8.52E-05	3.33E-06	-4.49E-07	1.76E-06
100	5	-2.27E-05	-3.78E-05	-2.52E-05	-4.64E-06	0.00E+00	0.00E+00	-2.58E-04	-3.67E-05	-8.11E-05	-2.98E-06	5.88E-07	-1.76E-06
100	10	-4.48E-05	-7.50E-05	-5.00E-05	-9.79E-06	1.04E-05	3.19E-04	-4.85E-04	-7.10E-05	-1.58E-04	-5.63E-06	1.31E-06	-3.54E-06
100	20	-8.75E-05	-1.47E-04	-9.90E-05	-1.96E-05	1.04E-05	3.19E-04	-8.66E-04	-1.34E-04	-3.03E-04	-1.00E-05	3.15E-06	-7.10E-06
200	-20	1.05E-04	1.88E-04	6.67E-05	1.50E-05	1.48E-04	0.00E+00	1.14E-03	2.64E-04	2.90E-04	1.40E-05	1.85E-05	-1.56E-07
200	-10	5.10E-05	9.35E-05	3.42E-05	8.33E-06	8.48E-05	0.00E+00	4.85E-04	1.20E-04	1.32E-04	5.67E-06	9.20E-06	-2.13E-07
200	-5	2.52E-05	4.65E-05	1.73E-05	4.16E-06	4.24E-05	0.00E+00	2.25E-04	5.76E-05	6.33E-05	2.53E-06	4.60E-06	-1.41E-07
200	5	-2.44E-05	-4.59E-05	-1.69E-05	-4.16E-06	-6.36E-05	0.00E+00	-1.95E-04	-5.32E-05	-5.81E-05	-1.95E-06	-4.59E-06	2.11E-07
200	10	-4.80E-05	-9.10E-05	-3.42E-05	-9.16E-06	-1.06E-04	0.00E+00	-3.65E-04	-1.03E-04	-1.11E-04	-3.36E-06	-9.17E-06	4.93E-07
200	20	-9.31E-05	-1.78E-04	-6.78E-05	-1.83E-05	-2.12E-04	0.00E+00	-6.40E-04	-1.91E-04	-2.05E-04	-4.65E-06	-1.83E-05	1.27E-06

Table D3.64 aqueous iron: effect of change in *c*

MHz	%	c 10nm	c 100nm	c 1um	c 10um	c 100um	c 1mm	a 10nm	a 100nm	a 1um	a 10um	a 100um	a 1mm
0.1	-20	-2.01E-01	-2.01E-01	-2.01E-01	-2.06E-01	-2.16E-01	-1.93E-01	2.45E-01	2.50E-01	2.50E-01	2.50E-01	2.49E-01	7.85E-01
0.1	-10	-1.01E-01	-1.01E-01	-1.01E-01	-1.04E-01	-1.10E-01	-9.86E-02	1.09E-01	1.11E-01	1.11E-01	1.11E-01	1.11E-01	2.99E-01
0.1	-5	-5.03E-02	-5.03E-02	-5.03E-02	-5.20E-02	-5.53E-02	-4.99E-02	5.13E-02	5.26E-02	5.26E-02	5.25E-02	5.25E-02	1.33E-01
0.1	5	5.03E-02	5.03E-02	5.04E-02	5.24E-02	5.62E-02	5.11E-02	-4.63E-02	-4.76E-02	-4.76E-02	-4.75E-02	-4.75E-02	-1.07E-01
0.1	10	1.01E-01	1.01E-01	1.01E-01	1.05E-01	1.13E-01	1.03E-01	-8.83E-02	-9.08E-02	-9.09E-02	-9.07E-02	-9.06E-02	-1.95E-01
0.1	20	2.02E-01	2.02E-01	2.02E-01	2.12E-01	2.30E-01	2.12E-01	-1.62E-01	-1.67E-01	-1.67E-01	-1.66E-01	-1.66E-01	-3.29E-01
1	-20	-2.01E-01	-2.01E-01	-2.02E-01	-2.12E-01	-1.93E-01	-3.12E-01	2.45E-01	2.50E-01	2.50E-01	2.49E-01	5.02E-01	2.23E-01
1	-10	-1.01E-01	-1.01E-01	-1.01E-01	-1.07E-01	-9.86E-02	-1.60E-01	1.09E-01	1.11E-01	1.11E-01	1.11E-01	2.00E-01	1.19E-01
1	-5	-5.03E-02	-5.03E-02	-5.07E-02	-5.38E-02	-4.99E-02	-7.98E-02	5.13E-02	5.26E-02	5.26E-02	5.25E-02	9.03E-02	6.03E-02
1	5	5.03E-02	5.03E-02	5.08E-02	5.45E-02	5.10E-02	7.74E-02	-4.63E-02	-4.76E-02	-4.76E-02	-4.75E-02	-7.57E-02	-5.96E-02
1	10	1.01E-01	1.01E-01	1.02E-01	1.10E-01	1.03E-01	1.52E-01	-8.83E-02	-9.08E-02	-9.09E-02	-9.06E-02	-1.40E-01	-1.16E-01
1	20	2.02E-01	2.02E-01	2.04E-01	2.22E-01	2.11E-01	2.95E-01	-1.62E-01	-1.67E-01	-1.67E-01	-1.66E-01	-2.43E-01	-2.16E-01
10	-20	-2.01E-01	-2.01E-01	-2.06E-01	-1.93E-01	-3.12E-01	-3.19E-01	2.45E-01	2.50E-01	2.50E-01	3.49E-01	2.24E-01	9.06E-02
10	-10	-1.01E-01	-1.01E-01	-1.04E-01	-9.86E-02	-1.60E-01	2.45E-02	1.08E-01	1.11E-01	1.11E-01	1.46E-01	1.18E-01	5.60E-02
10	-5	-5.03E-02	-5.03E-02	-5.20E-02	-4.98E-02	-7.98E-02	-1.33E-01	5.13E-02	5.26E-02	5.25E-02	6.75E-02	6.02E-02	9.88E-02
10	5	5.03E-02	5.04E-02	5.23E-02	5.08E-02	7.74E-02	6.79E-01	-4.63E-02	-4.76E-02	-4.75E-02	-5.87E-02	-5.96E-02	2.56E-02
10	10	1.01E-01	1.01E-01	1.05E-01	1.03E-01	1.52E-01	6.63E-01	-8.83E-02	-9.09E-02	-9.07E-02	-1.10E-01	-1.16E-01	1.23E-01
10	20	2.02E-01	2.02E-01	2.12E-01	2.10E-01	2.95E-01	5.14E-01	-1.61E-01	-1.67E-01	-1.66E-01	-1.97E-01	-2.16E-01	-4.00E-02
100	-20	-2.01E-01	-2.02E-01	-1.94E-01	-3.09E-01	-3.16E-01	-5.42E-01	2.45E-01	2.50E-01	2.90E-01	2.25E-01	9.13E-02	3.62E-03
100	-10	-1.01E-01	-1.01E-01	-9.86E-02	-1.59E-01	2.46E-02	-2.60E-01	1.08E-01	1.11E-01	1.25E-01	1.18E-01	5.56E-02	-4.96E-03
100	-5	-5.03E-02	-5.07E-02	-4.97E-02	-7.96E-02	-1.29E-01	-2.66E-01	5.12E-02	5.26E-02	5.87E-02	6.00E-02	9.75E-02	1.19E-04
100	5	5.03E-02	5.08E-02	5.04E-02	7.76E-02	6.70E-01	2.82E-01	-4.62E-02	-4.76E-02	-5.21E-02	-5.94E-02	2.40E-02	3.71E-03
100	10	1.01E-01	1.02E-01	1.02E-01	1.52E-01	6.58E-01	1.55E-01	-8.81E-02	-9.08E-02	-9.87E-02	-1.16E-01	1.19E-01	-1.10E-02
100	20	2.02E-01	2.04E-01	2.06E-01	2.96E-01	5.06E-01	9.18E-01	-1.61E-01	-1.66E-01	-1.79E-01	-2.16E-01	-4.08E-02	1.89E-02
200	-20	-2.01E-01	-2.03E-01	-1.73E-01	-4.85E-01	-4.90E-01	-1.02E+00	2.45E-01	2.50E-01	4.79E-01	9.70E-02	-1.41E-02	-2.61E-01
200	-10	-1.01E-01	-1.02E-01	-8.68E-02	-2.70E-01	-3.79E-01	-8.38E-01	1.08E-01	1.11E-01	1.95E-01	2.98E-02	-6.22E-02	-8.15E-02
200	-5	-5.03E-02	-5.09E-02	-4.36E-02	-1.42E-01	-5.05E-01	-5.78E-01	5.12E-02	5.26E-02	8.87E-02	1.10E-02	-2.68E-02	1.30E-02
200	5	5.03E-02	5.10E-02	4.41E-02	1.50E-01	-1.80E-01	1.06E-01	-4.62E-02	-4.76E-02	-7.51E-02	-6.19E-03	-8.19E-02	-8.18E-03
200	10	1.01E-01	1.02E-01	8.87E-02	3.04E-01	1.98E-01	-6.56E-02	-8.80E-02	-9.08E-02	-1.39E-01	-8.79E-03	2.16E-02	2.30E-02
200	20	2.02E-01	2.05E-01	1.80E-01	6.21E-01	9.16E-01	4.13E-02	-1.61E-01	-1.66E-01	-2.43E-01	-5.95E-03	-2.88E-03	3.48E-02

Table D3.65 aqueous iron: effect of change in *rho*

MHz	%	c 10nm	c 100nm	c 1um	c 10um	c 100um	c 1mm	a 10nm	a 100nm	a 1um	a 10um	a 100um	a 1mm
0.1	-20	2.32E-01	2.32E-01	2.39E-01	2.19E-01	2.24E-01	2.12E-01	2.57E-01	2.63E-01	3.10E-01	2.72E-01	2.26E-01	1.34E-01
0.1	-10	1.08E-01	1.08E-01	1.11E-01	1.03E-01	1.10E-01	1.05E-01	1.17E-01	1.20E-01	1.40E-01	1.23E-01	1.04E-01	6.21E-02
0.1	-5	5.21E-02	5.21E-02	5.36E-02	5.04E-02	5.46E-02	5.24E-02	5.60E-02	5.74E-02	6.65E-02	5.89E-02	4.99E-02	3.00E-02
0.1	5	-4.88E-02	-4.88E-02	-5.01E-02	-4.81E-02	-5.38E-02	-5.21E-02	-5.16E-02	-5.28E-02	-6.07E-02	-5.40E-02	-4.64E-02	-2.81E-02
0.1	10	-9.47E-02	-9.47E-02	-9.71E-02	-9.41E-02	-1.07E-01	-1.04E-01	-9.93E-02	-1.02E-01	-1.16E-01	-1.04E-01	-8.96E-02	-5.46E-02
0.1	20	-1.79E-01	-1.79E-01	-1.83E-01	-1.81E-01	-2.11E-01	-2.06E-01	-1.85E-01	-1.89E-01	-2.15E-01	-1.93E-01	-1.68E-01	-1.03E-01
1	-20	2.68E-01	2.68E-01	2.77E-01	2.97E-01	3.10E-01	2.42E-02	2.82E-01	3.00E-01	3.59E-01	2.62E-01	1.95E-01	-7.80E-03
1	-10	1.24E-01	1.24E-01	1.28E-01	1.44E-01	1.53E-01	1.19E-02	1.28E-01	1.36E-01	1.60E-01	1.20E-01	9.00E-02	-4.04E-03
1	-5	5.99E-02	5.99E-02	6.17E-02	7.11E-02	7.63E-02	5.94E-03	6.12E-02	6.49E-02	7.58E-02	5.74E-02	4.33E-02	-2.06E-03
1	5	-5.59E-02	-5.60E-02	-5.77E-02	-6.93E-02	-7.56E-02	-5.86E-03	-5.63E-02	-5.95E-02	-6.85E-02	-5.31E-02	-4.04E-02	2.12E-03
1	10	-1.08E-01	-1.08E-01	-1.12E-01	-1.37E-01	-1.51E-01	-1.17E-02	-1.08E-01	-1.14E-01	-1.31E-01	-1.02E-01	-7.81E-02	4.31E-03
1	20	-2.04E-01	-2.04E-01	-2.11E-01	-2.68E-01	-2.99E-01	-2.30E-02	-2.01E-01	-2.12E-01	-2.39E-01	-1.91E-01	-1.47E-01	8.86E-03
10	-20	3.15E-01	3.24E-01	3.54E-01	4.78E-01	2.96E-02	-1.59E-02	3.15E-01	3.77E-01	3.27E-01	2.53E-01	-8.49E-03	7.94E-04
10	-10	1.45E-01	1.49E-01	1.68E-01	2.35E-01	1.45E-02	-9.27E-03	1.42E-01	1.68E-01	1.48E-01	1.16E-01	-4.50E-03	-2.39E-05
10	-5	7.00E-02	7.17E-02	8.23E-02	1.17E-01	7.21E-03	-4.98E-03	6.79E-02	7.98E-02	7.04E-02	5.58E-02	-2.31E-03	-1.11E-04
10	5	-6.51E-02	-6.66E-02	-7.89E-02	-1.15E-01	-7.09E-03	5.66E-03	-6.22E-02	-7.23E-02	-6.44E-02	-5.17E-02	2.42E-03	2.96E-04
10	10	-1.26E-01	-1.29E-01	-1.55E-01	-2.29E-01	-1.41E-02	1.20E-02	-1.19E-01	-1.38E-01	-1.23E-01	-9.97E-02	4.94E-03	7.68E-04
10	20	-2.36E-01	-2.41E-01	-2.98E-01	-4.52E-01	-2.76E-02	2.67E-02	-2.21E-01	-2.53E-01	-2.28E-01	-1.86E-01	1.03E-02	2.20E-03
100	-20	3.82E-01	4.12E-01	7.20E-01	3.75E-02	-2.63E-02	-9.78E-02	3.65E-01	4.36E-01	3.14E-01	-6.80E-03	-8.01E-04	-6.21E-03
100	-10	1.76E-01	1.91E-01	3.51E-01	1.83E-02	-1.51E-02	-4.68E-02	1.64E-01	1.93E-01	1.43E-01	-3.90E-03	-9.42E-04	-3.25E-03
100	-5	8.44E-02	9.21E-02	1.73E-01	9.02E-03	-8.02E-03	-2.29E-02	7.79E-02	9.10E-02	6.83E-02	-2.07E-03	-5.96E-04	-1.66E-03
100	5	-7.83E-02	-8.61E-02	-1.69E-01	-8.79E-03	8.92E-03	2.17E-02	-7.09E-02	-8.17E-02	-6.28E-02	2.28E-03	8.29E-04	1.72E-03
100	10	-1.51E-01	-1.67E-01	-3.35E-01	-1.74E-02	1.87E-02	4.24E-02	-1.36E-01	-1.55E-01	-1.21E-01	4.75E-03	1.87E-03	3.50E-03
100	20	-2.82E-01	-3.15E-01	-6.56E-01	-3.39E-02	4.07E-02	8.10E-02	-2.49E-01	-2.82E-01	-2.24E-01	1.02E-02	4.56E-03	7.20E-03
200	-20	4.88E-01	6.21E-01	1.49E+00	-6.95E-02	-3.50E-02	-4.40E-02	4.23E-01	4.68E-01	2.55E-01	6.45E-03	-4.41E-03	-7.93E-03
200	-10	2.23E-01	2.91E-01	7.28E-01	-3.51E-02	-1.66E-02	-1.93E-02	1.88E-01	2.07E-01	1.16E-01	2.64E-03	-2.29E-03	-4.00E-03
200	-5	1.07E-01	1.41E-01	3.60E-01	-1.76E-02	-8.11E-03	-8.80E-03	8.92E-02	9.76E-02	5.54E-02	1.18E-03	-1.16E-03	-2.01E-03
200	5	-9.90E-02	-1.33E-01	-3.53E-01	1.78E-02	7.81E-03	8.25E-03	-8.06E-02	-8.76E-02	-5.10E-02	-9.08E-04	1.20E-03	2.02E-03
200	10	-1.91E-01	-2.59E-01	-6.99E-01	3.58E-02	1.53E-02	1.49E-02	-1.54E-01	-1.66E-01	-9.79E-02	-1.55E-03	2.45E-03	4.06E-03
200	20	-3.55E-01	-4.93E-01	-1.37E+00	7.22E-02	2.98E-02	2.48E-02	-2.80E-01	-3.02E-01	-1.81E-01	-2.08E-03	5.09E-03	8.15E-03

Table D3.66 aqueous iron: effect of change in *eta*

MHz	%	c 10nm	c 100nm	c 1um	c 10um	c 100um	c 1mm	a 10nm	a 100nm	a 1um	a 10um	a 100um	a 1mm
0.1	-20	-3.52E-08	-2.60E-05	-2.19E-02	-7.52E-02	-1.87E-02	-2.11E-03	2.40E-01	2.45E-01	1.56E-01	-1.07E-01	-1.06E-01	-5.69E-02
0.1	-10	-3.52E-08	-1.12E-05	-9.67E-03	-3.67E-02	-9.07E-03	-1.02E-03	1.07E-01	1.09E-01	7.26E-02	-5.20E-02	-5.17E-02	-2.76E-02
0.1	-5	0.00E+00	-5.24E-06	-4.56E-03	-1.81E-02	-4.47E-03	-5.06E-04	5.06E-02	5.17E-02	3.51E-02	-2.57E-02	-2.55E-02	-1.36E-02
0.1	5	0.00E+00	4.61E-06	4.10E-03	1.77E-02	4.36E-03	4.93E-04	-4.58E-02	-4.68E-02	-3.29E-02	2.50E-02	2.49E-02	1.33E-02
0.1	10	0.00E+00	8.68E-06	7.79E-03	3.51E-02	8.62E-03	9.74E-04	-8.73E-02	-8.95E-02	-6.38E-02	4.93E-02	4.92E-02	2.63E-02
0.1	20	0.00E+00	1.56E-05	1.42E-02	6.88E-02	1.69E-02	1.90E-03	-1.60E-01	-1.64E-01	-1.20E-01	9.63E-02	9.63E-02	5.14E-02
1	-20	-5.98E-07	-6.49E-04	-9.45E-02	-4.51E-02	-6.95E-03	-6.86E-04	2.37E-01	2.35E-01	-4.44E-02	-1.08E-01	-8.49E-02	-1.00E-03
1	-10	-2.46E-07	-2.79E-04	-4.53E-02	-2.19E-02	-3.38E-03	-3.34E-04	1.05E-01	1.05E-01	-1.92E-02	-5.25E-02	-4.13E-02	-4.86E-04
1	-5	-1.05E-07	-1.30E-04	-2.22E-02	-1.08E-02	-1.67E-03	-1.65E-04	4.99E-02	4.98E-02	-8.96E-03	-2.59E-02	-2.04E-02	-2.40E-04
1	5	1.05E-07	1.15E-04	2.14E-02	1.06E-02	1.63E-03	1.60E-04	-4.52E-02	-4.52E-02	7.74E-03	2.53E-02	1.99E-02	2.34E-04
1	10	2.11E-07	2.17E-04	4.19E-02	2.09E-02	3.21E-03	3.17E-04	-8.62E-02	-8.65E-02	1.44E-02	5.01E-02	3.93E-02	4.63E-04
1	20	3.87E-07	3.90E-04	8.07E-02	4.08E-02	6.28E-03	6.19E-04	-1.58E-01	-1.59E-01	2.47E-02	9.80E-02	7.68E-02	9.05E-04
10	-20	-1.50E-05	-1.39E-02	-8.06E-02	-2.07E-02	-2.31E-03	-1.38E-03	2.32E-01	1.79E-01	-1.06E-01	-9.96E-02	-3.42E-03	-1.24E-03
10	-10	-6.43E-06	-6.08E-03	-3.94E-02	-1.00E-02	-1.12E-03	-6.62E-04	1.03E-01	8.25E-02	-5.11E-02	-4.85E-02	-1.66E-03	-6.01E-04
10	-5	-3.02E-06	-2.86E-03	-1.95E-02	-4.96E-03	-5.52E-04	-3.26E-04	4.88E-02	3.96E-02	-2.52E-02	-2.39E-02	-8.21E-04	-2.97E-04
10	5	2.64E-06	2.55E-03	1.90E-02	4.83E-03	5.39E-04	3.26E-04	-4.41E-02	-3.67E-02	2.45E-02	2.33E-02	8.01E-04	2.89E-04
10	10	4.99E-06	4.84E-03	3.77E-02	9.55E-03	1.06E-03	6.31E-04	-8.42E-02	-7.09E-02	4.83E-02	4.61E-02	1.58E-03	5.72E-04
10	20	8.97E-06	8.76E-03	7.40E-02	1.87E-02	2.08E-03	1.23E-03	-1.54E-01	-1.32E-01	9.40E-02	9.03E-02	3.10E-03	1.12E-03
100	-20	-3.75E-04	-8.65E-02	-4.84E-02	-7.19E-03	-3.14E-03	6.14E-03	2.19E-01	-1.61E-02	-1.06E-01	-1.13E-02	-4.16E-03	-1.72E-03
100	-10	-1.61E-04	-4.10E-02	-2.36E-02	-3.49E-03	-1.50E-03	2.91E-03	9.77E-02	-5.19E-03	-5.18E-02	-5.51E-03	-2.02E-03	-8.33E-04
100	-5	-7.53E-05	-2.00E-02	-1.16E-02	-1.72E-03	-7.30E-04	1.29E-03	4.63E-02	-1.96E-03	-2.56E-02	-2.72E-03	-9.99E-04	-4.10E-04
100	5	6.64E-05	1.90E-02	1.13E-02	1.67E-03	6.99E-04	-1.62E-03	-4.20E-02	8.54E-04	2.50E-02	2.65E-03	9.74E-04	3.99E-04
100	10	1.25E-04	3.71E-02	2.24E-02	3.31E-03	1.37E-03	-3.23E-03	-8.02E-02	7.28E-04	4.94E-02	5.25E-03	1.92E-03	7.87E-04
100	20	2.25E-04	7.07E-02	4.39E-02	6.45E-03	2.63E-03	-6.14E-03	-1.47E-01	-2.02E-03	9.68E-02	1.03E-02	3.76E-03	1.53E-03
200	-20	-8.13E-04	-9.65E-02	-3.85E-02	-6.51E-03	1.10E-03	1.79E-02	2.10E-01	-5.43E-02	-9.31E-02	-1.22E-02	-4.40E-03	-1.79E-03
200	-10	-3.50E-04	-4.65E-02	-1.87E-02	-3.14E-03	6.16E-04	8.25E-03	9.35E-02	-2.43E-02	-4.54E-02	-5.96E-03	-2.13E-03	-8.57E-04
200	-5	-1.64E-04	-2.28E-02	-9.23E-03	-1.54E-03	3.18E-04	4.12E-03	4.43E-02	-1.15E-02	-2.24E-02	-2.94E-03	-1.05E-03	-4.20E-04
200	5	1.44E-04	2.20E-02	9.01E-03	1.50E-03	-3.40E-04	-4.81E-03	-4.02E-02	1.03E-02	2.19E-02	2.87E-03	1.02E-03	4.05E-04
200	10	2.72E-04	4.33E-02	1.78E-02	2.95E-03	-7.01E-04	-8.93E-03	-7.68E-02	1.94E-02	4.33E-02	5.68E-03	2.02E-03	7.97E-04
200	20	4.89E-04	8.37E-02	3.48E-02	5.73E-03	-1.49E-03	-1.72E-02	-1.41E-01	3.48E-02	8.48E-02	1.11E-02	3.95E-03	1.54E-03

Table D3.67 aqueous iron: effect of change in *kappa*

MHz	%	c 10nm	c 100nm	c 1um	c 10um	c 100um	c 1mm	a 10nm	a 100nm	a 1um	a 10um	a 100um	a 1mm
0.1	-20	0.00E+00	-7.03E-08	-1.41E-05	-1.66E-04	-4.52E-05	-5.00E-06	2.40E-04	2.32E-04	9.16E-05	-1.18E-04	-2.49E-04	-1.33E-04
0.1	-10	0.00E+00	-3.52E-08	-6.37E-06	-8.04E-05	-2.19E-05	-2.78E-06	1.06E-04	1.03E-04	4.27E-05	-5.58E-05	-1.20E-04	-6.42E-05
0.1	-5	0.00E+00	-3.52E-08	-3.03E-06	-3.95E-05	-1.04E-05	-1.67E-06	5.03E-05	4.90E-05	2.07E-05	-2.72E-05	-5.92E-05	-3.16E-05
0.1	5	0.00E+00	0.00E+00	2.77E-06	3.84E-05	1.04E-05	1.11E-06	-4.55E-05	-4.45E-05	-1.94E-05	2.58E-05	5.75E-05	3.07E-05
0.1	10	0.00E+00	0.00E+00	5.32E-06	7.55E-05	2.09E-05	2.22E-06	-8.67E-05	-8.51E-05	-3.77E-05	5.04E-05	1.13E-04	6.05E-05
0.1	20	0.00E+00	3.52E-08	9.81E-06	1.47E-04	4.03E-05	4.44E-06	-1.59E-04	-1.56E-04	-7.13E-05	9.64E-05	2.21E-04	1.18E-04
1	-20	0.00E+00	-9.51E-07	-8.60E-05	-1.16E-04	-1.60E-05	-2.17E-06	1.95E-04	1.60E-04	2.16E-05	-2.43E-04	-2.08E-04	-1.59E-06
1	-10	0.00E+00	-4.23E-07	-4.04E-05	-5.61E-05	-7.98E-06	-1.08E-06	8.64E-05	7.20E-05	1.13E-05	-1.17E-04	-1.01E-04	-7.68E-07
1	-5	0.00E+00	-2.11E-07	-1.96E-05	-2.77E-05	-3.73E-06	-5.42E-07	4.09E-05	3.43E-05	5.78E-06	-5.77E-05	-4.95E-05	-3.78E-07
1	5	0.00E+00	1.76E-07	1.86E-05	2.70E-05	3.73E-06	0.00E+00	-3.69E-05	-3.13E-05	-5.94E-06	5.59E-05	4.81E-05	3.67E-07
1	10	0.00E+00	3.17E-07	3.62E-05	5.32E-05	7.45E-06	5.42E-07	-7.03E-05	-6.01E-05	-1.20E-05	1.10E-04	9.48E-05	7.23E-07
1	20	0.00E+00	5.99E-07	6.87E-05	1.04E-04	1.44E-05	1.63E-06	-1.29E-04	-1.11E-04	-2.44E-05	2.14E-04	1.85E-04	1.41E-06
10	-20	-3.52E-08	-1.06E-05	-1.89E-04	-4.85E-05	-6.42E-06	0.00E+00	1.52E-04	8.20E-05	-1.20E-04	-2.61E-04	-5.47E-06	-3.38E-06
10	-10	0.00E+00	-4.76E-06	-9.11E-05	-2.35E-05	-3.21E-06	0.00E+00	6.76E-05	3.80E-05	-5.66E-05	-1.26E-04	-2.64E-06	-1.64E-06
10	-5	0.00E+00	-2.28E-06	-4.48E-05	-1.13E-05	-1.61E-06	0.00E+00	3.20E-05	1.83E-05	-2.75E-05	-6.20E-05	-1.30E-06	-8.05E-07
10	5	3.52E-08	2.02E-06	4.33E-05	1.13E-05	1.07E-06	1.05E-05	-2.88E-05	-1.71E-05	2.60E-05	6.01E-05	1.26E-06	7.81E-07
10	10	3.52E-08	3.90E-06	8.51E-05	2.21E-05	2.68E-06	1.05E-05	-5.50E-05	-3.31E-05	5.06E-05	1.19E-04	2.49E-06	1.54E-06
10	20	3.52E-08	7.19E-06	1.65E-04	4.33E-05	5.35E-06	1.05E-05	-1.00E-04	-6.22E-05	9.61E-05	2.31E-04	4.84E-06	2.99E-06
100	-20	-8.81E-07	-8.48E-05	-1.15E-04	-1.65E-05	-1.04E-05	0.00E+00	1.03E-04	1.89E-05	-3.04E-04	-2.08E-05	-1.13E-05	-3.58E-06
100	-10	-3.88E-07	-3.96E-05	-5.55E-05	-8.25E-06	-1.04E-05	0.00E+00	4.59E-05	1.01E-05	-1.47E-04	-1.00E-05	-5.47E-06	-1.73E-06
100	-5	-1.76E-07	-1.92E-05	-2.72E-05	-4.12E-06	0.00E+00	0.00E+00	2.17E-05	5.14E-06	-7.21E-05	-4.93E-06	-2.69E-06	-8.51E-07
100	5	1.76E-07	1.81E-05	2.65E-05	3.61E-06	0.00E+00	0.00E+00	-1.96E-05	-5.33E-06	6.98E-05	4.78E-06	2.61E-06	8.25E-07
100	10	3.17E-07	3.52E-05	5.24E-05	7.22E-06	1.04E-05	0.00E+00	-3.75E-05	-1.08E-05	1.37E-04	9.42E-06	5.15E-06	1.63E-06
100	20	5.64E-07	6.66E-05	1.02E-04	1.44E-05	1.04E-05	0.00E+00	-6.85E-05	-2.20E-05	2.67E-04	1.83E-05	1.00E-05	3.16E-06
200	-20	-2.05E-06	-1.34E-04	-7.66E-05	-6.66E-06	4.24E-05	0.00E+00	7.33E-05	-3.12E-05	-2.95E-04	-2.98E-05	-1.52E-05	-5.37E-06
200	-10	-9.20E-07	-6.33E-05	-3.71E-05	-3.33E-06	2.12E-05	0.00E+00	3.26E-05	-1.32E-05	-1.42E-04	-1.44E-05	-7.33E-06	-2.59E-06
200	-5	-4.24E-07	-3.09E-05	-1.84E-05	-1.67E-06	2.12E-05	0.00E+00	1.54E-05	-6.09E-06	-6.99E-05	-7.07E-06	-3.61E-06	-1.28E-06
200	5	3.89E-07	2.93E-05	1.76E-05	1.67E-06	0.00E+00	0.00E+00	-1.39E-05	5.19E-06	6.77E-05	6.85E-06	3.50E-06	1.24E-06
200	10	7.43E-07	5.72E-05	3.49E-05	3.33E-06	0.00E+00	0.00E+00	-2.65E-05	9.57E-06	1.33E-04	1.35E-05	6.89E-06	2.44E-06
200	20	1.38E-06	1.09E-04	6.78E-05	6.66E-06	-2.12E-05	0.00E+00	-4.83E-05	1.63E-05	2.59E-04	2.63E-05	1.34E-05	4.74E-06

Table D3.68 aqueous iron: effect of change in *Cp*

MHz	%	c 10nm	c 100nm	c 1um	c 10um	c 100um	c 1mm	a 10nm	a 100nm	a 1um	a 10um	a 100um	a 1mm
0.1	-20	5.37E-04	5.37E-04	5.53E-04	9.56E-04	2.51E-04	2.78E-05	1.79E-03	5.87E-04	4.39E-04	1.09E-03	1.40E-03	7.38E-04
0.1	-10	2.21E-04	2.21E-04	2.28E-04	4.06E-04	1.07E-04	1.17E-05	7.84E-04	2.41E-04	1.76E-04	4.56E-04	5.96E-04	3.14E-04
0.1	-5	1.01E-04	1.01E-04	1.04E-04	1.89E-04	4.97E-05	5.00E-06	3.69E-04	1.11E-04	7.99E-05	2.10E-04	2.77E-04	1.46E-04
0.1	5	-8.61E-05	-8.61E-05	-8.89E-05	-1.64E-04	-4.33E-05	-5.00E-06	-3.30E-04	-9.40E-05	-6.68E-05	-1.81E-04	-2.41E-04	-1.28E-04
0.1	10	-1.60E-04	-1.60E-04	-1.65E-04	-3.09E-04	-8.15E-05	-9.44E-06	-6.27E-04	-1.75E-04	-1.23E-04	-3.39E-04	-4.53E-04	-2.40E-04
0.1	20	-2.79E-04	-2.79E-04	-2.88E-04	-5.48E-04	-1.45E-04	-1.61E-05	-1.14E-03	-3.04E-04	-2.11E-04	-5.96E-04	-8.06E-04	-4.26E-04
1	-20	3.58E-04	3.58E-04	5.90E-04	4.27E-04	6.23E-05	7.05E-06	1.44E-03	3.58E-04	3.89E-04	9.82E-04	7.89E-04	6.10E-06
1	-10	1.47E-04	1.47E-04	2.45E-04	1.81E-04	2.66E-05	2.71E-06	6.30E-04	1.46E-04	1.57E-04	4.15E-04	3.35E-04	2.59E-06
1	-5	6.73E-05	6.72E-05	1.13E-04	8.41E-05	1.22E-05	1.08E-06	2.97E-04	6.66E-05	7.15E-05	1.92E-04	1.55E-04	1.20E-06
1	5	-5.71E-05	-5.70E-05	-9.69E-05	-7.30E-05	-1.06E-05	-1.63E-06	-2.66E-04	-5.63E-05	-5.99E-05	-1.67E-04	-1.35E-04	-1.04E-06
1	10	-1.06E-04	-1.06E-04	-1.80E-04	-1.37E-04	-1.97E-05	-2.71E-06	-5.05E-04	-1.04E-04	-1.11E-04	-3.13E-04	-2.54E-04	-1.96E-06
1	20	-1.84E-04	-1.84E-04	-3.16E-04	-2.44E-04	-3.51E-05	-4.34E-06	-9.20E-04	-1.80E-04	-1.90E-04	-5.54E-04	-4.51E-04	-3.47E-06
10	-20	2.37E-04	2.45E-04	5.00E-04	1.25E-04	1.55E-05	1.05E-05	1.17E-03	1.82E-04	5.32E-04	6.68E-04	1.40E-05	7.45E-06
10	-10	9.68E-05	1.00E-04	2.11E-04	5.27E-05	6.42E-06	0.00E+00	5.12E-04	7.30E-05	2.21E-04	2.82E-04	5.92E-06	3.17E-06
10	-5	4.42E-05	4.57E-05	9.75E-05	2.45E-05	3.21E-06	0.00E+00	2.41E-04	3.30E-05	1.02E-04	1.31E-04	2.74E-06	1.47E-06
10	5	-3.74E-05	-3.87E-05	-8.44E-05	-2.12E-05	-2.68E-06	0.00E+00	-2.17E-04	-2.76E-05	-8.69E-05	-1.14E-04	-2.38E-06	-1.28E-06
10	10	-6.92E-05	-7.16E-05	-1.58E-04	-3.96E-05	-4.82E-06	-1.05E-05	-4.12E-04	-5.07E-05	-1.62E-04	-2.13E-04	-4.46E-06	-2.41E-06
10	20	-1.20E-04	-1.24E-04	-2.78E-04	-6.97E-05	-8.56E-06	-1.05E-05	-7.51E-04	-8.71E-05	-2.83E-04	-3.76E-04	-7.88E-06	-4.28E-06
100	-20	1.54E-04	2.64E-04	1.94E-04	2.99E-05	2.07E-05	0.00E+00	9.77E-04	2.01E-04	5.21E-04	3.41E-05	1.77E-05	7.88E-06
100	-10	6.25E-05	1.08E-04	8.07E-05	1.24E-05	1.04E-05	0.00E+00	4.31E-04	8.29E-05	2.21E-04	1.45E-05	7.55E-06	3.37E-06
100	-5	2.85E-05	4.95E-05	3.69E-05	5.67E-06	0.00E+00	0.00E+00	2.03E-04	3.80E-05	1.02E-04	6.73E-06	3.51E-06	1.57E-06
100	5	-2.39E-05	-4.19E-05	-3.21E-05	-4.64E-06	0.00E+00	0.00E+00	-1.83E-04	-3.24E-05	-8.89E-05	-5.87E-06	-3.06E-06	-1.38E-06
100	10	-4.42E-05	-7.77E-05	-5.94E-05	-8.76E-06	0.00E+00	0.00E+00	-3.48E-04	-6.02E-05	-1.67E-04	-1.10E-05	-5.76E-06	-2.59E-06
100	20	-7.62E-05	-1.35E-04	-1.04E-04	-1.55E-05	-1.04E-05	0.00E+00	-6.36E-04	-1.05E-04	-2.95E-04	-1.96E-05	-1.03E-05	-4.63E-06
200	-20	9.73E-05	1.93E-04	8.48E-05	9.16E-06	-2.12E-05	-6.55E-04	8.20E-04	2.15E-04	3.29E-04	3.36E-05	8.37E-06	4.59E-06
200	-10	3.92E-05	7.82E-05	3.46E-05	3.33E-06	0.00E+00	-6.55E-04	3.63E-04	9.08E-05	1.40E-04	1.43E-05	3.29E-06	1.88E-06
200	-5	1.78E-05	3.56E-05	1.55E-05	1.67E-06	0.00E+00	-6.55E-04	1.71E-04	4.21E-05	6.53E-05	6.67E-06	1.47E-06	8.58E-07
200	5	-1.48E-05	-2.98E-05	-1.31E-05	-8.33E-07	0.00E+00	0.00E+00	-1.54E-04	-3.66E-05	-5.73E-05	-5.84E-06	-1.17E-06	-7.22E-07
200	10	-2.72E-05	-5.49E-05	-2.40E-05	-1.67E-06	0.00E+00	0.00E+00	-2.94E-04	-6.87E-05	-1.08E-04	-1.10E-05	-2.10E-06	-1.33E-06
200	20	-4.65E-05	-9.41E-05	-4.10E-05	-2.50E-06	0.00E+00	0.00E+00	-5.38E-04	-1.22E-04	-1.93E-04	-1.96E-05	-3.40E-06	-2.28E-06

Table D3.69 aqueous iron: effect of change in *alpha*

MHz	%	c 10nm	c 100nm	c 1um	c 10um	c 100um	c 1mm	a 10nm	a 100nm	a 1um	a 10um	a 100um	a 1mm
0.1	-20	0.00E+00	0.00E+00	0.00E+00	0.00E+00	0.00E+00	0.00E+00	-3.01E-03	-3.20E-05	-4.42E-07	-7.93E-08	-4.48E-07	-2.71E-06
0.1	-10	0.00E+00	0.00E+00	0.00E+00	0.00E+00	0.00E+00	0.00E+00	-1.52E-03	-1.60E-05	-2.21E-07	-3.97E-08	-2.24E-07	-1.36E-06
0.1	-5	0.00E+00	0.00E+00	0.00E+00	0.00E+00	0.00E+00	0.00E+00	-7.71E-04	-7.99E-06	-1.11E-07	-1.98E-08	-1.12E-07	-6.78E-07
0.1	5	0.00E+00	0.00E+00	0.00E+00	0.00E+00	0.00E+00	0.00E+00	7.53E-04	7.99E-06	1.11E-07	1.99E-08	1.12E-07	6.78E-07
0.1	10	0.00E+00	0.00E+00	0.00E+00	0.00E+00	0.00E+00	0.00E+00	1.50E-03	1.60E-05	2.21E-07	3.97E-08	2.24E-07	1.36E-06
0.1	20	0.00E+00	0.00E+00	0.00E+00	0.00E+00	0.00E+00	0.00E+00	3.01E-03	3.20E-05	4.42E-07	7.94E-08	4.48E-07	2.71E-06
1	-20	0.00E+00	3.52E-08	4.94E-07	0.00E+00	0.00E+00	1.63E-06	-3.03E-03	-3.43E-05	-1.03E-06	-1.64E-06	-1.27E-05	-3.62E-07
1	-10	0.00E+00	3.52E-08	2.82E-07	0.00E+00	0.00E+00	5.42E-07	-1.52E-03	-1.71E-05	-5.14E-07	-8.22E-07	-6.36E-06	-1.81E-07
1	-5	0.00E+00	3.52E-08	1.41E-07	0.00E+00	0.00E+00	5.42E-07	-7.59E-04	-8.57E-06	-2.57E-07	-4.11E-07	-3.18E-06	-9.05E-08
1	5	0.00E+00	0.00E+00	-1.41E-07	0.00E+00	0.00E+00	-5.42E-07	7.59E-04	8.57E-06	2.57E-07	4.11E-07	3.18E-06	9.05E-08
1	10	0.00E+00	0.00E+00	-2.82E-07	-3.59E-07	0.00E+00	-1.08E-06	1.52E-03	1.71E-05	5.14E-07	8.22E-07	6.36E-06	1.81E-07
1	20	0.00E+00	0.00E+00	-4.94E-07	-3.59E-07	0.00E+00	-1.63E-06	3.03E-03	3.43E-05	1.03E-06	1.64E-06	1.27E-05	3.62E-07
10	-20	0.00E+00	1.39E-06	4.35E-06	1.41E-06	1.50E-05	6.32E-05	-3.10E-03	-4.42E-05	-7.94E-06	-4.94E-05	-3.52E-06	2.18E-05
10	-10	0.00E+00	7.12E-07	2.27E-06	4.71E-07	7.49E-06	3.16E-05	-1.55E-03	-2.21E-05	-3.97E-06	-2.47E-05	-1.76E-06	1.09E-05
10	-5	0.00E+00	3.75E-07	1.13E-06	4.71E-07	3.75E-06	1.05E-05	-7.74E-04	-1.11E-05	-1.99E-06	-1.23E-05	-8.80E-07	5.45E-06
10	5	-3.52E-08	-3.37E-07	-9.46E-07	-4.71E-07	-3.75E-06	-2.11E-05	7.74E-04	1.11E-05	1.99E-06	1.23E-05	8.80E-07	-5.46E-06
10	10	-3.52E-08	-6.74E-07	-2.08E-06	-9.41E-07	-7.49E-06	-4.21E-05	1.55E-03	2.21E-05	3.97E-06	2.47E-05	1.76E-06	-1.09E-05
10	20	-3.52E-08	-1.35E-06	-4.16E-06	-1.41E-06	-1.50E-05	-7.37E-05	3.10E-03	4.42E-05	7.94E-06	4.94E-05	3.52E-06	-2.18E-05
100	-20	1.90E-06	5.13E-05	2.48E-05	1.48E-04	6.94E-04	-1.91E-03	-3.31E-03	-1.02E-04	-1.87E-04	-3.22E-05	2.13E-04	2.96E-05
100	-10	9.51E-07	2.56E-05	1.24E-05	7.42E-05	3.52E-04	-9.57E-04	-1.66E-03	-5.12E-05	-9.36E-05	-1.61E-05	1.06E-04	1.50E-05
100	-5	4.58E-07	1.28E-05	6.21E-06	3.71E-05	1.76E-04	-6.38E-04	-8.28E-04	-2.56E-05	-4.68E-05	-8.05E-06	5.32E-05	7.52E-06
100	5	-4.58E-07	-1.28E-05	-6.55E-06	-3.71E-05	-1.76E-04	6.38E-04	8.28E-04	2.56E-05	4.68E-05	8.05E-06	-5.33E-05	-7.60E-06
100	10	-9.51E-07	-2.57E-05	-1.28E-05	-7.42E-05	-3.52E-04	9.57E-04	1.66E-03	5.12E-05	9.36E-05	1.61E-05	-1.07E-04	-1.53E-05
100	20	-1.90E-06	-5.13E-05	-2.52E-05	-1.48E-04	-7.15E-04	1.91E-03	3.31E-03	1.02E-04	1.87E-04	3.22E-05	-2.13E-04	-3.09E-05
200	-20	7.36E-06	1.12E-04	9.78E-05	3.58E-05	-3.05E-03	-5.77E-02	-3.46E-03	-1.62E-04	-5.10E-04	1.44E-04	-4.55E-04	4.25E-04
200	-10	3.68E-06	5.60E-05	4.87E-05	1.75E-05	-1.53E-03	-3.02E-02	-1.73E-03	-8.12E-05	-2.55E-04	7.20E-05	-2.28E-04	2.21E-04
200	-5	1.84E-06	2.80E-05	2.44E-05	8.33E-06	-7.63E-04	-1.51E-02	-8.65E-04	-4.06E-05	-1.28E-04	3.60E-05	-1.14E-04	1.13E-04
200	5	-1.84E-06	-2.80E-05	-2.47E-05	-9.16E-06	7.63E-04	1.64E-02	8.65E-04	4.06E-05	1.28E-04	-3.60E-05	1.15E-04	-1.18E-04
200	10	-3.68E-06	-5.59E-05	-4.91E-05	-1.83E-05	1.53E-03	3.28E-02	1.73E-03	8.12E-05	2.55E-04	-7.20E-05	2.30E-04	-2.41E-04
200	20	-7.36E-06	-1.12E-04	-9.81E-05	-3.58E-05	3.09E-03	6.82E-02	3.46E-03	1.62E-04	5.10E-04	-1.44E-04	4.62E-04	-5.04E-04

Table D3.70 aqueous iron: effect of change in *beta*

MHz	%	c 10nm	c 100nm	c 1um	c 10um	c 100um	c 1mm	a 10nm	a 100nm	a 1um	a 10um	a 100um	a 1mm
0.1	-20	-3.27E-04	-3.27E-04	-3.39E-04	-7.42E-04	-2.00E-04	-2.22E-05	-2.17E-03	-3.60E-04	-2.21E-04	-7.45E-04	-1.11E-03	-5.87E-04
0.1	-10	-1.75E-04	-1.75E-04	-1.81E-04	-3.97E-04	-1.07E-04	-1.22E-05	-1.10E-03	-1.92E-04	-1.18E-04	-3.98E-04	-5.91E-04	-3.14E-04
0.1	-5	-9.03E-05	-9.03E-05	-9.35E-05	-2.05E-04	-5.52E-05	-6.11E-06	-5.57E-04	-9.91E-05	-6.10E-05	-2.06E-04	-3.05E-04	-1.62E-04
0.1	5	9.59E-05	9.60E-05	9.94E-05	2.18E-04	5.87E-05	6.11E-06	5.65E-04	1.05E-04	6.49E-05	2.19E-04	3.24E-04	1.72E-04
0.1	10	1.98E-04	1.98E-04	2.05E-04	4.49E-04	1.21E-04	1.33E-05	1.14E-03	2.16E-04	1.34E-04	4.50E-04	6.68E-04	3.55E-04
0.1	20	4.18E-04	4.18E-04	4.33E-04	9.49E-04	2.56E-04	2.83E-05	2.31E-03	4.56E-04	2.82E-04	9.52E-04	1.41E-03	7.51E-04
1	-20	-4.90E-04	-4.90E-04	-8.59E-04	-6.96E-04	-1.01E-04	-1.14E-05	-2.75E-03	-4.75E-04	-4.93E-04	-1.56E-03	-1.28E-03	-9.94E-06
1	-10	-2.62E-04	-2.61E-04	-4.58E-04	-3.71E-04	-5.38E-05	-5.96E-06	-1.40E-03	-2.52E-04	-2.63E-04	-8.32E-04	-6.84E-04	-5.31E-06
1	-5	-1.35E-04	-1.35E-04	-2.36E-04	-1.91E-04	-2.77E-05	-3.25E-06	-7.05E-04	-1.30E-04	-1.36E-04	-4.29E-04	-3.53E-04	-2.74E-06
1	5	1.43E-04	1.43E-04	2.50E-04	2.03E-04	2.93E-05	3.25E-06	7.14E-04	1.37E-04	1.44E-04	4.55E-04	3.74E-04	2.90E-06
1	10	2.94E-04	2.94E-04	5.15E-04	4.18E-04	6.07E-05	7.05E-06	1.44E-03	2.82E-04	2.96E-04	9.36E-04	7.69E-04	5.98E-06
1	20	6.21E-04	6.21E-04	1.09E-03	8.82E-04	1.28E-04	1.46E-05	2.91E-03	5.95E-04	6.24E-04	1.98E-03	1.62E-03	1.26E-05
10	-20	-7.29E-04	-7.55E-04	-1.64E-03	-4.15E-04	-5.24E-05	-4.21E-05	-3.49E-03	-5.33E-04	-1.68E-03	-2.21E-03	-4.69E-05	-2.47E-05
10	-10	-3.88E-04	-4.02E-04	-8.75E-04	-2.21E-04	-2.78E-05	-2.11E-05	-1.77E-03	-2.83E-04	-8.94E-04	-1.18E-03	-2.50E-05	-1.31E-05
10	-5	-2.00E-04	-2.07E-04	-4.51E-04	-1.14E-04	-1.44E-05	-1.05E-05	-8.90E-04	-1.45E-04	-4.60E-04	-6.07E-04	-1.29E-05	-6.75E-06
10	5	2.12E-04	2.19E-04	4.78E-04	1.20E-04	1.50E-05	1.05E-05	9.00E-04	1.53E-04	4.87E-04	6.42E-04	1.36E-05	7.12E-06
10	10	4.35E-04	4.51E-04	9.82E-04	2.48E-04	3.10E-05	2.11E-05	1.81E-03	3.14E-04	1.00E-03	1.32E-03	2.80E-05	1.46E-05
10	20	9.17E-04	9.50E-04	2.07E-03	5.23E-04	6.58E-05	4.21E-05	3.66E-03	6.60E-04	2.11E-03	2.78E-03	5.90E-05	3.07E-05
100	-20	-1.08E-03	-1.85E-03	-1.36E-03	-2.13E-04	-1.24E-04	0.00E+00	-4.45E-03	-1.30E-03	-3.47E-03	-2.27E-04	-1.14E-04	-4.83E-05
100	-10	-5.71E-04	-9.82E-04	-7.24E-04	-1.14E-04	-6.21E-05	0.00E+00	-2.25E-03	-6.84E-04	-1.84E-03	-1.20E-04	-6.05E-05	-2.56E-05
100	-5	-2.94E-04	-5.06E-04	-3.73E-04	-5.87E-05	-3.11E-05	0.00E+00	-1.13E-03	-3.50E-04	-9.44E-04	-6.18E-05	-3.11E-05	-1.32E-05
100	5	3.11E-04	5.36E-04	3.96E-04	6.23E-05	3.11E-05	-3.19E-04	1.14E-03	3.67E-04	9.95E-04	6.51E-05	3.27E-05	1.39E-05
100	10	6.39E-04	1.10E-03	8.15E-04	1.28E-04	7.25E-05	-3.19E-04	2.29E-03	7.52E-04	2.04E-03	1.34E-04	6.72E-05	2.86E-05
100	20	1.34E-03	2.32E-03	1.72E-03	2.72E-04	1.55E-04	-3.19E-04	4.63E-03	1.57E-03	4.28E-03	2.80E-04	1.41E-04	6.03E-05
200	-20	-1.58E-03	-3.13E-03	-1.37E-03	-2.12E-04	1.06E-04	6.57E-04	-5.59E-03	-2.67E-03	-4.11E-03	-4.21E-04	-1.64E-04	-7.13E-05
200	-10	-8.37E-04	-1.67E-03	-7.34E-04	-1.15E-04	4.24E-05	0.00E+00	-2.82E-03	-1.40E-03	-2.17E-03	-2.22E-04	-8.70E-05	-3.79E-05
200	-5	-4.30E-04	-8.59E-04	-3.79E-04	-5.99E-05	2.12E-05	0.00E+00	-1.42E-03	-7.16E-04	-1.11E-03	-1.14E-04	-4.47E-05	-1.95E-05
200	5	4.55E-04	9.10E-04	4.03E-04	6.33E-05	-4.24E-05	-6.57E-04	1.43E-03	7.48E-04	1.17E-03	1.20E-04	4.72E-05	2.06E-05
200	10	9.33E-04	1.87E-03	8.29E-04	1.32E-04	-6.36E-05	-6.57E-04	2.87E-03	1.53E-03	2.39E-03	2.46E-04	9.69E-05	4.23E-05
200	20	1.96E-03	3.94E-03	1.75E-03	2.80E-04	-1.27E-04	-1.31E-03	5.78E-03	3.19E-03	5.01E-03	5.16E-04	2.04E-04	8.90E-05

Appendix E: Table of physical properties of materials

Medium	c	ρ	μ or η	κ	C_p	α / f^2	β
polystyrene	2330 [1]	1053 [7]	1.27×10e+9 [7]	0.1151 [7]	1193.24 [7]	1.0×10^{-13} [7]	2.64×10^{-4} [7]
silica	5968 [2]	1970 [8]	$2.79\times\times10^{10}$ [2]	1.6 [2]	728.5 [2]	2.6×10^{-22} [11]	1.35×10^{-6} [2]
metallic iron	5900 [3]	7900 [9]	$6.56\times\times10^{10}$ [9]	80.4 [9]	443.8 [9]	5.7×10^{-14} [5]	1.2×10^{-5} [9]
350cSt silicone oil	1001.4 [16]	970.0 [15]	0.3395 [15]	0.159 [15]	1507.25 [15]	2.5×10^{-12} [16]	9.6×10^{-4} [15]
sample X	2100 [17]	1050 [17]	1.0×10^{9} [17]	0.65 [17]	3000 [17]	1.0×10^{-14} [17]	2.6×10^{-4} [17]
titanium dioxide AHR pigment	7900 [4]	3850 [10]	3.54×10^{10} [4]	3.5 [4]	930.1 [4]	1.2×10^{-16} [4]	8.61×10^{-6} [4]
soya oil	1450 [8]	908 [8]	0.05 [8]	0.220 [8]	1933 [8]	6.84×10^{-13} [8]	7.35×10^{-4} [8]
1-bromo-hexadecane	1299.4 [5]	1000 [5]	6.63×10^{-3} [5]	0.141 [13]	2090.8 [13]	1.45×10^{-13} [5]	7.75×10^{-4} [5]
hexadecane	1336 [5]	773.3 [6]	3.27×10^{-3} [5]	0.1405 [6]	2093.4 [6]	9×10^{-14} [5]	7×10^{-4} [5]
water at 25ºC	1496.7 [12]	997.1 [6]	8.91×10^{-4} [6]	0.6058 [6]	4179.60 [6]	2.30×10^{-14} [14]	2.57×10^{-4} [6]
water at 30ºC	1509.1 [12]	995.7 [6]	7.98×10^{-4} [6]	0.6135 [6]	4178.49 [6]	1.96×10^{-14} [14]	3.03×10^{-4} [6]

Table E1 Physical properties of continuous and dispersed media

E1.1 Key to abbreviations, property symbols and SI units used in Table E1

c	speed of sound (m/s)
ρ	density (kg/m^3)
η	shear viscosity (applicable to liquids) (Pas s)
μ	shear modulus (applicable to solids) (Pas)
κ	thermal conductivity (W/m/K)
C_p	specific heat at constant pressure (J/kg/K)
α/f^2	attenuation ($Np\ s^2/m$)
β	coefficient of expansion (1/K)

E1.2 Key to sources of property values used in Table E1

[1] Gladwell *et al* (1987)

[2] Kaye & Laby (1995)

[3] Ensminger (1988)

[4] Information supplied by DuPont Ltd, personal communication to UDSP Laboratory, University of Keele (1994)

[5] Experimentally determined by the UDSP Laboratory

[6] Weast (1988)

[7] Allegra & Hawley (1972)

[8] Information supplied by Malvern Instruments Ltd, personal communication to UDSP Laboratory, (1997)

[9] Information supplied by Goodfellow Corporation, products catalogue (1997-98)

[10] Information supplied by Tioxide Ltd, AHR product data sheet (Jan 1995)

[11] Gray (1963)

[12] Del Grosso & Mader (1972)

[13] Data for hexadecane used from Reference [6]

[14] Smith & Beyer (1948)

[15] Information supplied by Dow Corning Ltd, personal communication to UDSP Laboratory (1995)

[16] 350 cSt silicone oil refers to Dow Corning 200 Fluid, which possesses a kinematic viscosity of 350 centistokes and a frequency dependent complex wavenumber. Therefore, the velocity and attenuation figures are those measured experimentally at 2MHz.

[17] Sample X refers to a fictitious material used only for the purpose of simulation. It was conceived to possess a combination of physical properties that contrast with those of water in a way that is not reproducible with any known real and adequately categorized material.